

NASA CR-134710

PWA-5087

(NASA-CR-134710)	TWO-STAGE FAN. 2:	N75-10944
DATA AND PERFORMANCE WITH REDESIGNED		
SECOND STAGE ROTOR UNIFORM AND DISTORTED		
INLET FLOWS (Pratt and Whitney Aircraft)		
352 p HC \$10.00	CSCL 21E	G3/07 02758
		Unclas



**TWO-STAGE FAN  
 II. DATA AND PERFORMANCE WITH REDESIGNED  
 SECOND STAGE ROTOR UNIFORM AND  
 DISTORTED INLET FLOWS**

BY

H. E. Messenger  
 M. J. Keenan

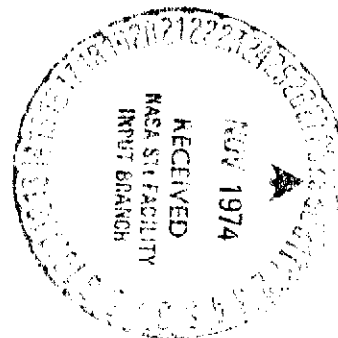
PRATT & WHITNEY AIRCRAFT DIVISION  
 UNITED AIRCRAFT CORPORATION

October 1974

prepared for

NATIONAL AERONAUTICS AND SPACE ADMINISTRATION

NASA Lewis Research Center  
 Contract NAS3-13494



1. Report No. NASA CR-134710	2. Government Accession No.	3. Recipient's Catalog No.	
4. Title and Subtitle TWO STAGE FAN - II DATA AND PERFORMANCE WITH REDESIGNED SECOND STAGE ROTOR, UNIFORM & DISTORTED INLET FLOWS		5. Report Date October 1974	6. Performing Organization Code
		8. Performing Organization Report No. PWA-5087	10. Work Unit No.
7. Author(s) H. E. Messenger M. J. Keenan		11. Contract or Grant No. NAS3-13494	
9. Performing Organization Name and Address PRATT & WHITNEY AIRCRAFT DIVISION UNITED AIRCRAFT CORPORATION EAST HARTFORD, CONNECTICUT 06108		13. Type of Report and Period Covered Contractor Report	
		14. Sponsoring Agency Code	
12. Sponsoring Agency Name and Address National Aeronautics and Space Administration, Washington, D.C. 20546		15. Supplementary Notes Project Manager, R. S. Ruggeri, Fluid System Components Division NASA-Lewis Research Center, Cleveland, Ohio 44135	
16. Abstract <p>A two-stage fan with a first rotor tip speed of 1450 ft/sec (441.96 m/sec) and no inlet guide vanes was tested with uniform and distorted inlet flows. The test was conducted with a redesigned second rotor having a part span shroud to prevent flutter, with variable-stagger stators set in nominal positions, and without rotor casing treatment.</p> <p>At design speed the fan achieved a pressure ratio of 2.8 at a corrected flow of 185.4 lbm/sec (84.0 kg/sec), an adiabatic efficiency of 85.0 percent, and a stall margin of 12 percent. The redesigned second rotor did not flutter.</p> <p>Tip radial distortion reduced the stall margin at intermediate speed, but had little effect on stall margin at high or low speeds. Hub radial distortion reduced the stall margin at design speed but increased stall margin at low speed. Circumferential distortion reduced stall pressure ratio and flow to give approximately the same stall line as with uniform inlet flow. Distortions were attenuated by the fan.</p>			
17. Key Words (Suggested by Author(s)) Two-Stage Fan Shrouded Rotors Distorted Inlet Flows Compressor		18. Distribution Statement  Unclassified - Unlimited	
19. Security Classif. (of this report) Unclassified	20. Security Classif. (of this page) Unclassified	21. No. of Pages	22. Price*

\* For sale by the National Technical Information Service, Springfield, Virginia 22151

## FOREWORD

This report was prepared for the National Aeronautics and Space Administration, Lewis Research Center, under Contract NAS3-13494 to present data and performance of a two-stage fan tested with a redesigned second stage rotor, resettable stators in their nominal positions, and without tip casing treatments, and to describe aerodynamic and mechanical details of the rotor redesign. Mr. R. S. Ruggeri was the NASA Project Manager for this effort, and Mr. H. V. Marman the Pratt & Whitney Aircraft Program Manager. This report was prepared by H. E. Messenger and M. J. Keenan, with contributions from B. Gray, T. Hodges, G. Burger, A. Merrow, J. Ruschak, A. Finke and other Pratt & Whitney Aircraft personnel.

## TABLE OF CONTENTS

	<b>Page</b>
SUMMARY	1
INTRODUCTION	2
APPARATUS AND PROCEDURE	3
Aerodynamic Design	3
Redesign of the Second-Stage Rotor	4
Velocity Vectors	5
Airfoil Design	6
Structural Design	8
Blade Stresses	8
Partspan Shroud Design	8
Blade Flutter	9
Blade Tip Chordwise Bending	9
Critical Speed Analysis	9
Test Facility	10
Instrumentation and Calibration	11
Test Procedure	13
Shakedown Tests	13
Overall and Blade Element Performance Mapping	14
Disassembly Inspection	14
Data Reduction Techniques	14
Data Correction and Averaging	14
Performance Parameter Calculations	16
RESULTS AND DISCUSSION	19
Uniform Inlet Flow	19
Fan Overall Performance	19
Overall Performance of First Stage, First Stage Rotor	20
Nondimensional Performance Data	20
Blade Element Data	21
First-Stage Rotor	22
First-Stage Stator	23
Second-Stage Rotor	23
Second-Stage Stator	23
Radially Distorted Inlet Flow	24
Tip Distorted Flow	24
Overall Performance	24
Blade Element Data	25
Hub Distorted Flow	26
Overall Performance	26
Blade Element Data	26

## TABLE OF CONTENTS (Cont'd)

	Page
Attenuation of Radial Distortion	27
Circumferentially Distorted Inlet Flow	28
Overall Performance	28
Circumferential Distributions of Flow Field Parameters	28
Remarks	30
Summary of Results	30
REFERENCES	32
FIGURES (1-98)	33-204
APPENDIXES	
A – Symbols and Performance Parameters	205
B – Airfoil Geometry on Conical Surfaces	215,
C – Design Values of Overall Performance and Blade Element Parameters for the Redesigned Stage	219
D – Airfoil Coordinates for Manufacturing Surfaces for the Redesigned Rotor 2	227
E – Overall Performance and Blade Element Data with Uniform Inlet Flow	233
F – Overall Performance and Blade Element Data with Tip Radially Distorted Inlet Flow	297
G – Overall Performance and Blade Element Data with Hub Radially Distorted Inlet Flow	307
H – Overall Performance and Velocity Vector Parameters for Circumferentially Distorted Inlet Flow	317
DISTRIBUTION LIST	339

## LIST OF FIGURES

Figure	Title	Page
1	Schematic of Two-Stage Fan Test Arrangement	33
2	Fan Flowpath	34
3	Photographs of Blades and Vanes	35
4	Stage 1 Efficiency Versus Span Showing Wake of the Part-Span Shroud	36
5	Design Total Pressure Ratio Versus Span at Rotor 2 Exit and Fan Exit	36
6	Design Inlet and Exit Relative Air Angle Versus Span for Original and Redesigned Rotor 2	37
7	Design Meridional Velocity Versus Span for Original and Redesigned Rotor 2	37
8	Design Relative Mach Number Versus Span for Original and Redesigned Rotor 2	38
9	Design Diffusion Factor Versus Span for Original and Redesigned Rotor 2	38
10	Stator Design Diffusion Factor Versus Span for Original and Redesigned Rotor 2	39
11	Stator 2 Design Mach Number Versus Span for Original and Redesigned Rotor 2	39
12	Stator 2 Design Inlet Air Angle Versus Span for Original and Redesigned Rotor 2	40
13	Redesigned Rotor 2 Inlet and Exit Metal Angles Versus Span	41
14	Redesigned Rotor 2 Incidence Angle Versus Span	42
15	Redesigned Rotor 2 Deviation Angles Versus Span	43
16	Redesigned Rotor 2 Front Camber Angles Versus Span	44
17	Redesigned Rotor 2 Minimum Channel Area Ratios Versus Span	44

## LIST OF FIGURES (Cont'd)

Figure	Title	Page
18	Redesigned Rotor 2 Channel Area Ratios Versus Axial Distance Percent Span at Blade Leading Edge	45
19	Chord Versus Span for Original and Redesigned Rotor 2	46
20	Front Chord Versus Span for Original and Redesigned Rotor 2	46
21	Solidity Versus Span for Original and Redesigned Rotor 2	46
22	Maximum Thickness/Chord Ratio Versus Span for Original and Redesigned Rotor 2	47
23	Chordwise Location of Airfoil Maximum Thickness Versus Span for Original and Redesigned Rotor 2	47
24	Redesigned Rotor 2 Combined Stress Compared to Successful Experience	48
25	Goodman Diagram for Redesigned Rotor 2	48
26	Resonance Diagram for Redesigned Rotor 2	49
27	Part-Span Shroud – Rotor 2	50
28	Resonance Diagram for Tip Chordwise Bending Modes of Redesigned Rotor 2	51
29	Spring-Mass Model for Critical Speed Analysis of Two-Stage Fan Rig	52
30	Vibrational Amplitude at No. 1 Bearing Showing Benefit of Oil-Damped Bearing	53
31	Schematic of Compressor Test Facility	54
32	Sketch of Distortion Screens	55
33	Photographs of Typical Instrumentation	56
34	Axial Locations of Instrumentation	57
35	Circumferential Locations of Instrumentation	58

## LIST OF FIGURES (Cont'd)

Figure	Title	Page
36	First-Stage Pressure Correlation Used for Radial Distortion Streamline Analysis Flowfield Calculation	59
37	Comparison of Measured and Calculated Static Pressure Versus Span at Rotor 1 Inlet	59
38	Calculated Static Pressure Versus Span at Stator 1 Inlet and Measured Static at Outer Wall	60
39	Measured and Calculated Static Pressure Versus Span at Stator 1 Exit	60
40	Calculated Static Pressure Versus Span at Stator 2 Inlet and Measured Wall Static Pressures	61
41	Measured and Calculated Static Pressure Versus Span at Stator 2 Exit	61
42	Fan Overall Performance with Uniform Inlet Flow	62
43	Fan Overall Performance at Design Speed with Uniform Inlet Flow	63
44	Operating Line Efficiency Versus Corrected Flow	64
45	Maximum Corrected Flow at Stator 2 Inlet Versus Pressure Ratio at Stator 2 Inlet	64
46	First Stage Performance With Uniform Inlet Flow	65
47	First Rotor Performance With Uniform Inlet Flow	66
48	Pressure Coefficient and Adiabatic Efficiency Versus Flow Coefficient For Uniform Inlet Flow Rotor 1	67
49	Pressure Coefficient and Adiabatic Efficiency Versus Flow Coefficient For Uniform Inlet Flow Stage 1	68
50	Pressure Coefficient and Adiabatic Efficiency Versus Flow Coefficient for Uniform Inlet Flow, Rotor 2	69
51	Pressure Coefficient and Adiabatic Efficiency Versus Flow Coefficient for Uniform Inlet Flow, Stage 2	70



## LIST OF FIGURES (Cont'd)

Figure	Title	Page
52	Rotor Adiabatic Efficiency Versus Span for Near Design Data Point	71
53	First Stage and Fan Overall Efficiency Versus Span for Near Design Data Point	72
54	Rotor Total Pressure Ratio Versus Span For Near Design Data Points	73
55	First Stage and Fan Overall Total Pressure Ratio Versus Span For Near Design Data Point	74
56	Loss Coefficient, Diffusion Factor, Deviation Angle, and Incidence Angle For Near Design Data Point – Rotor 1	75
57	Loss Coefficient, Diffusion Factor, Deviation Angle, and Incidence Angle For Near Design Data Point – Stator 1	76
58	Loss Coefficient, Diffusion Factor, Deviation Angle and Incidence Angle for Near Design Data Point – Rotor 2	77
59	Loss Coefficient, Diffusion Factor, Deviation Angle, and Incidence Angle for Near Design Data Point – Stator 2	78
60a-k	Blade Element Performance With Uniform Inlet Flow – Rotor 1	79-89
61a-k	Blade Element Performance With Uniform Inlet Flow – Stator 1	90-100
62a-k	Blade Element Performance With Uniform Inlet Flow – Rotor 2	101-111
63a-k	Blade Element Performance With Uniform Inlet Flow – Stator 2	112-122
64	Oscillograph Trace During Surge at Design Speed for Uniform Inlet Flow	123
65	First Rotor Inlet Total Pressure Ratio Versus Span for Radially Distorted Inlet Flow	124

## LIST OF FIGURES (Cont'd)

Figure	Title	Page
66	Inlet Total Pressure Distortion Parameter Versus Inlet Corrected Flow for Radial Distortions	125
67	Inlet Meridional Velocity Distortion Parameter Versus Inlet Corrected Flow for Radial Distortions	126
68	Fan Overall Performance with Tip Radially Distorted Inlet Flow	127
69	First Stage Performance with Tip Radially Distorted Inlet Flow	128
70	First Rotor Performance with Tip Radially Distorted Inlet Flow	129
71	Stall Margin Versus Corrected Speed for Uniform and Distorted Inlet Flows	130
72	Hot Film and Strain Gage Records at Stall, with Tip Radially Distorted Flow at 85 Percent Speed	131
73	Resonance Diagram for Rotor 1	132
74	Hot Film and Strain Gage Records at Stall with Tip Radially Distorted Flow at Design Speed	133
75	Spanwise Profiles of Stage 1 and Stage 2 Pressure Ratio for Uniform and Tip Radially Distorted Inlet Flows at Design Speed	134
76	Spanwise Profiles of Fan Efficiency for Uniform and Radially Distorted Inlet Flows at Design Speed	135
77a-e	Blade Element Performance with Tip Radial Distortion – Rotor 1	136-140
78a-e	Blade Element Performance with Tip Radial Distortion – Stator 1	141-145
79a-e	Blade Element Performance with Tip Radial Distortion – Rotor 2	146-150
80a-e	Blade Element Performance with Tip Radial Distortion – Stator 2	151-155

## LIST OF FIGURES (Cont'd)

Figure	Title	Page
81	Fan Overall Performance with Hub Radially Distorted Inlet Flow	156
82	First Stage Performance with Hub Radially Distorted Inlet Flow	157
83	First Rotor Performance with Hub Radially Distorted Inlet Flow	158
84	Spanwise Profiles of Stage 1 and Stage 2 Pressure Ratio for Uniform and Hub-Radially Distorted Inlet Flows at Design Speed	159
85a-e	Blade Element Performance with Hub Radial Distortion – Rotor 1	160-164
86a-e	Blade Element Performance with Hub Radial Distortion – Stator 1	165-169
87a-e	Blade Element Performance with Hub Radial Distortion – Rotor 2	170-174
88a-e	Blade Element Performance with Hub Radial Distortion – Stator 2	175-179
89	Total Pressure Ratio versus Span at Fan Inlet, First Stage Exit, and Fan Exit for Tip Radially Distorted Inlet Flow	180
90	Total Pressure Ratio versus Span at Fan Inlet, First Stage Exit, and Fan Exit for Hub Radially Distorted Inlet Flow	181
91	Circumferential Distributions of Total Pressure at Fan Inlet for Circumferentially Distorted Inlet Flow	182
92	Fan Overall Performance with Circumferentially Distorted Inlet Flow	183
93	First Stage Performance with Circumferentially Distorted Inlet Flow	184
94	Circumferential Distributions of Fan Inlet Static Pressure at the Hub for Tests with Circumferentially Distorted Inlet Flow at Design Speed	185

## LIST OF FIGURES (Cont'd)

Figure	Title	Page
95	Circumferential Distributions of Fan Inlet Static Pressure at the Tip for Tests with Circumferentially Distorted Inlet Flow at Design Speed	186
96a-f	Circumferential Distributions of Fan Inlet Total Pressure, Static Pressure, Absolute Mach Number, Relative Flow Angle, Absolute Flow Angle, and Meridional Velocity with Circumferential Inlet Flow Distortion	187-192
97a-f	Circumferential Distributions of First Stator Exit Total Pressure, Static Pressure, Absolute Mach Number, Total Temperature, Absolute Flow Angle, and Meridional Velocity with Circumferential Inlet Flow Distortion	193-198
98a-f	Circumferential Distributions of Fan Exit Total Pressure, Static Pressure, Absolute Mach Number Total Temperature, Absolute Flow Angle, and Meridional Velocity with Circumferential Inlet Flow Distortion	199-204

## LIST OF TABLES

Table	Title	Page
I	Design Performance	4
II	Blade and Vane Geometric Parameters	7
III	Partspan Shroud Parameters for Redesigned Rotor 2	8
IV	Predicted Vibration Amplitudes at Number 1 Bearing	10
V	Performance and Blade Element Instrumentation	12
VI	Stall Transient Instrumentation	13
VII	Parameters Input to Flowfield Program	16
VIII	Annulus Blockages	18
IX	Attenuation Parameters at Design Speed for Hub and Tip Radially Distorted Inlet Flow	27
X	Attenuation Parameters at Design Speed for Circumferentially Distorted Inlet Flow	29
XI	Airfoil Geometry on Conical Surfaces – Rotor 1	215
XII	Airfoil Geometry on Conical Surfaces – Stator 1	216
XIII	Airfoil Geometry on Conical Surfaces – Rotor 2 (Unshrouded)	216
XIV	Airfoil Geometry on Conical Surfaces – Rotor 2 (Redesign)	217
XV	Airfoil Geometry on Conical Surfaces – Stator 2	217
XVI	Spans and Diameters for Blade Element Data	219
XVII	Identification of Overall Performance and Blade – Element Data Table Column Headings	220
XVIII	Overall Performance and Blade Element Data	222
XIX	Airfoil Coordinates on Manufacturing Surfaces (Redesigned Rotor 2)	227

## LIST OF TABLES (Cont'd)

Table	Title	Page
XX	Fan Overall Performance (Uniform Inlet Flow)	233
XXI	Overall Performance and Blade Element Data (Uniform Inlet Flow)	234
XXII	Fan Overall Performance (Tip Radially Distorted Inlet Flow)	297
XXIII	Overall Performance and Blade Element Data (Tip Radially Distorted Flow)	298
XXIV	Fan Overall Performance (Hub Radially Distorted Flow)	307
XXV	Overall Performance and Blade Element Data (Hub Radially Distorted Flow)	308
XXVI	Fan Overall Performance (Circumferentially Distorted Inlet Flow)	317
XXVII	Velocity Vector Parameters at Rotor I Inlet (Circumferentially Distorted Inlet Flow)	318
XXVIII	Velocity Vector Parameters at Stator 1 Exit (Circumferentially Distorted Inlet Flow)	324
XXIX	Velocity Vector Parameters at Fan Exit (Circumferentially Distorted Inlet Flow)	330
XXX	First Stage Total Temperature Ratio (Circumferentially Distorted Inlet Flow)	336
XXXI	Circumferential Distributions of Total Pressure Ratio and Total Temperature Ratio at the Second-Stage Stator Exit	337

**TWO-STAGE FAN  
II. DATA AND PERFORMANCE WITH REDESIGNED  
SECOND STAGE ROTOR UNIFORM AND  
DISTORTED INLET FLOWS**

**H.E.Messenger and M.J.Keenan  
Pratt & Whitney Aircraft Division  
United Aircraft Corporation**

**SUMMARY**

Tests were conducted on a highly-loaded, two-stage fan with a 1st-stage rotor tip-speed of 1450 ft/sec [422 m/sec]. The purpose of the tests was to determine detailed aerodynamic performance of the basic configuration (i.e., with nominal stator settings and without tip-casing treatment) both with uniform and with distorted inlet flow. Good aerodynamic performance had been documented during earlier tests, but flutter encountered with the 2nd-stage rotor blades curtailed testing and led to a redesign of this rotor. A partspan shroud was added at 60 percent span from the hub of the new 2nd-stage rotor which, together with other minor geometric changes, eliminated flutter in the fan operating range. The redesigned 2nd-stage rotor also incorporated a radially skewed (negatively sloped) exit total pressure profile to increase hub velocity, thereby reducing critical loadings to increase stall margin.

With uniform inlet flow at design speed and pressure ratio, the fan with the redesigned rotor achieved an adiabatic efficiency of 85.0% which is 1.3% above the redesign value and 0.7% below the value attained in tests with the unshrouded rotor 2. A fan flow of 185.4 lbm/sec [84.0 kg/sec] was achieved which is 0.7% above the design value of 184.2 lbm/sec [83.5 kg/sec]. Fan stall margin was approximately 12% based on operation at design pressure ratio, about 2% higher than in the earlier tests. Peak fan efficiencies over the operating range from 50 to 100 percent speed were above 83%; efficiencies at overspeed decreased to a peak value of 79.2% at 110 percent of design speed.

Hub and tip radial distortions, each covering approximately 40 percent of the inlet annulus area and having distortion parameters,  $(P_{\max} - P_{\min})/P_{\max}$ , of 0.14 at design speed, caused small changes in fan efficiency relative to uniform inlet flow but more significant changes in fan stall margin. Relative to a constant throttle operating line through the design point, the tip-radial distortion reduced fan stall margin to 7% at 85 percent of design speed but had little effect on the stall line at 70 and 100 percent speeds. The hub-radial distortion caused reductions in fan maximum flow of 1% to 3% and reduced stall margin at design speed to 6%, half the value obtained with uniform inlet flow. A gain in stall margin of seven percentage points was noted at 70 percent speed. At design speed, fan attenuation of tip-radial distortion was nearly complete; hub-radial distortion was slightly overattenuated. Circumferential distortion covered approximately a 90-degree segment at the fan inlet with a peak distortion parameter of 0.14 at design speed. Stall occurred at a lower pressure ratio with this distortion than with uniform inlet flow but at a lower flow so that the stall line was essentially unchanged. The fan significantly attenuated this distortion except at the hub.

## INTRODUCTION

Fans and compressors for advanced aircraft engines must have light weight, high efficiency, adequate stall margin, and tolerance to inlet flow distortions. For advanced aircraft which fly mixed supersonic-subsonic missions, turbofan engines having low bypass ratios and high fan pressure ratios are required. Inasmuch as multistage fans are required, the use of high tip speeds and high blade loadings permits reductions in the number of fan stages.

NASA has conducted an extensive in-house and contractual research program on high-speed, highly-loaded fan stages. Fan stages with tip speeds from 800 to 1800 ft/sec [244 to 549 m/sec] and design pressure ratios from 1.15 to 2.28 have been tested (ref. 1 to 8). This research program has proven that high-speed, highly-loaded stages can give good performance. Based on these results, a two-stage, highly-loaded, high-speed fan has been designed, fabricated, and tested. The objectives of the two-stage-fan program are to evaluate the stage matching problems, distortion tolerance, response to stator adjustment, and effectiveness of casing treatment for such a fan. Design tip speed for the two-stage fan is 1450 ft/sec [442 m/sec], design pressure ratio is 2.8, tip diameter is 31 in. [0.787 m], design corrected flow is 184.2 lbm/sec [83.55 kg/sec], and inlet hub-tip ratio is 0.4. Details of the aerodynamic and mechanical design were presented in an earlier report (ref. 9).

Good aerodynamic performance was demonstrated during the first test of this two-stage fan. At design speed and pressure ratio, the measured flow closely matched the design value. Efficiency at this design operating point was 85.7% and stall margin was 10%. Measured rotor losses were about equal to design values, but stator losses were less than design values. This first test effort was curtailed due to flutter on the 2nd-stage rotor blades and cracking of stator vane root leading edges. First bending, subsonic stall flutter was encountered near the stall limit at speeds between 77 and 93 percent of the design value. Supersonic stall flutter was encountered at speeds above 105 percent of design. Failure of one 1st-stage stator vane root leading edge section was attributed to a locally thin section, and failure of one 2nd-stage stator vane root leading edge was attributed to a stress concentration resulting from a brazed-on leading edge sensor. The results of the first test were reported by Ruggeri and Benser of NASA (ref 10).

Because of the problems encountered during the first test effort, the 2nd-stage rotor was redesigned. A partspan shroud was added to the rotor blades to eliminate flutter. The 2nd-stage rotor was also redesigned to provide a radially skewed exit total pressure profile (i.e., higher total pressure at the hub than at the tip) to increase stall margin by raising hub exit velocities, thereby reducing aerodynamic loadings at the hub. The 2nd-stage stator was predicted to operate satisfactorily with this revised pressure ratio profile. Additional 1st-stage vanes were fabricated to insure that a sufficient number of vanes meeting design thickness specifications were available for the second test of the fan. Data obtained from the first test (i.e., before the redesign) showed that the stator-exit instrumentation provides the same information as the 2nd-stage stator leading edge sensors with good accuracy. Therefore, these 2nd-stage sensors were eliminated from the rebuild, avoiding the resulting stress concentrations.†

---

† Instrumentation was not installed on the leading edge of the 1st-stage stator vanes in either the first or second test of the fan.



Tests of this modified two-stage fan were run with uniform inlet flow at 50, 70, 85, 95, 100, 105, and 110 percent of design speed, and data were obtained between open throttle and stall at each speed except at 110 percent speed where the fan was not stalled. Overall and blade element performance data were obtained at 70, 85, and 100 percent of design speed with tip radially distorted and hub radially distorted inlet flows. Overall performance data with circumferentially distorted inlet flow were obtained at 70, 90, and 100 percent of design speed; 90 percent speed was used rather than 85 percent speed to avoid a 1st-stage rotor first-bending 4E resonance that had been encountered during shakedown testing with circumferentially distorted inlet flow. Measurements were made to determine overall performance and velocity distribution data at the fan inlet, first-stage exit, and fan exit.

This report presents the details of the aerodynamic and mechanical redesigns and the results of testing the two-stage fan with the redesigned 2nd-stage rotor. Special terms, abbreviations, and symbols used in this report are defined in Appendix A.

## APPARATUS AND PROCEDURE

### AERODYNAMIC DESIGN

A schematic of the two-stage fan test rig is shown in Figure 1. The fan was designed to provide a pressure ratio of 2.8 with a 1st-stage rotor tip speed of 1450 ft/sec [442 m/sec], an adiabatic efficiency of 83.9%, and a flow rate of 184.2 lbm/sec [83.54 kg/sec]. The fan was designed without inlet-guide-vanes (IGV) but with the provision for adding a variable-camber IGV at a later date. Both stators were designed to give axial exit flow. The hub-tip ratio was 0.4, and the specific flow at the 1st-stage rotor was set at 42.0 lbm/sec-ft<sup>2</sup> [205 kg/sec-m<sup>2</sup>]. The average Mach number at the fan exit was approximately 0.5, a practical value for thrust augmentation. Flowpath convergence and wall curvature between inlet and exit were used to control velocity profiles and blade aerodynamic loadings (diffusion factors) near the walls. Design loadings were similar to those for which good single-stage performance had been obtained during earlier programs.

The 1st-stage rotor inlet tip-diameter was selected as 31 in. [0.787 m] to permit use of existing hardware and to allow adequate horsepower margin for the drive engine. With a required 1st-stage rotor tip-speed of 1450 ft/sec [442 m/sec], the design speed corrected to standard inlet conditions was 10,720 rpm. The inlet inner case diameter was held at 10 in. [0.254 m] minimum to permit clearance for the front bearing compartment.

As shown in the flowpath drawing presented in Figure 2, axial spacings between the rotor and stator of the first-stage and between the rotor and stator of the second-stage were held to a minimum which is in line with actual engine design practice. A spacing of slightly more than one inch [0.0254 meters] was allowed between stages to provide room for radial and tangential traverse instrumentation at the exit of the 1st-stage stator.

## REDESIGN OF THE SECOND-STAGE ROTOR

The 2nd-stage rotor was redesigned to prevent the flutter that occurred in the operating regime of the fan during testing of the original configuration and to improve stall margin. Vector diagrams calculated for this redesign were checked to determine whether the existing designs of the 1st-stage rotor and stator and the 2nd-stage stator would operate satisfactorily with the redesigned rotor. It was found that satisfactory operating conditions would be obtained without modifying these blade rows. The geometry of the 2nd-stage rotor was selected and checked for structural integrity. Details of the redesign are given in the following sections.

Performance parameters at the design point for the original and redesigned fans are summarized in Table I. Photographs of the blades and vanes are shown in Figure 3.

TABLE I  
DESIGN PERFORMANCE

corrected speed  $N/\sqrt{\theta} = 10,720$  rpm  
corrected flow  $W/\sqrt{\theta}/\delta = 184.2$  lbm/sec [83.55 kg/sec]

	Pressure Ratio		Adiabatic Efficiency (%)	
	Local	Cumulative	Local	Cumulative
Rotor 1	1.787 (1.786)	1.787 (1.786)	89.4	89.4
Stator 1	0.977 (.976)	1.744 (1.742)	-----	85.4 (85.3)
Rotor 2	1.646 (1.655)	2.872 (2.884)	89.2 (89.9)	86.2 (86.5)
Stator 2	0.975 (.971)	2.80 (2.80)	-----	83.9 (83.7)

(Redesign Values in Parentheses)

The primary purpose of redesigning rotor 2, as previously stated, was to move the region of 1st bending-mode flutter out of the fan operating range. To accomplish this, a partspan shroud was added to the blade at 60 percent of span. The spanwise location of the shroud was selected to satisfy structural requirements and to minimize its loss by placing it in the wake generated by the 1st-stage rotor shroud. The efficiency profile calculated from inter-stage measurements in tests of the original configuration is shown in Figure 4.

A second objective of the redesign was to increase the stall range of the 2nd-stage stator and rotor by raising their exit hub velocities and thereby reducing their hub aerodynamic loading levels. To achieve these lower loadings, the 2nd-stage rotor was redesigned to provide a radially skewed exit total pressure profile (a total pressure approximately 12% higher at the hub than at the tip) while retaining the average fan overall pressure ratio of 2.80 (Figure 5).

## Velocity Vectors

Except for small adjustments in position of the leading and trailing edges of the 2nd-stage rotor, the fan flowpath (Figure 2) was unchanged from the original design. The changes listed in Figure 2 resulted from changes in the axial locations of the blade edges at the hub and tip. Design losses for the 2nd-stage rotor were assumed to be unchanged since changes in Mach number and solidity were small.

Blockages were included in the aerodynamic design to account for boundary layer growth on the casing walls. Boundary layer displacement thickness at the inlet to the 1st-stage rotor was assumed to be equal to that measured downstream of inlet bellmouths used in PWA research programs. Growth of the wall displacement thickness through the blade rows was estimated using a correlation developed by W. T. Hanley (ref. 11) wherein growth along the casing walls is chiefly a function of wall static pressure gradient.

Blockages were also included to account for the presence of partspan shrouds. For each rotor, a blockage equal to the percent of total annulus area occupied by the shroud was applied at the exit of that rotor and the inlet of the following stator and half this amount was used at the inlet plane of the rotor. No allowance for shroud blockage was applied at either the 1st-stage or 2nd-stage stator exits. Total blockage input to the streamline analysis calculation at various axial locations was computed as the sum of endwall blockages and shroud blockages and applied equally to all stream-tubes. The blockages used in the flowfield calculation for the original design were used for the redesign with the addition of the increments required to account for the blockage and wake of the 2nd-stage rotor partspan shroud. The magnitudes of these blockage increments were the same as these used for the 1st-rotor partspan shroud. These design values of blockage at the 1st-stage rotor inlet and exit were verified by flowfield calculations of test data points in which the calculated wall static pressures agreed with measured values (ref. 10).

Flowfield calculations for the original design had been made using a computer program that required a concentration of streamlines near the hub. Streamline analyses for the redesign were made using an improved program which permitted a more even radial distribution of streamlines. Recalculation of the original design aerodynamics using the improved program showed some differences (e.g., velocity changes up to 30 ft/sec [9.1 m/sec]); the comparisons of aerodynamic parameters for the original design and the redesign shown in Figures 6 through 12 are based on the results obtained with the improved program. Inlet relative air-angles (Figure 6) for the redesigned rotor 2 are slightly smaller than those for the original rotor 2 primarily to account for the added blockage of the partspan shroud. The exit relative air-angle decreased by 9.5 degrees at the hub (increased turning) and increased slightly at the tip (less turning) to achieve the skewed (negatively sloped) total pressure profile incorporated in the redesign (Figure 5).

Distributions of velocity and Mach number at the leading and trailing edges of the rotor (Figures 7 and 8) showed increased rotor exit hub velocity with the negatively sloped total pressure profile, which reduced rotor hub aerodynamic loadings (Figure 9) by 0.028 from the calculated value for the original design. The rather high hub loadings of the 2nd-stage stator also decreased somewhat (Figure 10) while tip loadings increased, giving a more balanced

spanwise loading distribution. Stator 2 hub Mach numbers (Figure 11) were somewhat higher for the redesign, and stator 2 inlet air-angles (Figure 12) differed by as much as two degrees from the original design. These changes in angle are considered small in relation to the low-loss incidence range demonstrated in tests with the original design (ref. 10). Because of this and the fact that the redesigned 2nd-stage rotor gave larger angles (higher incidence) into the hub of the 2nd-stage stator and smaller angles (lower incidence) into the tip, no adjustment was made to the 2nd-stage stator settings. Smaller incidence angle changes were calculated for the other blade rows. The maximum change for the 1st-stage rotor was a 0.86 degree lower incidence at ten percent span from the hub. The 1st-stage stator incidence increased by a maximum of 0.23 degrees at ten percent span. The maximum 2nd-stage rotor incidence change was a 1.22 degree lower incidence at five percent span. The maximum incidence changes on the 2nd-stage stator were an increase of 2.5 degrees at five percent span and a decrease of 2.7 degrees at 90 percent span. Based on these small angle changes, it was concluded that the original 1st-stage rotor and 2nd-stage stator would operate satisfactorily with the redesigned 2nd-stage rotor.

Variable positioning of stator-stagger was available to optimize fan performance if needed. However, results reported herein were obtained using the original design stagger settings on both stators. A complete tabulation of aerodynamic parameters for the redesign at blade row leading and trailing edges is given in Appendix C, Tables XVI to XVIII.

### Airfoil Design

Rotor and stator blade sections for both stages of the fan were multiple-circular-arc (MCA) airfoils designed on conical surfaces approximating stream surfaces of revolution. Blade setting angles were determined from design flow-angles and from incidence and deviation angle criteria described in an earlier report (ref. 9). Blade chords were chosen to be consistent with moderate axial lengths, acceptable rotor loadings, and structural requirements. Airfoil leading and trailing edge radii and blade thicknesses were chosen to provide mechanical integrity while maintaining adequate flow area.

Leading and trailing edge metal angles for the redesigned rotor (Figure 13) were determined from redesign velocity vectors and the application of the same incidence and deviation criteria used in the original design. Rotor incidence angles and deviation angles are shown in Figures 14 and 15, respectively. Although data from tests of the original configuration indicated that deviation angles at the rotor 2 hub were higher than had been anticipated (up to 5 deg. higher at ten percent span from the hub), no attempt was made to alter deviation criteria for the redesign since experience has shown that it is difficult to determine accurate deviation angles at rotor hubs. Blade front camber angles (Figure 16) were chosen at values which, in combination with specified incidence and total camber angles, provided minimum critical channel area ratios  $A/A^*$  similar to those of the original design as shown in Figure 17. Distributions of flow area ratios through the blade channels for several percents of span for the redesigned rotor 2 are shown in Figure 18.

Airfoil geometry on design conical surfaces for all blades and vanes, including both the original and redesigned rotor 2 is summarized in Appendix B, Tables XI through XV. Details of rotor 1, stator 1, rotor 2 (original), and stator 2 designs, including manufacturing sections defined on planes normal to the stacking line, were provided in a previous report (ref. 9). Manufacturing sections for the redesigned rotor 2 are given in Appendix D. A summary of important geometric design parameters for the blades and vanes is given in Table II below.

**TABLE II**  
**BLADE AND VANE GEOMETRIC PARAMETERS**

	ROTOR 1	STATOR 1	ROTOR 2 Redesign	STATOR 2
Number of Airfoils	28	46	60	59
Aspect Ratio†	2.48	2.75	2.63	2.20
Hub Chord-inch	3.62 [0.092m]	2.75 [0.070m]	2.10 [0.053m]	2.22 [0.056m]
Tip Chord-inch	4.55 [0.116m]	3.10 [0.079m]	1.89 [0.048m]	2.45 [0.062m]
Hub Solidity	2.38	2.52	2.24	2.25
Tip Solidity	1.33	1.55	1.27	1.66

† Average length/axially – projected – root – chord

The redesign of the rotor included changes to the blade chord and thickness-to-chord ratio dictated by structural requirements. To avoid a 1st-bending 4E resonance in the operating range, the blade chord, originally constant, was decreased ten percent at the tip, fairing to no taper between the location of the partspan shroud and the hub (Figure 19). The front chord and blade solidity (Figures 20 and 21) were decreased correspondingly. These changes reduced the blade mass above the shroud and, thereby, moved the predicted 1st-bending 4E resonance point above 110 percent of design speed. To increase chordwise bending frequency, which had been excited by a 46E resonance during tests of the original configuration, airfoil sections were stiffened by increasing tip maximum thickness from 2.5% to 3% of chord (Figure 22) and by moving the chordwise location of maximum thickness of most of the sections toward the leading edge (Figure 23).

## Structural Design

### Blade Stresses

Blade structural data for the 1st-stage rotor and stator, the original 2nd-stage rotor, and the 2nd-stage stator were provided in the earlier report (ref. 9). Combined centrifugal, untwist, and restraint stresses were calculated for the redesigned rotor at 110 percent of design speed. The results (Figure 24) showed that the rotor 2 combined stresses would be below those of other comparable NASA fan blade designs. A Goodman diagram for the blade (Figure 25) showed an allowable continuous vibratory stress of approximately 11,350 lbf/in.<sup>2</sup> [ $7.8 \times 10^7$  N/m<sup>2</sup>] at the maximum predicted combined steady-stress of 58,000 lbf/in.<sup>2</sup> [ $4.0 \times 10^8$  N/m<sup>2</sup>] which would provide an adequate vibratory stress margin since predicted critical resonances did not occur within the operating range.

### Partspan Shroud Design

The redesigned blades were provided with a partspan shroud at 60 percent span to eliminate the bending flutter encountered during testing of the original two-stage fan. This shroud, coupled with a 10% chordal taper from the shroud to the blade tip and a tip thickness increase from 2.5% to 3% of chord, also removed a critical 4E resonance from the operating range, providing a 6.8% margin on 1st-bending resonance at 110 percent of design speed (Figure 26). Shroud parameters are summarized in Table III, and a sketch of the shroud is shown in Figure 27.

TABLE III

PARTSPAN SHROUD PARAMETERS FOR REDESIGNED ROTOR 2

Shroud Chord - inch	0.725 [0.0184m]
Shroud Contact Angle from plane of rotation - degrees	60
Shroud Location - Percent Span From Hub	60
Shroud Thickness - inch	0.118 [0.003m]
Bearing Stress Predicted - lbf/in. <sup>2</sup>	2980 [ $2.06 \times 10^7$ N/m <sup>2</sup> ]
Bearing Stress Allowable - lbf/in. <sup>2</sup>	5000 [ $3.45 \times 10^7$ N/m <sup>2</sup> ]
Bending Stress Predicted - lbf/in. <sup>2</sup>	49,000 [ $3.38 \times 10^8$ N/m <sup>2</sup> ]
Bending Stress Allowable - lbf/in. <sup>2</sup>	70,000 [ $4.83 \times 10^8$ N/m <sup>2</sup> ]

## Blade Flutter

Flutter is a self-excited and self-sustaining vibration which occurs in either a torsional or bending mode or a combination of both. Flutter parameters for the redesigned 2nd-stage rotor blade were calculated at 110 percent of design speed and compared with results from previous tests. The peak predicted coupled mode flutter parameter  $\psi c/d$  of 0.175 lies within the range of experience where flutter problems have not been encountered. The predicted value of supersonic torsional flutter parameter,  $24V'c\omega_t$ , of 1.66 also lies within the envelope of successful (no flutter) experience.

## Blade Tip Chordwise Bending

In tests of the original fan configuration, the tip of the unshrouded 2nd-stage blade was identified as a potential failure area due to high vibratory stresses associated with a 46E resonance in the tip chordwise 2nd-bending mode. The 46 vanes of the 1st-stage stator formed the source of excitation. A resonance diagram for the 1st and 2nd tip chordwise bending modes for the redesigned blade (Figure 28) shows that the changes in blade design moved the predicted 46E resonance out of the high operating range. The second mode 59E resonance at 85 percent of design speed was not anticipated to be a problem since the 59 vanes of the 2nd-stage stator did not appear to be a strong source of excitation (no 59E response had been observed during tests with the original blade).

## Critical Speed Analysis

Excessive vibrations were measured on the front bearing housing at approximately 10,550 rpm during tests of the original fan. Critical speed analysis had predicted modes at 9,000 rpm and 13,100 rpm, and subsequent improvements to the analytical model shifted the 9,000 rpm mode to 9600 rpm. In considering methods of eliminating possible excessive rig vibration, it was assumed that either predicted mode might be encountered during testing with the redesigned 2nd-stage rotor. Using variations on the mathematical model shown in Figure 29, forced response analyses were conducted and the sensitivity at the No. 1 bearing to a one oz-in. [0.007 N-m] imbalance located at various positions was evaluated. Table IV shows that the predicted vibration amplitude at the original No. 1 bearing is highest for the 9,600 rpm mode when the one oz-in [0.007 N-m] imbalance is located at the rear diaphragm. Maximum amplitude for the 13,100 rpm mode is caused by imbalance at either the 1st-stage or 2nd-stage rotor plane. An oil-damped front bearing was incorporated in the test rig to minimize rig vibrations and to eliminate a potential need for trim balancing. Figure 30 indicates that use of oil damped No. 1 bearing reduced the 9600 rpm mode amplitude 72% and eliminated the 13,100 rpm mode.

**TABLE IV**  
**PREDICTED VIBRATION AMPLITUDES AT NUMBER 1 BEARING**  
 (Imbalance One oz-in. [0.007 N-m])

LOCATION OF IMBALANCE	VIBRATION AMPLITUDE AT NO. 1 BEARING LOCATION	
	9,600 rpm Mode	13,100 rpm Mode
Rotor 1	4.5 x 10 <sup>-3</sup> in [1.14 x 10 <sup>-4</sup> m]	6.2 x 10 <sup>-3</sup> in. [1.58 x 10 <sup>-4</sup> m]
Rotor 2	1.6 x 10 <sup>-3</sup> in. [0.41 x 10 <sup>-4</sup> m]	6.3 x 10 <sup>-3</sup> in. [1.60 x 10 <sup>-4</sup> m]
Rear Diaphragm	13.6 x 10 <sup>-3</sup> in. [3.45 x 10 <sup>-4</sup> m]	4.5 x 10 <sup>-3</sup> in. [1.14 x 10 <sup>-4</sup> m]

#### TEST FACILITY

The test program was carried out in a sea-level compressor test stand (Figure 31). The stand was equipped with a gas turbine drive-engine with a 2.1:1 gearbox to provide speed range capability. Airflow entered the rig through a calibrated nozzle, and a 72-ft [21.9 m] straight section of 42 in. [1.07 m] diameter pipe ran from the nozzle to a 90 in. [2.29 m] diameter inlet plenum. A wire mesh screen and an "egg-crate" structure located in the plenum provided a uniform total pressure profile to the compressor. The airflow was exhausted from the compressor into a toroidal collector and then into a 6 ft [1.83 m] diameter discharge stack which contained a 6 ft [1.83 m] diameter valve to provide backpressure or throttling for the test compressor. A 24-in. [0.61 m] and a 12 in. [0.35 m] valve was located in bypass lines to provide fine adjustment of backpressure.

For tests with distorted inlet flow, the desired inlet distortion patterns were generated by means of screens attached to a 1 in. x 1 in. [.0254 m x .0254 m] mesh base screen of 1/8 in. [.0032 m] diameter wire. A rotatable case with 12 struts located 33 in. [0.84 m] upstream of the rotor leading edge was used to support the base screen. Sketches of the hub-radial, tip-radial, and circumferential distortion screens are shown in Figure 32.

Ten struts located 14 in. [0.356 m] upstream of the rotor leading edge (Figure 1) supported the forward bearing and the assembly for the strain-gage slip-ring. Eight struts located 11 in. [0.28 m] downstream of the stator trailing edge supported the rear bearing. Rotor strain-gage and inlet hub static pressure instrumentation leads were routed through the nonrotating nose fairing.



## INSTRUMENTATION AND CALIBRATION

Airflow to the compressor was measured by means of a calibrated nozzle designed to ISO<sup>†</sup> standards. Airflow measurements were within one percent accuracy. The compressor speed was measured by means of an impulse type pick-up. The pick-up was an electromagnetic device which counted the number of gear teeth that passed within an interval of time and converted the count to RPM. The accuracy between 4,000 rpm and 12,000 rpm was within 0.2%.

All temperatures were measured with chromel-alumel, type-K thermocouples and were recorded in millivolts by means of an automatic data-acquisition system. Temperature elements were calibrated for Mach numbers over their full operating range. Effects of total pressure level on temperature recovery were accounted for by using the corrections given by Glawe, Simms, and Stickney (ref.12). The thermocouple leads were calibrated for each temperature element. Overall rms temperature accuracy was estimated to be  $\pm 1.0^\circ\text{R}$  ( $\pm 0.56^\circ\text{K}$ ). Wedge probes for measuring total pressure, static pressure, and air angle were calibrated for Mach number as a function of indicated ratio of static-pressure-to-total-pressure with pitch angle as a parameter. Total pressure recovery and yaw-angle deviation were calibrated as functions of Mach number and pitch angle. Accuracy of the measured air-angles was within 1.0 degree.

The pressures sensed by probes, fixed rakes, and static taps were measured by means of transducers and recorded in millivolts by an automatic data-acquisition system. The accuracy of the pressure was  $\pm 0.1\%$  of the full-scale value. The pressures from sensors located upstream of the rotor 1 trailing edge were measured using  $15 \text{ lbf/in.}^2$  [ $1.033 \times 10^5 \text{ N/m}^2$ ] full-scale transducers. Pressures from the trailing edge of rotor 1 and from all downstream locations were measured using  $50 \text{ lbf/in.}^2$  [ $3.46 \times 10^5 \text{ N/m}^2$ ] full-scale transducers.

Two proximity detectors located over the tips of each rotor blade at midchord were used to monitor blade tip clearance.

Photographs of typical instrumentation are shown in Figure 33, and the axial and circumferential positions of the instrumentation are shown in Figures 34 and 35, respectively. Instrumentation for measuring overall and blade-element performance data is listed in Table V.

The eleven radial positions at each axial station were defined by the intersection of the axial station and the redesign streamlines which pass through 5, 10, 15, 30, 50, 60, 65, 70, 85, 90, and 95 percent of the passage height at the 1st-stage rotor trailing edge. For tests with radially distorted inlet flow, five radial positions on the streamlines which pass through 10, 30, 50, 70, and 90 percent of the passage height at the trailing edge of the 1st-stage rotor were used. The radial locations at which these streamlines passed the leading and trailing edges of each blade row are given in Appendix C, Table XVII.

Table VI lists the parameters that were recorded continually during excursions into stall or surge and to detect and evaluate rotating stall. Two hot-film probes, located at the fan inlet and exit (Station 6 and 16) and with sensors at 25, 50, and 85 percent of passage height from the hub, were used to record velocity fluctuations continuously on a multichannel tape recorder when operating near or within the stall region.

---

<sup>†</sup>International Organization for Standardization

TABLE V  
PERFORMANCE AND BLADE ELEMENT INSTRUMENTATION

INSTRUMENT PLANE LOCATION	PARAMETER	TYPE AND QUANTITY
Sta. 0 -- Inlet Plenum Chamber	p	6 pressure taps on plenum wall
	T	6 bare wire chromel-alumel thermocouples
Sta. 6 -- Rotor 1 Inlet (2.25 in. [0.0673 m] upstream of Rotor 1)	p	6 O.D. and I.D. wall static taps.
	†P, p & air angle $\beta$	2 wedge radial traverse probes spaced 180° apart circumferentially.
	P	two radial rakes with sensors at 10, 30, 50, 70, and 90 percent span (distortion tests only)
Sta. 8 -- Rotor 1 Exit (approx. halfway between Rotor 1 T.E. and Stator 1 L.E.)	††p	4 O.D. wall static taps approximately equally spaced circumferentially.
Sta. 11 -- Stator 1 Exit (halfway between T.E. of Stator 1 and L.E. of Rotor 2)	††p	4 O.D. and 4 I.D. wall static taps, approximately equally spaced circumferentially.
	†T, P, p, & air angle $\beta$	Two NASA combination probes - one with circumferential traverse of one vane gap, plus radial traverse, and second probe with radial traverse at midgap.
Sta. 14 -- Rotor 2 Exit	††p	4. O.D. and I.D. wall static taps, approximately equally spaced circumferentially.
Sta. 16 -- Fan Discharge (within ½ chord downstream of Stator 2)	††p	4 O.D. and 4 I.D. wall static taps approximately equally spaced circumferentially.
	†P, p, & air angle $\beta$	2 wedge probes, radial traverse, approximately 180° apart and located at vane midchannel.
	†T	2 wake rakes located approximately 180° apart, radially traversed, 10 elements across stator gap.
	†p	2 wake rakes located approximately 180° apart, radially traversed, 13 elements across stator gaps.
Sta. 17 -- Rig Exit	P	One circumferential P rake, 5 stations located at 50 percent span (used for setting points).

† 11 radial locations for uniform inlet flow tests (5, 10, 15, 30, 50, 60, 65, 70, 85, 90, and 95% of passage height); 5 radial locations for distorted inlet flow tests (10, 30, 50, 70, and 90% of passage height).

†† Static pressure taps ahead of and behind stators are located on approximate extensions of mean channel streamlines.

REPRODUCIBILITY OF THE ORIGINAL PAGE IS POOR

**TABLE VI**  
**STALL TRANSIENT INSTRUMENTATION**

INSTRUMENTATION PLANE LOCATION	PARAMETER	TYPE AND QUANTITY
Inlet Nozzle	p	1 static tap downstream and 1 static tap upstream of inlet nozzle
	$\Delta p$	A $\Delta p$ transducer sensing the differential pressure between the upstream and downstream nozzle static pressures
	T	One nozzle temperature
Sta. 0 – Plenum	p	One plenum static tap
	T	One plenum temperature
Sta. 6 – Rotor Inlet	V	One hot-film probe
Rotor 1, Stator 1, and Rotor 2 Exit	p	One O.D. static tap each location
Rotor Blades	Stress	Various strain-gages
Stator Blades	Stress	Various strain-gages
Sta. 16 – Fan Discharge	p	One O.D. static tap
	V	One hot-film probe
Sta. 17 – Fan Discharge	P	One circumferential pressure rake at 50 percent span
Gearbox	N	Impulse pick-up

Accelerometers were used to measure shaft vibration, and stationary and rotating critical parts were instrumented with strain-gages to determine levels of vibratory stress over the operating range of the compressor.

## TEST PROCEDURE

### Shakedown Tests

Shakedown tests were conducted with uniform inlet flow to establish the mechanical integrity of the compressor and to locate stress boundaries that might limit the operating range over which tests could be conducted. During the shakedown tests, the stability limits of the fan were determined for a range from 50 to 110 percent of design speed. The redesigned 2nd-

stage rotor had no stability problems, and flutter was not encountered on any blades or vanes. Shaft vibration problems were not encountered, and the rig was cleared for tests between 50 and 110 percent of design speed. Running tip clearances on rotors 1 and 2 at design speed were approximately 0.026 in. [0.00066 m] and 0.018 in. [0.00046 m], respectively.

For speeds of 50, 70, 85, 95, 100, and 105 percent of design, rotating stall or surge surveys were conducted. Readings from the hot-film probes and selected rotor and stator strain-gages were recorded along with a speed signal and stator exit O.D. static pressure. These readings were recorded simultaneously by a multichannel tape recorder. Readings of the other transient parameters shown in Table VI were recorded every 1.5 seconds as the fan stage was throttled toward stall; approximately 100 scans were made by the automatic recording system from wide-open throttle to the minimum flow condition.

### **Overall and Blade Element Performance Mapping**

Fan overall and blade element performance data were obtained at speeds from 50 to 110 percent of design for uniform inlet flow. At each speed, data points were taken between the maximum flow attainable and the low-flow stability limit except at 110 percent speed where points were spread between open throttle and high pressure ratio but stall point was not obtained.

Overall and blade element performance data were obtained at 70, 85, and 100 percent of design speed with tip radially distorted and hub radially distorted inlet flow. Overall performance data with circumferentially distorted inlet flow were obtained at 70, 90, and 100 percent of design speed. With circumferential distortion, a first bending 4E resonance was encountered on the 1st-stage rotor at 85 percent speed. Stresses did not exceed allowable values, but potential problems were avoided by substituting 90 percent speed in place of 85 percent speed for this test.

### **Disassembly Inspection**

Following the test program, which included stator setting optimization and casing treatment studies (not reported herein), the 1st-stage blade-tip rub-strip (composite material) failed while taking a post-test check point. The failure caused a sudden drop in flow, pressure ratio, and efficiency. No deterioration in performance had been seen prior to the final check point, and routine inspection did not show any indication that there had been a rubstrip or blade damage prior to this failure.

## **DATA REDUCTION TECHNIQUES**

### **Data Correction and Averaging**

All steady-state performance data were automatically recorded in millivolts on computer cards. These data were then converted to engineering units, corrected, and used to calculate overall and blade element parameters as described in the following sections. Data obtained from impact tube type total pressure probes (fixed radial rakes and traversing wake rakes) were

corrected for shock loss when located in supersonic flow. Wedge probes were used to measure total pressure, air angle, and static pressure. Mach number was determined from calibrations of measured total and static pressures. The measured total pressure and flow angle from these probes were corrected using Mach number calibration curves for individual probes. The resulting calibrated Mach number and corrected total pressure were then used in conjunction with standard tables of air properties to calculate static pressure.

Combination probes were used to measure total pressure, air angle, static pressure, and total temperature. Corrections were based on probe calibrations similar to those previously described for wedge probes but with an additional calibration of total temperature recovery versus Mach number. The temperature calibration was consistent with the general method for temperature correction described below.

Thermocouple signals were converted to temperature measurements using wire calibrations for individual sensors. These temperature measurements were converted into total temperature using Mach number calibrations for individual sensors and the pressure-level corrections given by Glawe, Simms, and Stickney (ref. 12).

For tests with uniform inlet flow, circumferential distributions of total pressure obtained at the 1st-stage and 2nd-stage stator exits were mass-flow averaged at each radial position using the corresponding measured distribution of total temperature and a constant circumferential static pressure that was determined by linearly interpolating static pressure data from the wall or wedge probe. The arithmetic average of the three highest values from the circumferential total pressure distribution measured across the passage between adjacent stator vanes at each radial location was chosen to represent the free-stream or stator inlet pressure at the appropriate percent of span. A circumferential mass-flow average total temperature was also calculated at each radial position using the total temperatures and pressures given by the measured circumferential distributions and static pressures linearly interpolated between wedge probe or inner and outer wall static tap measurements. Circumferentially mass-flow-averaged temperatures from the two temperature wake rakes at the 2nd-stage stator exit were arithmetically averaged at each radial location. One pressure wake rake did not traverse properly on some data points. Comparison of measurements showed excellent agreement when both rakes were functioning properly. On the basis of this agreement, the only data used for the analysis were from the pressure rake which worked consistently.

Air angles measured by circumferential traverses at the 1st-stage stator exit were mass-flow-averaged at each radial location. Air angles measured by the two wedge probes at the 2nd-stage stator exit were arithmetically averaged at each radial location.

For tests with distorted inlet flows, radial traverses at the exit of the 1st-stage stator were made at the midgap instead of the combined circumferential and radial traverses used for uniform inlet flow tests. Ratios of gapwise mass-flow-averaged total pressure and temperature and of free-stream total pressure to midgap measurements were correlated for uniform inlet flow data. These correlations were then used to calculate performance and blade element parameters for the 1st-stage rotor and stator with distorted inlet flow. An example of one of the pressure correlations is shown in Figure 36. This type of correlation was checked using data from a previous single-stage fan test (ref. 2) and found to give good agreement with mid-

range†, radial distortion data. The major disadvantage of this method is that the calculated total pressure loss for stator 1 does not vary with incidence angle. The resulting error is greatest for data points at open-throttle and near-stall. Fan overall performance data were not affected by inaccuracies inherent in this method.

For tests with circumferentially distorted inlet flow, fan inlet total pressure was calculated by radially mass-flow-averaging the measurements made by each fixed rake and by arithmetically averaging these radial mass-flow averages. This arithmetic average included inlet rake measurements made at all rotations of the circumferential inlet distortion screen.

First-stage exit radial traverses of temperature and pressure were corrected using the correlations of gap-average versus midgap values. These corrected pressures and temperatures were then radially mass-flow averaged for each probe position relative to the distortion screen. First-stage exit overall total pressure and temperature were calculated by arithmetically averaging these radially mass-flow averaged temperatures and pressures. Fan exit total pressures and temperatures were measured by wake rake traverses at all rotations of the distortion screen. Total pressures and temperatures were each circumferentially mass-flow averaged for each rake at each radial location. These values were radially mass flow averaged at each rake position relative to the screen. Overall average total pressure and temperature were calculated by arithmetically averaging the circumferentially and radially mass-flow averaged values for each wake rake position.

#### Performance Parameter Calculations

Overall and blade element performance parameters for uniform and radially distorted inlet flows were calculated by means of a flowfield analysis computer program. All parameters were corrected to standard-day conditions. Inputs to the flowfield program are listed in Table VII.

TABLE VII  
PARAMETERS INPUT TO FLOWFIELD PROGRAM

LOCATION	PARAMETERS
Compressor Inlet (Station 0, Figure 34)	1) Corrected mass flow 2) Corrected rotor speed
Rotor 1 Inlet Instrument Plane (Station 6)	1) Total pressure ratio †† versus radius 2) Constant radial blockage factor

† Not wide open throttle or near stall.

†† Ratio = 1.0 for uniform inlet flow. For radial distortions, ratio is local value of total pressure divided by mass-flow-average of total pressure at Station 6.

TABLE VII (Cont'd)

## PARAMETERS INPUT TO FLOWFIELD PROGRAM

LOCATION	PARAMETERS
Stator 1 Inlet (Station 8)	1) Total pressure ratio versus radius 2) Constant radial blockage factor
Stator 1 Exit Instrument Plane (Station 11)	1) Total temperature ratio versus radius 2) Total pressure ratio versus radius 3) Constant radial blockage factor 4) Absolute air angle versus radius
Stator 2 Inlet (Station 14)	1) Total pressure ratio versus radius 2) Constant radial blockage factor
Stator 2 Exit Instrument Plane (Station 16)	1) Total temperature ratio versus radius 2) Total pressure ratio versus radius 3) Constant radial blockage factor 4) Absolute air angle versus radius

Total pressures and temperatures were ratioed to compressor inlet values (station 6). Compressor inlet total pressure was assumed equal to the inlet plenum pressure for tests with uniform inlet flow. For tests with distorted inlet flows, overall pressures were ratioed to the mass-flow average of the total pressures measured by the rakes at the fan inlet. Temperatures were always ratioed to the inlet plenum temperature.

A flow blockage factor was used at each axial location to improve the accuracy of the static pressure and velocity calculations of the flowfield program. Blockages were applied equally to all stream tubes at each of the axial locations. Axial distributions of flow blockage factors were selected so that the hub and tip static pressures obtained from the flowfield calculations gave the best agreement with the wall average static pressure for a representative midthrottle operating point at design speed. As shown in Table VIII, the flow blockage factors used in the data reduction flowfield calculations were the same as those blockages used in the redesign except at the stator 2 trailing edge where 3% blockage was added to the calculation for data reduction. Figures 37 through 41 show that the measured and calculated statics for a near design data point agreed quite well at axial locations upstream of each rotor and at the fan exit and that there was lesser agreement for locations downstream of each rotor.

Traverses were not made at rotor-exit instrumentation stations and, therefore, only wall static pressure measurements were available for comparison with calculated values. However, the radial gradient of static pressure indicated by wall static pressures at the exit of rotor 2 (Figure 40) did not seem to be compatible with swirl determined by temperature rise and with streamline curvature limited by flowpath walls. No hub wall static pressure measurements were made at the exit of rotor 1 due to the difficulty in leading tubing out through variable geometry stators. Static pressure in the unmixed boundary layer and core flows from rotor blades would be expected to be lower than the pressure calculated by the axisymmetric-flow-field streamline calculation.

Other criteria used to set blockage indicate that proper values were applied in reducing the data. Calculated rotor exit relative air-angles are in reasonable agreement with deviation-rules derived using test data from many rotors. Stator loss versus incidence curves also appear to be reasonable. In particular, the onset of choke losses appear to have occurred at the right combinations of Mach number and flow angle.

The blockage selection method is consistent with the method used in reducing the data in other programs (ref. 1, 2, 3, 9 & 13). The successful use of these data in the design of the subject two-stage fan is further justification of this method.

TABLE VIII  
ANNULUS BLOCKAGES

STATION	DATA REDUCTION (%)	REDESIGN (%)
Rotor 1 Leading Edge	2.4	2.4
Rotor 1 Trailing Edge	4.1	4.1
Stator 1 Leading Edge	4.1	4.1
Stator 1 Trailing Edge	2.8	2.8
Rotor 2 Leading Edge	2.8	2.8
Rotor 2 Trailing Edge	5.3	5.3
Stator 2 Leading Edge	5.3	5.3
Stator 2 Trailing Edge and Downstream	6.5	3.5



All static pressure distributions and air angles behind the rotor were calculated by assuming axisymmetric flow and using mass-flow continuity, radial equilibrium, and energy equations. Curvature, enthalpy, and entropy gradient terms were included in the equilibrium calculations. Aerodynamic conditions at the blade edges were calculated by translating the measured data from the instrument plane along streamlines to blade edges. Blade element parameters were calculated for airfoil sections lying on conical surfaces defined by the intersections of design streamlines and the blade edges. Calculations were made on streamlines passing through the rotor 1 trailing edge at 5, 10, 15, 30, 50, 60, 65, 70, 85, 90, and 95 percent of the passage height for uniform inlet flow and 10, 30, 50, 70, and 90 percent for radially distorted inlet flow. Blade-edge stations for the flowfield calculation (Figure 2) were input as slanted straight-lines which closely approximate the meridional profiles of the manufactured blade edges. In addition to the blade element parameters, the output of the flowfield analysis program included overall performance of the 1st-stage rotor, the 1st-stage, the 2nd-stage rotor, and the complete two-stage fan. Blade element performance data for uniform and radially distorted flow tests are tabulated in Appendices E, F, and G. Accumulated overall performance to the exit of each blade row is tabulated at the bottom of the blade element data sheet for that blade row.

## RESULTS AND DISCUSSION

### UNIFORM INLET FLOW

#### Fan Overall Performance

The overall performance of the two-stage fan is shown in Figure 42, and the performance at design speed is shown on an expanded scale in Figure 43. Overall performance parameters are listed in Appendix E, Table XX. Performance of the original fan with the unshrouded 2nd-stage rotor (ref. 10) is also plotted on these figures. Adiabatic efficiency was 85.0% at design speed and pressure ratio, which is 1.3 percentage points above the redesign value but 0.7 percentage points below the efficiency attained in tests with the unshrouded 2nd-stage rotor. Peak efficiency at design speed was 85.4% and occurred at a pressure ratio of 2.93. The fan exhibited peak efficiencies above 83% over the speed range from 50 to 100 percent speed. As speed was increased beyond the design value, however, maximum efficiency decreased rather rapidly, and peak values occurred at the highest levels of back pressure tested. At 110 percent of design speed, an efficiency higher than the peak test value of 79.2% would likely have resulted from testing the fan at higher back pressures, but the risk of excessive stresses associated with an overspeed surge outweighed the utility of such data. Stall margin was calculated for all speeds using the constant throttle operating line shown in Figure 42. This operating line passes through the design point and corresponds to a fixed area fan nozzle. Nozzle Mach numbers were determined by a ratio of static-pressure to total-pressure equal to the reciprocal of the fan overall total pressure ratio. The nozzle flow was corrected to inlet conditions based on the selected pressure ratio and a temperature ratio derived from test efficiencies. Efficiency data were interpolated to obtain the plot of operating-line efficiency versus corrected flow presented in Figure 44. Peak adiabatic efficiency on the operating line exceeded 85.5% and was obtained in the speed range between 85 and 95 percent of design speed. Efficiency then dropped gradually with decreasing speed to 83% at 50 percent speed. Operating line efficiency decreased to 82% at 105 percent speed and to 78.5% at 110 percent speed.

The redesigned 2nd-stage rotor provided higher overall fan pressure ratios at all speeds and flow rates. This higher pressure ratio also increased maximum flow rates when flow was limited by system resistance or by stator 2 choke. At 85 percent of design speed and below, maximum flow was limited by system resistance, as shown by Figure 45. At higher speeds the increased pressure ratio gave a lower corrected flow into stator 2 for a given fan-inlet corrected flow. This delayed stator 2 choke and permitted higher fan inlet flows. Figure 45 shows that stator choke and system resistance limits in tests with the redesigned rotor were the same as in tests with the original rotor.

At design speed and pressure ratio, the flow was 185.4 lbm/sec [84.0 kg/sec], about 0.7% above the design flow of 184.2 lbm/sec [kg/sec]. At all speeds less than design, maximum flows exceeded values obtained in the previous test, with a 2.5% increase at 70 and 85 percent of design speed (Figure 42).

A five percentage point improvement in fan stall margin (based on the assumed operating line) at design speed was one of the goals of the redesign. Rotor 2 was redesigned with a higher total pressure ratio at the hub than at the tip in order to keep rotor 2 and stator 2 exit hub velocities high, thereby reducing their hub aerodynamic loadings. The stall margin actually achieved at design speed was approximately 12% based on the operating line shown in Figure 42, about two percentage points higher than that obtained in tests with the original 2nd-stage rotor.

Minimum flow at all speeds tested up to and including 105 percent of design speed was limited by fan surge with a cycle period of approximately one second. Momentary rotating stall was detected at the fan exit during both the decreasing flow and the recovery portion of the surge cycle. Stall margin (based on the assumed operating line) was lowest at design speed, increased to 15% at 105 percent speed, and increased steadily with decreasing speed to a value of 22% at 50 percent of design speed. A complete listing of stall flows and pressure ratios for uniform inlet flow is included in Appendix E, Table XX.

#### **Overall Performance of First Stage, First-Stage Rotor**

Overall performance of the 1st-stage and of the 1st-stage rotor with uniform inlet flow is shown in Figures 46 and 47, respectively. These plots each show a pressure-flow characteristic curve at design speed that very nearly passed through the design point. At the operating point closest to design flow and pressure ratio, the 1st-stage rotor adiabatic efficiency of 91.2% was approximately 1.8% higher than the design value, and 1st-stage efficiency of 87.3% was about 2.0% higher than design. At low speeds the curves of efficiency versus flow show that the 1st-stage operated on the stall side of peak efficiency because the flow capacity of the 2nd-stage limited the maximum flow and efficiency attainable by the 1st-stage rotor and the 1st-stage.

#### **Nondimensional Performance Data**

Nondimensional plots of pressure coefficients and adiabatic efficiency versus flow coefficient for the 1st-stage rotor, the 1st-stage, the 2nd-stage rotor, and the 2nd-stage are presented in Figures 48 through 51. These plots are qualitatively similar to those from tests of the fan

with the unshrouded 2nd-stage rotor, (ref. 10). The spread of curves for different speeds for rotor 1 and stage 1 shows the marked compressibility effects characteristic of high pressure ratio, high specific flow stages. At low speeds, rotor 1 and stage 1 pressure coefficients increased steadily with decreasing flow coefficient although operating on the stall (low flow-coefficient) side of peak efficiency. At design speed and higher speeds, points are clustered at the low pressure-coefficient ends of the 1st-stage characteristic curves, showing that the 2nd-stage limited maximum flow at high speeds also. Rotor 1 efficiency remained fairly constant between 50 and 100 percent of design speed but diminished rapidly with overspeed. A comparison of rotor 1 and stage 1 characteristics shows that stator 1 losses were not severe. There are no indications of stator 1 choke.

The flattening of the pressure coefficient-flow coefficient curves at high speeds for rotor 2 and stage 2 at high values of pressure coefficient, in contrast to the more sloped curves for rotor 1 and stage 1, indicates that the 2nd-stage had approached a loading limit and had set the stall flow of the fan.

As speed increased, maximum flow-coefficient decreased (Figures 50 and 51). Maximum flow-coefficient at 110 percent speed was 5% lower than at design speed. The open-throttle point at 110 percent speed (shaded symbol in Figure 50) had a flow coefficient that was no higher than the point represented by the half-shaded symbol which had a higher pressure coefficient. Stator 2 was choked at the open throttle point, as shown by Figure 45, but it could not have been choked at the other point which had the same flow but a higher rotor pressure ratio. The large efficiency drop between the half-shaded and fully shaded symbol data points on Figure 50 indicates that rotor 2 was choked. Rotor 2 choke is the most probable cause of flow limits at high speeds.

#### **Blade Element Data**

The spanwise efficiencies for the near-design data points (Figures 52 and 53) showed generally good agreement with design predictions. Efficiency profiles for both the 1st-stage rotor and the 1st-stage (Figures 52 and 53) exhibited a region of low efficiency which extended as much as ten percent of the passage height on either side of the location of the rotor partspan shroud. The 2nd-stage rotor efficiency profile for the same data point did not exhibit a comparable low efficiency region near the location of its partspan shroud, perhaps because its shroud was designed to lie in the wake of the 1st-stage rotor shroud.

The average efficiency for the 2nd-stage rotor for the data point presented is approximately 0.5 percentage points lower than the design value due to less-than-design efficiencies in the tip region of the blade. The decreased efficiency in the tip region may be the result of taper at the tip of the redesigned rotor blade, which decreases its solidity relative to the original untapered blade. This solidity effect has been described by W. A. Benser of NASA (ref. 13).

Pressure ratio profiles for the near-design data point (Figures 54 and 55) show effects of partspan shrouds consistent with those of the efficiency profiles described above. The 2nd-stage rotor and overall fan pressure ratios followed in general the negatively sloped profile of the rotor 2 redesign, which was included in an attempt to increase fan stall margin.

Figure 55 shows that the spanwise gradient of overall pressure ratio was approximately equal to the design value, except for the region of low pressure in the wake of the partspan shrouds. The pressure ratio of the 1st-stage and of the 1st-stage rotor was higher at the hub and lower at the tip than the design values, and the opposite was true for the 2nd-stage rotor (Figure 54). The spanwise region of high pressure ratio at the exit of the 1st-stage resulted in a decreased incidence on rotor 2 and resulted in lower-than-design work at this spanwise location for the rotor. Conversely, regions of low pressure ratio in rotor 1 were regions of high work in rotor 2. In this manner, the 2nd-stage rotor corrected the total pressure profile to obtain the desired gradient at the fan exit.

The two measurement stations added at 55 percent and 60 percent of span gave a better definition of 1st-stage rotor shroud losses than was obtained in tests of the original fan with unshrouded 2nd-stage rotor, as shown by the pressure ratio profiles in Figure 54. Figure 54 also shows that the measured exit pressure profile of the 1st-stage rotor with the redesigned 2nd-stage rotor was very nearly the same as with the original 2nd-stage rotor (flat pressure profile).

Figures 56 through 59 give spanwise profiles of loss, diffusion factor, deviation angle, and suction surface leading edge incidence angle for each of the four fan blade rows for a near design data point. With certain exceptions, blade element data for the near-design data point showed good agreement with the predicted design performance. Losses for the four blade-rows were somewhat below design values except for the higher values for the 1st-stage rotor in the area of its partspan shroud and for 1st-stage stator and 2nd-stage rotor from 60 percent span to the tip. Deviation angles for the data point were higher than design for both the 1st-stage and 2nd-stage rotors near the location of their partspan shrouds and near the hub of the 2nd-stage rotor and generally about two degrees lower than design for the 1st-stage stator. Incidence angles for blade elements for the 1st-stage stator and the 2nd-stage rotor were low in spanwise regions where the 1st-stage rotor pressure ratio was higher than design, and were high in regions where the 1st-stage rotor pressure ratio was below the design level. The 2nd-stage stator, which was designed for a constant spanwise inlet total pressure, had low incidence angles at the hub and high incidence angles at the tip when used with the redesigned rotor. Loss coefficients were reasonably low on all blade elements despite the somewhat skewed radial profiles of incidence angle.

Blade element plots of loss, diffusion factor, and deviation angle versus incidence for all data obtained with uniform inlet flow are presented for eleven radial locations in Figures 60 through 63. Complete tabulations of blade element data for uniform inlet flow are given in Appendix E, Table XXI.

#### First-Stage Rotor

The blade element data for the 1st-stage rotor (Figure 60) showed trends typical of a moderately high speed fan rotor. At speeds at and above design, the range of rotor incidence angle was quite small. At lower speeds, the range of incidence angle increased and the level of minimum loss decreased. The blade appeared to have run somewhat stalled at low speeds, particularly at the tip as indicated by high losses and diffusion factors at high incidence angles. Negative loss coefficients were calculated for the 1st-stage rotor for blade elements

near the hub for certain data points. These negative losses were attributed to two causes: 1) low temperature rise at low speeds magnified the effect of temperature measurement errors (at 50 percent speed a 1°F [0.555°K] error would change efficiency by approximately 8%) and 2) temperature and pressure sensors were offset radially, and the interpolations in regions of steep radial gradients may not have matched temperatures and pressures accurately. Distribution of loss between rotors and stators is not believed to be the source of the problem since stator losses appear to be reasonable for these points.

#### First-Stage Stator

The blade element data for the 1st-stage stator (Figure 61) showed a lack of any trend of loss with changes in incidence angle or speed except at spans that were affected by the part-span shroud and near the hub where Mach numbers were highest. Loss levels were slightly lower than design predictions for the inner half of the vane span and slightly higher than design for the outer half. For points near stall, the stator attained loading levels (diffusion factors) of between 0.55 and 0.60 near the hub at design speed and 0.62 at 70 percent speed near the tip.

#### Second-Stage Rotor

The blade element data for the 2nd-stage rotor (Figure 62) showed deviation and diffusion factor levels similar to those of the previously tested unshrouded rotor. Deviation angles near the hub were several degrees higher than design values for all speeds, but values for the outer 75 percent of span of the blade agreed well with design levels. Diffusion factors were also quite high near the hub, reaching 0.64 at 8 percent of span at design speed. Since 0.65 is sometimes considered a stall limit for rotor blades, this rotor may have been involved in initiation of surge at design speed. This hypothesis is consistent with strain-gage activity recorded during stall which indicated that either the 2nd-stage rotor or the 2nd-stage stator had initiated fan stall (Figure 64). The data for this rotor showed a rather narrow incidence angle range near the tip, particularly at high speeds, but a wider range near the hub, with well-defined minimum loss levels at several speeds. High losses in the hub region may indicate choking at high speeds.

#### Second-Stage Stator

The blade element data for the 2nd-stage stator (Figure 63) reflected strong evidence of choking near the hub, extending over the lower half of the vane span at all speeds, as shown by a rapid increase of loss with decreasing incidence. This rise in loss to levels up to three times design values was accompanied by abrupt decreases in deviation angles to values considerably lower than design. These low indicated deviation angles may be the result of large stator wakes reaching the gapwise location of the probe and affecting the angle measurement. The data also indicated that this stator underwent quite a rapid rise in loading with increasing incidence angle at high speeds, reaching diffusion factors of approximately 0.60 near the hub (3 percent span) and in the area of partspan shroud wakes. The rapid rate at which loading was increasing with incidence angle and the strain-gage record (Figure 64) indicate that the stator might have set the stall limit at high speeds. Peak loadings were, however, lower than values attained in tests of the fan with the unshrouded rotor (0.67 at 10 percent span at design speed), indicating that the negatively sloped total pressure profile of the re-designed rotor successfully reduced critical loadings to increase stall margin.

## RADIALLY DISTORTED INLET FLOW

Radial distortion screens (Figure 32) were used to generate patterns that covered approximately the inner and outer 40 percent of the 1st-stage rotor inlet annulus area and provided distortion parameters,  $(P_{\max.} - P_{\min.})/P_{\max.}$ , of 0.14 with the discharge throttle wide open at design speed. Figure 65 shows the spanwise total pressure profiles at the measurement plane of the 1st-stage rotor inlet for the wide-open and near-stall throttle conditions at design speed. Figure 66 shows the distortion parameter plotted as a function of fan inlet corrected flow for hub and tip radial distortions. The distortion expressed in terms of a meridional velocity defect  $(V_{\max.} - V_{\min.})/V_{\max.}$  is plotted versus corrected flow in Figure 67. This velocity defect parameter governs the changes in incidence angles caused by the distortions. Although the total pressure distortion parameter (Figure 66) decreased with flow (and therefore with speed), the velocity defect parameter of Figure 67 shows that the changes in incidence angle were largest at low speed and smallest at high speed.

### Tip Distorted Flow

#### Overall Performance

Overall performance for the fan, the 1st-stage, and the 1st-stage rotor with tip radially distorted inlet flow is shown in Figures 68, 69, and 70, respectively. Overall performance parameters are listed in Appendix F, Table XXII along with stall flows and pressure ratios for each speed. Performance with uniform inlet flow is included in the figures as dashed lines for comparison.

At design speed, the tip-radial distortion increased stall margin by approximately two percentage points relative to the undistorted flow stall line (Figure 71). Stall margin was reduced by eight percentage points at 85 percent speed and did not change at 70 percent speed. The tip distortion at design speed apparently relieved the hub loadings that caused stall with uniform inlet flow, resulting in the small gain (two percentage points) in stall margin. Tip-radial distortion had been expected to reduce the stall margin severely at 70 percent speed since tip loadings were the probable cause of stall with undistorted flow. At this speed, the stall line was unchanged but stall occurred at a lower flow and lower pressure ratio than with undistorted flows. Pressure ratio dropped slightly as stall was approached in contrast to the steadily increasing pressure with undistorted flow. These trends of pressure ratio versus flow can also be seen in the performance maps for the 1st-stage rotor and for the 1st-stage. The large reduction in stall line at 85 percent speed appears out of line with the stall margin changes at 70 and 100 percents of design speed (Figure 71). Strain-gage and hot-film data recorded at the time of stall at 85 percent speed (Figure 72) show evidence of rotating stall before major instabilities and stresses occurred. A strong vibratory stress can be seen on rotor 1 just before indications of major instabilities. The flow-instability time shown in Figure 72 was selected as the first indication that the relatively quiet periodic rotating stall was developing into a major flow instability. This first bending mode vibration resonance with 4 excitations per revolution is consistent with the predicted resonance diagram (Figure 73). Figure 74 shows that at design speed, rotating stall indications were similar to those at 85 percent speed, but that the first bending mode vibrations occurred after major instabilities

had already begun. It is not known whether or not this vibration actually contributed to aerodynamic instability, but it is believed to be a possible explanation for the unique response of the fan to tip-radial distortion at 85 percent speed. Pressure ratios were higher with the tip distortion than with uniform inlet flow for a given speed and corrected flow, except near stall at 70 percent speed. This indicates that rotor tips were not severely stalled and that they produced higher pressure ratios at the higher incidence angles. Increased maximum flow rates at part-speeds were a result of increased pressure ratio on the system-resistance pressure ratio (Figure 45).

Efficiencies appeared to have been higher with tip-radially distorted flow than with uniform flow (Figure 68). Most of this increase in efficiency occurred in the 1st-stage rotor. The reduced number of measurements for distortion tests (five radial locations instead of eleven used in undistorted flow tests) did not include all endwall region and partspan shroud region losses. The effect on overall performance was checked by recalculating a near-design uniform inlet flow data point with input data profiles specified at five radial locations. The reduced sampling increased calculated efficiency by approximately one percent.

#### Blade Element Data

A major effect of the tip-radial distortion was to increase the pressure ratio of the 1st-stage and to decrease pressure ratio of the 2nd-stage for a given overall pressure ratio. This redistribution is illustrated by Figure 75 which shows spanwise profiles of pressure ratio along streamlines. The 1st-stage pressure ratio profile was about the same when operating with distorted flow at a fan overall pressure ratio of 2.683 as when operating with undistorted flow at a fan overall pressure ratio of 2.860. For the same data points, the 2nd-stage pressure ratio was much lower than for uniform inlet flow. The 2nd-stage pressure profile was about the same when operating with distorted flow at fan overall pressure ratio of 3.041 as when operating with undistorted flow at a pressure ratio of 2.860. The spanwise distributions of pressure ratio were not changed as much as the pressure ratio levels. Fan overall efficiency profiles were also nearly the same for distorted and undistorted flow tests, as shown by Figure 76.

Blade element performance parameters for each blade row at five radial positions are shown in Figures 77 through 80. The 1st-stage rotor tip (90 percent of span from the hub) operated at high positive incidence due to the low axial velocity caused by the tip distortion. The maximum loading level for any blade row did not exceed 0.6. The highest diffusion factor (0.59) occurred at the tip of the 1st-stage rotor at 70 percent of design speed. The loss of stall margin at 85 percent speed apparently cannot be explained by high diffusion factors (maximum  $D = 0.54$ ). As also noted in the uniform inlet flow data, the blade element data for tip radially distorted inlet flow showed choking losses on the 2nd-stage stator at low back pressures and deviation angles near the hub of the 2nd-stage rotor were several degrees higher than design values. Calculated losses for the 2nd-stage rotor were negative at 25 percent span for some part-speed points. This anomaly does not appear to have resulted from an improper division of loss between rotor and stator of the 2nd-stage but is more likely associated with temperatures from the correlated 1st-stage exit data as explained in the section "Data Correction and Averaging".

## Hub Distorted Flow

### Overall Performance

Overall performance for the fan, the 1st-stage, and the 1st-stage rotor with hub radially distorted inlet flow is shown in Figures 81, 82, and 83, and overall performance parameters are listed in Appendix G, Table XXIV. Hub-radial distortion caused a reduction in maximum flow at all speeds tested, ranging from 3% at design speed to less than 1% at 70 percent speed. At design speed, where excessive loadings at the hub caused stall with uniform inlet flow, the hub distortion increased stall margin. In particular, stall margin at design speed with respect to a constant throttle operating line through the design point decreased to 6%, half the value achieved with uniform inlet flow. A smaller decrease in stall margin was noted at 85 percent of design speed, and a 7% gain was attained at 70 percent (Figure 71). Efficiency levels were similar to values with uniform inlet flow but at design speed peak fan efficiency occurred near stall. At 85 percent speed, only two data points were obtained, an insufficient number to determine a peak efficiency. As can be seen in the plots of performance for the 1st-stage and 1st-stage rotor, the rise in pressure ratio achieved with the hub distortion was rather small compared to the rise achieved with uniform inlet flow as the fan was back-pressured from wide open throttle to stall, particularly at low speeds.

### Blade Element Data

The spanwise profiles of total pressure ratio for hub-radially distorted and undistorted flows presented in Figure 84 show that the 1st-stage had a higher pressure ratio at the hub with the distortion for near-operating-line data points. The profiles of the midspan and tip regions of the 1st-stage and the complete profile of the 2nd-stage are similar in shape to profiles with undistorted flow.

Pressure ratio at the hub of the 1st-stage decreased at all speeds as the fan was throttled toward stall. For example, at design speed the 1st-stage pressure ratio at 10 percent span from the hub was 1.986 at the open-throttle point and 1.945 at the near stall point. This trend, associated with past-axial exit relative flow angles, caused a small rise in pressure ratio as the fan was throttled. The spanwise efficiency profile presentation (Figure 76) shows efficiency lower in the distorted region and higher in the undistorted region than with uniform inlet flow.

Blade element data for each blade row at five radial positions are shown in Figures 85 through 88. As expected, the 1st-stage rotor and the 1st-stage stator operated at high incidence angles near the hub due to the reduced axial velocities associated with the hub distortion. The 1st-stage rotor hub losses and diffusion factors increased substantially at low speeds as the fan operated towards stall; the rotor attained a diffusion factor of 0.72 at 30 percent span at 70 percent of design speed. At 70 and 85 percent speeds and near-stall operating conditions, the 1st-stage stator loadings also exceeded design predicted levels over the inner half of the vane span (Figure 86). In general, the blade element data from tests with the hub distortion aligned reasonably well with undistorted flow data. Rotor loss data have more scatter, with negative loss coefficients calculated at 10 percent span for both rotors (100%N for R1 and 70%N for R2). Deviation data for the 2nd-stage stator have more scatter than with undistorted flow, particularly for points having high loss coefficients.



## Attenuation of Radial Distortion

Attenuations of radial distortions through the two-stage fan were calculated for three data points with hub distortion, and three points with tip distortion at design speed. To account for the radial variation in total pressure present in the design (uniform inlet flow) profiles at the fan exit and 1st-stage exit, an attenuation parameter,  $A_r$ , at a given axial location  $x$  was defined as:

$$\frac{(A_r)_x}{100} = 1 - \frac{\left[ \left( \frac{\Delta P}{P} \right)_x - \left( \frac{\Delta P}{P} \right)_{\text{Design}} \right]}{\left( \frac{\Delta P}{P} \right)_{\text{Inlet}}}$$

where  $\Delta P/P = (P_{\text{max}} - P_{\text{min}})/P_{\text{max}}$ , and where a negative sign is attached to each  $\Delta P/P$  for which the pressure in the hub region exceeds the pressure in the tip region. Thus the  $(\Delta P/P)_{\text{design}}$  was negative since the design exit total pressure was higher at the hub than at the tip. The  $\Delta P/P$  at the inlet was positive for hub distortions, and negative for tip distortions. Any time the test  $\Delta P/P$  at the fan exit matched the design  $\Delta P/P$  at the fan exit, the distortion was considered fully attenuated and the value of  $A_r$  was 100. Negative values of  $A_r$  represent amplified distortions, values of  $A_r$  between 0 and 100 represent the percentages of attenuation, and values greater than 100 represent over-attenuated distortions.

Table IX presents a summary of attenuation parameters calculated at design speed for hub and tip radially distorted inlet flow, and Figures 89 and 90 give pressure profiles at the fan inlet, 1st-stage exit, and fan exit for these data points. These profiles indicate that the fan attenuated radial distortions well; in fact, the fan slightly over-attenuated hub-radial distortion.

TABLE IX  
ATTENUATION PARAMETERS AT DESIGN SPEED FOR HUB AND TIP  
RADIALLY DISTORTED INLET FLOW

TYPE OF DISTORTION	POINT NUMBER	FIRST-STAGE ROTOR INLET			FIRST-STAGE EXIT			FAN EXIT		
		$(\Delta P/P)$ Test	$(\Delta P/P)$ Design	$A_{r6}$ %	$(\Delta P/P)$ Test	$(\Delta P/P)$ Design	$A_{r11}$ %	$(\Delta P/P)$ Test	$(\Delta P/P)$ Design	$A_{r16}$ %
Tip Radial	6-10-31	-0.1440	0	0	-0.1143	.0213	5.8	-.1427	-.0922	65.0
	6-10-32	-0.1430	0	0	-0.1104	.0213	7.9	-.1494	-.0922	60.0
	6-10-34	-0.1373	0	0	-.0468	.0213	-50.4	-.1104	-.0922	86.7
Hub Radial	5-10-01	0.1426	0	0	-.0632	.0213	159.3	-.1322	-.0922	128.0
	5-10-03	0.1415	0	0	-.0401	.0213	143.3	-.0752	-.0922	87.9
	5-10-04	0.1444	0	0	-.0618	.0213	157.6	-.1134	-.0922	114.7

## CIRCUMFERENTIALLY DISTORTED INLET FLOW

Circumferential distortion screens (Figure 32) were used to generate distortion patterns covering approximately a 90-degree segment of the 1st-stage rotor inlet annulus area and provided distortion parameters,  $(P_{\max} - P_{\min})/P_{\max}$ , of 0.118, 0.142, and 0.143 at 12, 52, and 93 percent of span, respectively, at a near-design data point (Figure 91).

### Overall Performance

Overall performance with circumferentially distorted inlet flow is shown in Figures 92 and 93 for the fan and first stage, and overall performance parameters are listed in Table XXVI, Appendix H. On these plots, filled symbols are used to designate data points based on six screen positions (data 30-degree increments), open symbols are used based on two screen-positions (90-degree increments), and dashed lines are used to indicate performance with uniform inlet flow. Data were taken at 90 percent of design speed instead of 85 percent to avoid high rotor 1 stresses associated with a first bending 4E resonance detected at 85 percent speed.

Fan and first stage overall performance appears to have been relatively unaffected by the circumferential inlet flow distortions employed in this test. The fan stall lines shown in the figures are nearly identical to those of uniform inlet flow and only minor changes in maximum flow are apparent. Some flattening of the pressure-flow characteristic occurs at design speed with circumferential distortion and indicated fan peak efficiencies decrease somewhat. Some of the difference in efficiency may be due to the non-flowfield program method of calculating efficiency values for circumferential distortion. The extremely high efficiencies shown in Figure 93 for the first stage are two-screen-position data points and are not considered to be as accurate as the lower efficiency six-screen-position data points.

### Circumferential Distributions of Flow Field Parameters

The circumferential distributions of static pressure at design speed are shown in Figures 94 and 95. The pressures were measured by means of taps located on the outer case and inner hub at five axial-planes between the distortion screen and the 1st-stage rotor inlet. The profiles show regions of lower static pressure behind the screen, which is consistent with the results obtained during other fan test programs (ref. 2 & 3); however, in general the circumferential variation of pressure is less than had been observed in the tests of the other fans.

At both the hub and the tip, differences between maximum and minimum static pressures measured around the circumference were highest at the two axial-locations nearest the rotor leading edge, almost as high just downstream of the distortion screen, and lowest at the two axial-stations in between. The circumferential extent of the region of low static pressure decreased in the direction of flow, which gave steeper circumferential gradients of static pressure as the rotor was approached.

Circumferential distributions of total pressure ratio, static pressure ratio, absolute Mach number, relative air-angle, absolute air-angle, and meridional velocity at the 1st-stage rotor inlet are shown in Figure 96 at 10, 50, and 90 percent span for data points at design speed for wide-open and near-stall throttle settings. Distributions of total pressure ratio, static pressure ratio, absolute Mach number, total temperature ratio, absolute air-angle, and meridional velocity at the first-stage exit and fan exit are presented in Figures 97 and 98, respectively. Of interest in these plots is the attenuation of total pressure distortion at 50 percent and 90 percent of span and the apparent amplification at the hub. These plots also reflect the potential inaccuracies in performance based on two screen-positions instead of the six used throughout previous programs. Where parameters are known to vary significantly around the circumference, appreciable differences in calculated average values may have resulted, as suggested by the plots of inlet total pressure (Figure 96).

The rather improbable "sawtooth" distribution of absolute air-angle at the fan exit (Figure 96) is probably due to disagreement in readings of the two wedge-probes rather than actual angle variation. Table X summarizes attenuations for the two design-speed points based on six screen-positions, indicating that the first stage amplified distortion, while the second stage attenuated it with a sizable net attenuation by the fan except at the hub. The attenuation parameter,  $A_c$ , at a given station,  $x$ , is defined as:

$$\frac{(A_c)_x}{100} = 1 - \frac{\left(\frac{P_{\max.} - P_{\min.}}{P_{\max.}}\right)_x}{\left(\frac{P_{\max.} - P_{\min.}}{P_{\max.}}\right)_{\text{inlet}}}$$

Negative values of  $A_c$  represent amplified distortions and positive values represent percentages of attenuation.

Additional velocity vector parameters are given in Appendix H, Tables XXVII, XXVIII, and XXIX. Also given are circumferential distributions of total temperature ratio at first-stator exit and fan exit (Tables XXX and XXXI).

TABLE X  
ATTENUATION PARAMETERS AT DESIGN SPEED  
FOR CIRCUMFERENTIALLY DISTORTED INLET FLOW

PERCENT SPAN	POINT 007-10-02			POINT 007-10-03		
	$\left(\frac{P_{\text{MAX.}} - P_{\text{MIN.}}}{P_{\text{MAX.}}}\right)_6$	(Ac) 11	(Ac) 16	$\left(\frac{P_{\text{MAX.}} - P_{\text{MIN.}}}{P_{\text{MAX.}}}\right)_6$	(Ac) 11	(Ac) 16
10	0.1176	-264	0.6	0.1024	-139	-41.3
50	0.1416	- 18.2	39.1	0.1327	- 44.4	67.6
90	0.1429	- 9.7	46.9	0.1266	- 10.6	31.1

Station 6: Fan Inlet  
Station 11: First-Stage Exit  
Station 16: Fan Exit

## REMARKS

The two-stage fan was well matched at design speed, and it is unlikely that resetting the stators would have improved overall efficiency. The loadings of the second-stage hub appear to have caused stall, but it could not be determined whether the 2nd-stage rotor or the stator instigated the stall. If the stator initiated stall, it is probable that stall margin can be increased by closing stator 2 to reduce its loading and incidence angles.

The rapid decrease in efficiency at speeds above design, indicates mismatched incidence angles, which generate high losses. The high Mach numbers entering each blade row at over-speed operation reduced the low-loss incidence ranges of the blade rows, accentuating the importance of incidence angle matching. It is probable that resetting the stators will improve high-speed efficiency significantly.

At part-speed, the first stage was highly loaded while the second stage was relatively lightly loaded. It may be possible to delay stall by redistributing loadings between stages through the use of variable stator settings. Redistribution of loading is more easily obtained with a variable inlet guide vane, which was not available on this rig. Improvements in efficiency would be difficult to obtain since the ranges of low-loss incidence covered most of the operating range of all blades rows at part-speed.

Rotor tip casing treatment over the 1st-stage rotor would probably increase tip-loading capability and delay stall at low speed, particularly with tip radially distorted inlet flow. The calculated loadings at the tip of the 2nd-stage rotor do not appear to have been sufficiently high to have caused stall, and it is unlikely that casing treatment over this rotor would improve stall margin.

## SUMMARY OF RESULTS

Tests of the two-stage fan having a 1st-stage rotor tip speed of 1450 ft/sec [442 m/sec] (and the redesigned 2nd-stage rotor) produced the following significant results:

1. A corrected flow of 185.4 lbm/sec [84.0 kg/sec] and a pressure ratio of 2.8 were achieved at design speed at an adiabatic efficiency of 85.0% and a stall margin of 12%.
2. The addition of a partspan shroud on the redesigned 2nd-stage rotor prevented flutter at all operating conditions.
3. Peak operating-line adiabatic efficiency was 85.5% and was obtained at 85 percent and 95 percent of design speed. Operating line efficiency dropped to 83.0% at 50 percent speed and dropped rapidly with overspeed to values of 82.0% and 78.5% at 105 percent and 110 percent design of speed, respectively.

4. Losses due to the 2nd-stage rotor partspan shroud reduced fan efficiency. At design speed and pressure ratio, overall adiabatic efficiency was 85% compared to 85.7% in a previous test with a shroudless 2nd-stage rotor.
5. Stall margin was 21% at 50 percent speed, dropping monotonically to 12% at design speed. Stall margin then increased to 15% at 105 percent speed. Stalls were initiated by high loadings at the tip of the first stage at low speeds and by high loadings at the hub of the second stage at high speeds.
6. The skewed pressure-ratio profile of the redesigned 2nd-stage rotor, with higher pressure at the hub than at the tip, gave two percentage points more stall margin at design speed than the constant radial pressure profile of the original rotor.
7. The fan maintained at least 6% stall margin when operating with severe tip-radial, hub-radial, and circumferential distortions. The hub distortion reduced stall margin at design speed, where excessive hub loadings caused stall with undistorted flow. At low speeds, where excessive tip loadings caused stall with undistorted flow, the hub distortion increased stall margin. The tip distortion increased stall margin at high speeds by relieving hub loadings. At 85 percent of design speed, the tip distortion reduced stall margin but had little effect at 70 percent speed. The circumferential distortion had little effect on stall margin at all speeds tested.
8. Radial distortions were always attenuated. Circumferential distortions were also attenuated except for the near-stall data points where distortion at the hub was amplified.

## REFERENCES

1. Harley, K. G. and Burdsall, E. A.: "High Loading Low Speed Fan Study - Unslotted Blades and Vanes," NASA CR-72667, PWA-3653, 1970.
2. Sulam, D. H.; Keenan, M. J. and Flynn, J. T.: "Single Stage Evaluation of Highly Loaded High Mach Number Compressor Stages - II Data and Performance, Multi-Circular-Arc Rotor", NASA CR-72694, PWA-3772, 1970.
3. Morris, A. L. and Sulam, D. H.: "High Loading, 1800 Ft/Sec Tip Speed Transonic Compressor Stage - II Final Report," NASA CR-120991, PWA-4463, 1972.
4. Gostelow, J. P.; Krabacher, K. W. and Smith, L. H., Jr.: "Performance Comparisons of High Mach Number Compressor Rotor Blading," NASA CR-1256, 1968.
5. Bilwakesh, K. R.; Kock, C. C. and Prince, D. C.: "Evaluation of Range and Distortion Tolerance for High Mach Number Transonic Fan Stages - Final Report on Task II: Performance of 1500 Ft/Sec Tip Speed Transonic Fan Stage With Variable Geometry Inlet Guide Vanes and Stator", NASA CR-72880, G. E. R7AEG195, 1972.
6. Urasek, D. C.; Moore, R. D. and Osborn, W. M.: "Performance of a Single Stage Transonic Compressor With a Blade Tip Solidity of 1.3," NASA TM X-2645, 1972.
7. Ball, C. L.; Janetzke, D. C. and Reid, L.: "Performance of a 1380 Foot Per Second Tip Speed Axial Flow Compressor Rotor With Blade Tip Solidity of 1.5," NASA TM S-2379, 1971.
8. Janetzke, D. C.; Ball, C. L. and Hager, R. D.: "Performance of a 1380 Foot Per Second Tip Speed Axial Flow Compressor Rotor With a Blade Tip Solidity of 1.1," NASA TM X-2449, 1972.
9. Messenger, H. E. and Kennedy, E. E.: "Two-Stage Fan-1: Aerodynamic and Mechanical Design," NASA CR-120859, PWA=4148, 1972.
10. Ruggeri, R. S. and Benser, W. A.: "Performance of a Highly Loaded Two-Stage Axial Flow Fan," NASA TM X-3076, 1974.
11. Hanley, W. T.: "A Correlation of Endwall Losses in Plane Compressor Cascades," *Journal of Engineering for Power*, Trans. ASME, Vol. 90, Series A, No. 3, July 1968, pp. 251-257.
12. Glawe, G. E.; Simms, F. S. and Stickney, T. N.: "Radiation and Recovery Corrections and Time Constants of Several Chromel-Alumel Thermocouple Probes at High Temperatures in High Velocity Gas Streams," NACA TN 3766, Oct. 1956.
13. Benser, W. A.: NASA SP304, "Fluid Mechanics, Acoustics and Design of Turbo-Machinery from Symposium on Fluid Mechanics and Design of Turbo Machinery." Penn. State University, Sept. 1970.

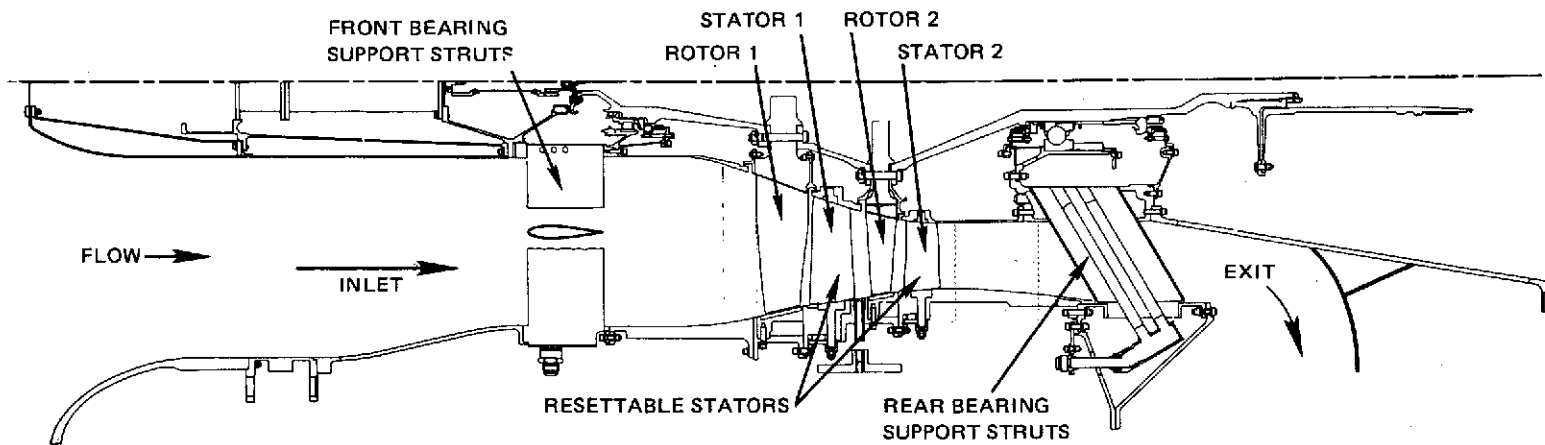


Figure 1 Schematic of Two-Stage Fan Test Arrangement

REPRODUCIBILITY OF THE  
ORIGINAL PAGE IS POOR

DIMENSION IN INCHES  
(METERS)

STA	DIAMETER		AXIAL DISTANCE FROM ROTOR 1 LEADING EDGE	
	I.D.	O.D.	z - I.D.	z - O.D.
4	10.00 (0.254)	32.48 (0.825)	-5.20 (-0.132)	-5.20 (-0.132)
5	10.26 (0.261)	32.33 (0.821)	-3.70 (-0.094)	-3.70 (-0.094)
6	10.94 (0.278)	31.96 (0.811)	-2.245 (-0.057)	-2.245 (-0.057)
7	12.40 (0.315)	31.00 (0.787)	0.0 (0.0)	0.42 (0.011)
8	14.84 (0.377)	29.93 (0.760)	3.30 (0.084)	2.75 (0.070)
9	15.22 (0.387)	29.67 (0.754)	3.80 (0.097)	3.45 (0.088)
10	16.85 (0.428)	28.96 (0.736)	6.15 (0.156)	6.33 (0.161)
11	17.18 (0.436)	28.82 (0.752)	6.75 (0.172)	6.75 (0.172)
*12	17.39 (0.442)	28.58 (0.726)	7.23 (0.184)	7.57 (0.192)
** 12	17.39 (0.442)	28.55 (0.725)	7.23 (0.184)	7.65 (0.194)
*13	18.35 (0.467)	28.12 (0.714)	9.20 (0.234)	8.82 (0.224)
** 13	18.37 (0.467)	28.14 (0.715)	9.27 (0.236)	8.76 (0.223)
14	18.58 (0.472)	27.90 (0.709)	9.80 (0.249)	9.59 (0.244)
15	18.90 (0.480)	27.60 (0.701)	11.85 (0.301)	11.93 (0.303)
16	18.90 (0.480)	27.60 (0.701)	13.50 (0.343)	13.50 (0.343)

\*ORIGINAL } DENOTES CHANGES IN  
\*\*REDESIGN } AXIAL POSITION DUE TO REDESIGN

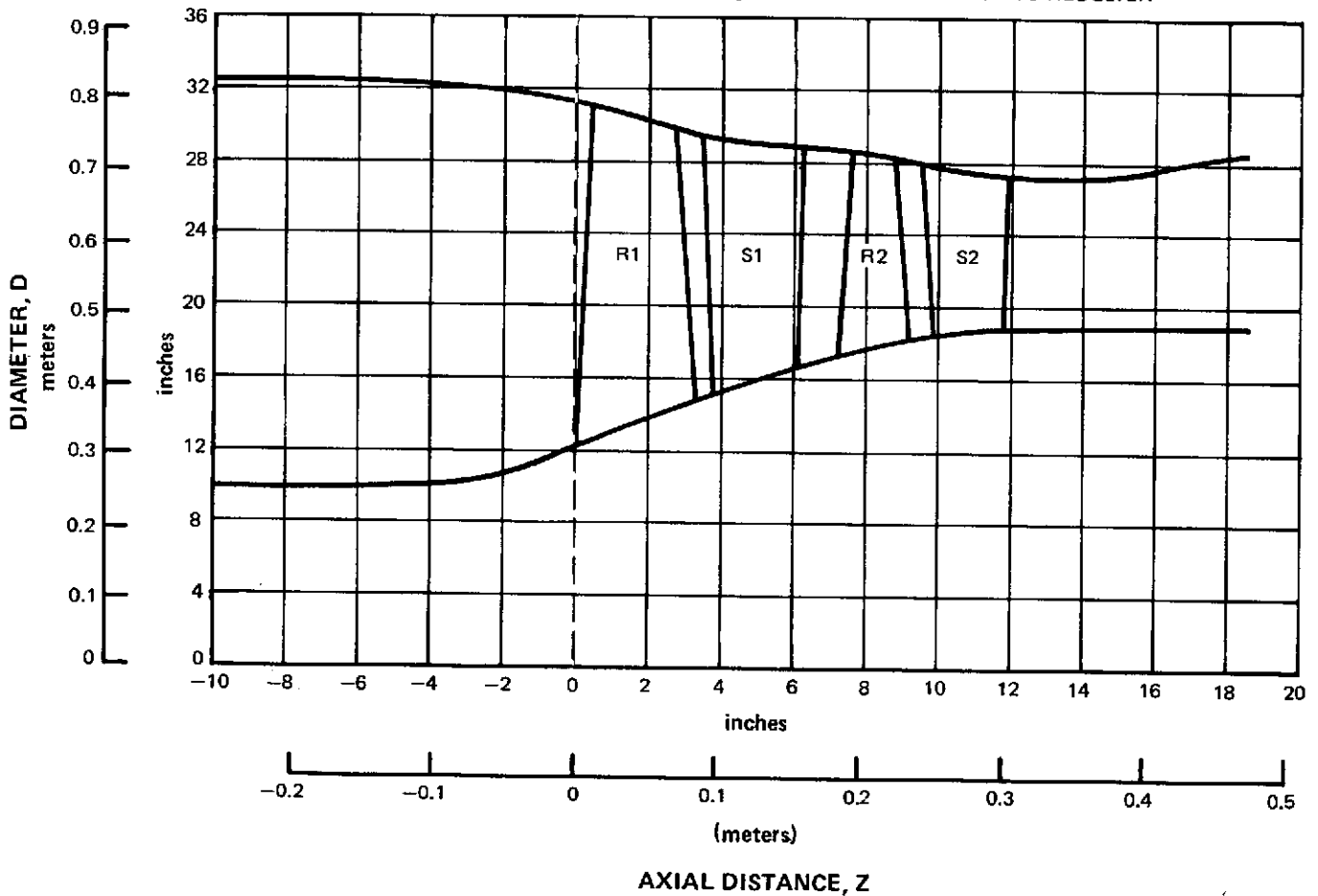
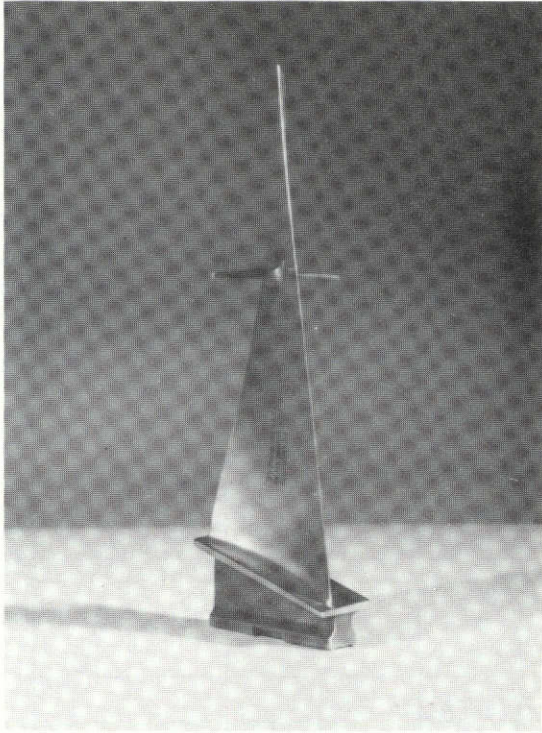
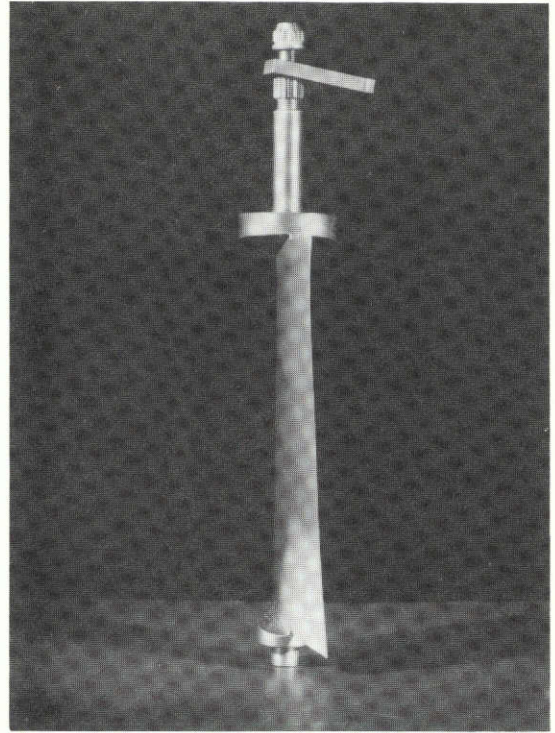


Figure 2 Fan Flowpath

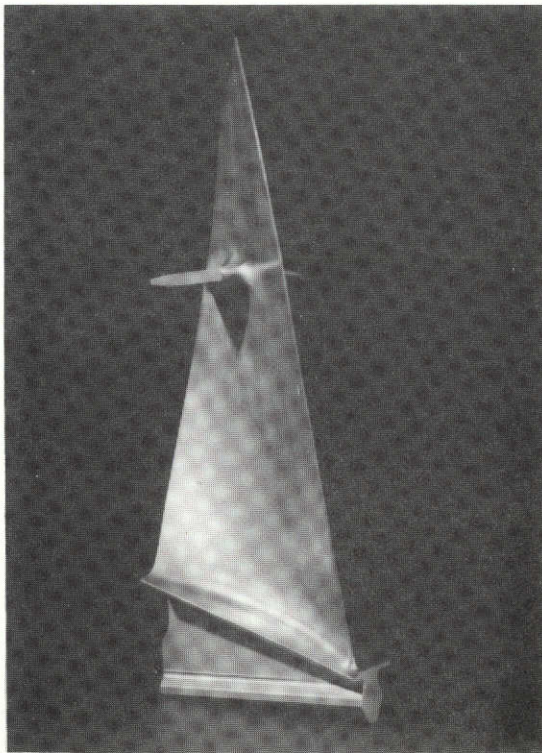




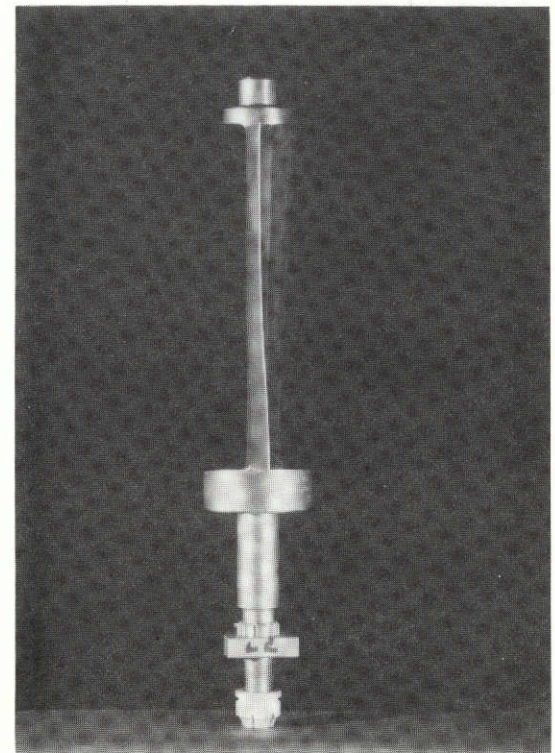
First-Stage Blade



First-Stage Vane



Second-Stage Redesigned Blade



Second-Stage Vane

Figure 3 Photographs of Blades and Vanes

REPRODUCIBILITY OF THE  
ORIGINAL PAGE IS POOR

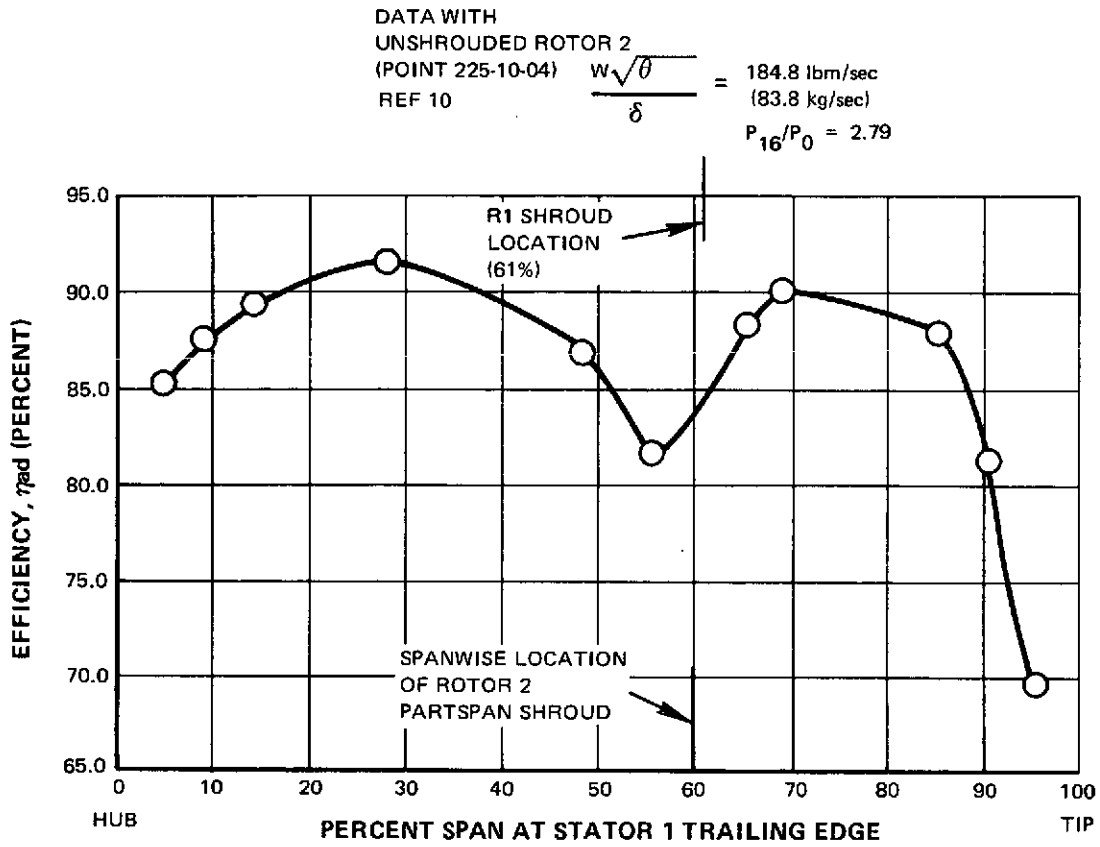


Figure 4 Stage 1 Efficiency Versus Span Showing Wake of the Part-Span Shroud

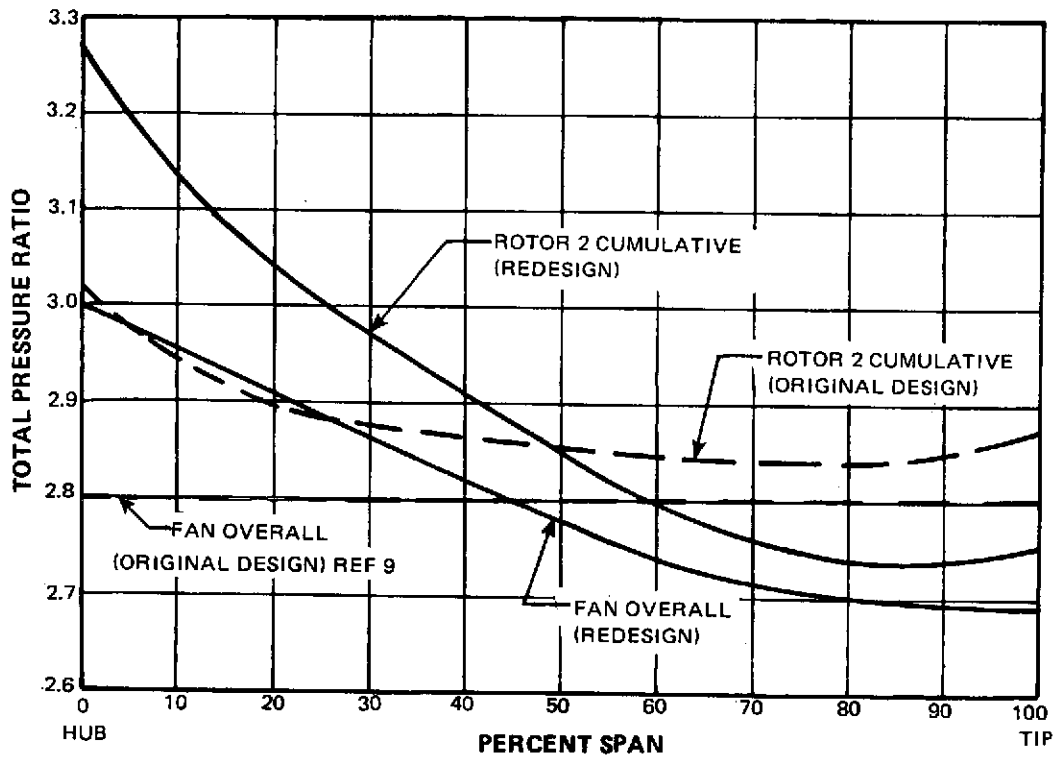


Figure 5 Design Total Pressure Ratio Versus Span at Rotor 2 Exit and Fan Exit

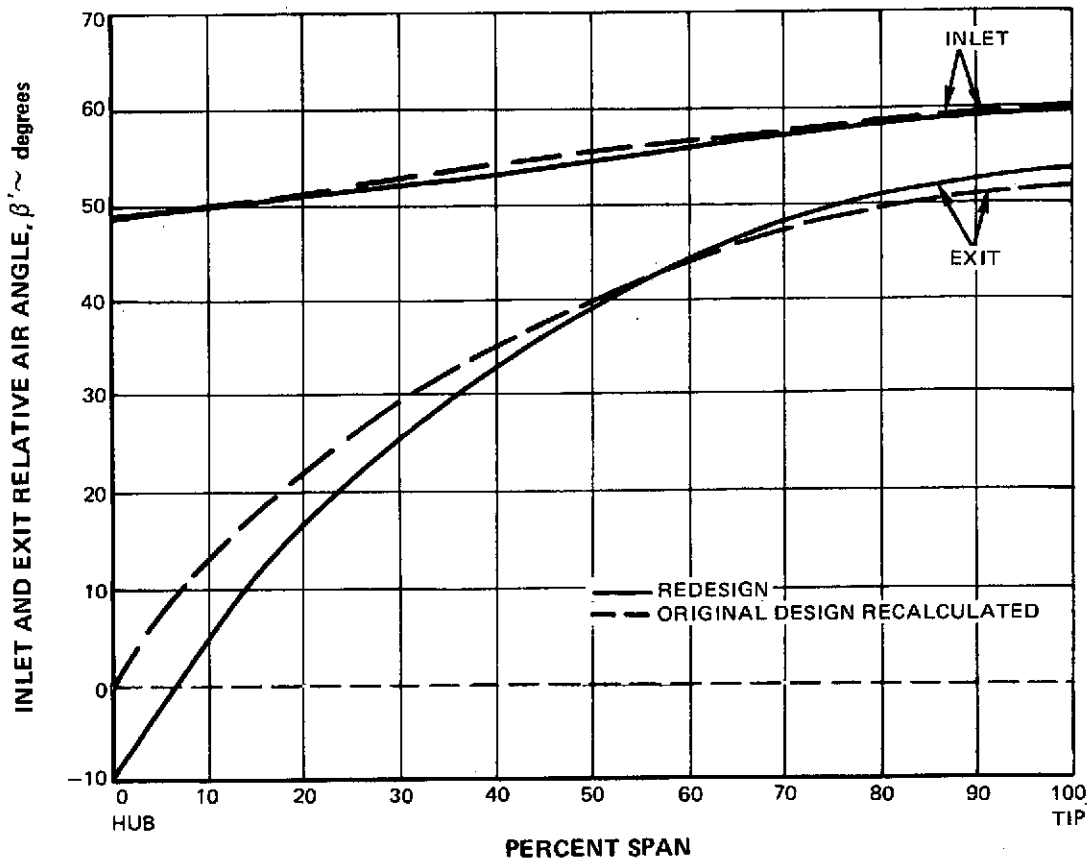


Figure 6 Design Inlet and Exit Relative Air Angle Versus Span for Original and Redesigned Rotor 2

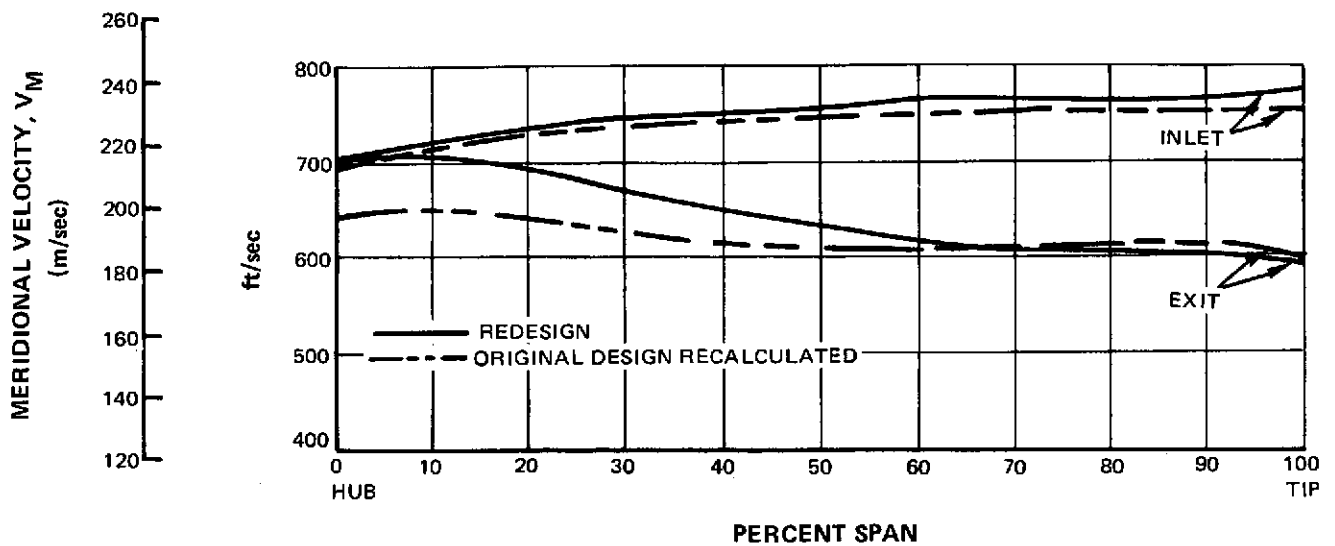


Figure 7 Design Meridional Velocity Versus Span for Original and Redesigned Rotor 2

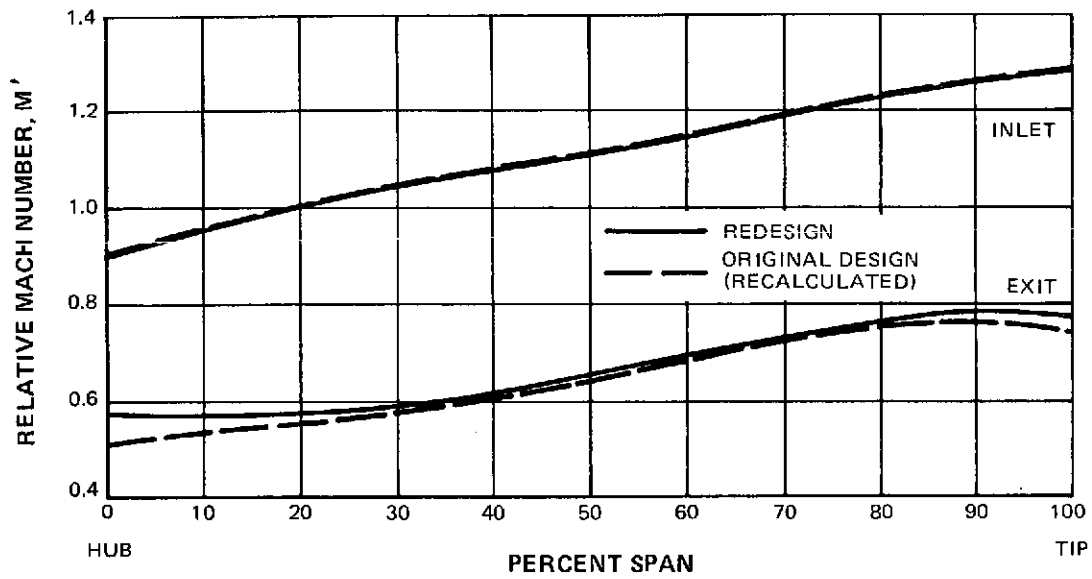


Figure 8 Design Relative Mach Number Versus Span for Original and Redesigned Rotor 2

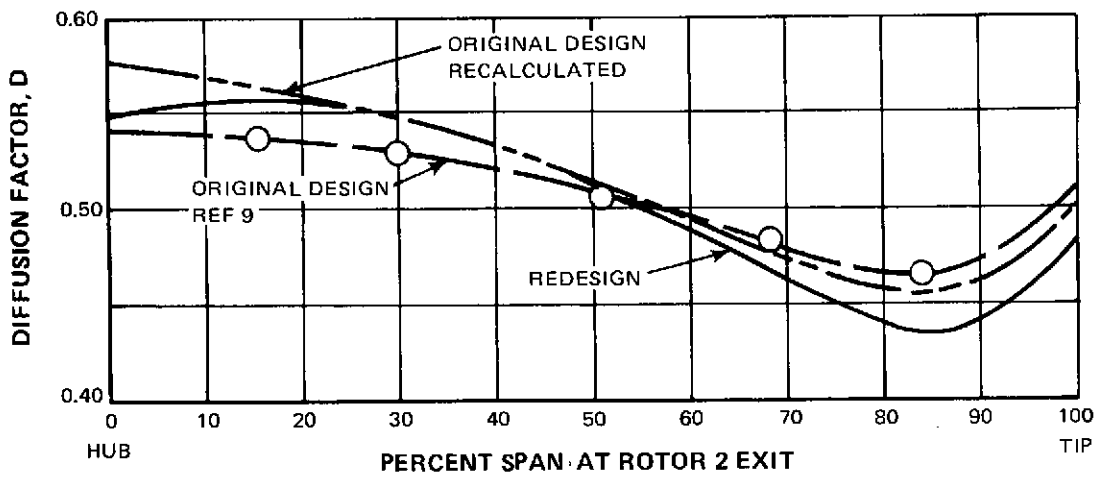


Figure 9 Design Diffusion Factor Versus Span for Original and Redesigned Rotor 2

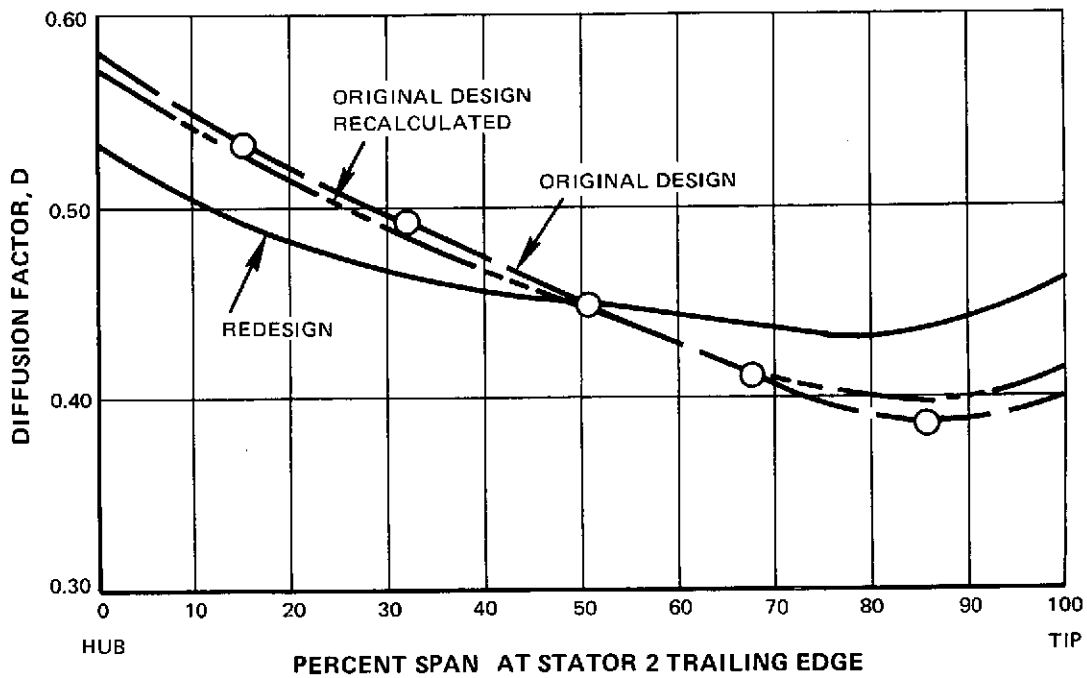


Figure 10 Stator Design Diffusion Factor Versus Span for Original and Redesigned Rotor 2

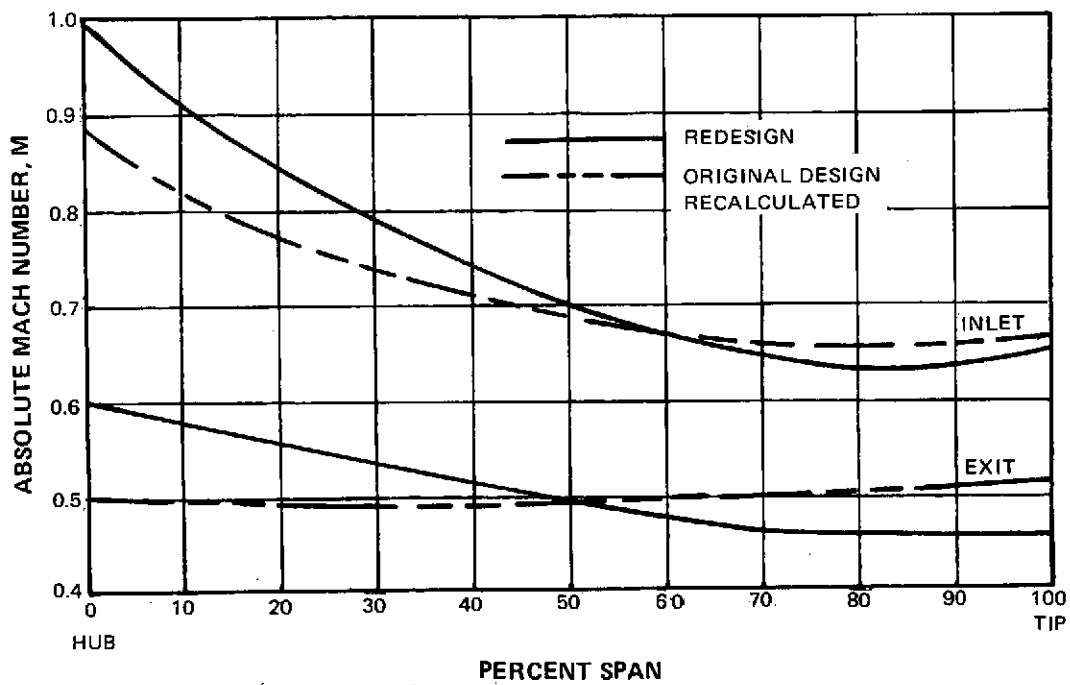


Figure 11 Stator 2 Design Mach Number Versus Span for Original and Redesigned Rotor 2

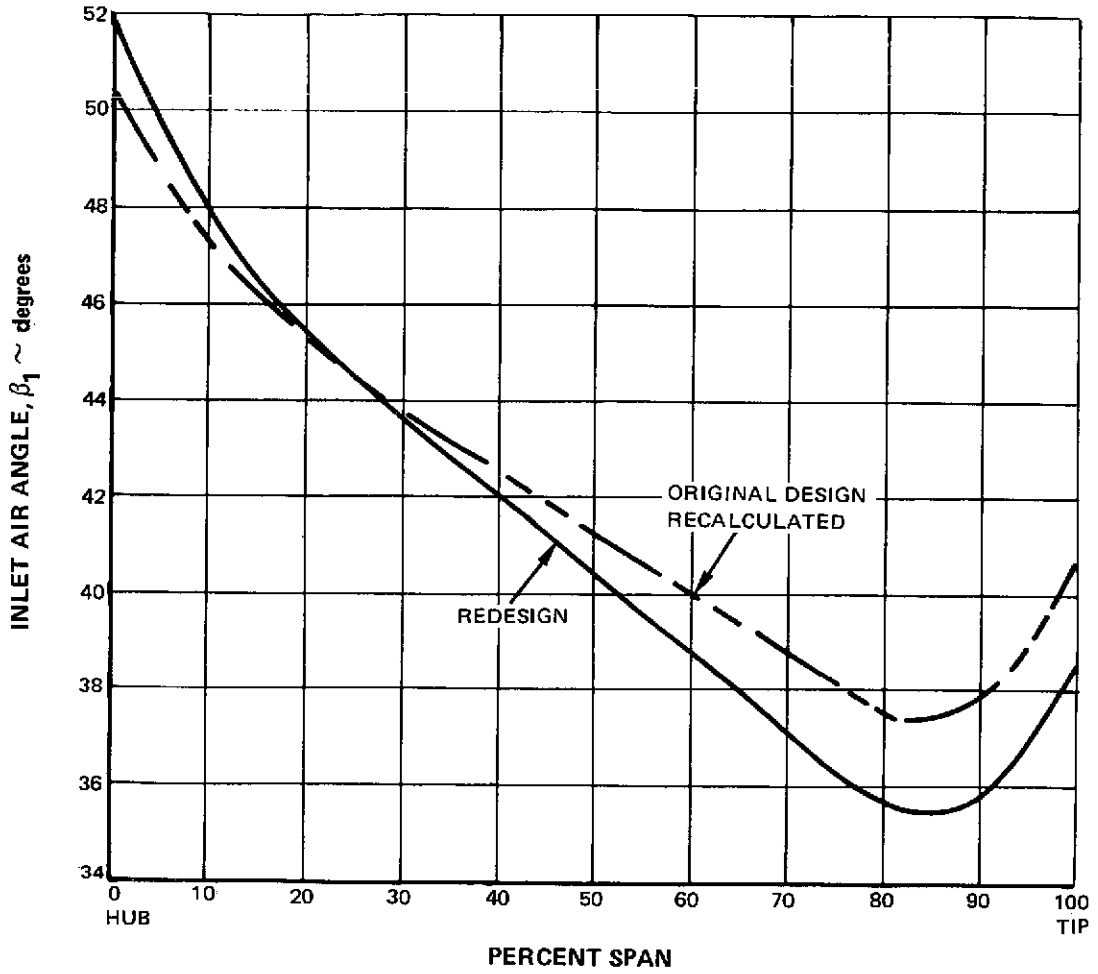


Figure 12 Stator 2 Design Inlet Air Angle Versus Span for Original and Redesigned Rotor 2

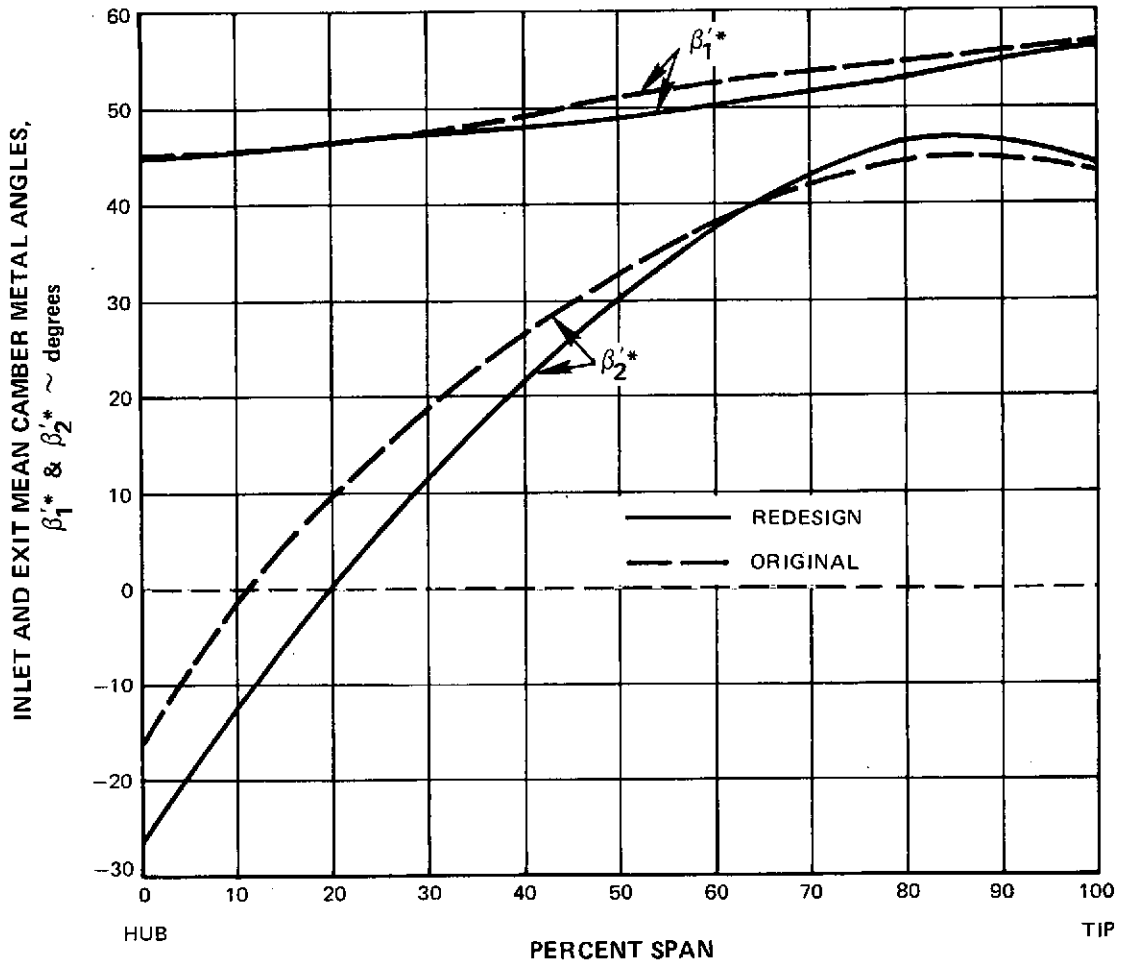


Figure 13 Redesigned Rotor 2 Inlet and Exit Metal Angles Versus Span

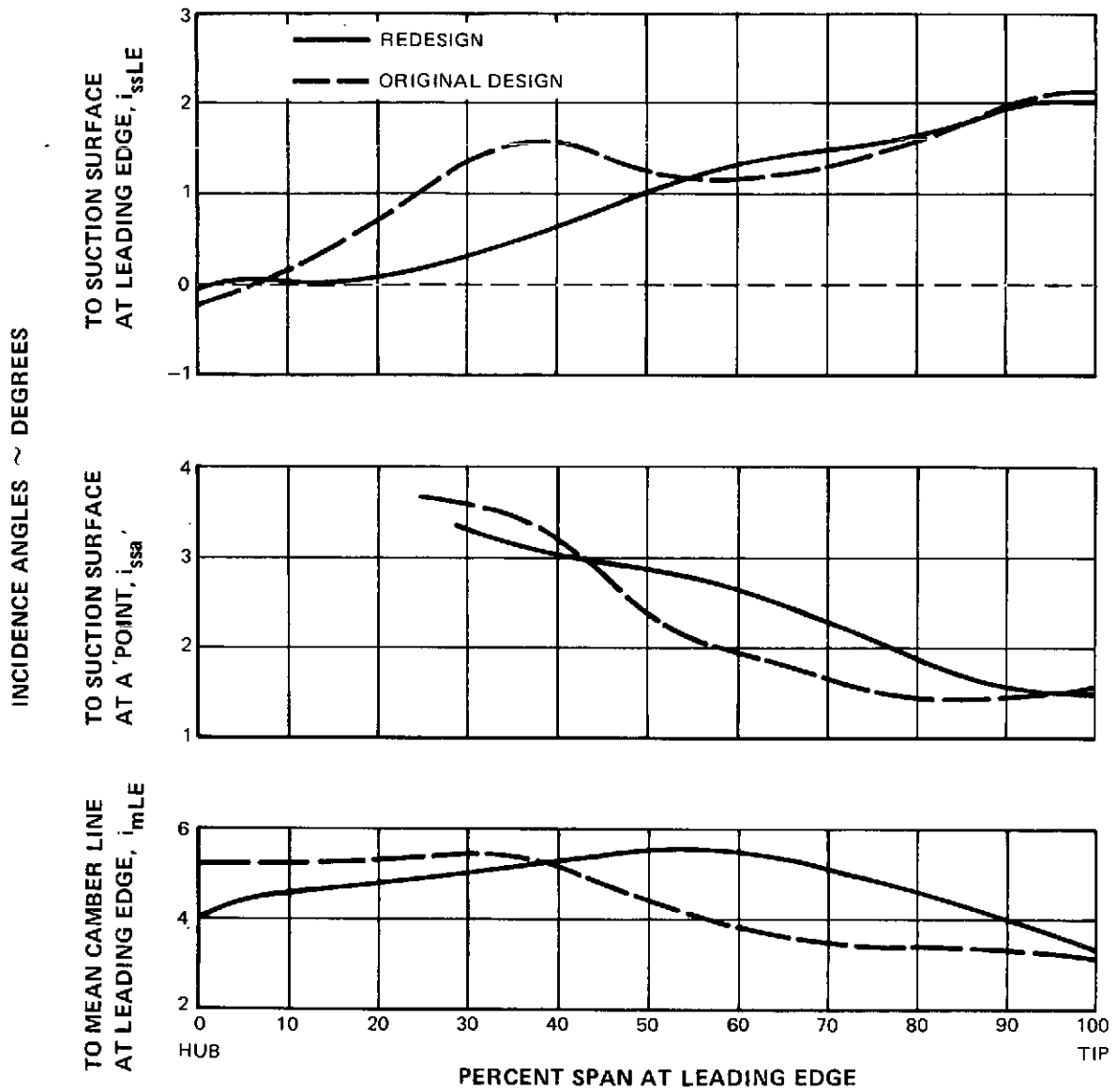


Figure 14 Redesigned Rotor 2 Incidence Angle Versus Span



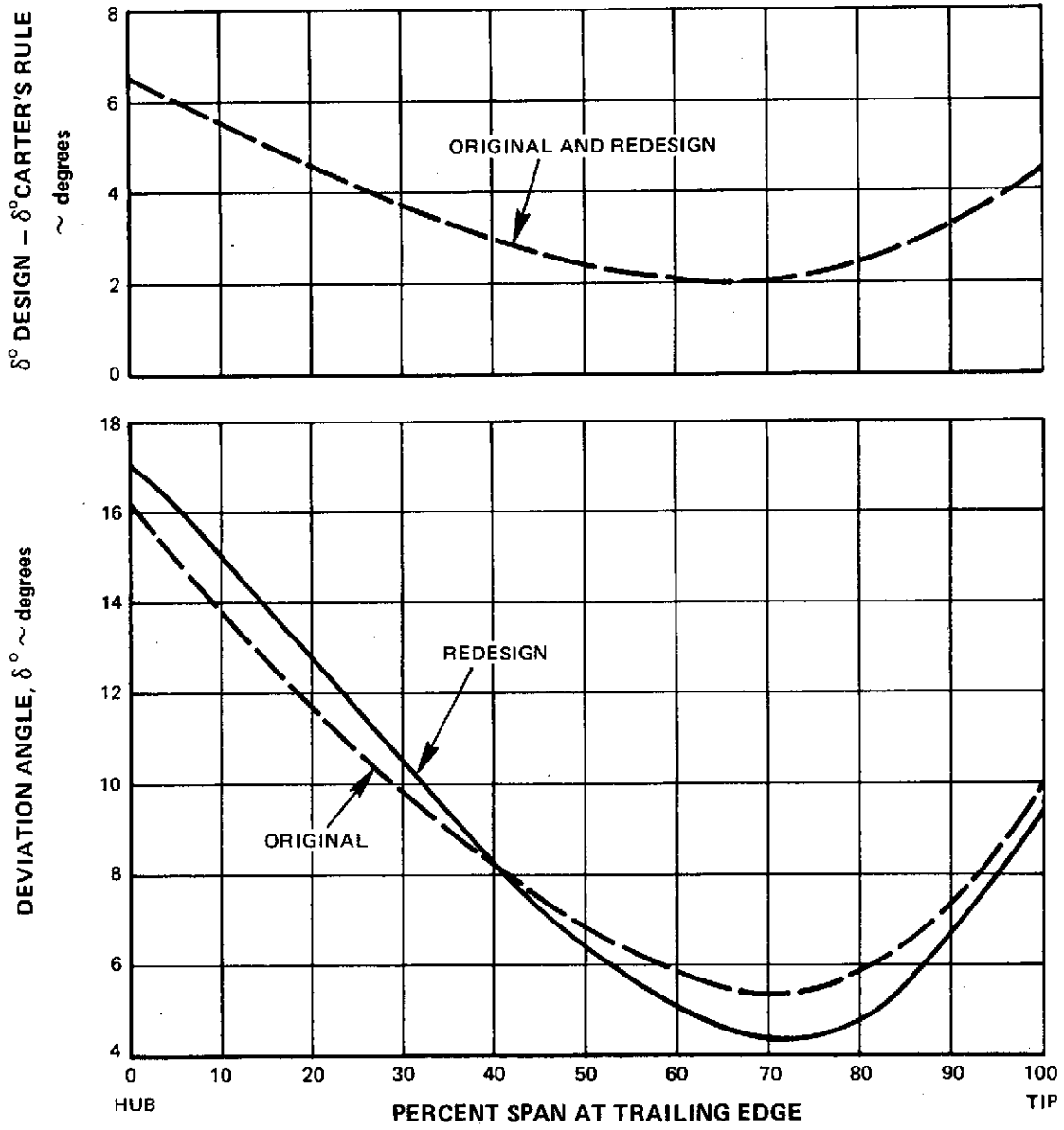


Figure 15 Redesigned Rotor 2 Deviation Angles Versus Span

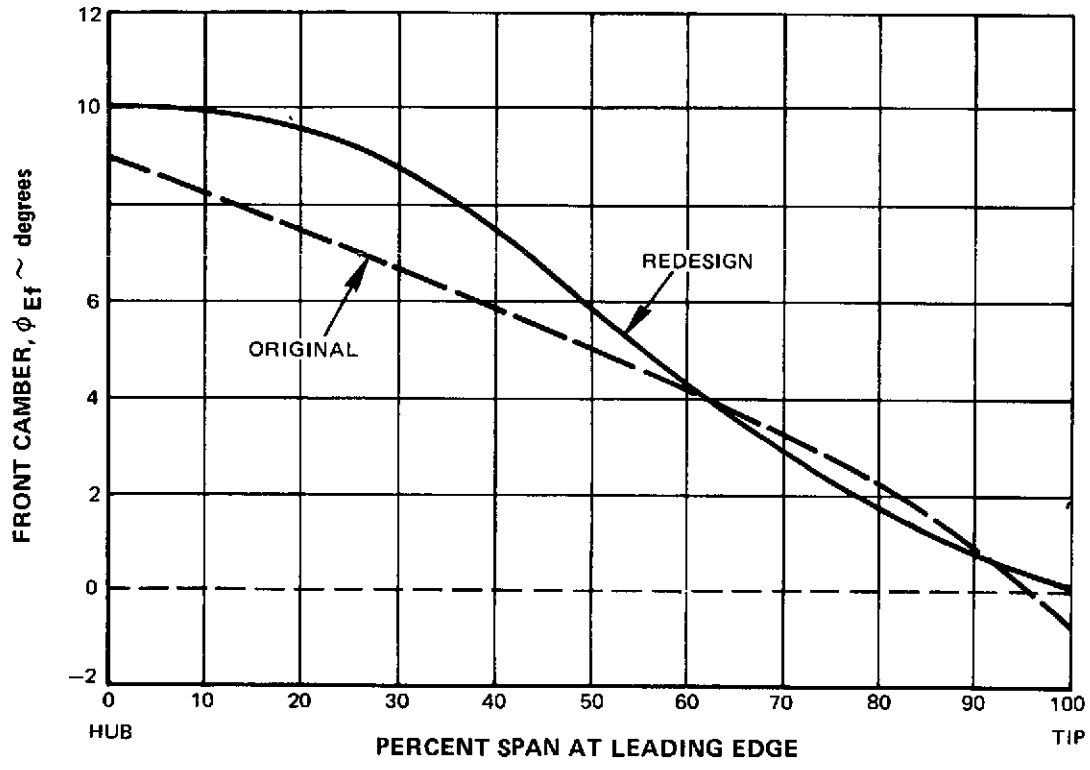


Figure 16 Redesigned Rotor 2 Front Camber Angles Versus Span

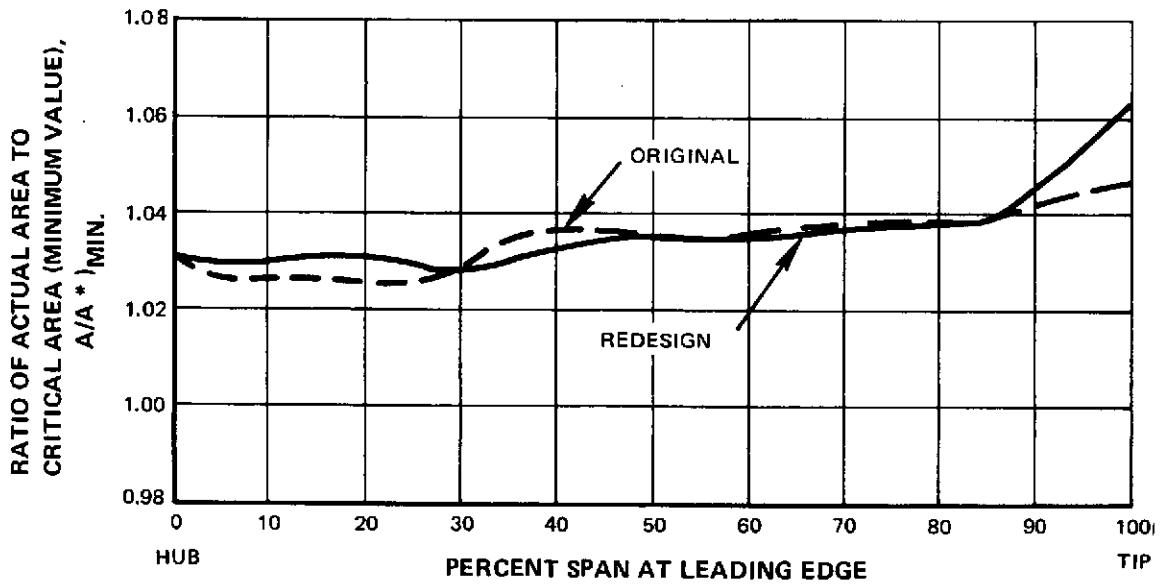


Figure 17 Redesigned Rotor 2 Minimum Channel Area Ratios Versus Span

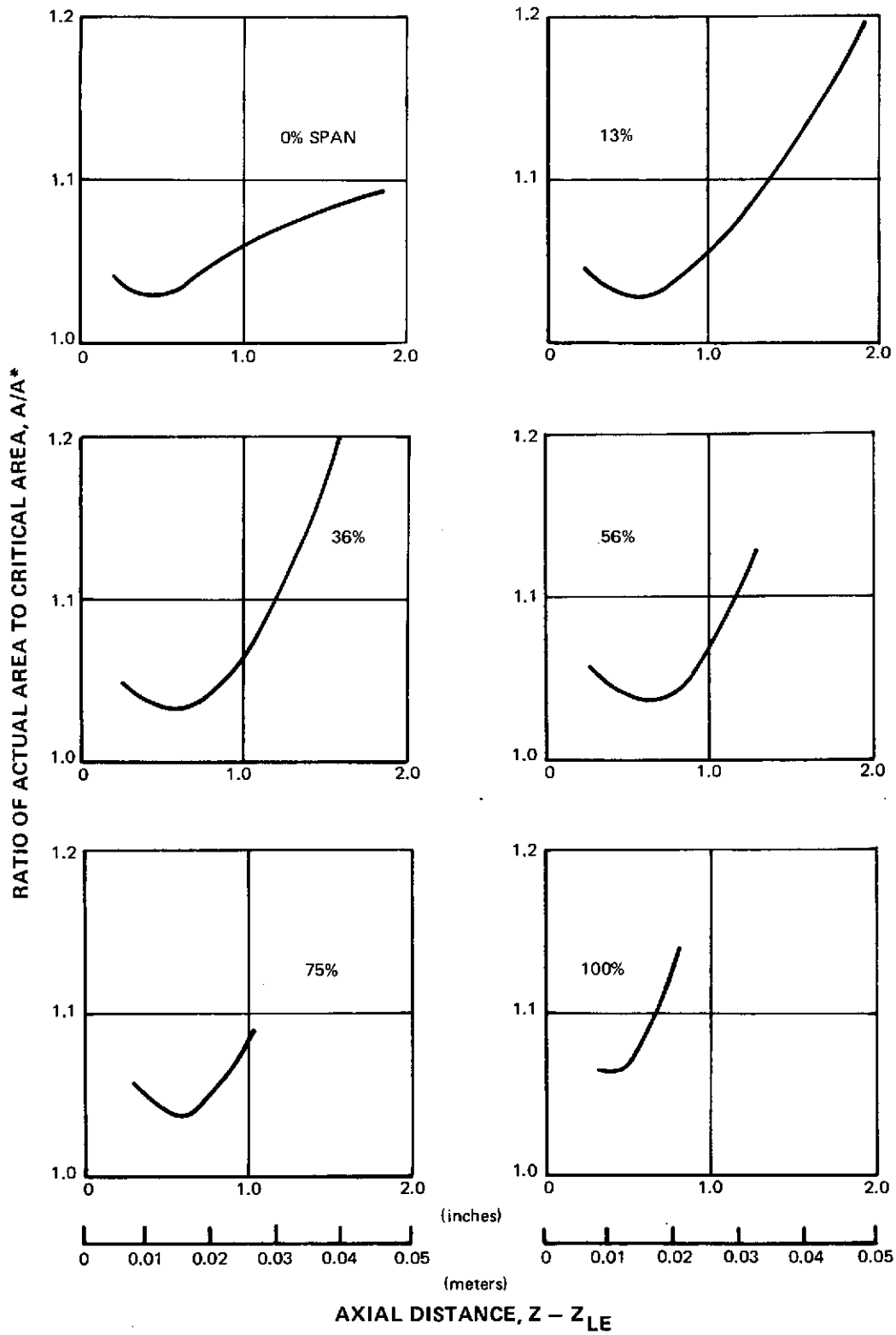


Figure 18 Redesigned Rotor 2 Channel Area Ratios Versus Axial Distance Percent Span at Blade Leading Edge

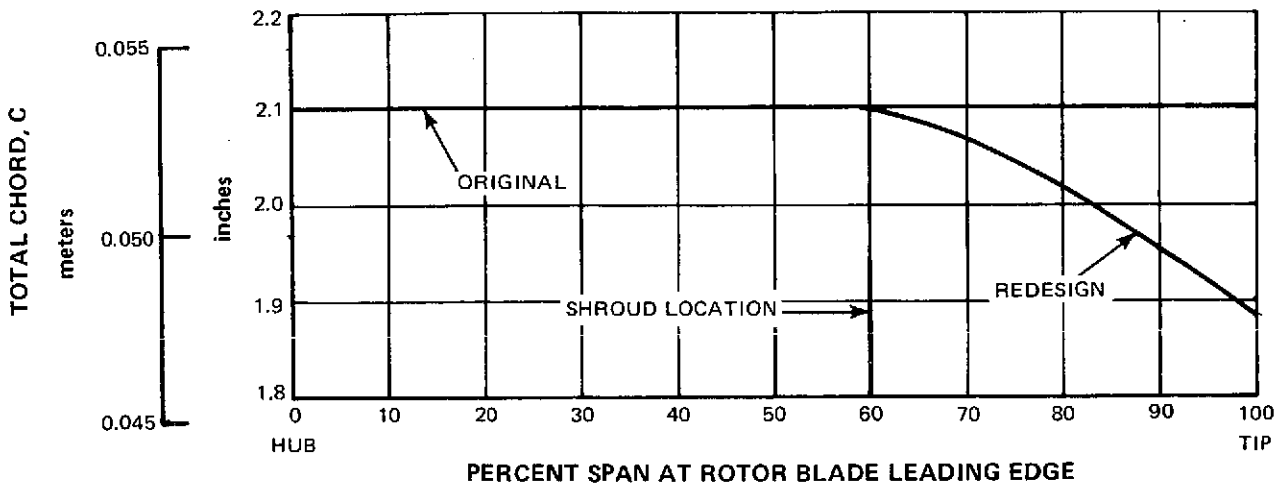


Figure 19 Chord Versus Span for Original and Redesigned Rotor 2

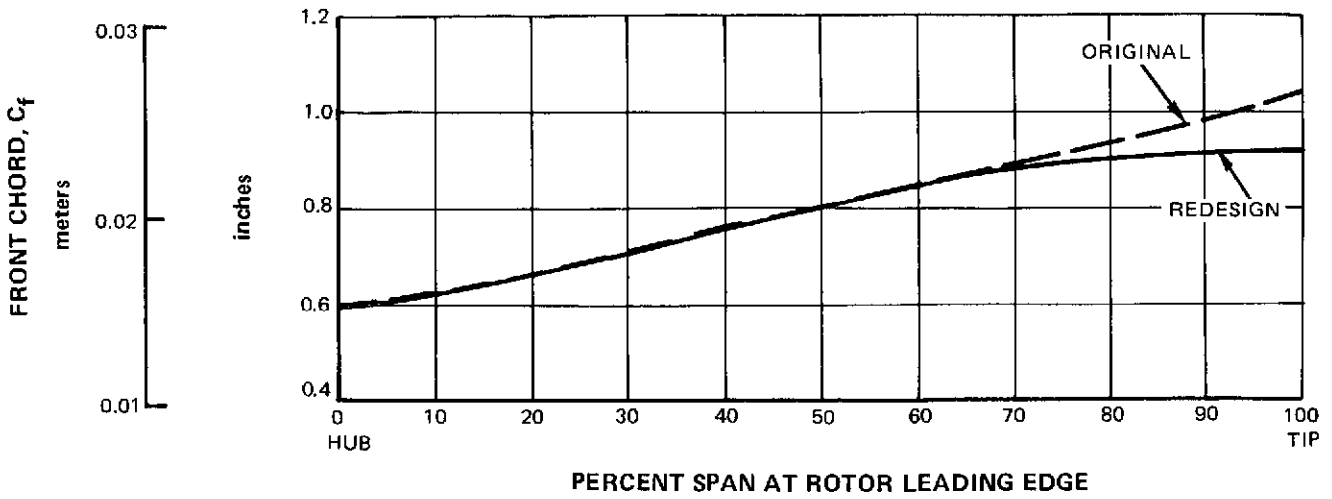


Figure 20 Front Chord Versus Span for Original and Redesigned Rotor 2

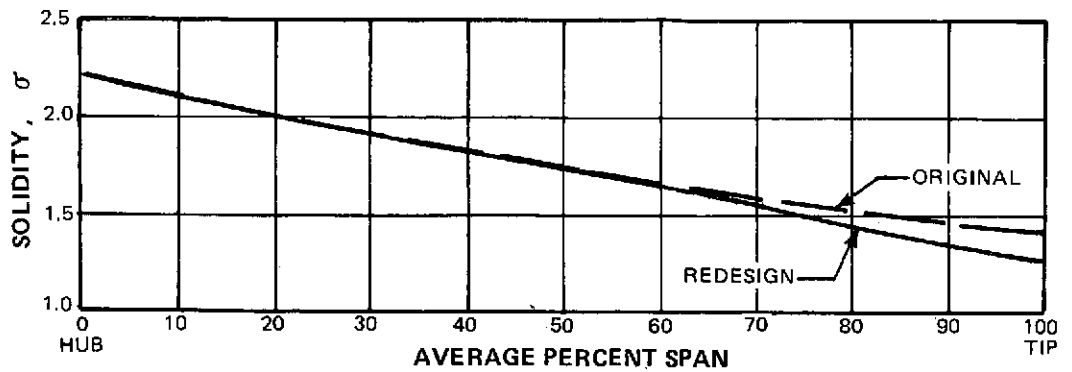


Figure 21 Solidity Versus Span for Original and Redesigned Rotor 2

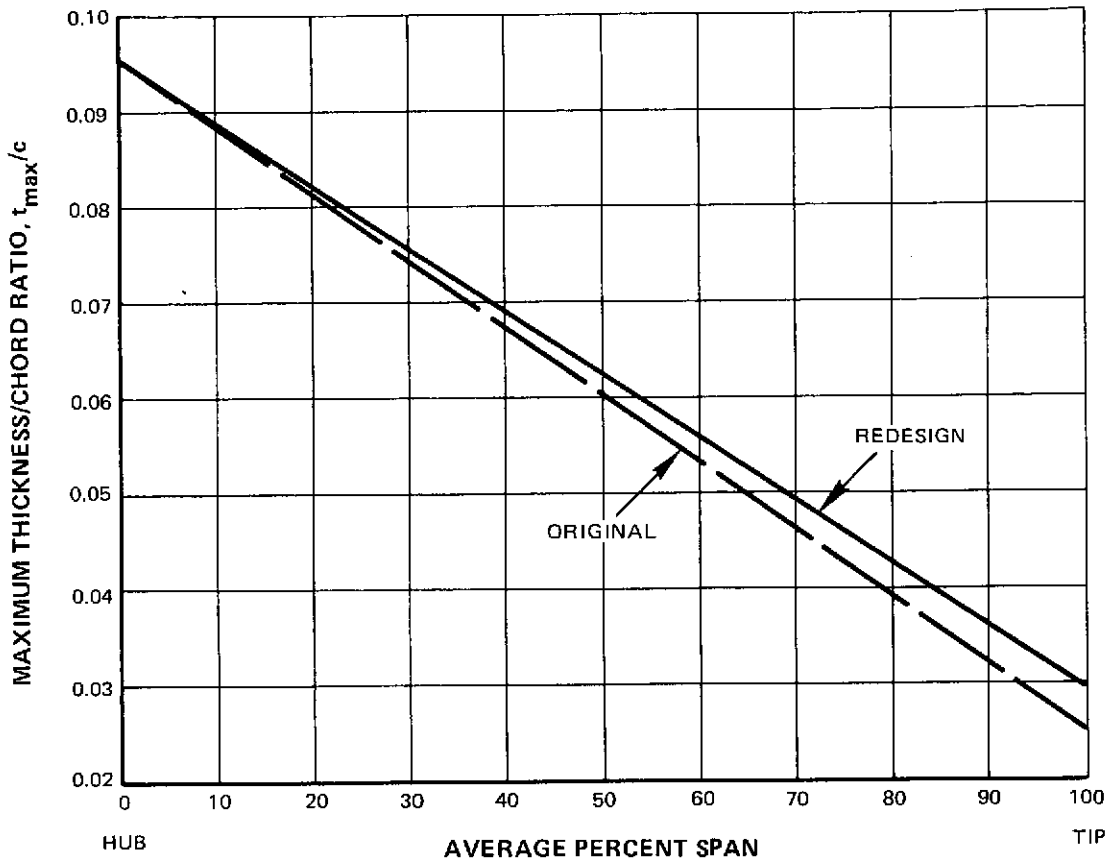


Figure 22 Maximum Thickness/Chord Ratio Versus Span for Original and Redesigned Rotor 2

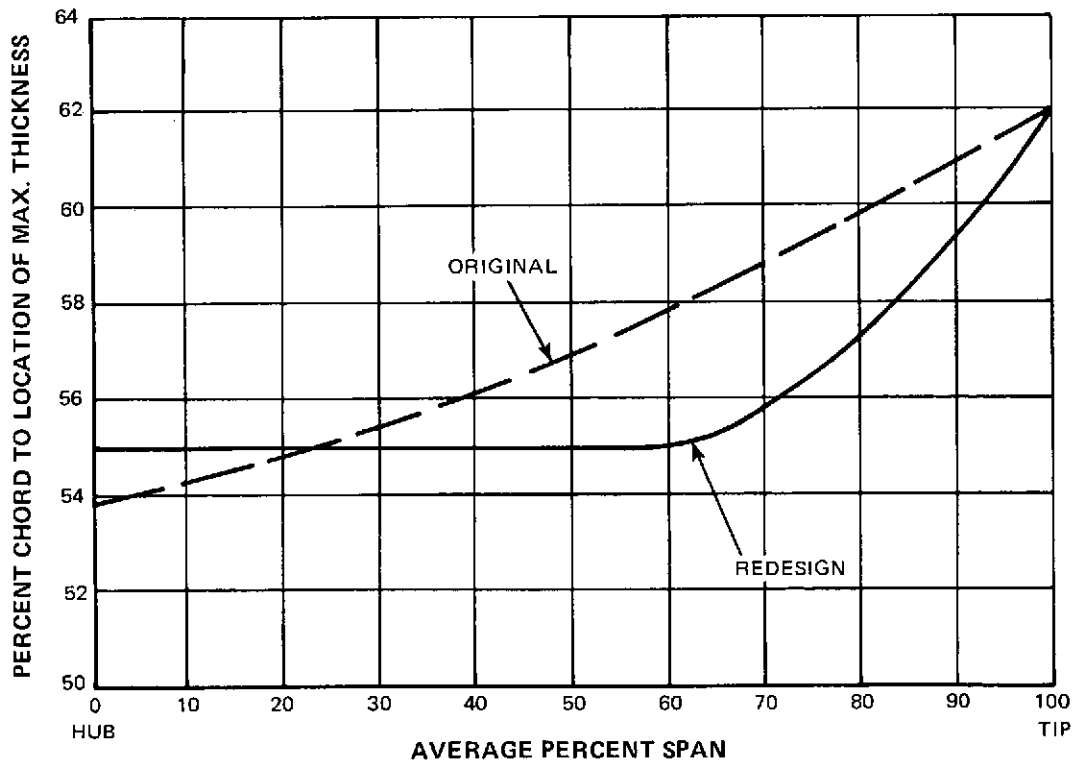


Figure 23 Chordwise Location of Airfoil Maximum Thickness Versus Span for Original and Redesigned Rotor 2

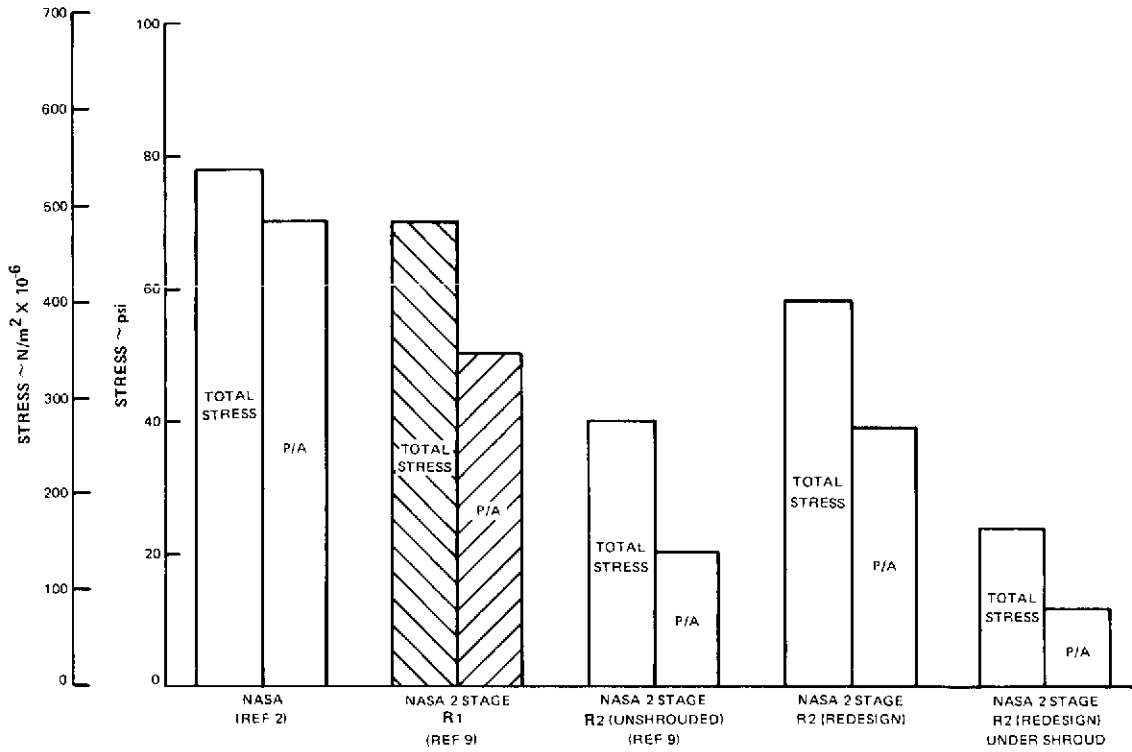


Figure 24 Redesigned Rotor 2 Combined Stress Compared to Successful Experience

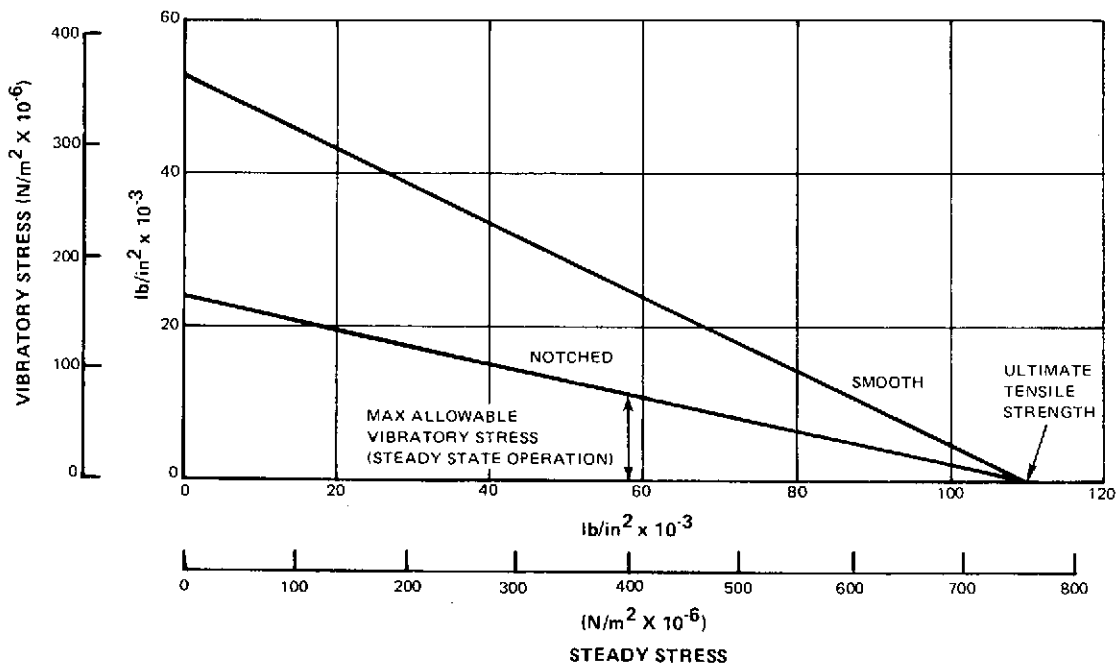


Figure 25 Goodman Diagram for Redesigned Rotor 2

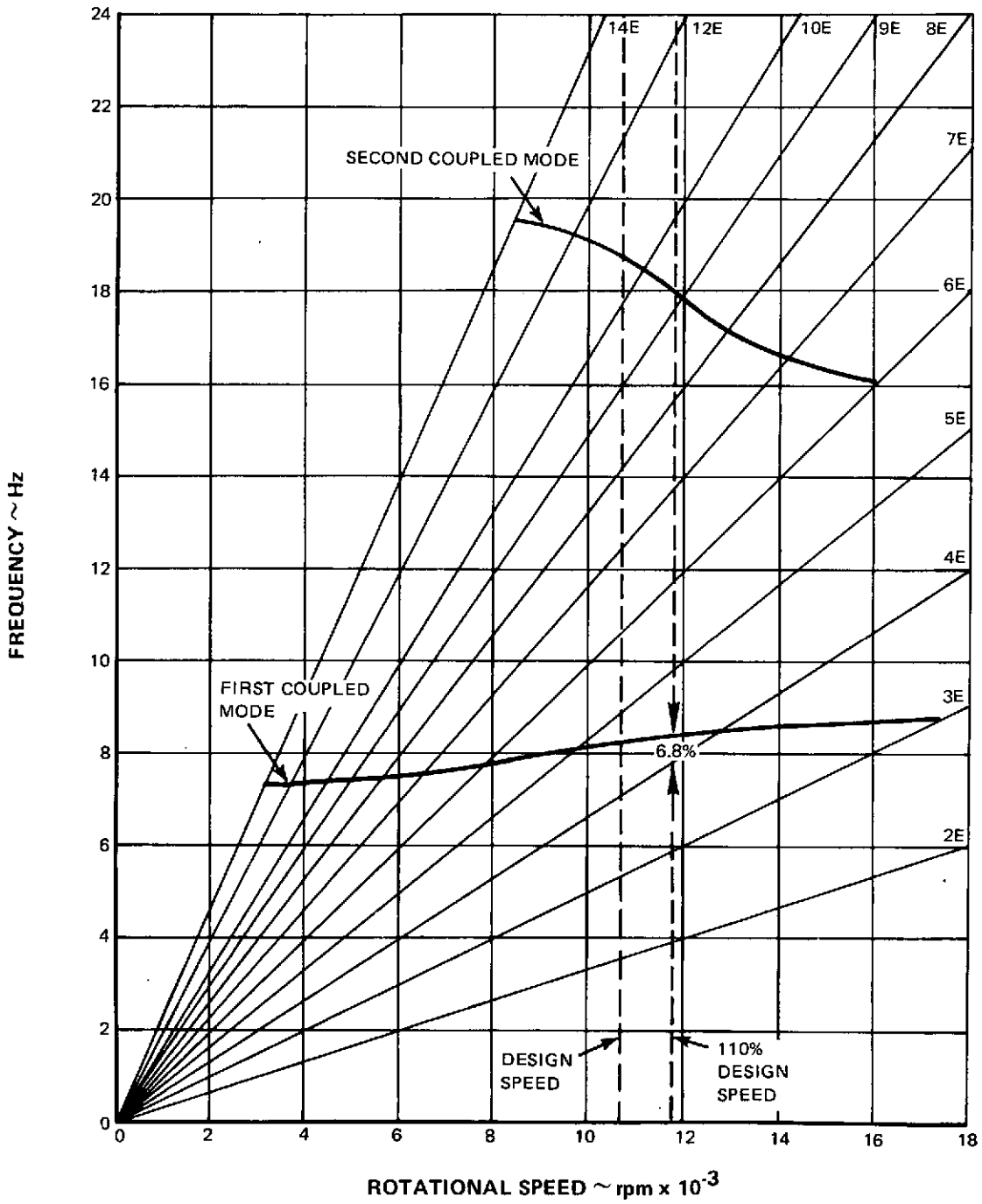
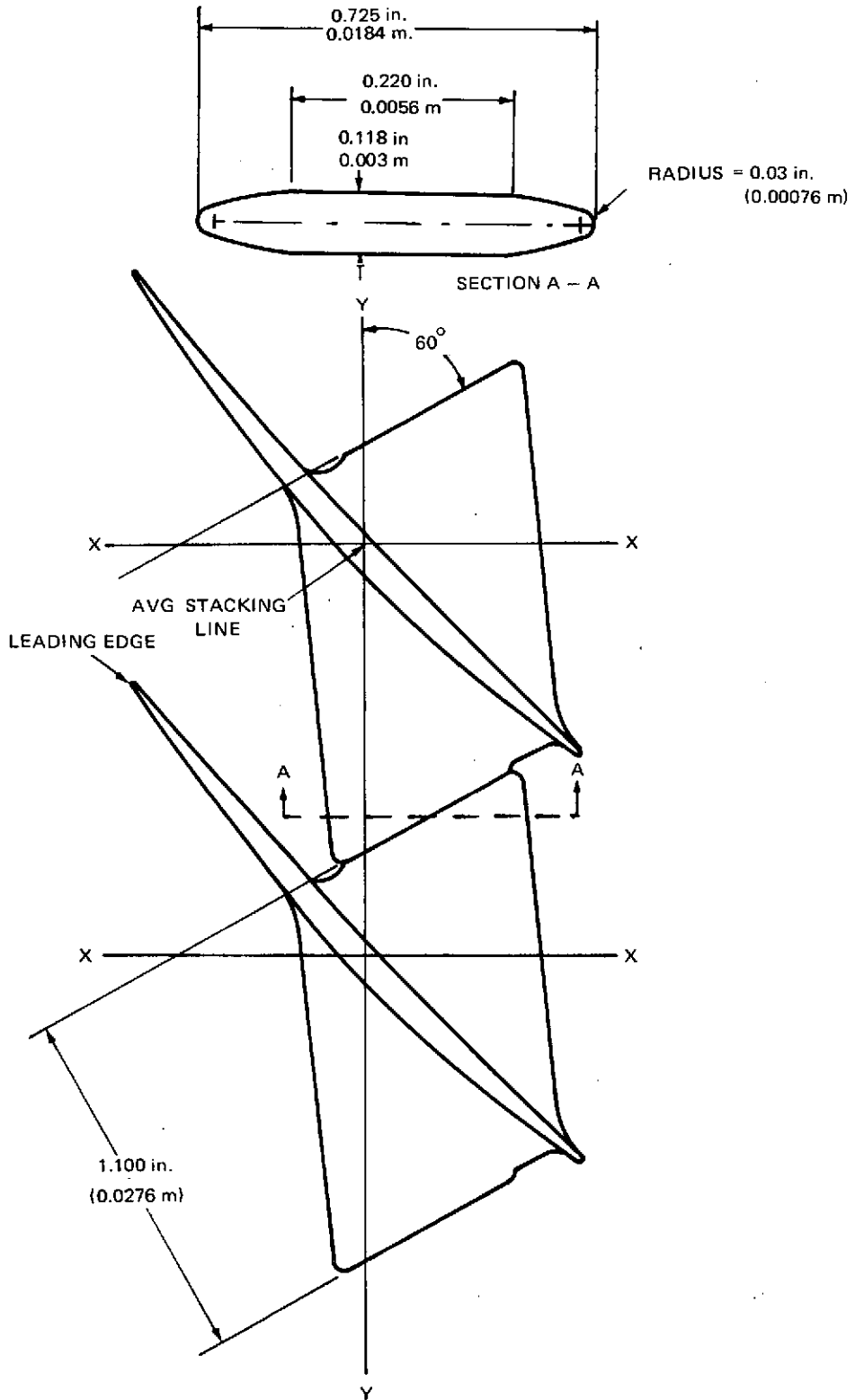


Figure 26 Resonance Diagram for Redesigned Rotor 2



REPRODUCIBILITY OF THE ORIGINAL PAGE IS POOR

Figure 27 Part-Span Shroud – Rotor 2 (Not to Scale)



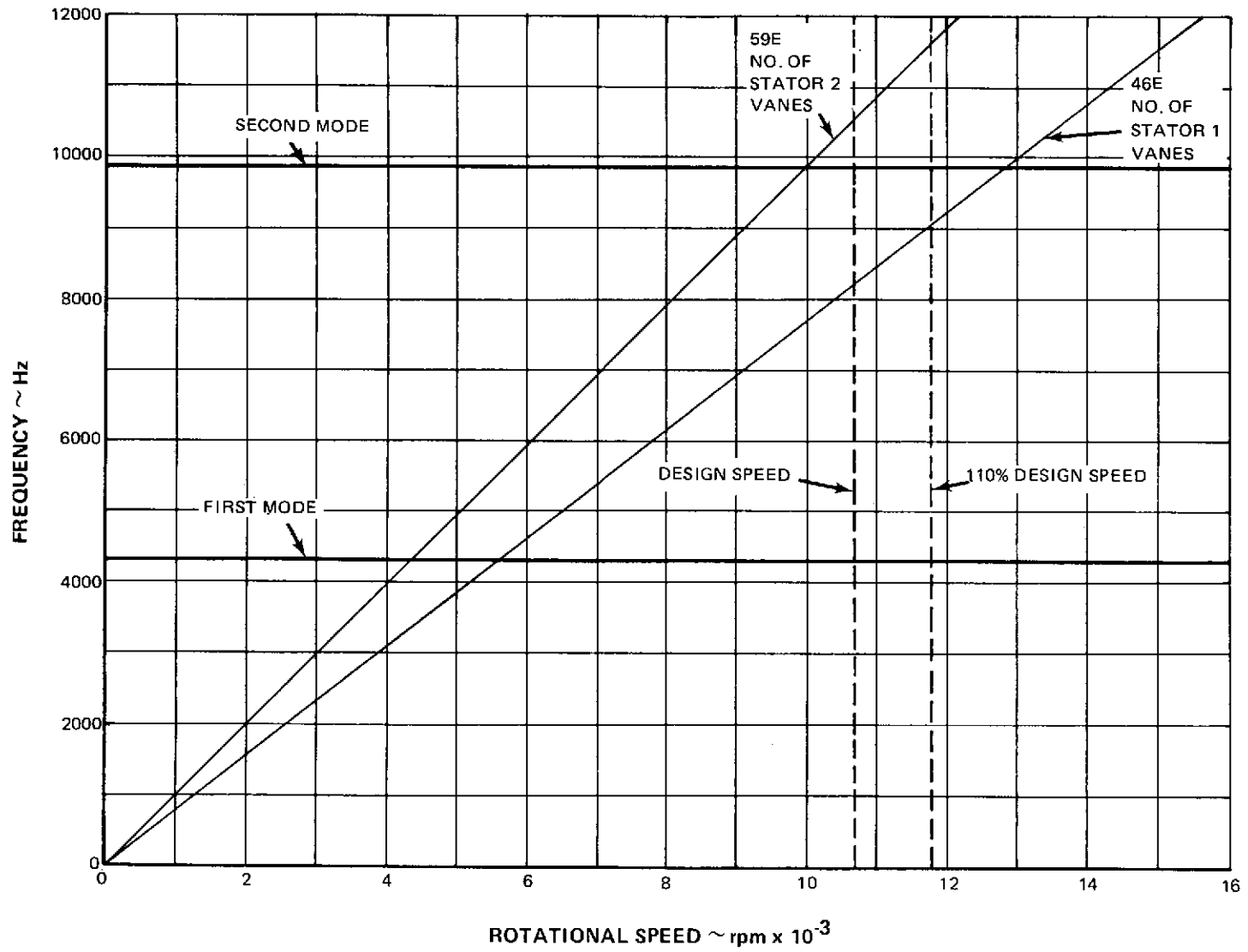
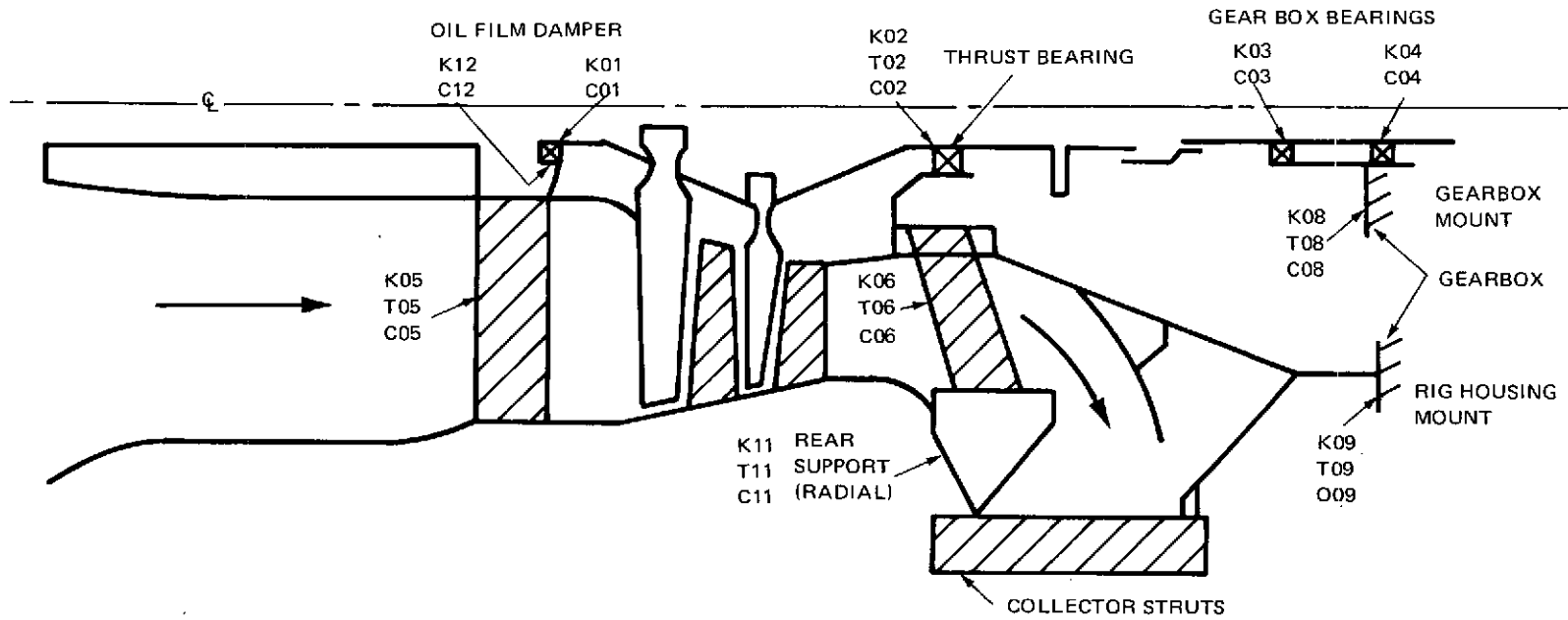


Figure 28 Resonance Diagram for Tip Chordwise Bending Modes of Redesigned Rotor 2



_LINEAR SPRINGS lb/in. X 10 <sup>-8</sup>		N/m X 10 <sup>-10</sup>	TORSIONAL SPRINGS in-lb/deg X 10 <sup>-8</sup>		m-N/rad X 10 <sup>-8</sup>	DAMPER CONSTANTS lb-sec/in.		N-sec/m X 10 <sup>-2</sup>
K01	0.042	0.073	T02	0.005	.032	C01	10	17.5
K02	0.018	0.036	T05	1.500	9.7	C02	10	17.5
K03	0.005	0.009	T06	0.220	1.43	C03	10	17.5
K04	0.010	0.017	T08	10.000	64.8	C04	10	17.5
K05	0.020	0.035	T09	10.000	64.8	C05	100	175
K06	0.190	0.33	T11	12.700	82.3	C06	100	175
K08	1.000	1.75				C08	200	350
K09	1.000	1.75				C09	200	350
K11	0.179	0.314				C11	100	175

Figure 29 Spring-Mass Model for Critical Speed Analysis of Two-Stage Fan Rig

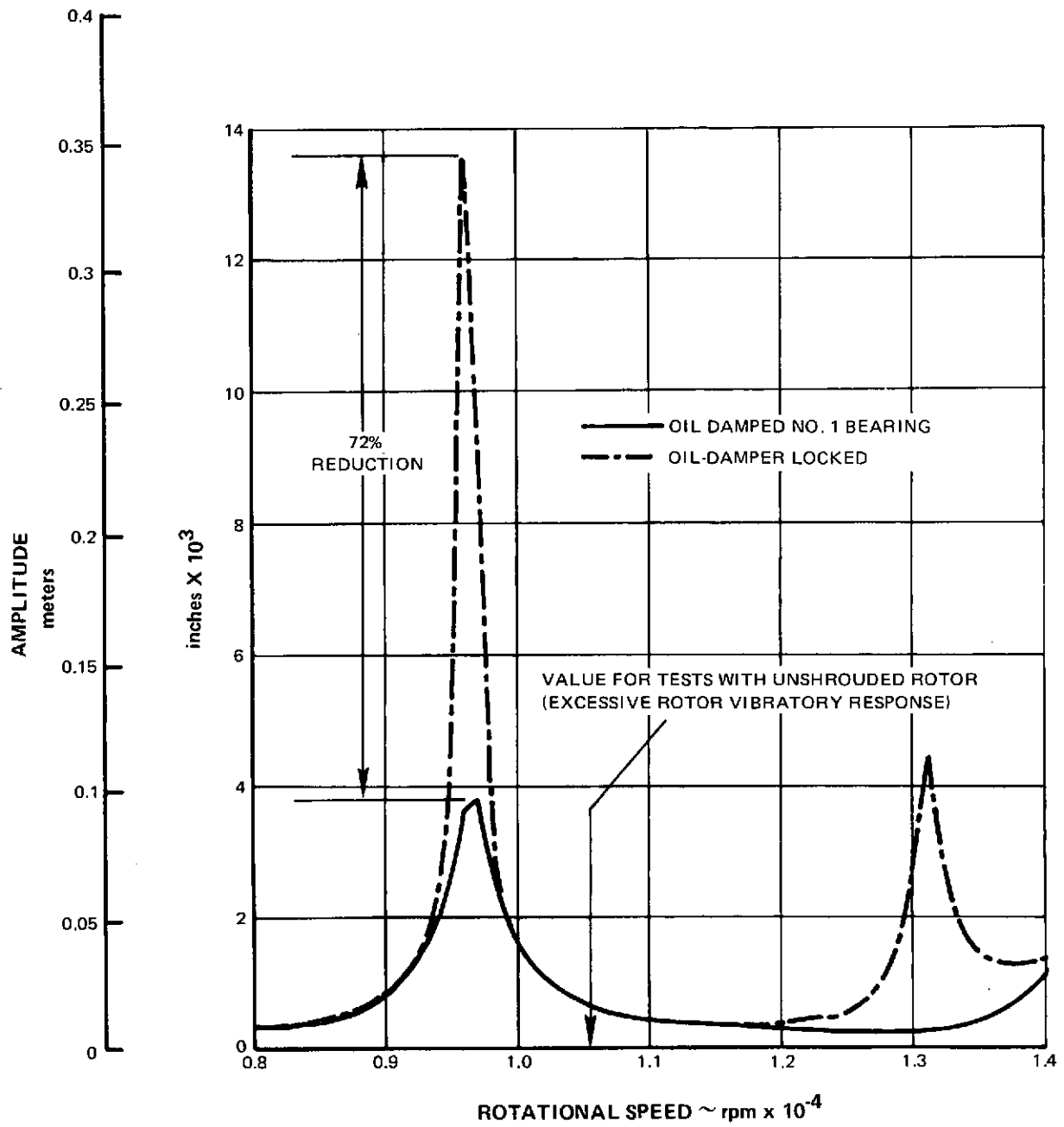


Figure 30 Vibrational Amplitude at No. 1 Bearing Showing Benefit of Oil-Damped Bearing

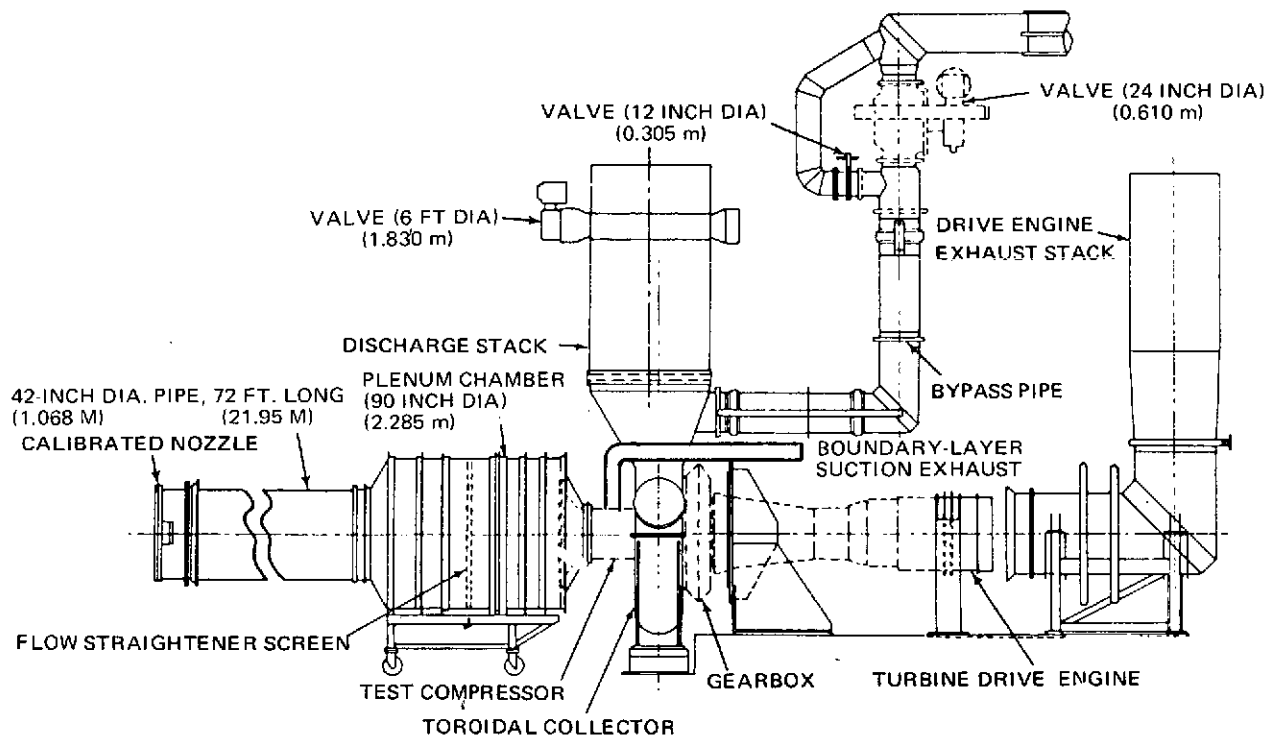
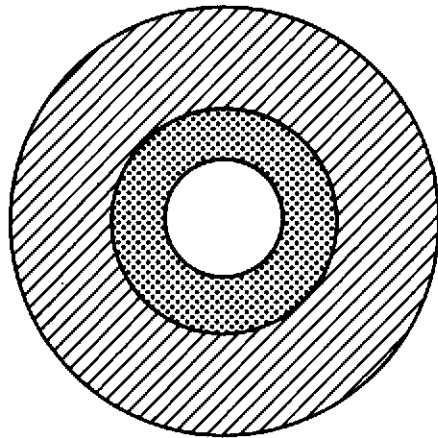


Figure 31 Schematic of Compressor Test Facility

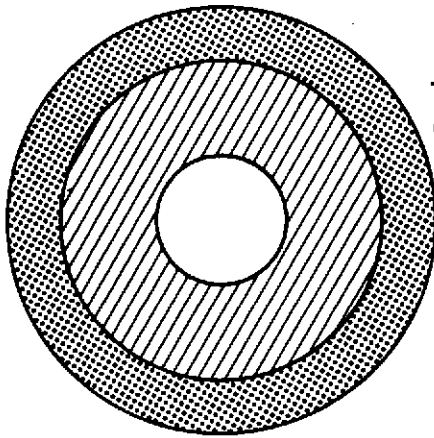
REPRODUCIBILITY OF THE ORIGINAL PAGE IS POOR



**HUB RADIAL SCREEN**  
(31.1% OF ANNULAR AREA COVERED)

CONSISTING OF:

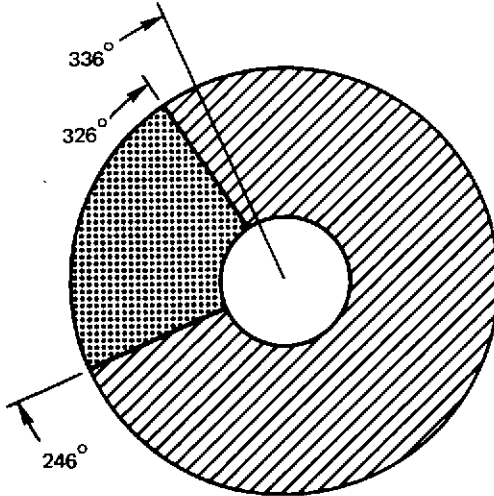
- BASE SCREEN 1 X 1 X 0.125 IN. (0.0254 X 0.0254 X 0.0032 m)
- 1 SCREEN 0.5 X 0.5 X 0.062 IN. (0.0127 X 0.0127 X 0.0016 m)
- 1 SCREEN 0.25 X 0.25 X 0.062 IN. (0.0064 X 0.0064 X 0.0016 m)
- 4 SCREENS 0.0625 X 0.0625 X 0.017 IN. (0.0016 X 0.0016 X 0.0004 m)



**TIP RADIAL SCREEN**  
(39.8% OF ANNULAR AREA COVERED)

CONSISTING OF:

- BASE SCREEN 1 X 1 X 0.125 IN. (0.0254 X 0.0254 X 0.0032 m)
- 1 SCREEN 0.5 X 0.5 X 0.062 IN. (0.0127 X 0.0127 X 0.0016 m)
- 1 SCREEN 0.25 X 0.25 X 0.062 IN. (0.0064 X 0.0064 X 0.0016 m)
- 2 SCREENS 0.0625 X 0.0625 X 0.017 IN. (0.0016 X 0.0016 X 0.0004 m)

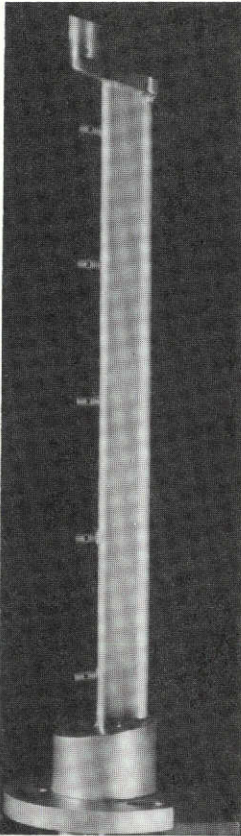


**CIRCUMFERENTIAL SCREEN**  
(22.9% OF ANNULUS AREA COVERED)

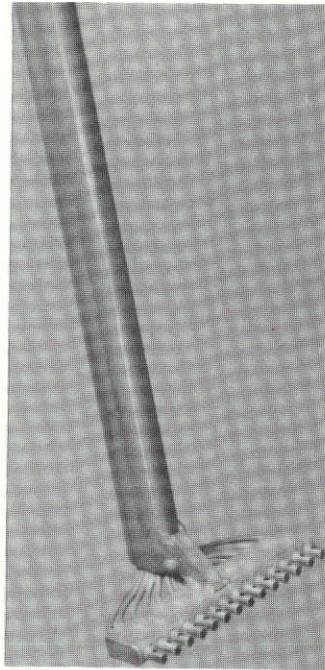
CONSISTING OF:

- BASE SCREEN 1 X 1 X 0.125 IN. (0.0254 X 0.0254 X 0.0032 m)
- 1 SCREEN 0.5 X 0.5 X 0.062 IN. (0.0127 X 0.0127 X 0.0016 m)
- 1 SCREEN 0.25 X 0.25 X 0.062 IN. (0.0064 X 0.0064 X 0.0016 m)
- 4 SCREENS 0.0625 X 0.0625 X 0.017 IN. (0.0016 X 0.0016 X 0.0004 m)
- 2 SCREENS 0.0625 X 0.0625 X 0.017 IN. (0.0016 X 0.0016 X 0.0004 m)  
(COVERING 0-20% SPAN)

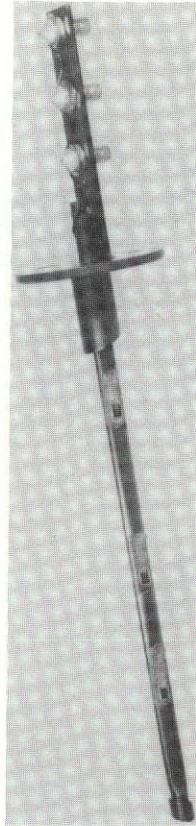
Figure 32 Sketch of Distortion Screens



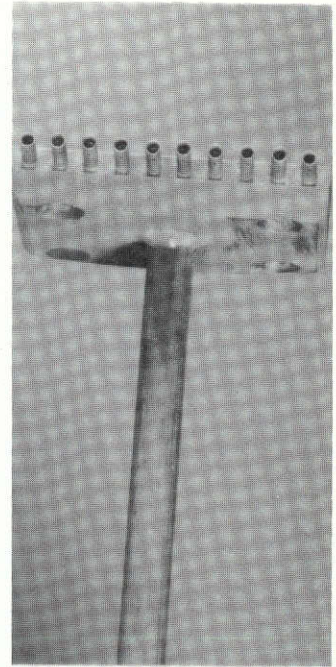
A. Fan Inlet  
Total Pressure  
Rake Probe



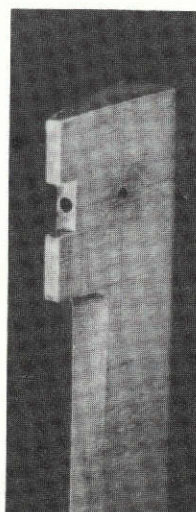
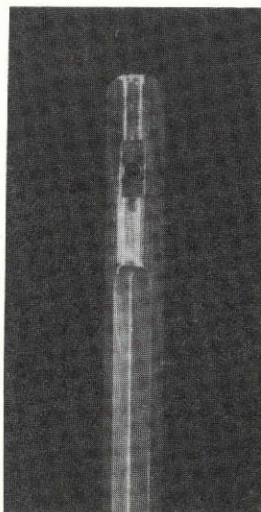
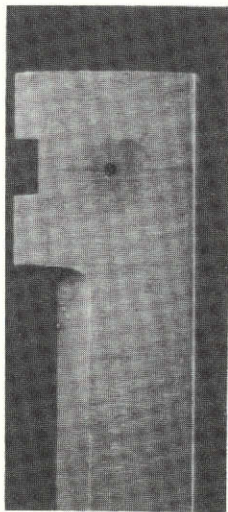
B. Stator 2 Exit Total Pressure  
Wake Probe



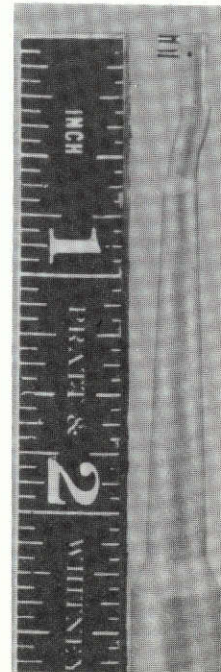
C. Fan Inlet  
Hot Film  
Probe



D. Stator 2 Exit Total Tempera-  
ture Wake Rake



E. Fan Inlet & Static Exit Traverse Wedge Probes



F. Stator 1 Exit  
NASA Combination Probe

REPRODUCIBILITY OF THE  
ORIGINAL PAGE IS POOR.

Figure 33 Photographs of Typical Instrumentation

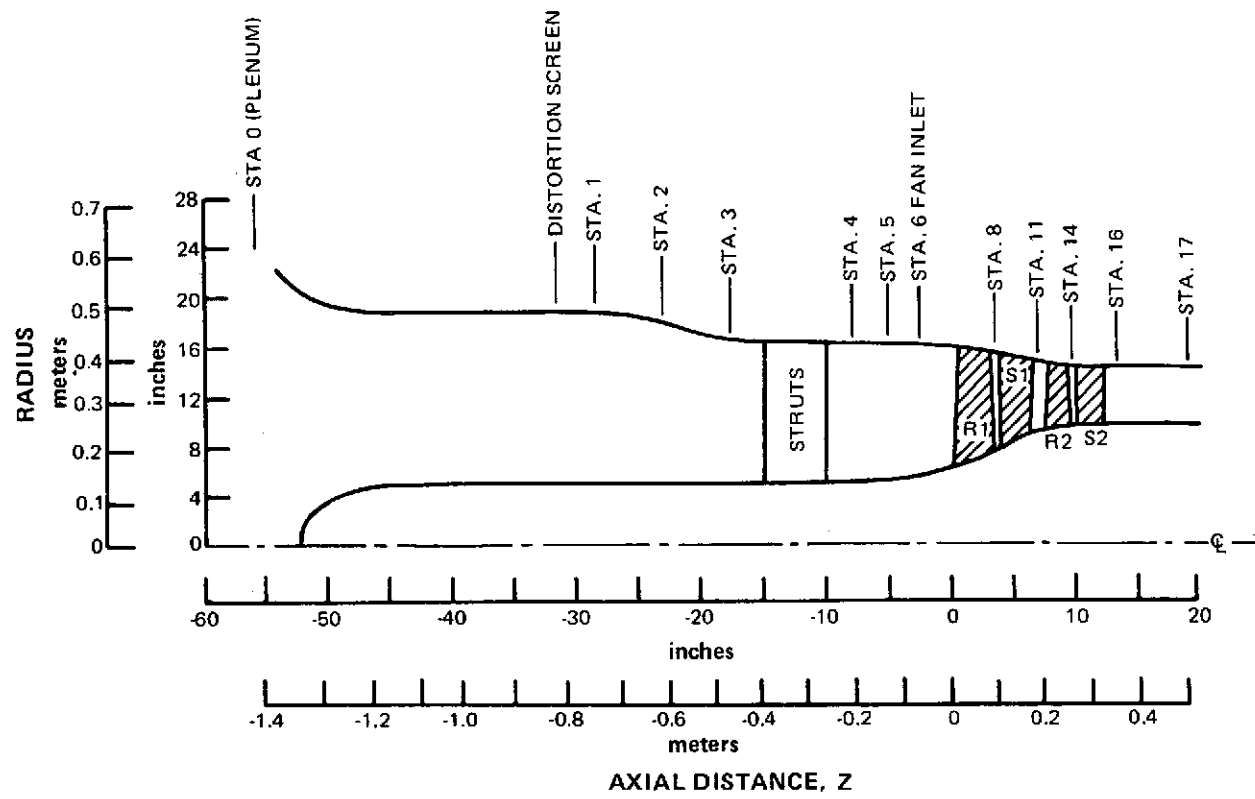


Figure 34 Axial Locations of Instrumentation

VIEW LOOKING DOWNSTREAM

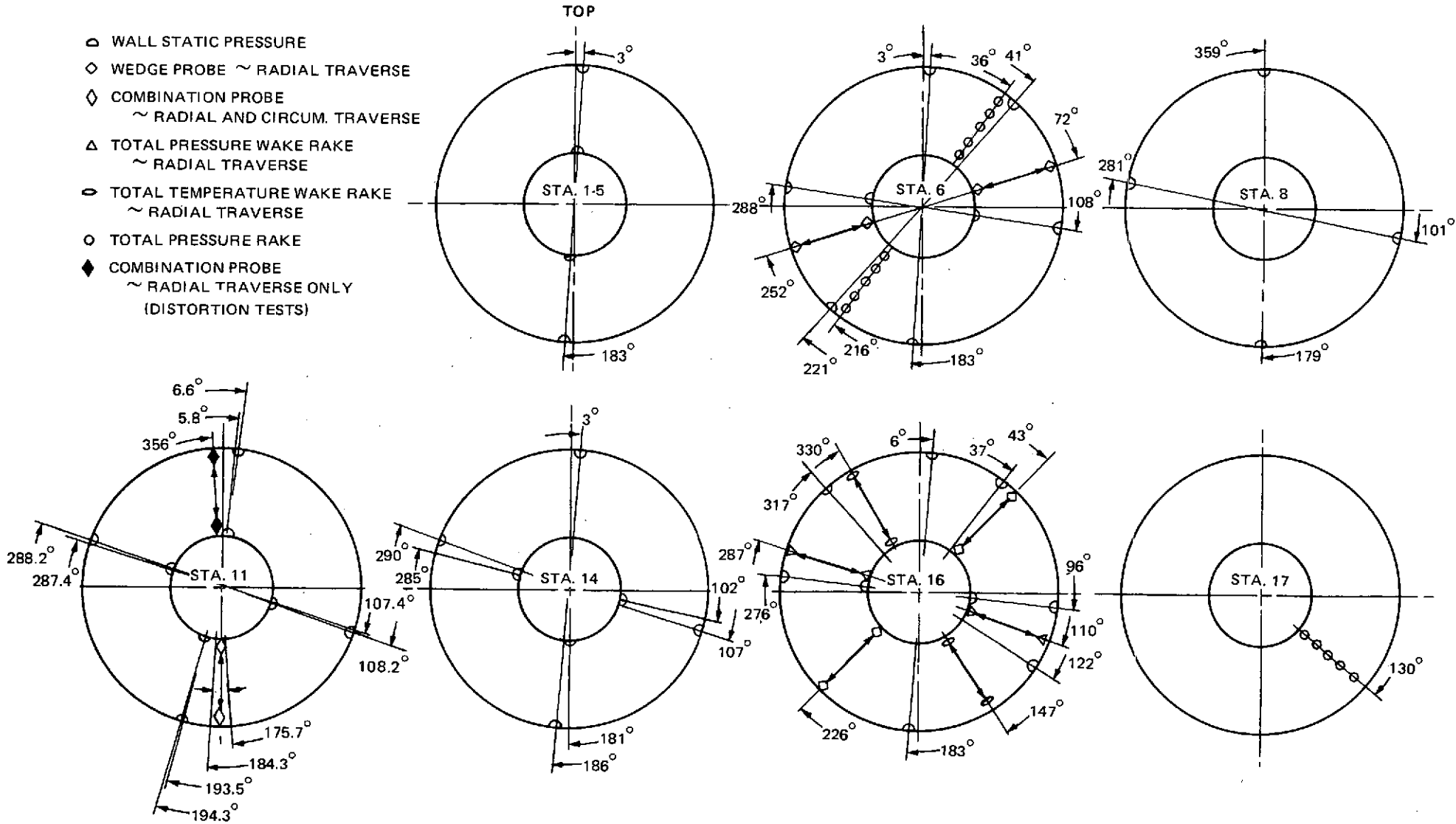


Figure 35 Circumferential Locations of Instrumentation



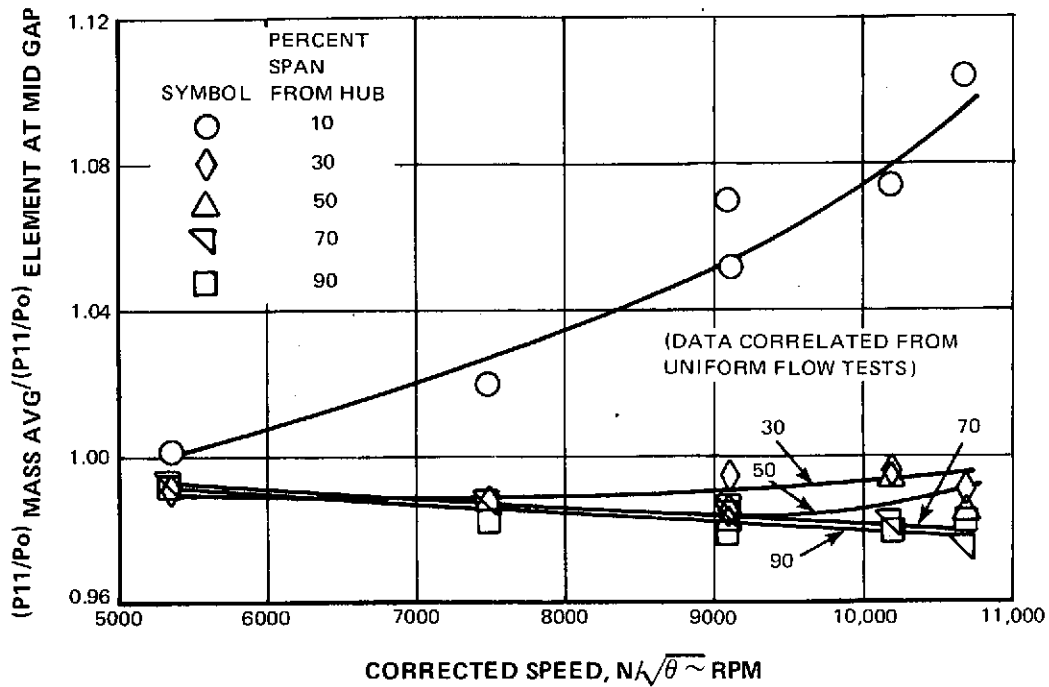


Figure 36 First Stage Pressure Correlation Used for Radial Distortion Streamline Analysis Flowfield Calculation

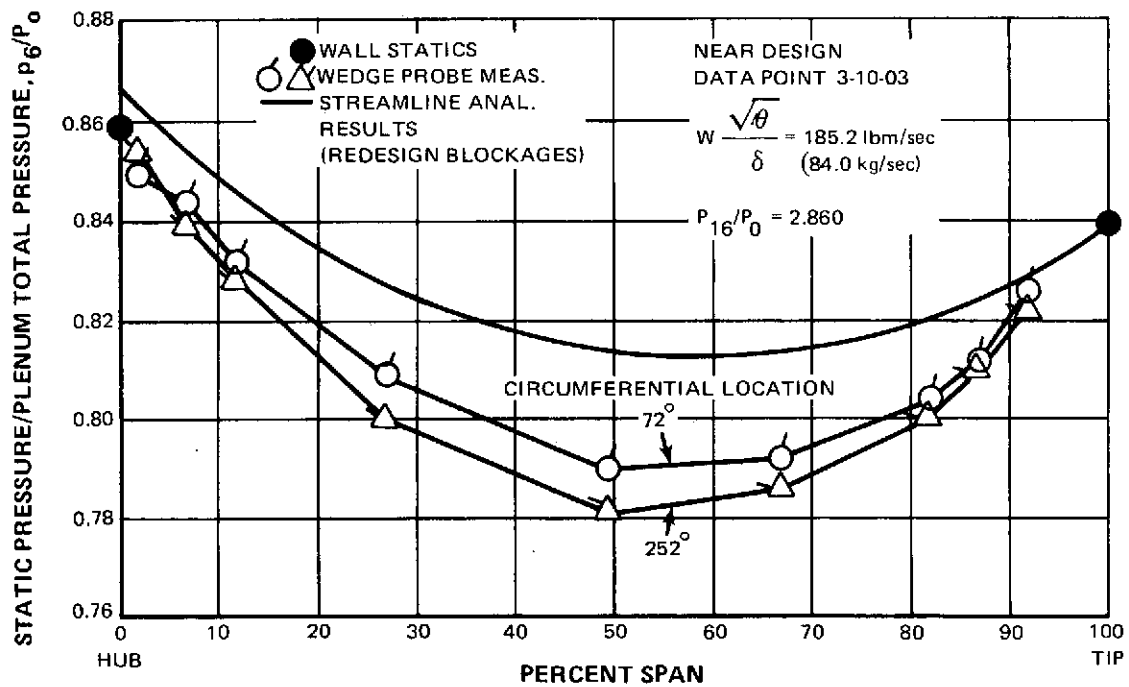


Figure 37 Comparison of Measured and Calculated Static Pressure Versus Span at Rotor 1 Inlet

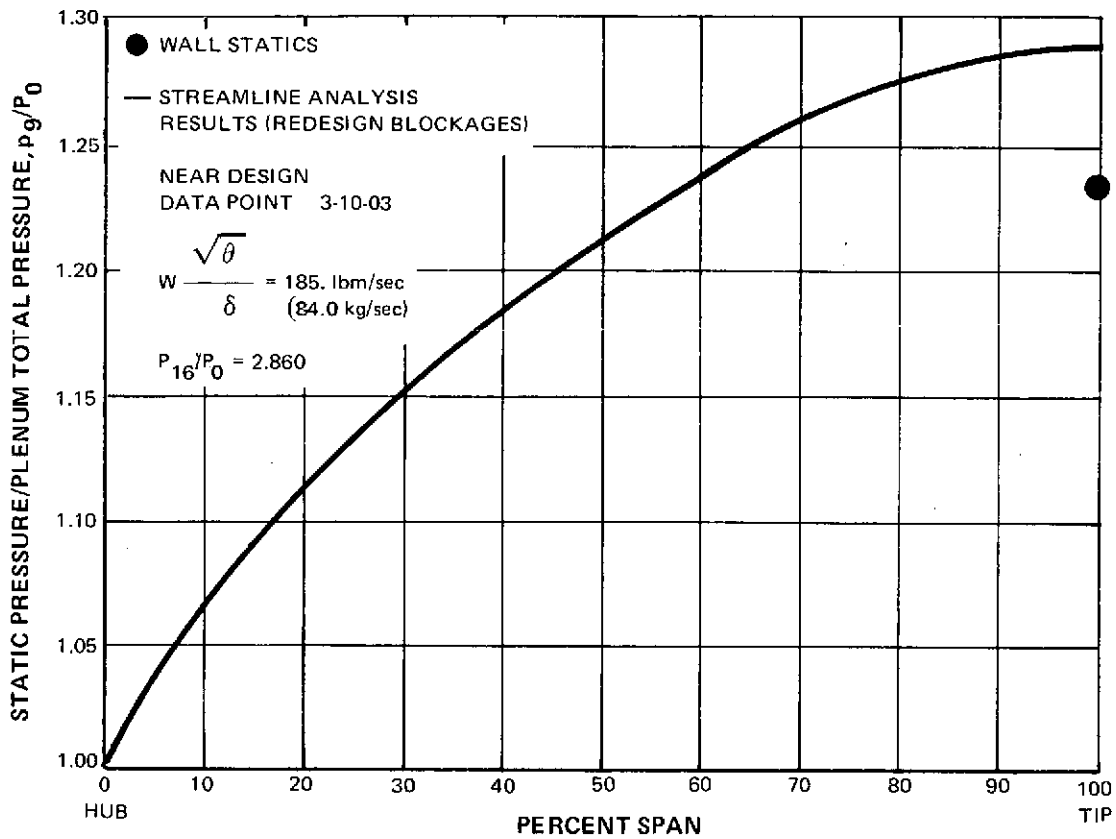


Figure 38 Calculated Static Pressure Versus Span at Stator 1 Inlet and Measured Static at Outer Wall

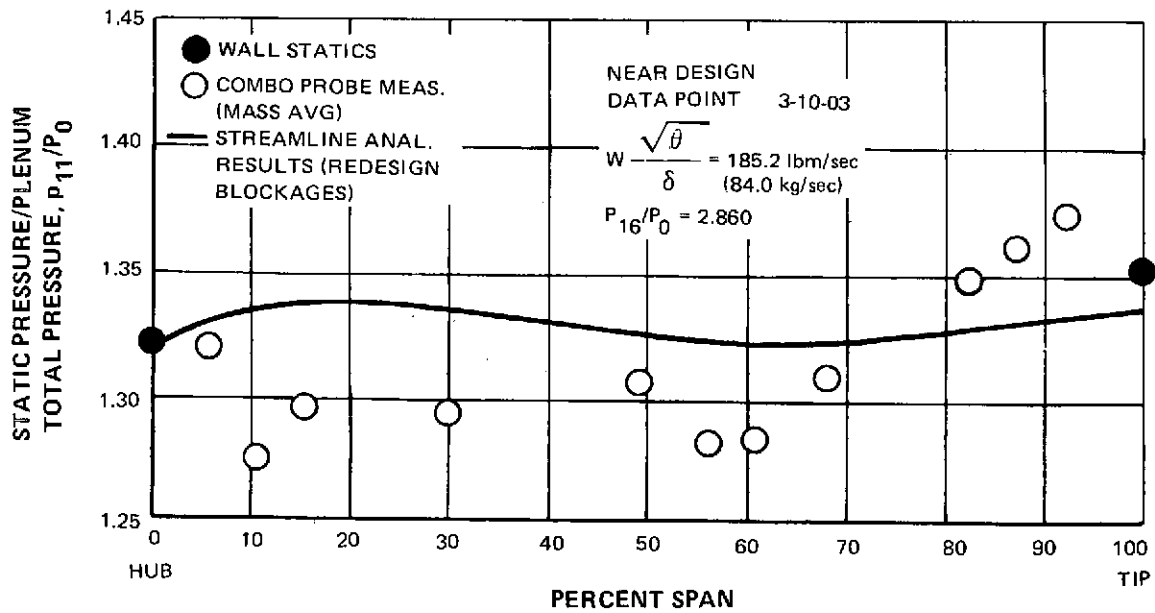


Figure 39 Measured and Calculated Static Pressure Versus Span at Stator 1 Exit

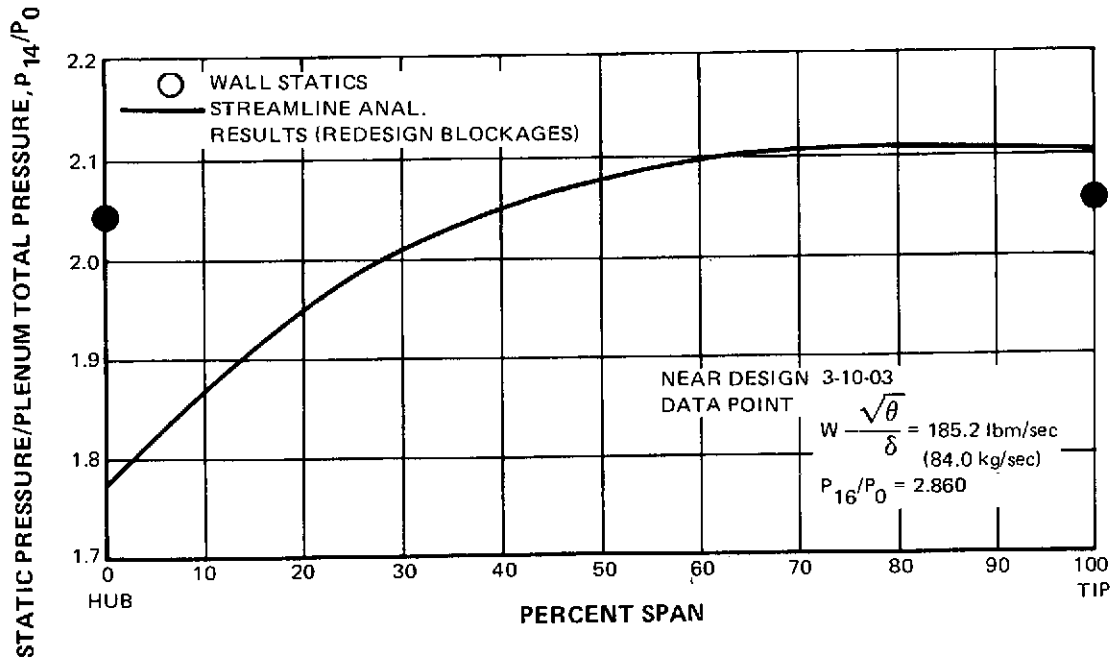


Figure 40 Calculated Static Pressure Versus Span at Stator 2 Inlet and Measured Wall Static Pressures

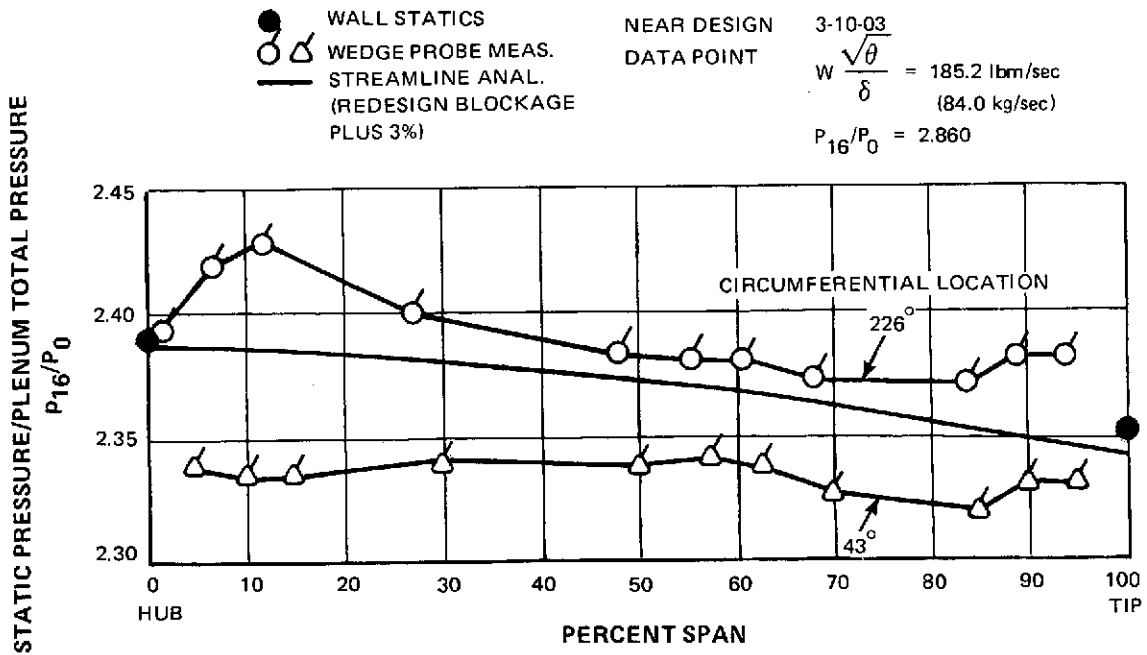


Figure 41 Measured and Calculated Static Pressure Versus Span at Stator 2 Exit

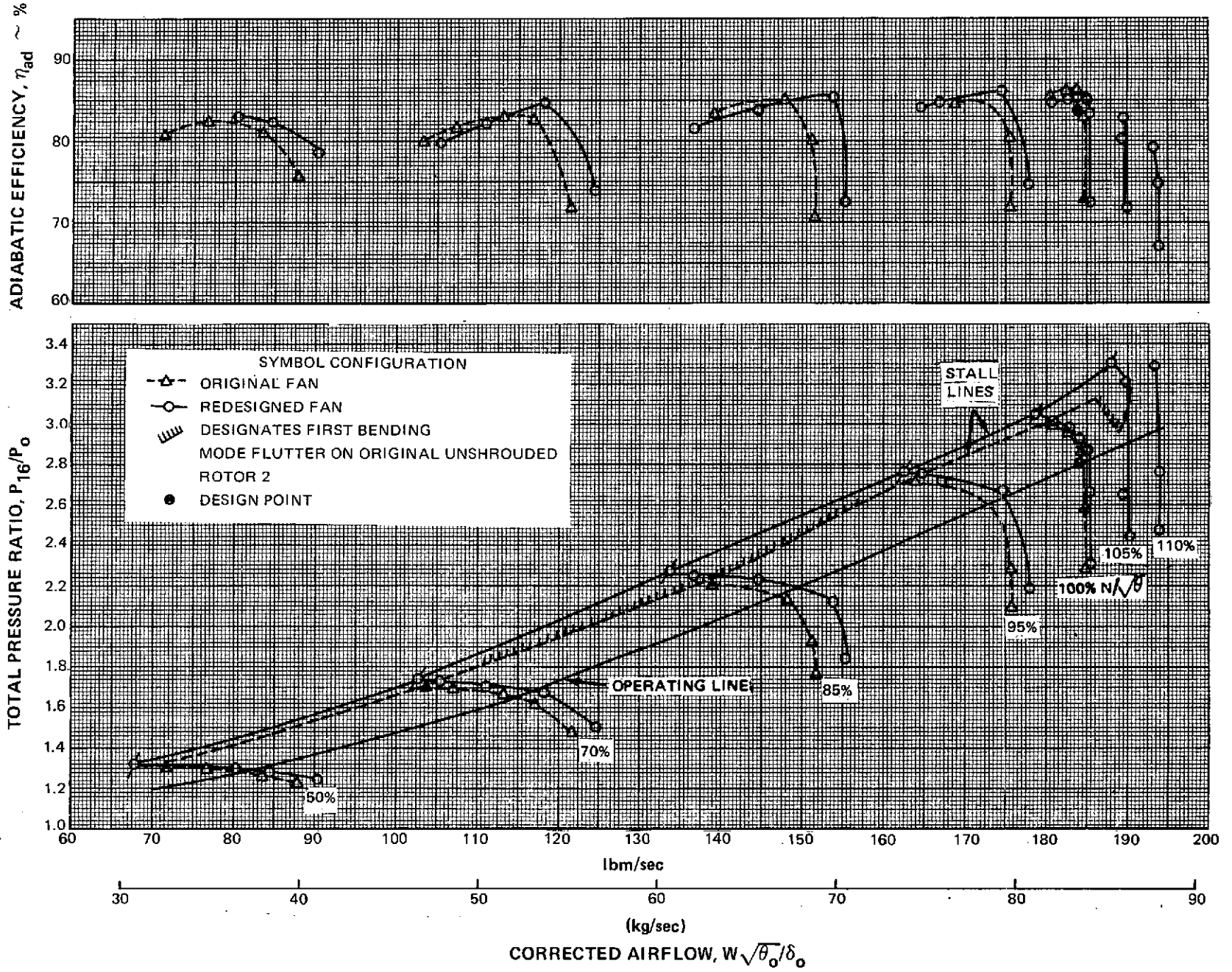


Figure 42 Fan Overall Performance with Uniform Inlet Flow

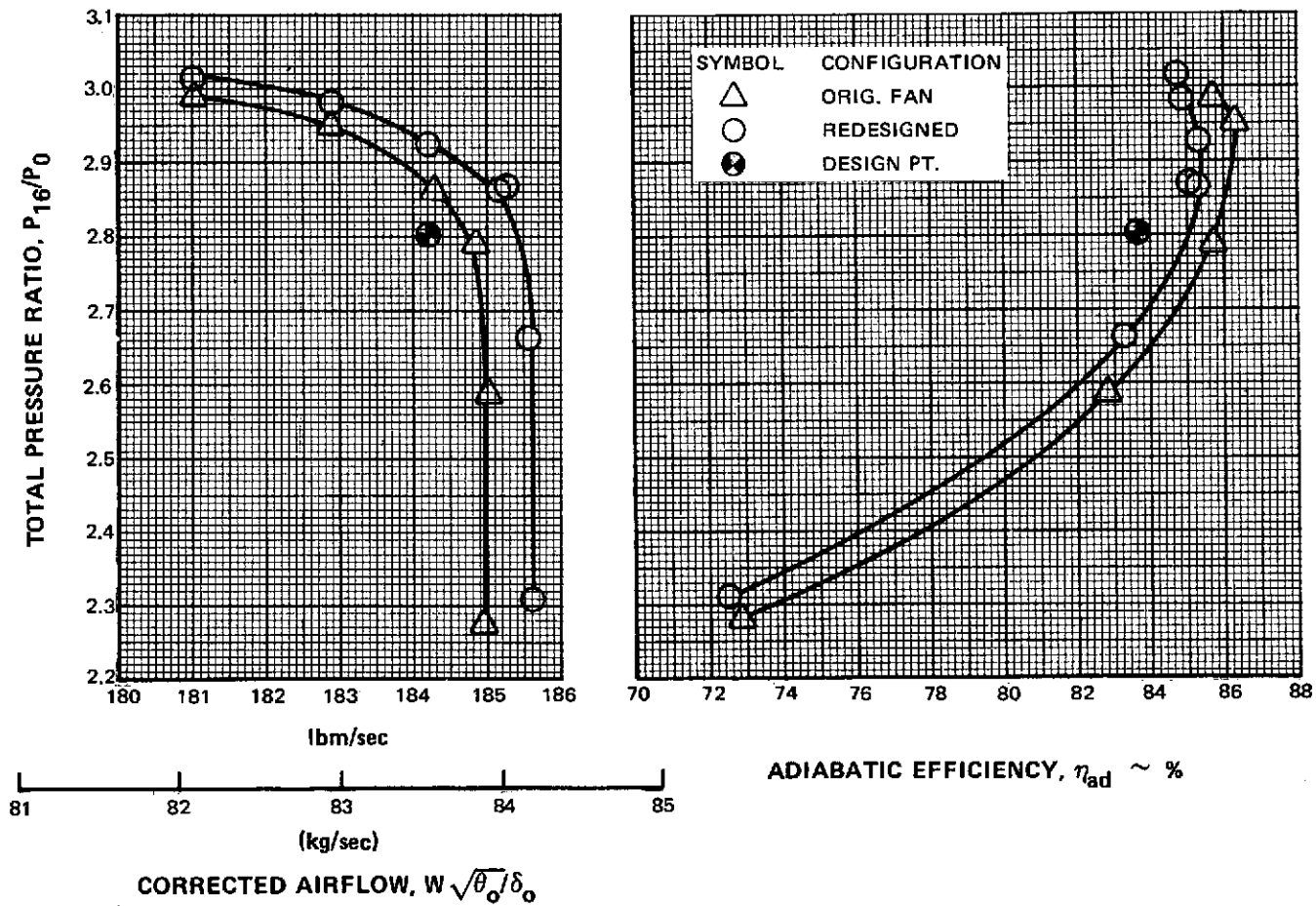


Figure 43 Fan Overall Performance at Design Speed with Uniform Inlet Flow

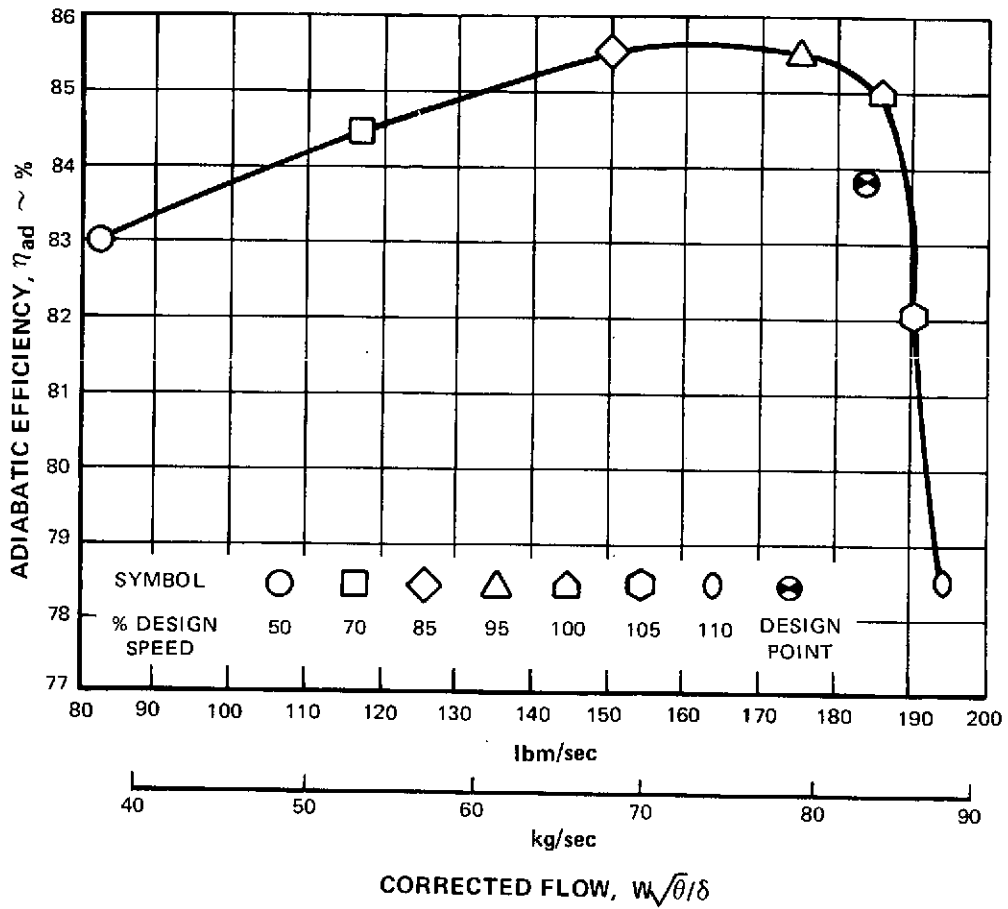


Figure 44 Operating Line Efficiency Versus Corrected Flow

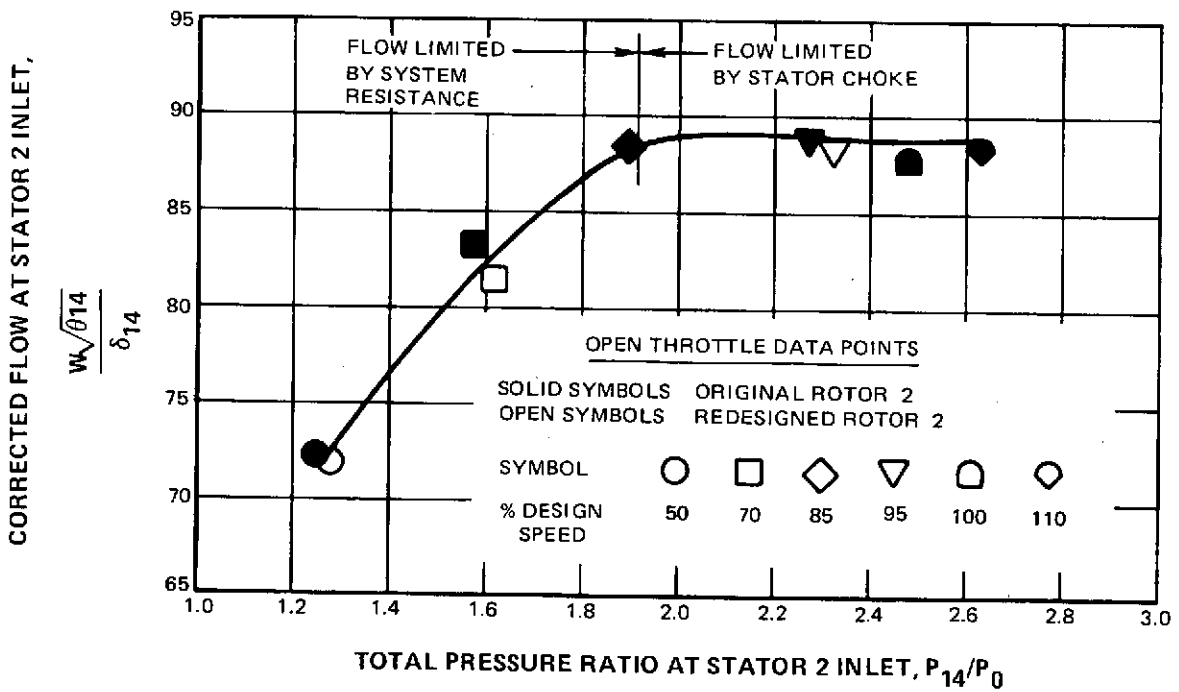


Figure 45 Maximum Corrected Flow at Stator 2 Inlet Versus Pressure Ratio at Stator 2 Inlet

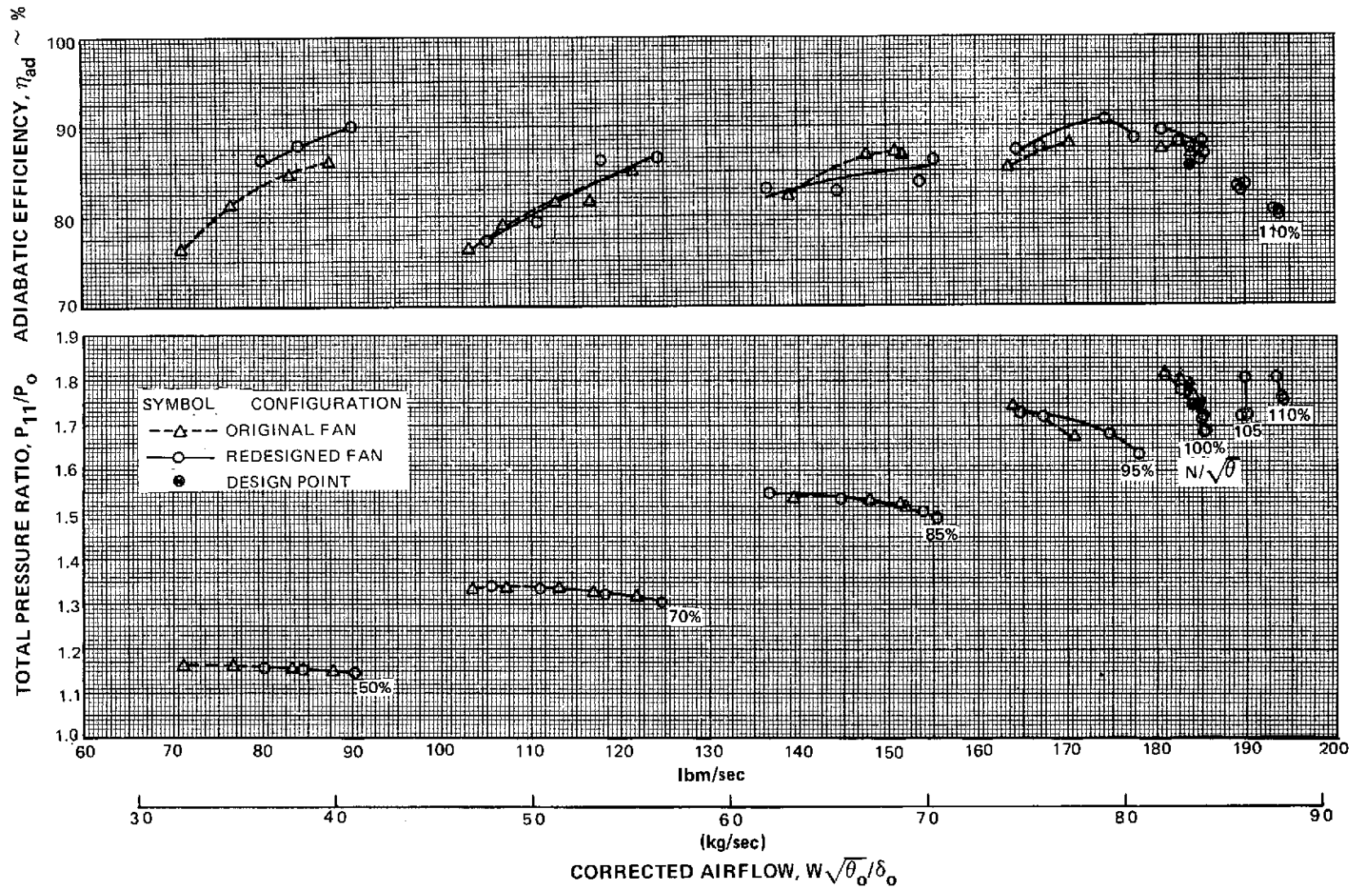


Figure 46 First Stage Performance With Uniform Inlet Flow

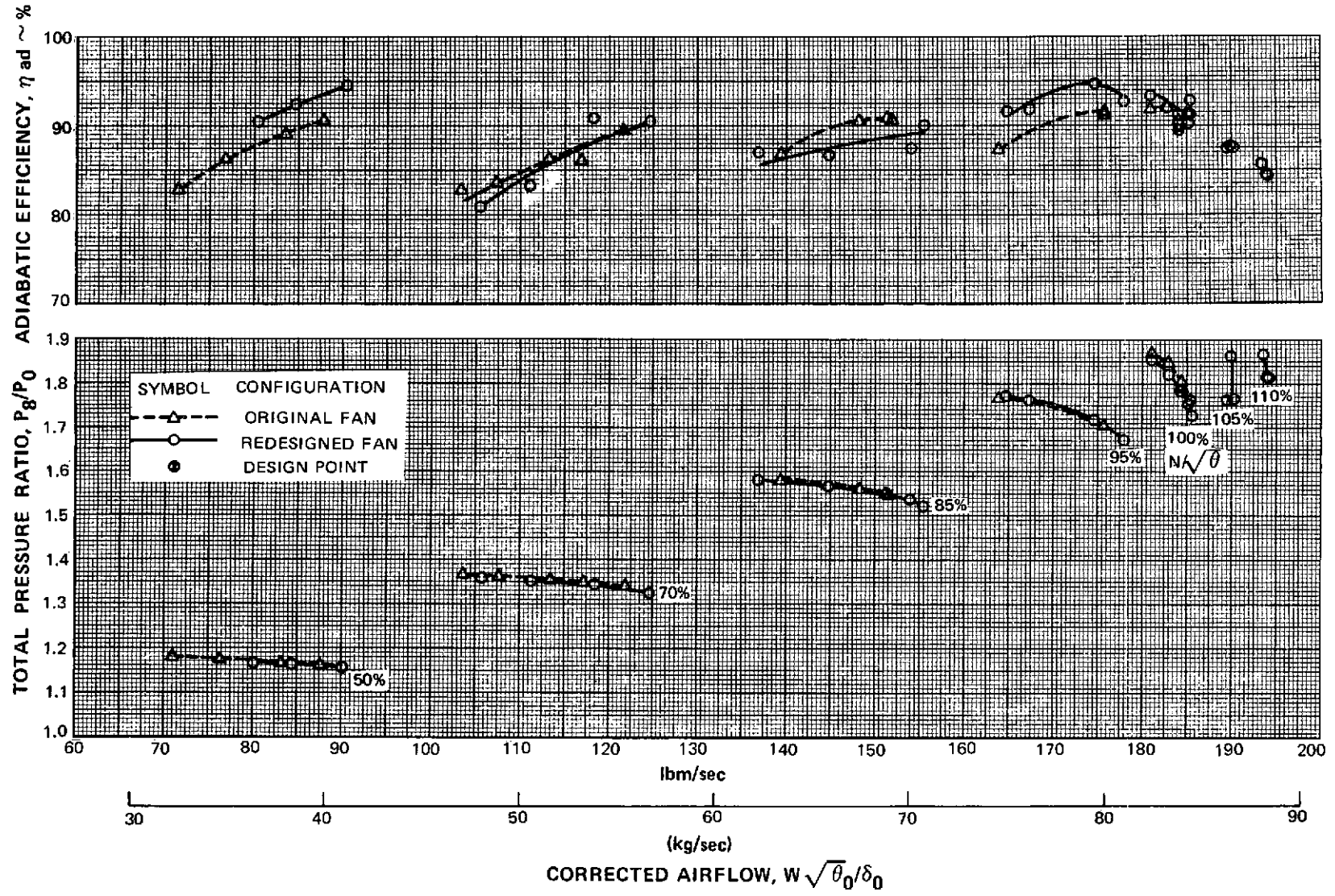


Figure 47 First Rotor Performance With Uniform Inlet Flow



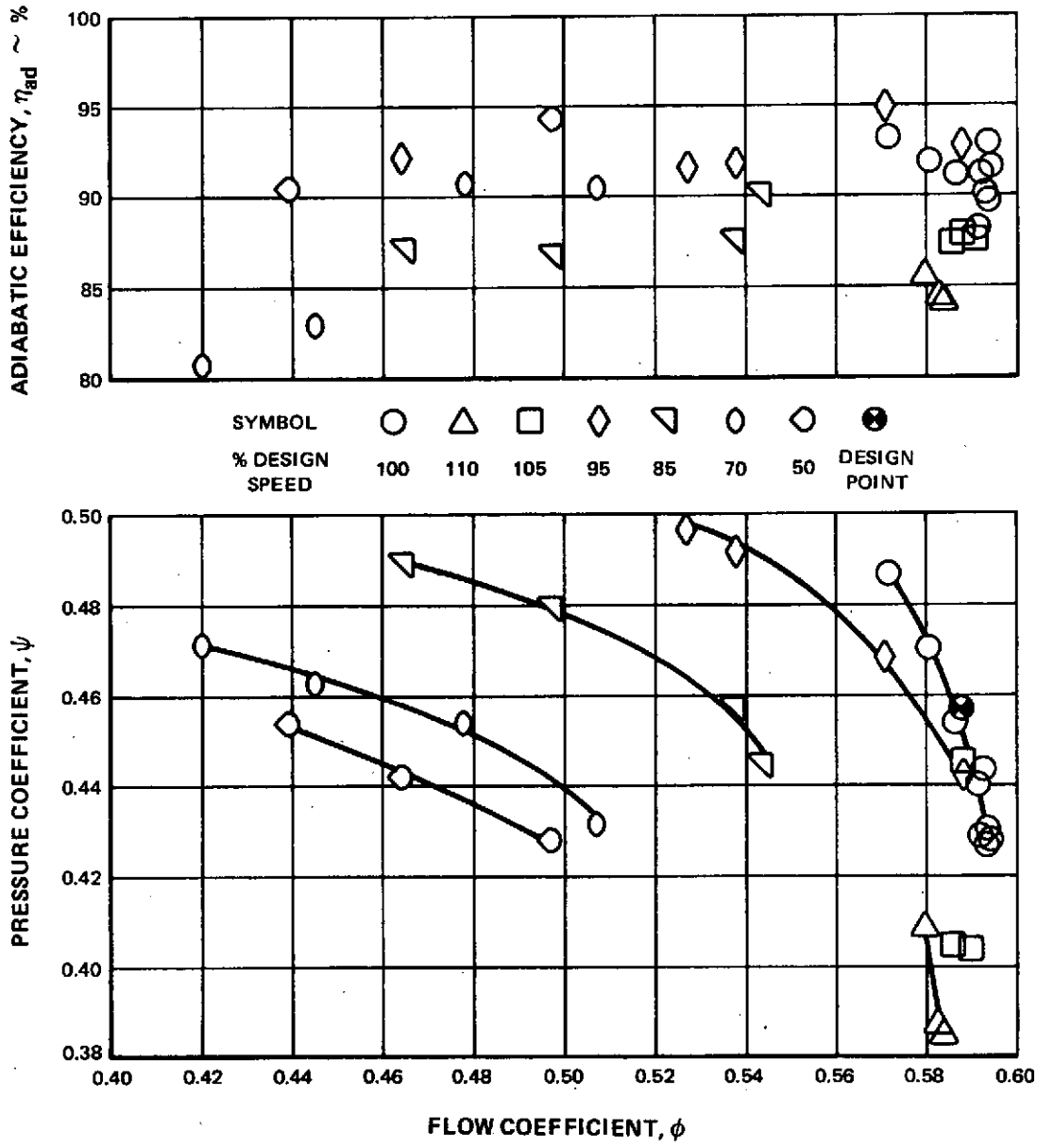


Figure 48 Pressure Coefficient and Adiabatic Efficiency Versus Flow Coefficient For Uniform Inlet Flow Rotor 1

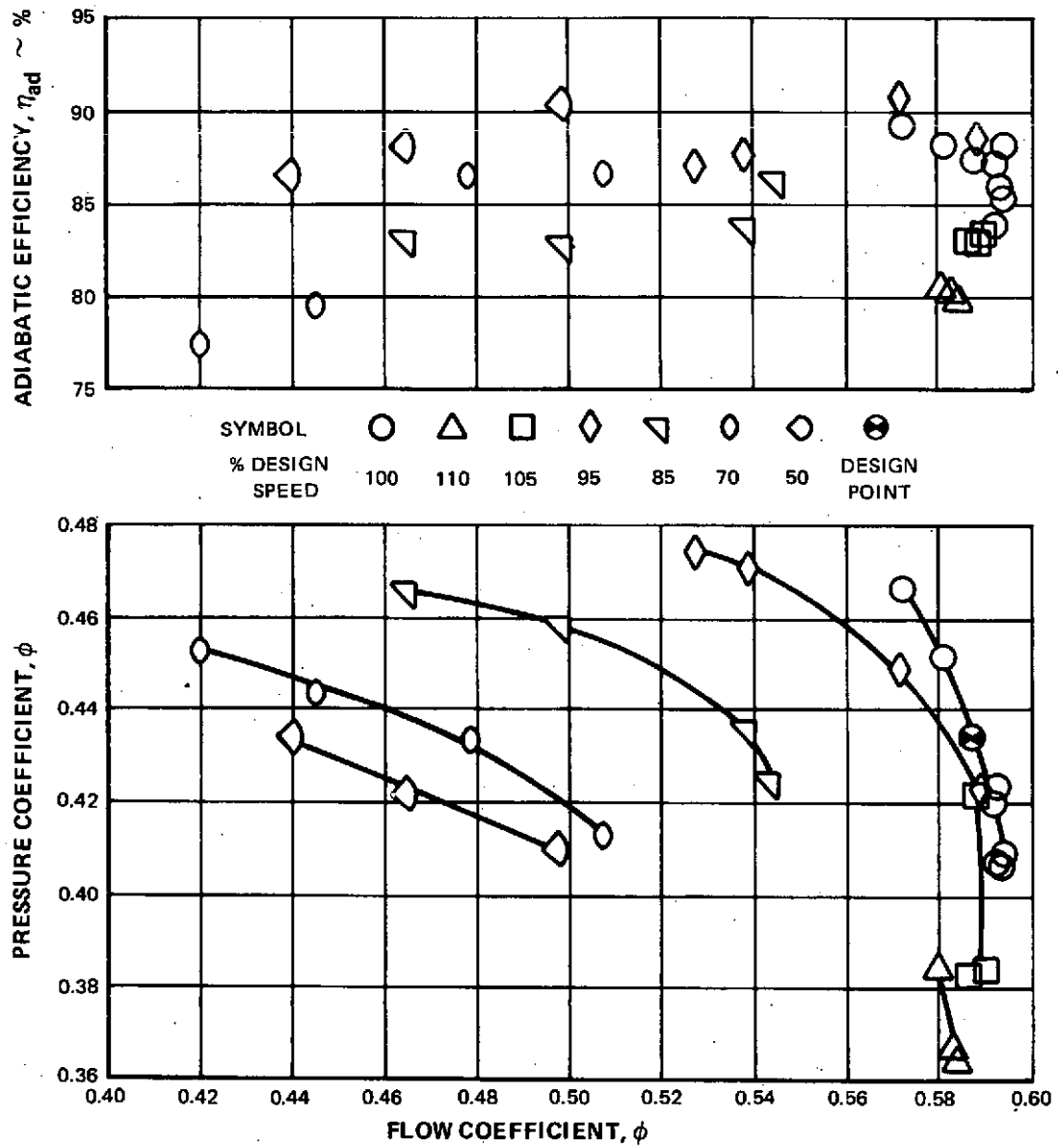


Figure 49 Pressure Coefficient and Adiabatic Efficiency Versus Flow Coefficient For Uniform Inlet Flow Stage 1

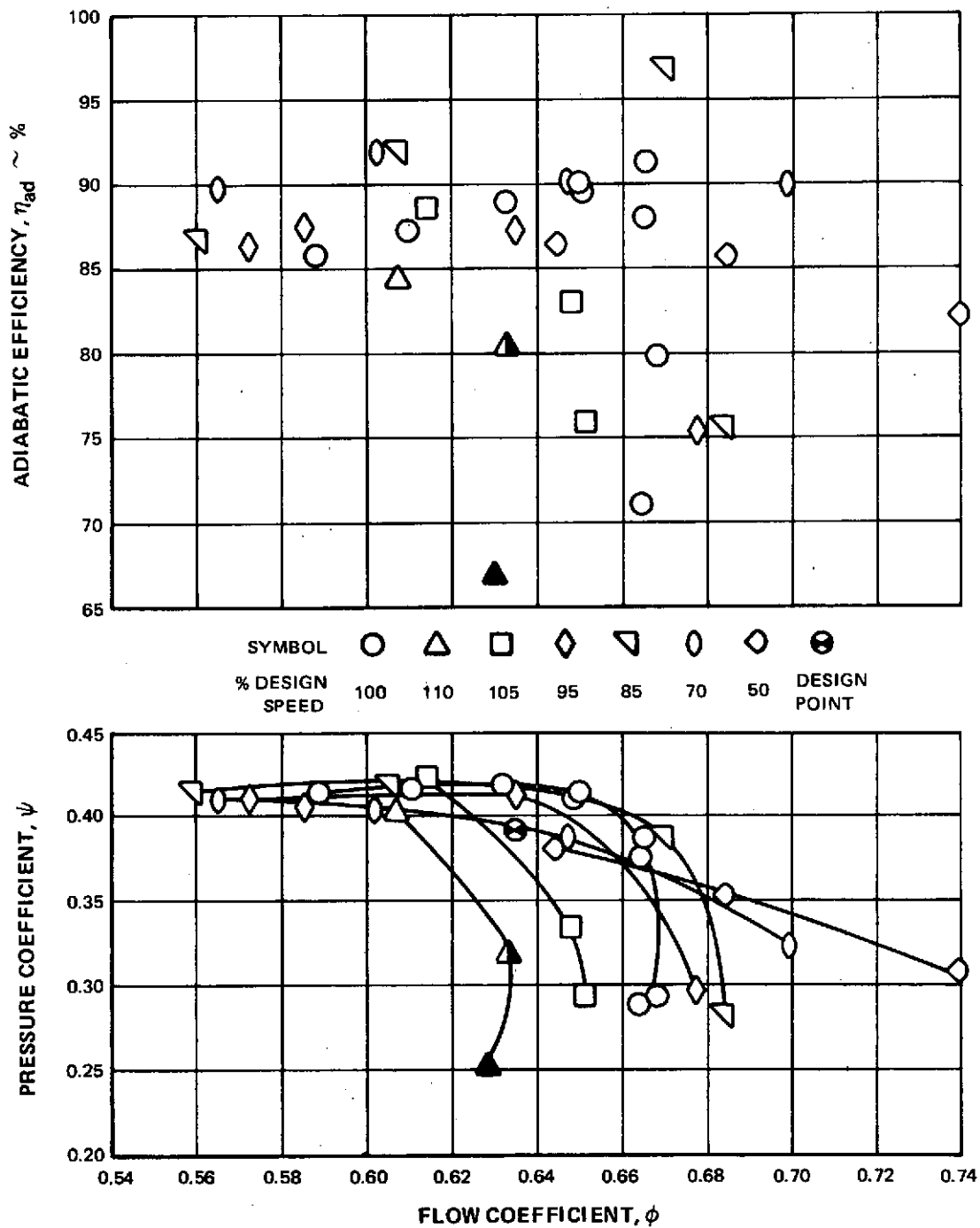


Figure 50 Pressure Coefficient and Adiabatic Efficiency Versus Flow Coefficient for Uniform Inlet Flow, Rotor 2

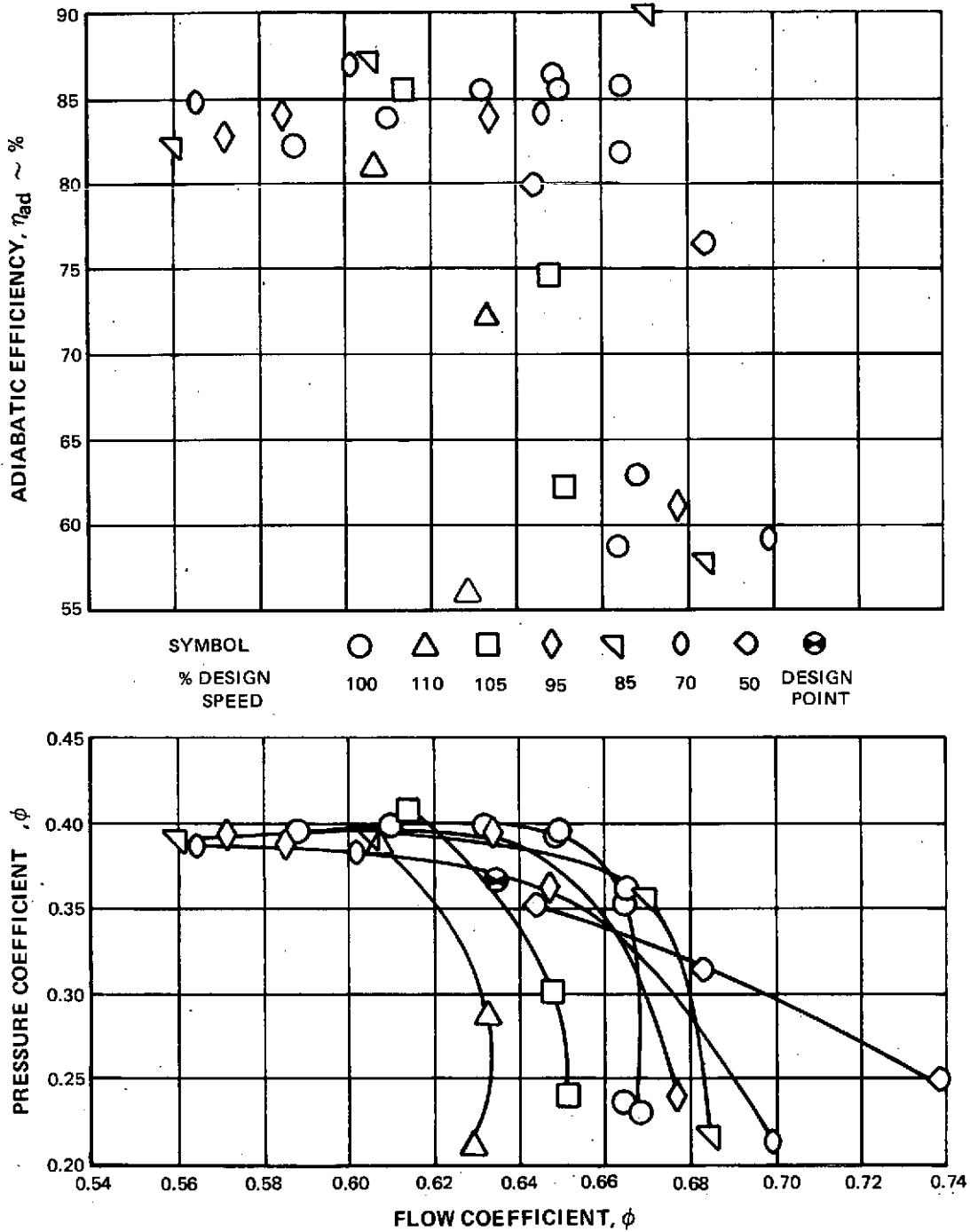


Figure 51 Pressure Coefficient and Adiabatic Efficiency Versus Flow Coefficient for Uniform Inlet Flow, Stage 2

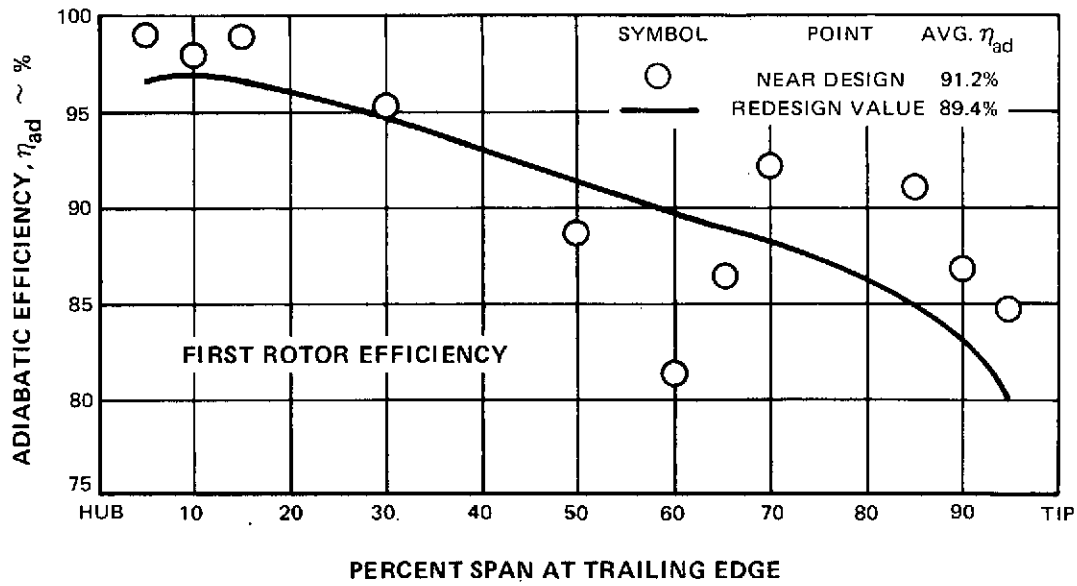
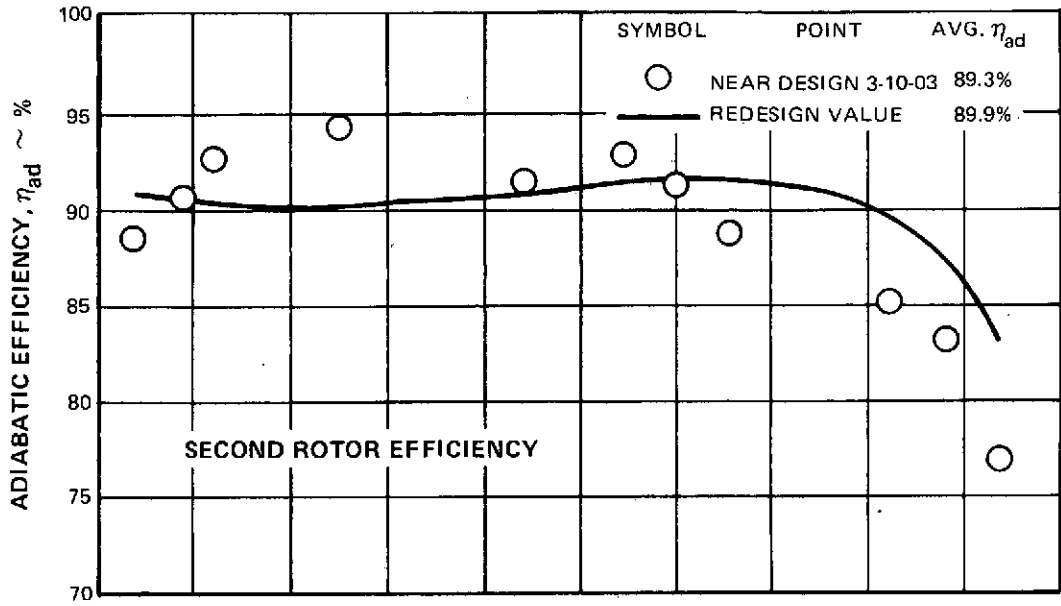


Figure 52 Rotor Adiabatic Efficiency Versus Span for Near Design Data Point

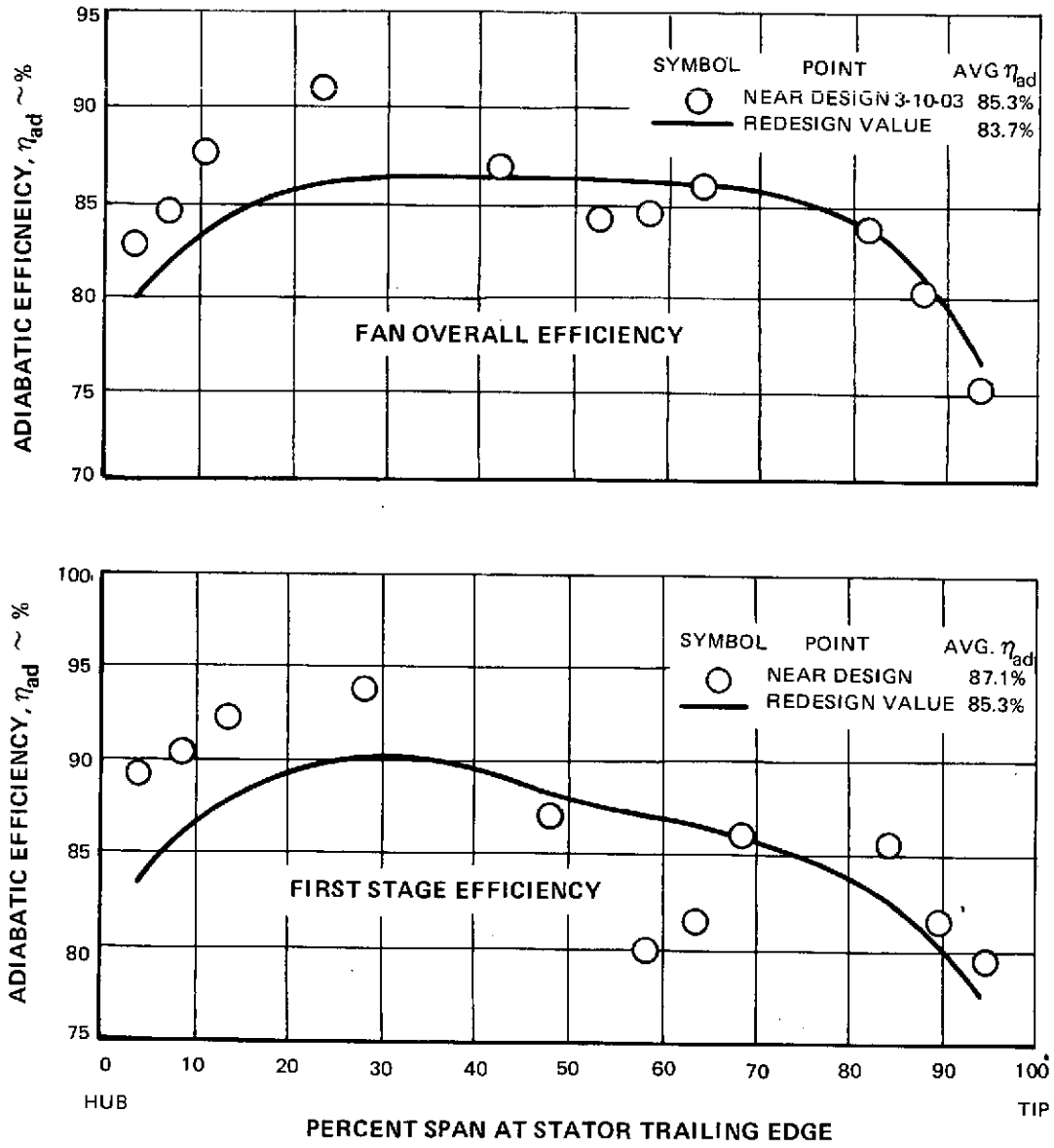


Figure 53 First Stage and Fan Overall Efficiency Versus Span for Near Design Data Point

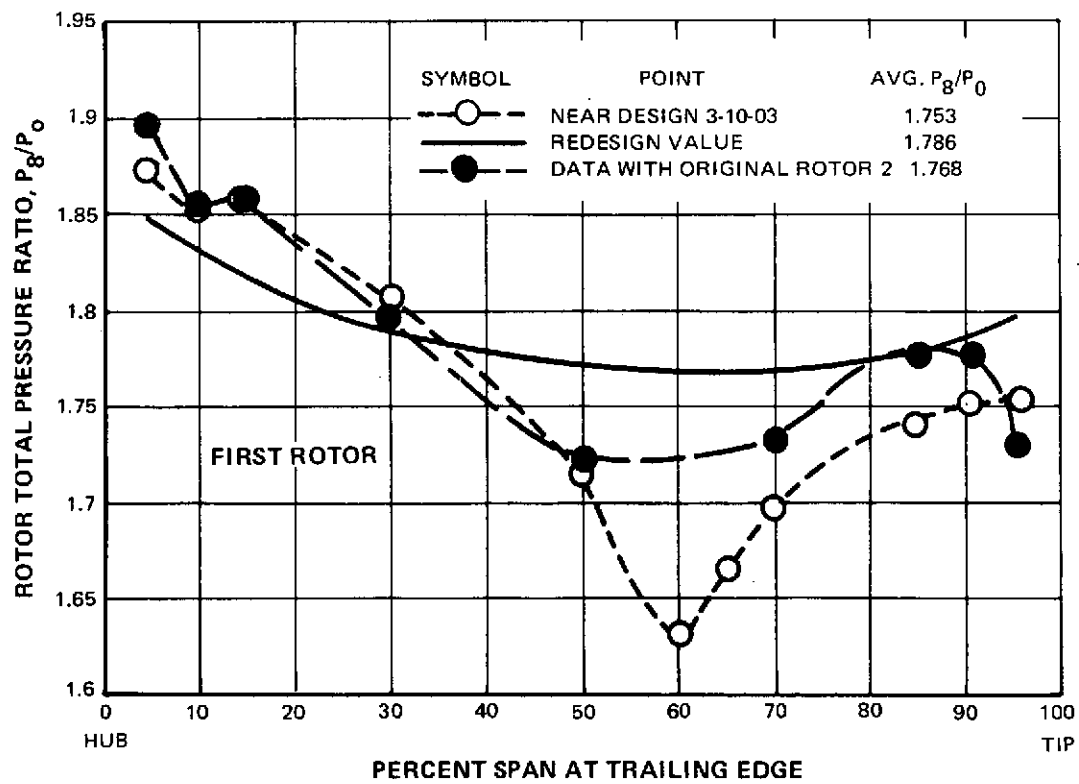
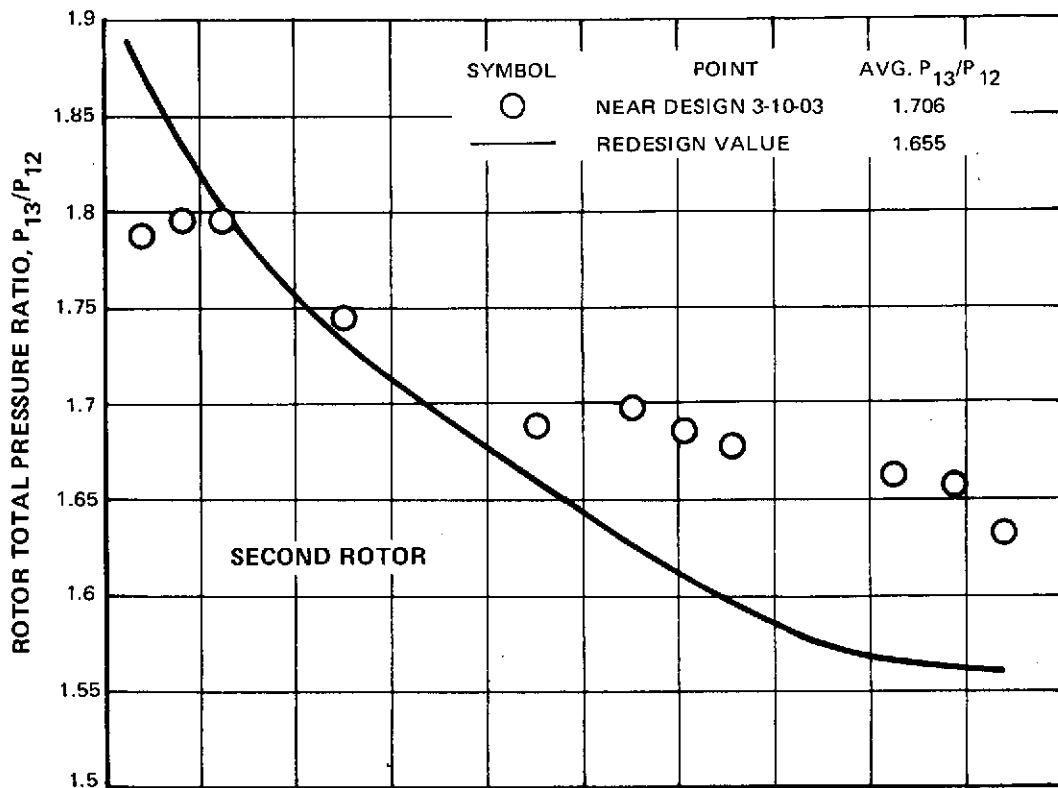


Figure 54 Rotor Total Pressure Ratio Versus Span For Near Design Data Points

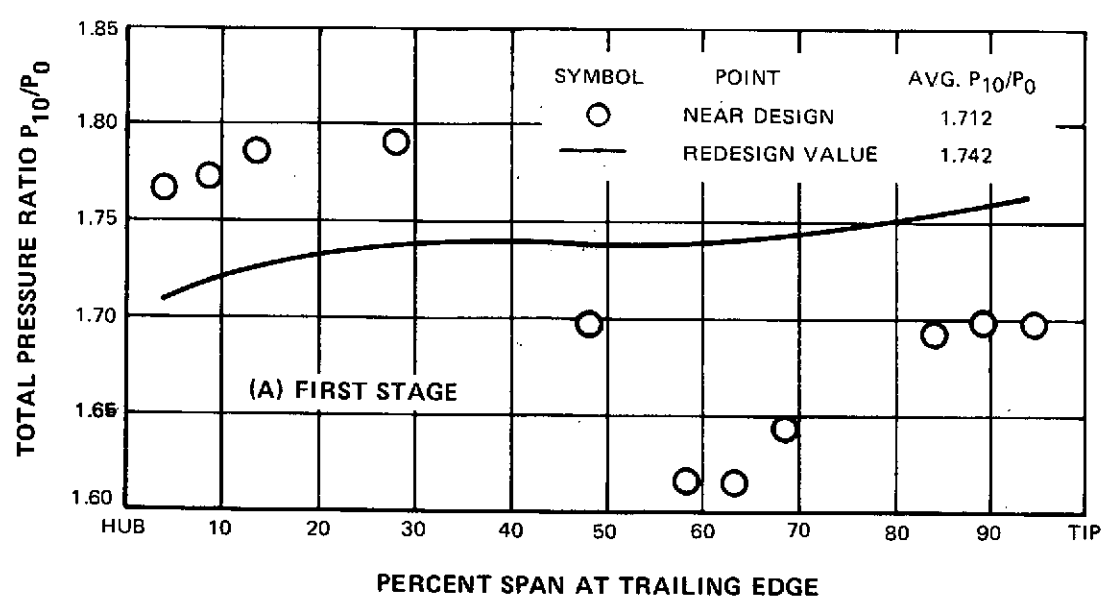
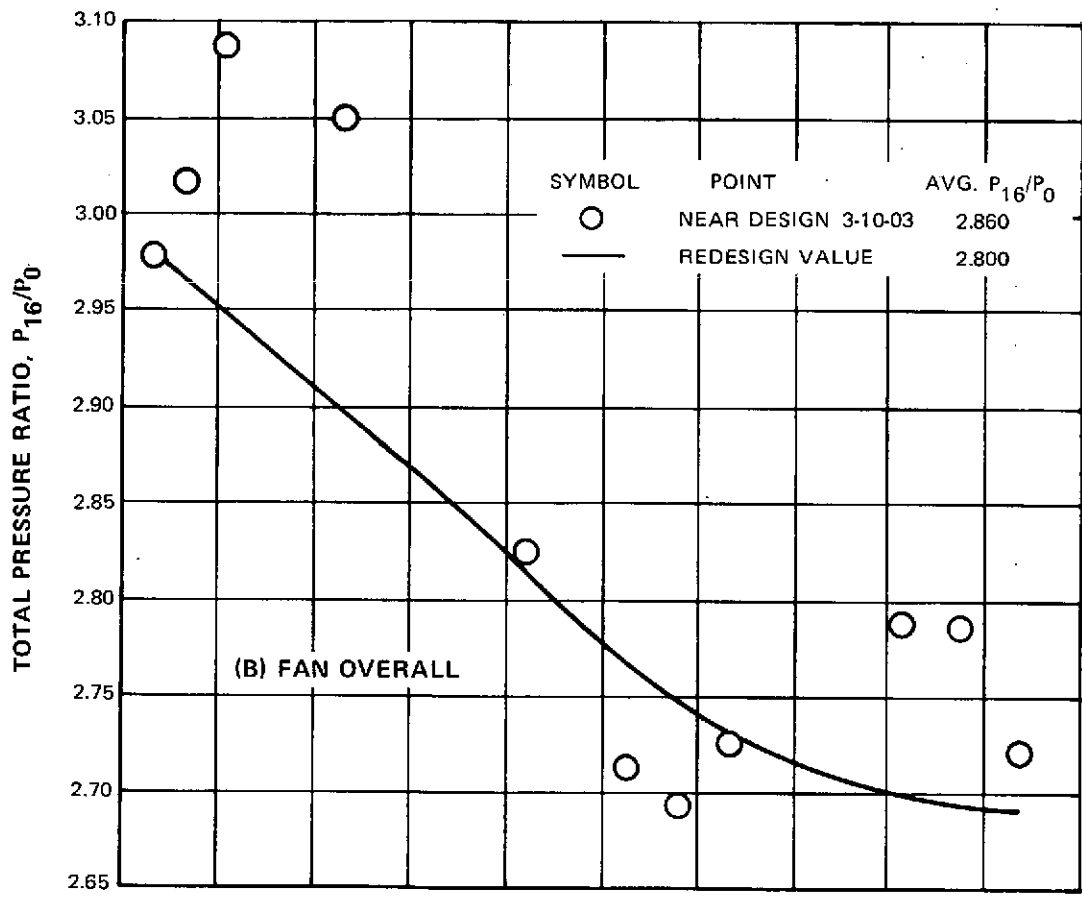


Figure 55 First Stage and Fan Overall Total Pressure Ratio Versus Span For Near Design Data Point



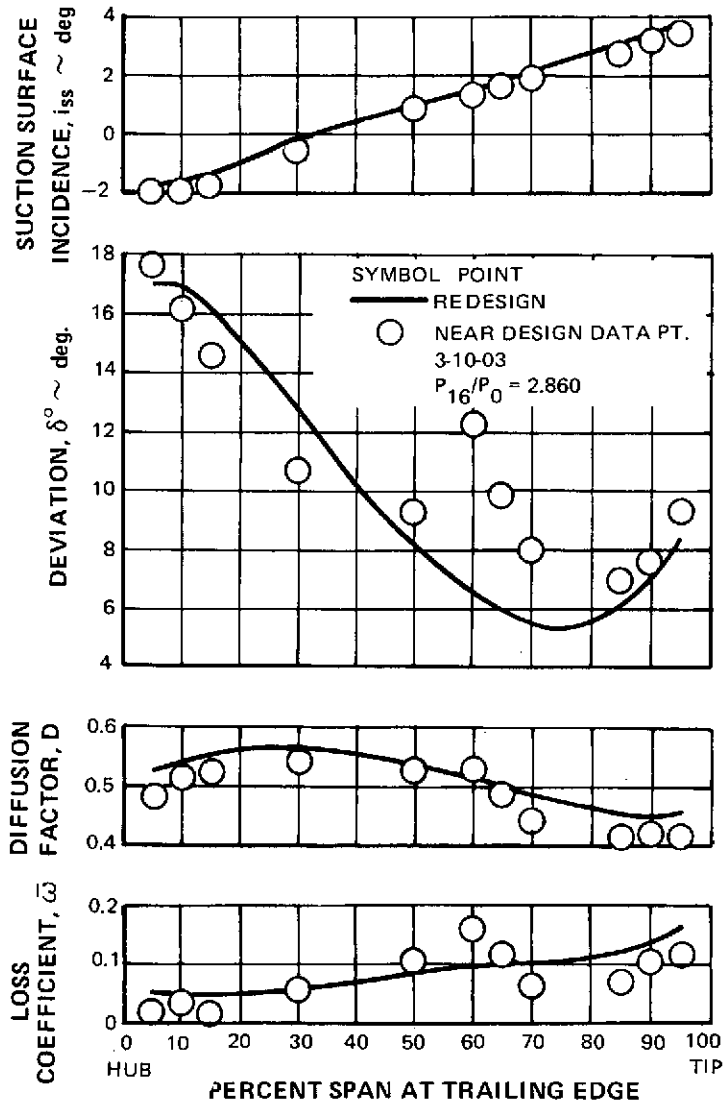


Figure 56 Loss Coefficient, Diffusion Factor, Deviation Angle, and Incidence Angle For Near Design Data Point-Rotor 1

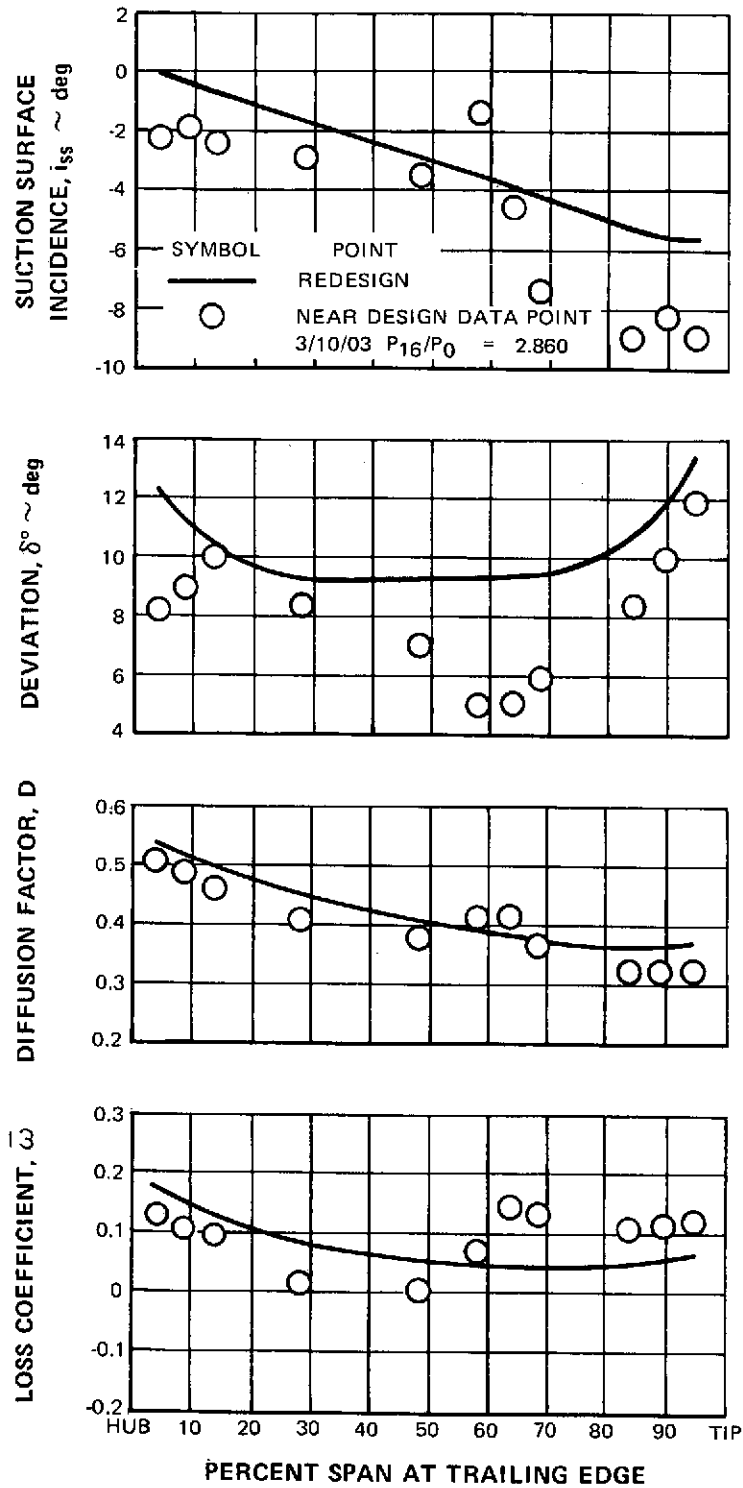


Figure 57 Loss Coefficient, Diffusion Factor, Deviation Angle and Incidence Angle For Near Design Data Point – Stator 1

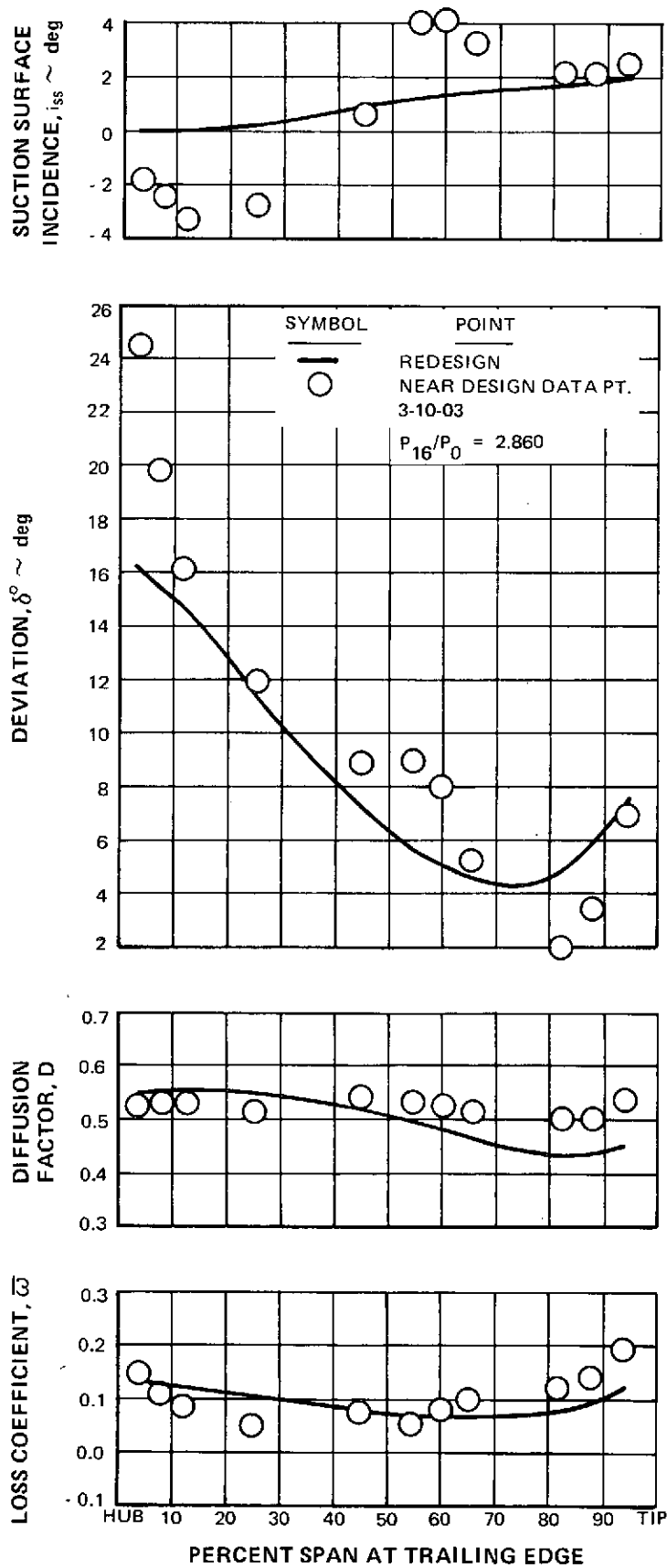


Figure 58 Loss Coefficient, Diffusion Factor, Deviation Angle and Incidence Angle for Near Design Data Point – Rotor 2

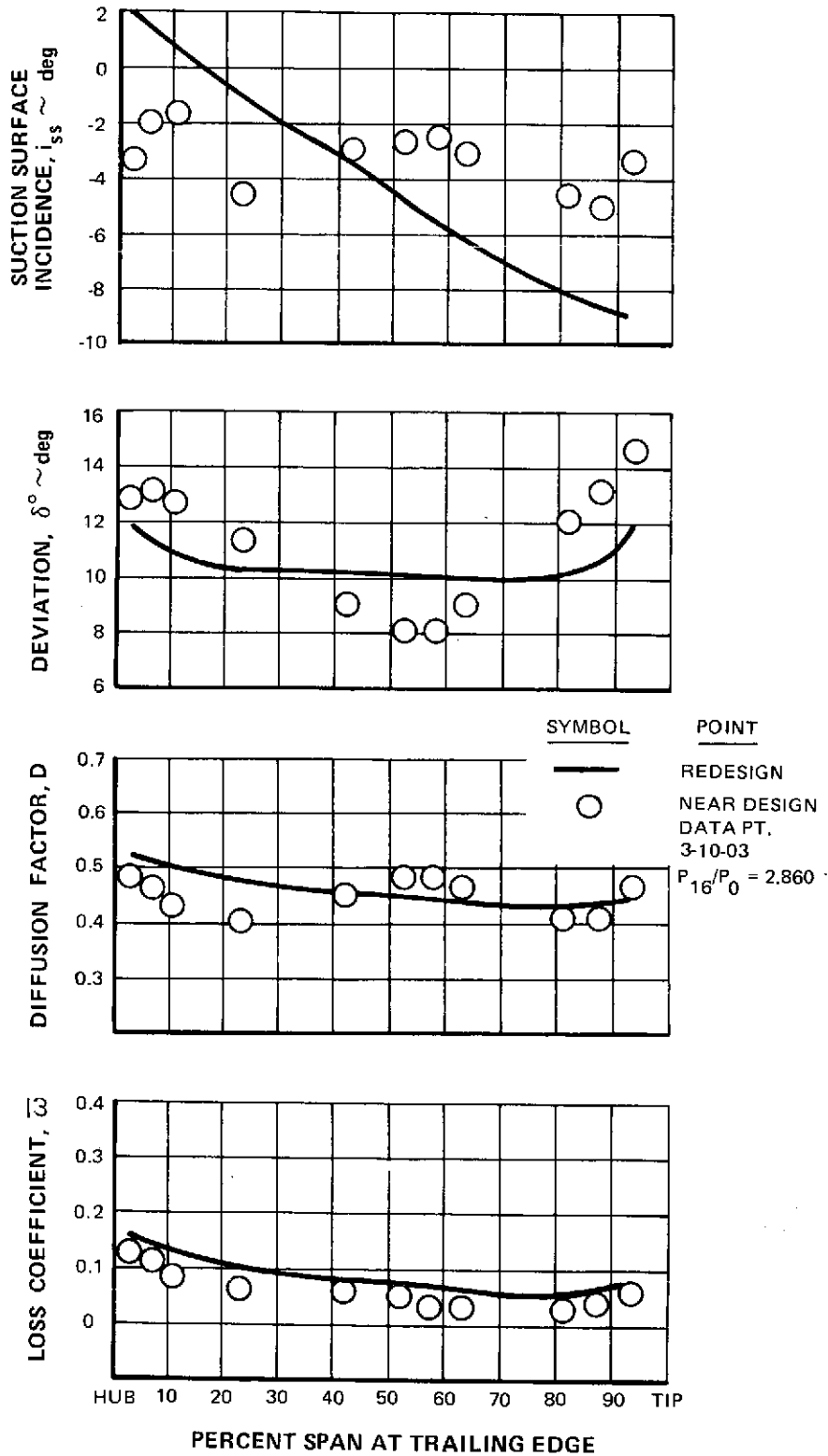


Figure 59 Loss Coefficient, Diffusion Factor, Deviation Angle, and Incidence Angle for Near Design Data Point – Stator 2

REPRODUCIBILITY OF THIS  
 ORIGINAL PAGE IS POOR

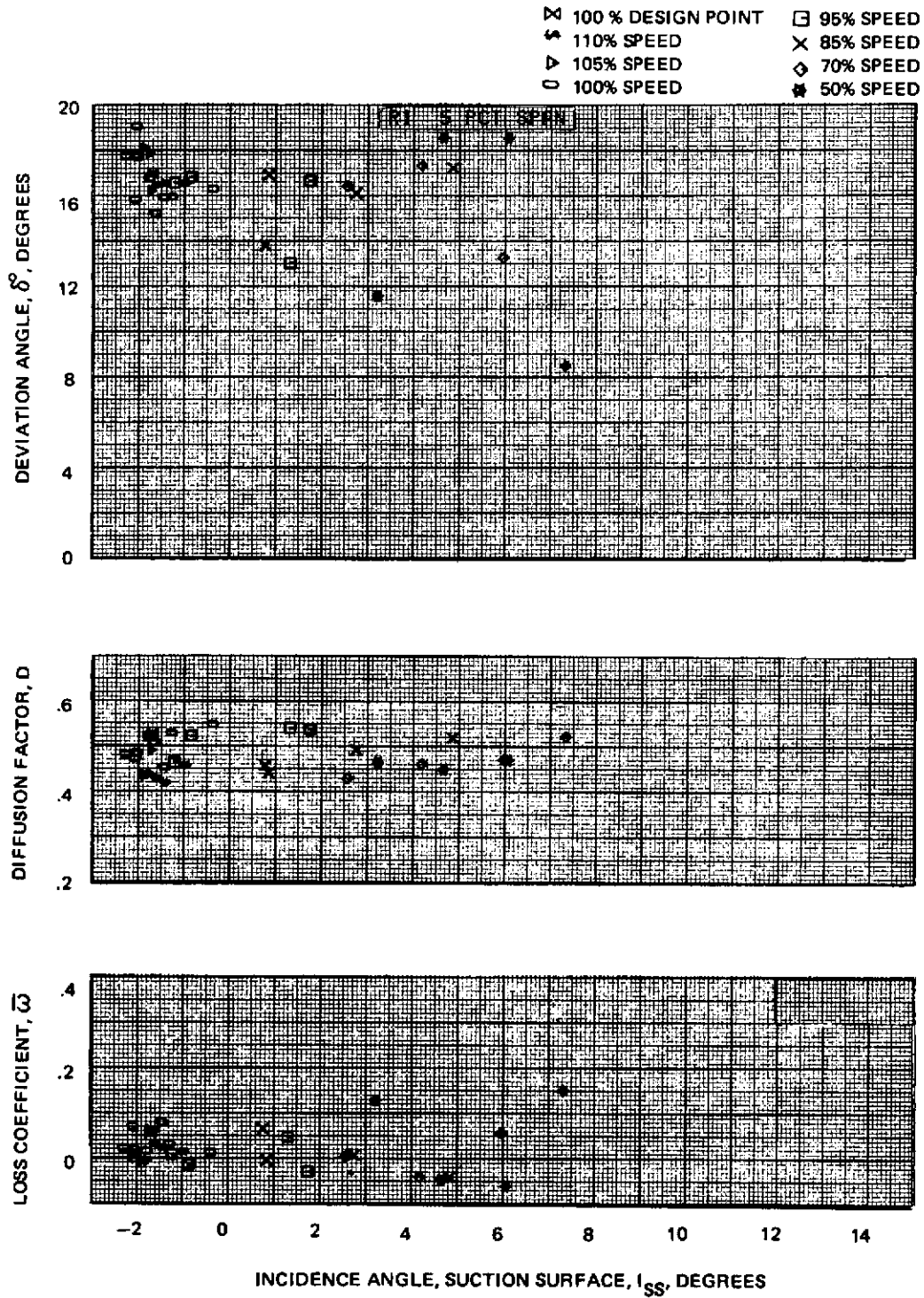


Figure 60a Blade Element Performance with Uniform Inlet Flow – Rotor 1  
5% Span

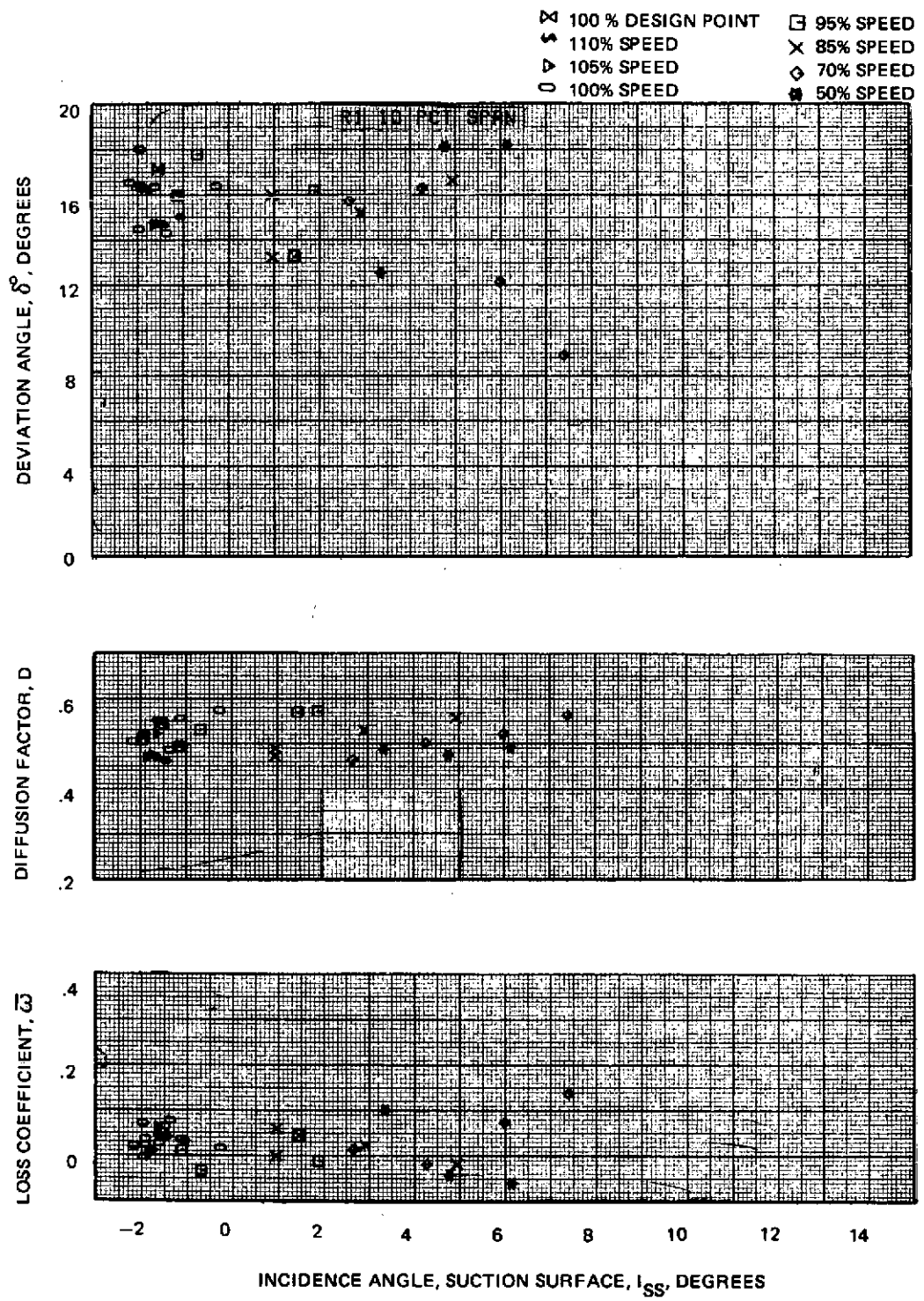


Figure 60b Blade Element Performance with Uniform Inlet Flow – Rotor 1  
10% Span

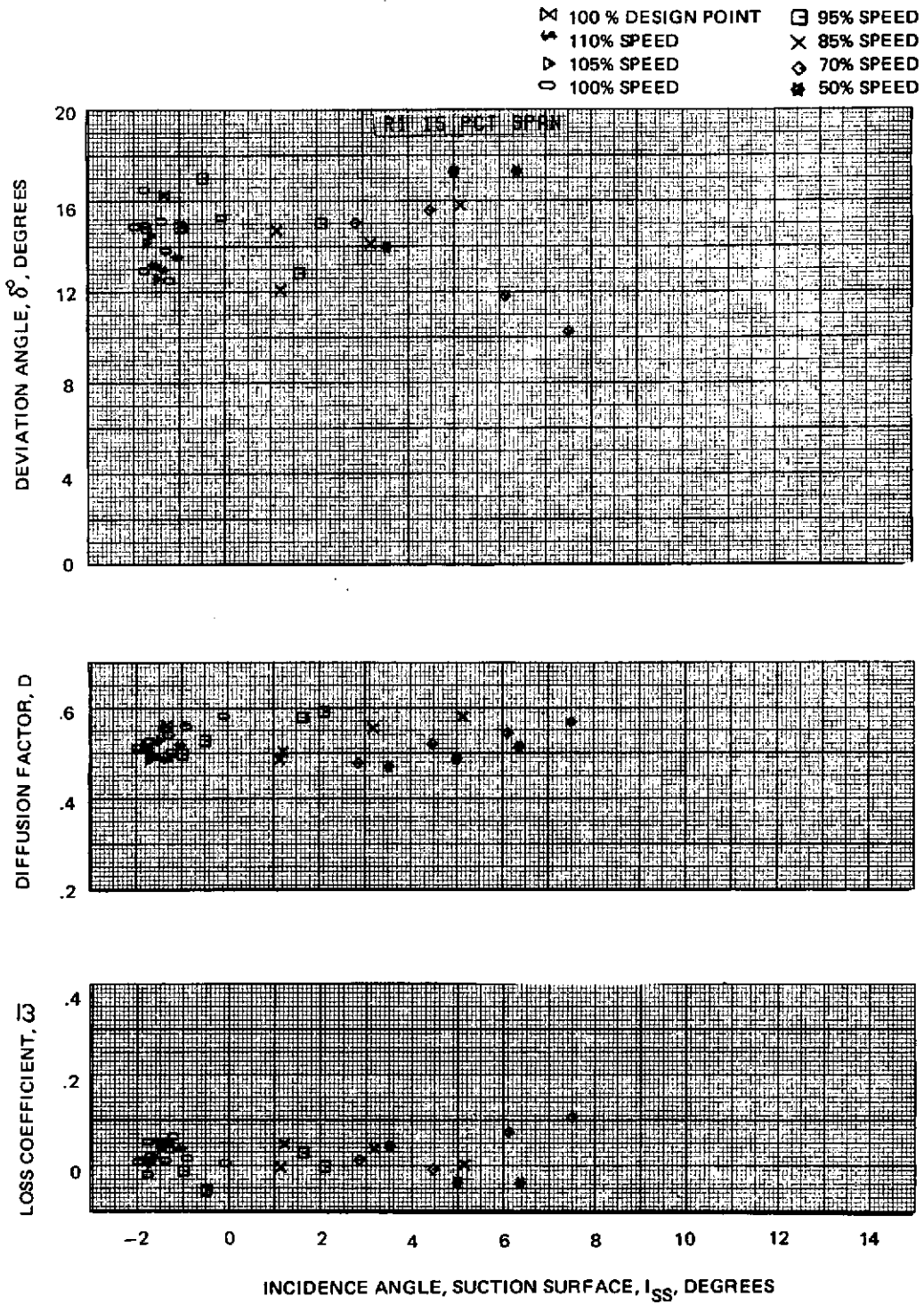


Figure 60c Blade Element Performance with Uniform Inlet Flow – Rotor 1  
15% Span

REPRODUCIBILITY OF THE  
 ORIGINAL PAGE IS POOR

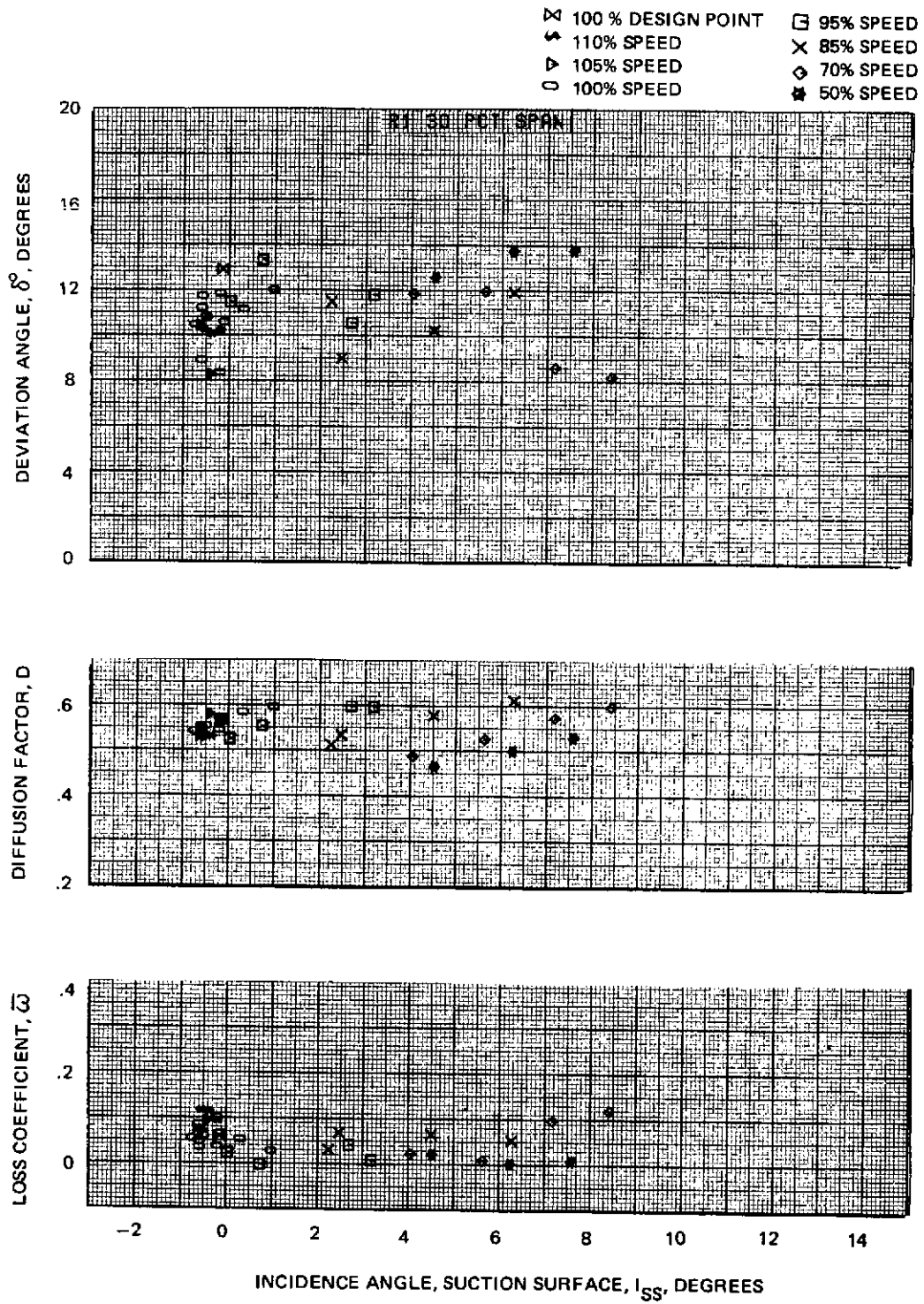


Figure 60d Blade Element Performance with Uniform Inlet Flow – Rotor 1  
30% Span



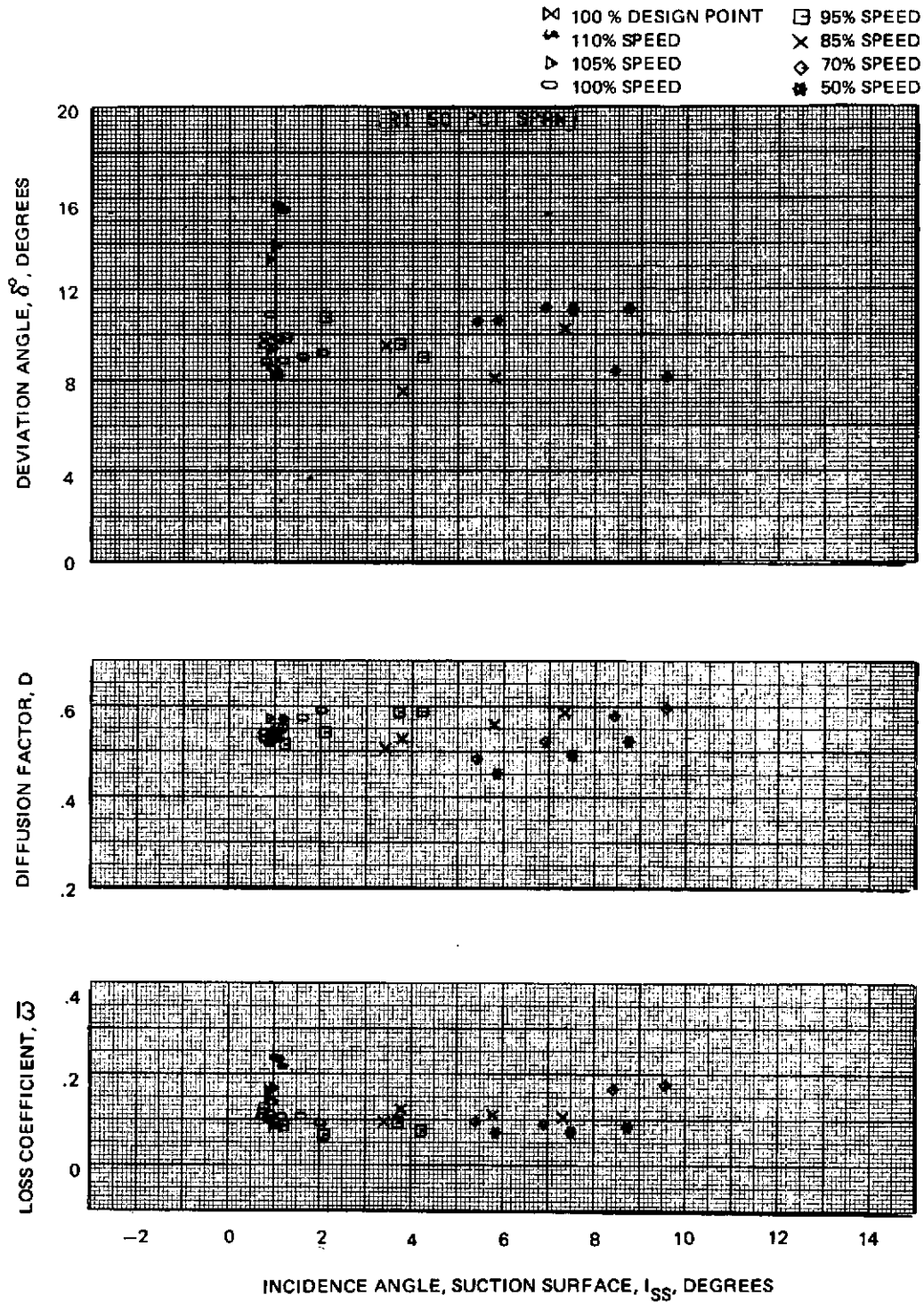


Figure 60e Blade Element Performance with Uniform Inlet Flow – Rotor 1  
50% Span

REPRODUCIBILITY OF THE  
 ORIGINAL PAGE IS POOR

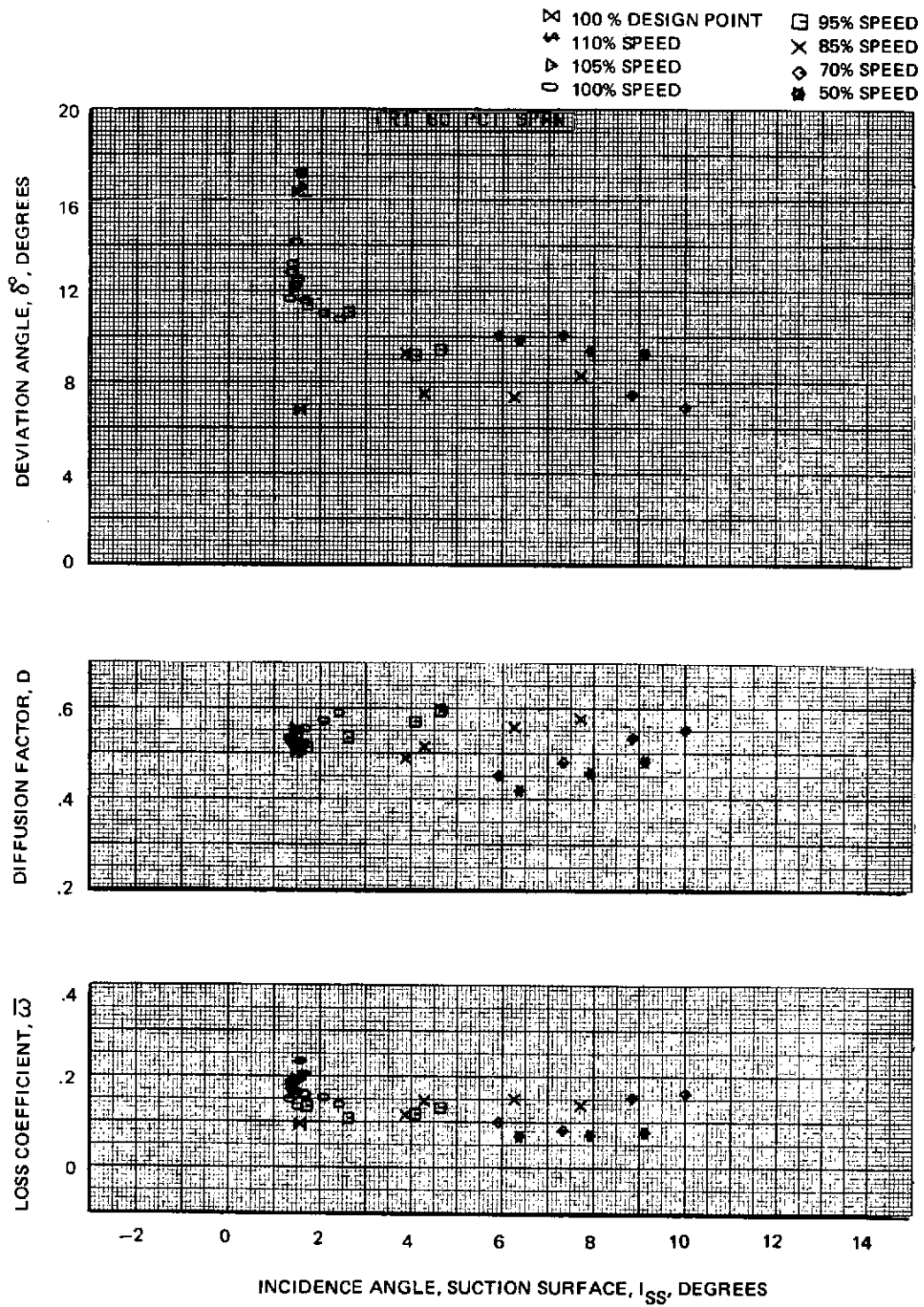


Figure 60f Blade Element Performance with Uniform Inlet Flow – Rotor 1  
60% Span

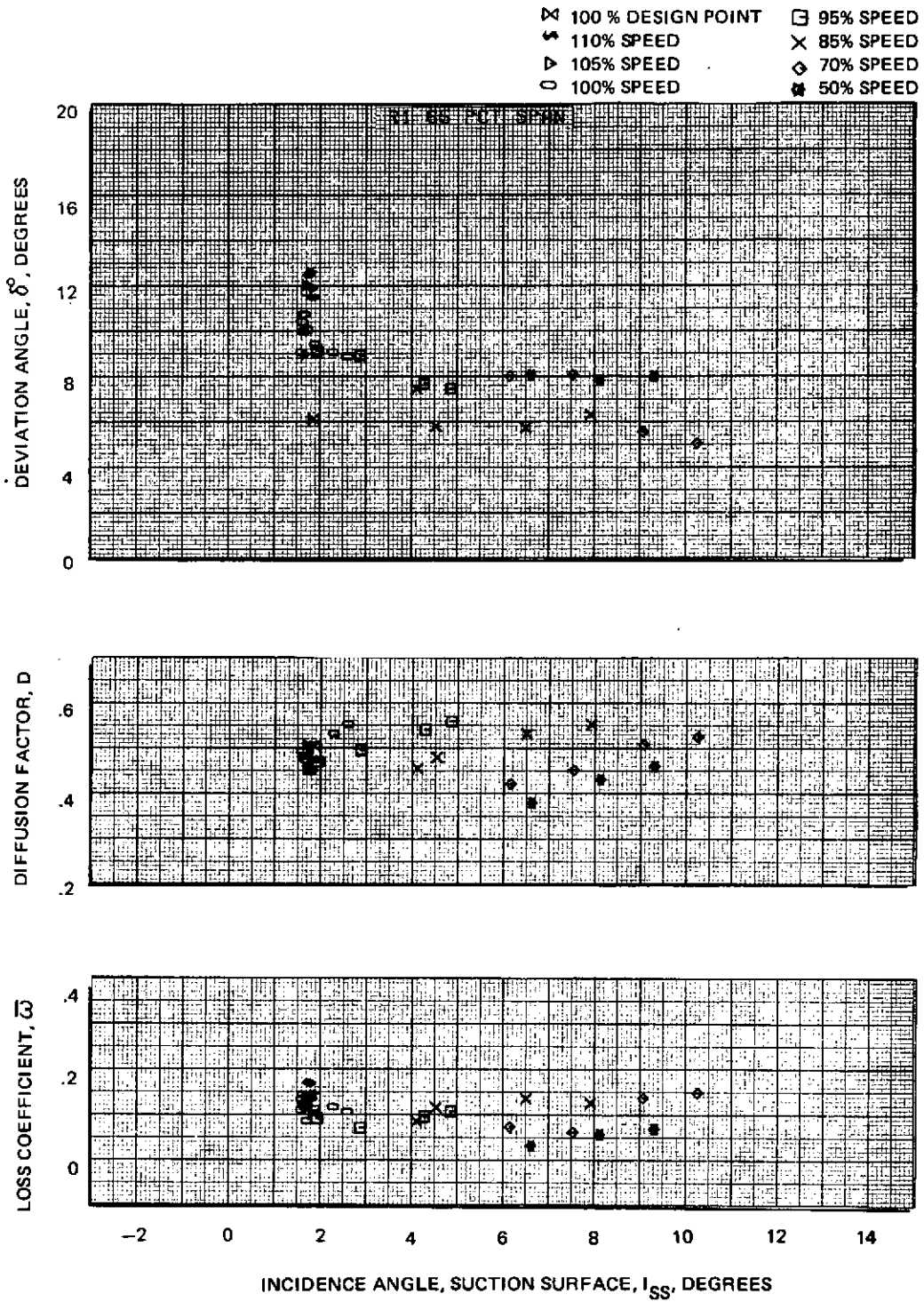


Figure 60g Blade Element Performance with Uniform Inlet Flow – Rotor 1  
65% Span

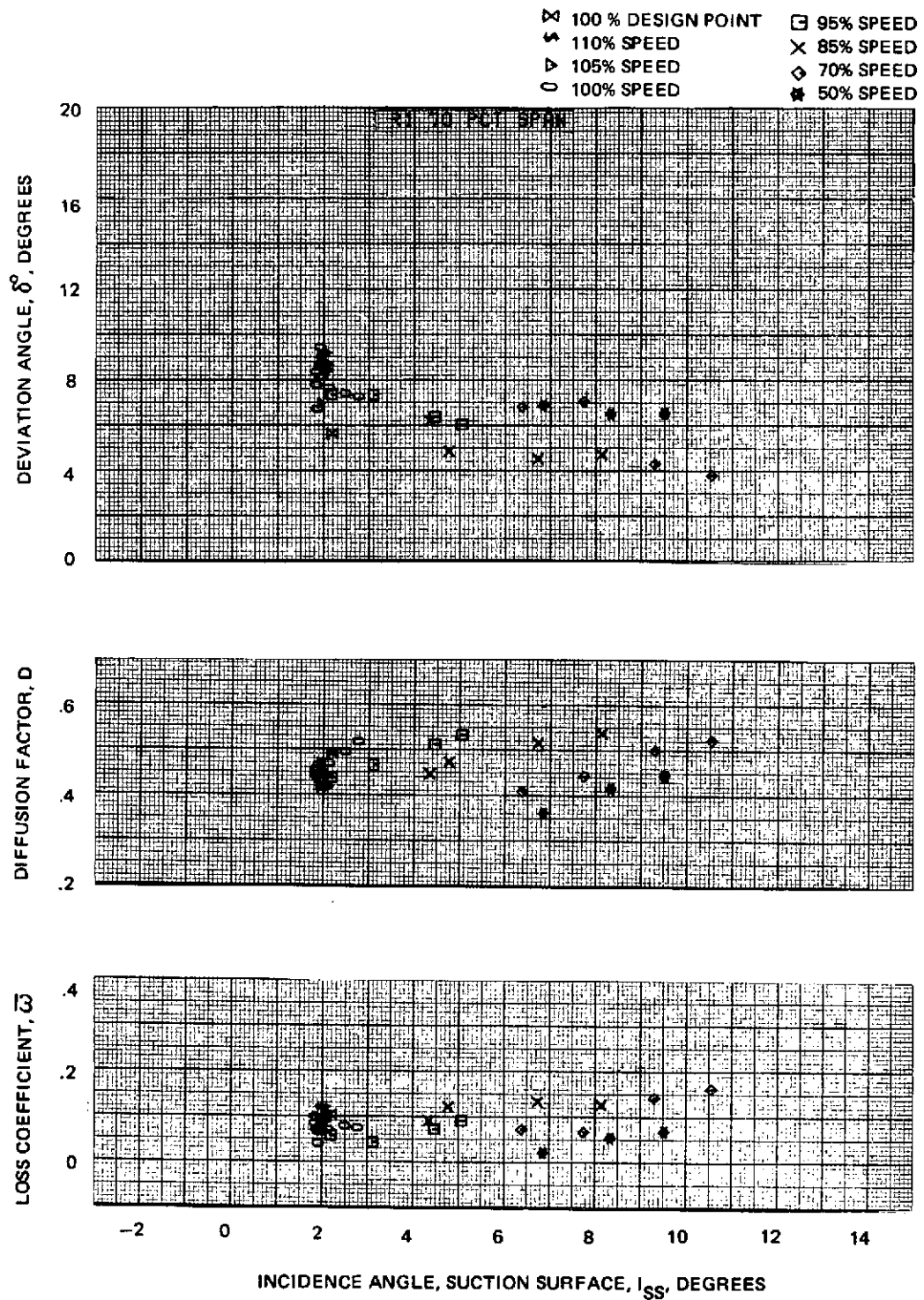


Figure 60h Blade Element Performance with Uniform Inlet Flow – Rotor 1  
70% Span

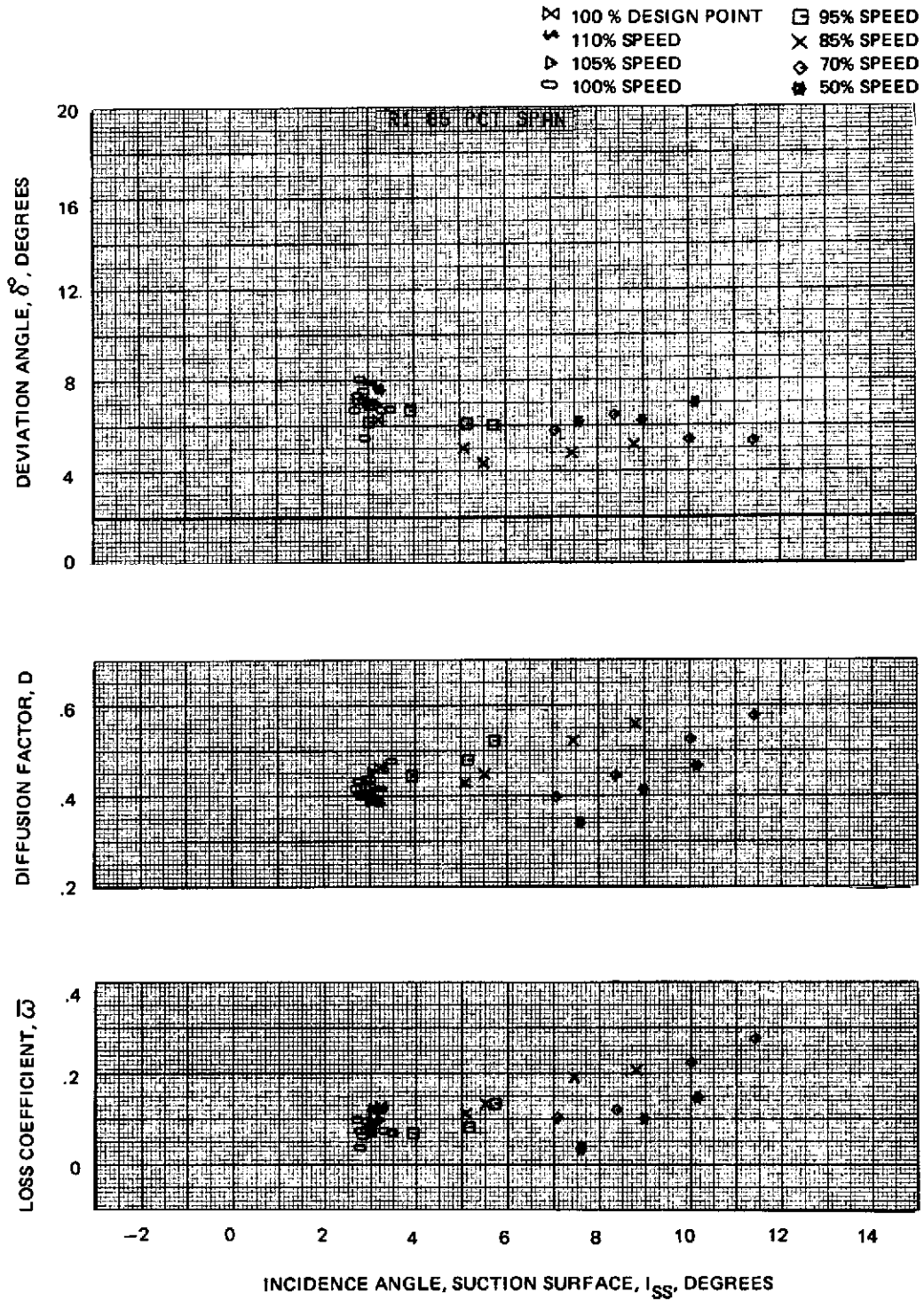


Figure 60i Blade Element Performance with Uniform Inlet Flow – Rotor 1  
85% Span

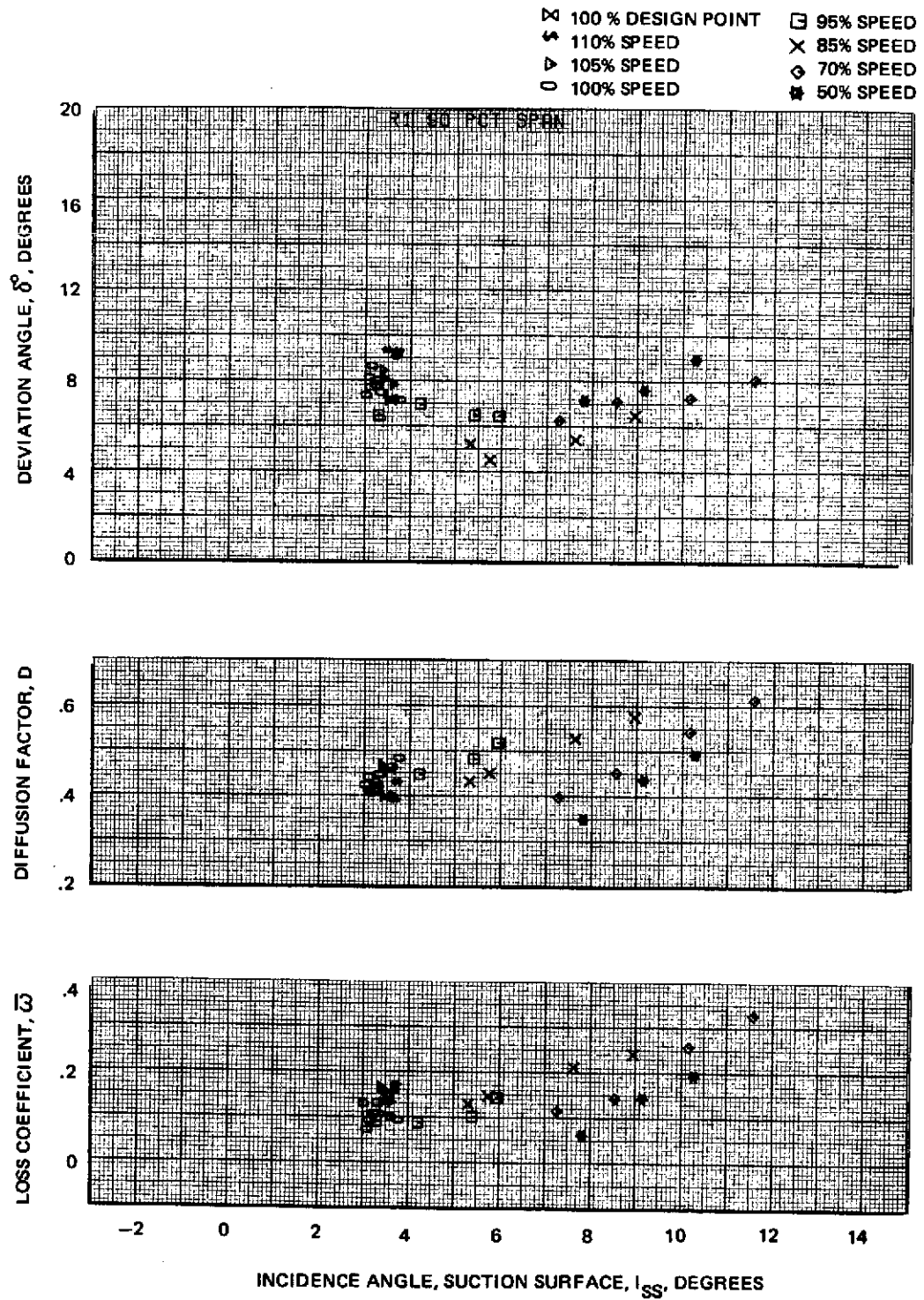


Figure 60j Blade Element Performance with Uniform Inlet Flow – Rotor 1  
90% Span

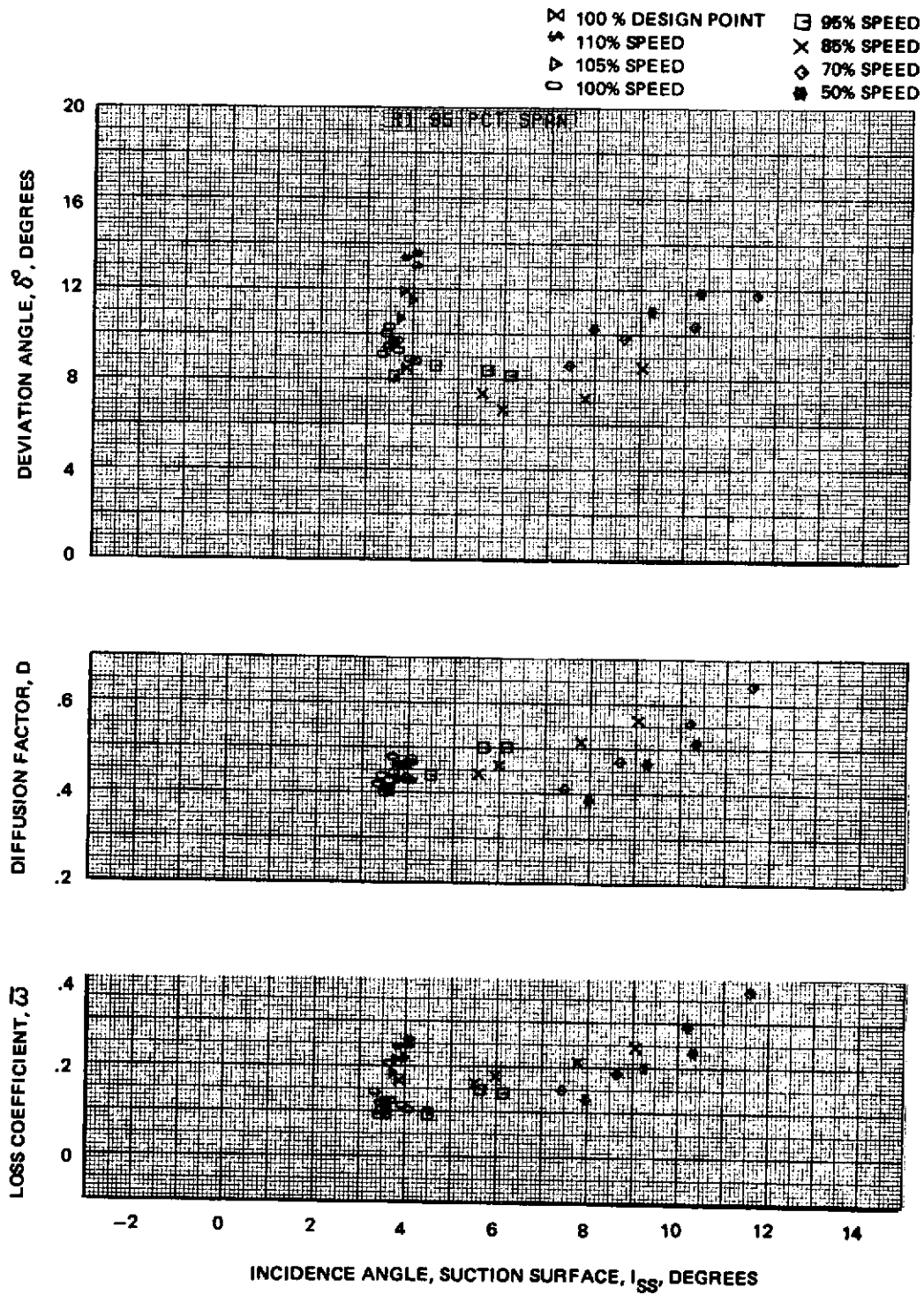


Figure 60k Blade Element Performance with Uniform Inlet Flow – Rotor 1  
95% Span

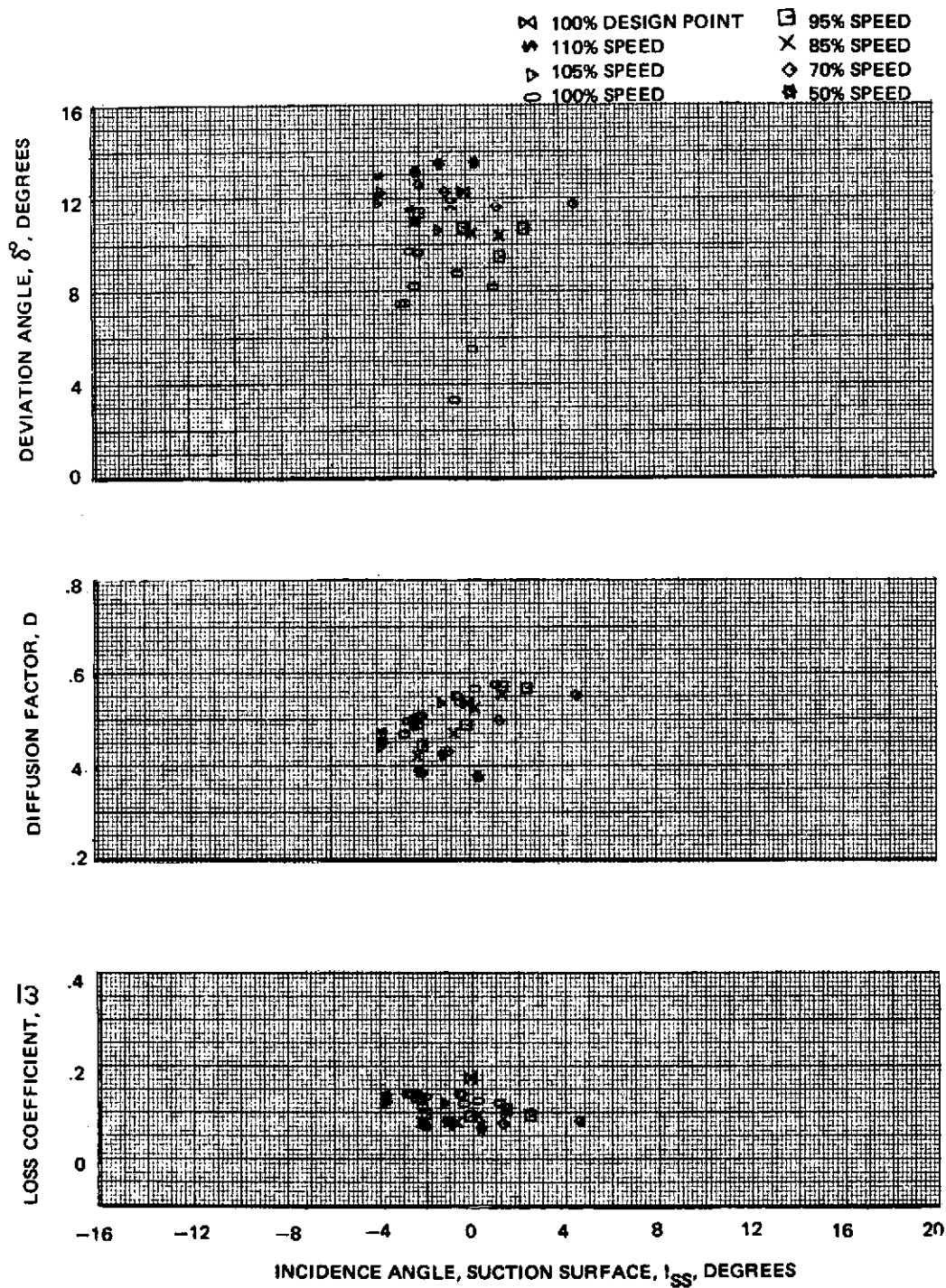


Figure 61a Blade Element Performance with Uniform Inlet Flow – Stator 1  
4% Span



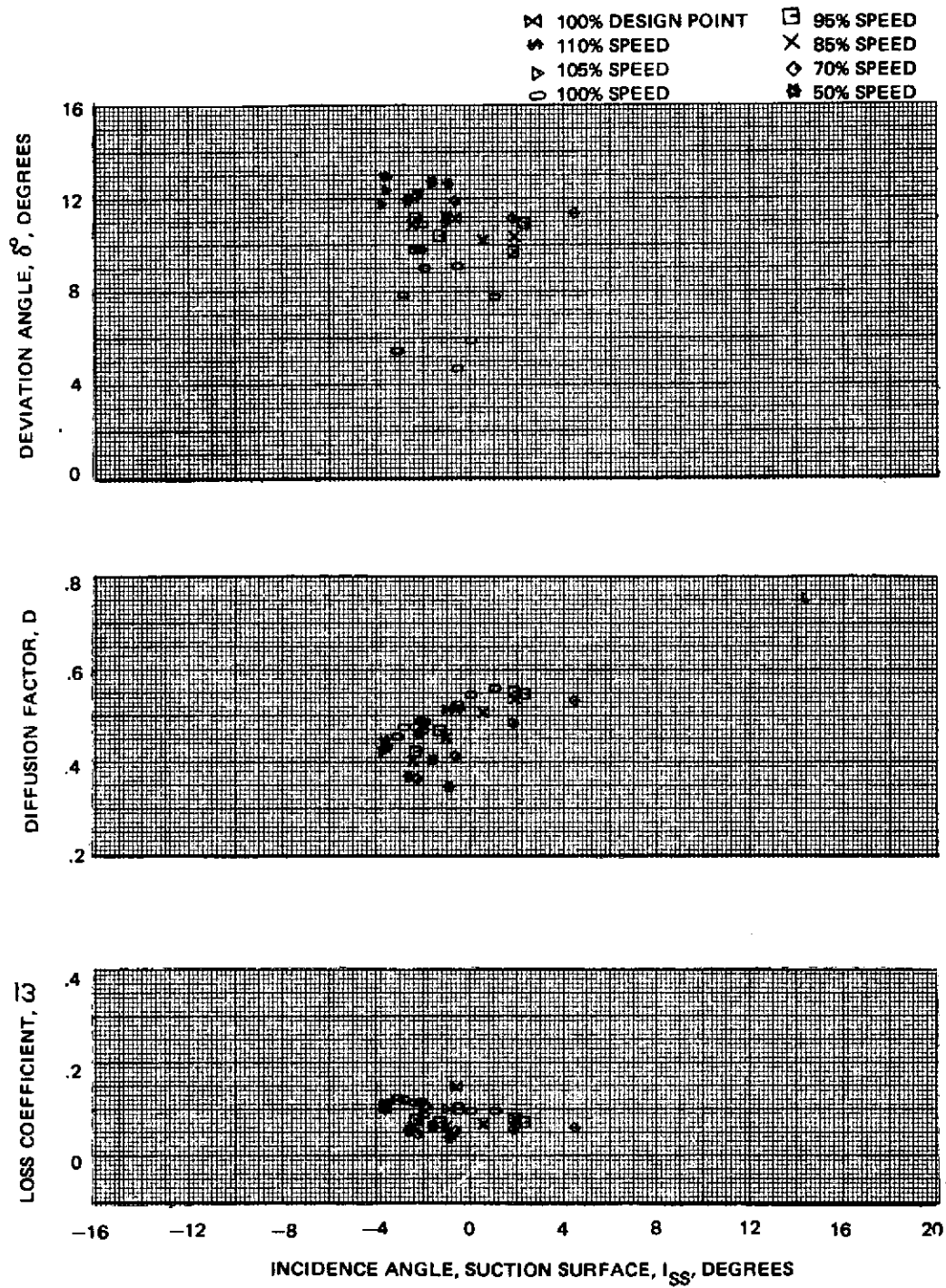


Figure 61b Blade Element Performance with Uniform Inlet Flow – Stator 1  
9% Span

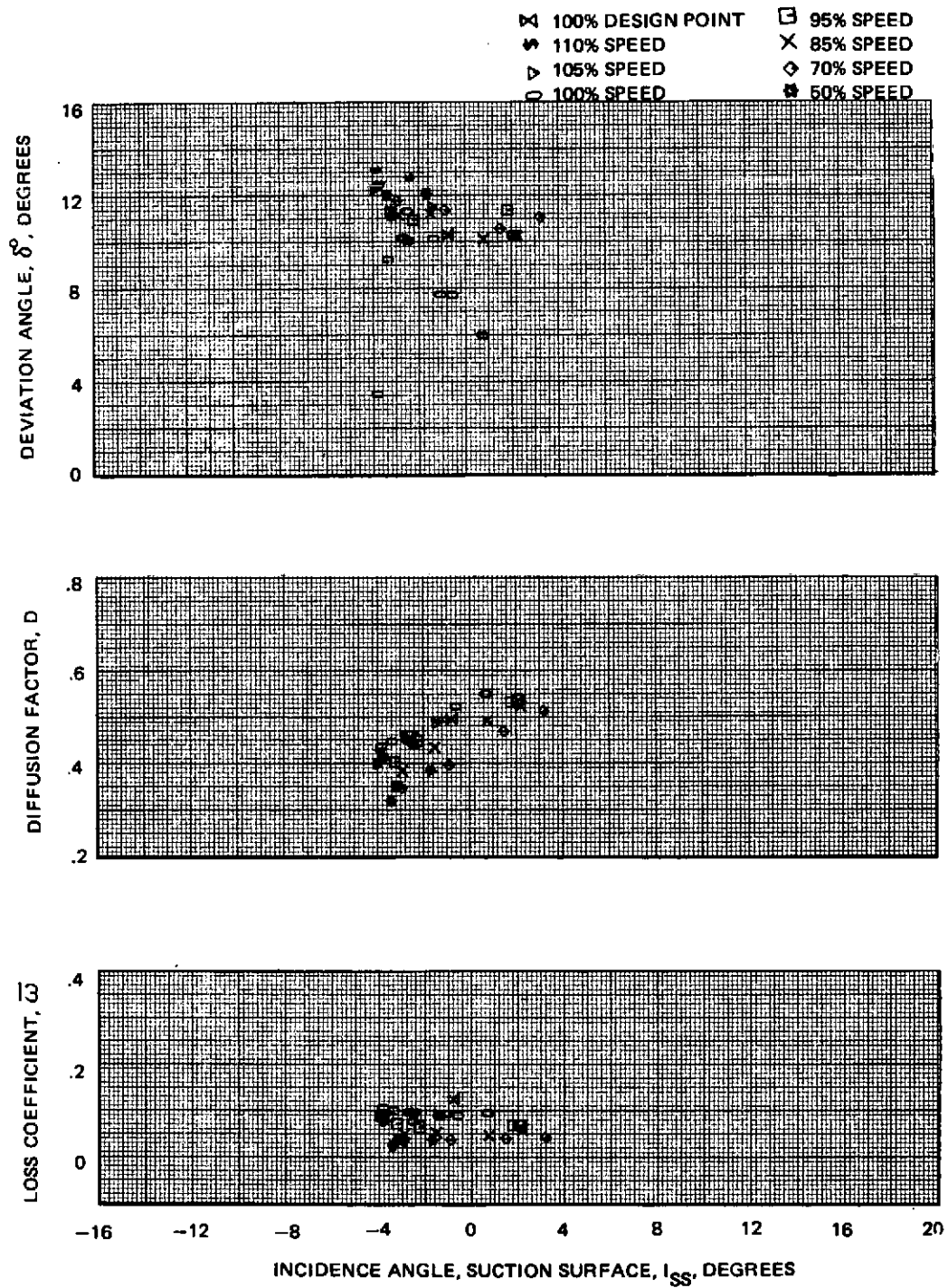


Figure 61c Blade Element Performance with Uniform Inlet Flow – Stator 1  
14% Span

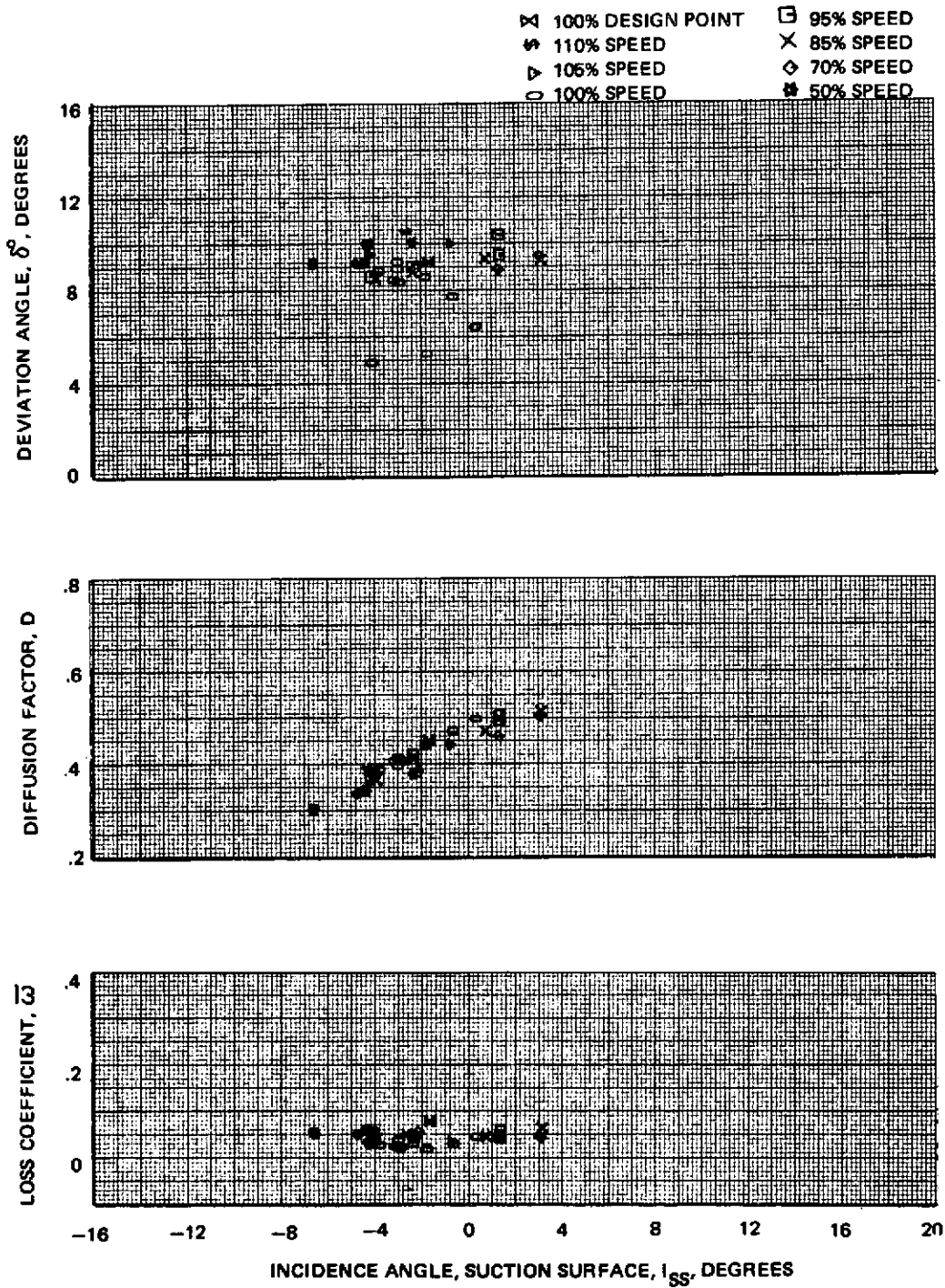


Figure 61d Blade Element Performance with Uniform Inlet Flow – Stator 1  
28% Span

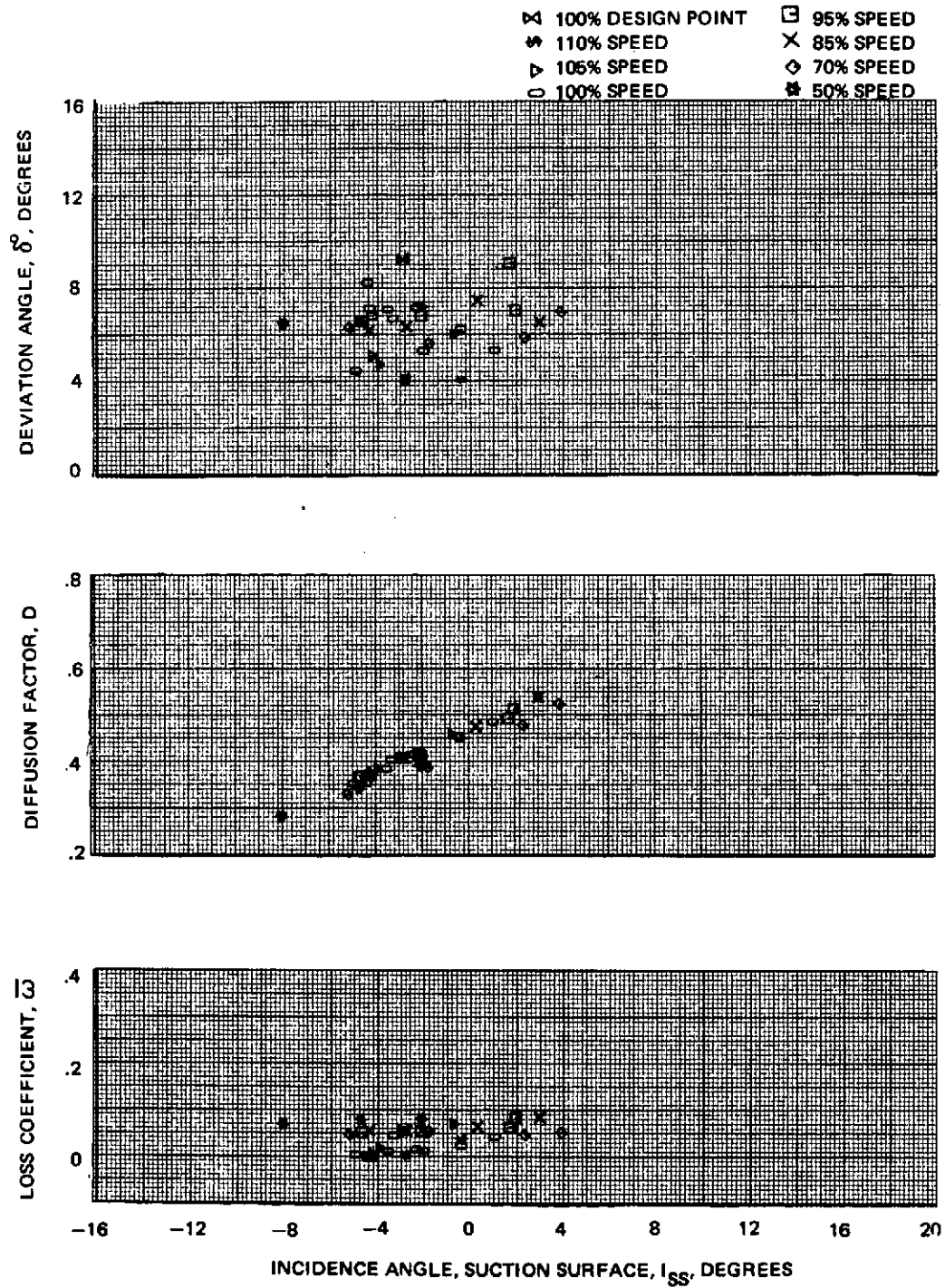


Figure 61e Blade Element Performance with Uniform Inlet Flow – Stator 1  
48% Span

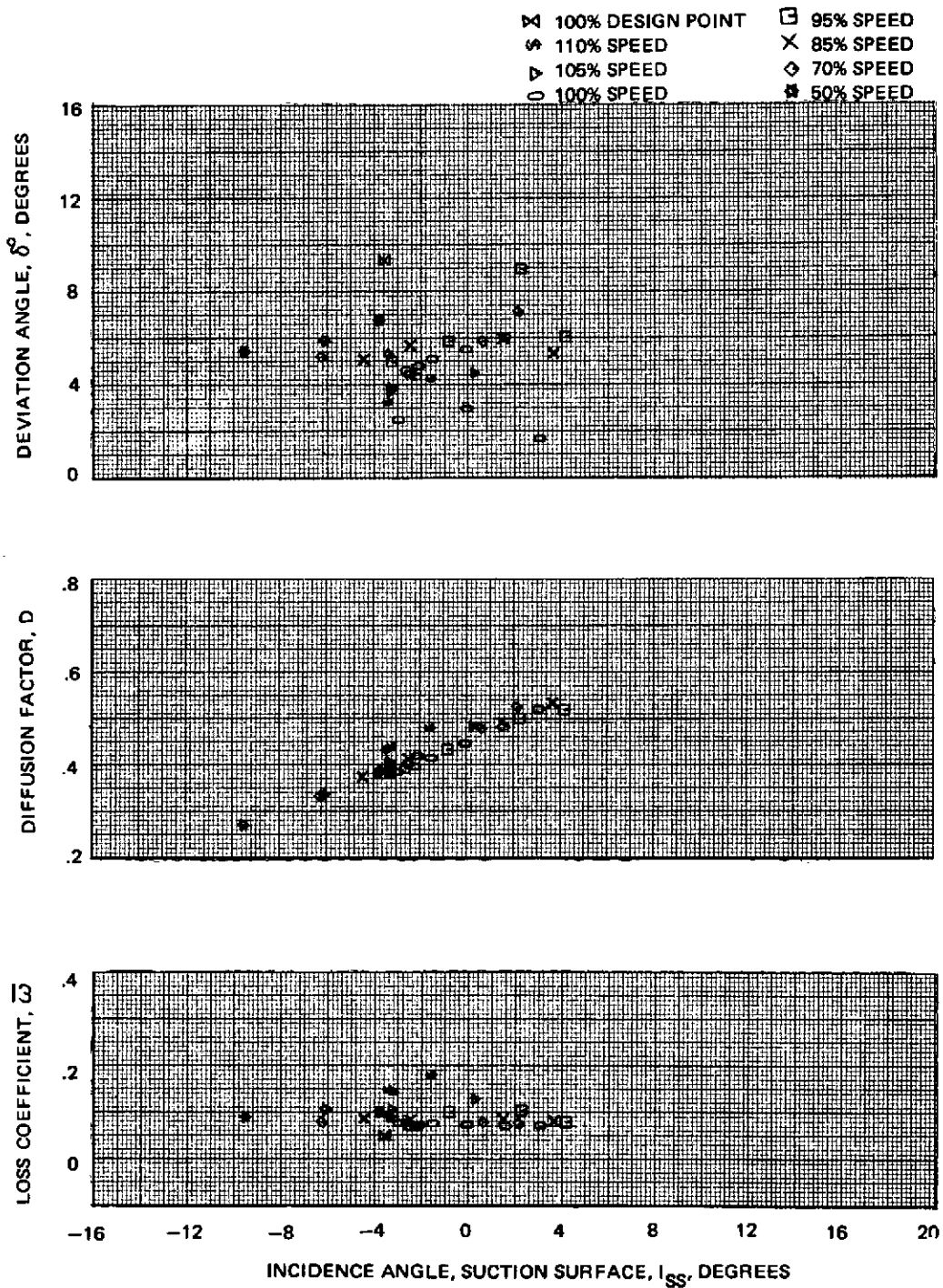


Figure 61f Blade Element Performance with Uniform Inlet Flow — Stator 1  
58% Span

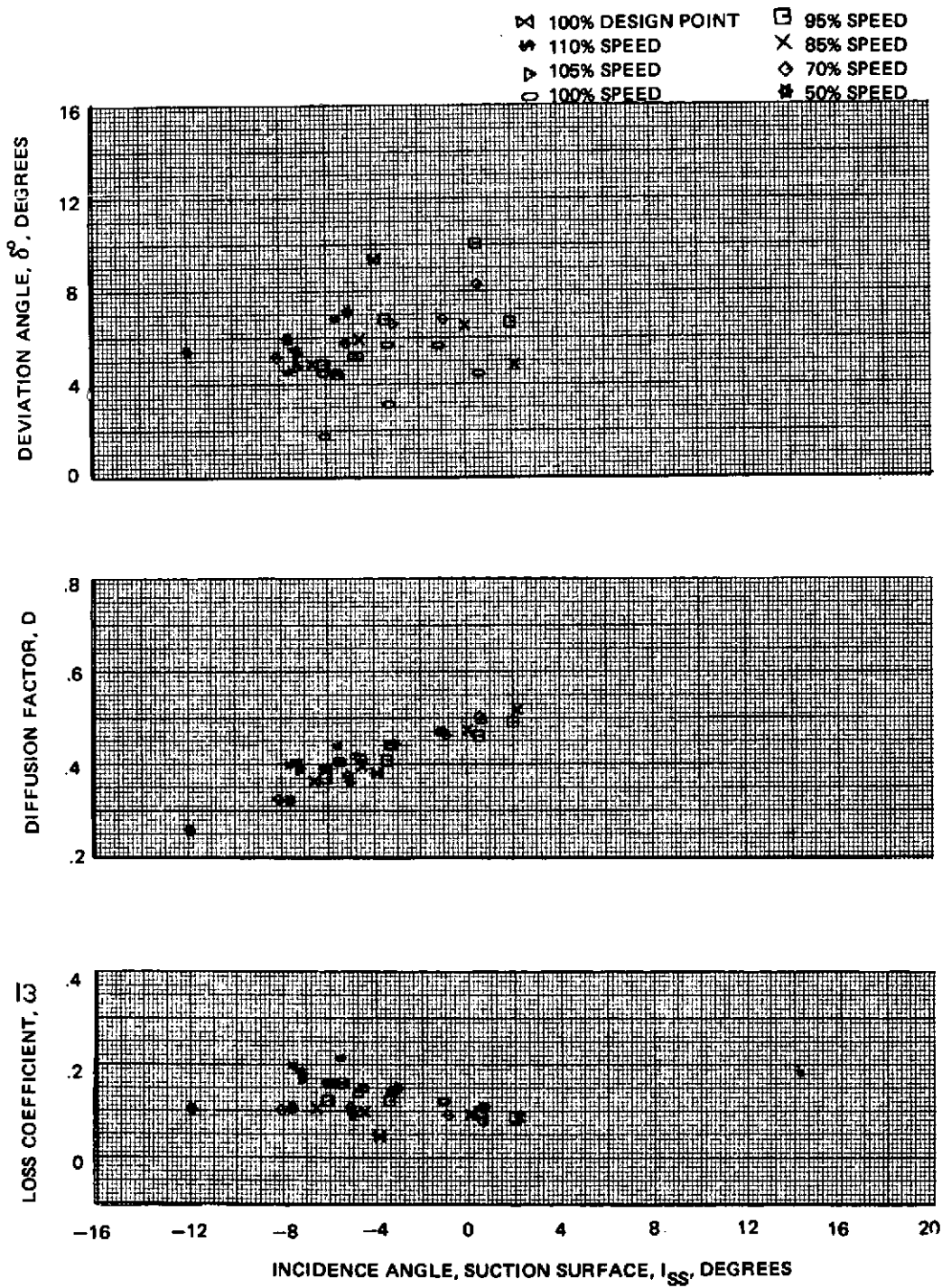


Figure 61g Blade Element Performance with Uniform Inlet Flow – Stator 1  
64% Span

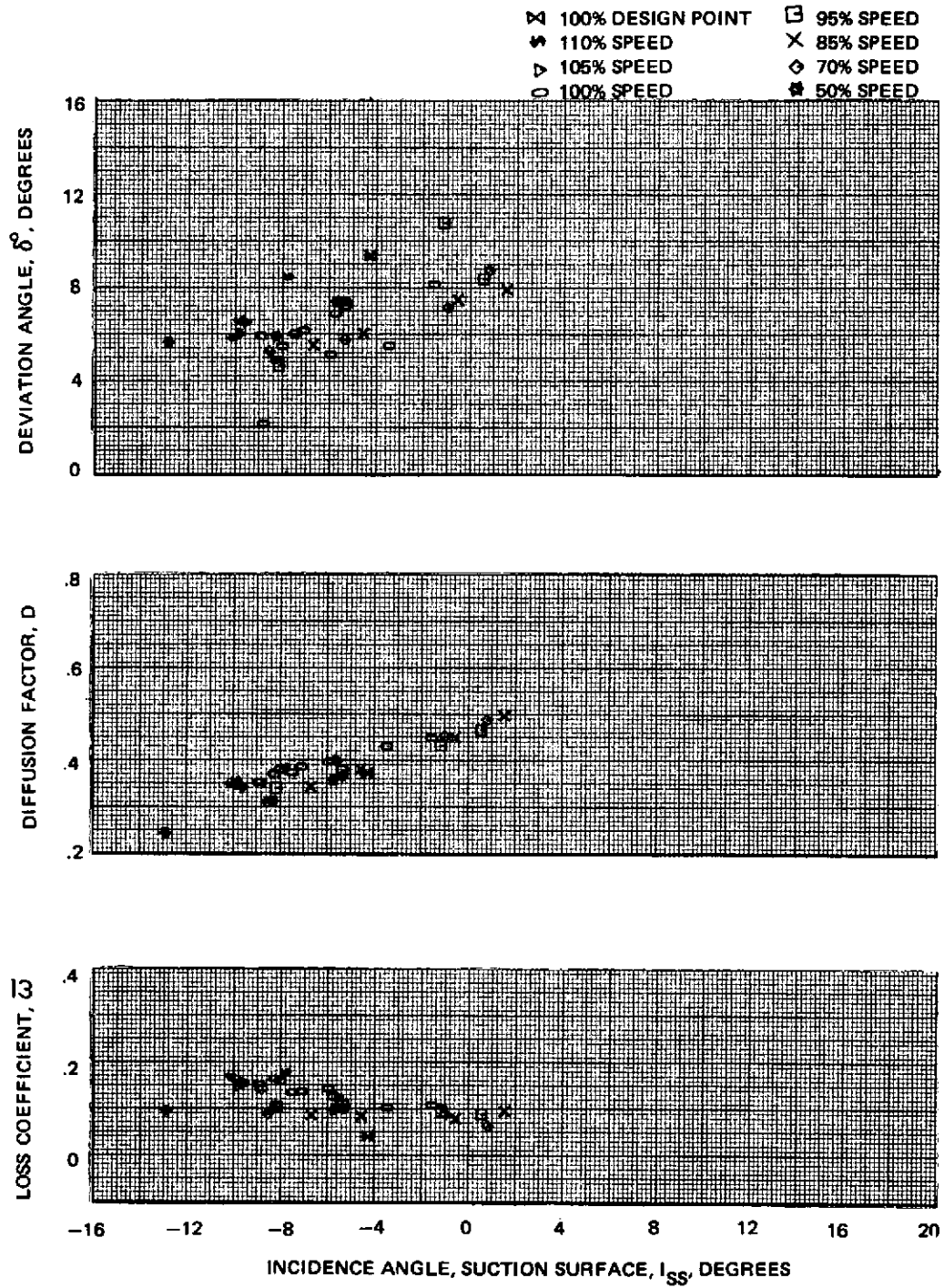


Figure 61h Blade Element Performance with Uniform Inlet Flow – Stator 1  
69% Span

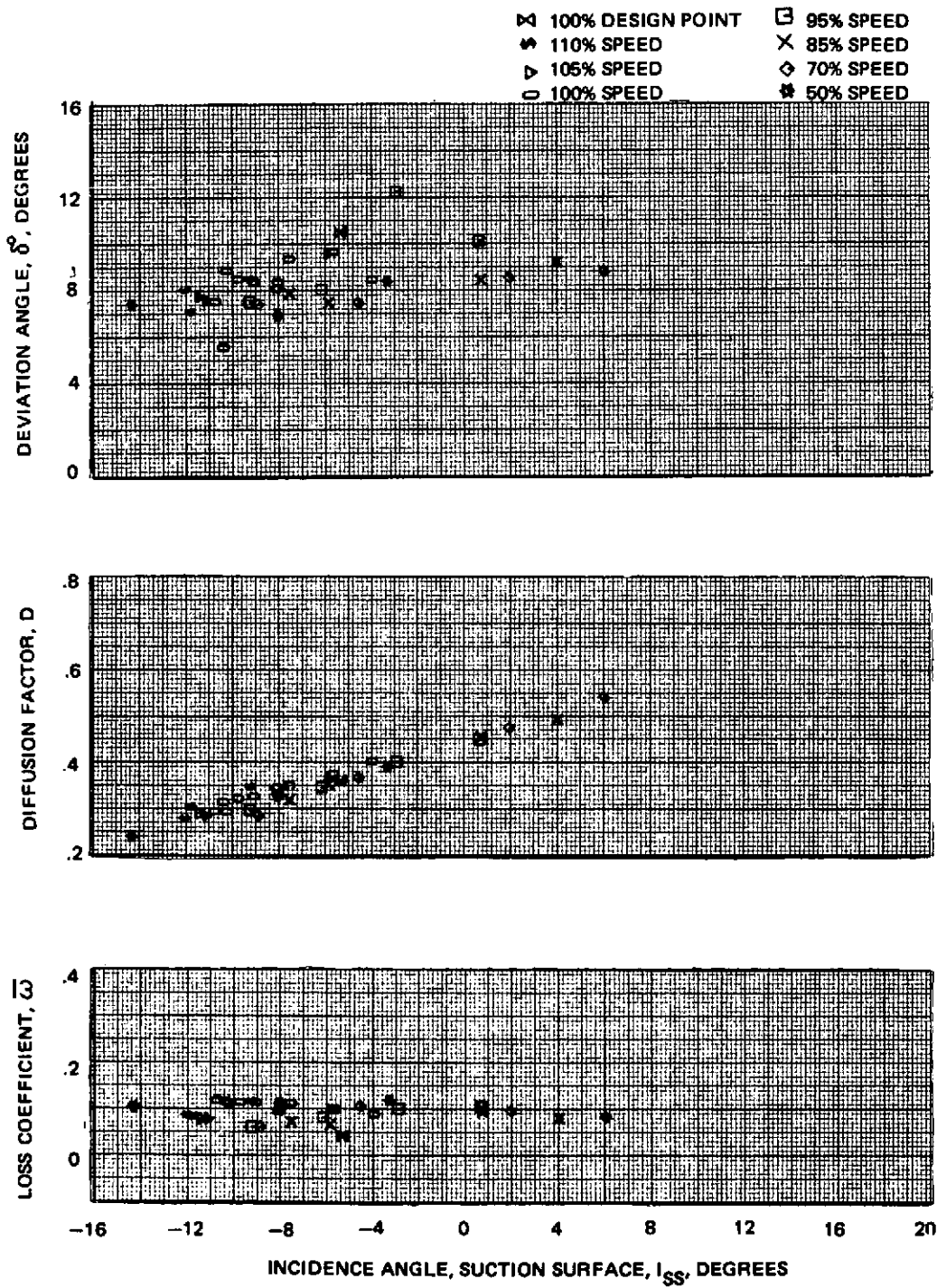


Figure 61i Blade Element Performance with Uniform Inlet Flow – Stator 1  
84% Span



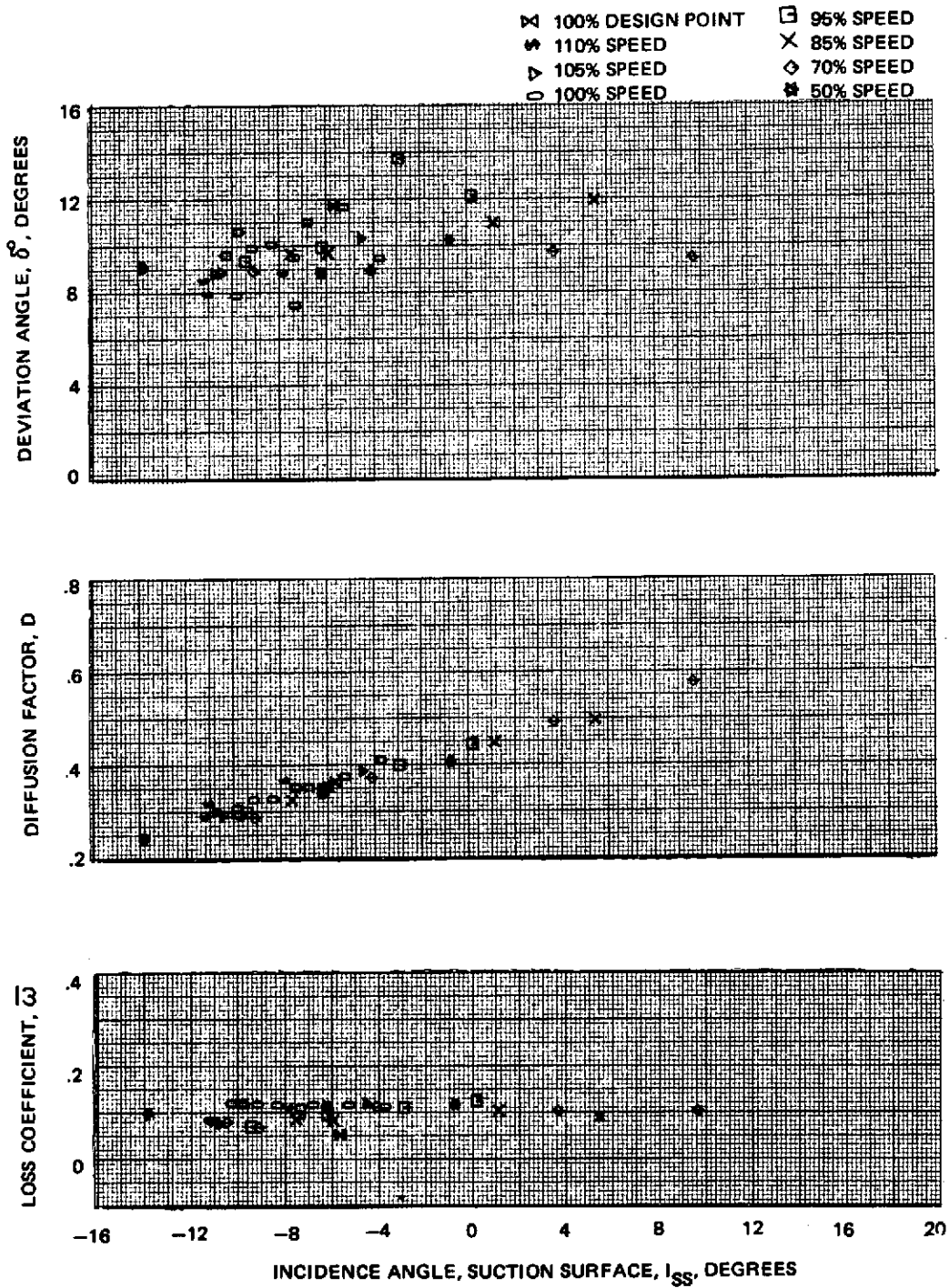


Figure 61j Blade Element Performance with Uniform Inlet Flow – Stator 1  
90% Span

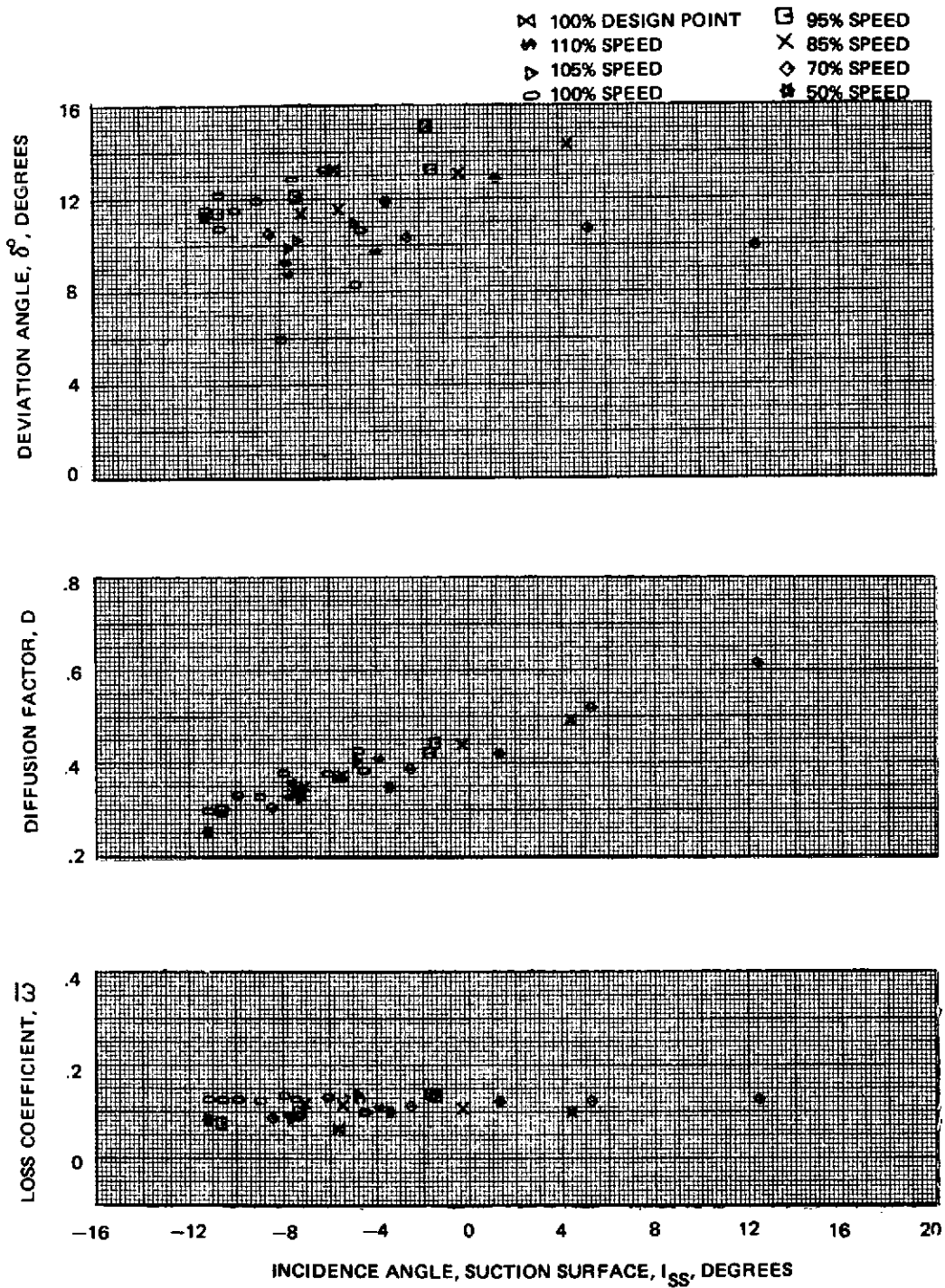


Figure 61k Blade Element Performance with Uniform Inlet Flow – Stator 1  
 95% Span

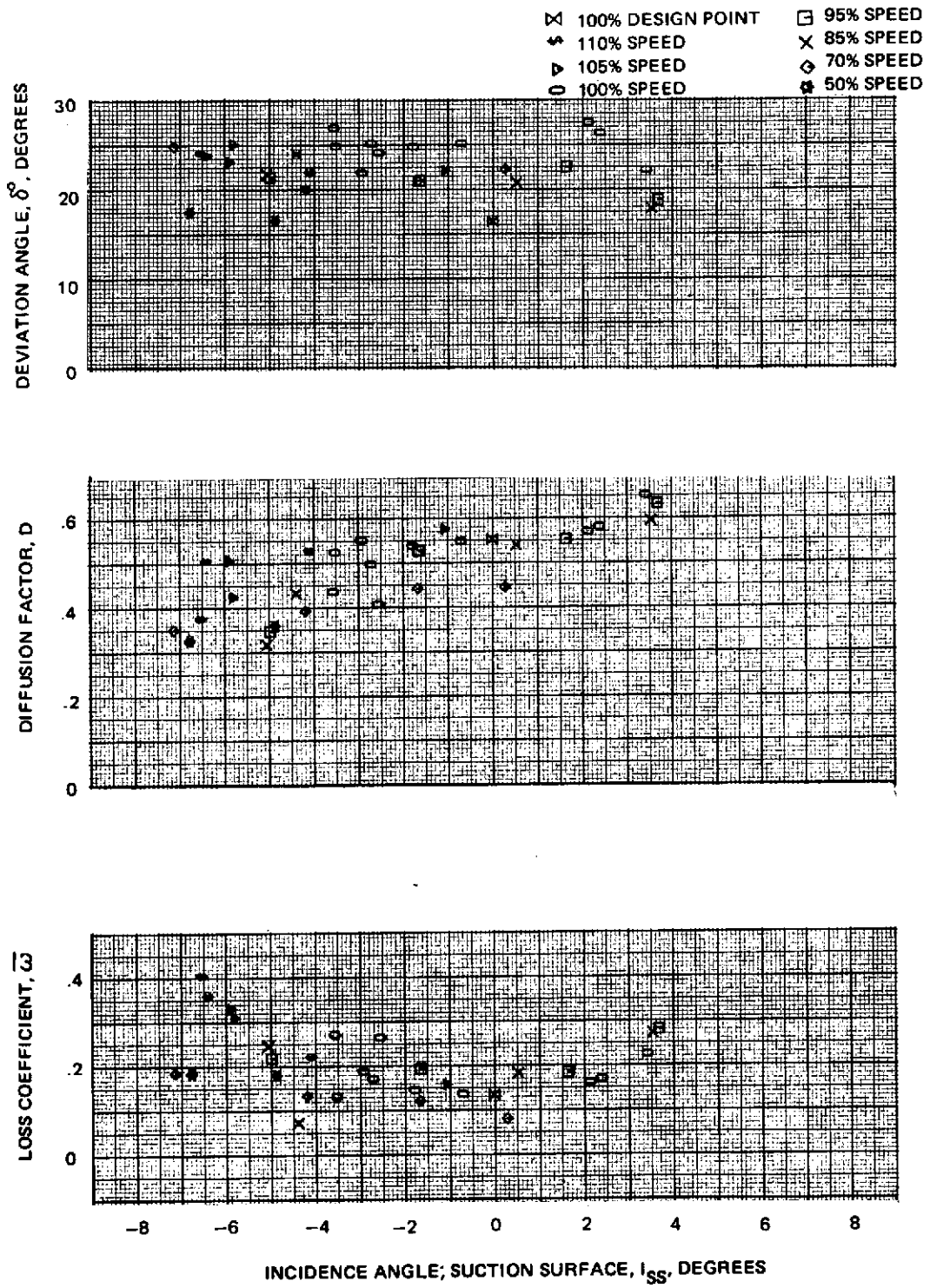


Figure 62a Blade Element Performance With Uniform Inlet Flow – Rotor 2  
4% Span

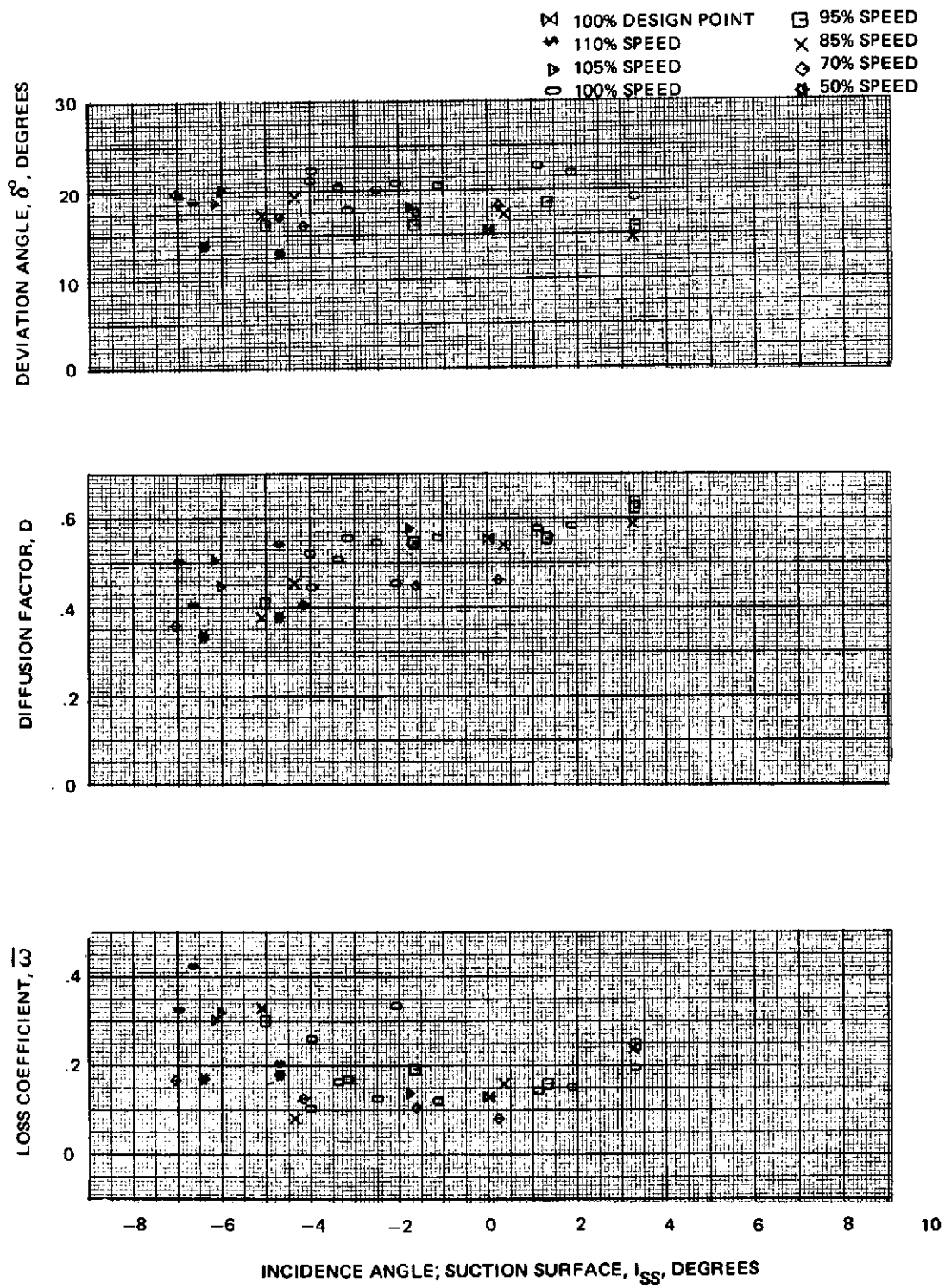


Figure 62b Blade Element Performance With Uniform Inlet Flow – Rotor 2  
8% Span

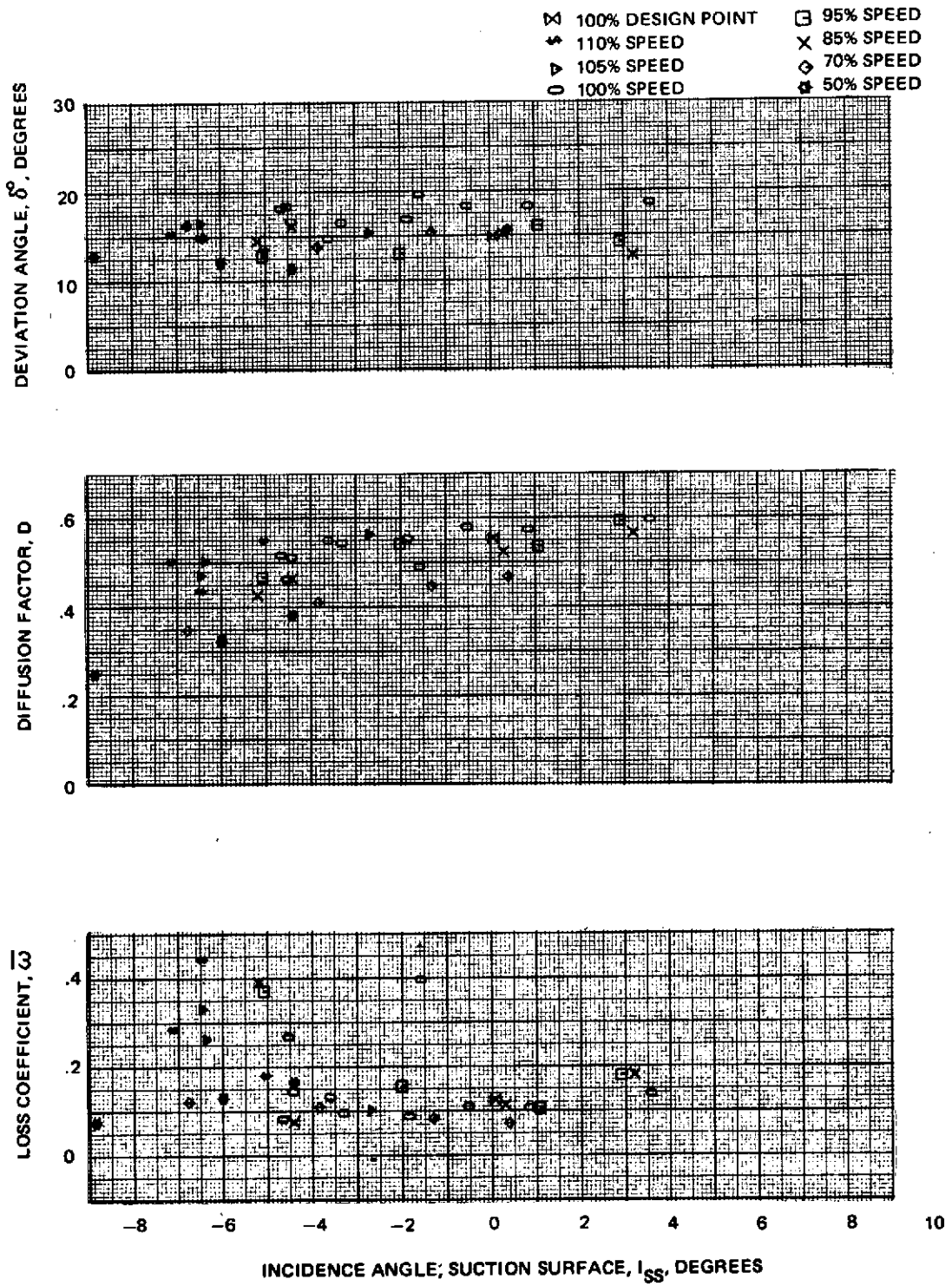


Figure 62c Blade Element Performance With Uniform Inlet Flow – Rotor 2  
 12% Span

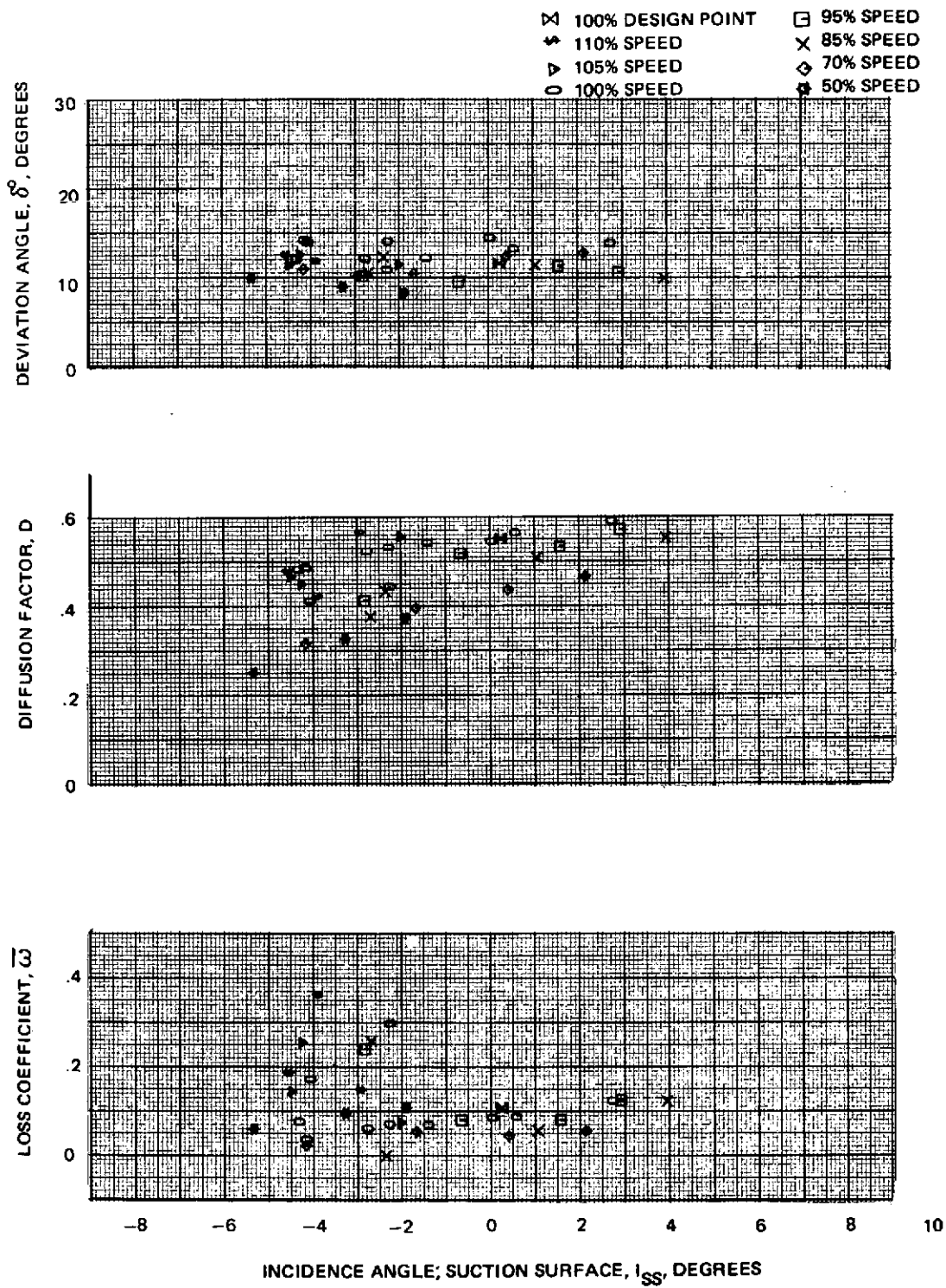


Figure 62d Blade Element Performance With Uniform Inlet Flow – Rotor 2  
25% Span

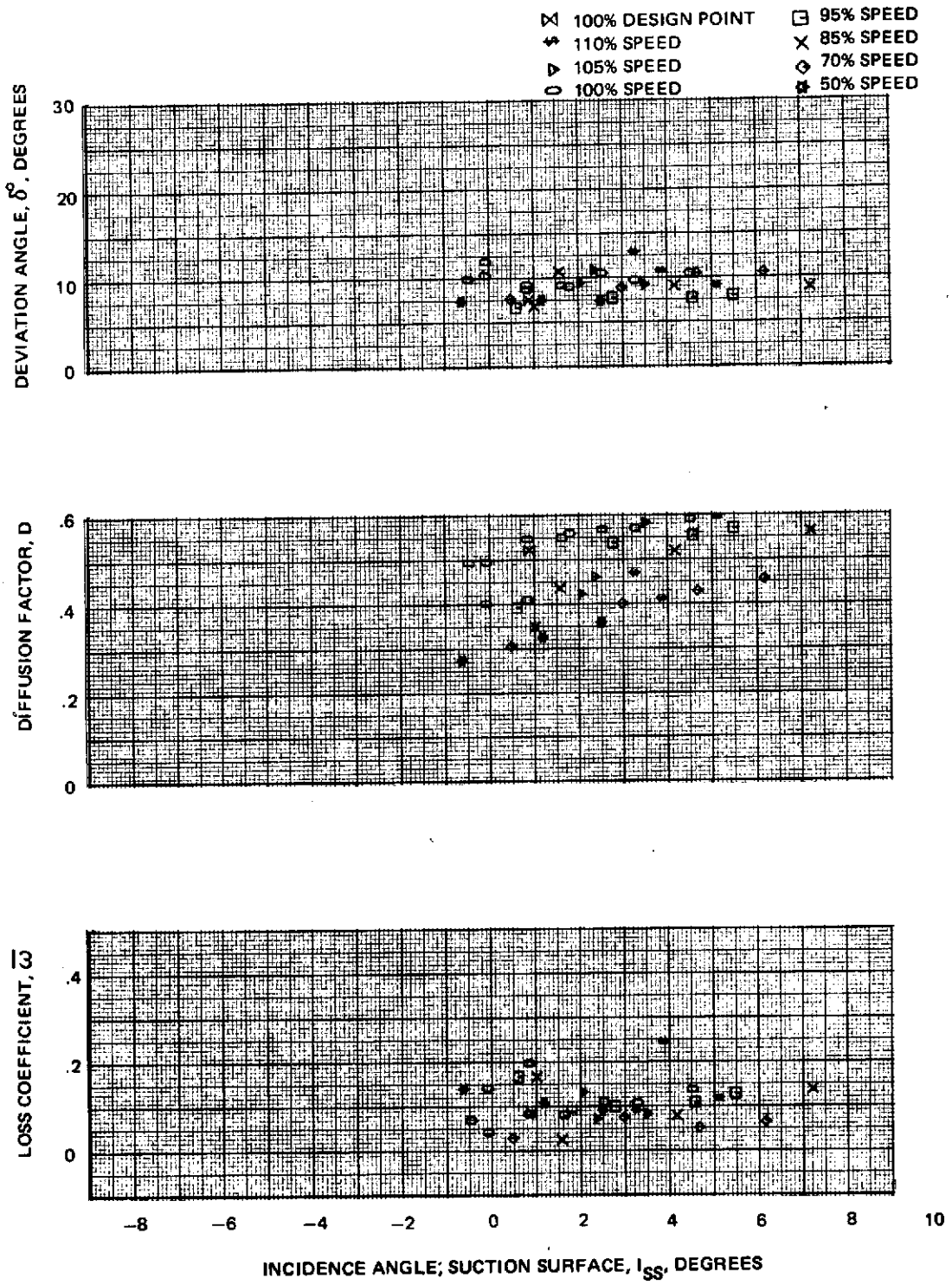


Figure 62e Blade Element Performance With Uniform Inlet Flow – Rotor 2  
45% Span

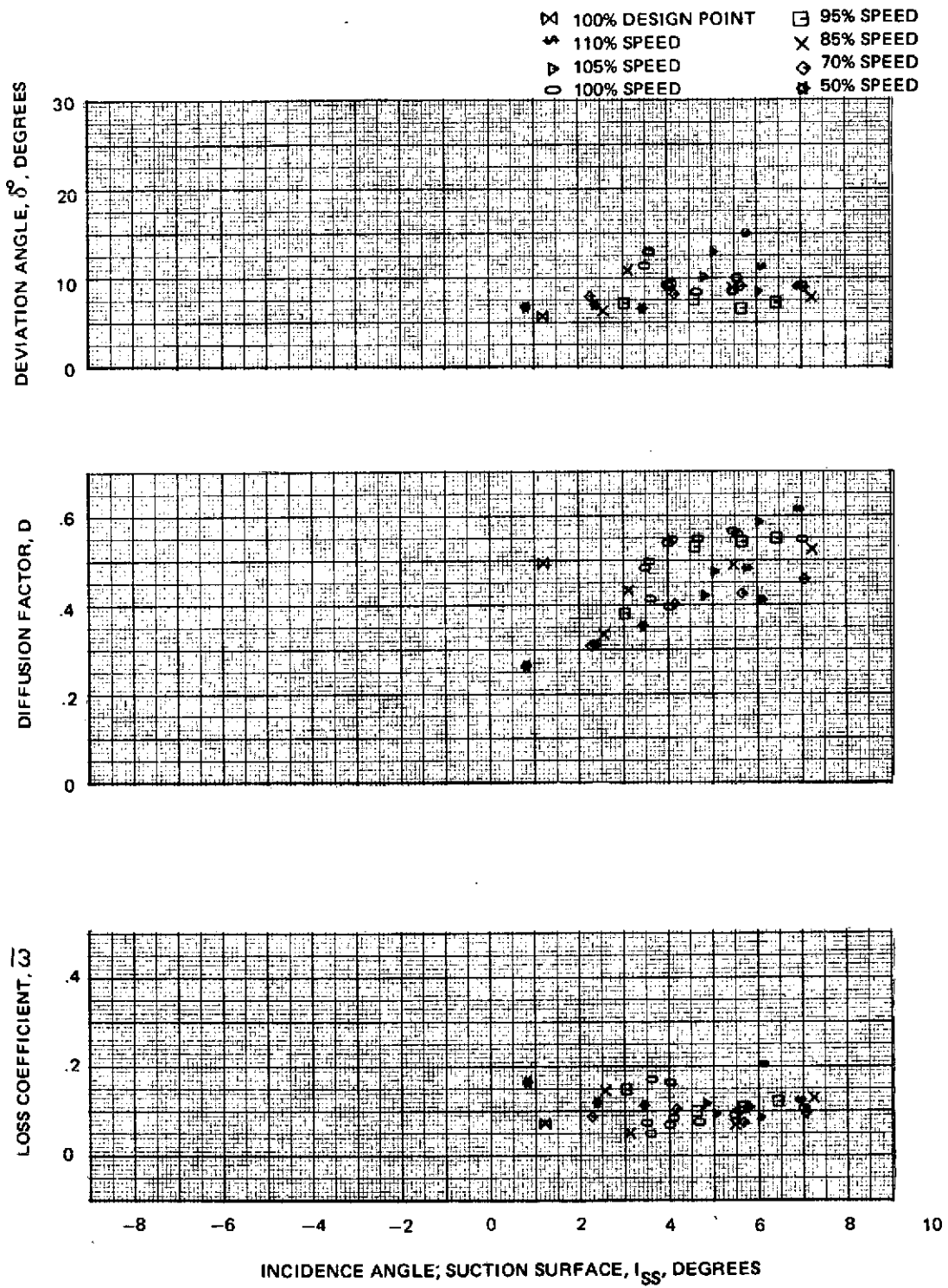


Figure 62f Blade Element Performance With Uniform Inlet Flow -- Rotor 2  
55% Span



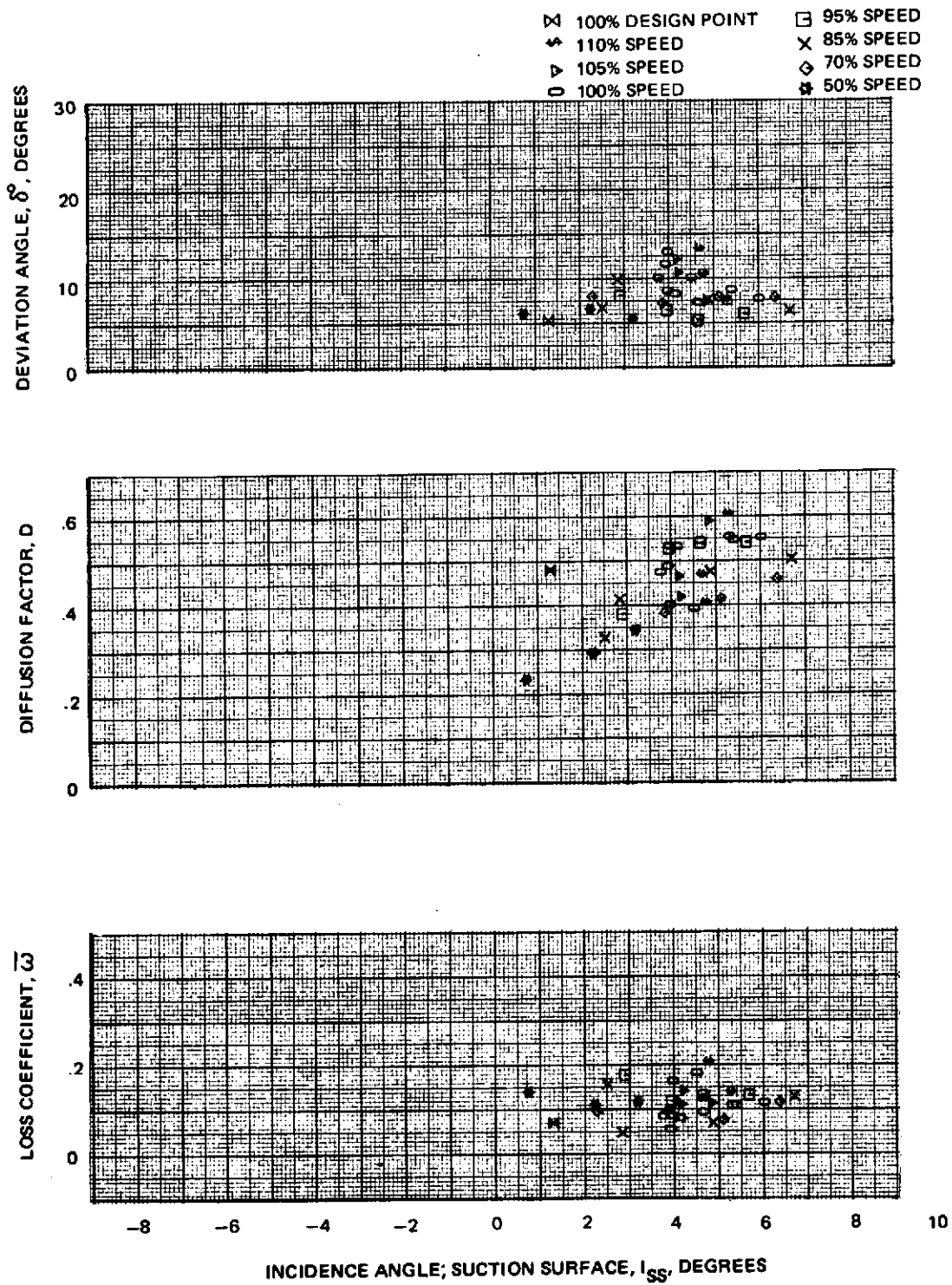


Figure 62g Blade Element Performance With Uniform Inlet Flow – Rotor 2  
60% Span

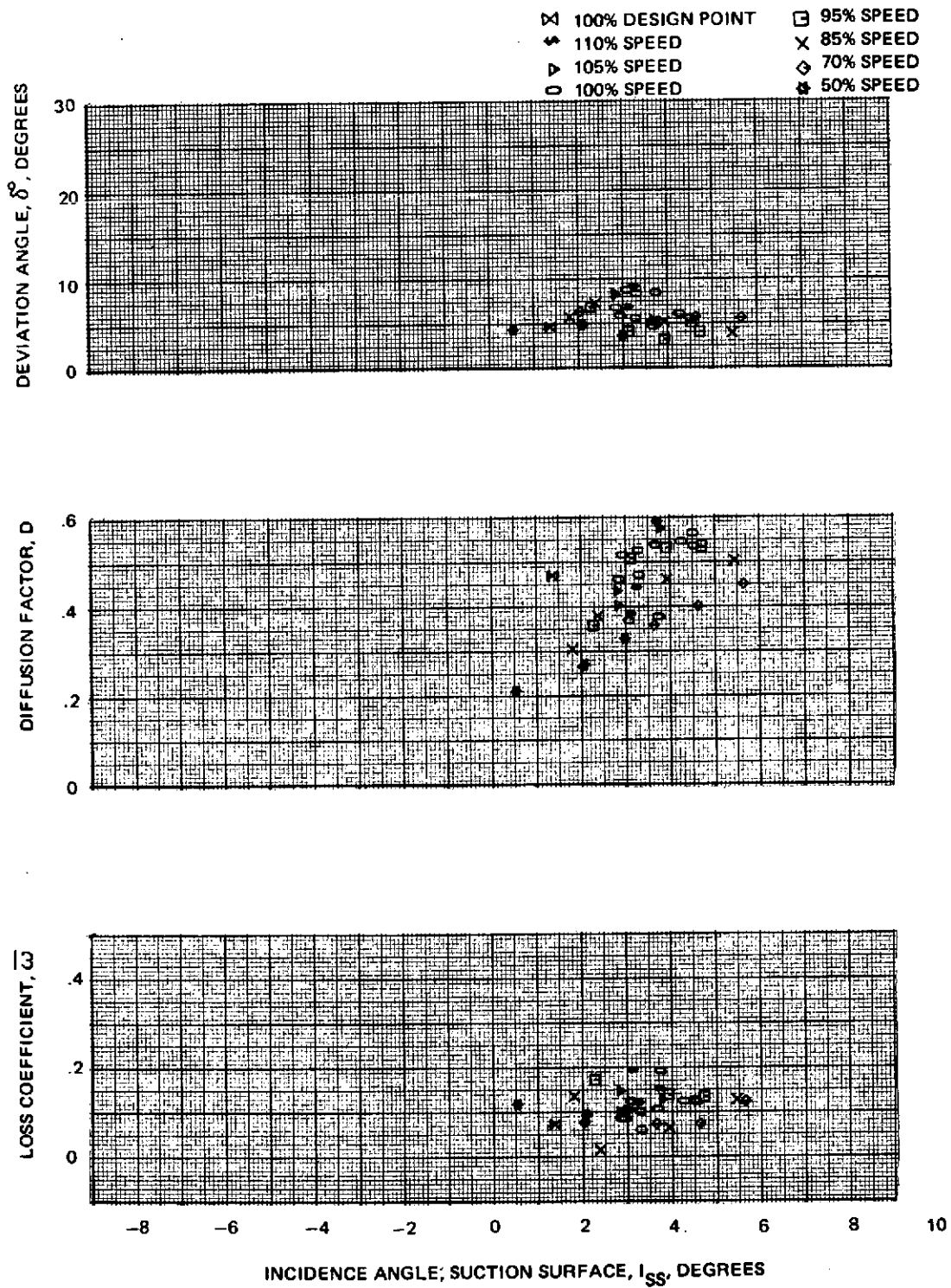


Figure 62h Blade Element Performance With Uniform Inlet Flow – Rotor 2  
66% Span

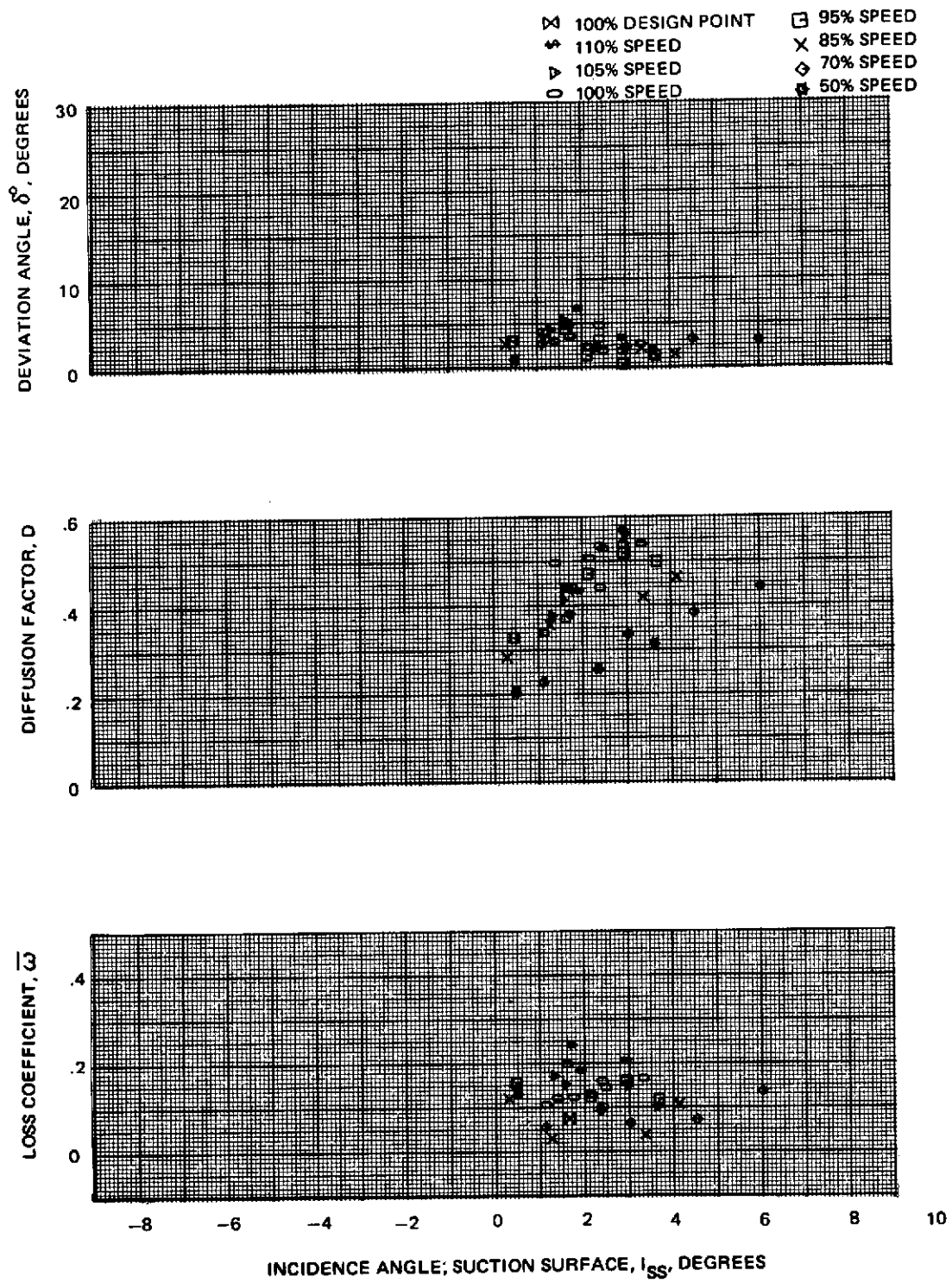
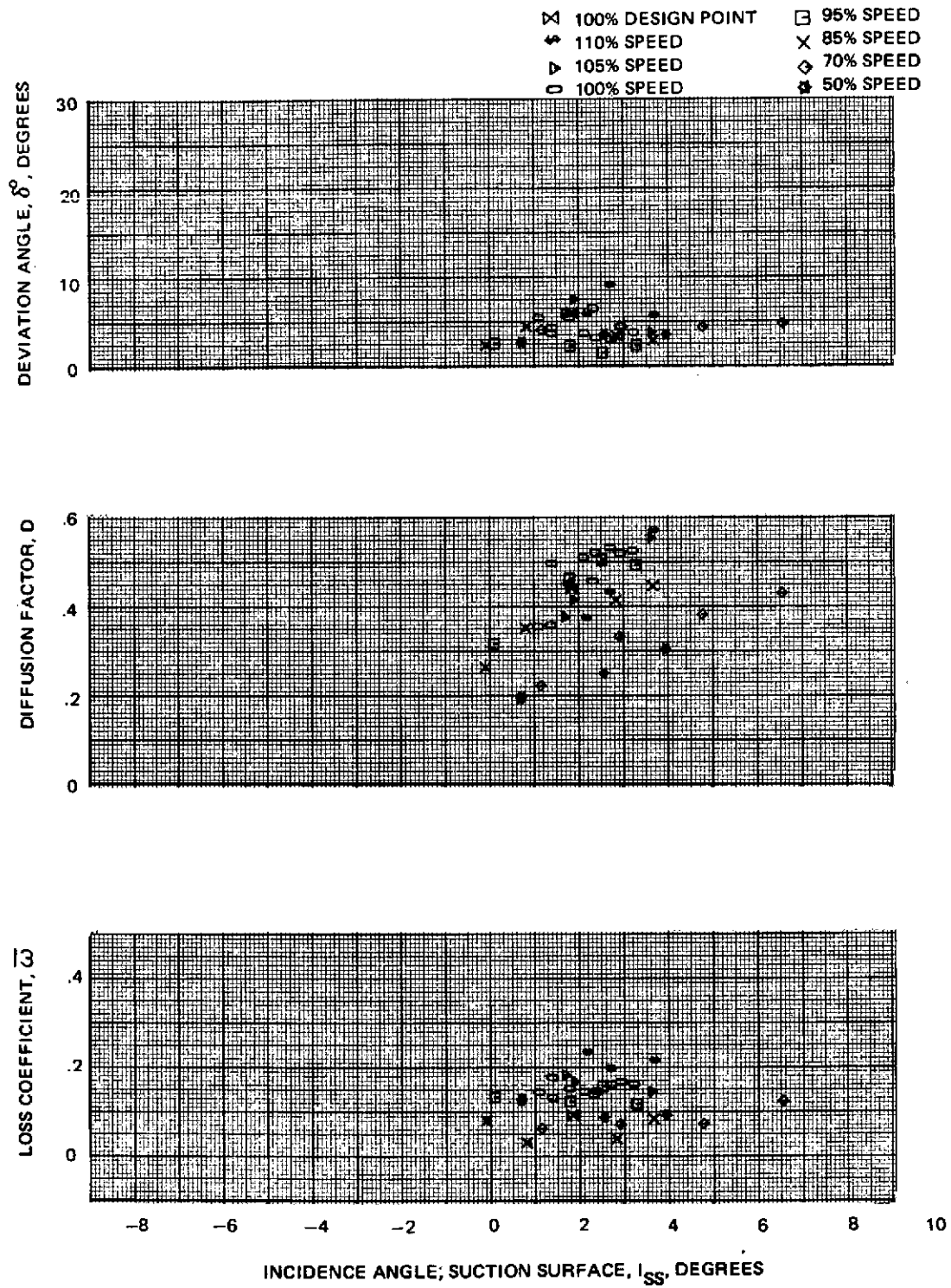


Figure 62i Blade Element Performance With Uniform Inlet Flow – Rotor 2  
'82% Span



110 Figure 62j Blade Element Performance With Uniform Inlet Flow – Rotor 2  
88% Span

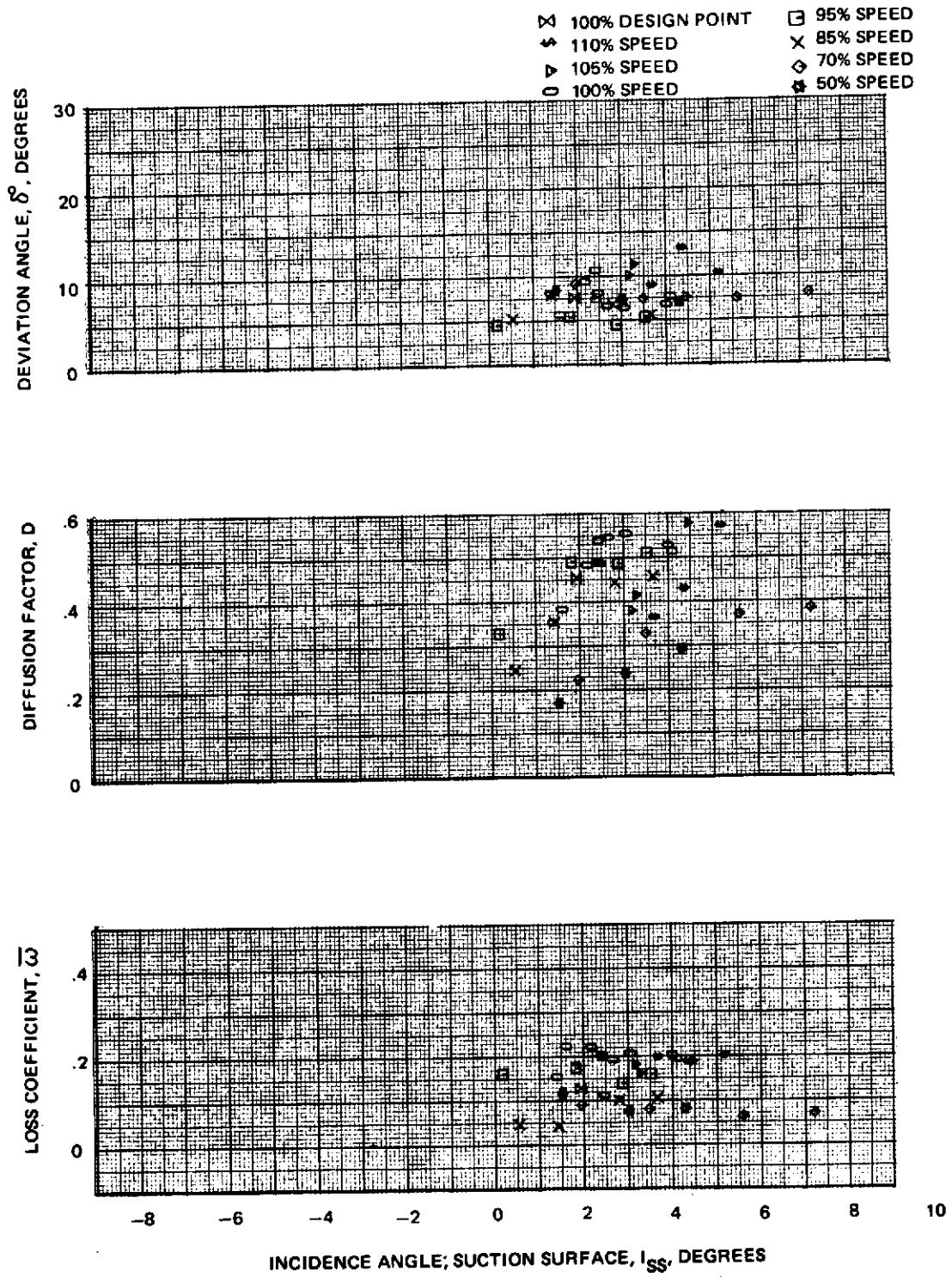


Figure 62k Blade Element Performance With Uniform Inlet Flow – Rotor 2  
 94% Span

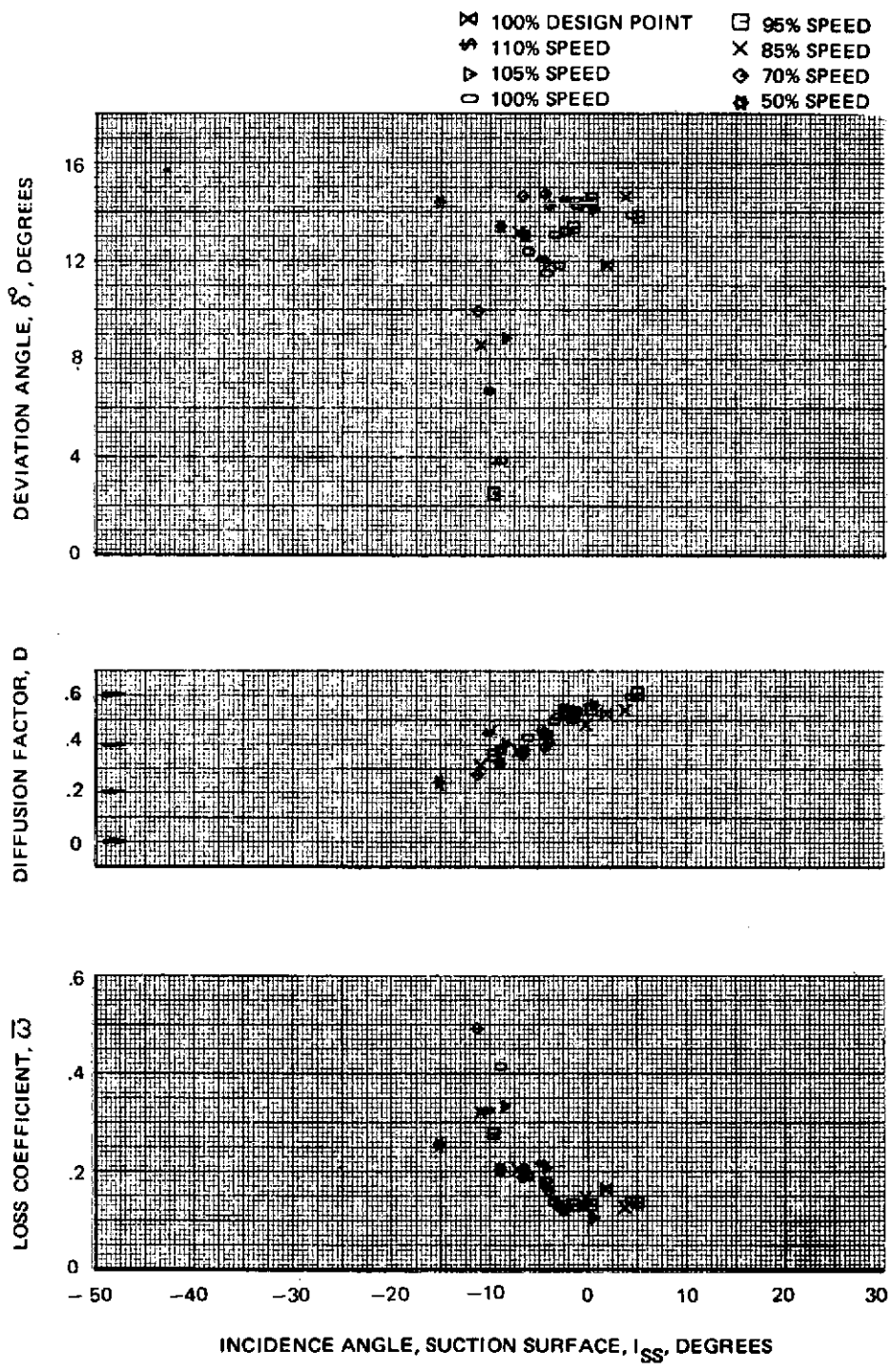
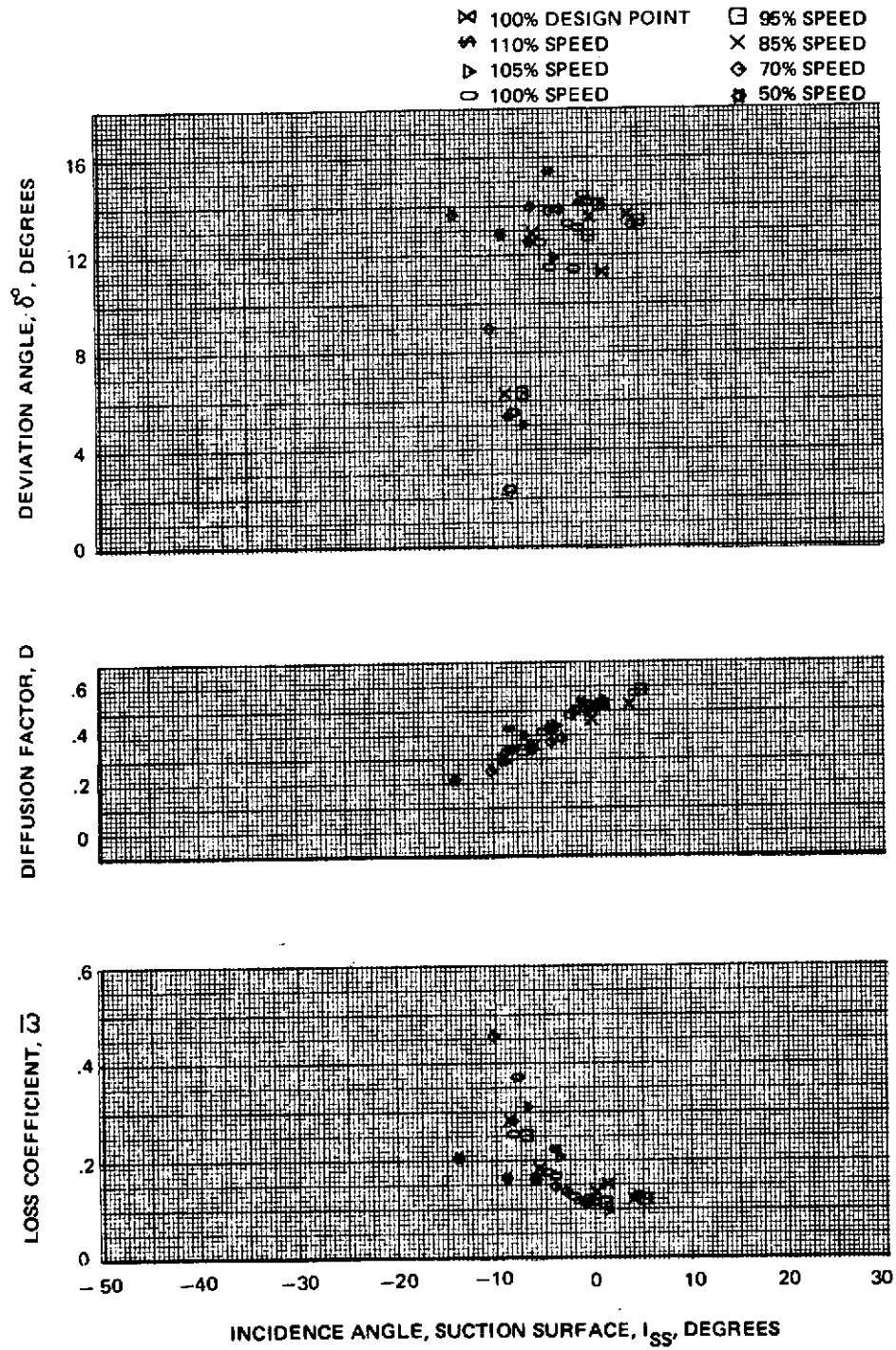


Figure 63a Blade Element Performance With Uniform Inlet Flows – Stator 2  
3% Span



REPRODUCIBILITY OF THE ORIGINAL PAGE IS POOR

Figure 63b Blade Element Performance With Uniform Inlet Flows -- Stator 2  
7% Span

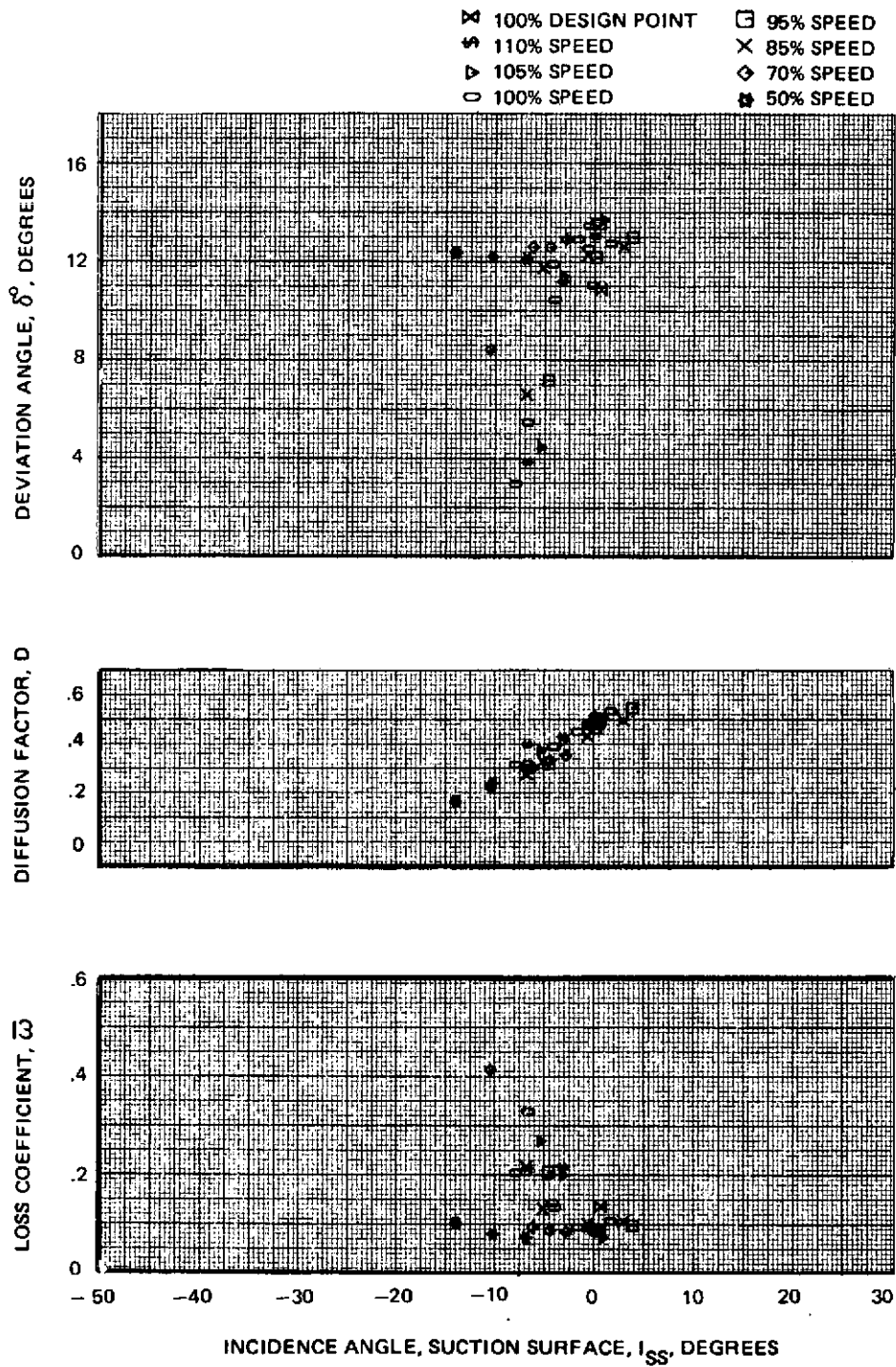


Figure 63c Blade Element Performance With Uniform Inlet Flows – Stator 2  
11% Span



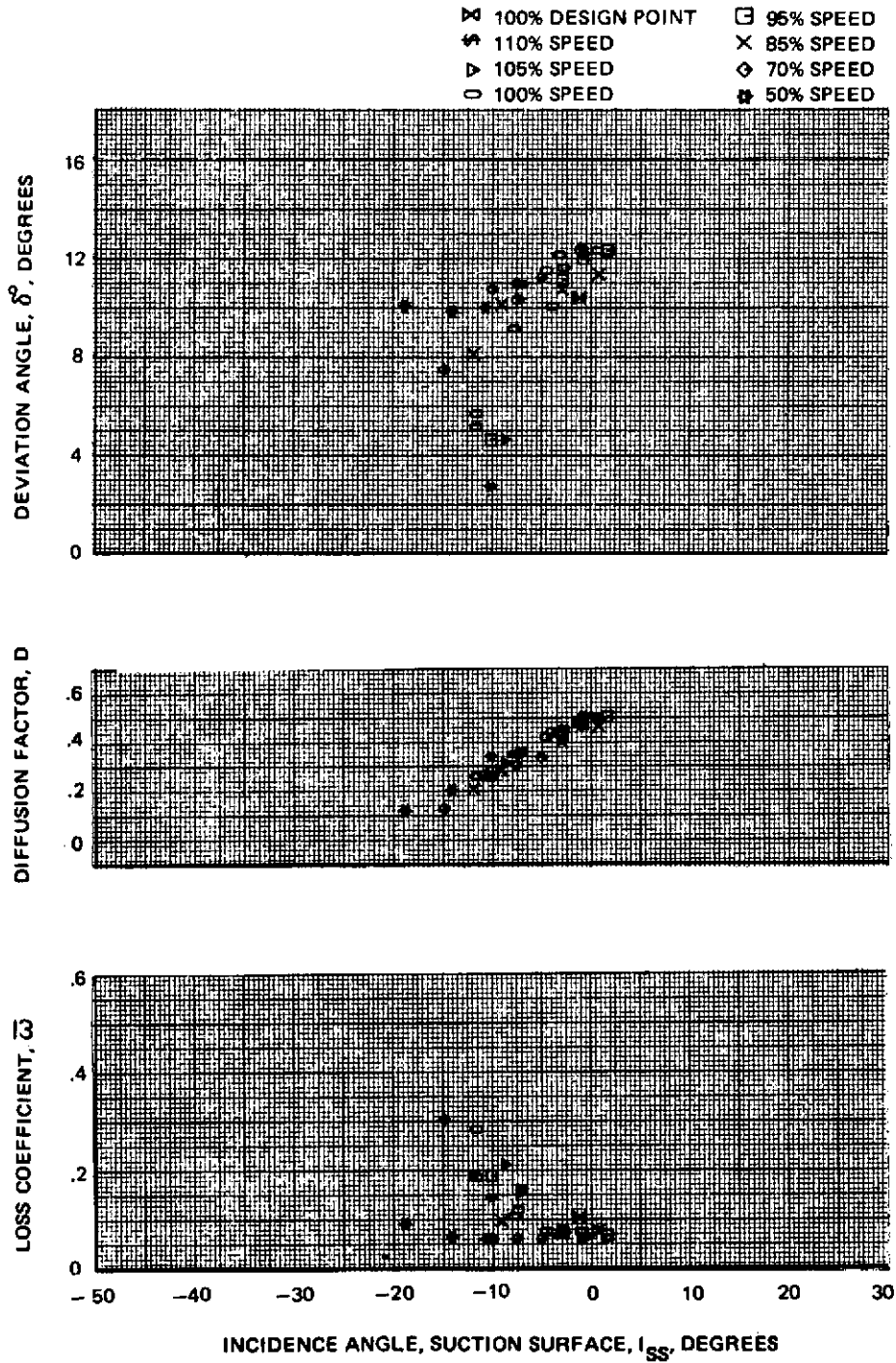


Figure 63d Blade Element Performance With Uniform Inlet Flows – Stator 2  
23% Span

REPRODUCIBILITY OF THE  
 ORIGINAL PAGE IS POOR

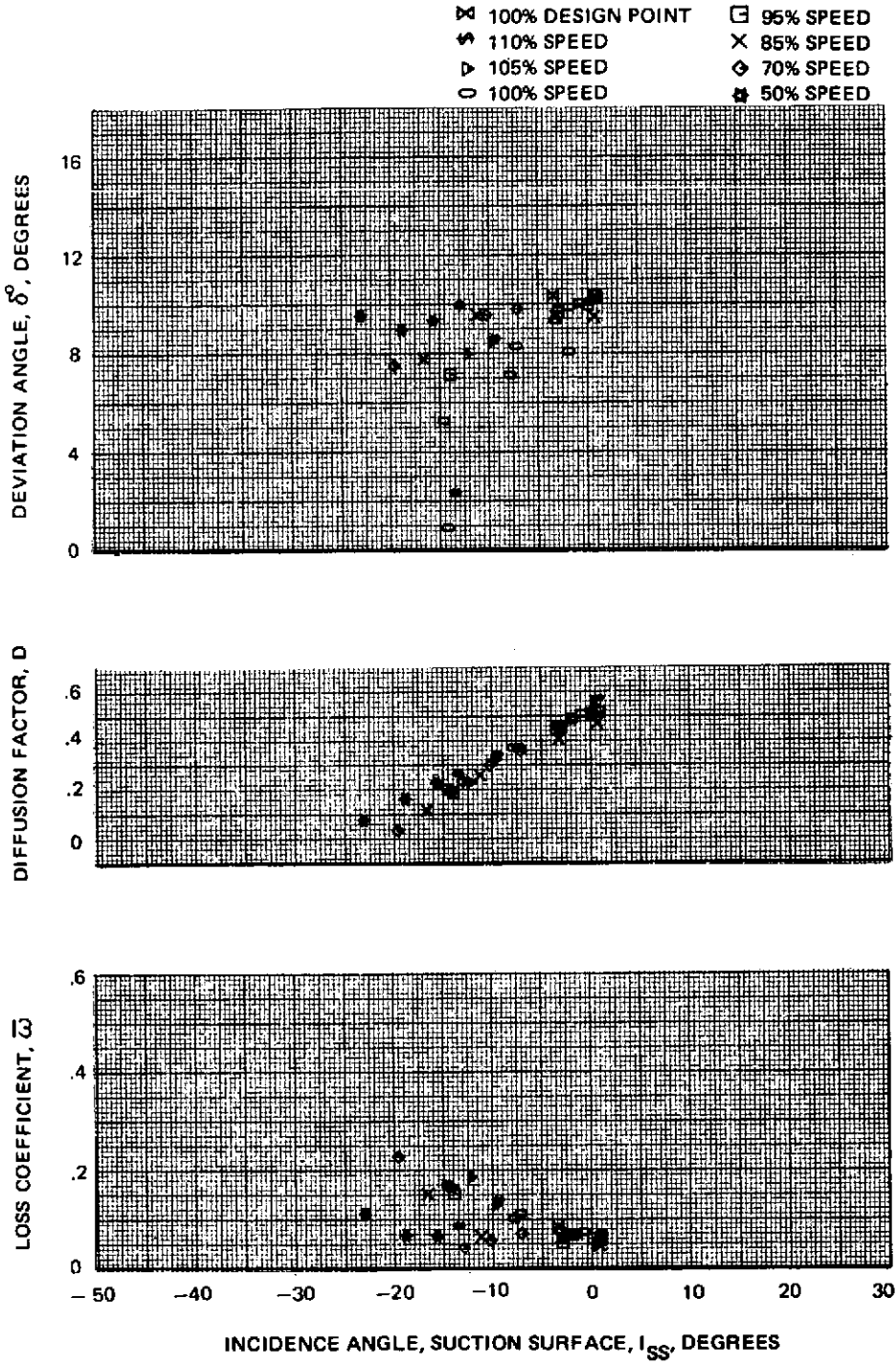
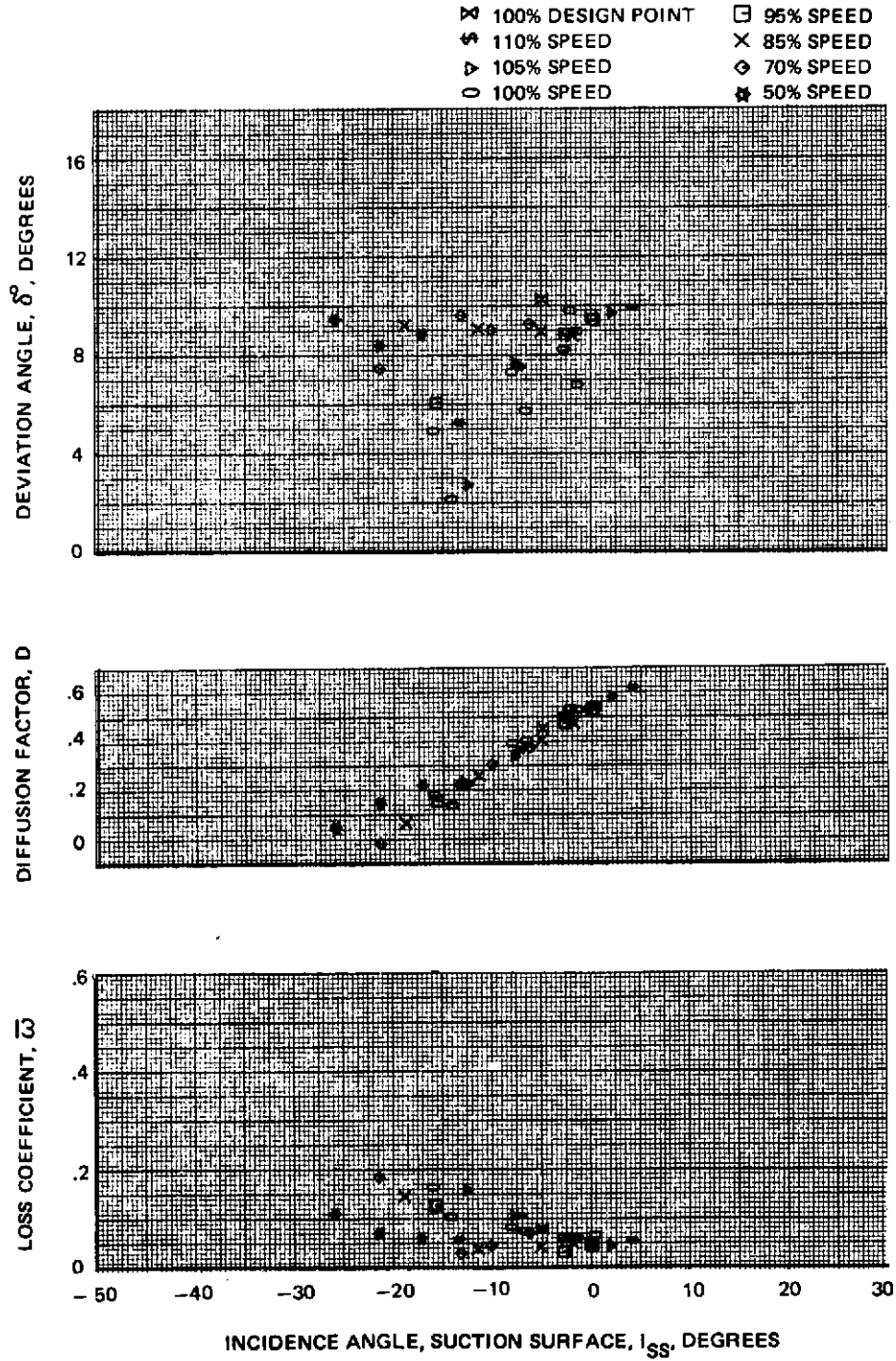


Figure 63e Blade Element Performance With Uniform Inlet Flows – Stator 2  
42% Span



**Figure 63f** Blade Element Performance With Uniform Inlet Flows – Stator 2  
53% Span

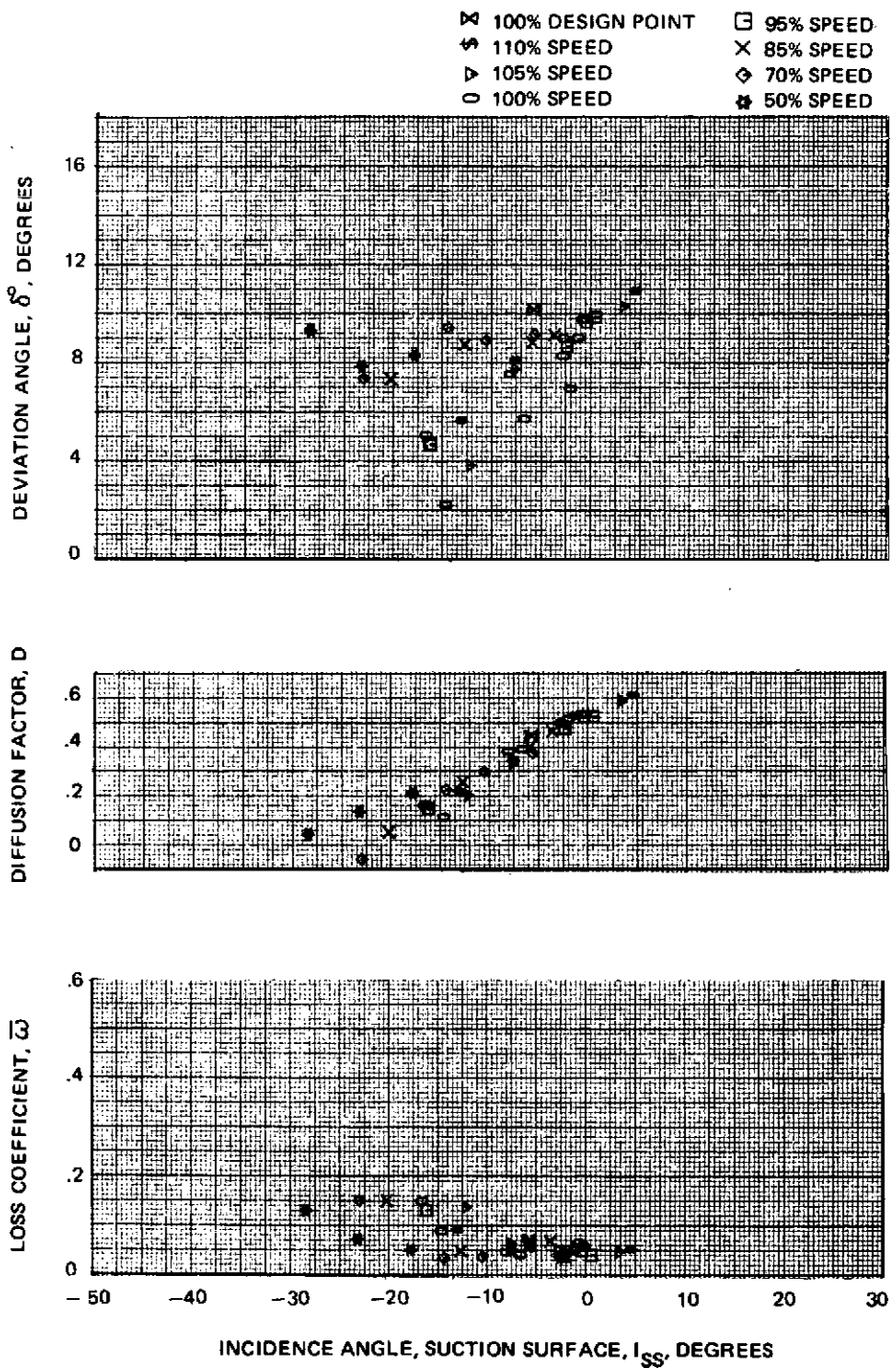
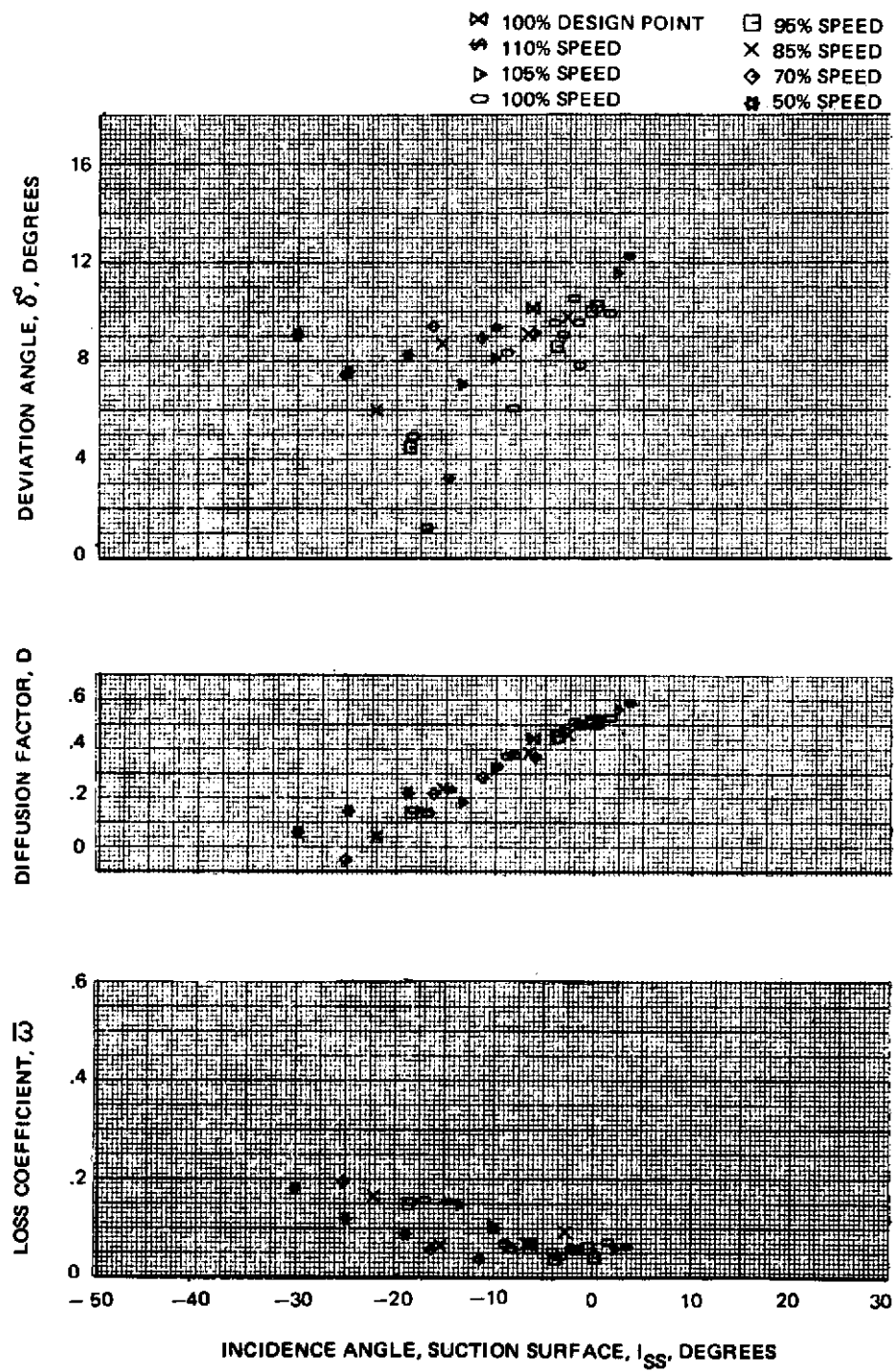


Figure 63g Blade Element Performance With Uniform Inlet Flows – Stator 2  
58% Span



**Figure 63h** Blade Element Performance With Uniform Inlet Flows – Stator 2  
64% Span

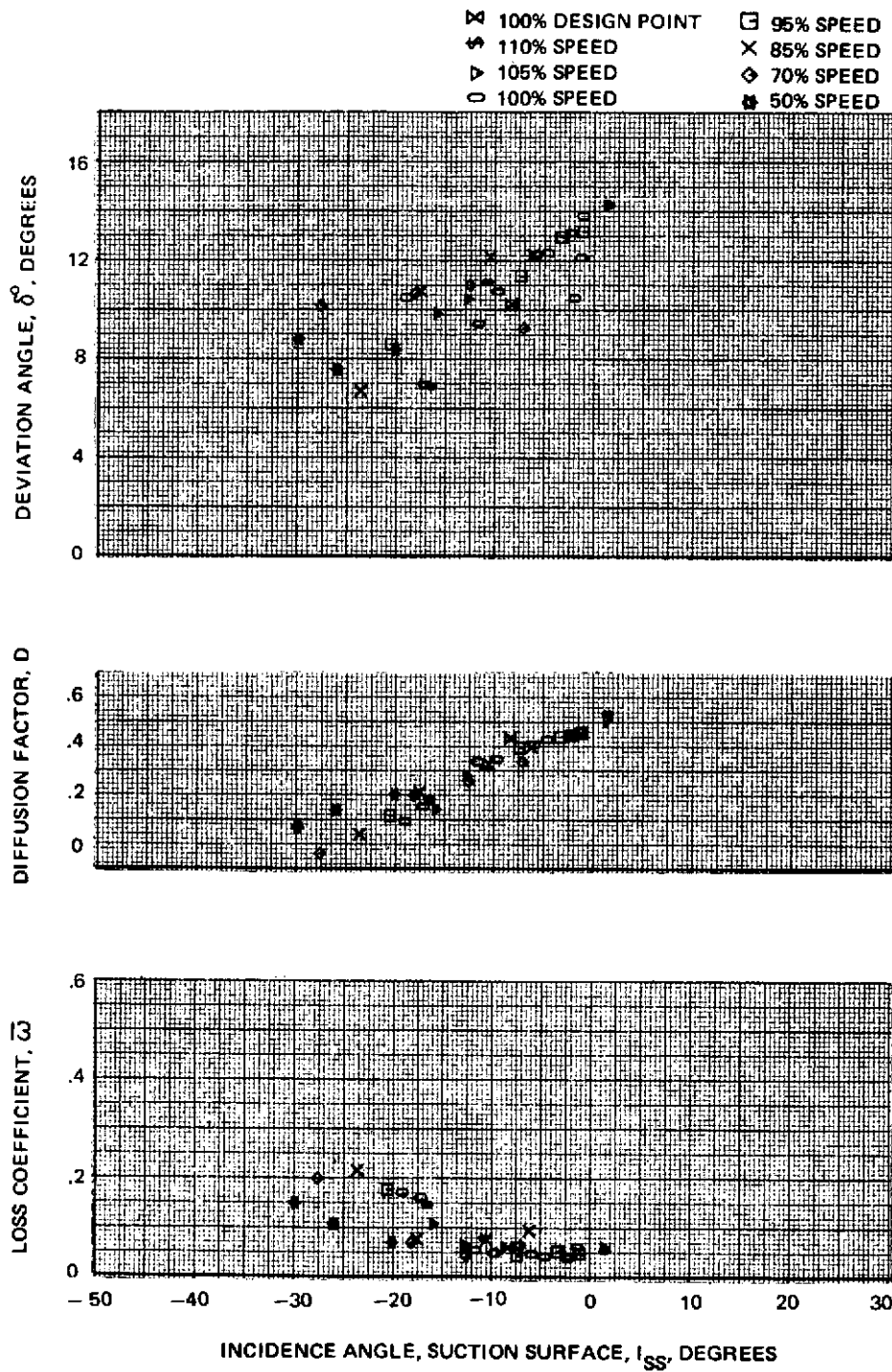


Figure 63i Blade Element Performance With Uniform Inlet Flows – Stator 2  
82% Span

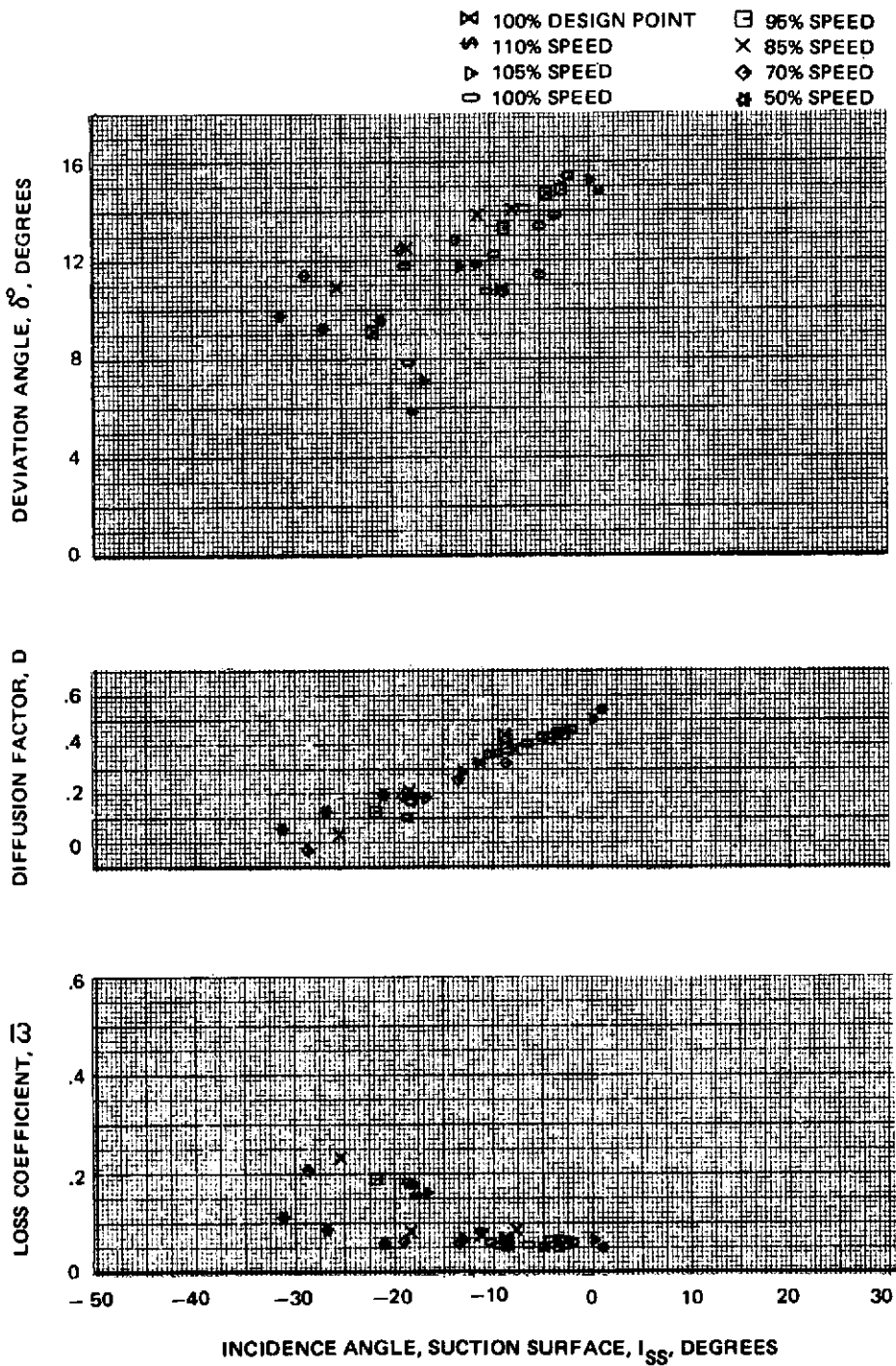


Figure 63j Blade Element Performance With Uniform Inlet Flows – Stator 2  
88% Span

REPRODUCTION OF THE  
ORIGINAL PAGE IS POOR

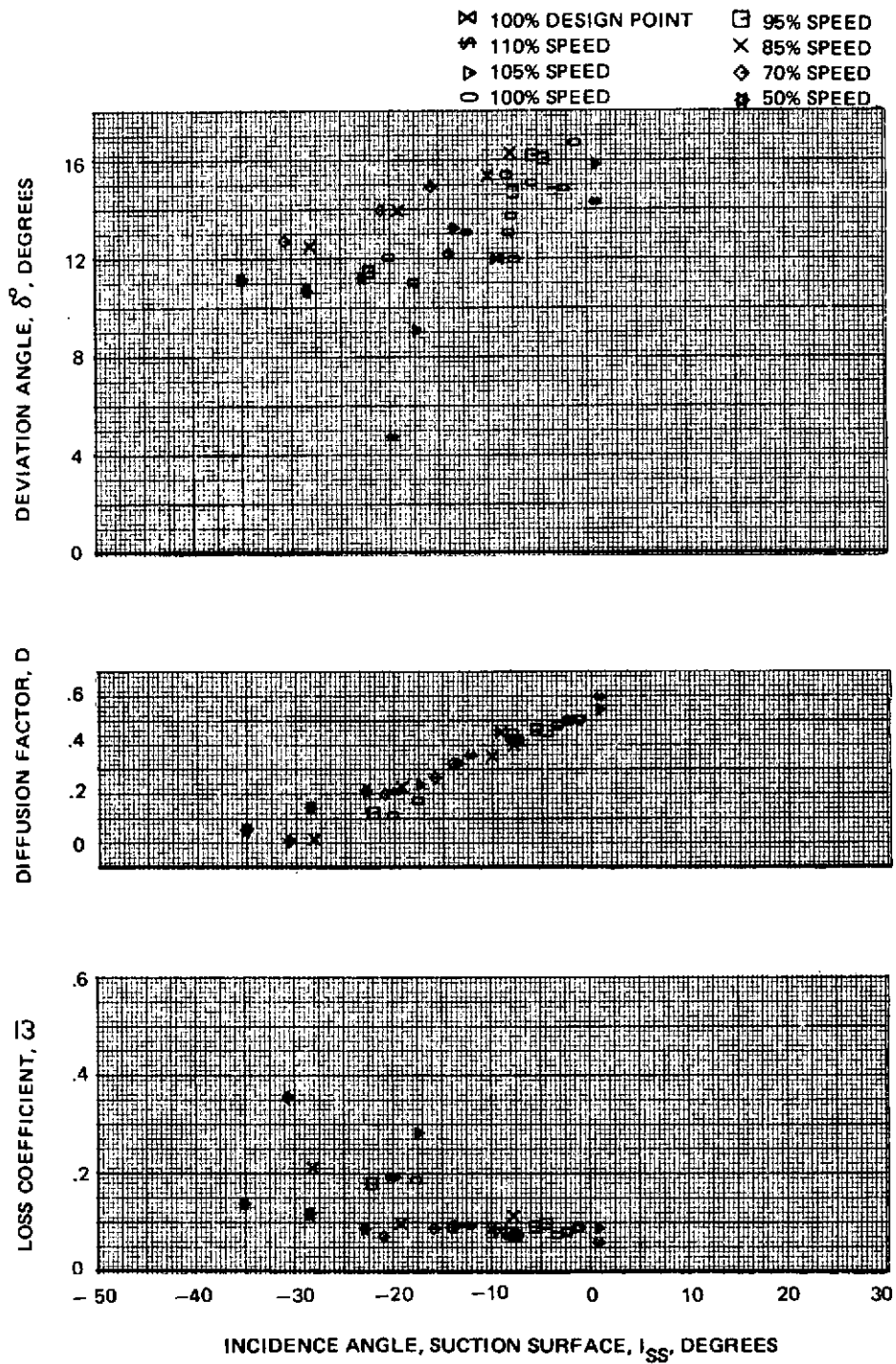


Figure 63k Blade Element Performance With Uniform Inlet Flows – Stator 2  
94% Span



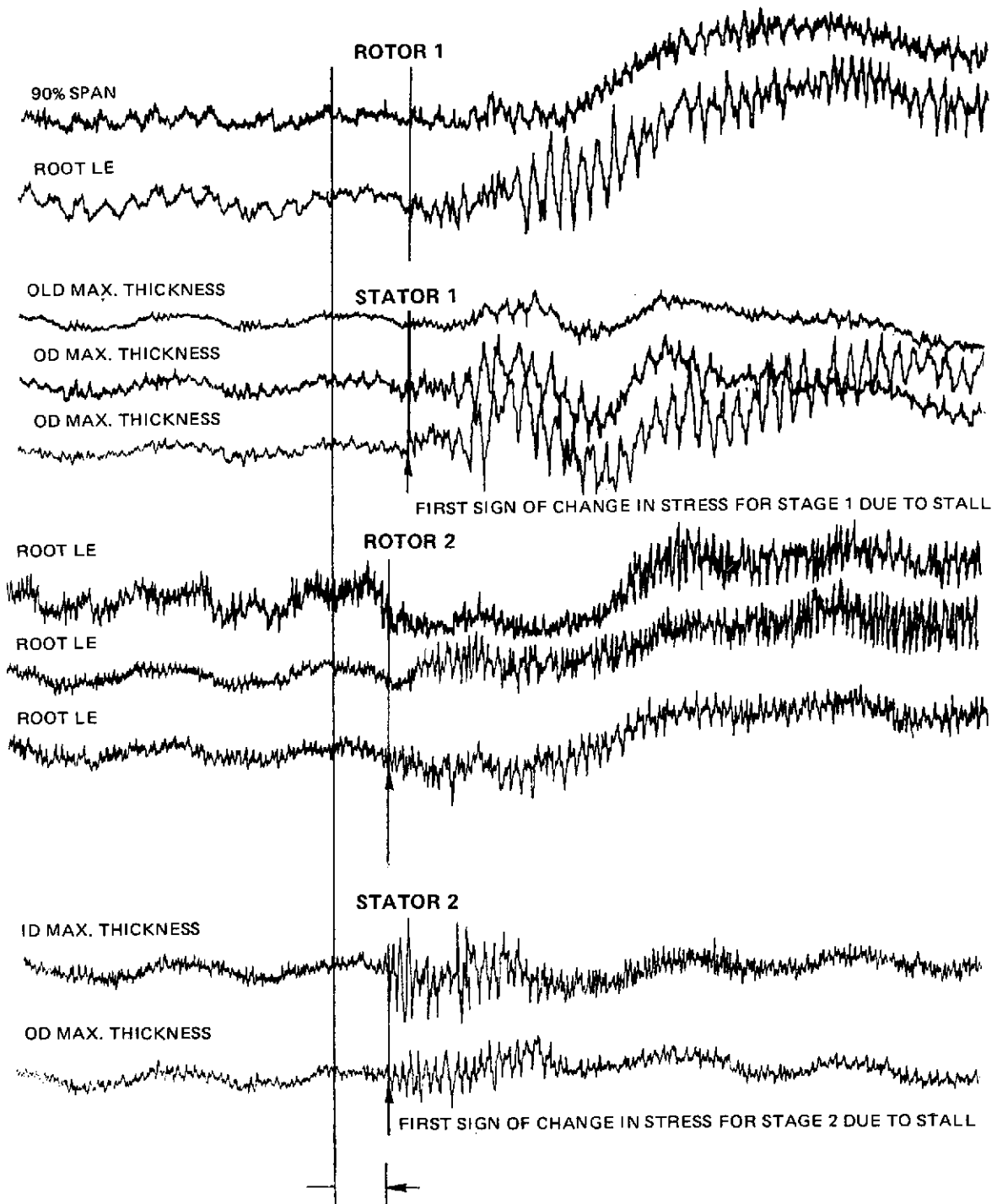


Figure 64 Oscillograph Trace During Surge at Design Speed for Uniform Inlet Flow

REPRODUCIBILITY OF THE  
ORIGINAL PAGE IS POOR

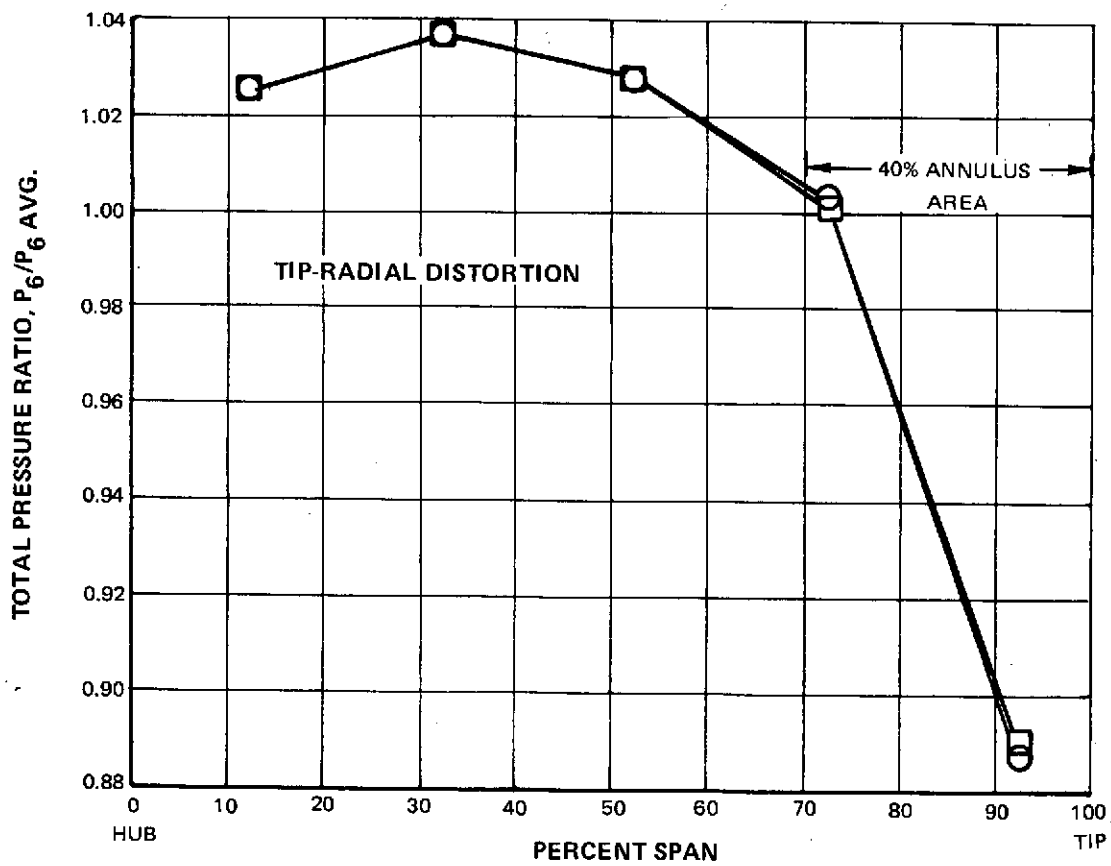
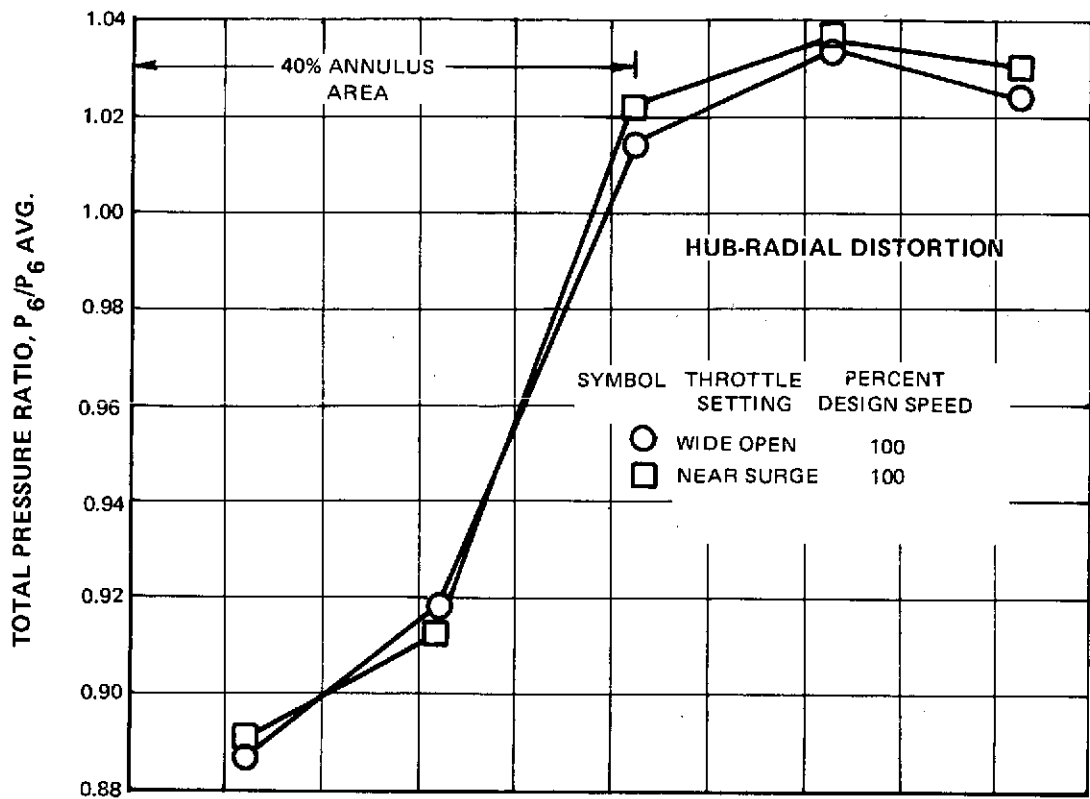


Figure 65 First Rotor Inlet Total Pressure Ratio Versus Span for Radially Distorted Inlet Flow

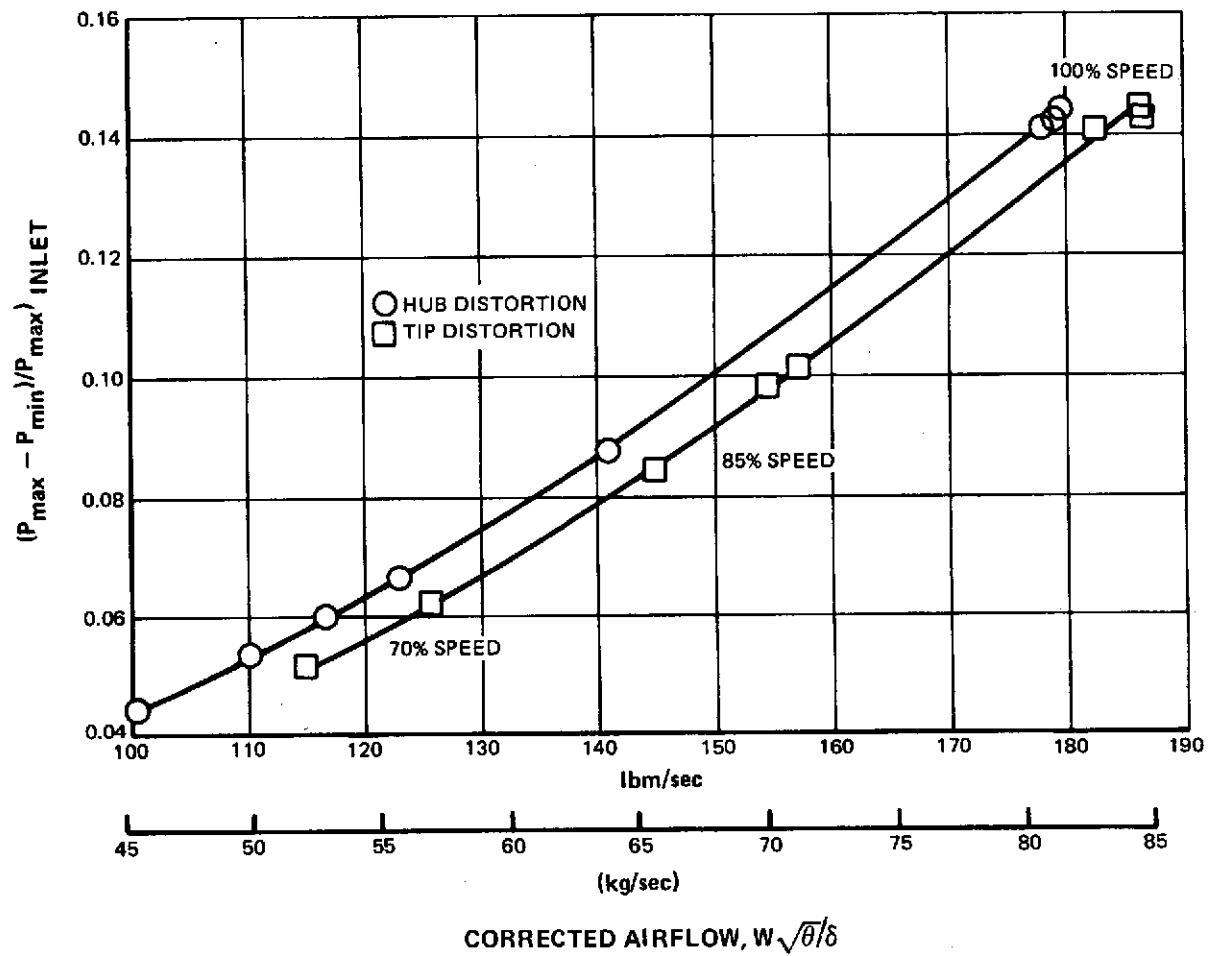


Figure 66 Inlet Total Pressure Distortion Parameter Versus Inlet Corrected Flow for Radial Distortions

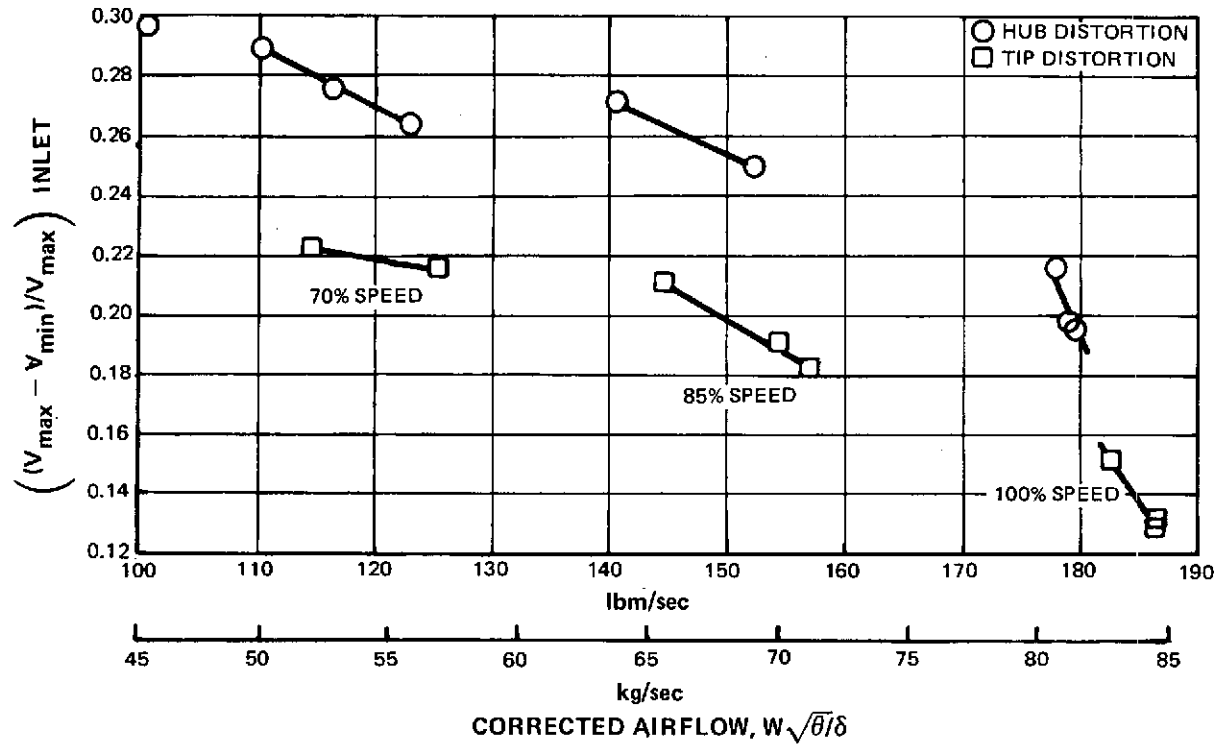


Figure 67 Inlet Meridional Velocity Distortion Parameter Versus Inlet Corrected Flow for Radial Distortions

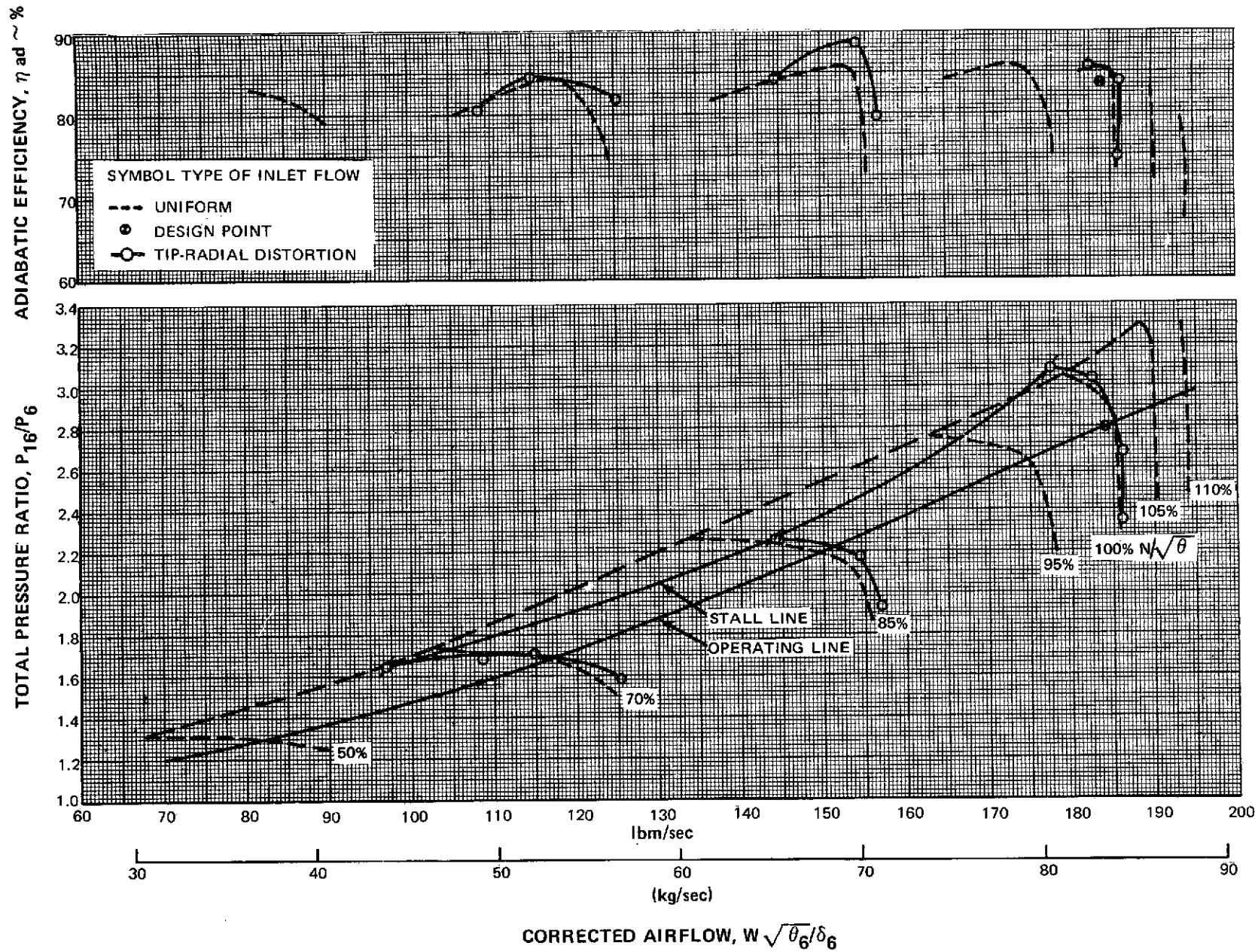


Figure 68 Fan Overall Performance with Tip Radially Distorted Inlet Flow

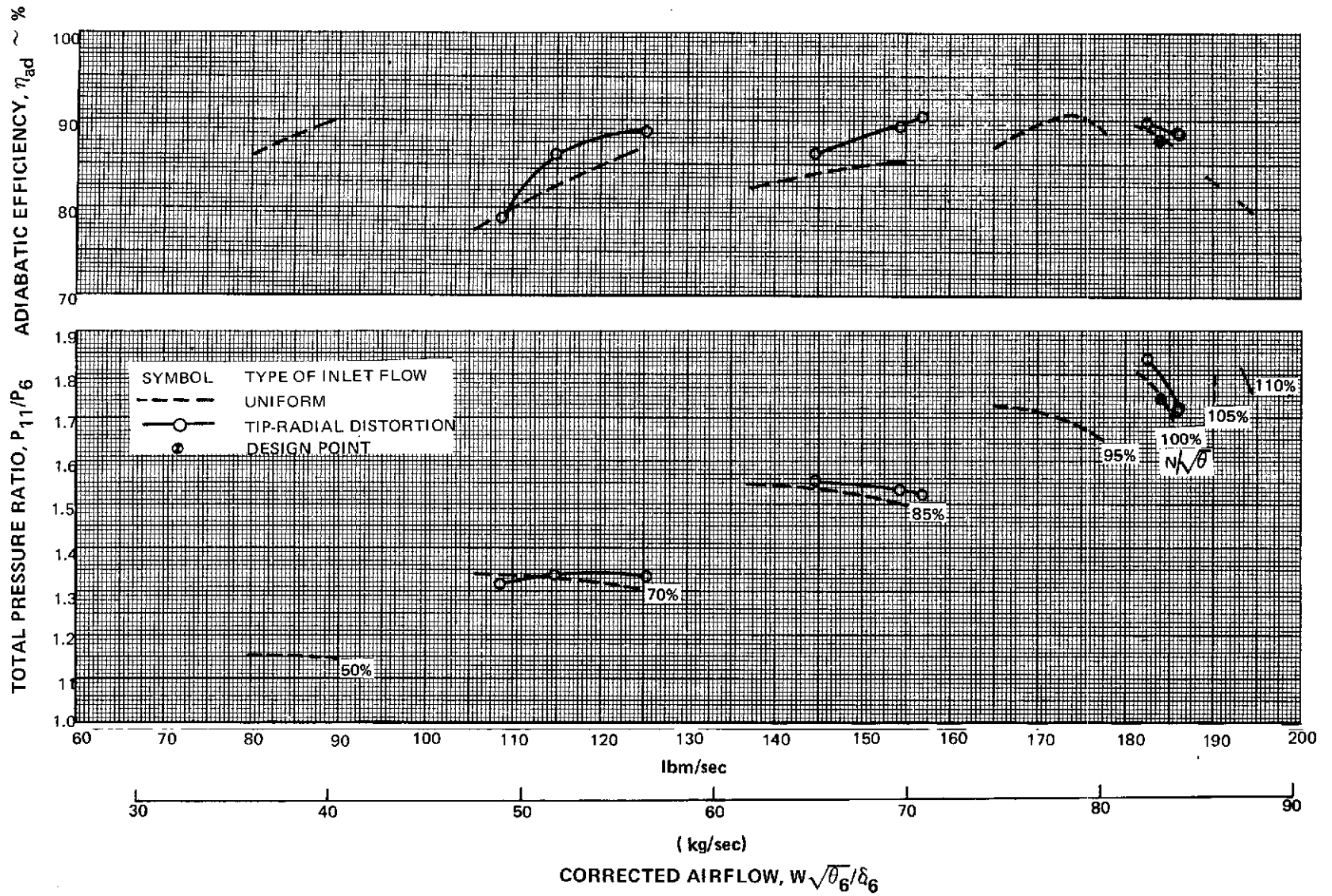


Figure 69 First Stage Performance with Tip Radially Distorted Inlet Flow

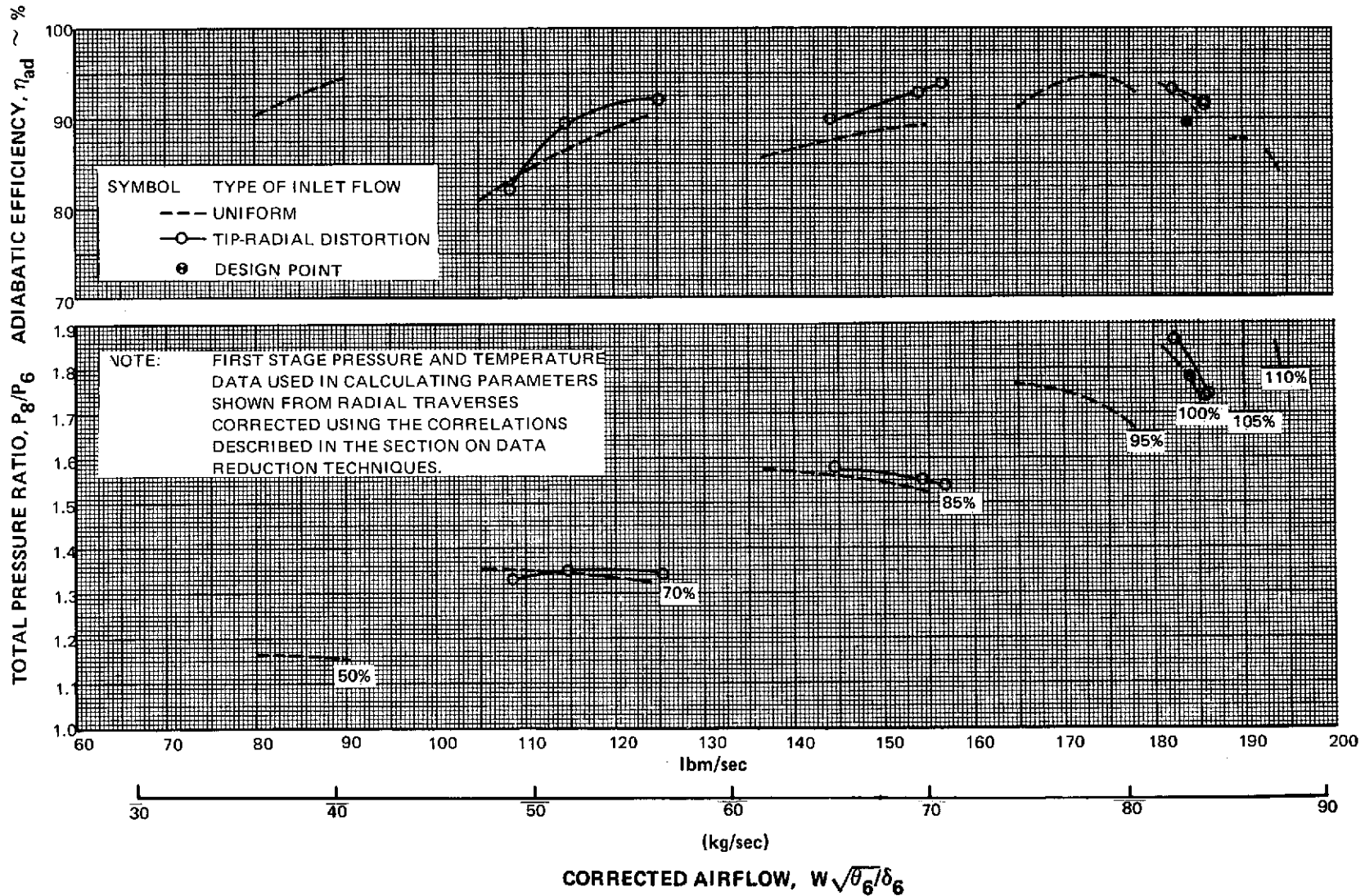


Figure 70 First Rotor Performance with Tip Radially Distorted Inlet Flow

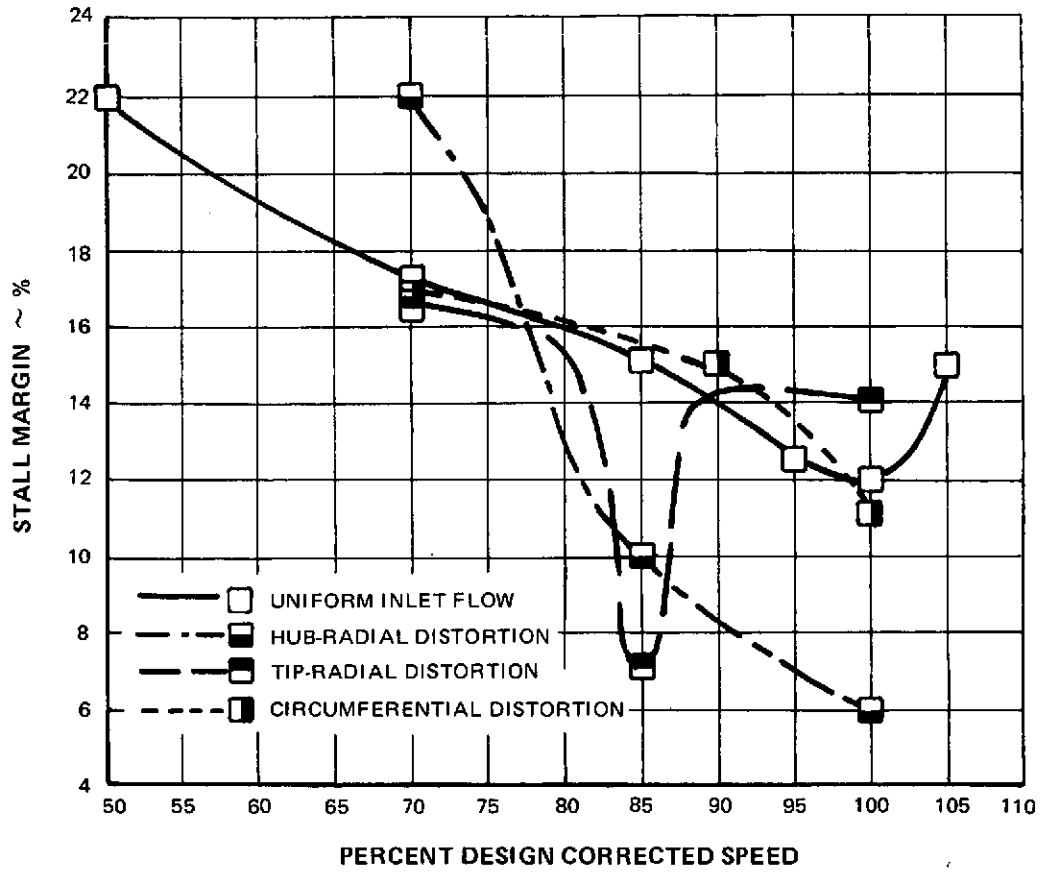


Figure 71 Stall Margin Versus Corrected Speed for Uniform and Distorted Inlet Flows



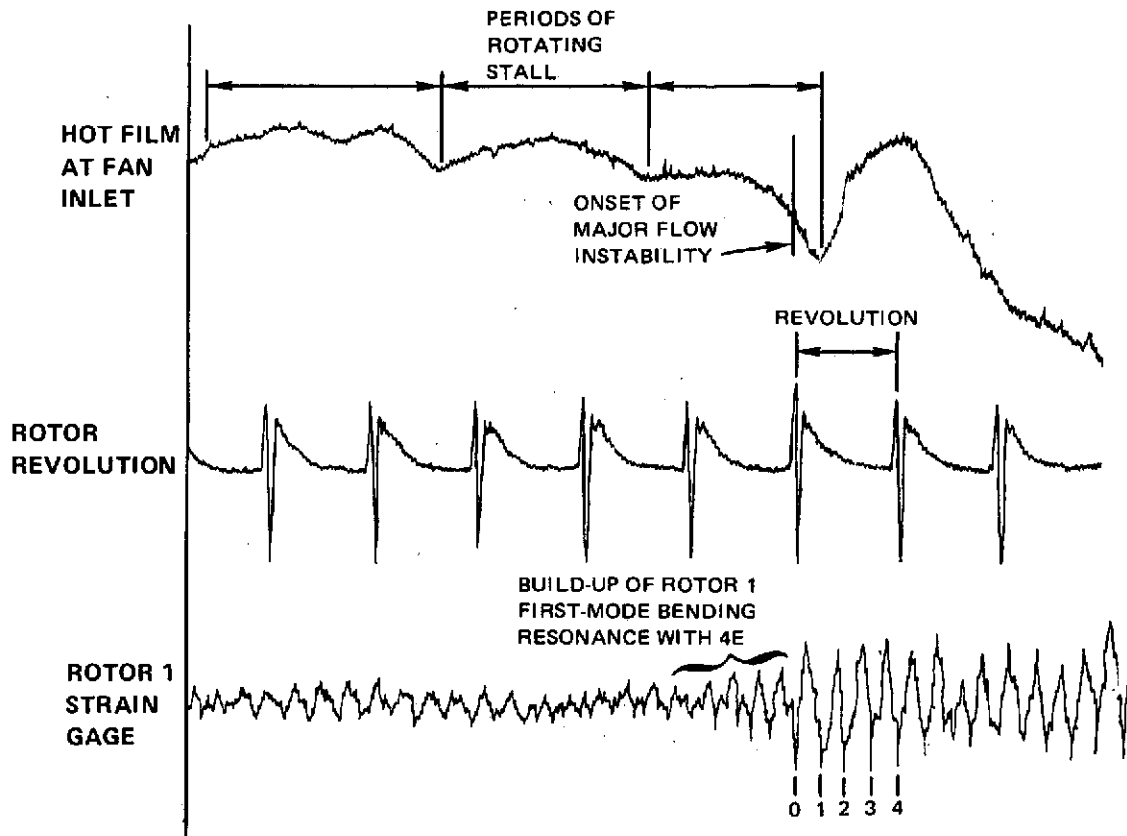


Figure 72 Hot Film and Strain Gage Records at Stall, with Tip Radially Distorted Flow at 85 Percent Speed

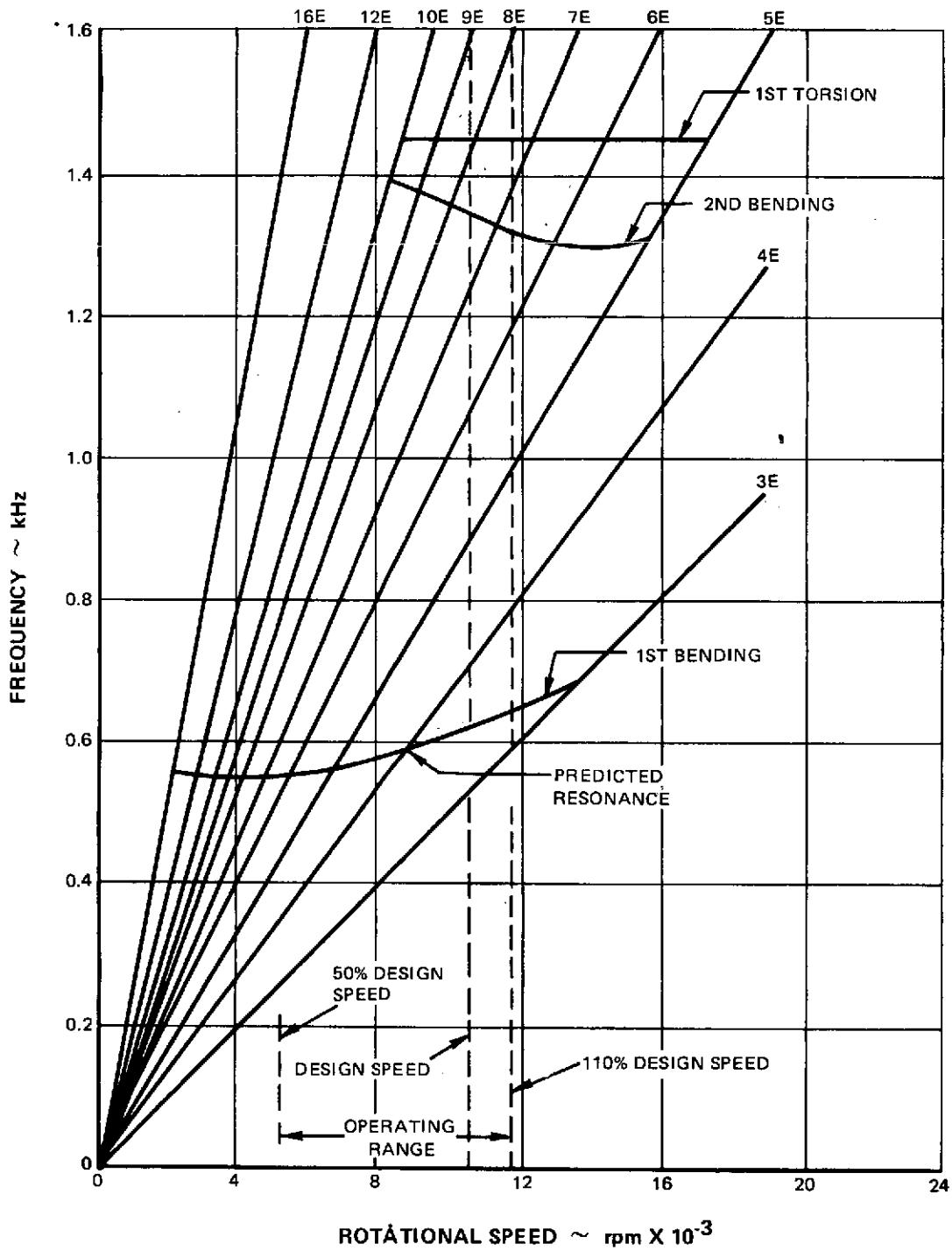


Figure 73 Resonance Diagram for Rotor 1

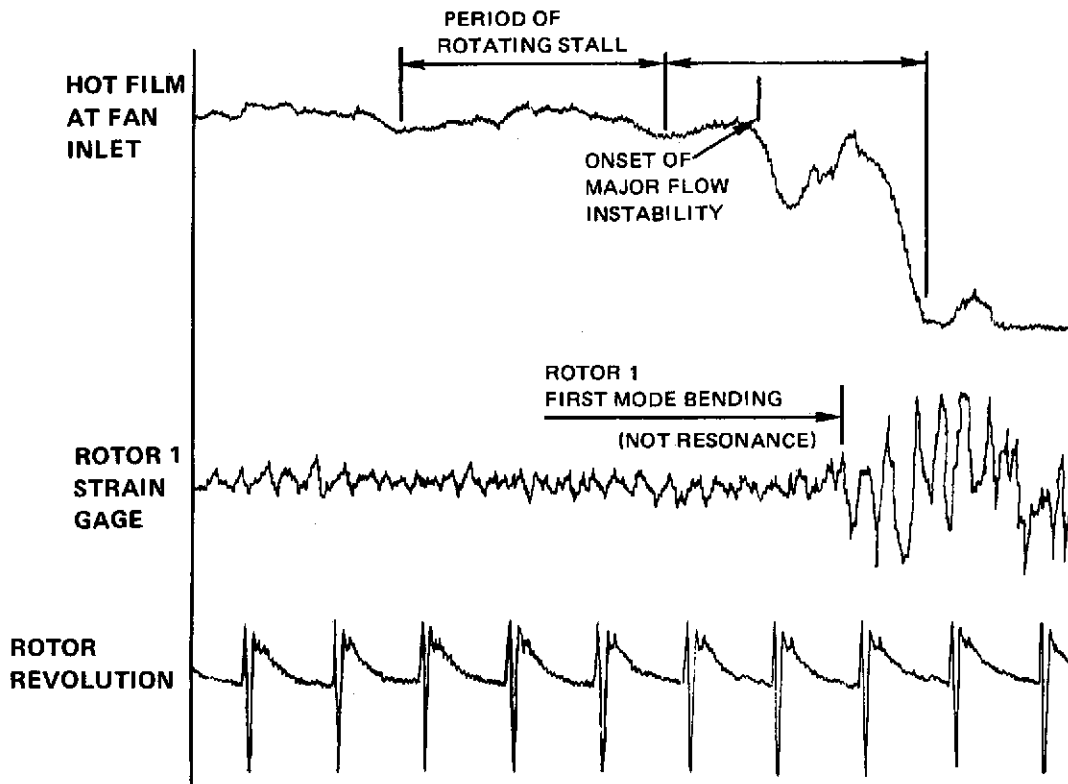


Figure 74 Hot Film and Strain Gage Records at Stall with Tip Radially Distorted Flow at Design Speed

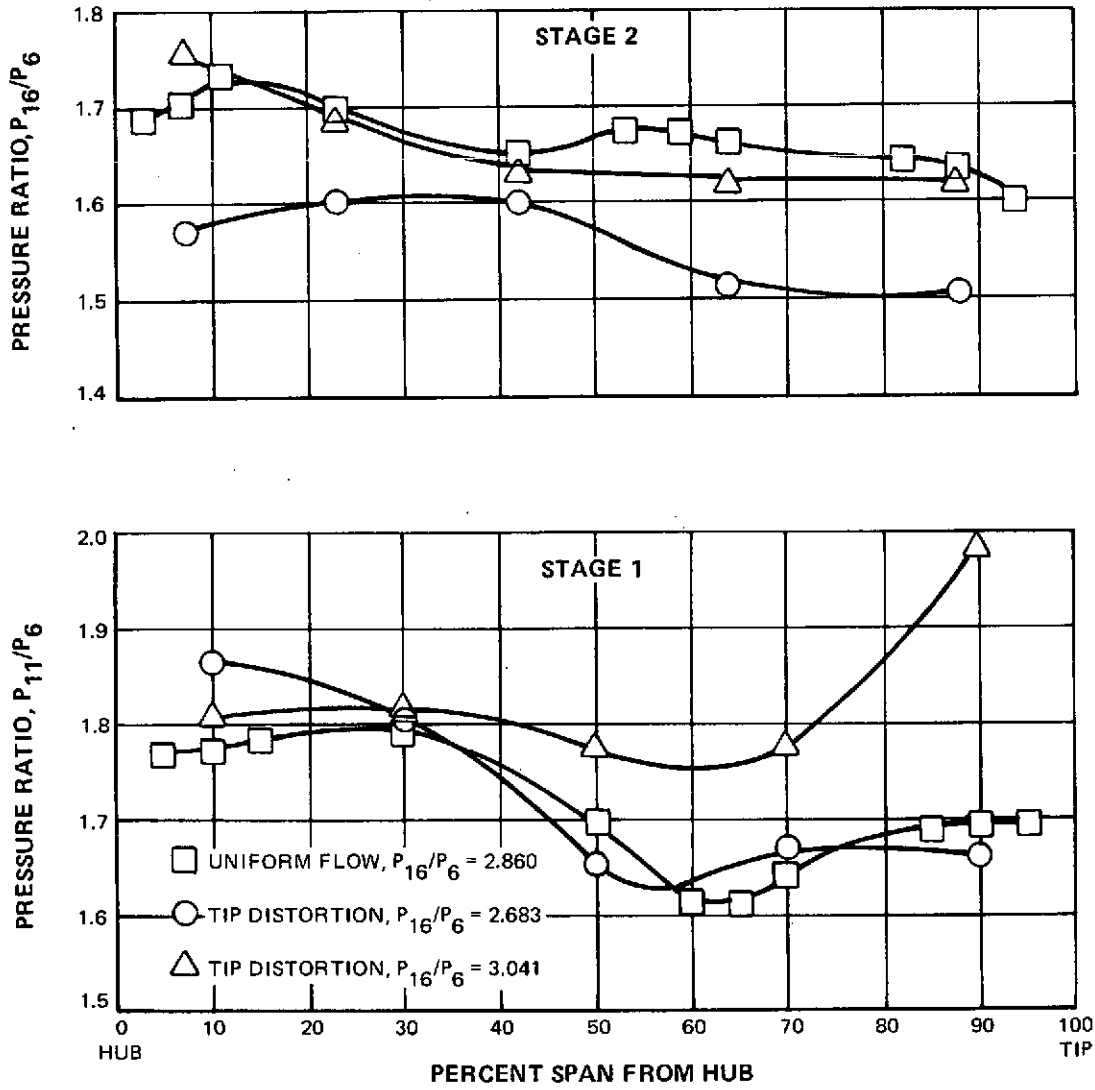


Figure 75 Spanwise Profiles of Stage 1 and Stage 2 Pressure Ratio for Uniform and Tip Radially Distorted Inlet Flows at Design Speed

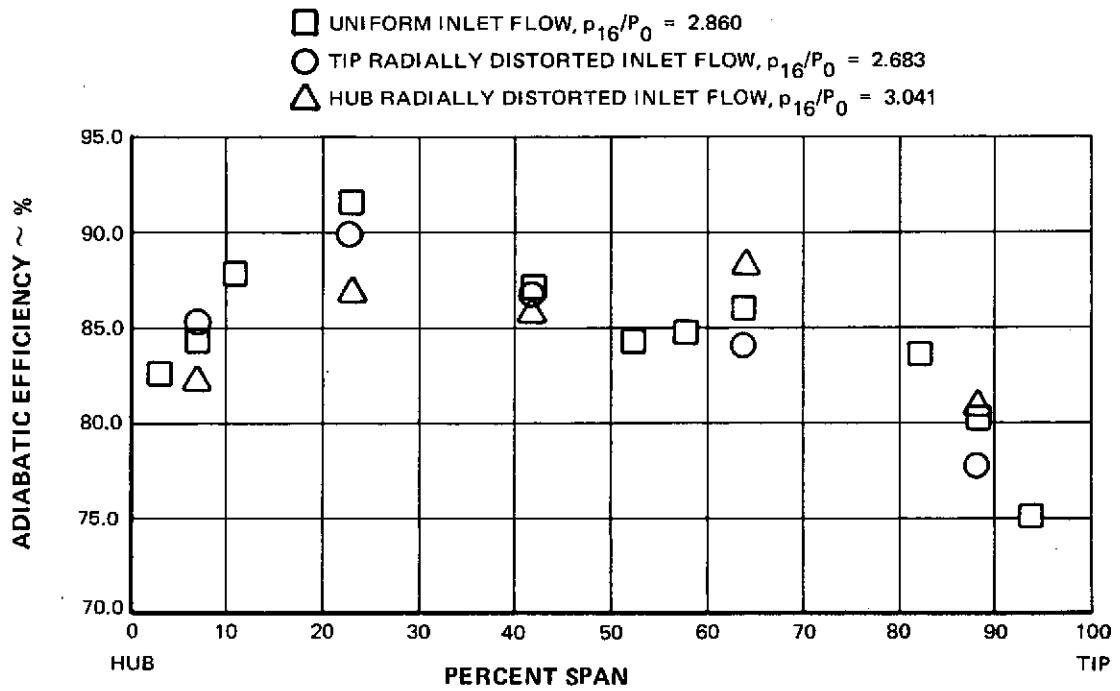


Figure 76 Spanwise Profiles of Fan Efficiency for Uniform and Radially Distorted Inlet Flows at Design Speed

NOTE: First Stage Pressure and Temperature Data Used In Calculating Parameters Shown Is From Radial Traverses Corrected Using The Correlations Described In The Section On Data Reduction Techniques

- 100% SPEED
- × 85% SPEED
- ◇ 70% SPEED
- ⊠ 100% DESIGN POINT

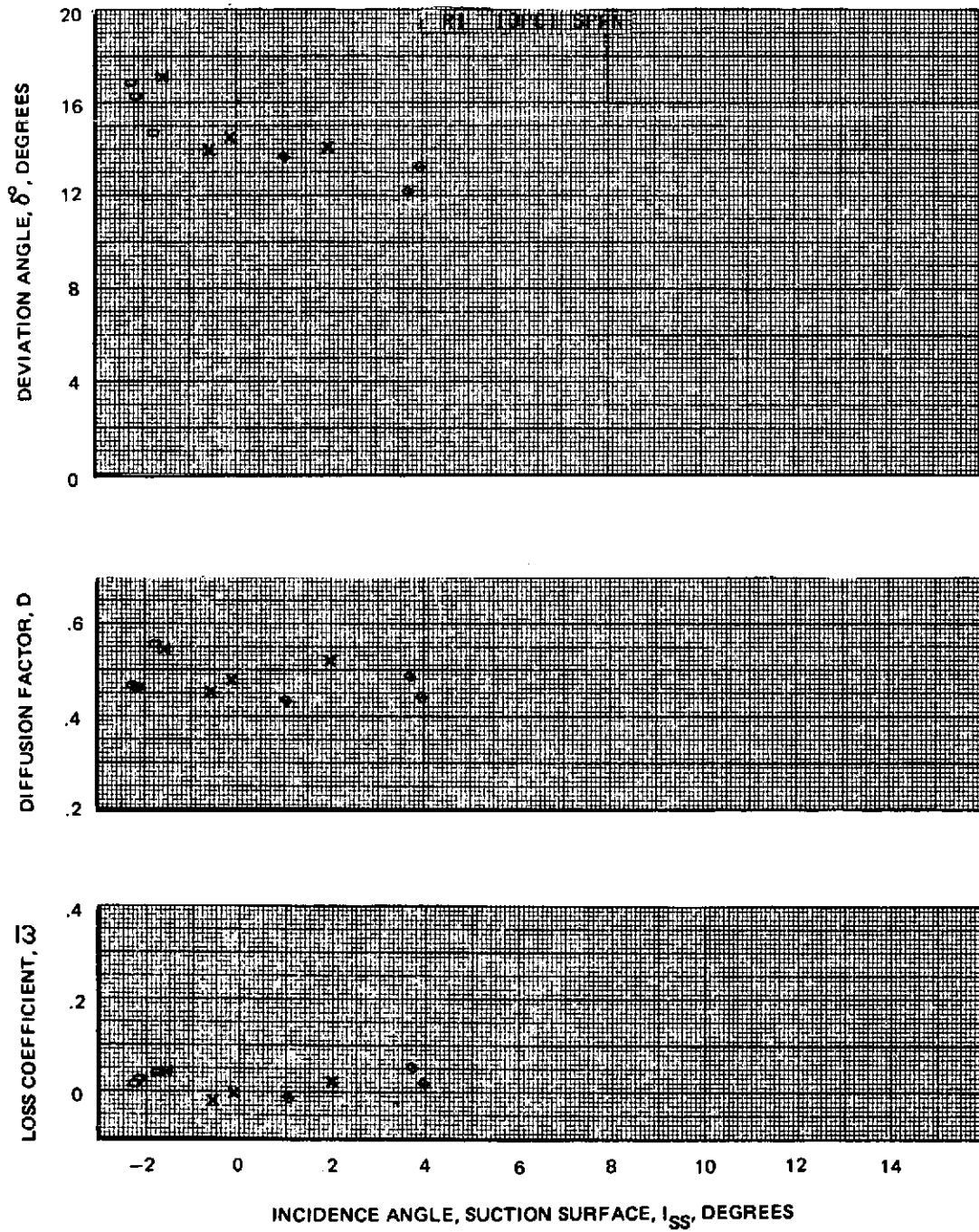


Figure 77a Blade Element Performance With Tip Radial Distortion – Rotor 1  
10% Span

NOTE: First Stage Pressure and Temperature Data Used In Calculating Parameters Shown Is From Radial Traverses Corrected Using The Correlations Described In The Section On Data Reduction Techniques

- 100% SPEED
- × 85% SPEED
- ◇ 70% SPEED
- ⊠ 100% DESIGN POINT

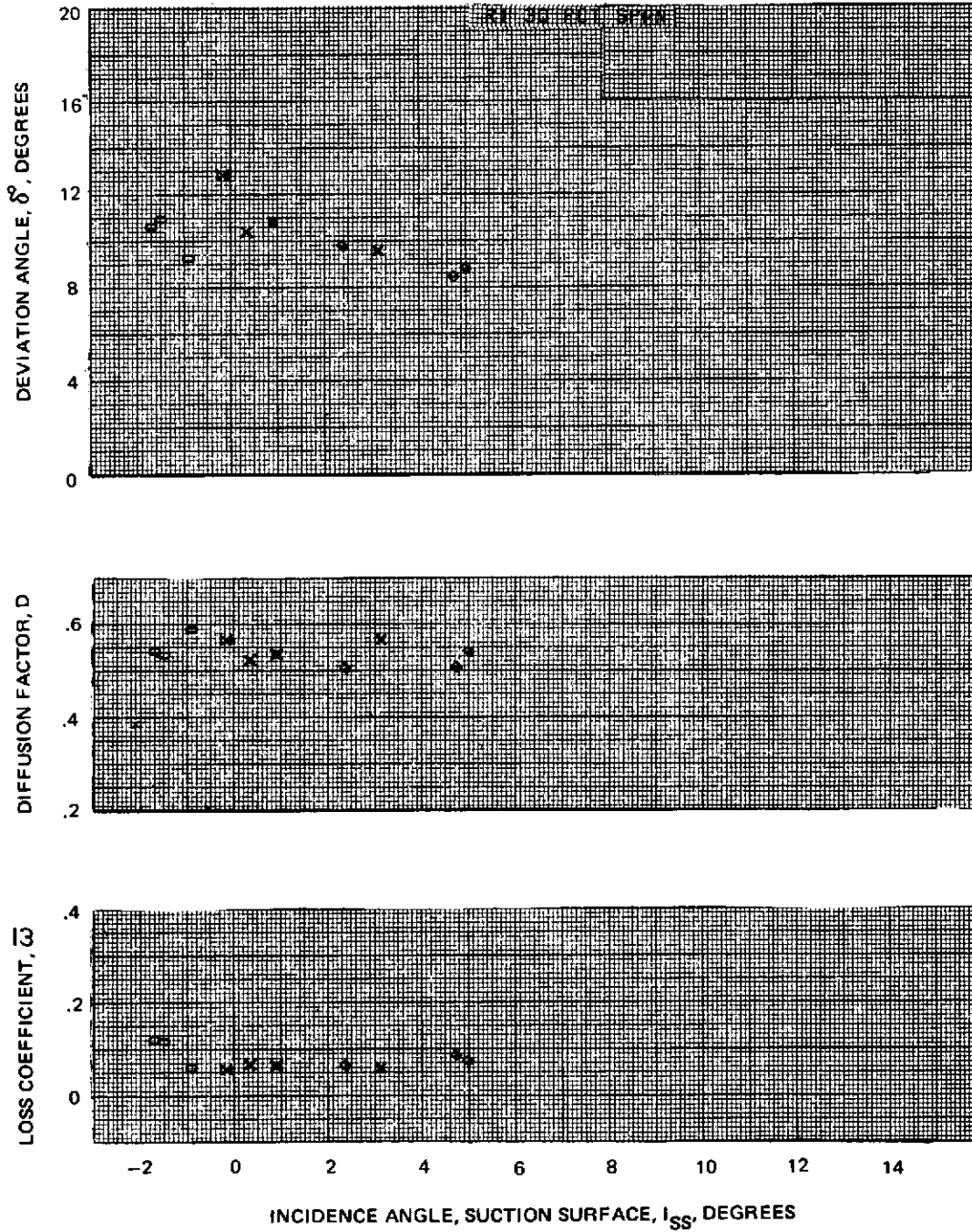


Figure 77b Blade Element Performance With Tip Radial Distortion – Rotor 1  
30% Span

NOTE: First Stage Pressure and Temperature Data Used In Calculating Parameters Shown Is From Radial Traverses Corrected Using The Correlations Described In The Section On Data Reduction Techniques

○ 100% SPEED  
 X 85% SPEED  
 ◇ 70% SPEED  
 ⊠ 100% DESIGN POINT

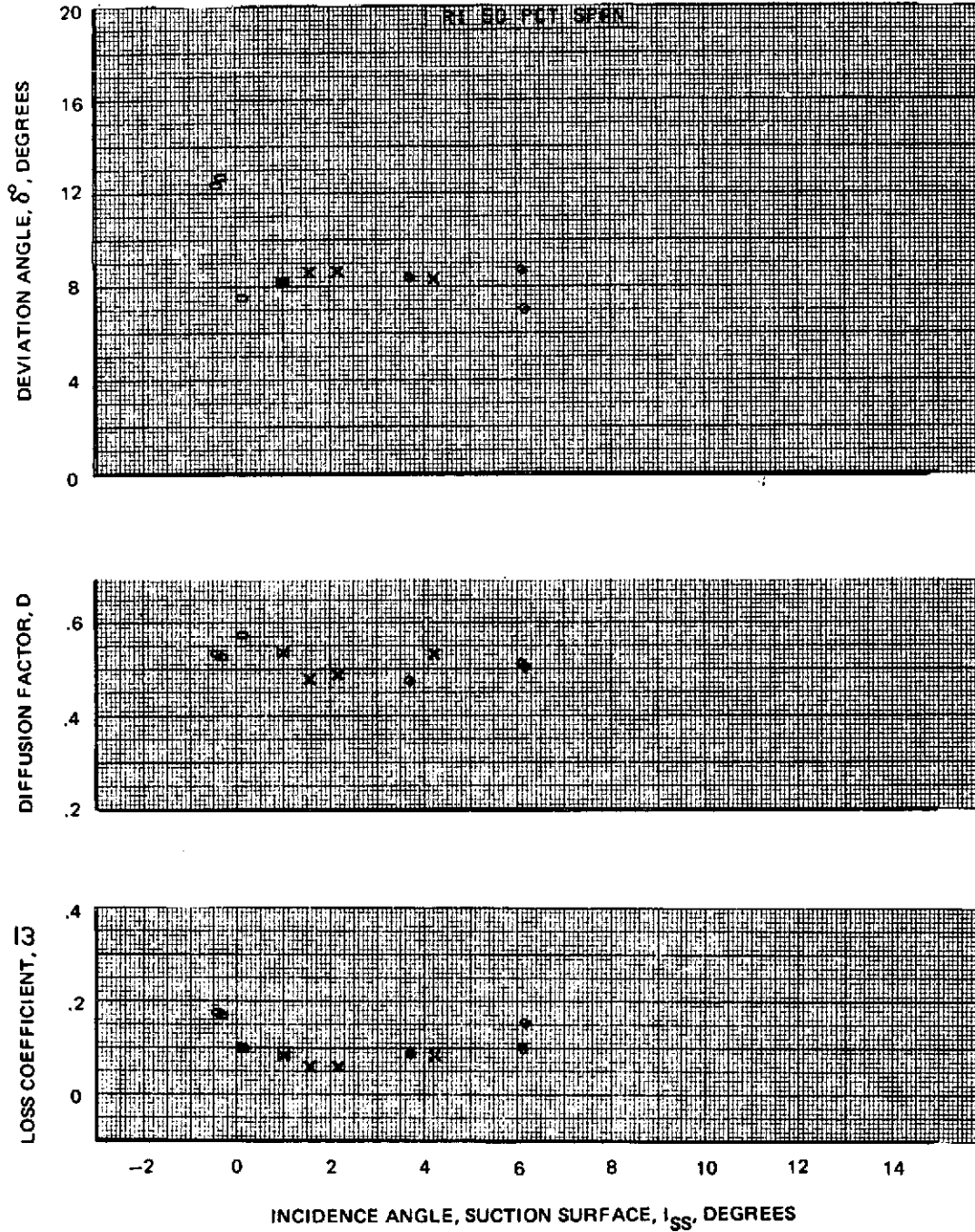


Figure 77c Blade Element Performance With Tip Radial Distortion – Rotor 1  
 50% Span



NOTE: First Stage Pressure and Temperature Data Used In Calculating Parameters Shown Is From Radial Traverses Corrected Using The Correlations Described In The Section On Data Reduction Techniques

- 100% SPEED
- × 85% SPEED
- ◇ 70% SPEED
- ⊠ 100% DESIGN POINT

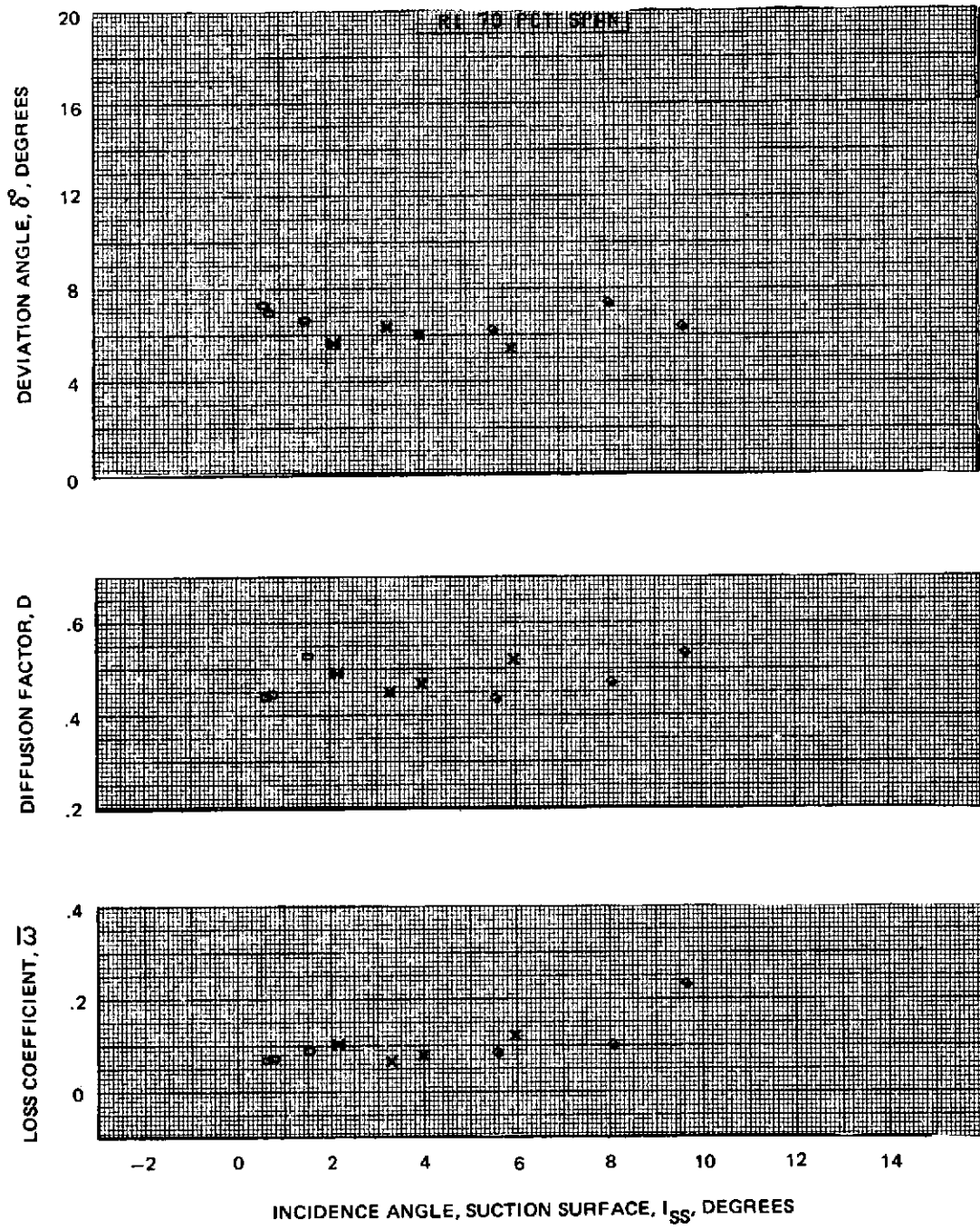


Figure 77d Blade Element Performance With Tip Radial Distortion – Rotor 1  
70% Span

NOTE: First Stage Pressure and Temperature Data Used In Calculating Parameters Shown Is From Radial Traverses Corrected Using The Correlations Described In The Section On Data Reduction Techniques

○ 100% SPEED  
 X 85% SPEED  
 ◇ 70% SPEED  
 ⊠ 100% DESIGN POINT

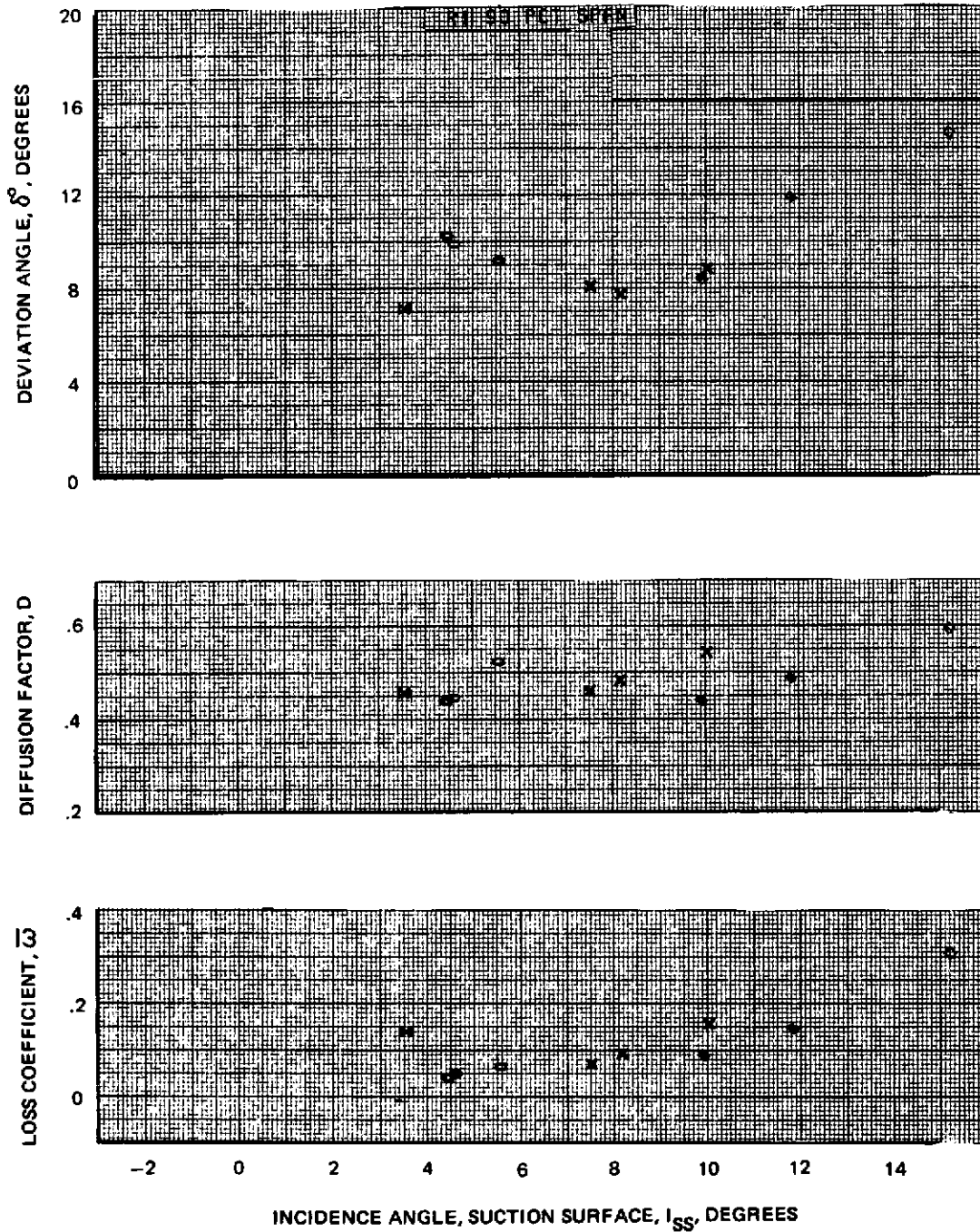


Figure 77e Blade Element Performance With Tip Radial Distortion – Rotor 1 90% Span

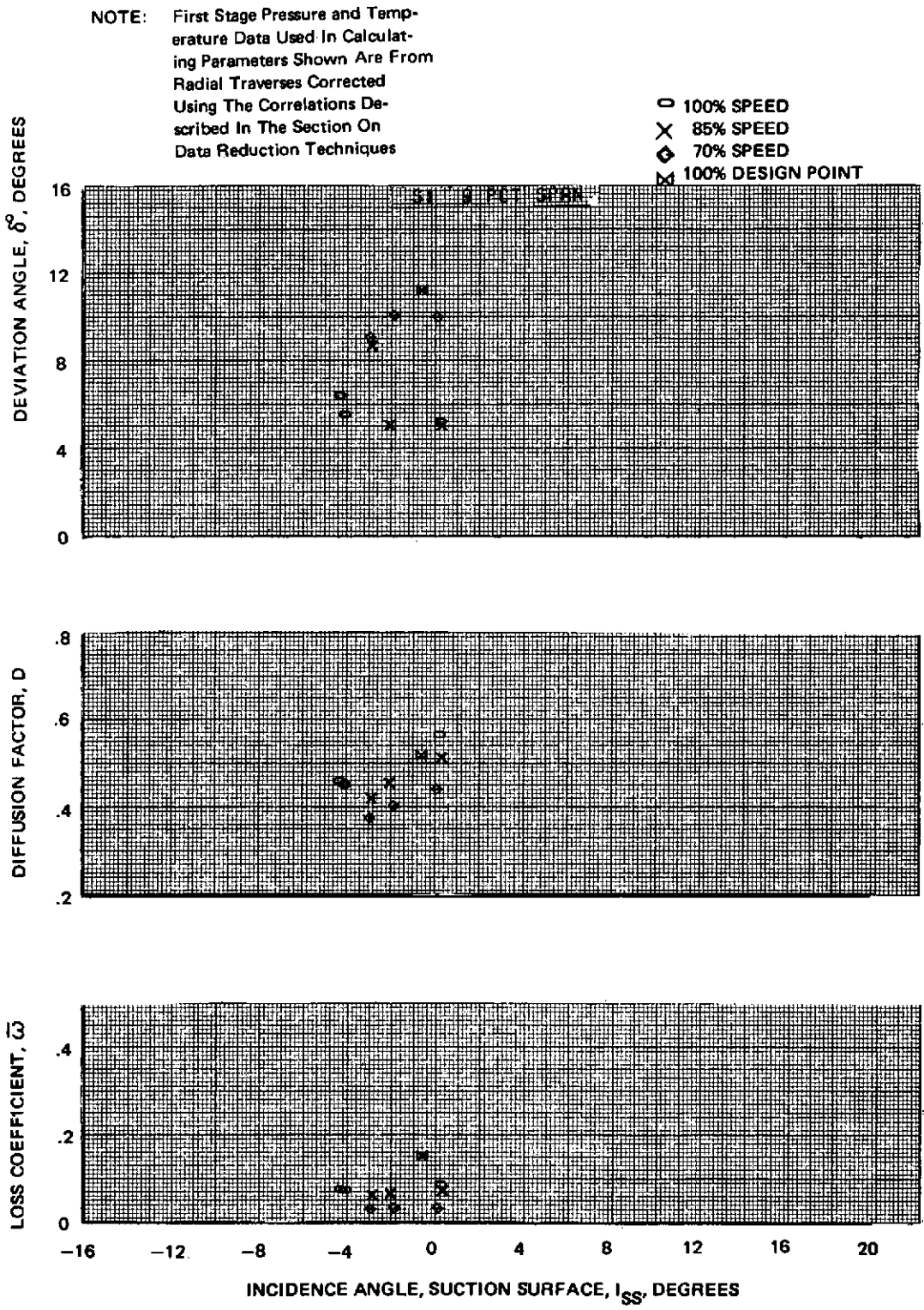


Figure 78a Blade Element Performance With Tip Radial Distortion – Stator 1  
9% Span

NOTE: First Stage Pressure and Temperature Data Used In Calculating Parameters Shown Are From Radial Traverses Corrected Using The Correlations Described In The Section On Data Reduction Techniques

- 100% SPEED
- × 85% SPEED
- ◇ 70% SPEED
- ⊠ 100% DESIGN POINT

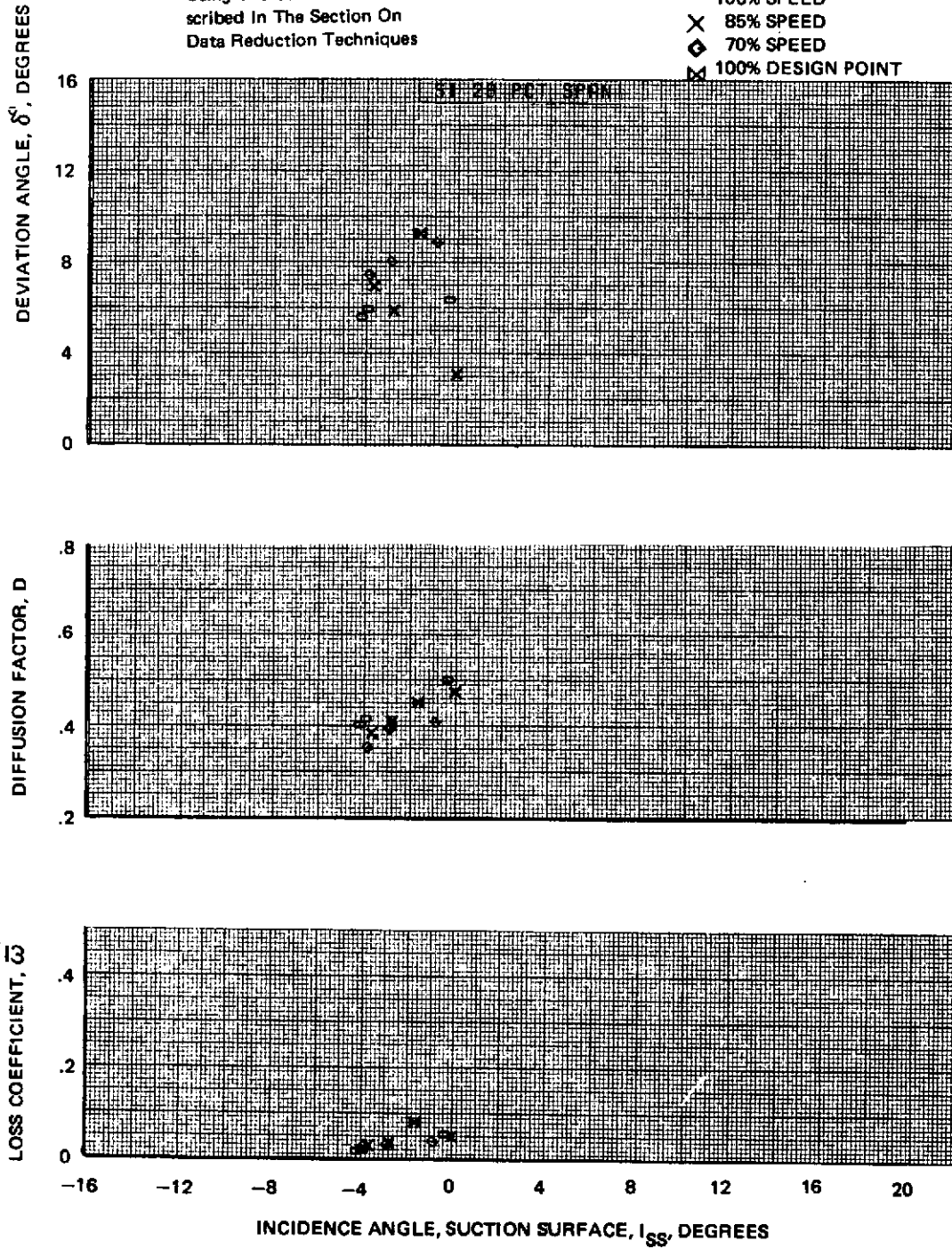


Figure 78b Blade Element Performance With Tip Radial Distortion – Stator 1  
28% Span

NOTE: First Stage Pressure and Temperature Data Used In Calculating Parameters Shown Are From Radial Traverses Corrected Using The Correlations Described In The Section On Data Reduction Techniques

○ 100% SPEED  
 × 85% SPEED  
 ◇ 70% SPEED  
 ⊠ 100% DESIGN POINT

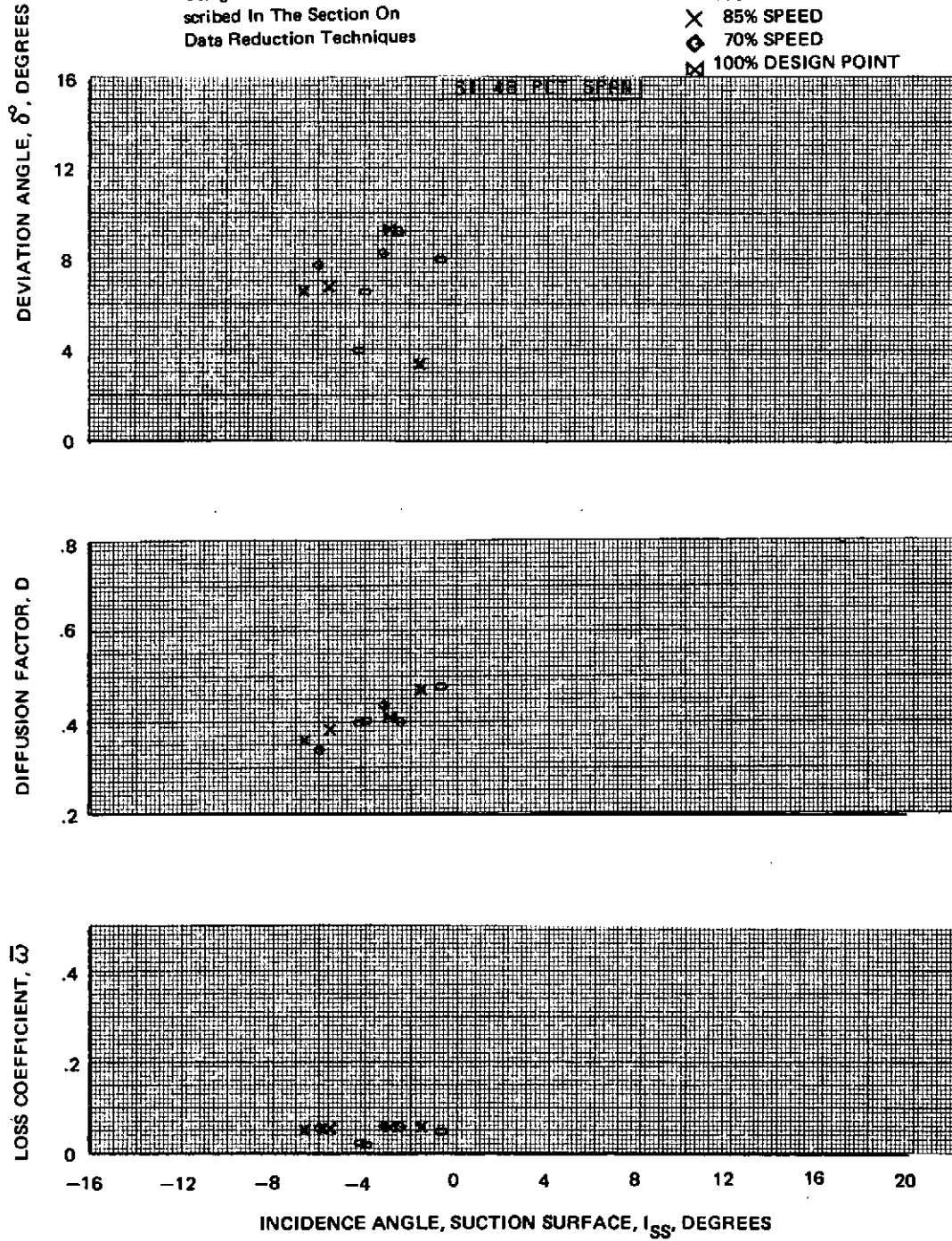
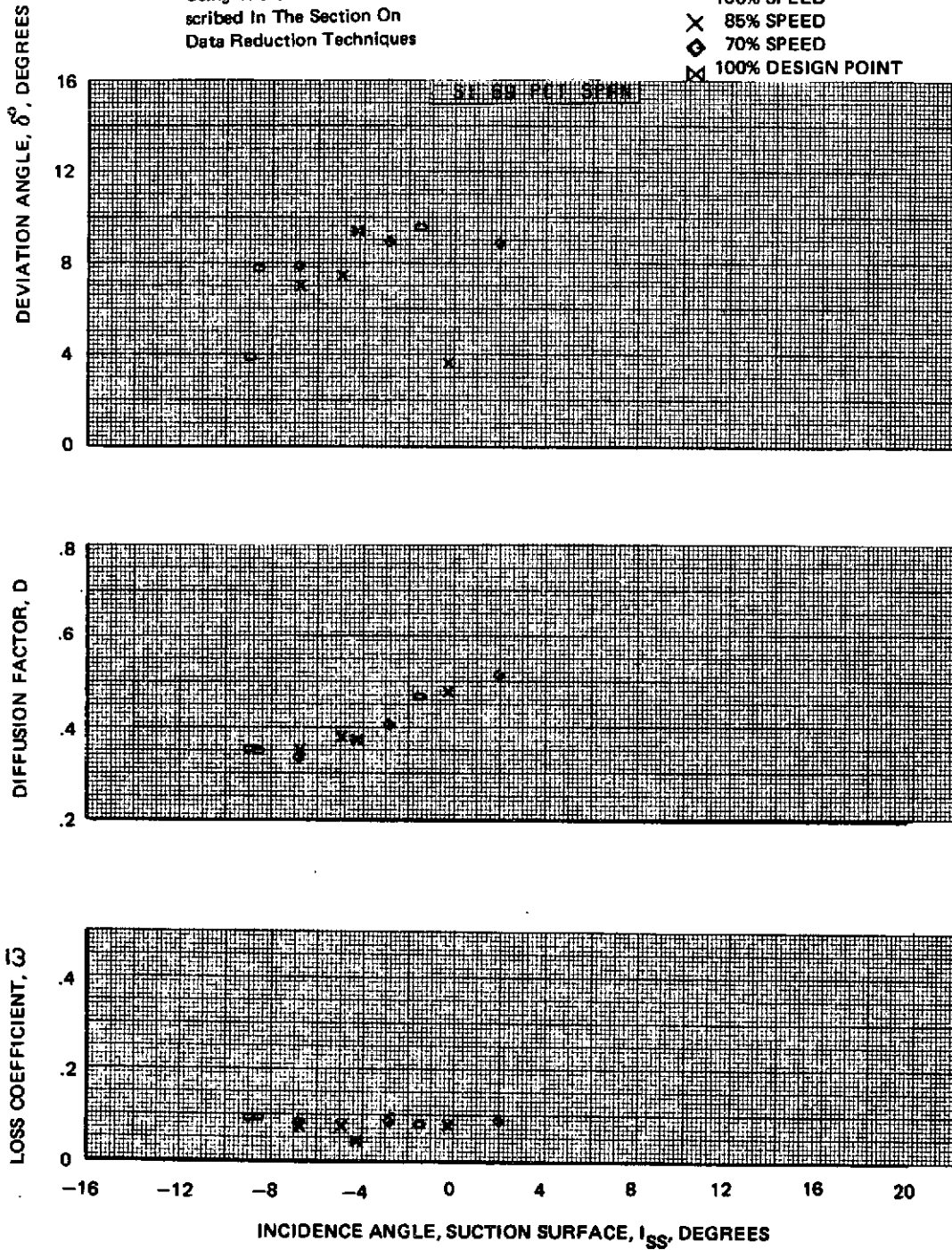


Figure 78c Blade Element Performance With Tip Radial Distortion – Stator 1  
 48% Span

NOTE: First Stage Pressure and Temperature Data Used In Calculating Parameters Shown Are From Radial Traverses Corrected Using The Correlations Described In The Section On Data Reduction Techniques

- 100% SPEED
- × 85% SPEED
- ◇ 70% SPEED
- △ 100% DESIGN POINT



NOTE: First Stage Pressure and Temperature Data Used In Calculating Parameters Shown Are From Radial Traverses Corrected Using The Correlations Described In The Section On Data Reduction Techniques

- 100% SPEED
- × 85% SPEED
- ◇ 70% SPEED
- ⊠ 100% DESIGN POINT

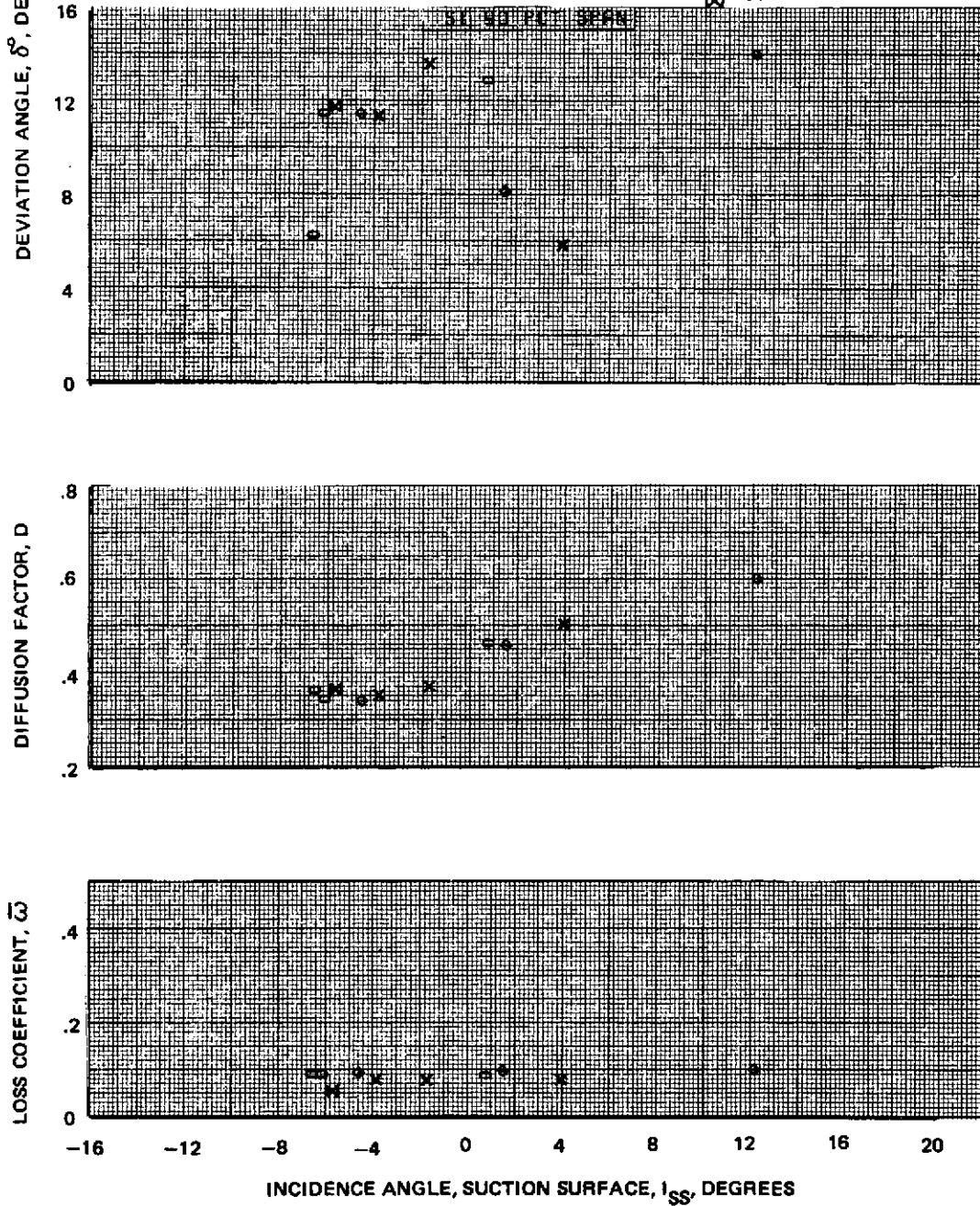
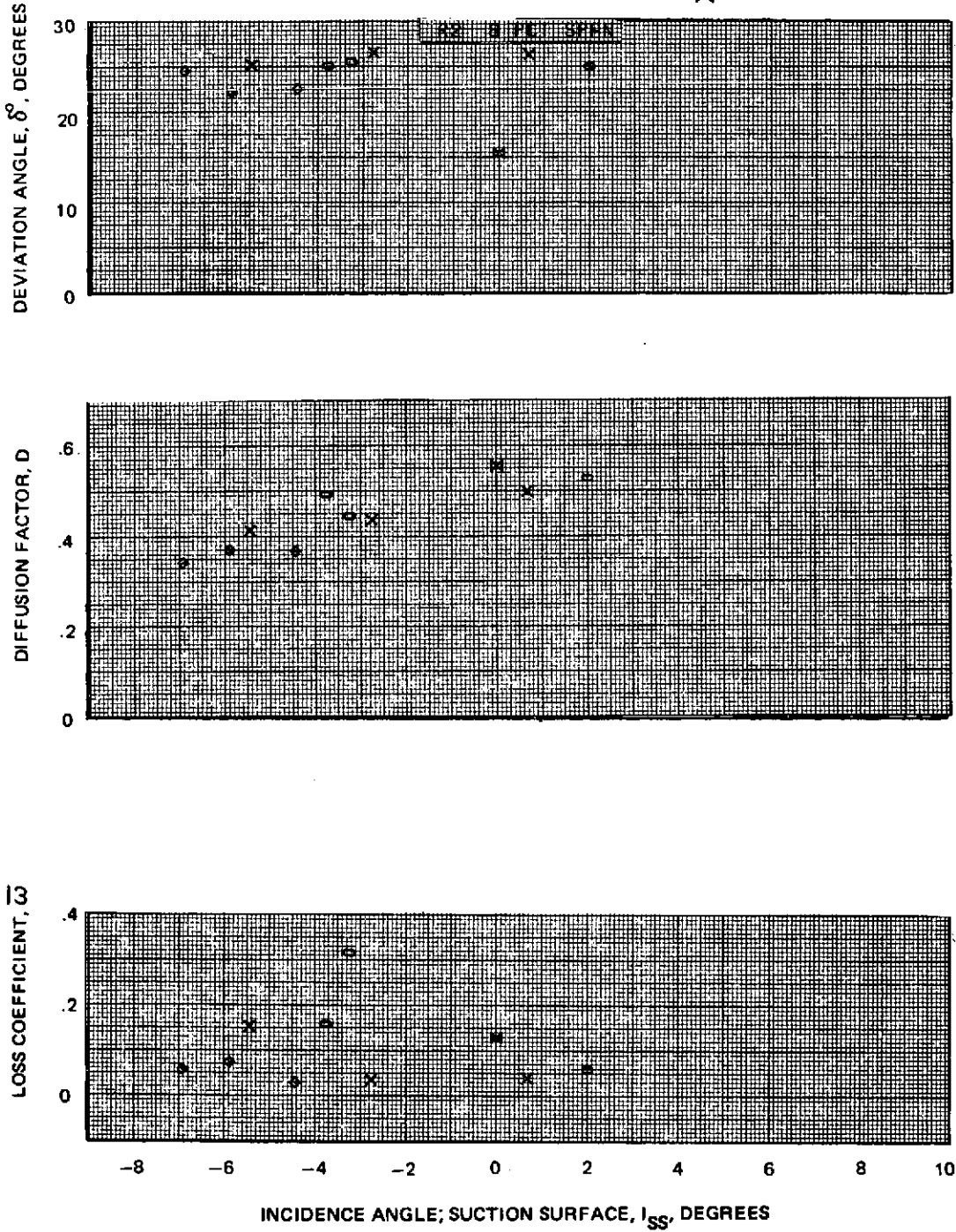


Figure 78e Blade Element Performance With Tip Radial Distortion – Stator 1  
90% Span

NOTE: First Stage Pressure and Temperature Data Used In Calculating Parameters Shown Is From Radial Traverses Corrected Using The Correlations Described In The Section On Data Reduction Techniques

○ 100% SPEED  
 × 85% SPEED  
 ◇ 70% SPEED  
 ⊗ 100% DESIGN POINT





NOTE: First Stage Pressure and Temperature Data Used In Calculating Parameters Shown Is From Radial Traverses Corrected Using The Correlations Described In The Section On Data Reduction Techniques

- 100% SPEED
- × 85% SPEED
- ◇ 70% SPEED
- ⊠ 100% DESIGN POINT

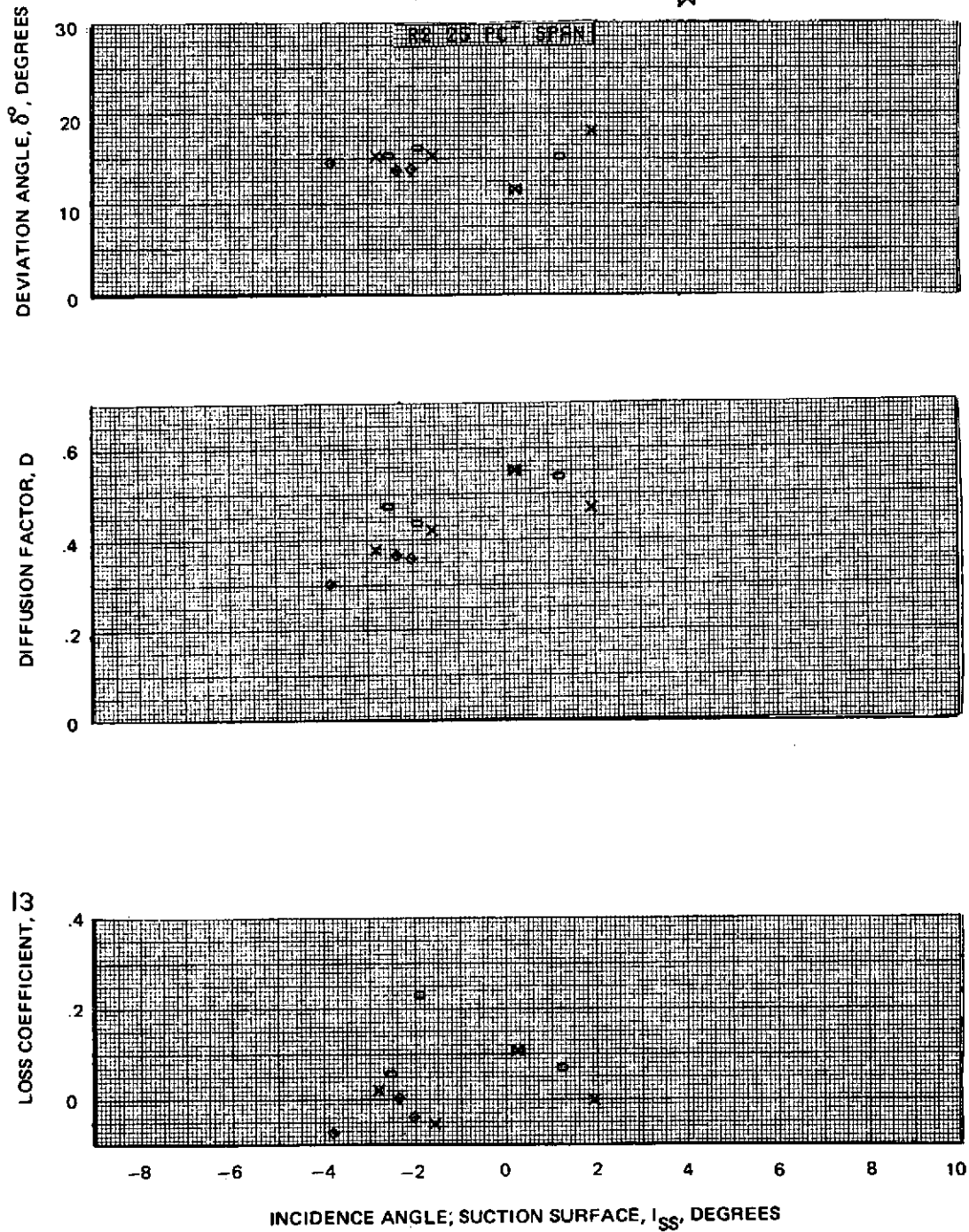


Figure 79b Blade Element Performance With Tip Radial Distortion Rotor 2  
25% Span

NOTE: First Stage Pressure and Temperature Data Used In Calculating Parameters Shown Is From Radial Traverses Corrected Using The Correlations Described In The Section On Data Reduction Techniques

- 100% SPEED
- × 85% SPEED
- ◇ 70% SPEED
- ⊠ 100% DESIGN POINT

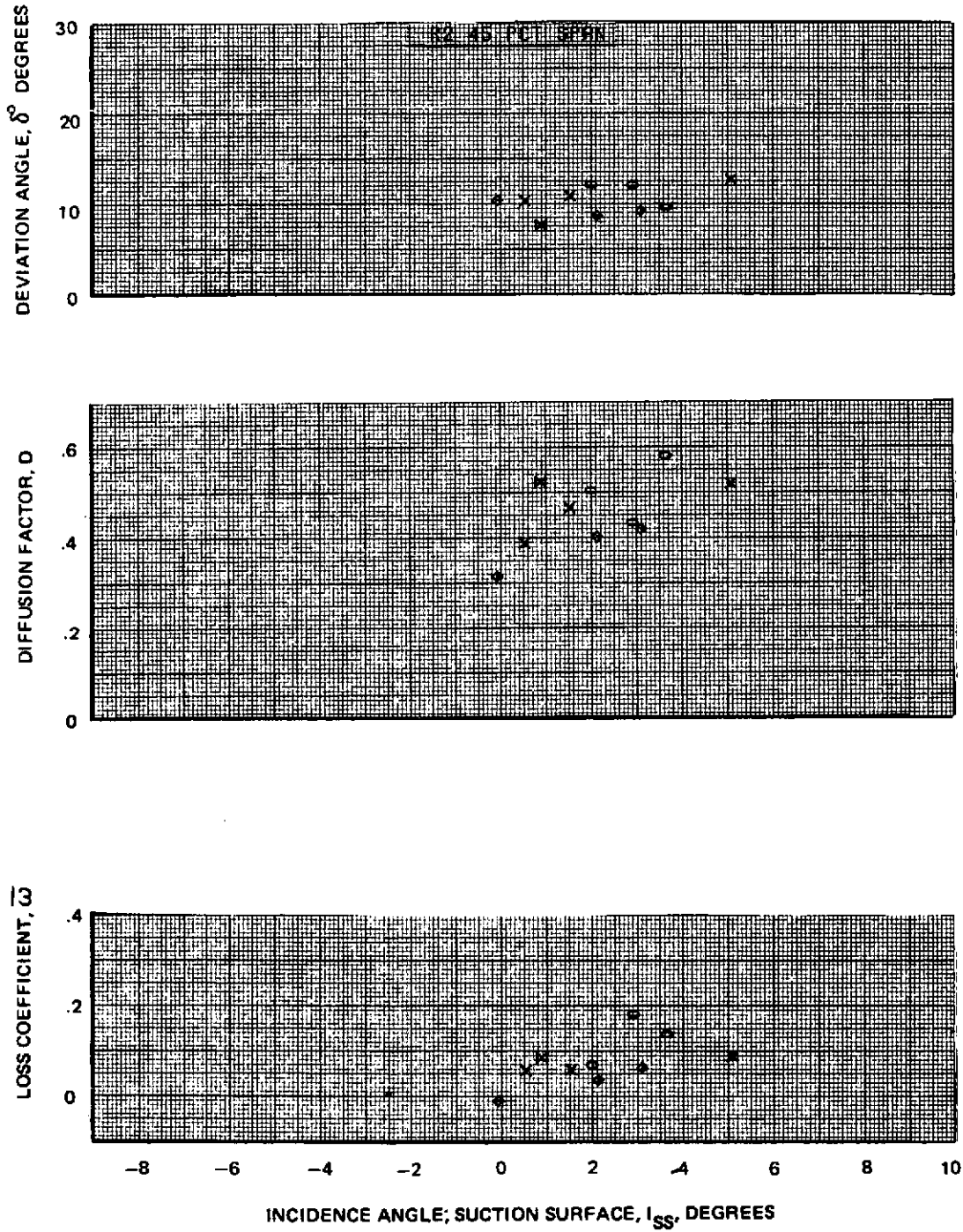


Figure 79c Blade Element Performance With Tip Radial Distortion- Rotor 2 45% Span

NOTE: First Stage Pressure and Temperature Data Used In Calculating Parameters Shown Is From Radial Traverses Corrected Using The Correlations Described In The Section On Data Reduction Techniques

- 100% SPEED
- × 85% SPEED
- ◇ 70% SPEED
- ⊠ 100% DESIGN POINT

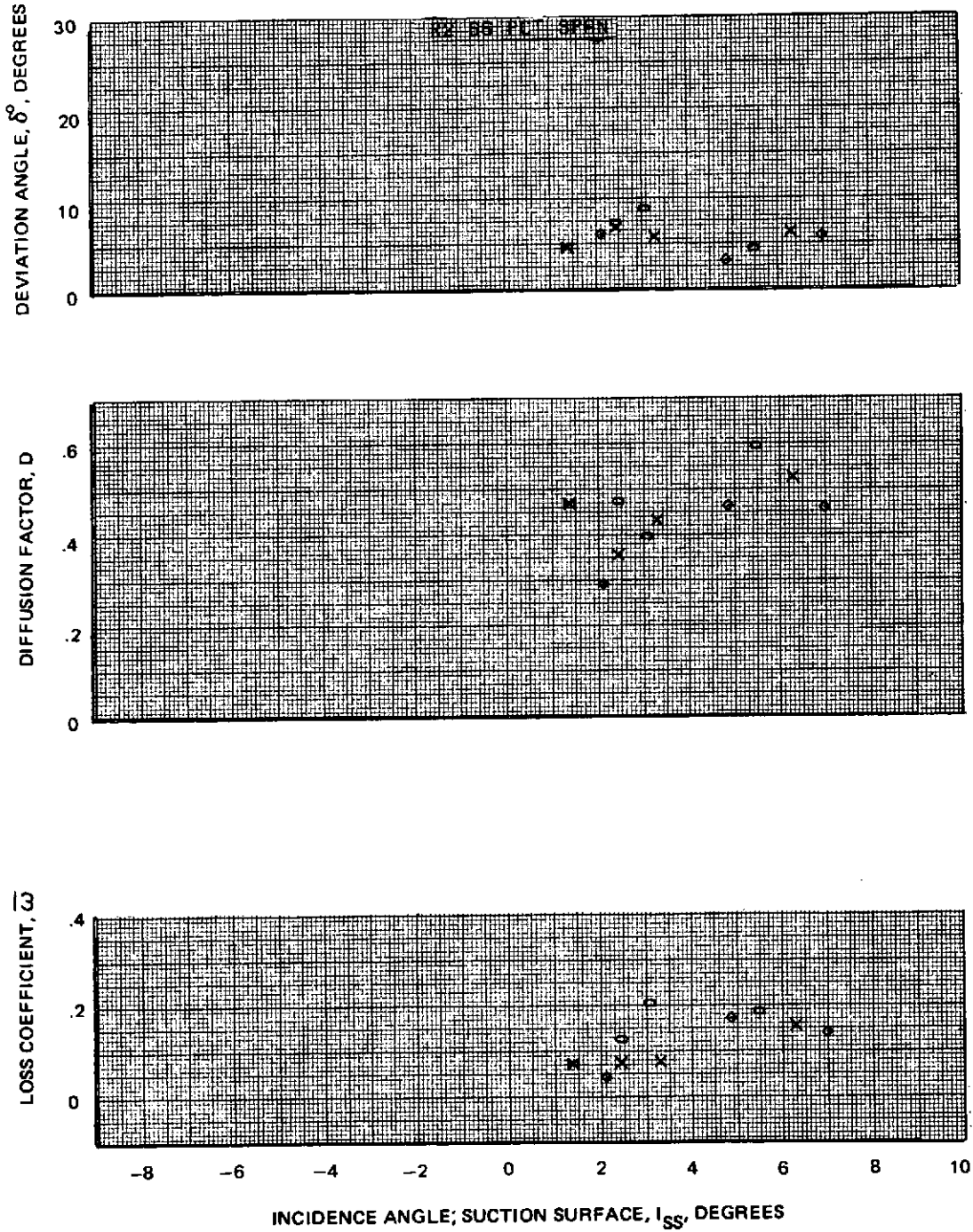


Figure 79d Blade Element Performance With Uniform Inlet Flow – Rotor 2  
66% Span

NOTE: First Stage Pressure and Temperature Data Used In Calculating Parameters Shown Is From Radial Traverses Corrected Using The Correlations Described In The Section On Data Reduction Techniques

- 100% SPEED
- × 85% SPEED
- ◇ 70% SPEED
- ⊠ 100% DESIGN POINT

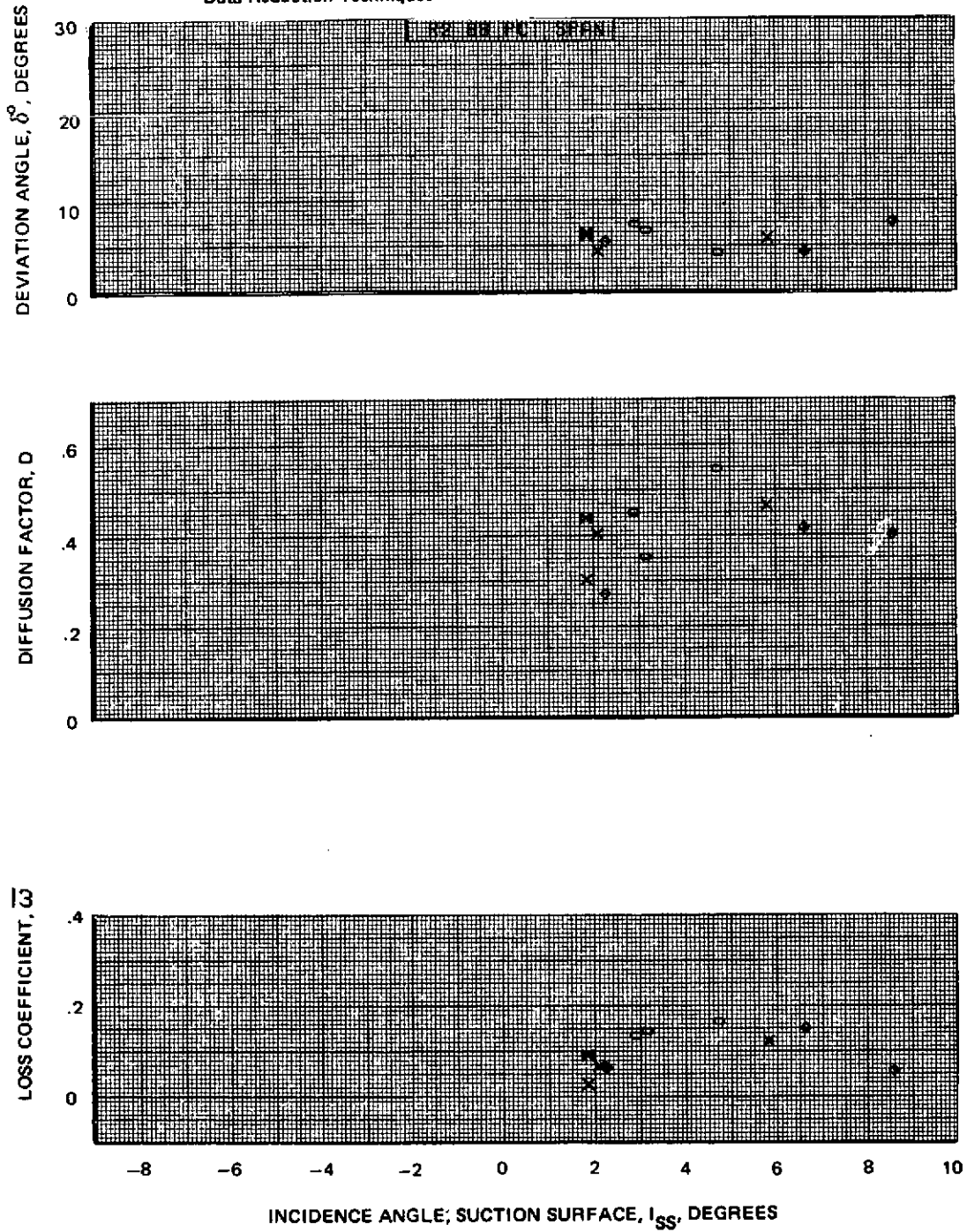


Figure 79e Blade Element Performance With Tip Radial Distortion- Rotor 2  
88% Span

NOTE: First Stage Pressure and Temperature Data Used In Calculating Parameters Shown Are From Radial Traverses Corrected Using The Correlations Described In The Section On Data Reduction Techniques

○ 100% SPEED  
 × 85% SPEED  
 ◊ 70% SPEED  
 ⊗ 100% DESIGN POINT

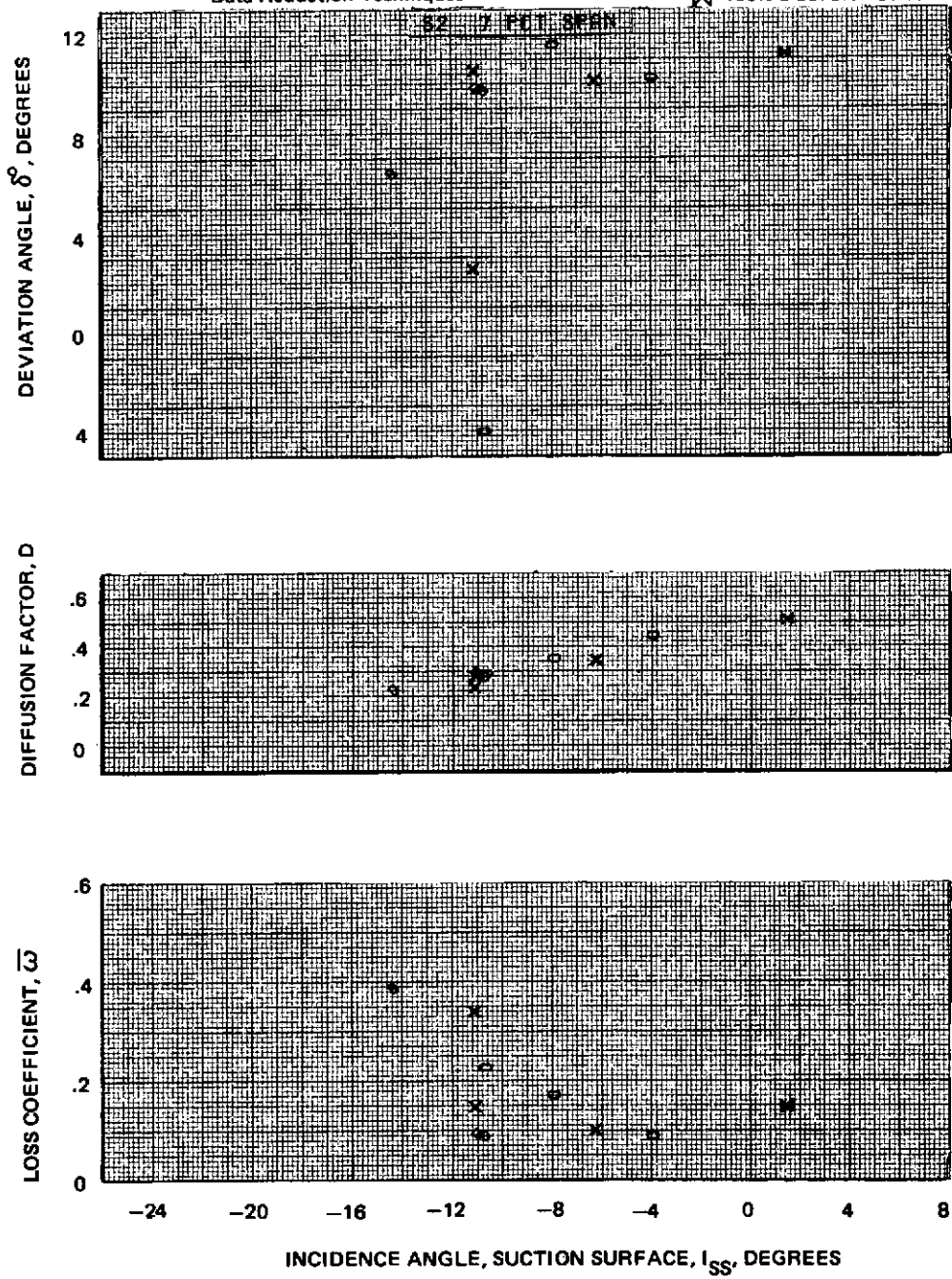


Figure 80a Blade Element Performance With Tip Radial Distortion – Stator 2  
 7% Span

NOTE: First Stage Pressure and Temperature Data Used In Calculating Parameters Shown Are From Radial Traverses Corrected Using The Correlations Described In The Section On Data Reduction Techniques

○ 100% SPEED  
 X 85% SPEED  
 ◇ 70% SPEED  
 ⊠ 100% DESIGN POINT

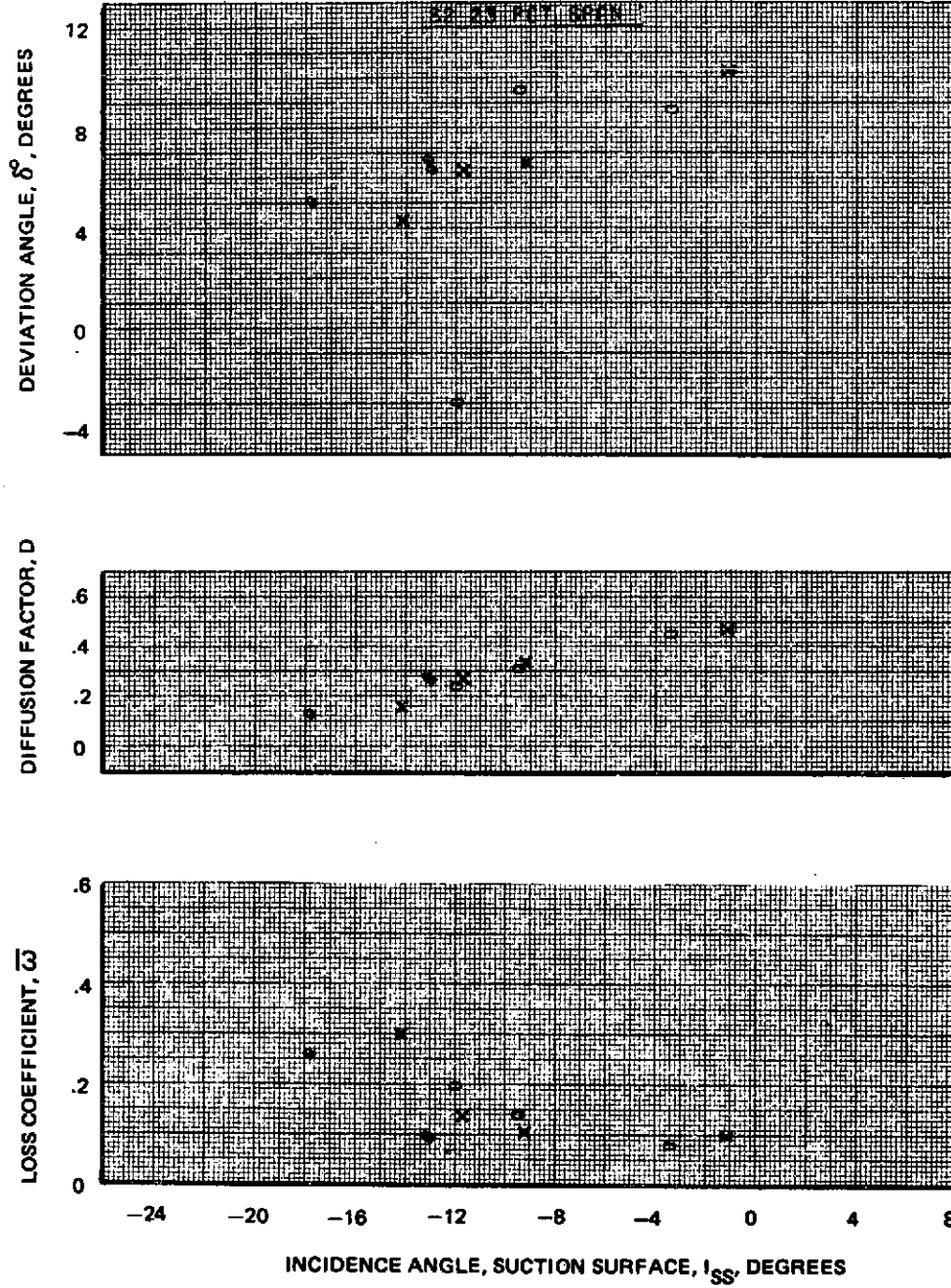


Figure 80b Blade Element Performance With Tip Radial Distortion – Stator 2  
 23% Span

NOTE: First Stage Pressure and Temperature Data Used In Calculating Parameters Shown Are From Radial Traverses Corrected Using The Correlations Described In The Section On Data Reduction Techniques

○ 100% SPEED  
 X 85% SPEED  
 ◇ 70% SPEED  
 ⊠ 100% DESIGN POINT

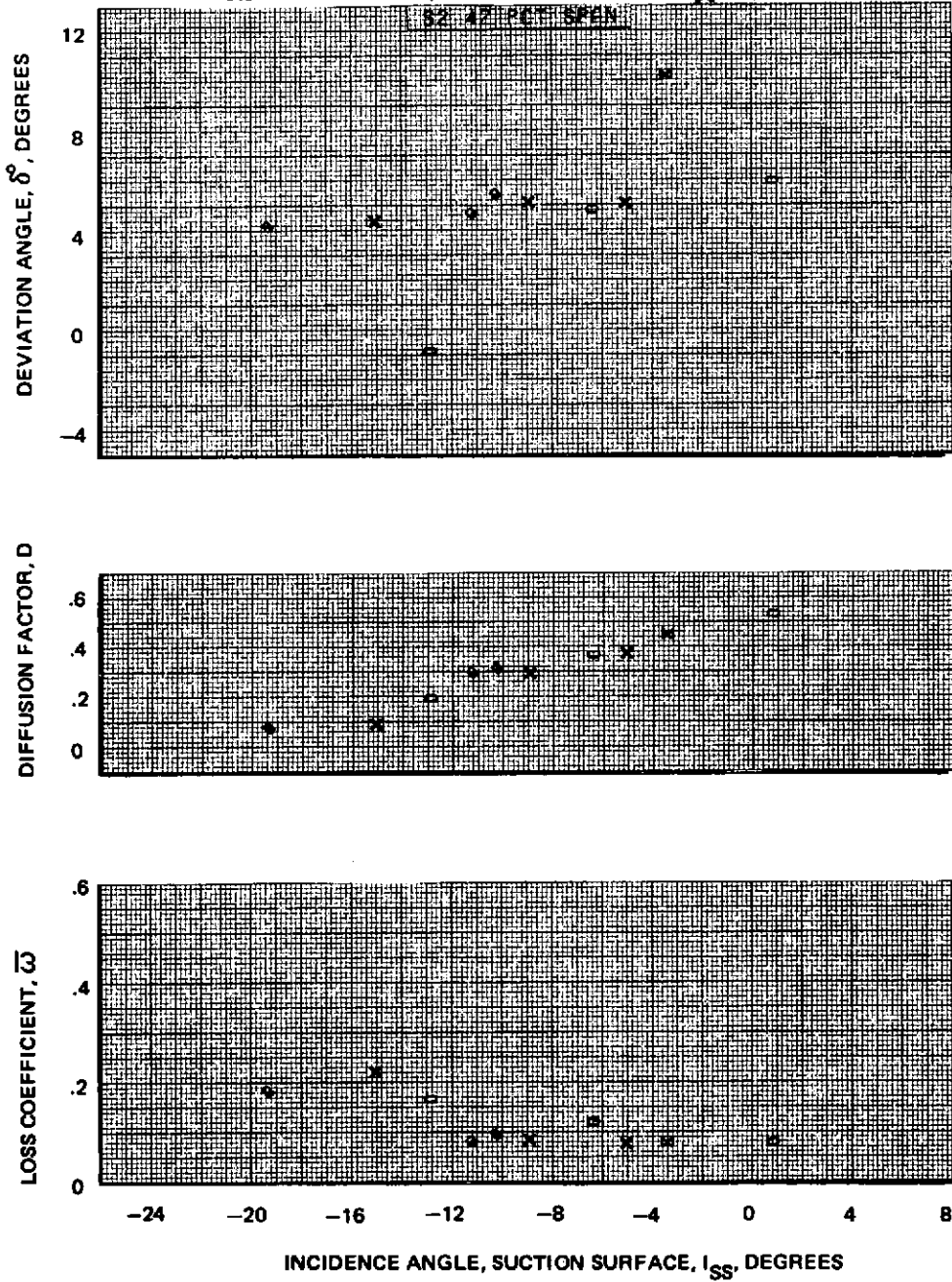


Figure 80c Blade Element Performance With Tip Radial Distortion – Stator 2  
 42% Span

NOTE: First Stage Pressure and Temperature Data Used In Calculating Parameters Shown Are From Radial Traverses Corrected Using The Correlations Described In The Section On Data Reduction Techniques

- 100% SPEED
- × 85% SPEED
- ◇ 70% SPEED
- ⊠ 100% DESIGN POINT

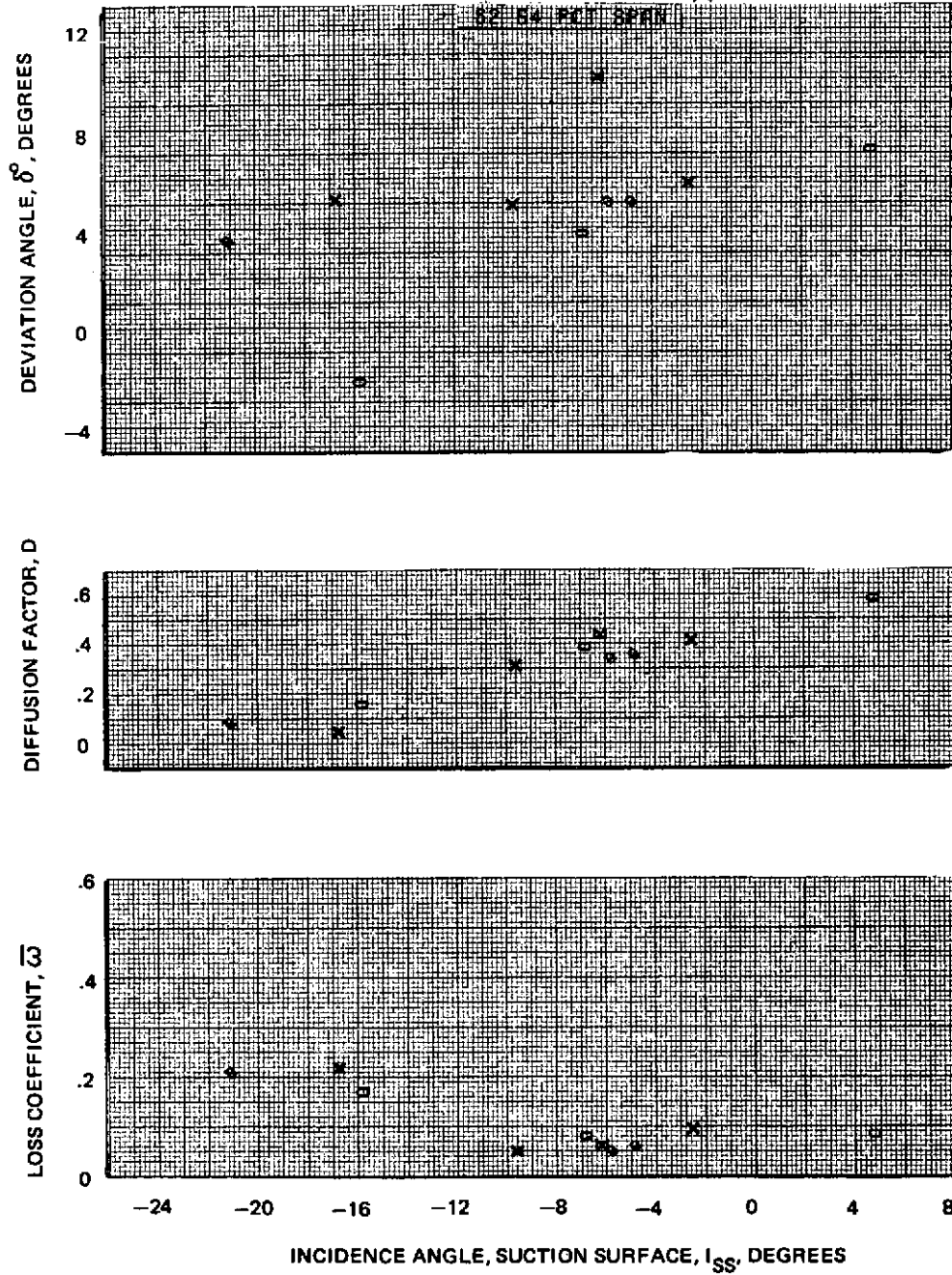


Figure 80d Blade Element Performance With Tip Radial Distortion – Stator 2  
64% Span



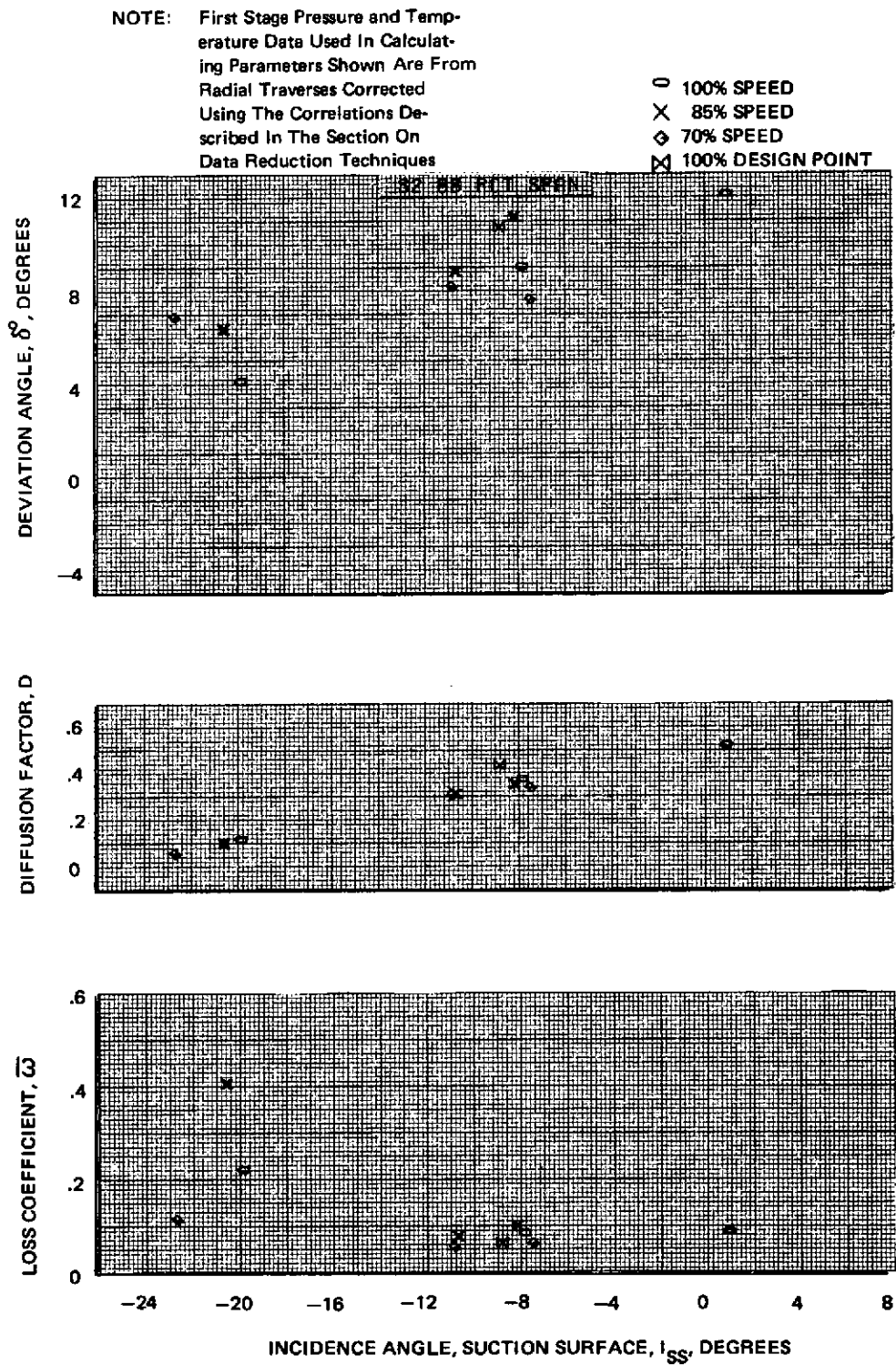


Figure 80e Blade Element Performance With Tip Radial Distortion – Stator 2  
88% Span

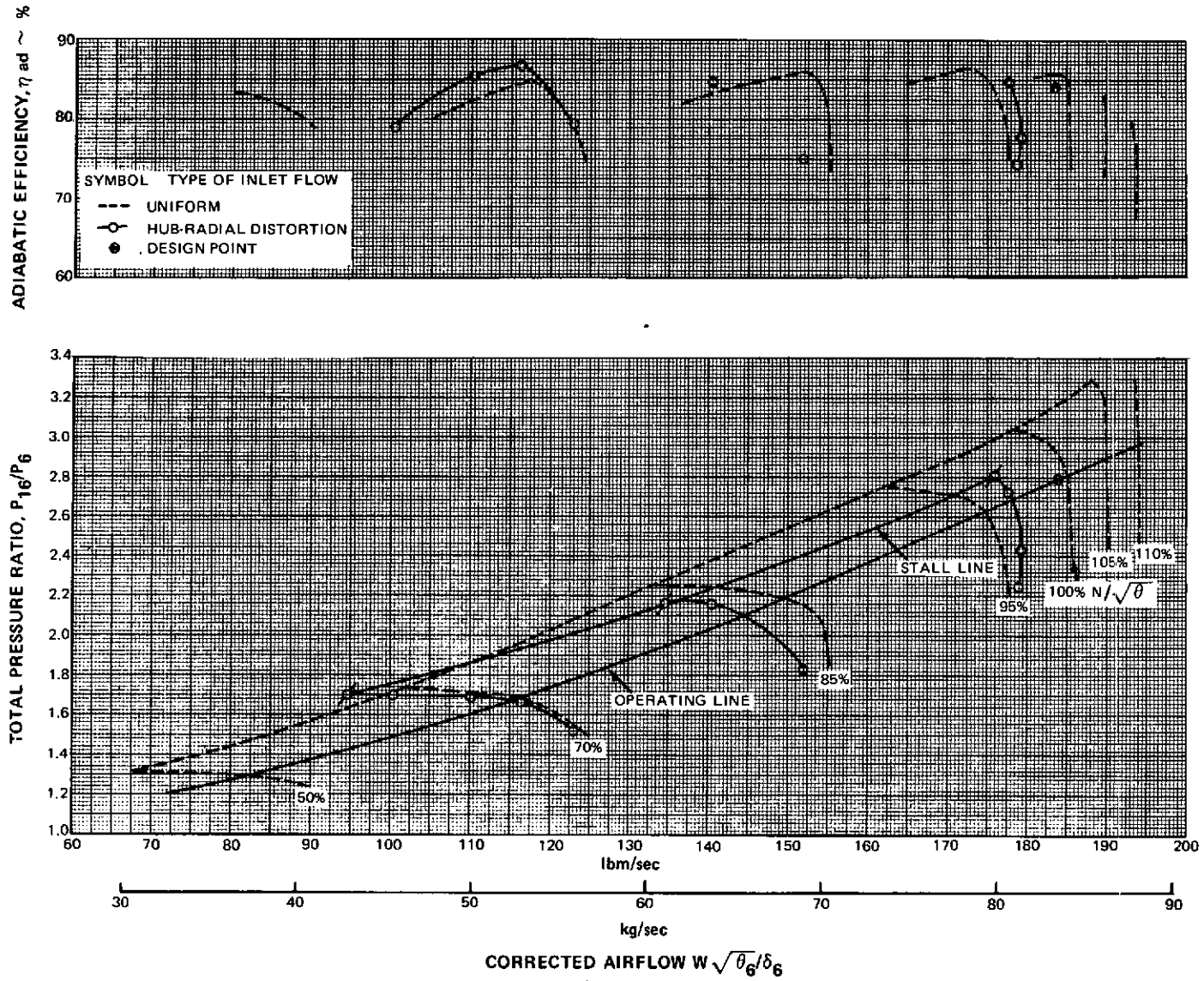


Figure 81 Fan Overall Performance with Hub Radially Distorted Inlet Flow

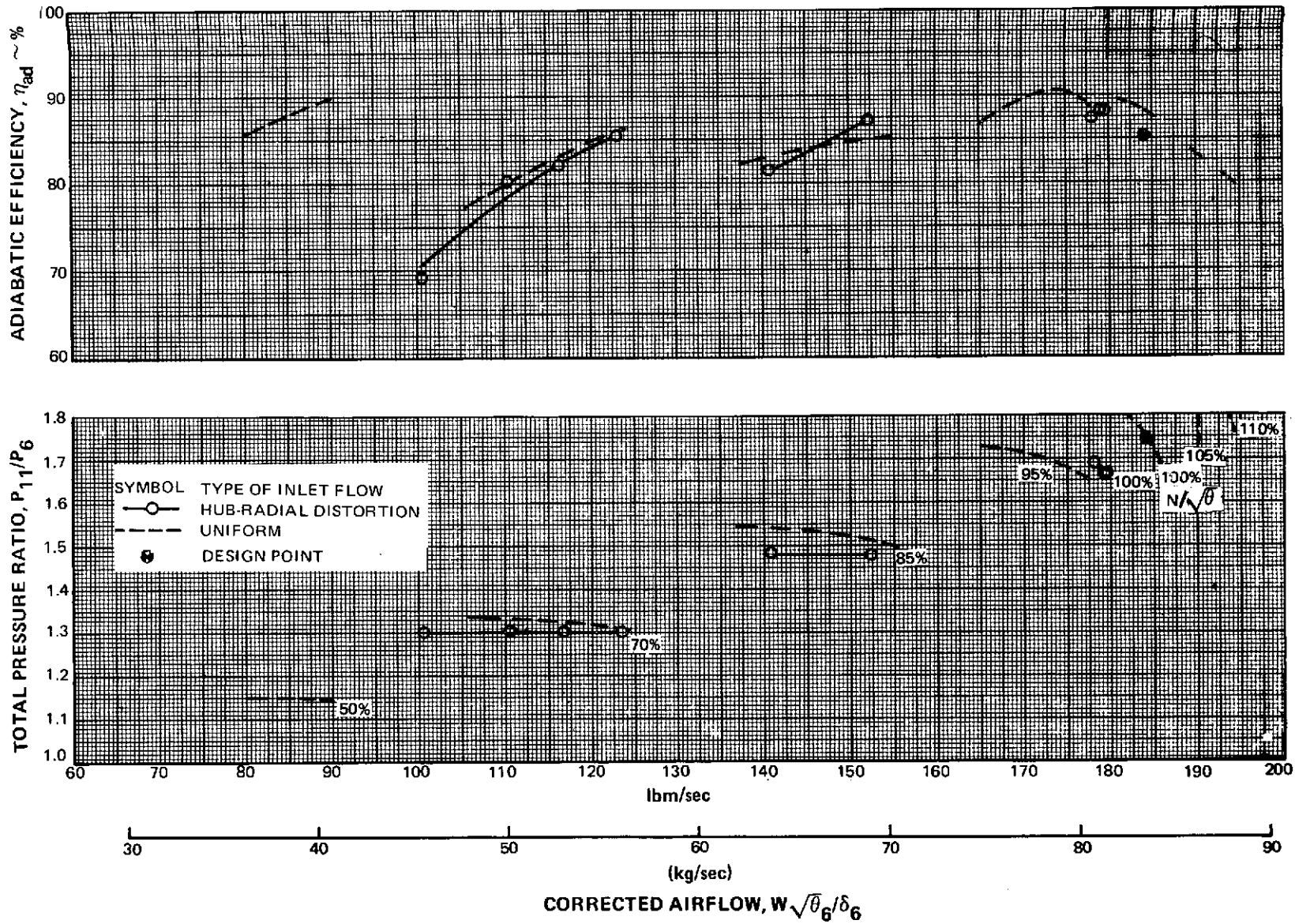


Figure 82 First Stage Performance with Hub Radially Distorted Inlet Flow

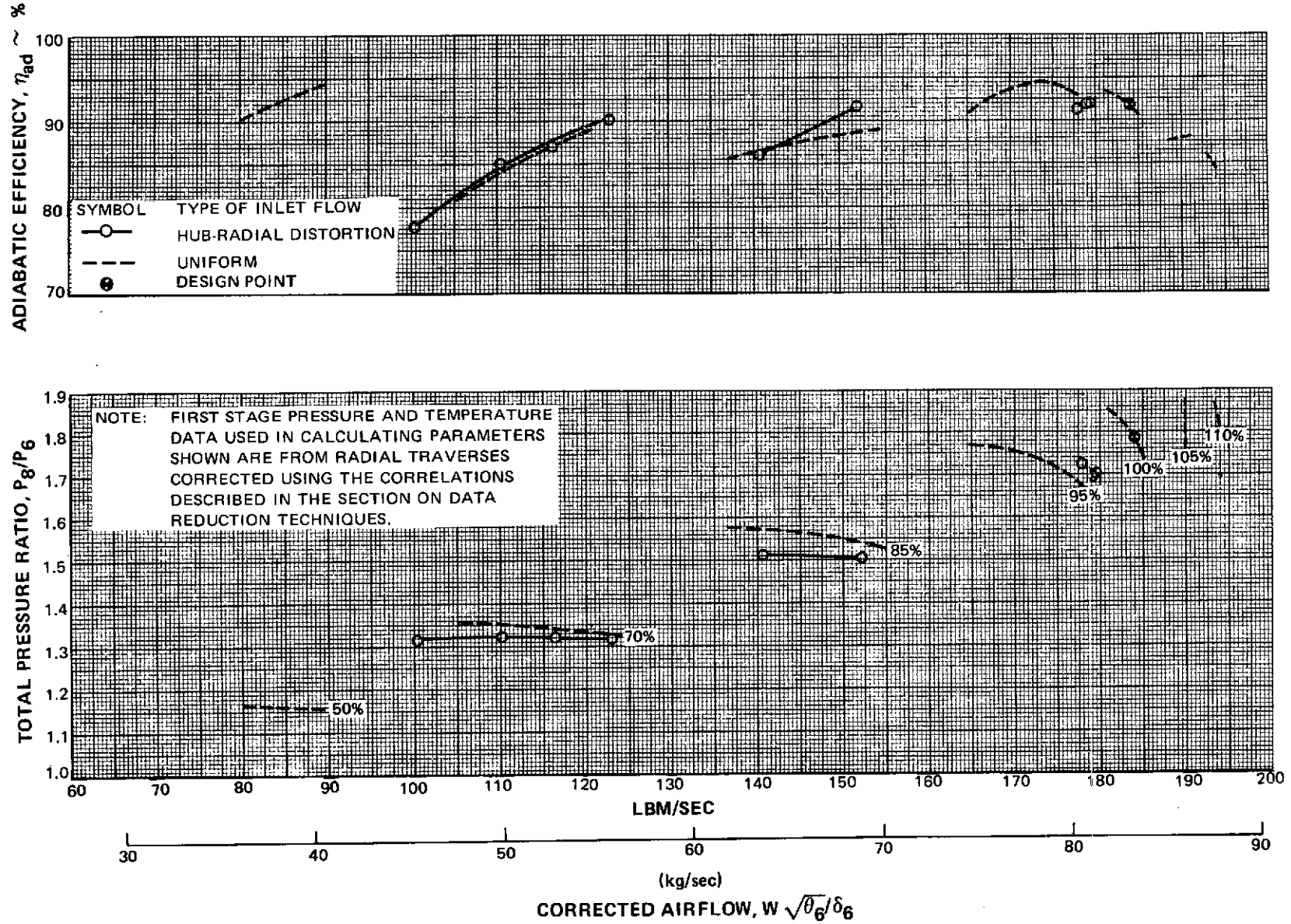


Figure 83 First Rotor Performance with Hub Radially Distorted Inlet Flow

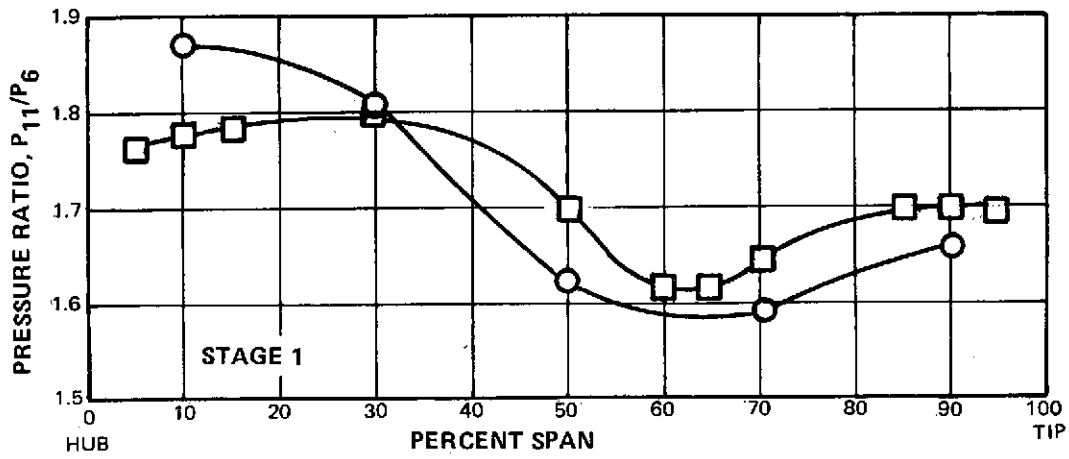
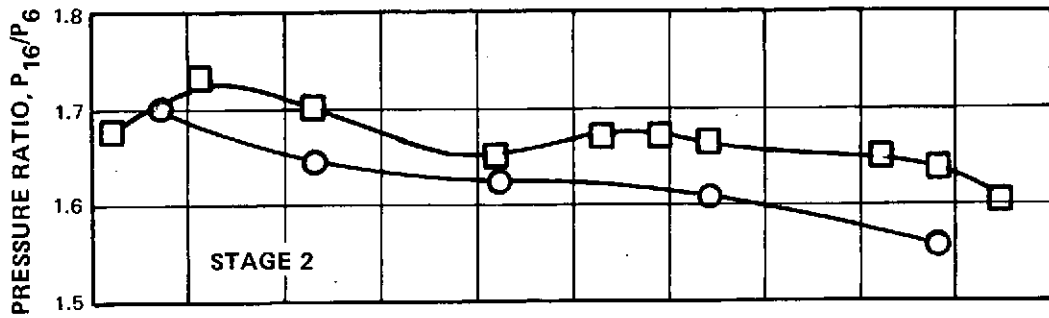


Figure 84 Spanwise Profiles of Stage 1 and Stage 2 Pressure Ratio for Uniform and Hub-Radially Distorted Inlet Flows at Design Speed

NOTE: First Stage Pressure and Temperature Data Used In Calculating Parameters Shown Is From Radial Traverses Corrected Using The Correlations Described In The Section On Data Reduction Techniques

- 100% SPEED
- × 85% SPEED
- ◇ 70% SPEED
- ⊠ 100% DESIGN POINT

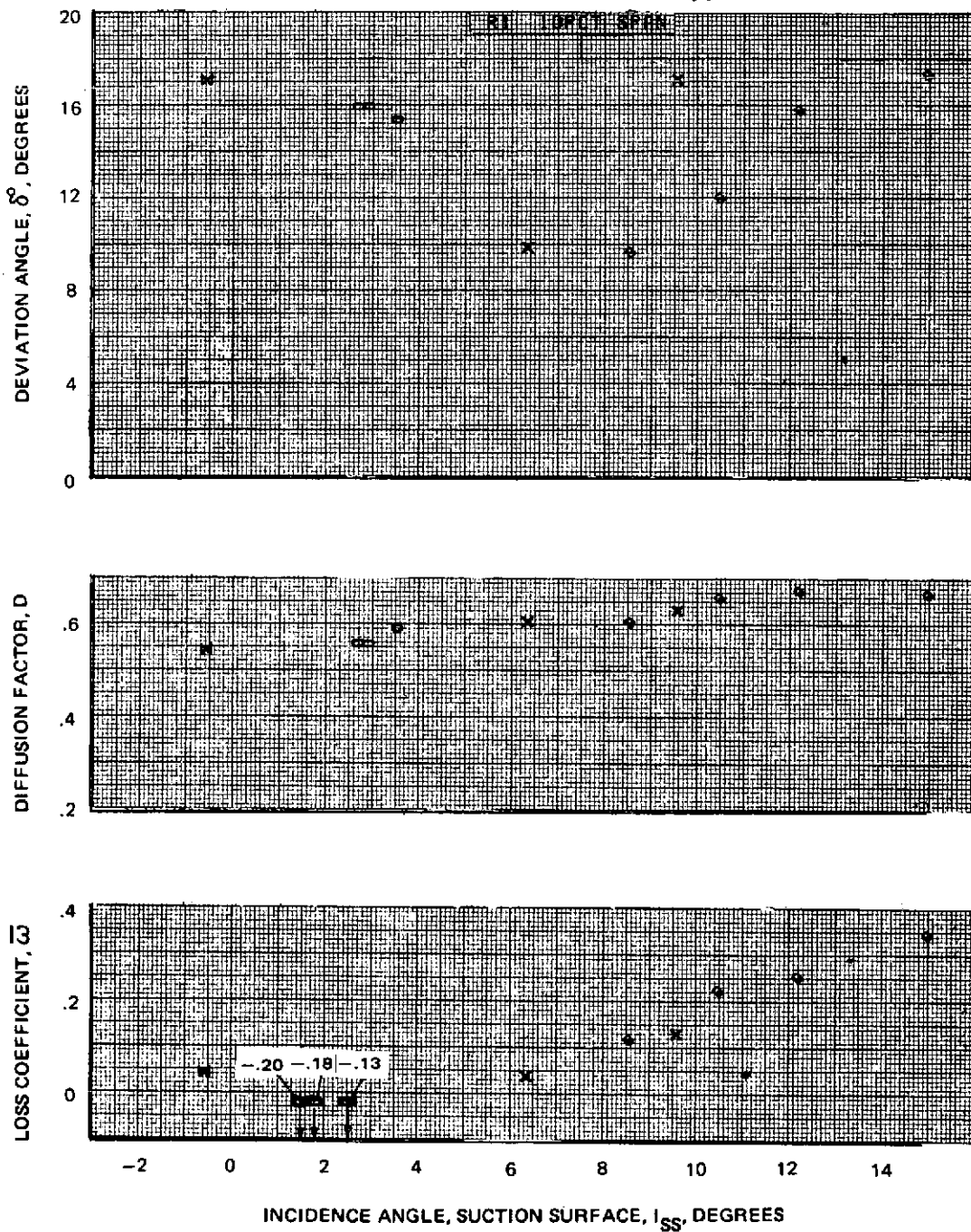


Figure 85a Blade Element Performance With Hub Radial Distortion – Rotor 1  
10% Span

NOTE: First Stage Pressure and Temperature Data Used In Calculating Parameters Shown Is From Radial Traverses Corrected Using The Correlations Described In The Section On Data Reduction Techniques

- 100% SPEED
- × 85% SPEED
- ◇ 70% SPEED
- ⊠ 100% DESIGN POINT

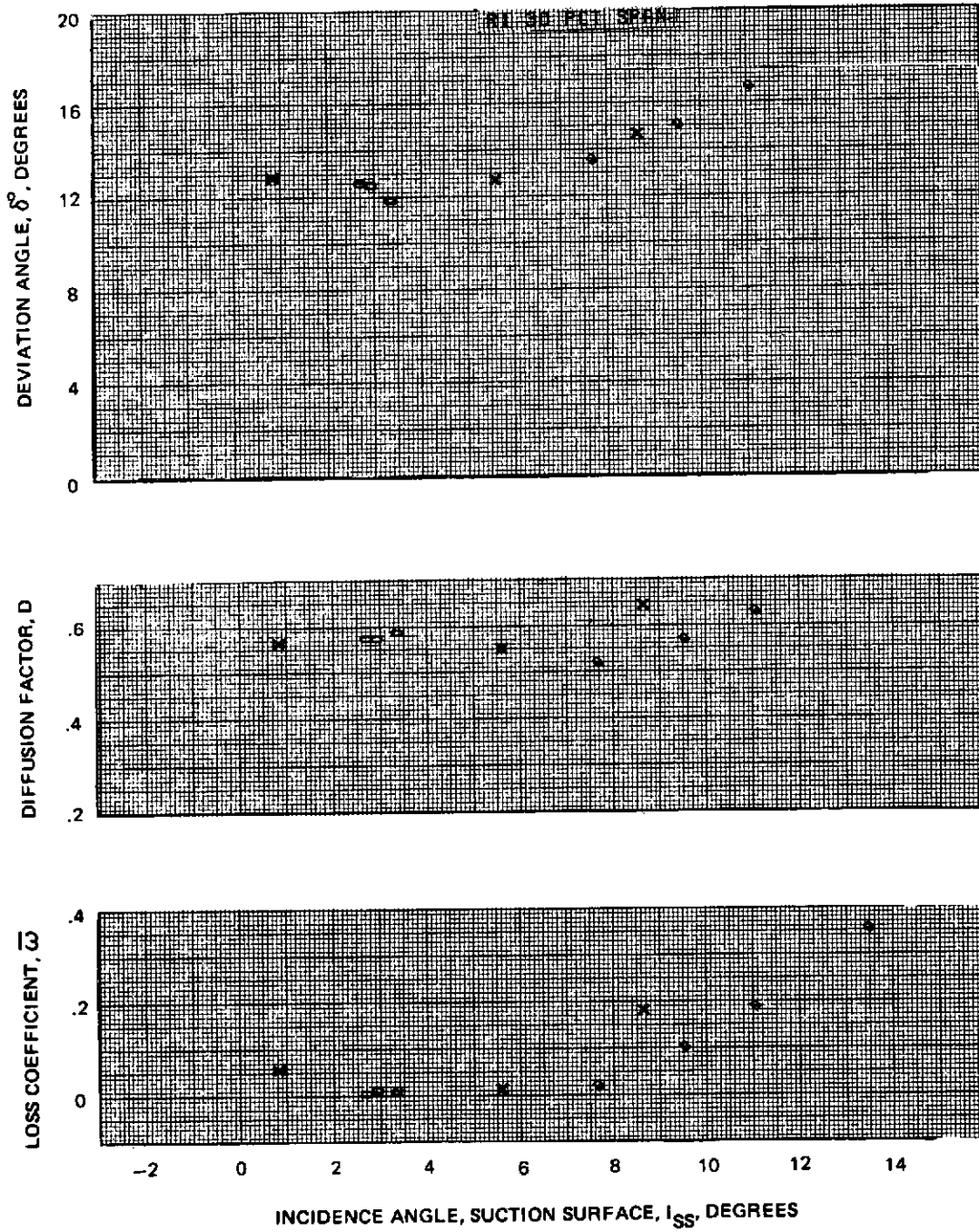


Figure 85b Blade Element Performance With Hub Radial Distortion – Rotor 1 30% Span

NOTE: First Stage Pressure and Temperature Data Used In Calculating Parameters Shown Is From Radial Traverses Corrected Using The Correlations Described In The Section On Data Reduction Techniques

○ 100% SPEED  
 × 85% SPEED  
 ◇ 70% SPEED  
 ⊠ 100% DESIGN POINT

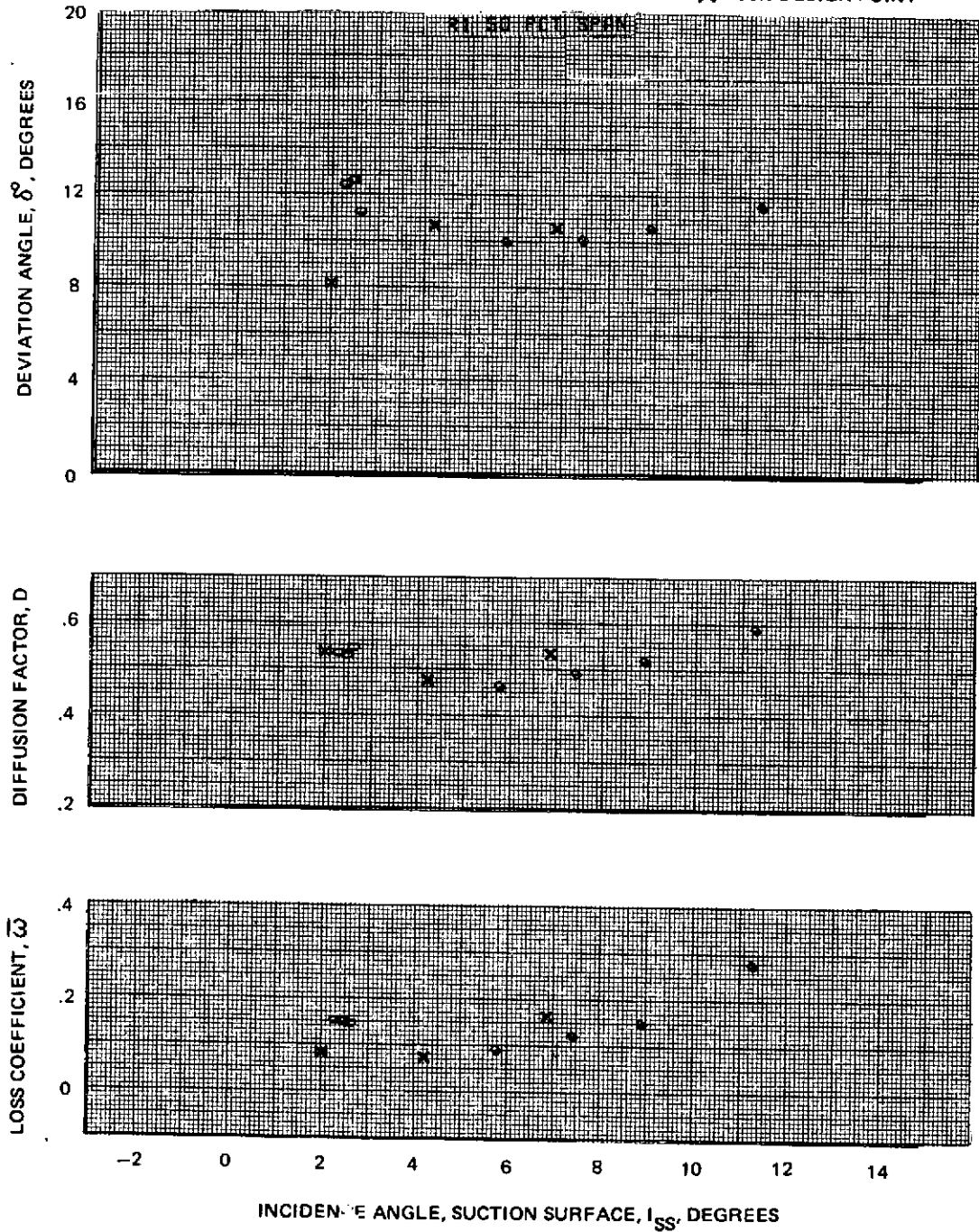


Figure 85c Blade Element Performance With Hub Radial Distortion – Rotor 1  
 50% Span



NOTE: First Stage Pressure and Temperature Data Used In Calculating Parameters Shown Is From Radial Traverses Corrected Using The Correlations Described In The Section On Data Reduction Techniques

- 100% SPEED
- × 85% SPEED
- ◇ 70% SPEED
- ⊠ 100% DESIGN POINT

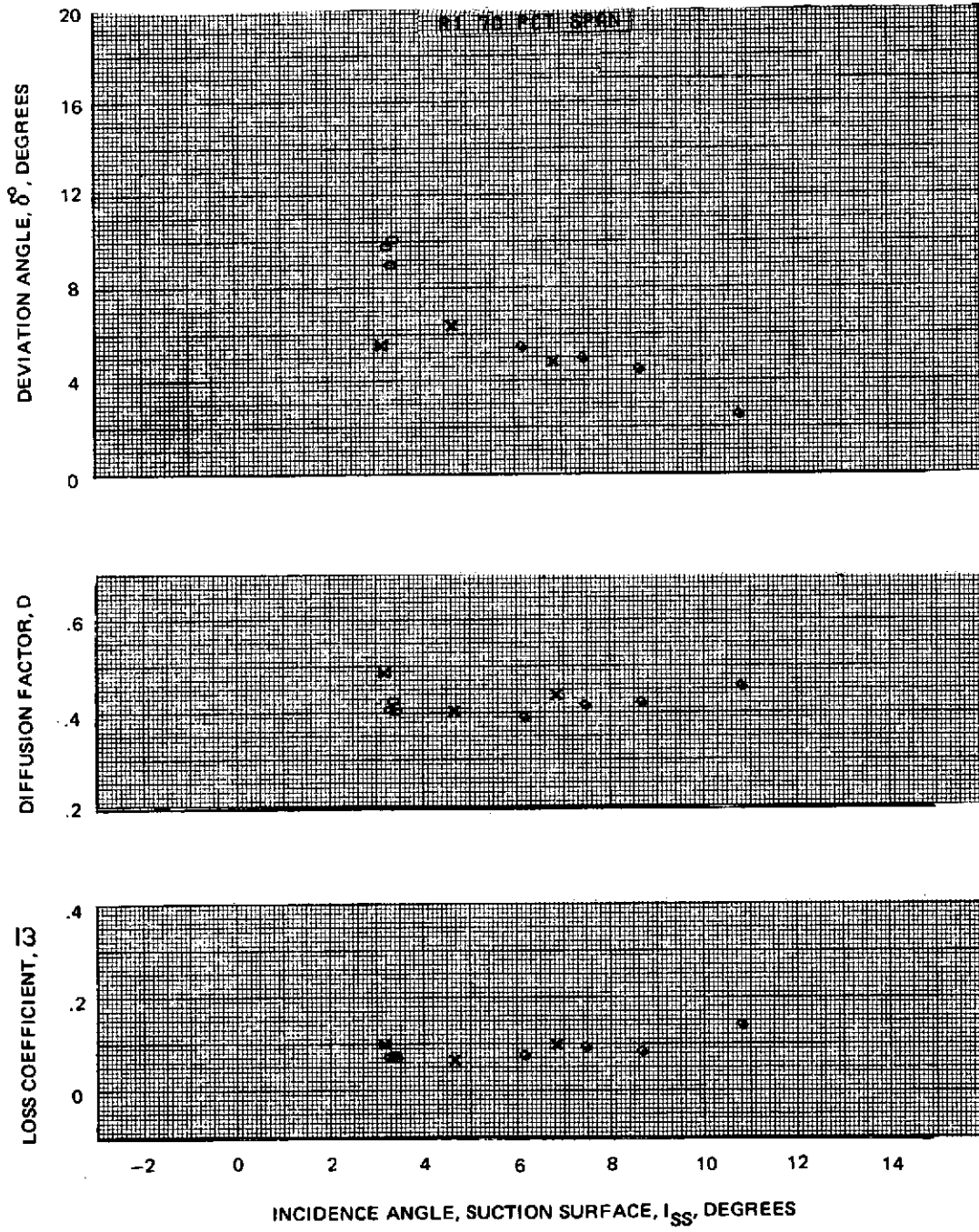


Figure 85d Blade Element Performance With Hub Radial Distortion – Rotor 1  
70% Span

NOTE: First Stage Pressure and Temperature Data Used In Calculating Parameters Shown Is From Radial Traverses Corrected Using The Correlations Described In The Section On Data Reduction Techniques

- 100% SPEED
- × 85% SPEED
- ◇ 70% SPEED
- ⊠ 100% DESIGN POINT

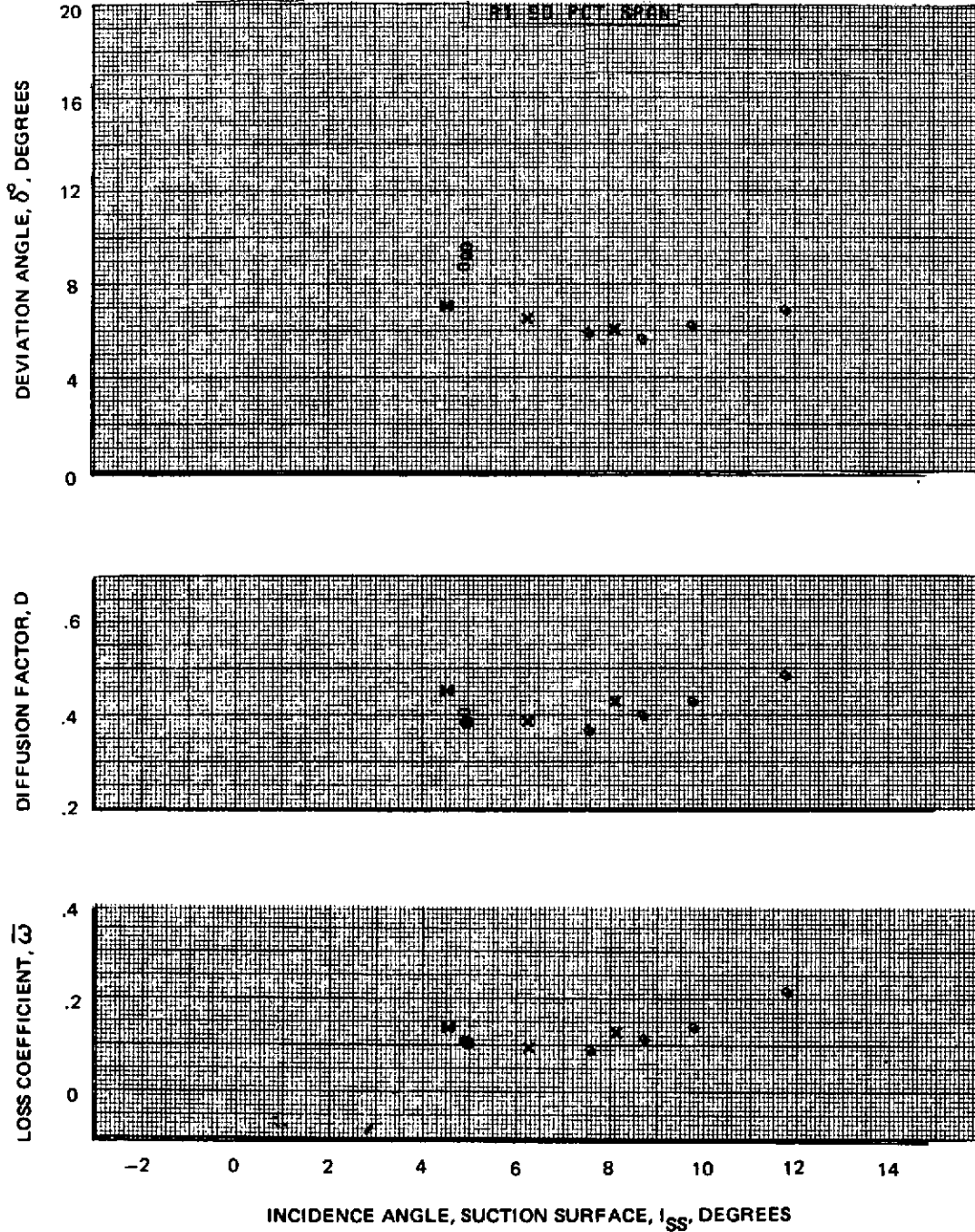


Figure 85e Blade Element Performance With Hub Radial Distortion – Rotor 1  
90% Span

NOTE: First Stage Pressure and Temperature Data Used In Calculating Parameters Shown Are From Radial Traverses Corrected Using The Correlations Described In The Section On Data Reduction Techniques

□ 100% SPEED  
 X 85% SPEED  
 ◇ 70% SPEED  
 △ 100% DESIGN POINT

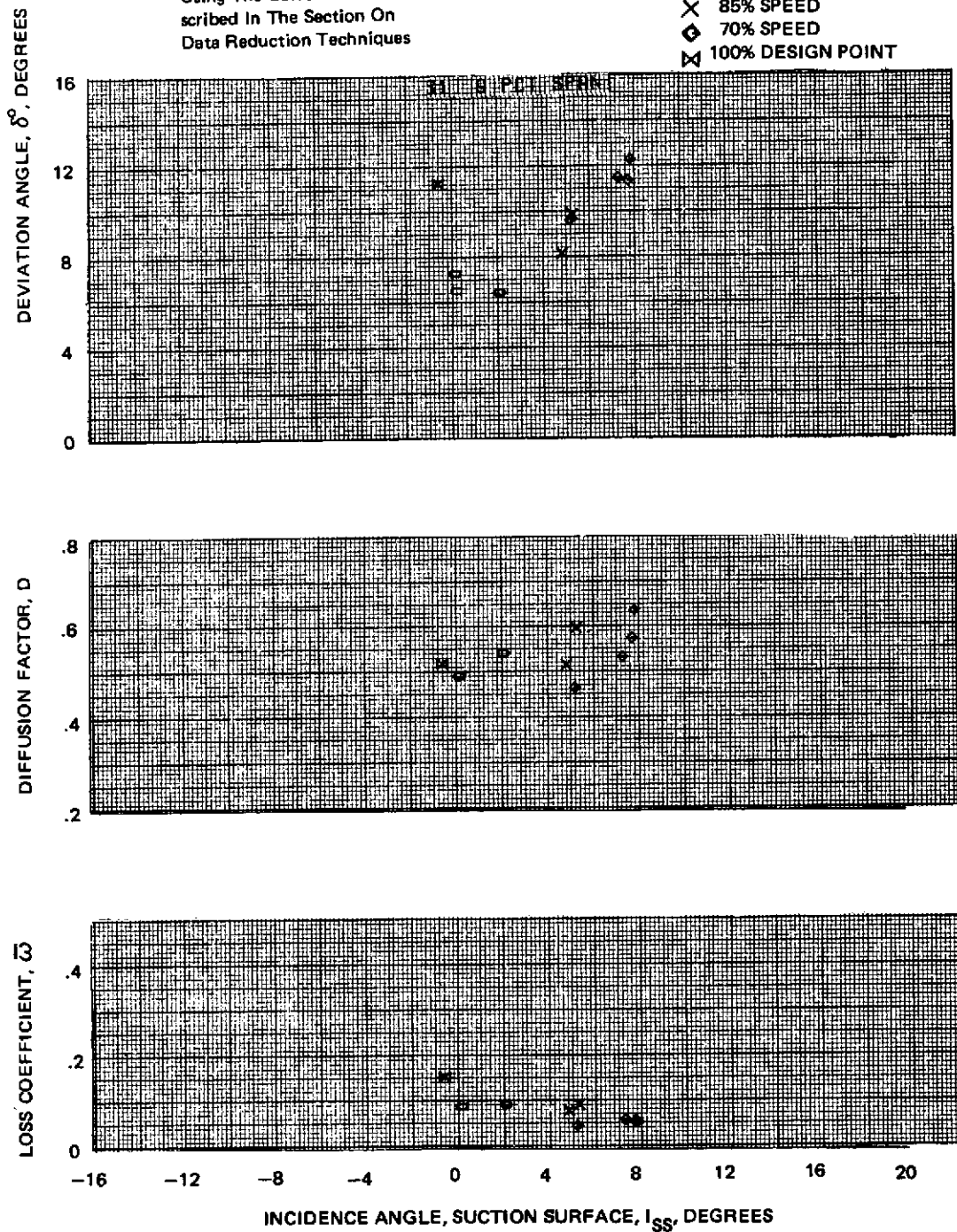


Figure 86a Blade Element Performance With Hub Radial Distortion – Stator 1  
 9% Span

NOTE: First Stage Pressure and Temperature Data Used In Calculating Parameters Shown Are From Radial Traverses Corrected Using The Correlations Described In The Section On Data Reduction Techniques

- 100% SPEED
- × 85% SPEED
- ◇ 70% SPEED
- ⊠ 100% DESIGN POINT

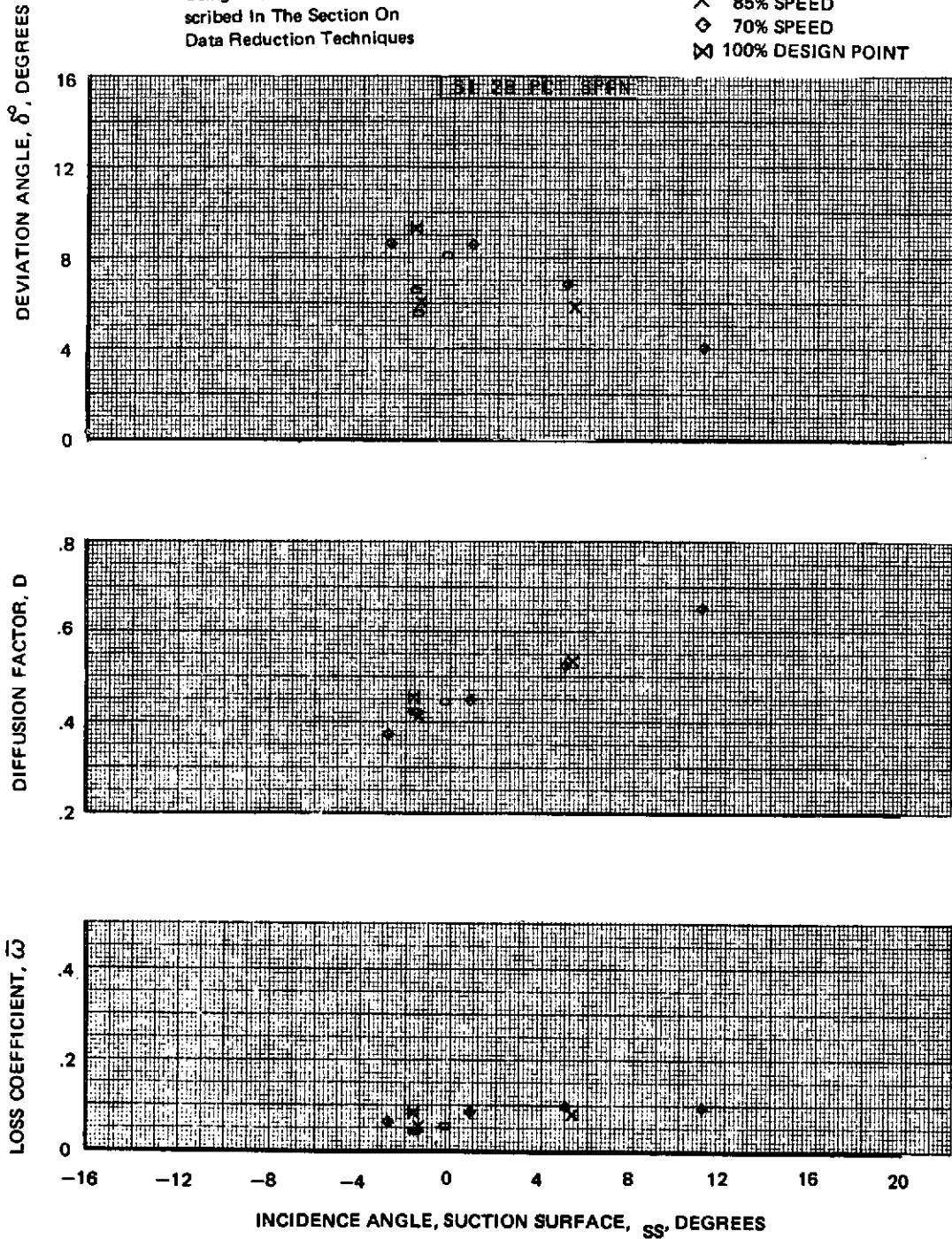


Figure 86b Blade Element Performance With Hub Radial Distortion – Stator 1  
28% Span

NOTE: First Stage Pressure and Temperature Data Used In Calculating Parameters Shown Are From Radial Traverses Corrected Using The Correlations Described In The Section On Data Reduction Techniques

- 100% SPEED
- × 85% SPEED
- ◇ 70% SPEED
- ⊠ 100% DESIGN POINT

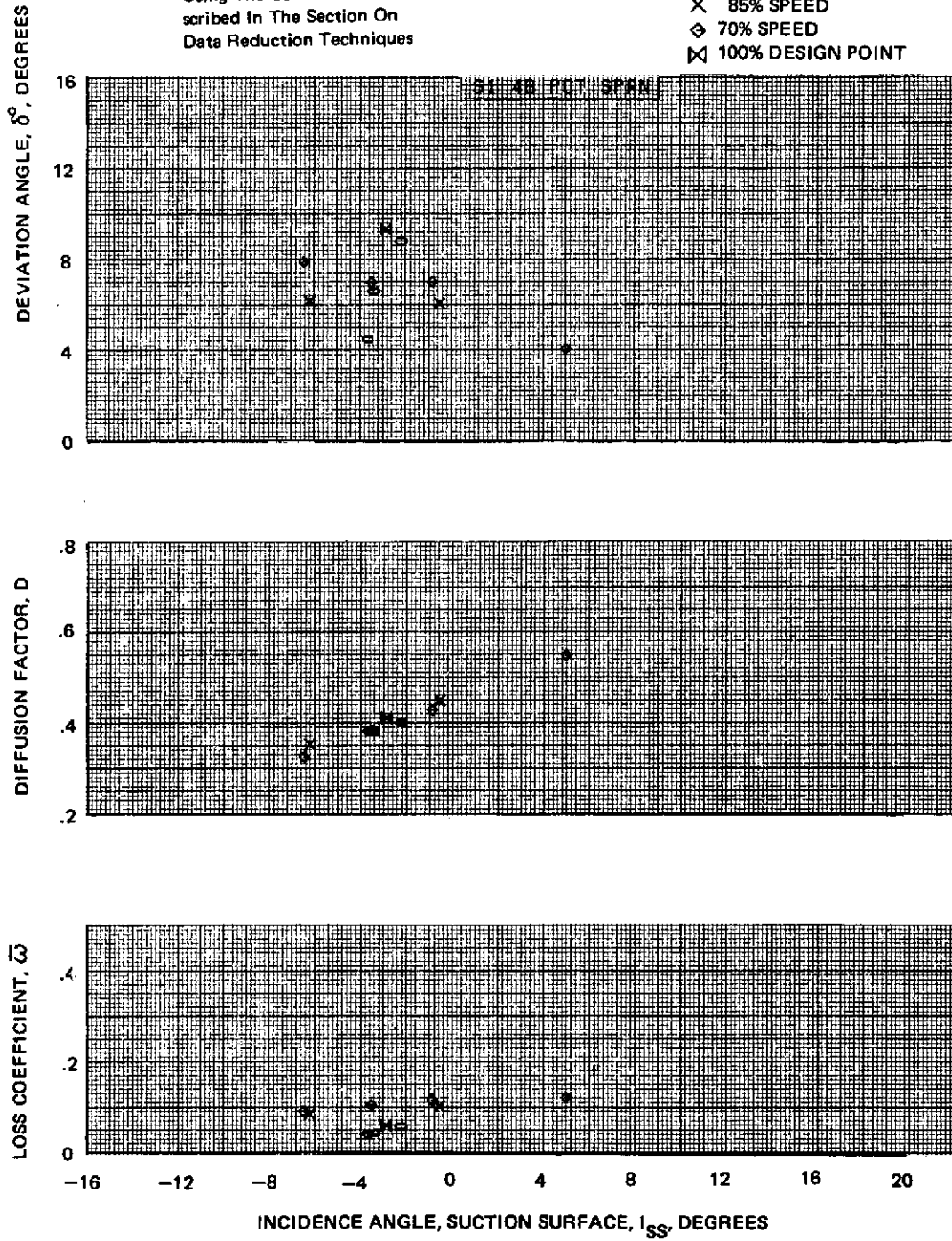


Figure 86c Blade Element Performance With Hub Radial Distortion – Stator 1  
48% Span

NOTE: First Stage Pressure and Temperature Data Used In Calculating Parameters Shown Are From Radial Traverses Corrected Using The Correlations Described In The Section On Data Reduction Techniques

- 100% SPEED
- × 85% SPEED
- ◇ 70% SPEED
- ⊗ 100% DESIGN POINT

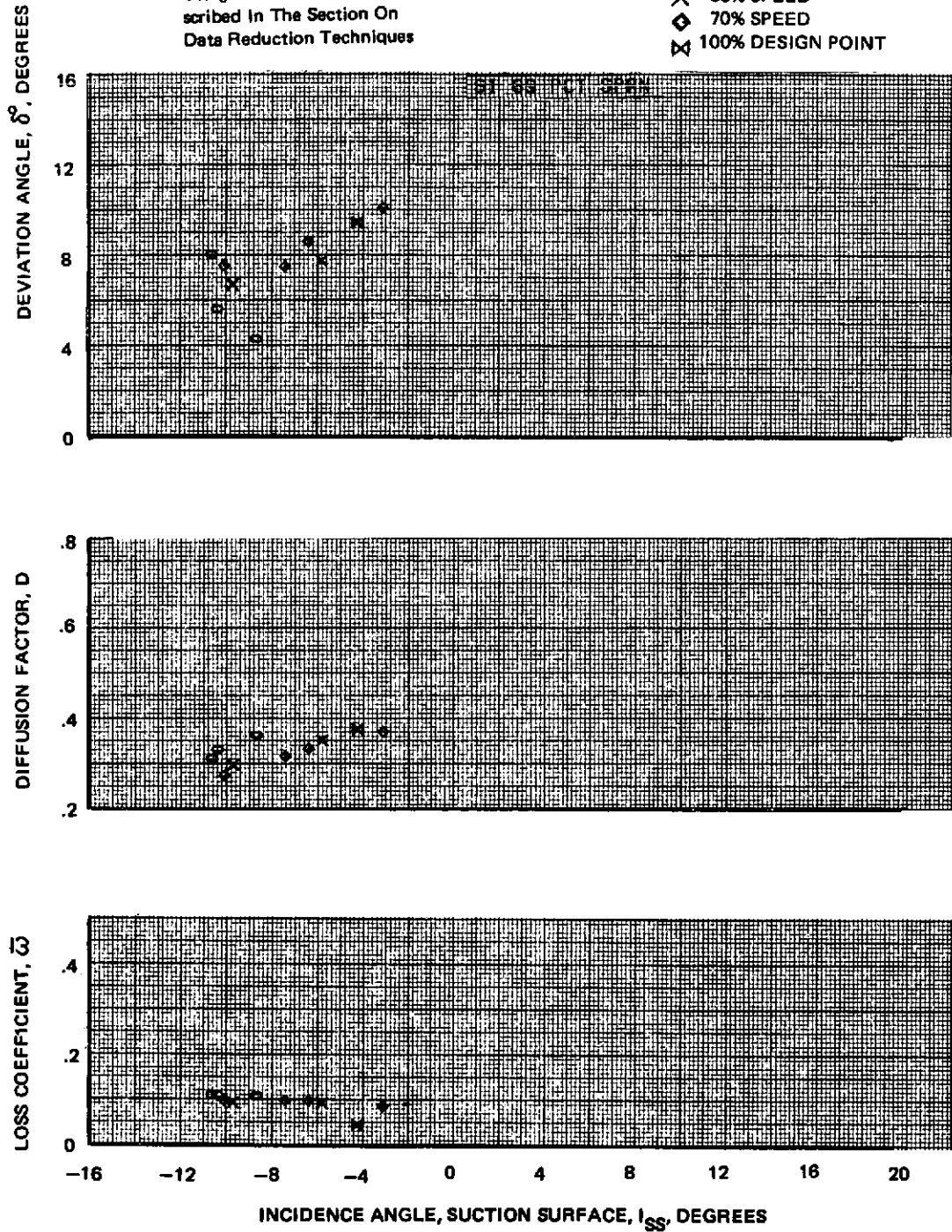


Figure 86d. Blade Element Performance With Hub Radial Distortion – Stator 1  
69% Span

NOTE: First Stage Pressure and Temperature Data Used In Calculating Parameters Shown Are From Radial Traverses Corrected Using The Correlations Described In The Section On Data Reduction Techniques

- 100% SPEED
- × 85% SPEED
- ◇ 70% SPEED
- ⊠ 100% DESIGN POINT

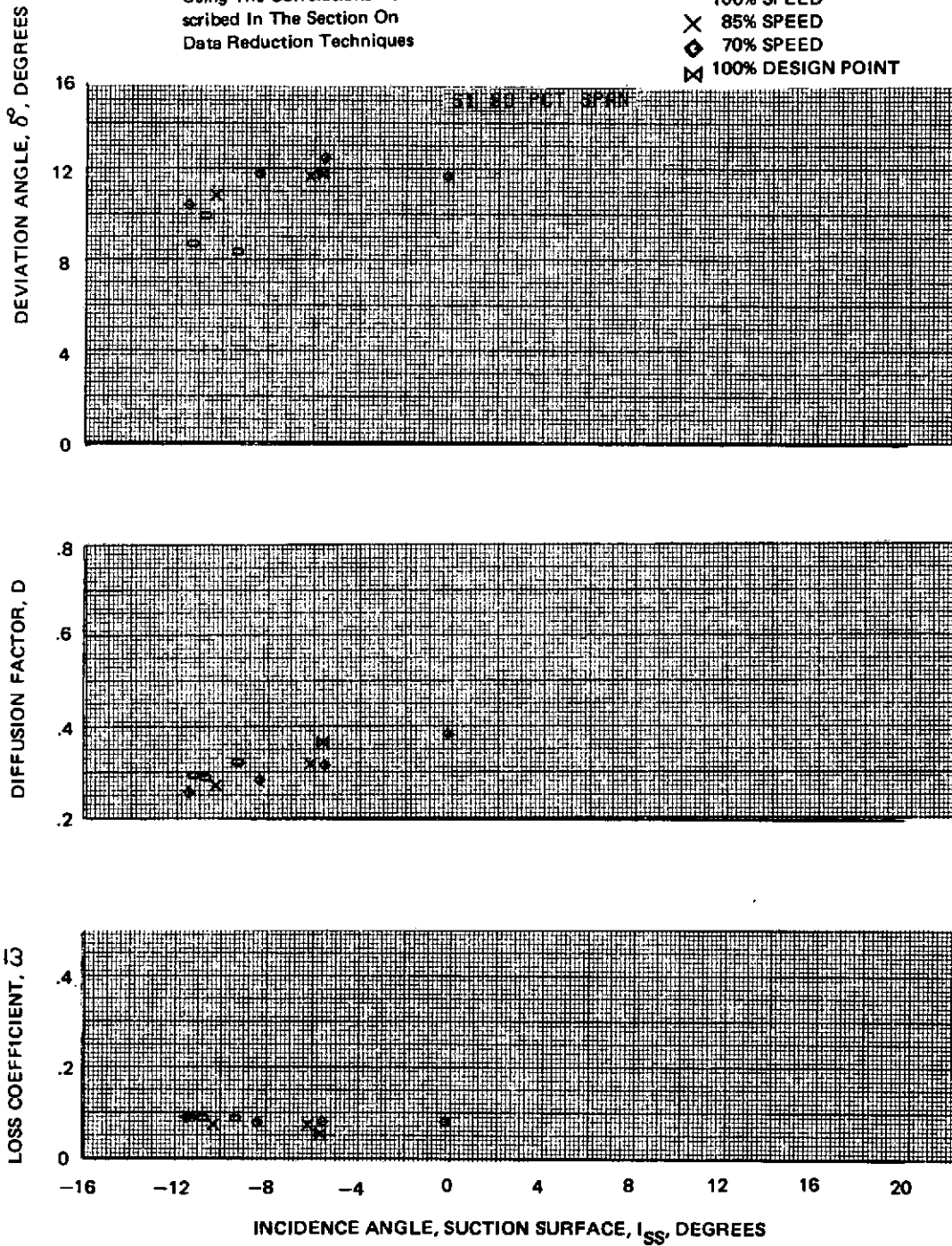


Figure 86e Blade Element Performance With Hub Radial Distortion – Stator 1  
90% Span

NOTE: First Stage Pressure and Temperature Data Used In Calculating Parameters Shown Are From Radial Traverses Corrected Using The Correlations Described In The Section On Data Reduction Techniques

○ 100% SPEED  
 × 85% SPEED  
 ◇ 70% SPEED  
 ⊠ 100% DESIGN POINT

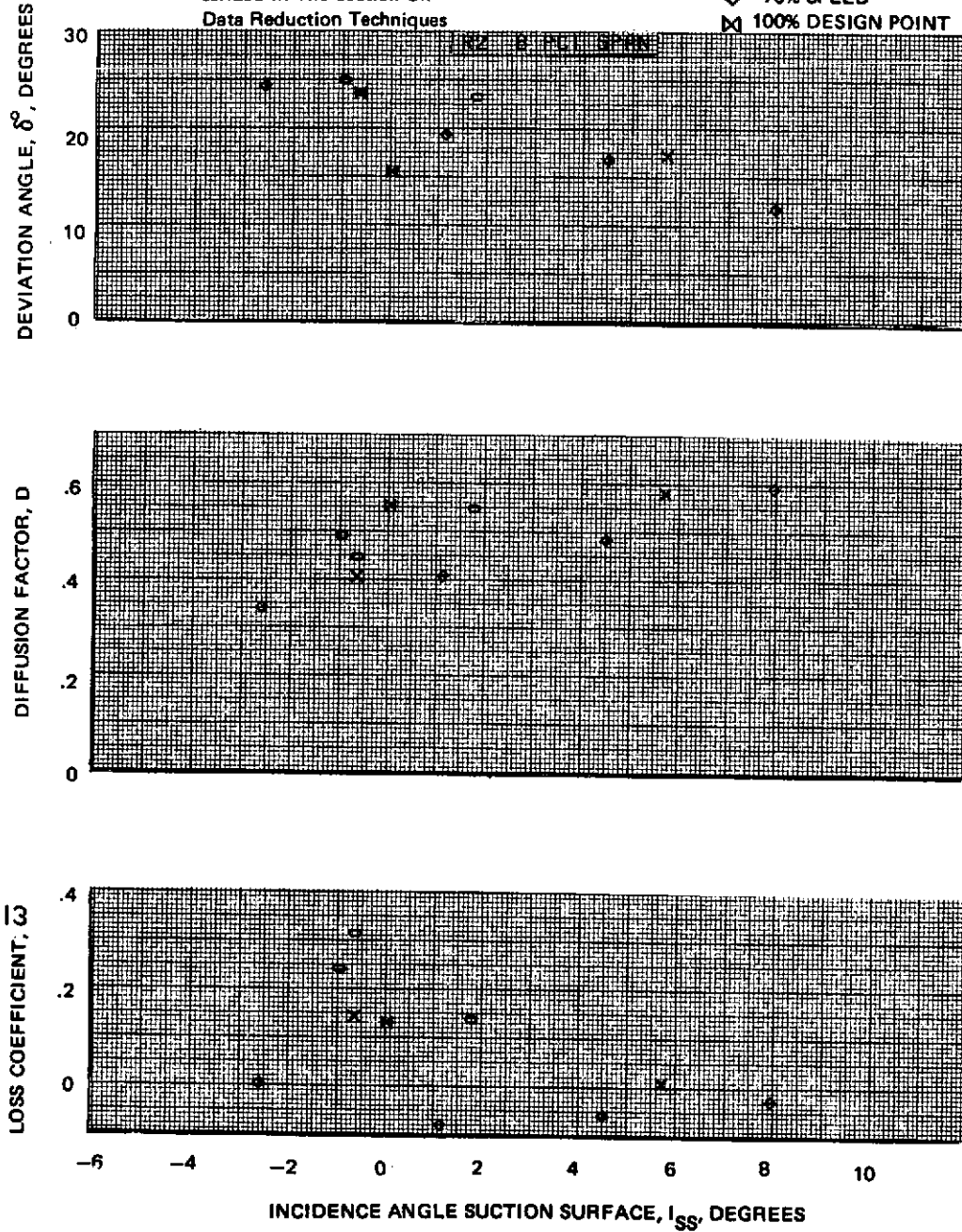


Figure 87a Blade Element Performance With Hub Radial Distortion – Rotor 2  
 8% Span



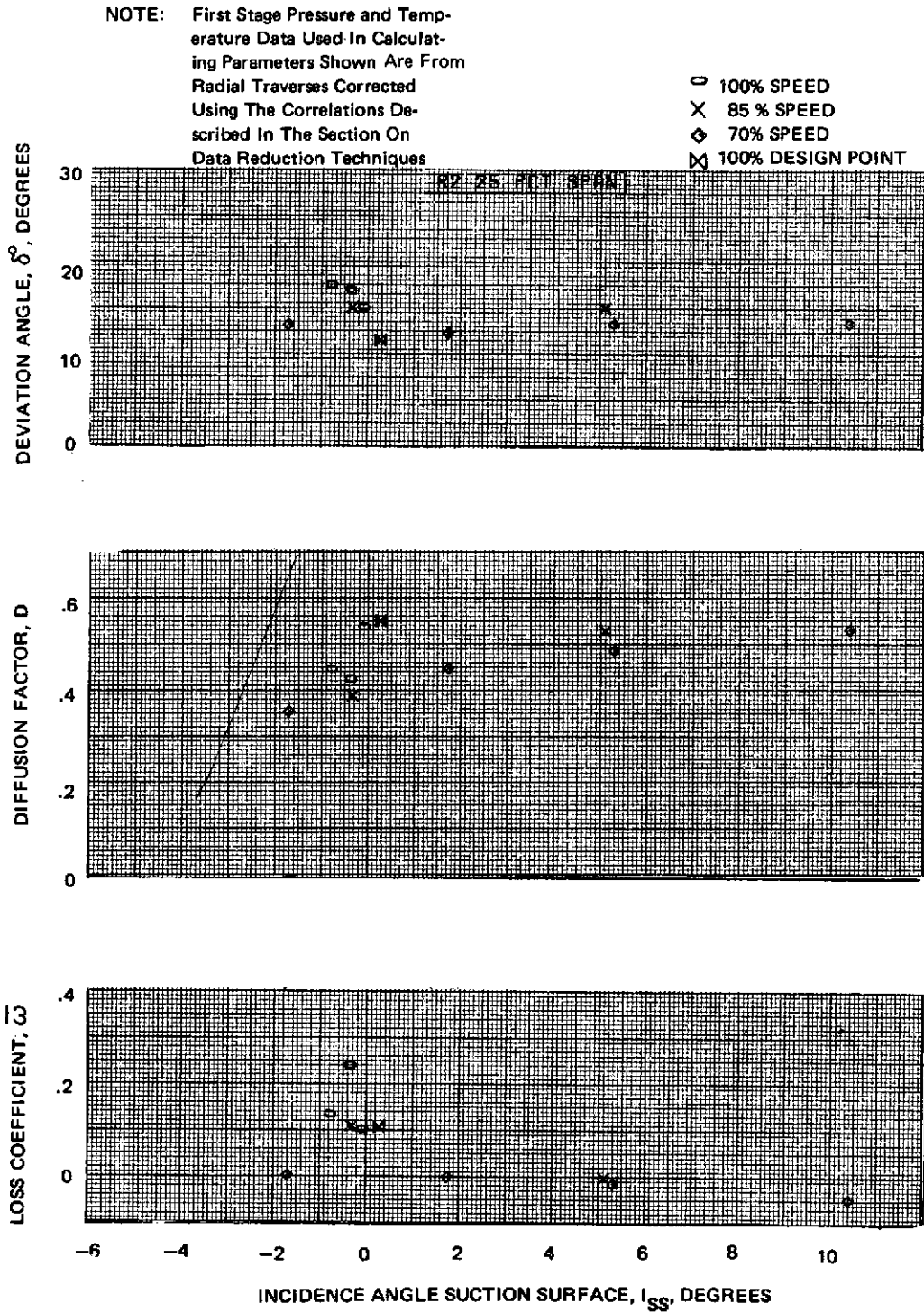


Figure 87b Blade Element Performance With Hub Radial Distortion – Rotor 2  
25% Span

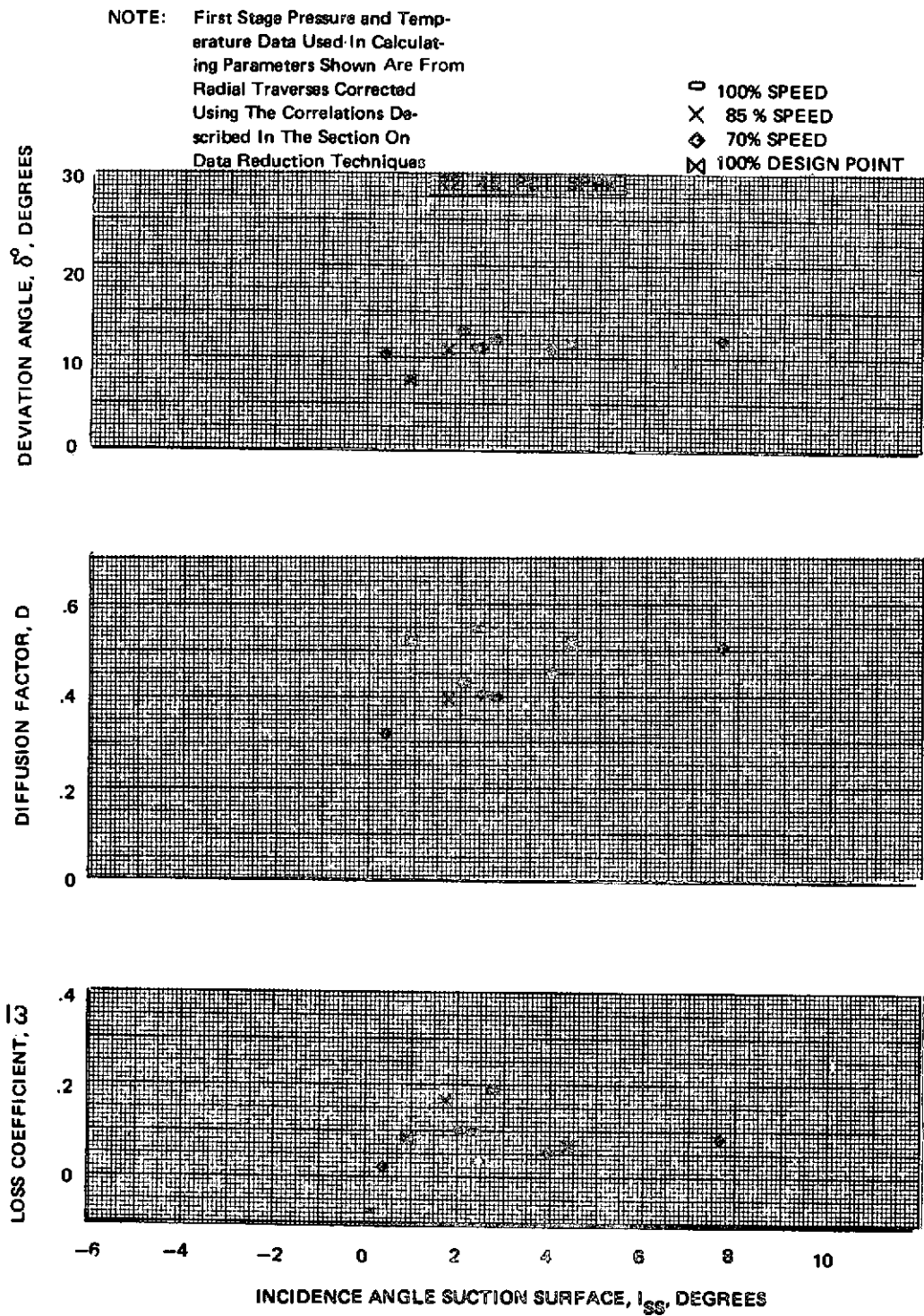


Figure 87c Blade Element Performance With Hub Radial Distortion – Rotor 2  
45% Span

NOTE: First Stage Pressure and Temperature Data Used In Calculating Parameters Shown Are From Radial Traverses Corrected Using The Correlations Described In The Section On Data Reduction Techniques

- 100% SPEED
- × 85% SPEED
- ◇ 70% SPEED
- ⊠ 100% DESIGN POINT

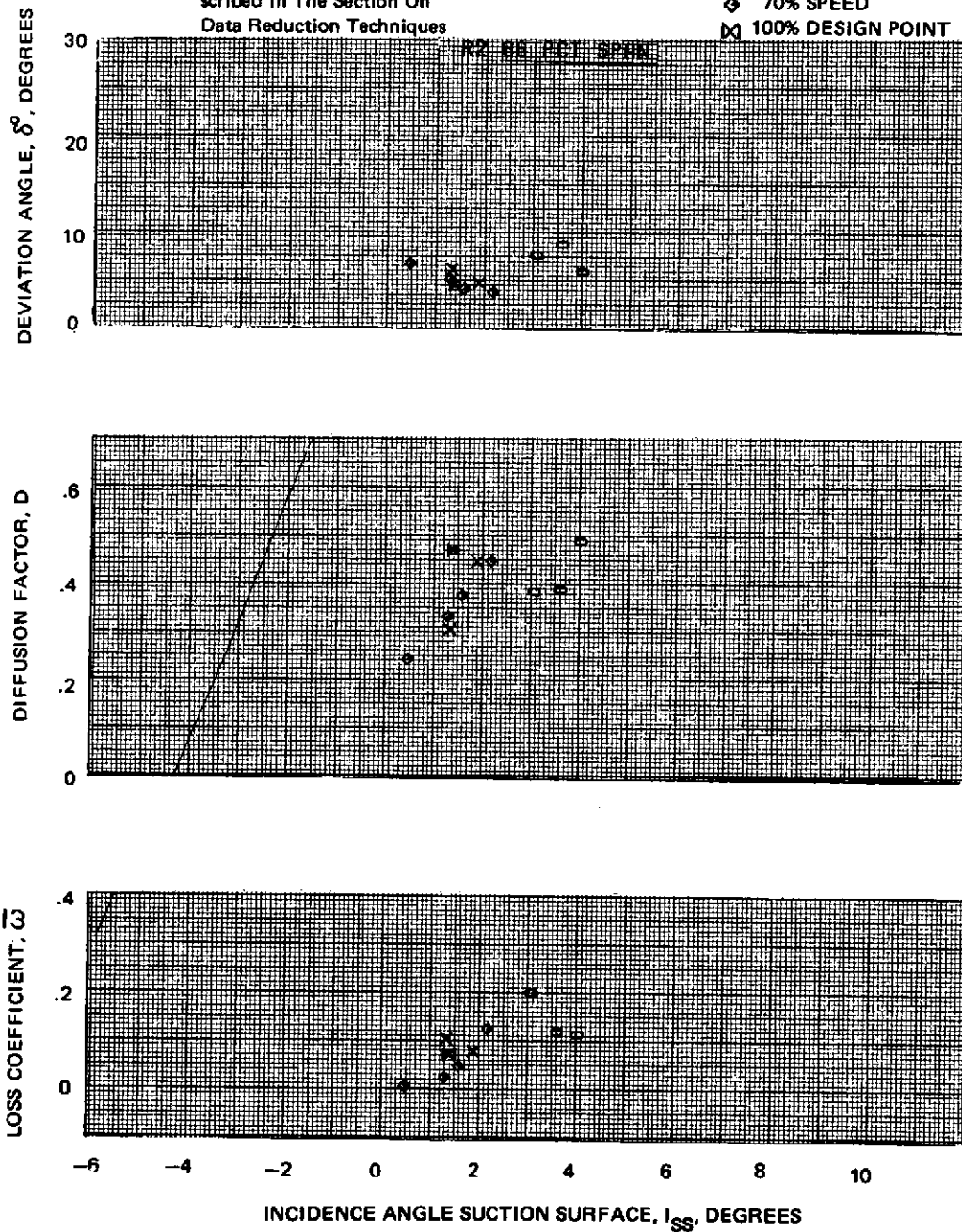


Figure 87d Blade Element Performance With Hub Radial Distortion – Rotor 2  
66% Span

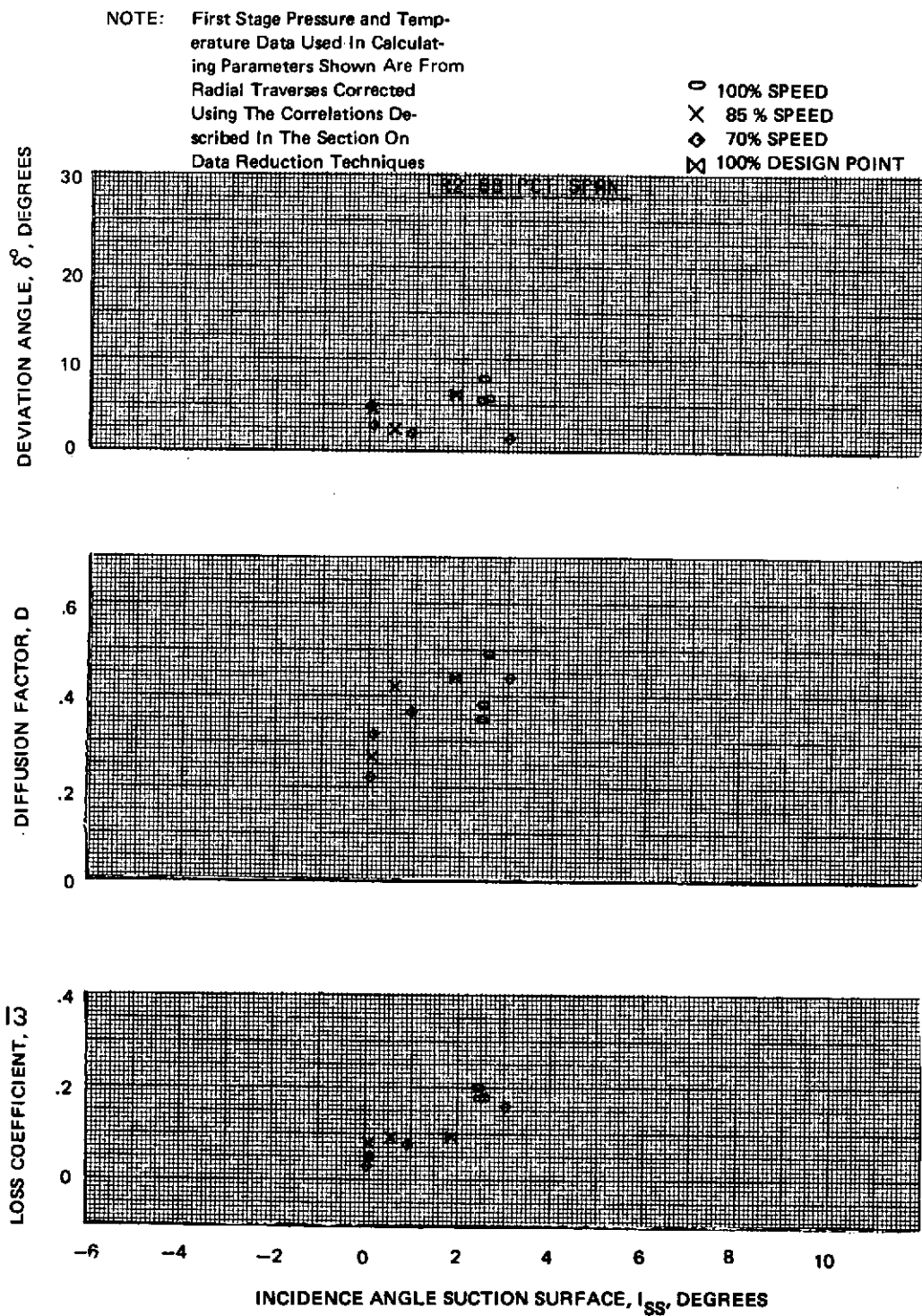


Figure 87e Blade Element Performance With Hub Radial Distortion – Rotor 2  
88% Span

NOTE: First Stage Pressure and Temperature Data Used In Calculating Parameters Shown Is From Radial Traverses Corrected Using The Correlations Described In The Section On Data Reduction Techniques

- 100% SPEED
- × 85% SPEED
- ◇ 70% SPEED
- ⊠ 100% DESIGN POINT

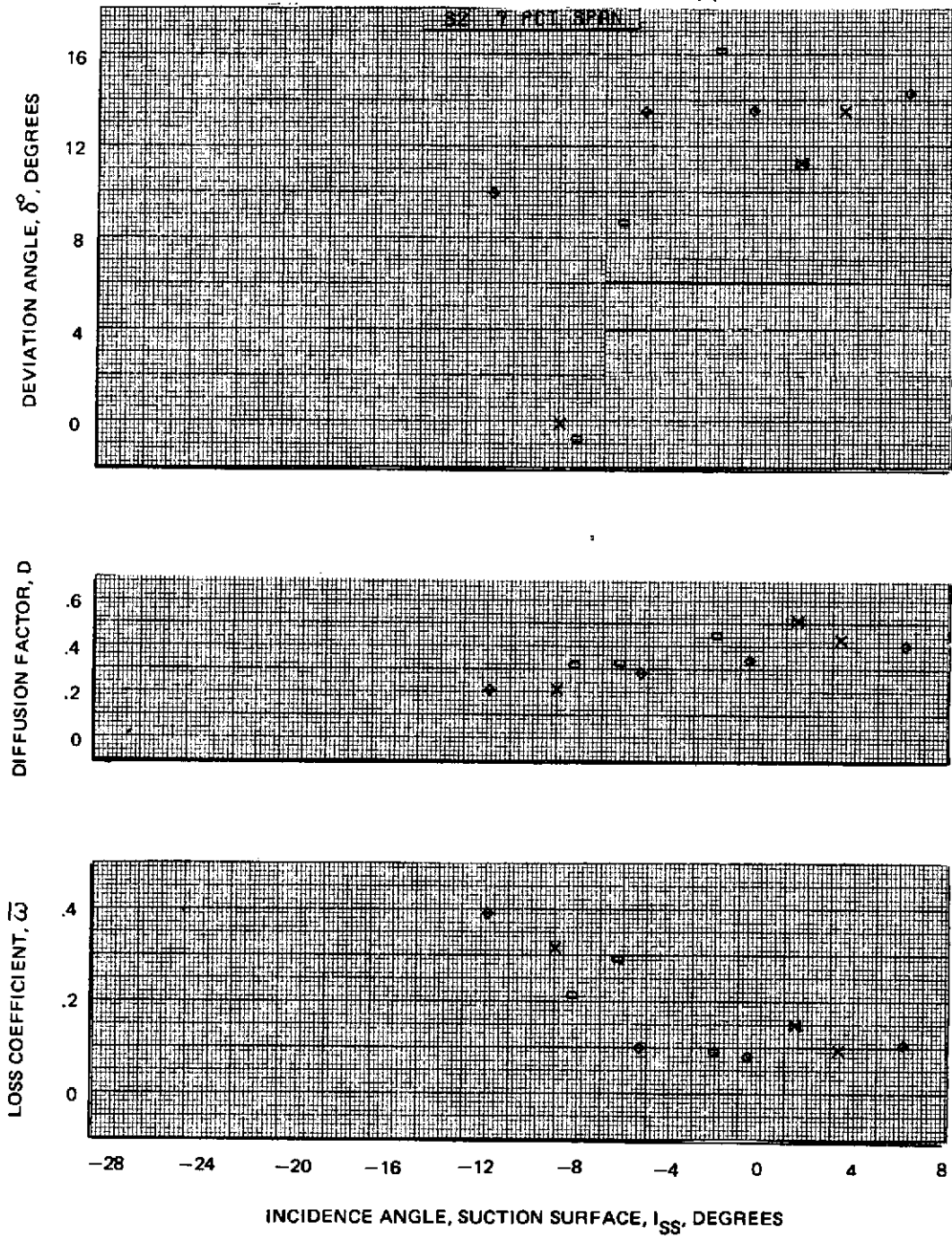


Figure 88a Blade Element Performance With Hub Radial Distortion – Stator 2  
7% Span

NOTE: First Stage Pressure and Temperature Data Used In Calculating Parameters Shown Is From Radial Traverses Corrected Using The Correlations Described In The Section On Data Reduction Techniques

- 100% SPEED
- × 85% SPEED
- ◇ 70% SPEED
- ⊗ 100% DESIGN POINT

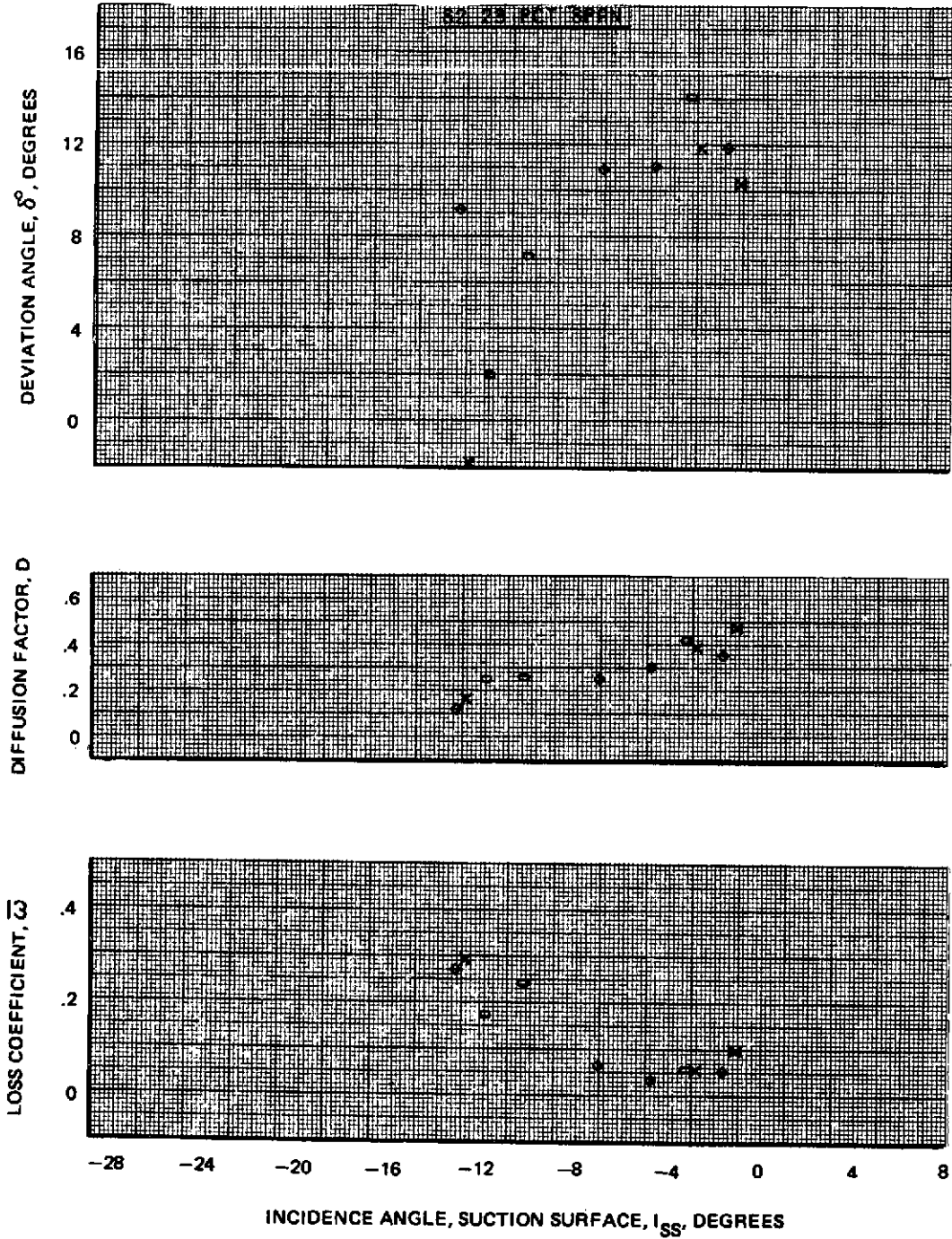


Figure 88b Blade Element Performance With Hub Radial Distortion – Stator 2  
23% Span

NOTE: First Stage Pressure and Temperature Data Used In Calculating Parameters Shown Is From Radial Traverses Corrected Using The Correlations Described In The Section On Data Reduction Techniques

○ 100% SPEED  
 × 85% SPEED  
 ◇ 70% SPEED  
 ⊠ 100% DESIGN POINT

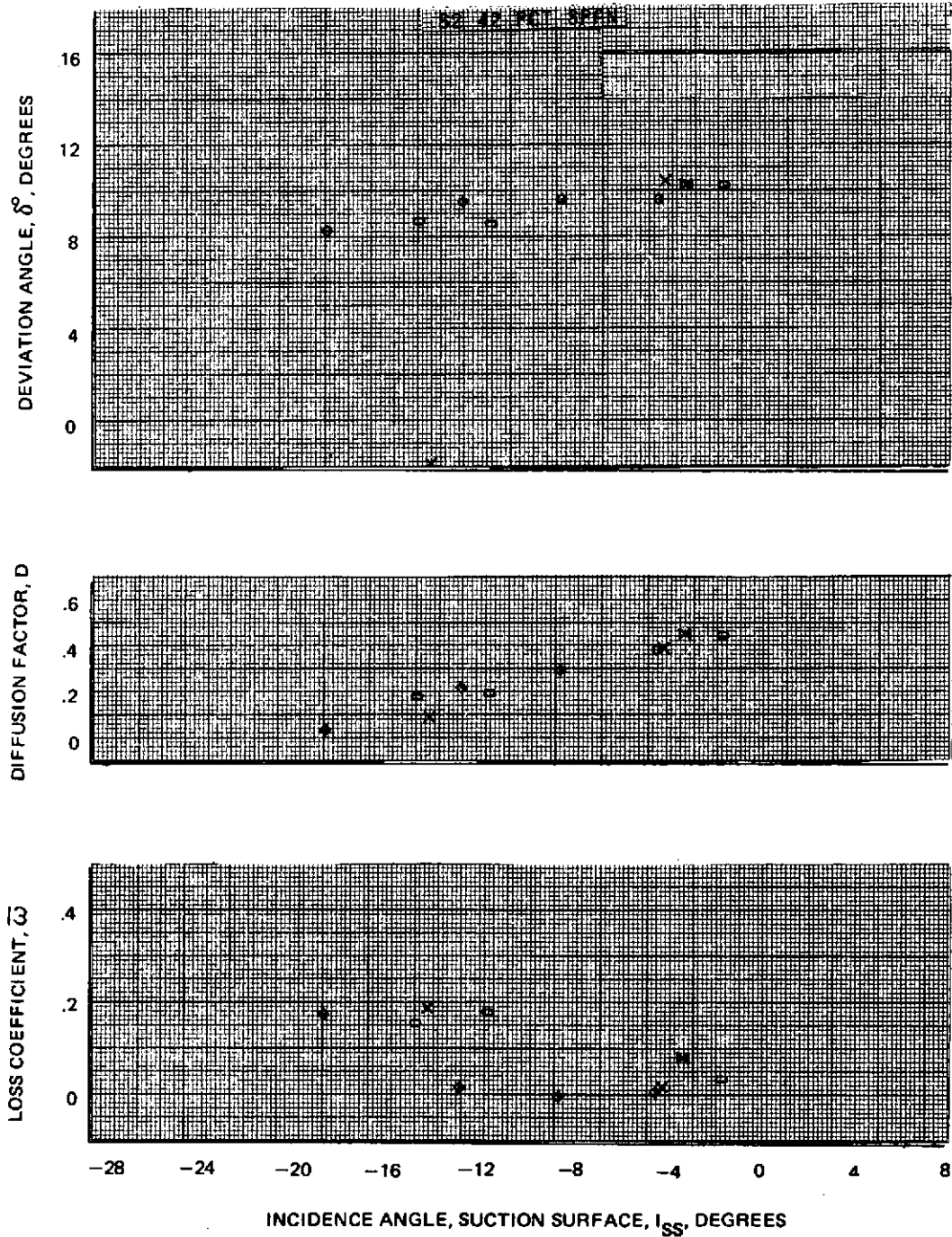


Figure 88c Blade Element Performance With Hub Radial Distortion – Stator 2  
 42% Span

NOTE: First Stage Pressure and Temperature Data Used In Calculating Parameters Shown Is From Radial Traverses Corrected Using The Correlations Described In The Section On Data Reduction Techniques

- 100% SPEED
- × 85% SPEED
- ◇ 70% SPEED
- ⊠ 100% DESIGN POINT

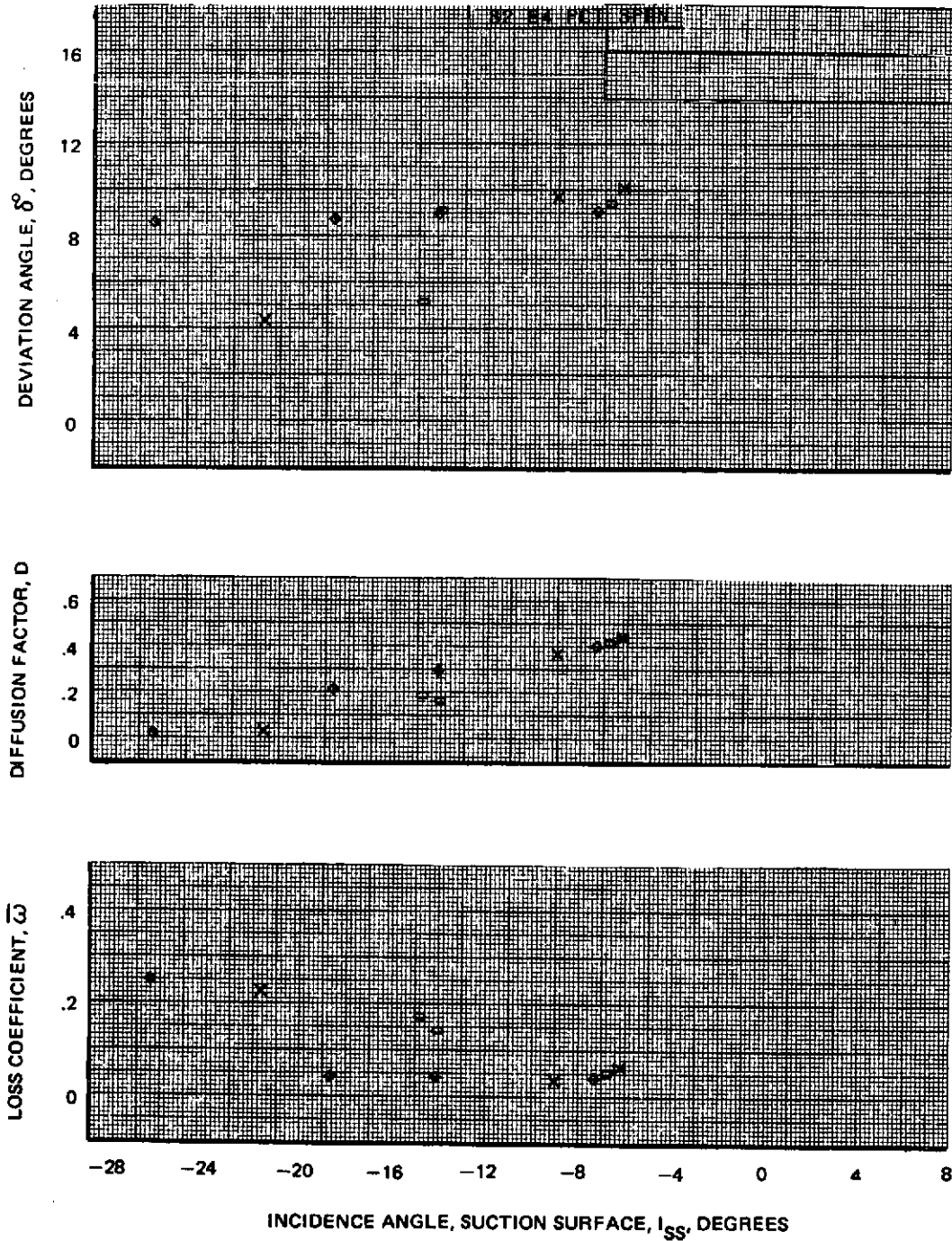


Figure 88d Blade Element Performance With Hub Radial Distortion – Stator 2  
64% Span



NOTE: First Stage Pressure and Temperature Data Used In Calculating Parameters Shown Is From Radial Traverses Corrected Using The Correlations Described In The Section On Data Reduction Techniques

- 100% SPEED
- × 85% SPEED
- ◇ 70% SPEED
- ⊠ 100% DESIGN POINT

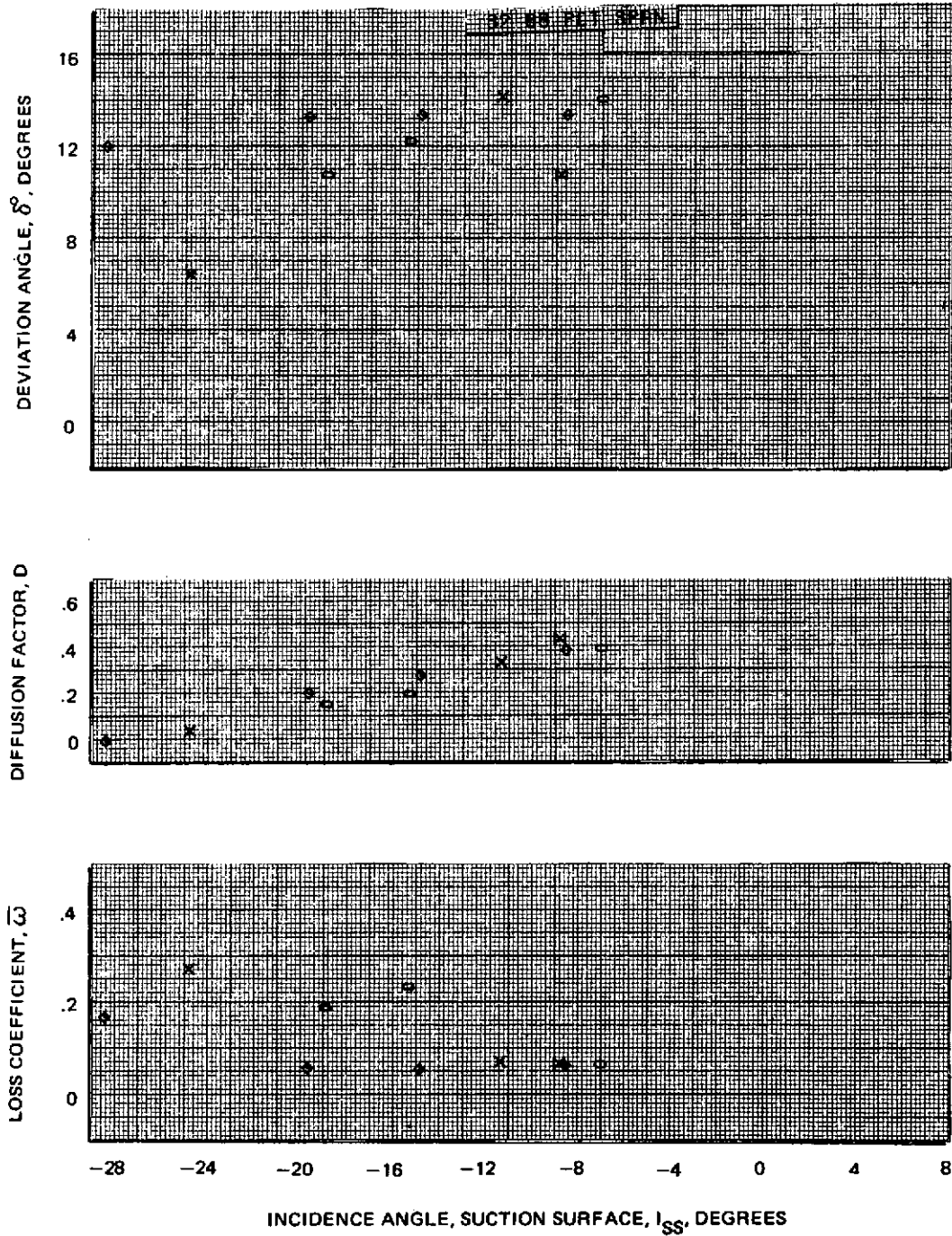


Figure 88e Blade Element Performance With Hub Radial Distortion – Stator 2  
88% Span

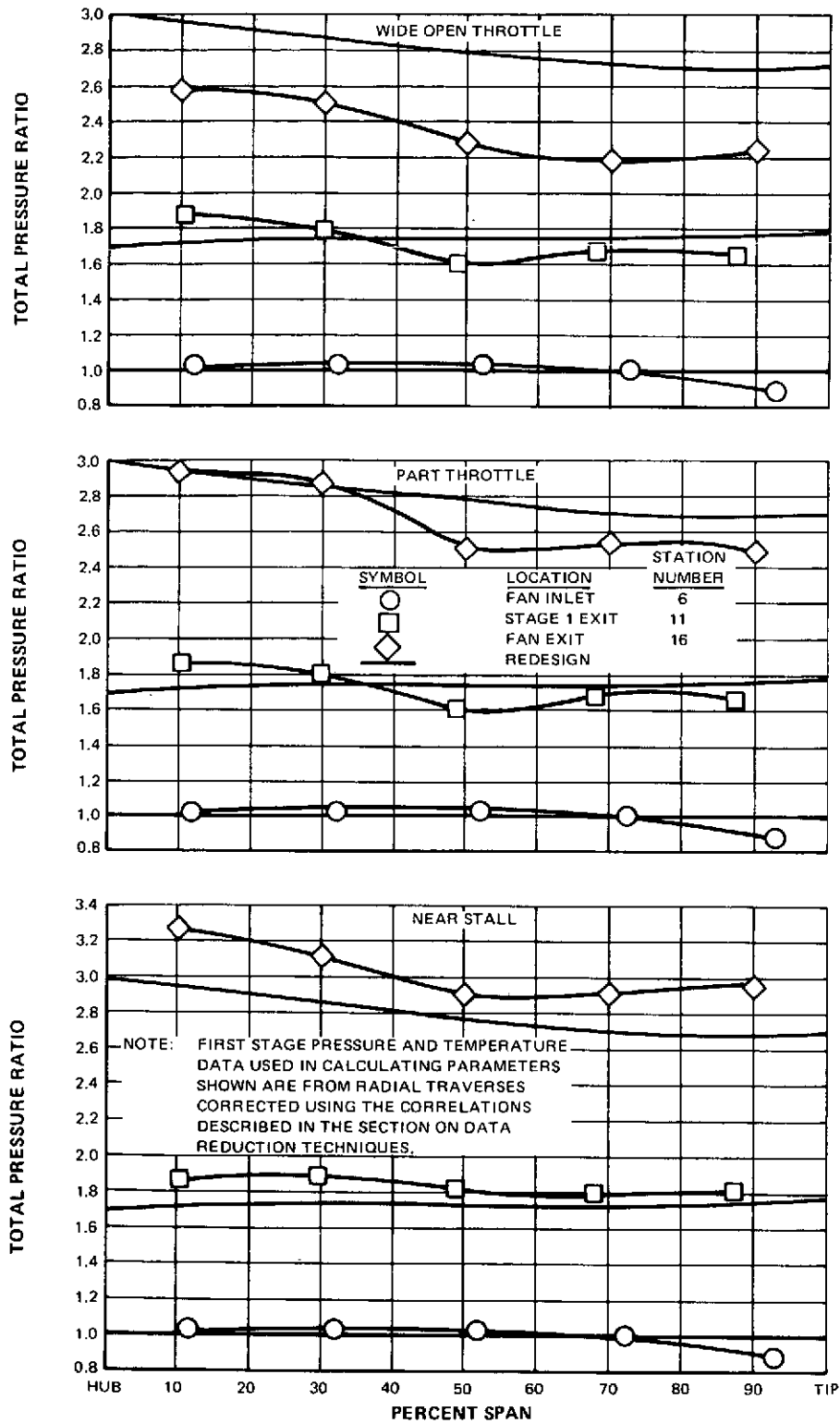


Figure 89 Total Pressure Ratio versus Span at Fan Inlet, First Stage Exit, and Fan Exit for Tip Radially Distorted Inlet Flow

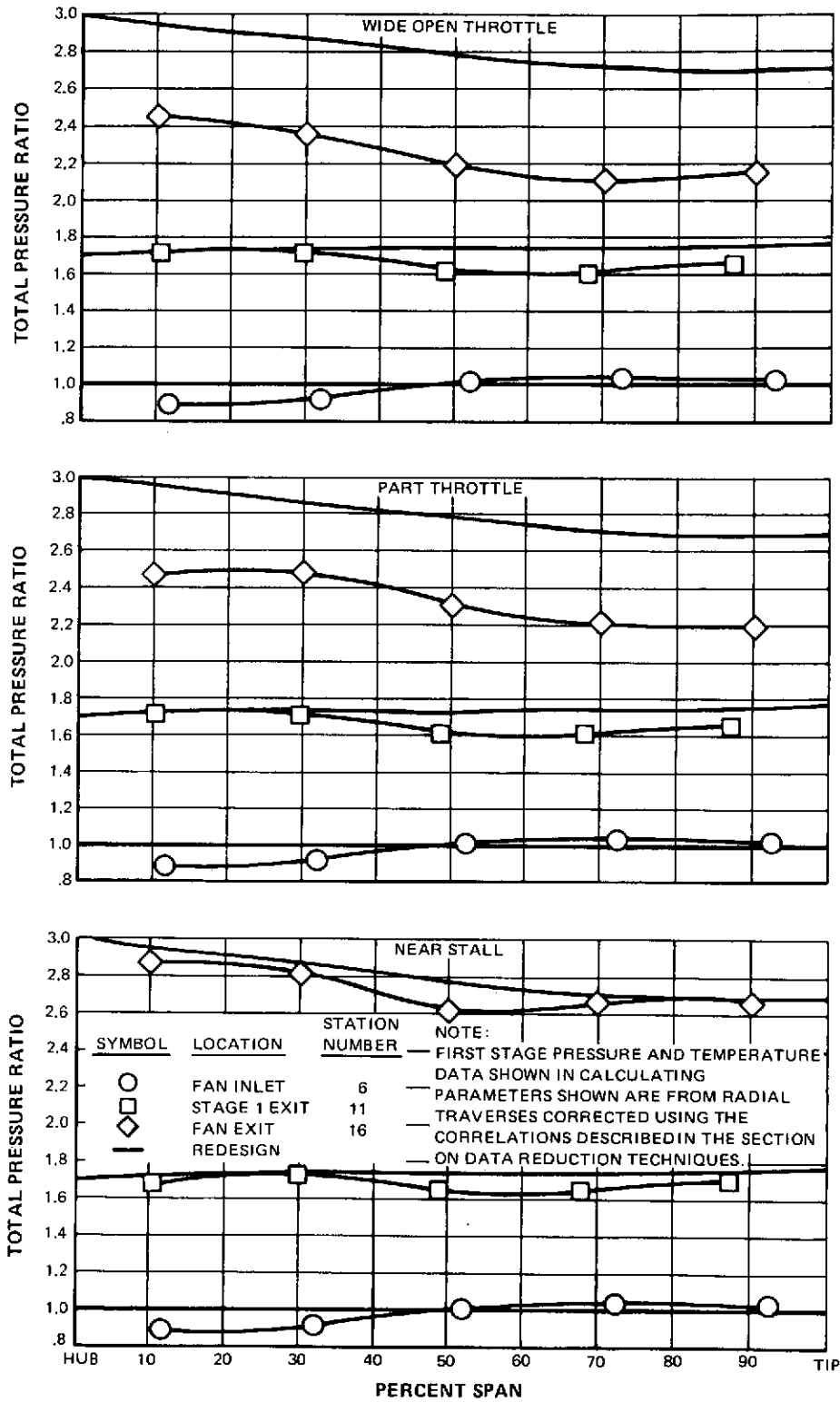


Figure 90 Total Pressure Ratio versus Span at Fan Inlet, First Stage Exit, and Fan Exit for Hub Radially Distorted Inlet Flow

C-3

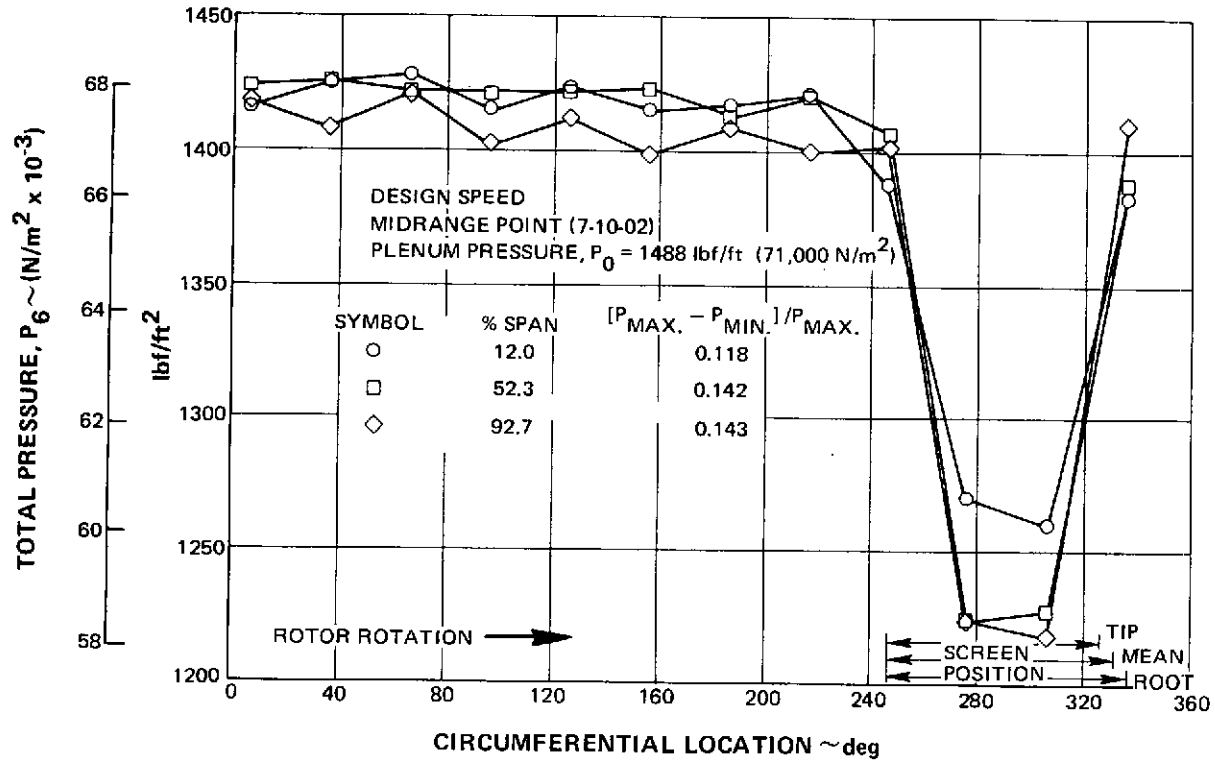


Figure 91 Circumferential Distributions of Total Pressure at Fan Inlet for Circumferentially Distorted Inlet Flow

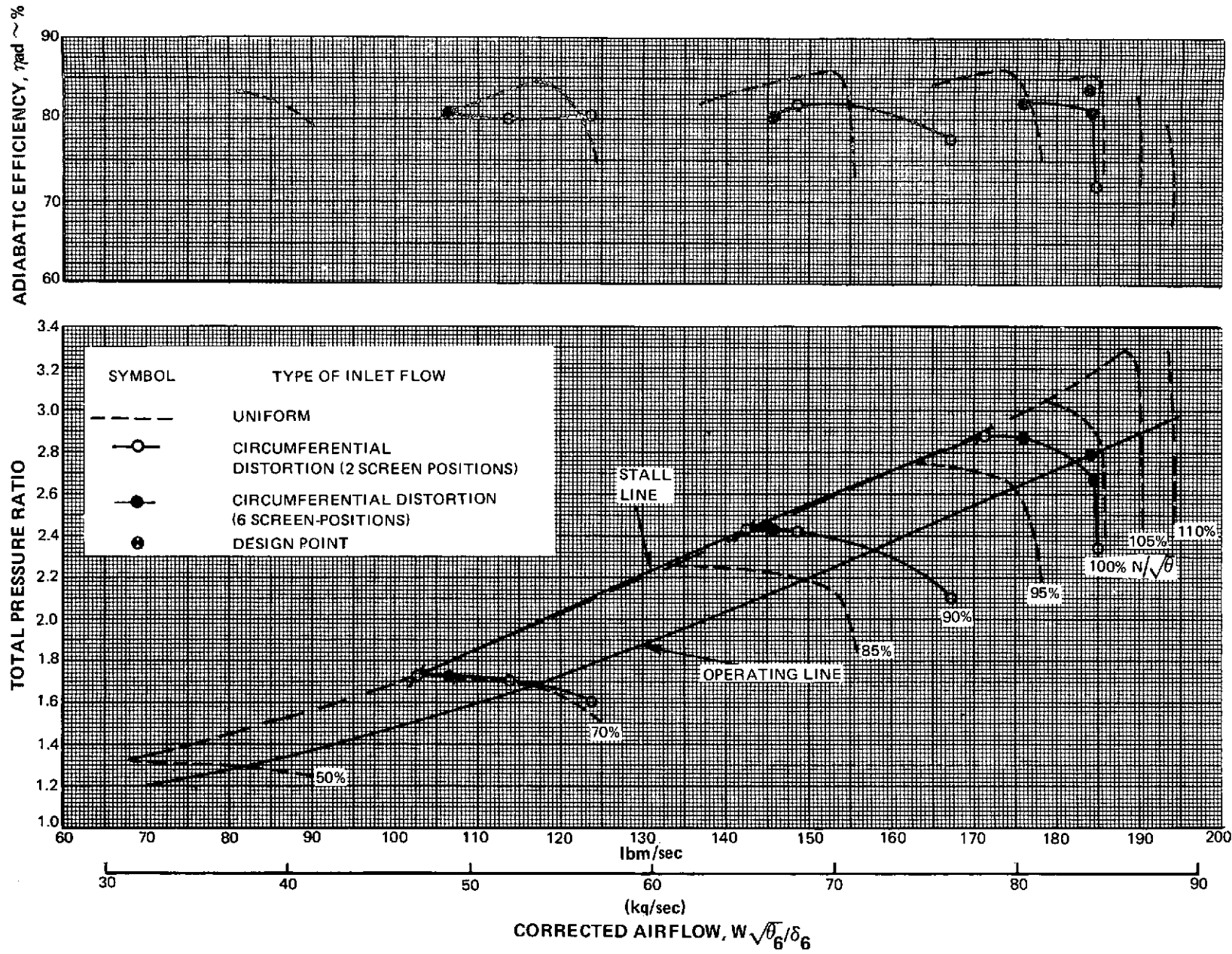


Figure 92 Fan Overall Performance with Circumferentially Distorted Inlet Flow

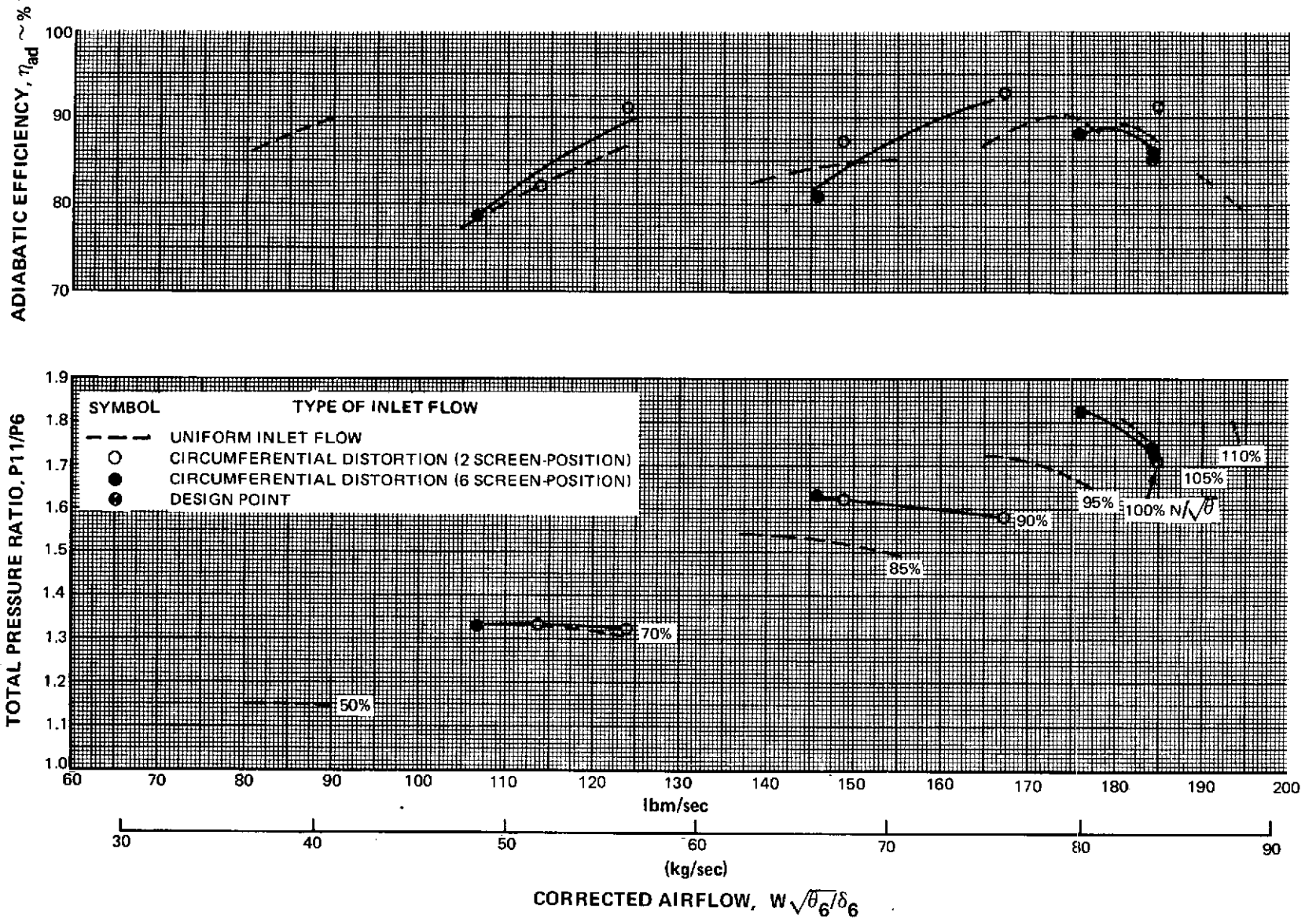


Figure 93 First Stage Performance with Circumferentially Distorted Inlet Flow

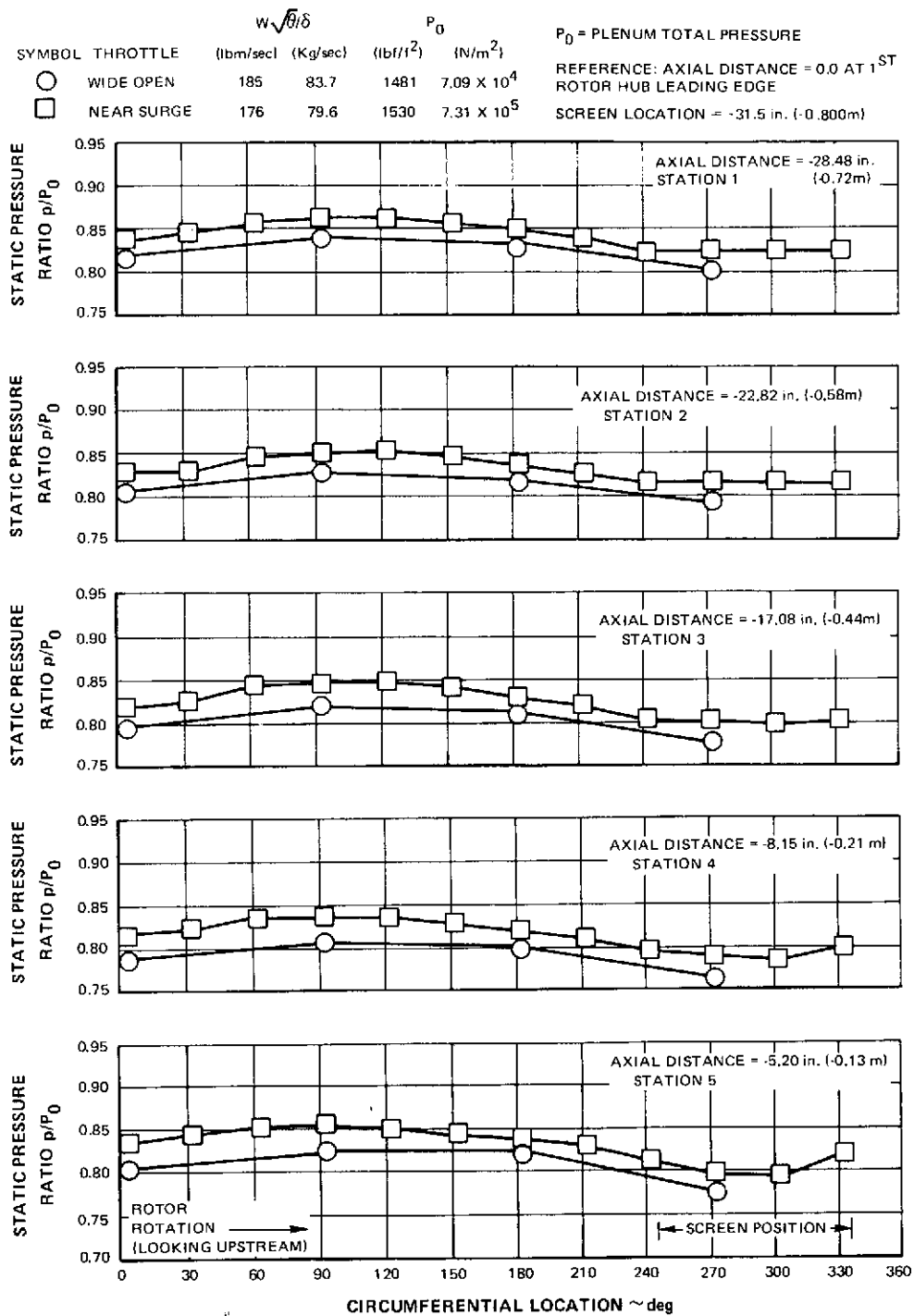


Figure 94 Circumferential Distributions of Fan Inlet Static Pressure at the Hub for Tests with Circumferentially Distorted Inlet Flow at Design Speed

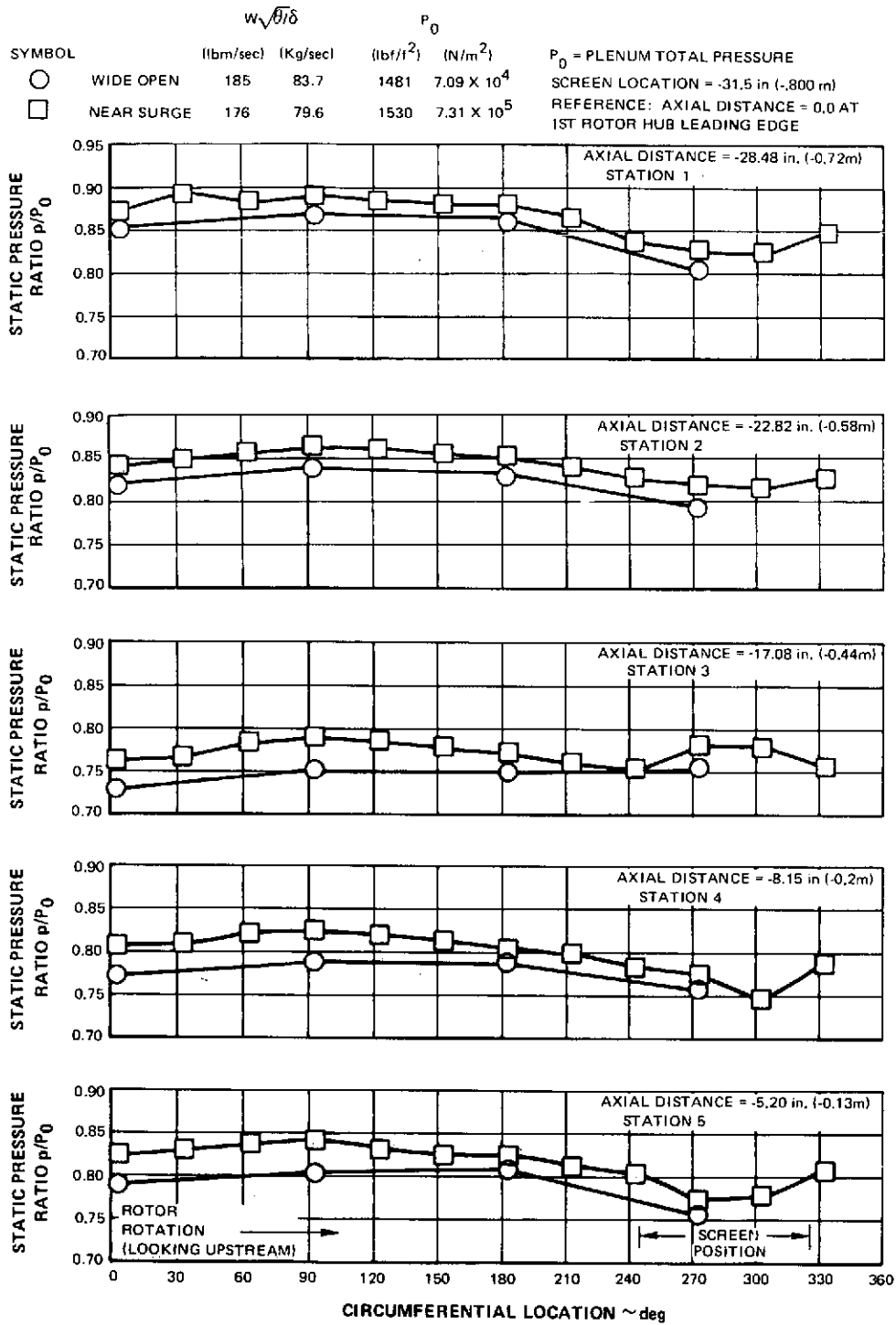


Figure 95 Circumferential Distributions of Fan Inlet Static Pressure at the Tip for Tests with Circumferentially Distorted Inlet Flow at Design Speed



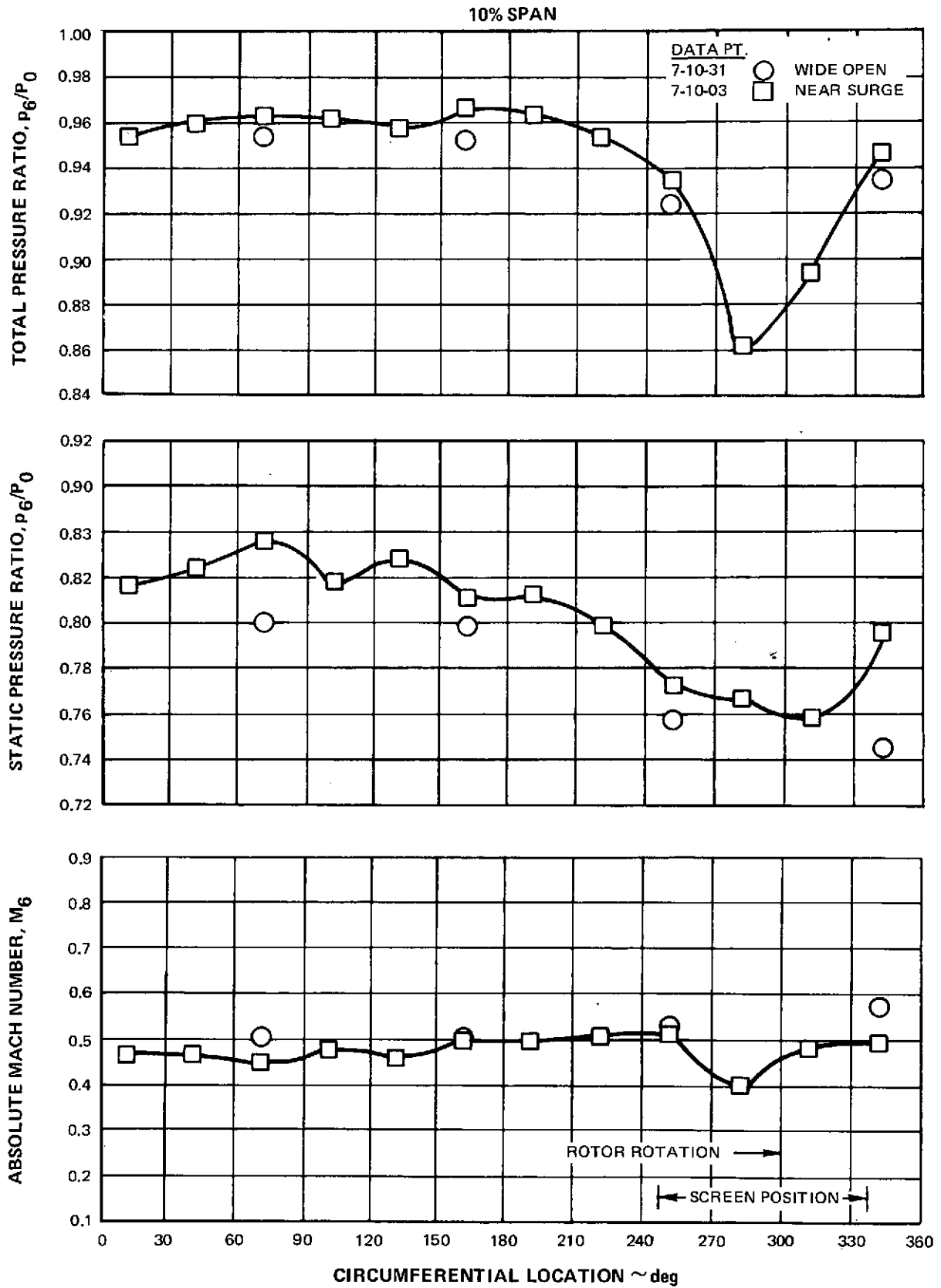


Figure 96a Circumferential Distributions of Fan Inlet Total Pressure, Static Pressure, Absolute Mach Number, Relative Flow Angle, Absolute Flow Angle, and Meridional Velocity with Circumferential Inlet Flow Distortion

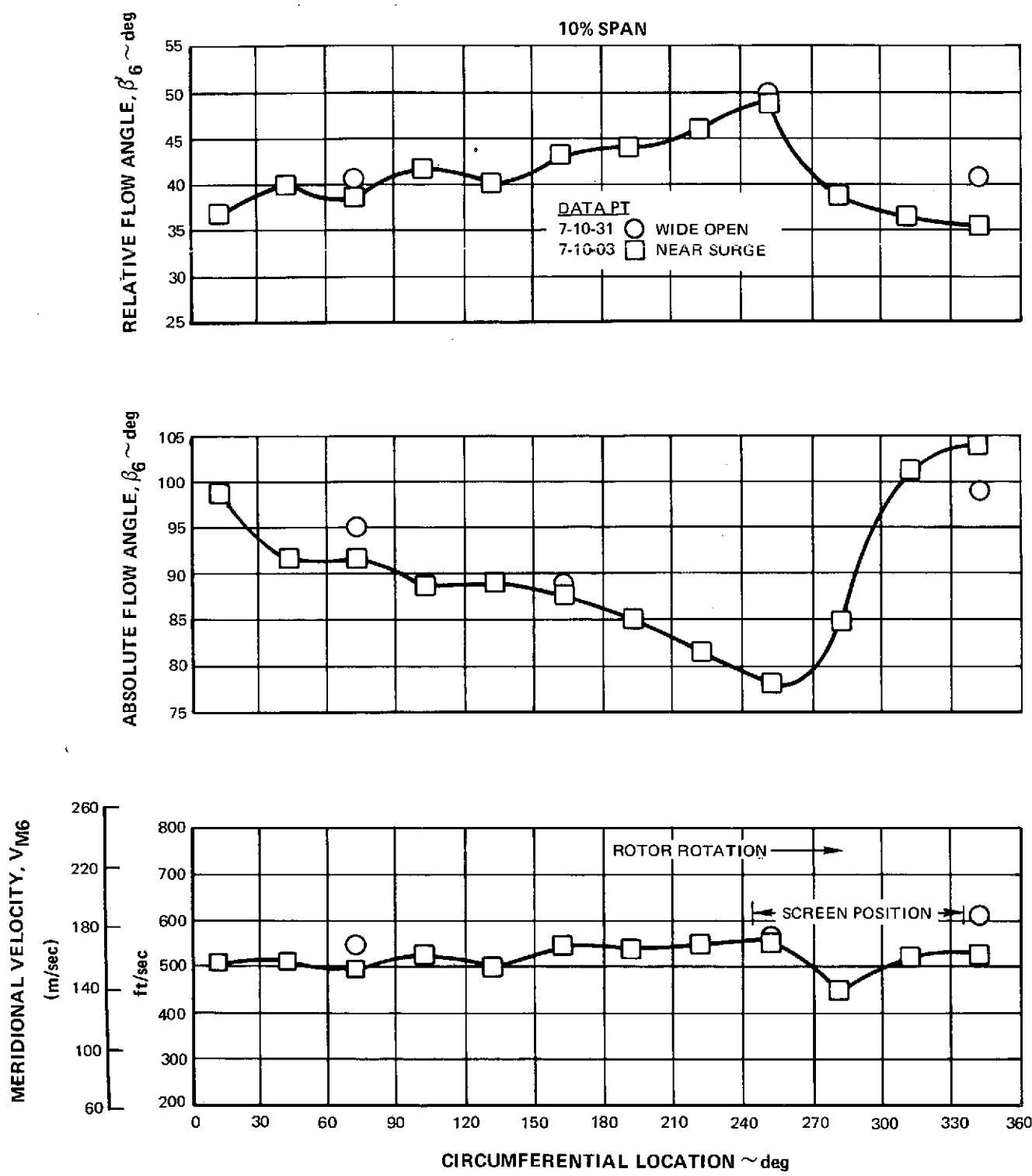


Figure 96 b Circumferential Distributions of Fan Inlet Total Pressure, Static Pressure, Absolute Mach Number, Relative Flow Angle, Absolute Flow Angle, and Meridional Velocity with Circumferential Inlet Flow Distortion

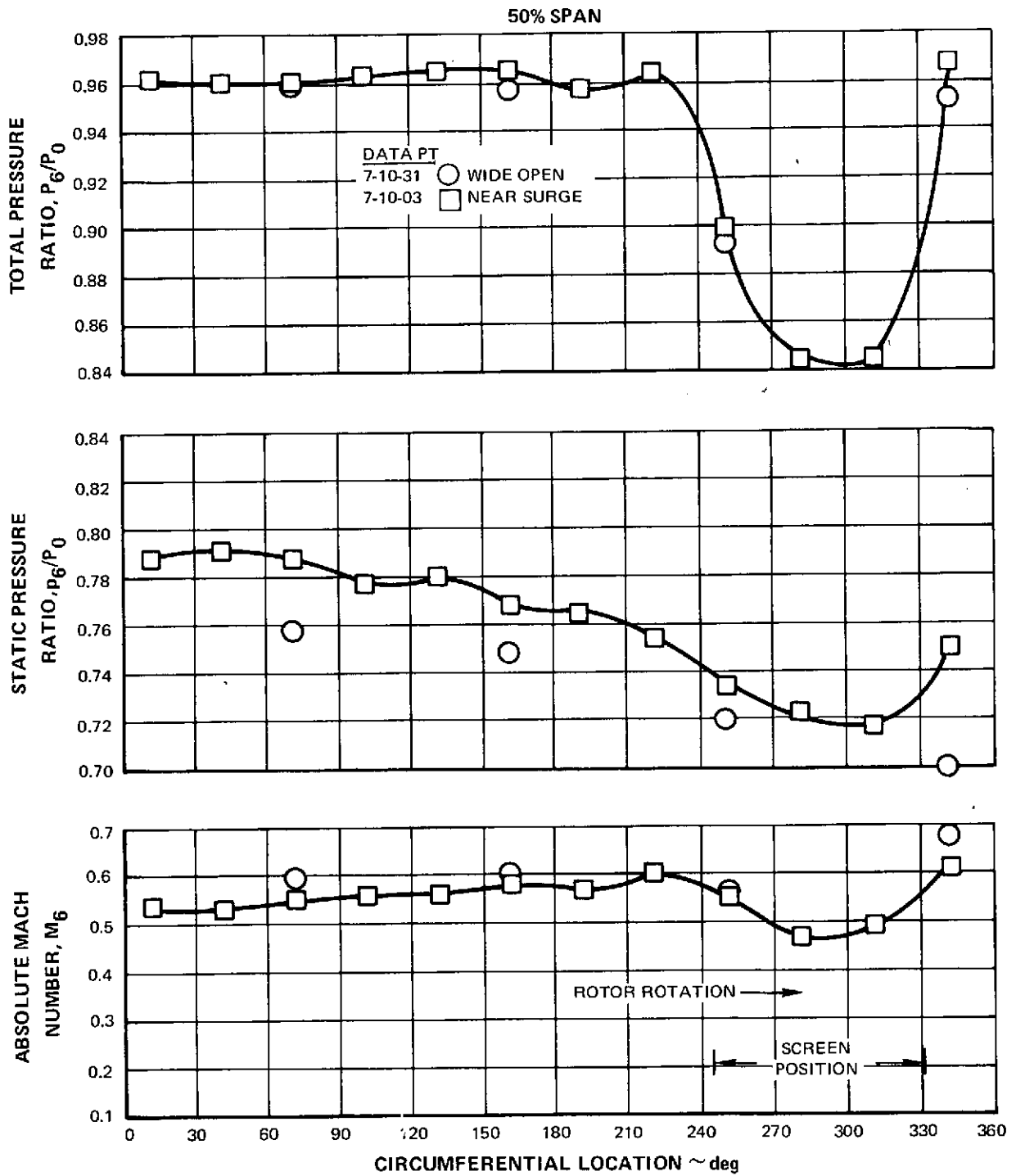


Figure 96 c Circumferential Distributions of Fan Inlet Total Pressure, Static Pressure, Absolute Mach Number, Relative Flow Angle, Absolute Flow Angle, and Meridional Velocity with Circumferential Inlet Flow Distortion

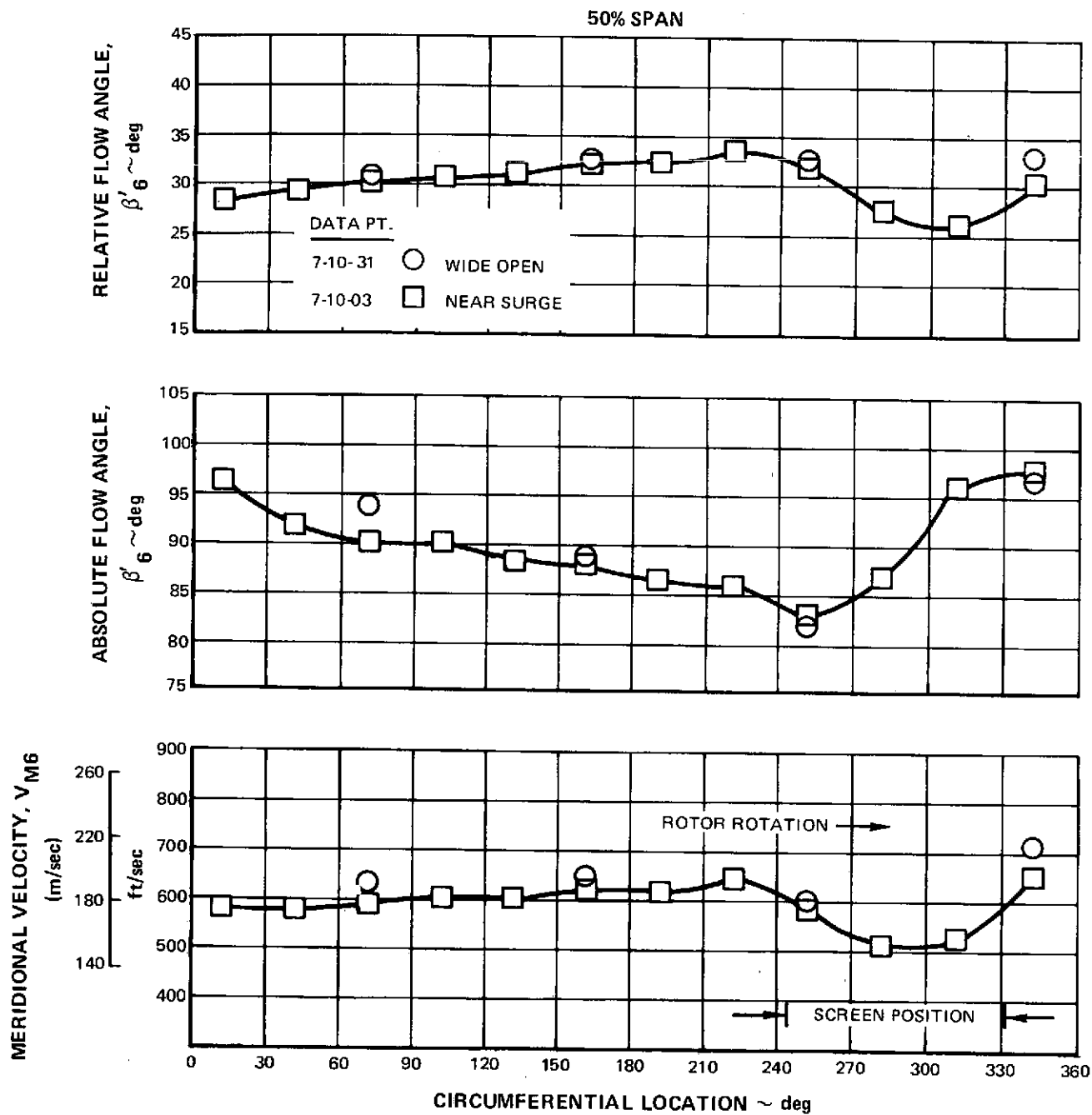


Figure 96 d Circumferential Distributions of Fan Inlet Total Pressure, Static Pressure, Absolute Mach Number, Relative Flow Angle, Absolute Flow Angle, and Meridional Velocity with Circumferential Inlet Flow Distortion

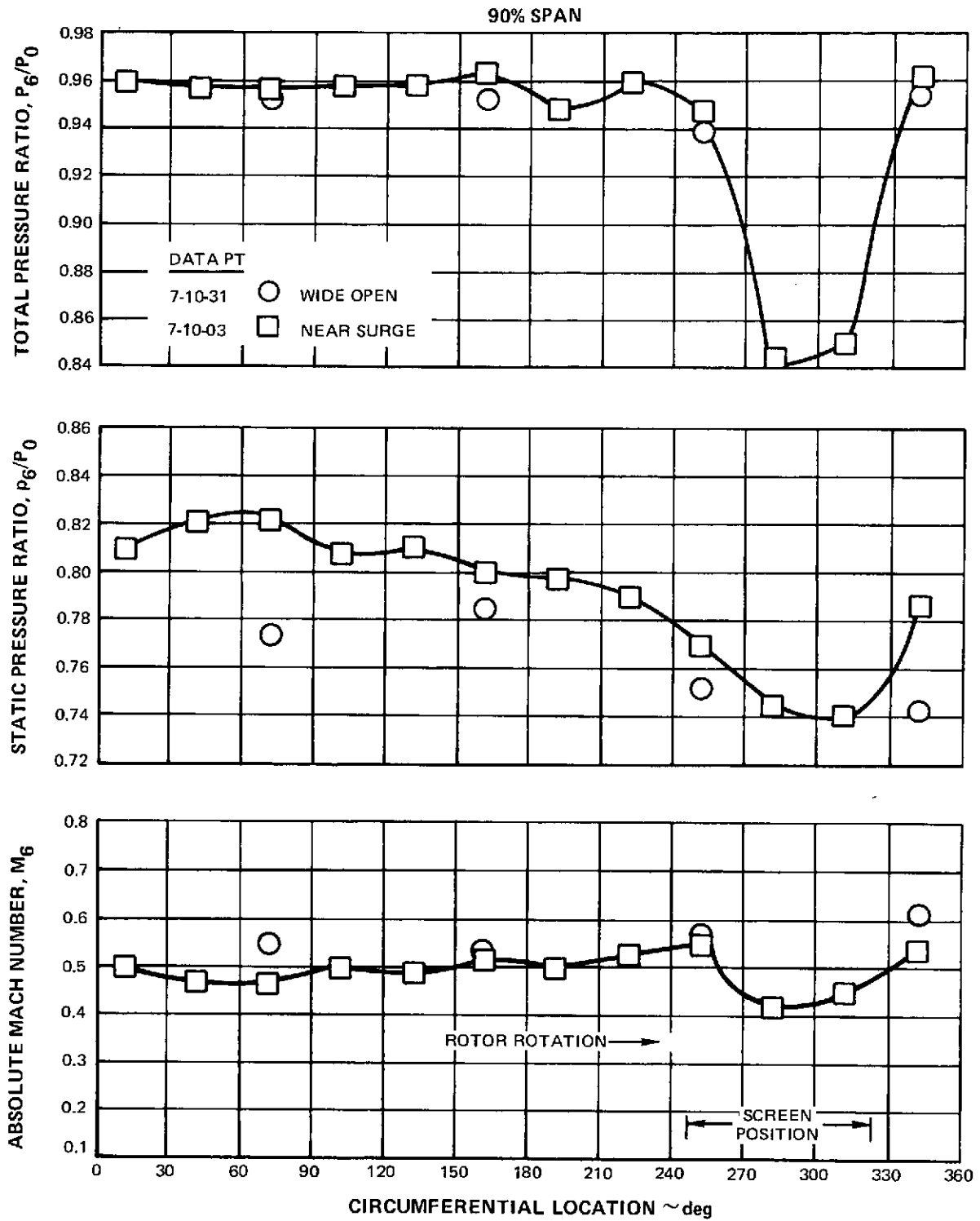


Figure 96 e Circumferential Distributions of Fan Inlet Total Pressure, Static Pressure, Absolute Mach Number, Relative Flow Angle, Absolute Flow Angle, and Meridional Velocity with Circumferential Inlet Flow Distortion

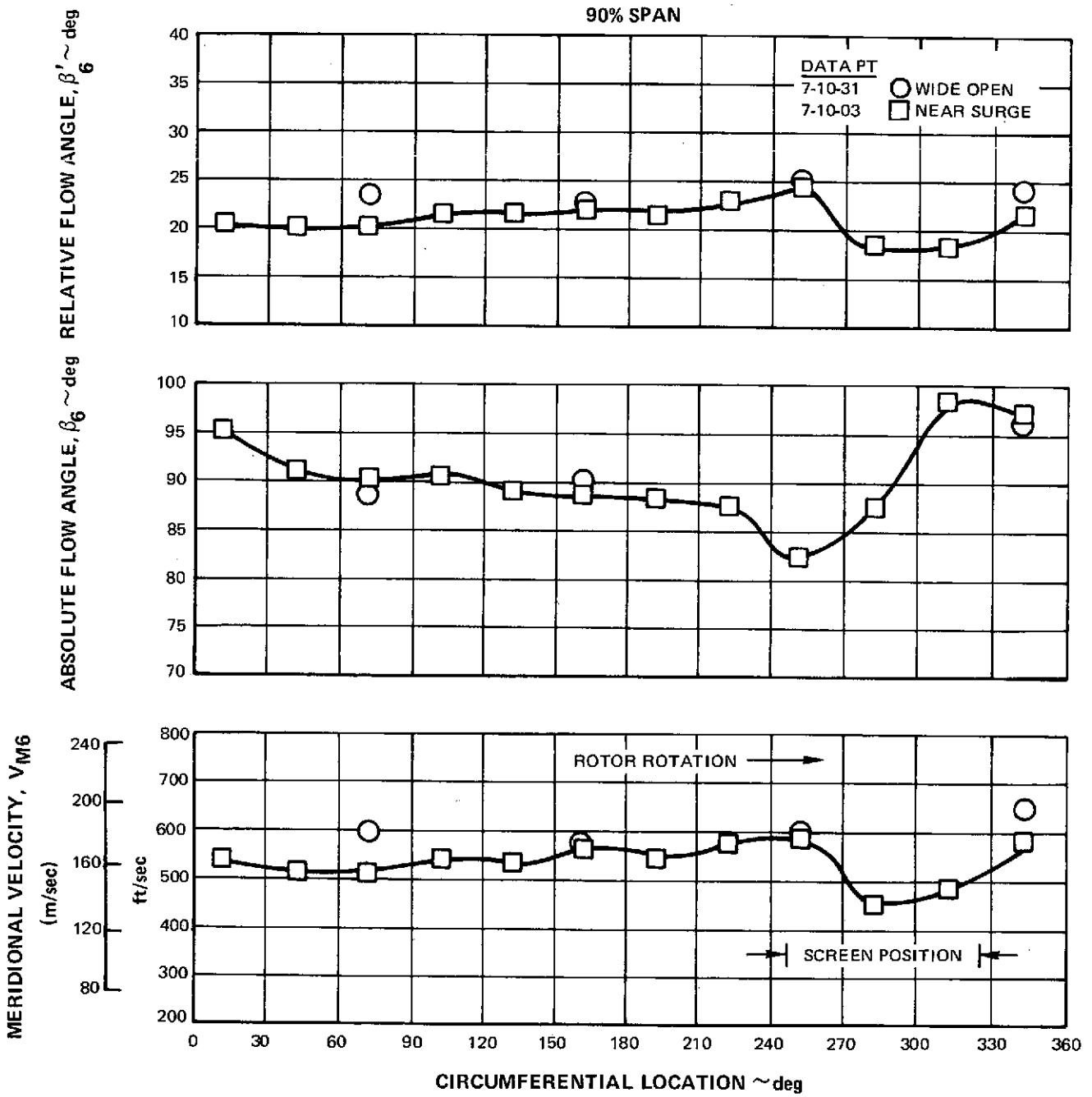


Figure 96f Circumferential Distributions of Fan Inlet Total Pressure, Static Pressure, Absolute Mach Number, Relative Flow Angle, Absolute Flow Angle, and Meridional Velocity with Circumferential Inlet Flow Distortion

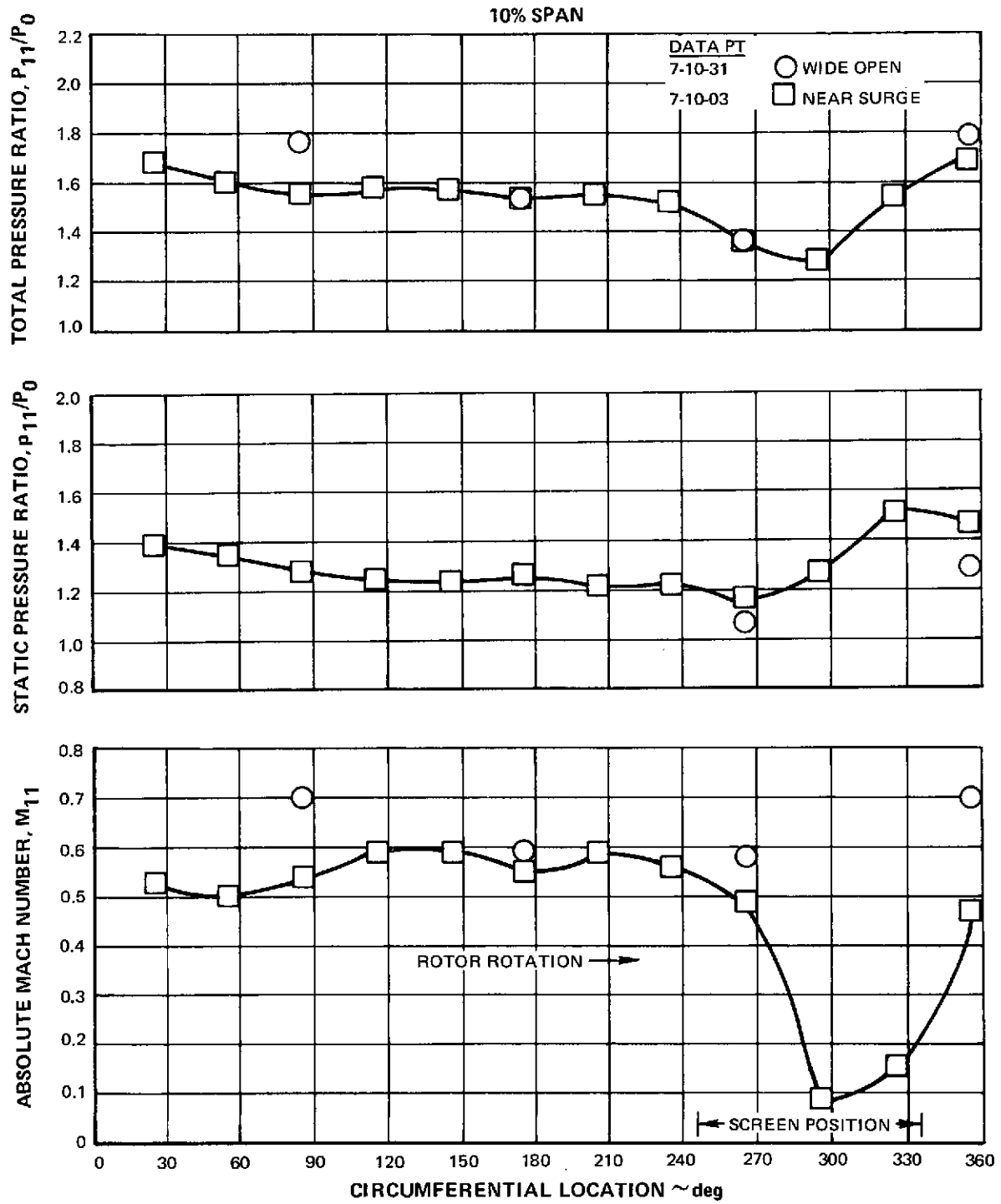


Figure 97a Circumferential Distributions of First Stator Exit Total Pressure, Static Pressure, Absolute Mach Number, Total Temperature, Absolute Mach Number, Total Temperature, Absolute Flow Angle, and Meridional Velocity with Circumferential Inlet Flow Distortion

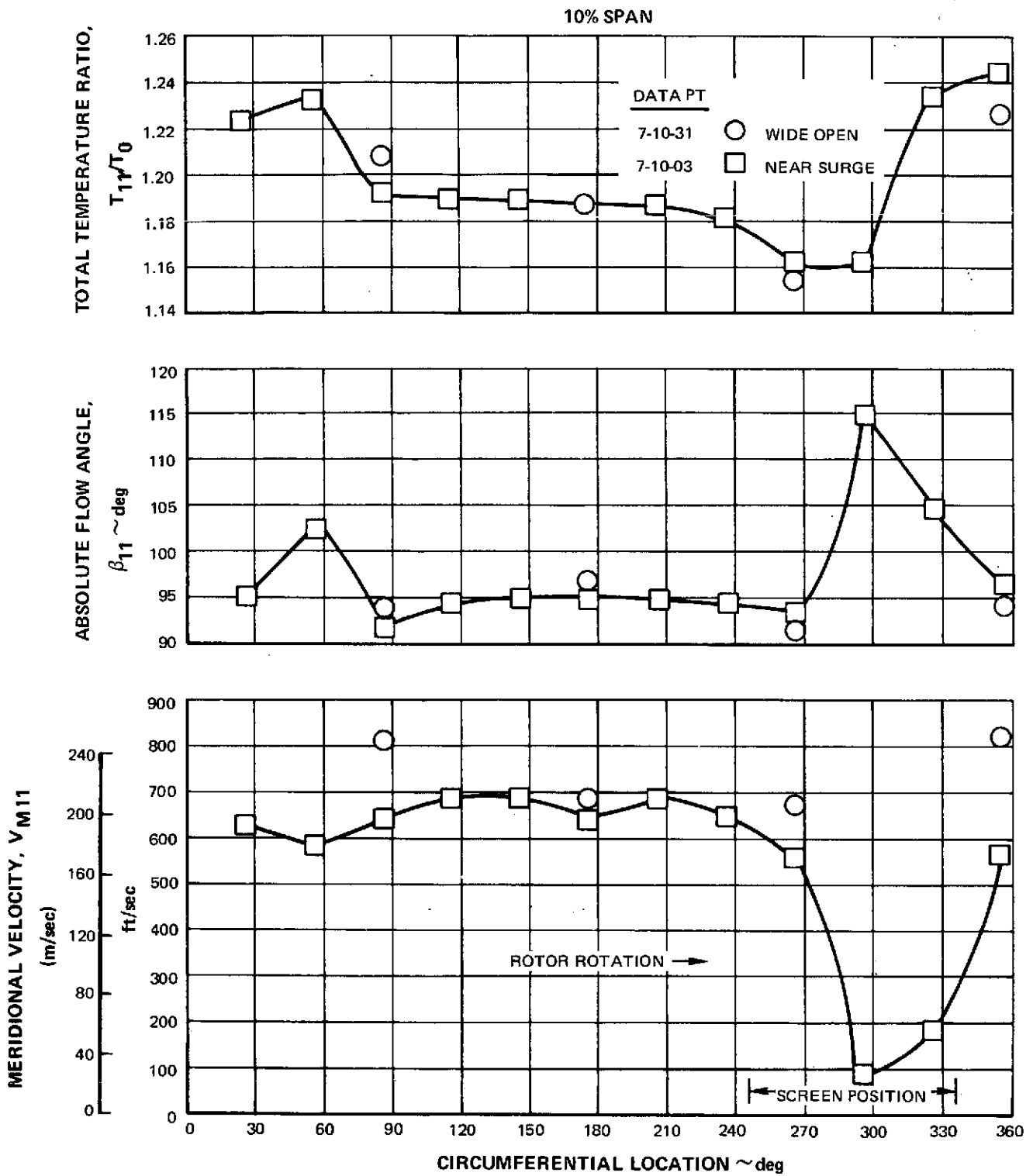


Figure 97b Circumferential Distributions of First Stator Exit Total Pressure, Static Pressure, Absolute Mach Number, Total Temperature, Absolute Mach Number, Total Temperature, Absolute Flow Angle, and Meridional Velocity with Circumferential Inlet Flow Distortion



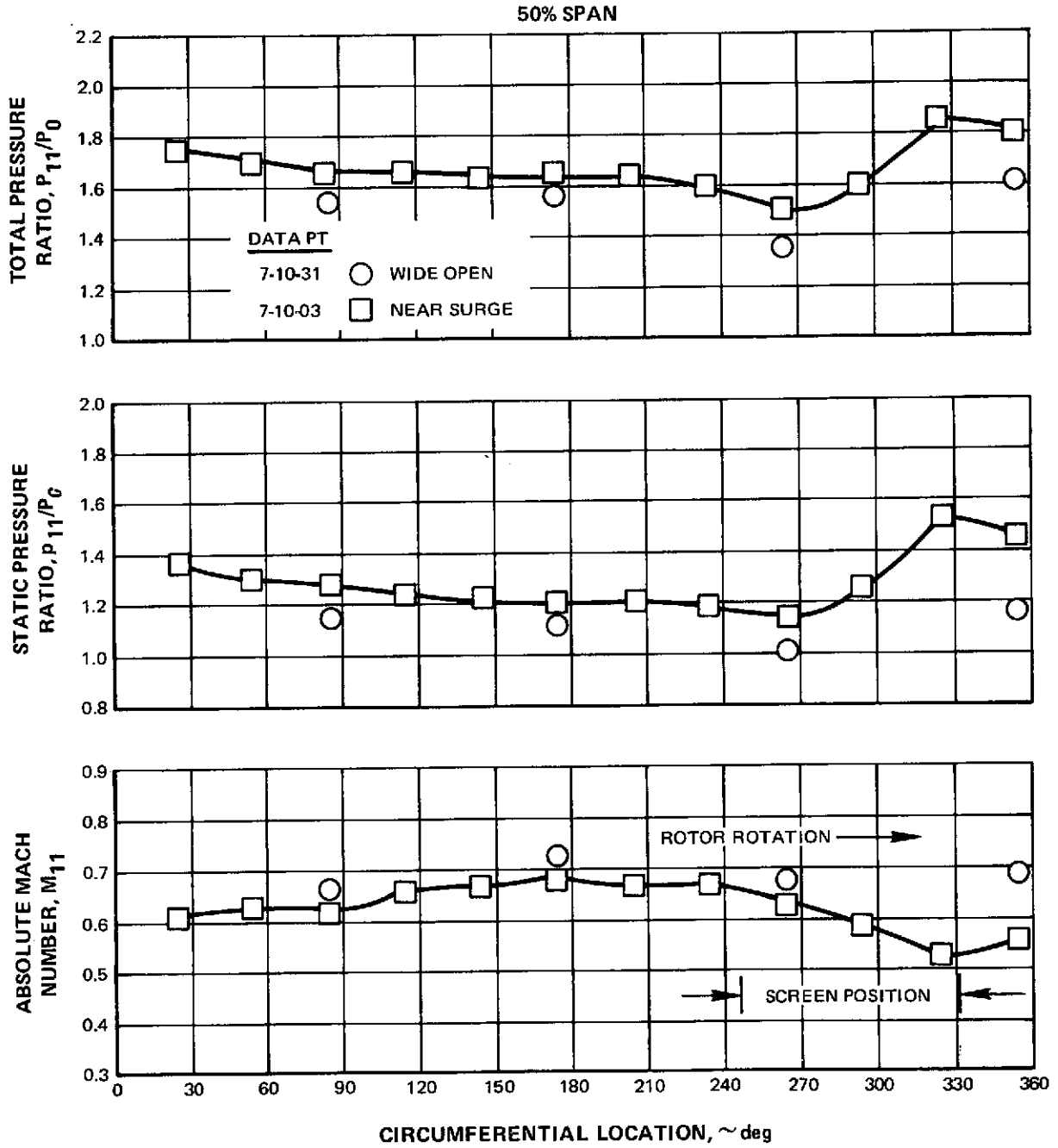


Figure 97c Circumferential Distributions of First Stator Exit Total Pressure, Static Pressure, Absolute Mach Number, Total Temperature, Absolute Mach Number, Total Temperature, Absolute Flow Angle, and Meridional Velocity with Circumferential Inlet Flow Distortion

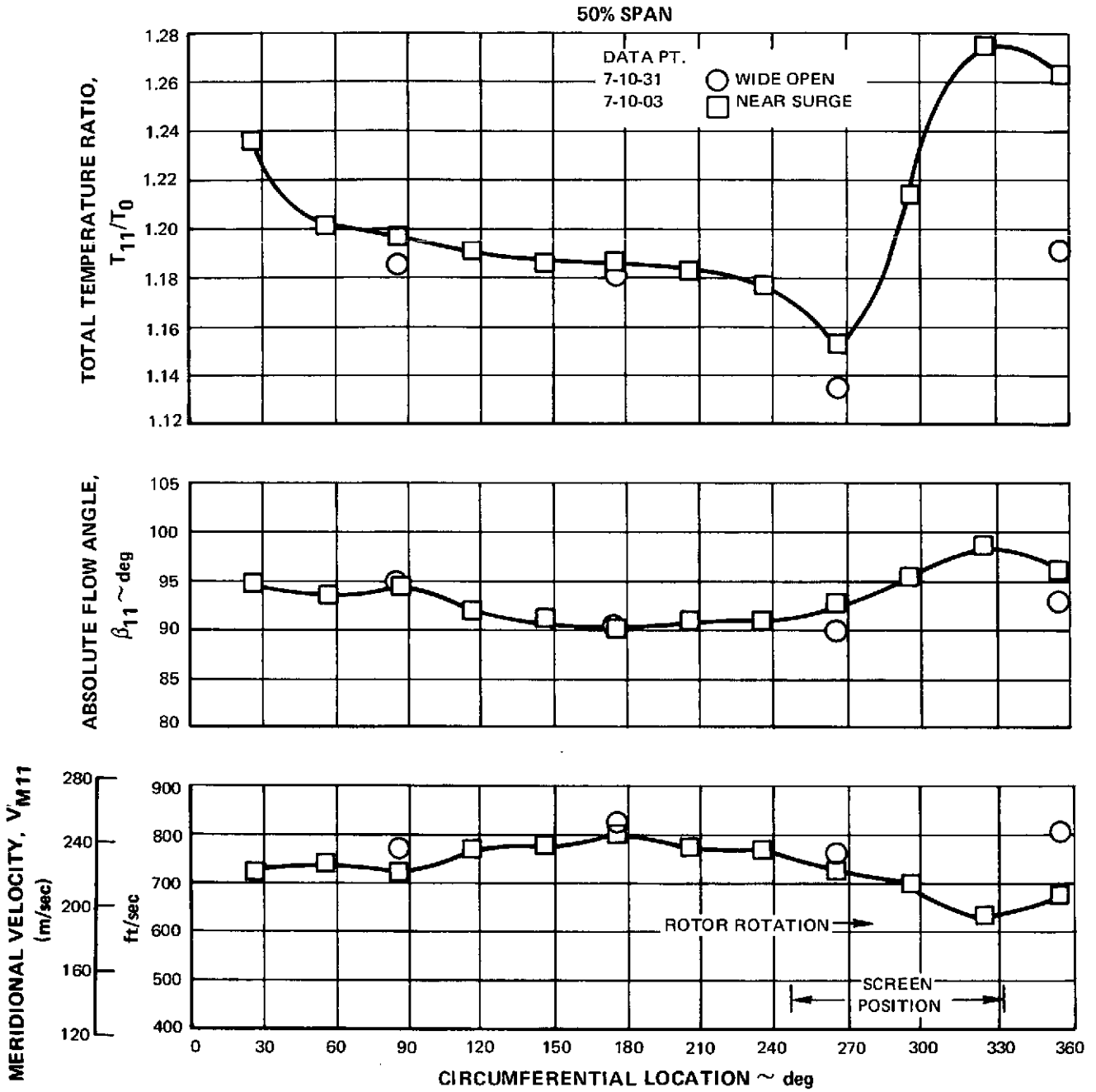


Figure 97d Circumferential Distributions of First Stator Exit Total Pressure, Static Pressure, Absolute Mach Number, Total Temperature, Absolute Mach Number, Total Temperature, Absolute Flow Angle, and Meridional Velocity with Circumferential Inlet Flow Distortion

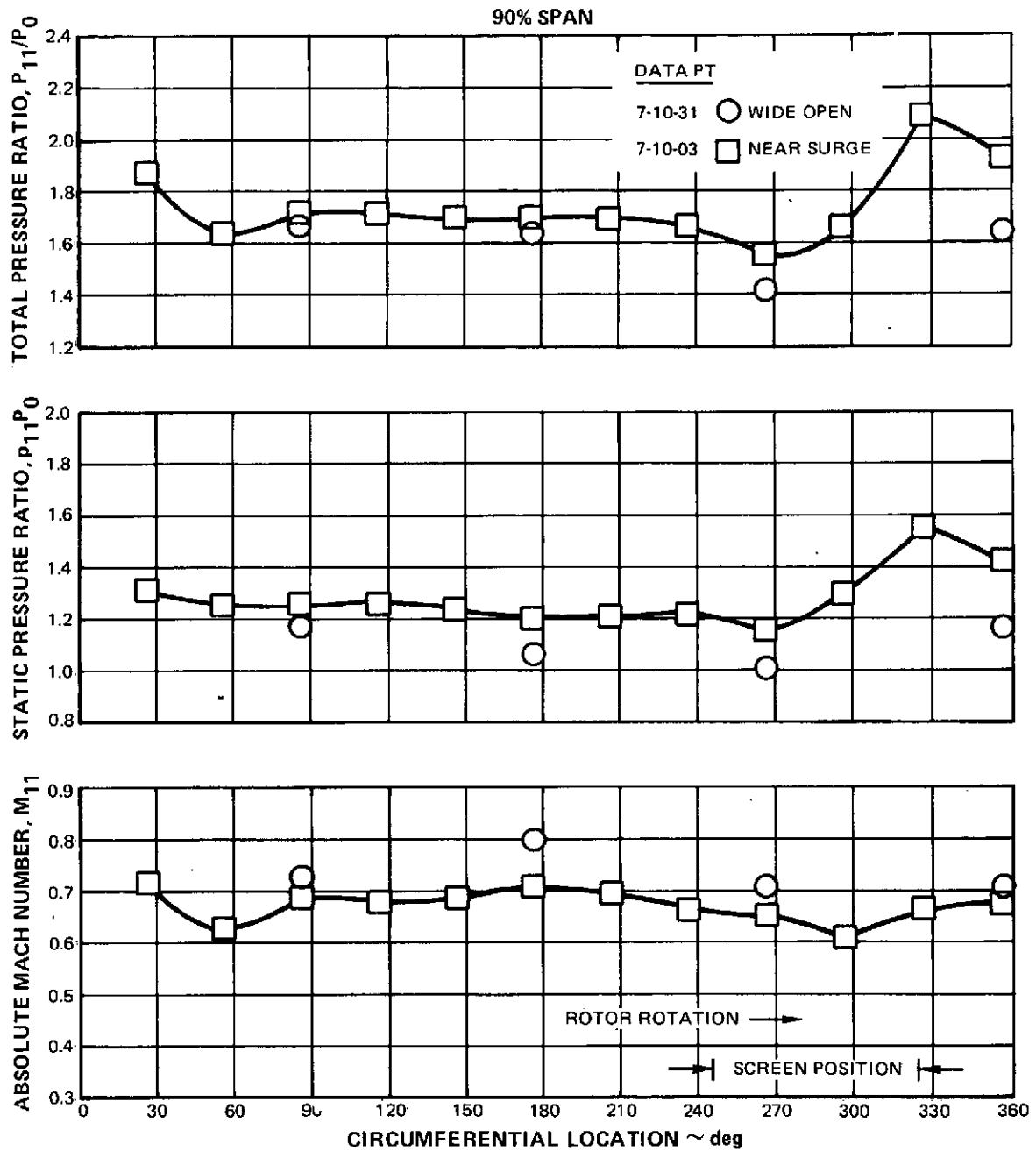


Figure 97e Circumferential Distributions of First Stator Exit Total Pressure, Static Pressure, Absolute Mach Number, Total Temperature, Absolute Mach Number, Total Temperature, Absolute Flow Angle, and Meridional Velocity with Circumferential Inlet Flow Distortion

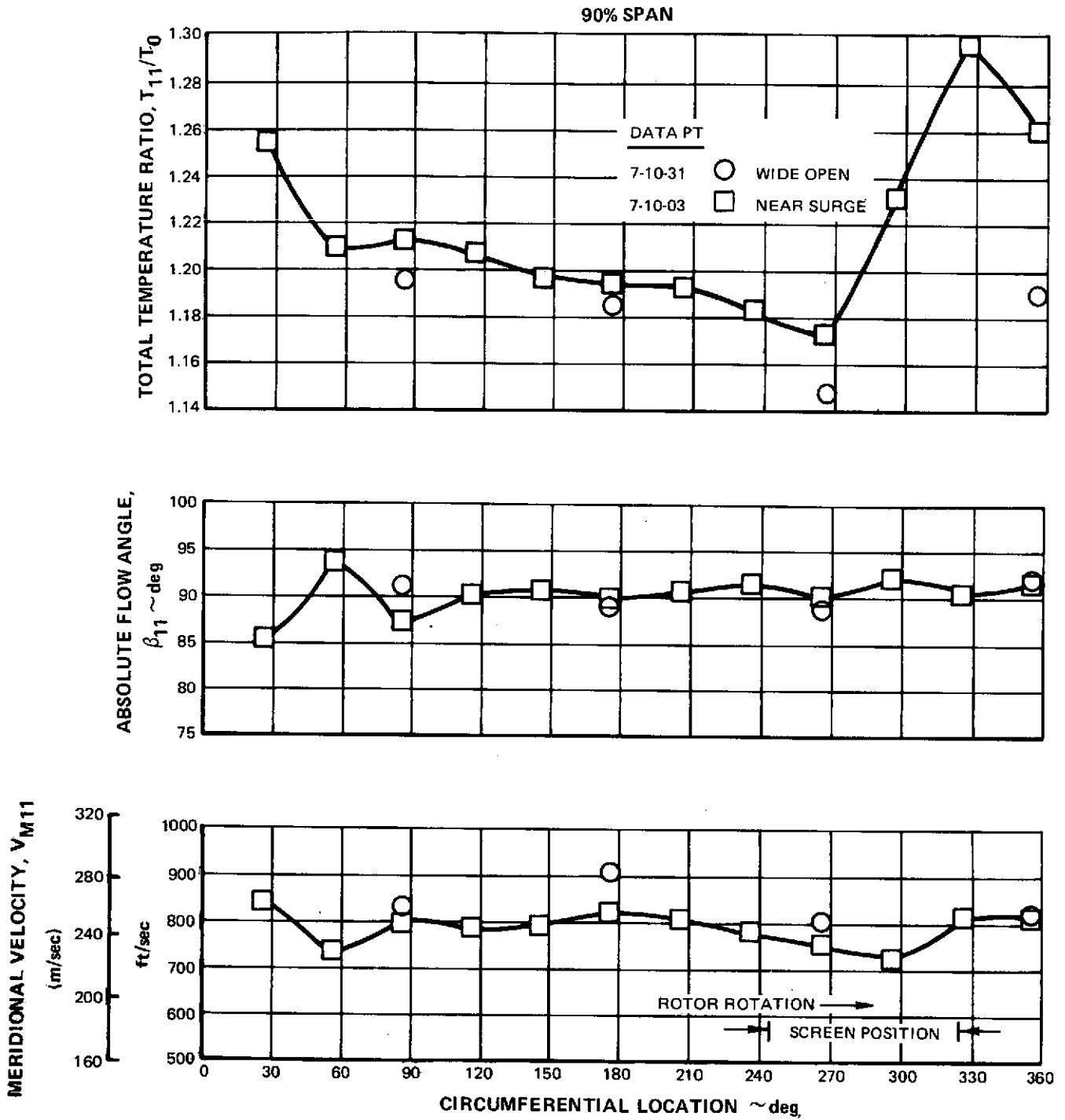


Figure 97f Circumferential Distributions of First Stator Exit Total Pressure, Static Pressure, Absolute Mach Number, Total Temperature, Absolute Flow Angle and Meridional Velocity with Circumferential Inlet Flow Distortion

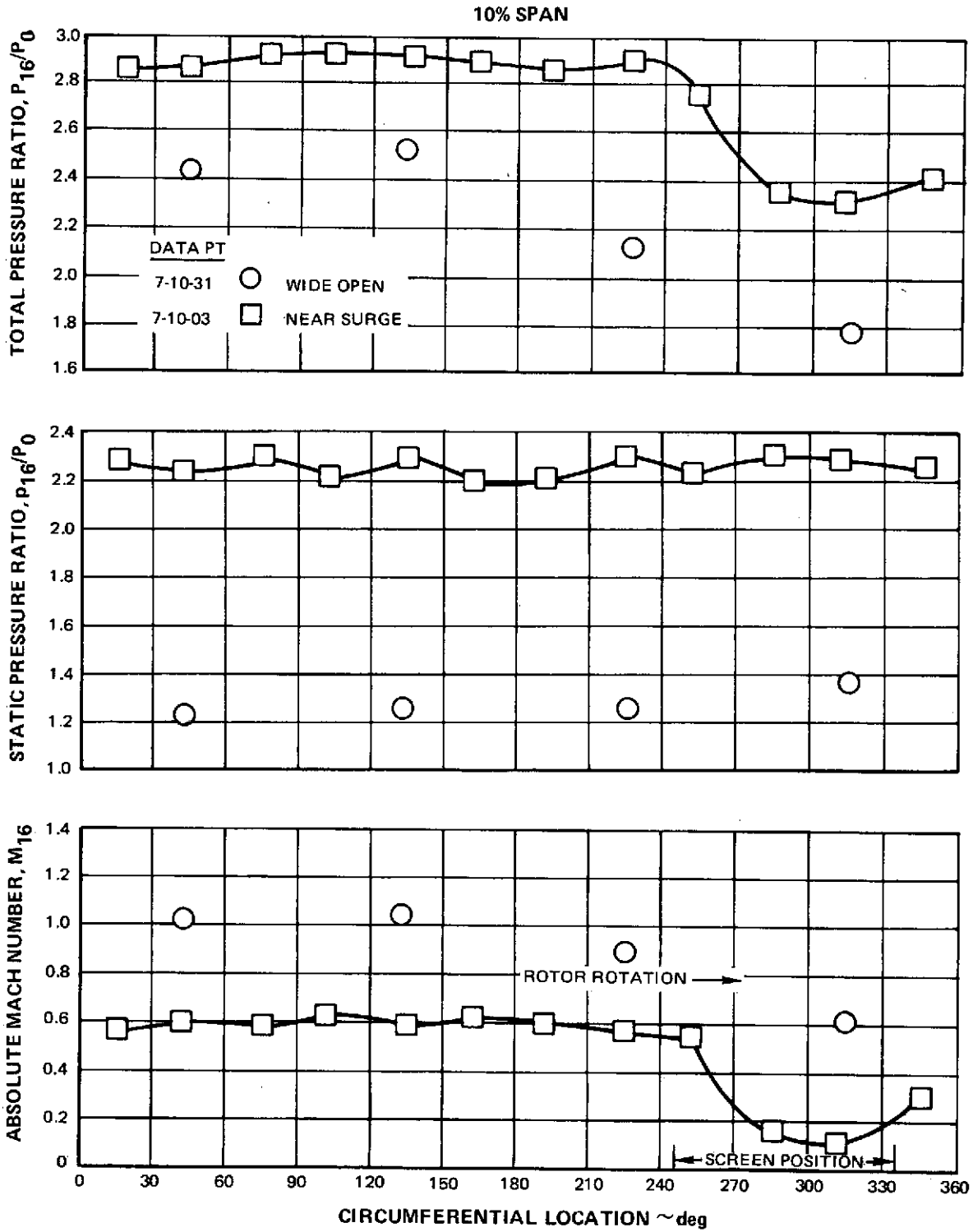


Figure 98a Circumferential Distributions of Fan Inlet Total Pressure, Static Pressure, Absolute Mach Number, Relative Flow Angle, Absolute Flow Angle, and Meridional Velocity with Circumferential Inlet Flow Distortion

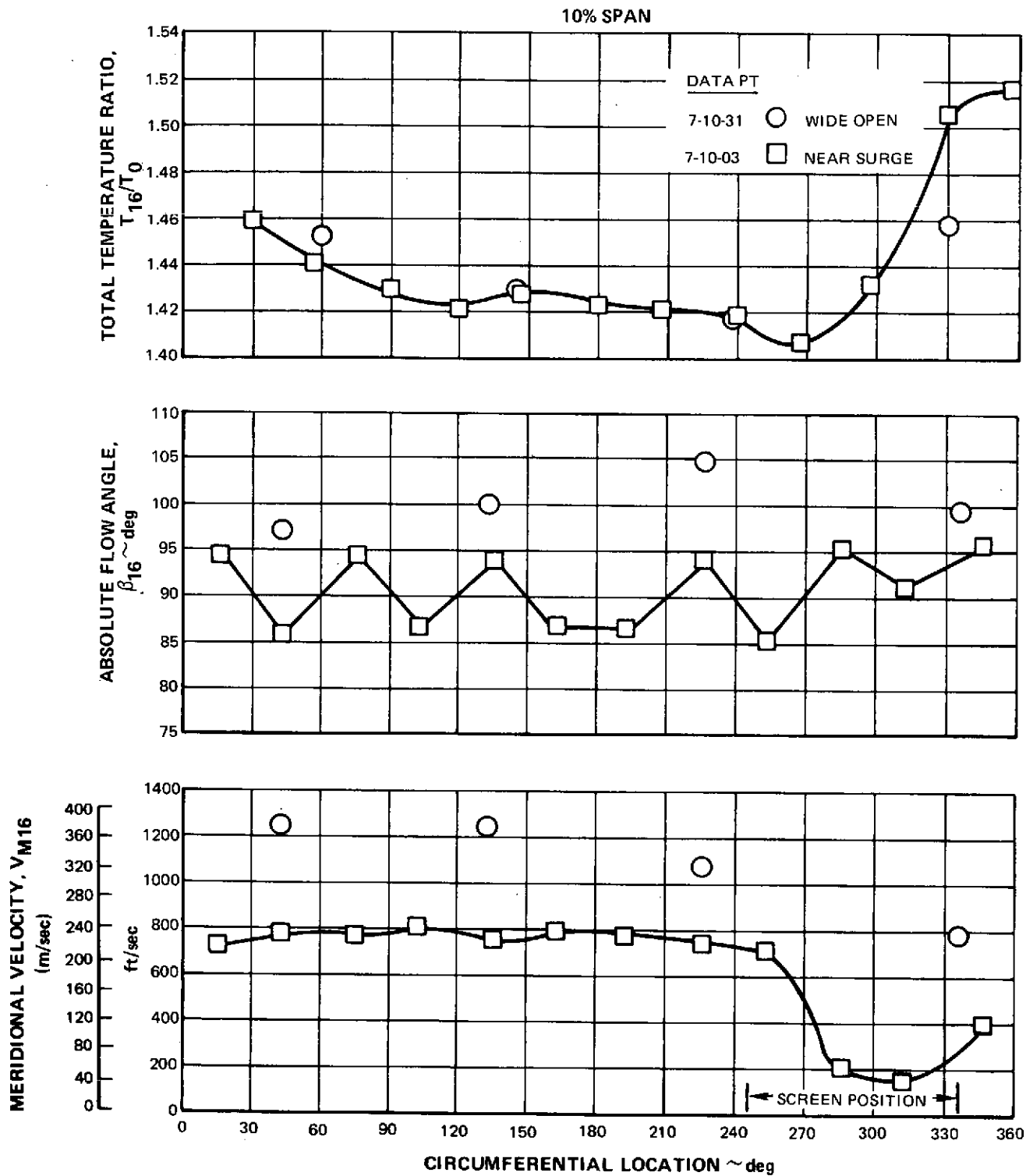


Figure 98b Circumferential Distributions of Fan Exit Total Pressure, Static Pressure, Absolute Mach Number, Total Temperature, Absolute Flow Angle, and Meridional Velocity with Circumferential Inlet Flow Distortion

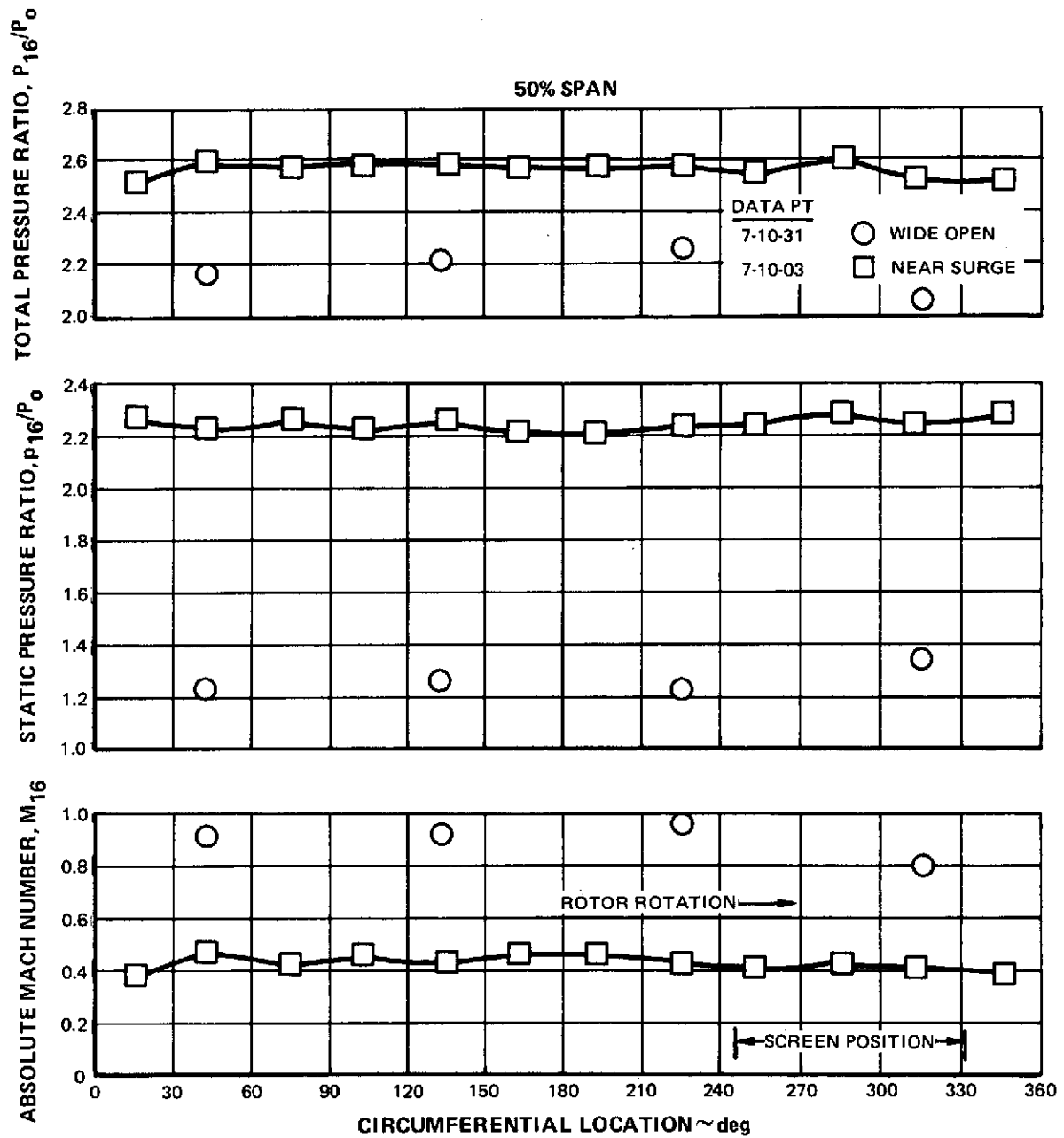


Figure 98c Circumferential Distributions of Fan Exit Total Pressure, Static Pressure, Absolute Mach Number, Total Temperature, Absolute Flow Angle, and Meridional Velocity with Circumferential Inlet Flow Distortion

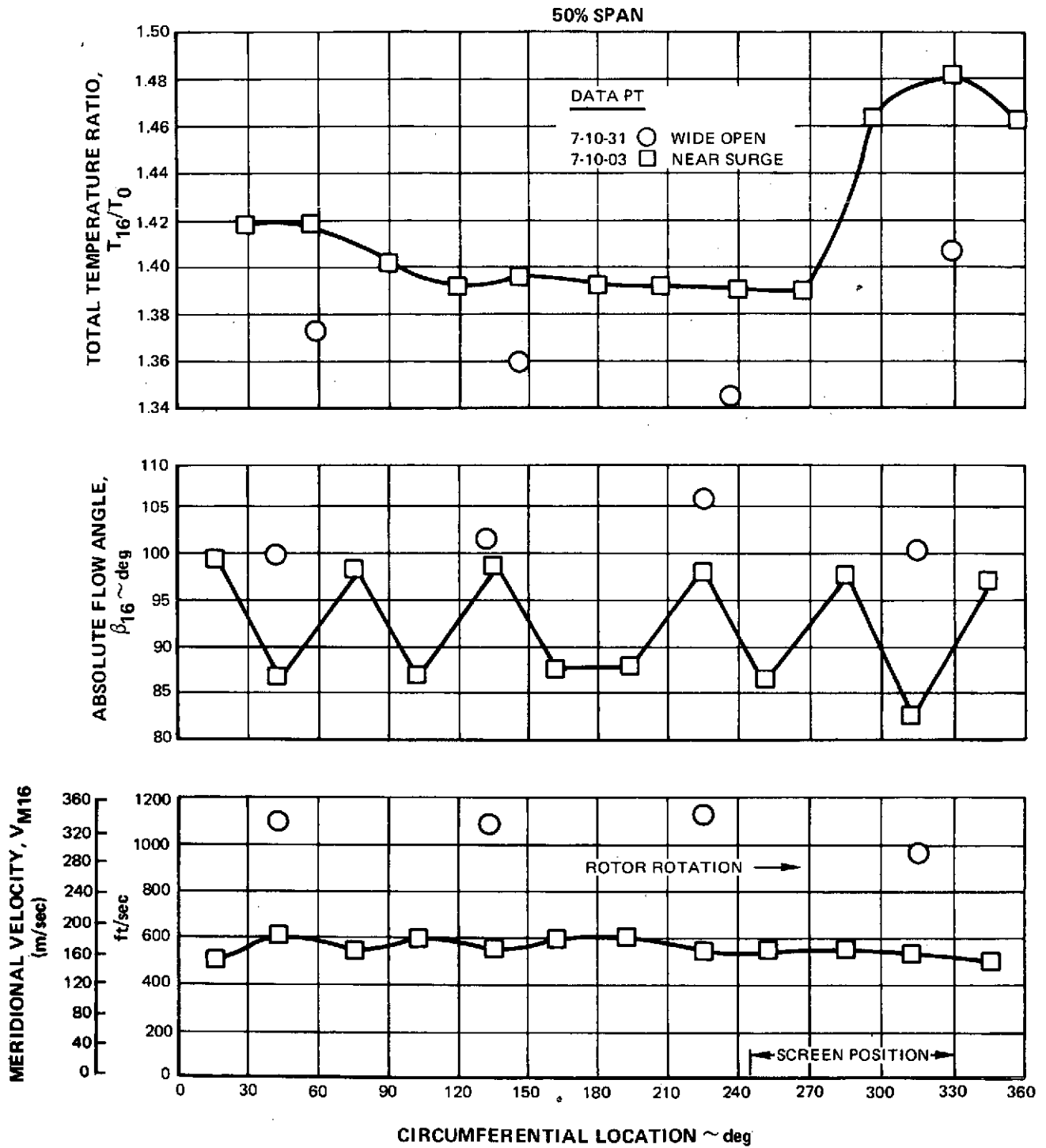


Figure 98d Circumferential Distributions of Fan Exit Total Pressure, Static Pressure, Absolute Mach Number, Total Temperature, Absolute Flow Angle, and Meridional Velocity with Circumferential Inlet Flow Distortion



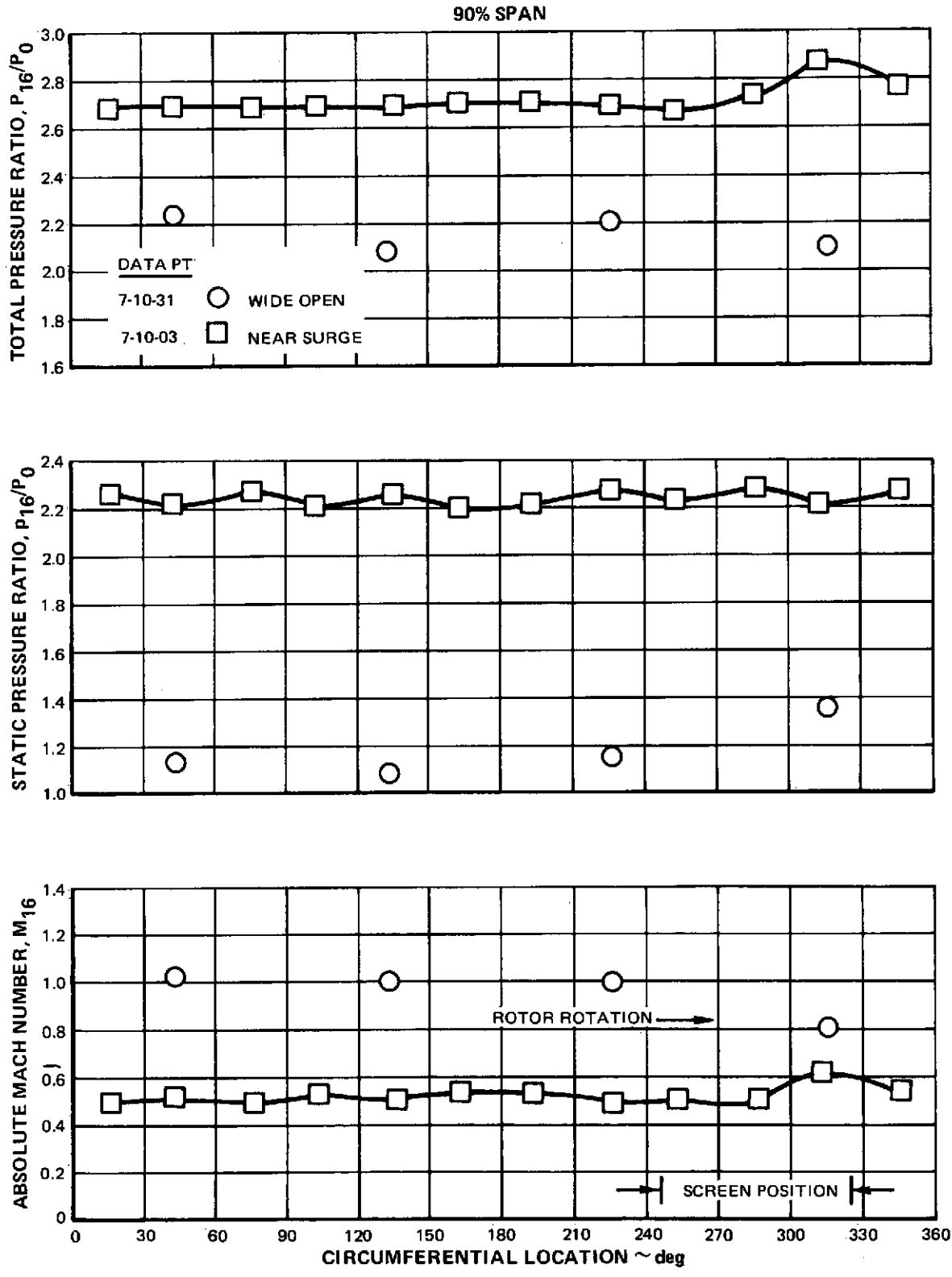


Figure 98e Circumferential Distributions of Fan Exit Total Pressure, Static Pressure, Absolute Mach Number, Total Temperature, Absolute Flow Angle, and Meridional Velocity with Circumferential Inlet Flow Distortion

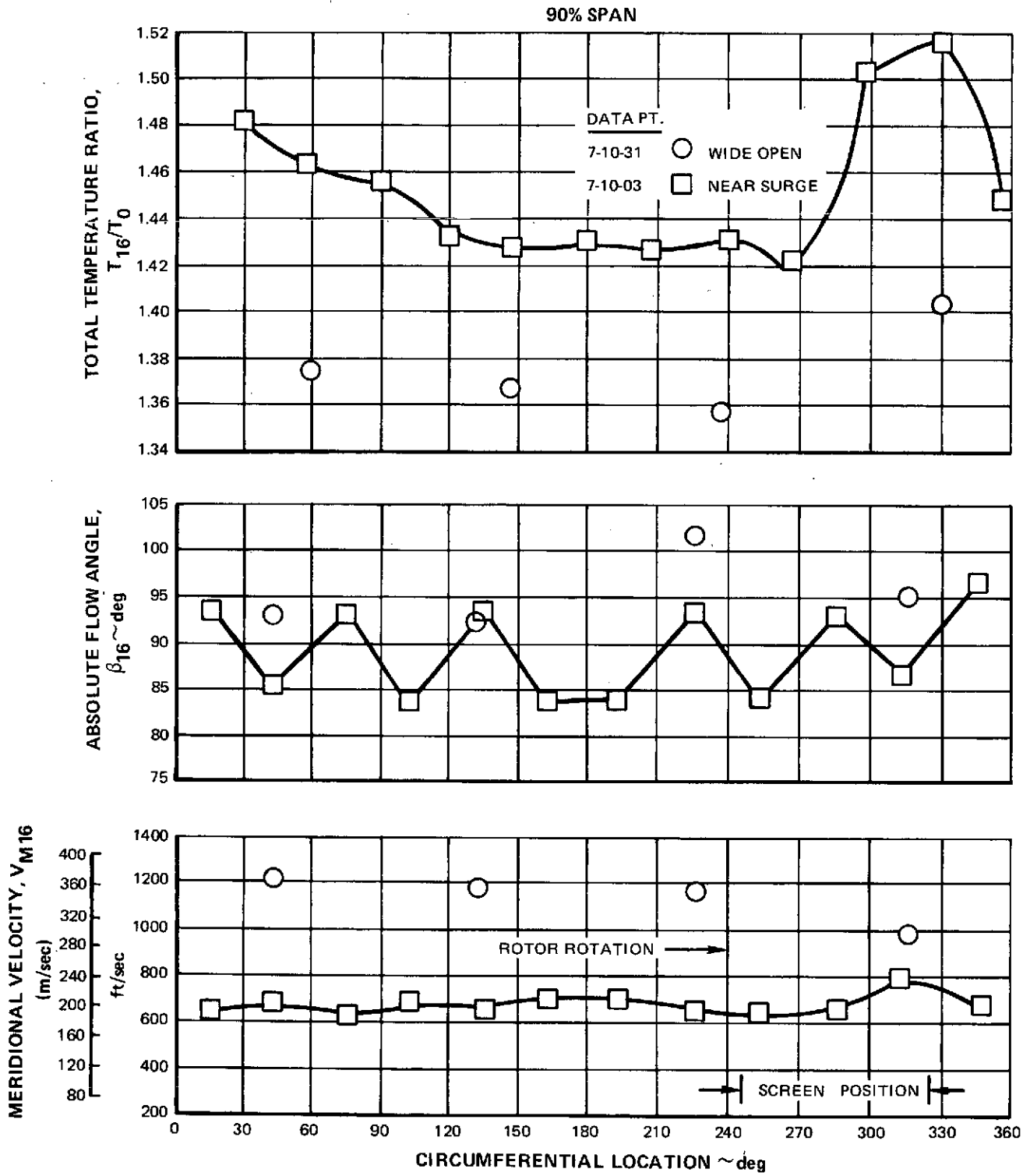


Figure 98f Circumferential Distributions of Fan Exit Total Pressure, Static Pressure, Absolute Mach Number, Total Temperature, Absolute Flow Angle, and Meridional Velocity with Circumferential Inlet Flow Distortion

## APPENDIX A

## SYMBOLS

A	–	area - inches <sup>2</sup> [meters <sup>2</sup> ]
A <sub>c</sub>	–	attenuation parameter for circumferentially distorted inlet flow
A/A*	–	ratio of actual area to critical area (where local Mach number is 1.0)
A <sub>r</sub>	–	attenuation parameter for radially distorted inlet flow
a	–	distance along chord from leading edge of airfoil to point of maximum elevation of airfoil above chord line - inches (meters)
a'	–	a point on the suction surface of a blade halfway between the leading edge and the point from which a Mach wave emanates that meets the leading edge of the following blade
C	–	damper coefficient – lb-sec/in [N-sec/m]
c	–	chord (aerodynamic on flow surface) - inches [meters]
c <sub>p</sub>	–	ratio of specific heats – BTU/lbm-°R [joule/kg-°k]
D	–	diffusion factor
d	–	amplitude of vibrational displacement in the direction normal to the minimum moment of inertia axis - inches [meters]
E	–	ε, the angle between rays drawn to a conical design surface, one ray to the leading edge of an airfoil section, the second to some other point on the airfoil - degrees (radians)
	–	excitations per rotor revolution
g <sub>c</sub>	–	conversion factor, 32.17 lb <sub>m</sub> ft/lb sec <sup>2</sup>
ID	–	inside diameter inches [meters]
i <sub>m</sub>	–	incidence angle, angle between inlet air direction and line tangent to blade mean camber line at leading edge, degrees (labelled INCM, Table XVI)
i <sub>ss</sub>	–	incidence angle, angle between inlet air direction and line tangent to blade suction surface at leading edge, degrees (labelled INCS, Table XVI)

APPENDIX A

J	–	Conversion Factor – 778 Ft - lbf/Btu [ 1.00m-kg/Joule]
$\bar{K}$	–	blockage factor = Effective area/total area
K	–	linear spring constants - lb/in [N/m]
M	–	Mach number
MCA	–	Multiple-circular-arc
N	–	rotor speed, rpm ( $N/\sqrt{\theta}$ labelled NCORR, table XVI)
OD	–	outside diameter, inches or meters
P	–	total pressure lbs/ft <sup>2</sup> or n/m <sup>2</sup>
p	–	static pressure, lbs/ft <sup>2</sup> or n/m <sup>2</sup>
R	–	distance from apex of design conical surface to point on blade - inches [meters]
	–	gas constant for air
r	–	radius measured from rig centerline - inches [meters]
r, $\theta$ , z	–	cylindrical coordinate system, with z axis as rig centerline
s	–	blade spacing – inches [meters]
SL	–	streamline number
T	–	total temperature - °R [°K]
	–	torsional spring constant – in-lb/degree [m-N/radian]
t	–	static temperature, °R or °K
	–	blade maximum thickness - inches [meters]
U	–	rotor speed - ft/sec [meters/sec]
V	–	air velocity - ft/sec [meters/sec]
• Vm	–	meridional velocity ( $V_r^2 + V_z^2$ ) <sup>1/2</sup> , ft/sec [m/sec] (labelled VM, Table XVI)
W	–	mass flow rate - lbm/sec [kg/sec]

$z$	— axial distance - inches [meters]
$\beta$	— absolute air angle, $\cot^{-1} (V_m/V\theta)$ , degrees (labelled B, Table XVI)
$\beta'$	— relative air angle, $\cot^{-1} (V_m/V\theta')$ , degrees (labelled B', Table XVI)
$\Delta\beta$	— air turning angle - degrees [radians]
$\gamma$	— blade chord angle, angle between a chord line and axial direction (measured in a plane parallel to z-axis) - degrees [radians]; — ratio of specific heats for air
$\delta$	— ratio of total pressure to standard pressure of 2116 lbs/ft <sup>2</sup> [1.0125 x 10 <sup>5</sup> N/m <sup>2</sup> ]
$\delta^\circ$	— deviation angle, exit air angle minus tangent to blade mean camber line at trailing edge - degrees [radians]
$\epsilon$	— angle between tangent to streamline projected on meridional plane and axial direction - degrees [radians]
$\eta$	— efficiency (percent)
$\theta$	— ratio of total temperature to standard temperature of 518.7°R [288.16°K]
$\rho$	— mass density - lbm/ft <sup>3</sup> [kg/meters <sup>3</sup> ]
$\sigma$	— solidity, ratio of aerodynamic chord to gap between blades
$\phi$	— blade camber angle, difference between blade angles at leading and trailing edges on conical surface, $\beta_1^* - \beta_2^*$ for rotors and $\beta_2^* - \beta_3^*$ for stators — degrees [radians],
$\phi_E$	— blade camber angle on plane of “unwrapped” conical surface $\beta_1^* - \beta_2^* - E_{TE}$ for rotors and $\beta_2^* - \beta_3^* - E_{TE}$ for stators- degrees [radians]
$\psi$	— amplitude of torsional vibration, radians
$\omega$	— angular velocity of rotor, radians/sec
$\omega_b$	— bending vibrational frequency (cycles/sec)
$\omega_t$	— torsional vibrational frequency (radians/sec)
$\bar{\omega}$	— total press loss coefficient

## APPENDIX A

### Subscripts

ad	–	adiabatic
E	–	refers to camber definitions which include epse angle E
f	–	front
Ef	–	refers to front camber definitions which include epse angle E
in	–	inlet
m	–	meridional (velocity); mean camber line (angle)
n	–	selected operating point
p	–	profile (loss; polytropic (efficiency))
r	–	radial direction
	–	ratio (e.g. $P_r$ = total pressure ratio)
ss	–	suction surface
sh	–	shock
t	–	transition
z	–	axial component
$\theta$	–	tangential component
o	–	plenum chamber
6	–	instrument plane upstream of rotor 1
7	–	station at rotor 1 leading edge
8	–	station at rotor 1 trailing edge
9	–	station at stator 1 leading edge
10	–	station at stator 1 trailing edge
11	–	instrument plane downstream stator 1

- 12        –    station at rotor 2 leading edge
- 13        –    station at rotor 2 trailing edge
- 14        –    station at stator 2 leading edge
- 15        –    station at stator 2 trailing edge
- 16        –    instrument plane downstream stator 2

#### Superscripts

- relative to rotor
- \*    –    blade metal (angle);
- critical, at Mach number unity (area)

## PERFORMANCE PARAMETERS

a) Relative total temperature

$$T'_7 = t_7 \left[ 1 + \frac{\gamma - 1}{2} (M'_7)^2 \right] \quad (\text{rotor 1) IN}$$

$$T'_8 = T'_7 + \left[ \frac{(\omega r_8)^2 - (\omega r_7)^2}{\frac{2\gamma}{\gamma - 1} R_{g_c}} \right] \quad (\text{rotor 1) OUT}$$

b) Incidence angle based on mean camber line

$$i_m = \beta'_7 - \beta'^*_7 \quad (\text{rotor 1})$$

$$i_m = \beta_9 - \beta'^*_9 \quad (\text{stator 1})$$

Incidence angle based on suction surface metal angle

$$i_{ss} = \beta'_7 - \beta'^*_{ss7} \quad (\text{rotor 1})$$

$$i_{ss} = \beta_9 - \beta'^*_{ss9} \quad (\text{stator 1})$$

c) Deviation angle

$$\delta^\circ = \beta'_8 - \beta'^*_8 \quad (\text{rotor 1})$$

$$\delta^\circ = \beta_{10} - \beta'^*_{10} \quad (\text{stator 1})$$

d) Diffusion factor

$$D = 1 - \frac{V'_8}{V'_7} + \frac{r_8 V_{\theta 8} - r_7 V_{\theta 7}}{(r_8 + r_7) \sigma V'_7} \quad (\text{rotor 1})$$

$$D = 1 - \frac{V_{10}}{V_9} + \frac{r_9 V_{\theta 9} - r_{10} V_{\theta 10}}{(r_9 + r_{10}) \sigma V_9} \quad (\text{stator 1})$$



e) Loss coefficient

$$\bar{\omega} = \frac{P'_7 \left[ \frac{T'_8}{T'_7} \right]^{\frac{\gamma}{\gamma-1}} - P'_8}{P'_7 - p_7} \quad (\text{rotor 1})$$

$$\bar{\omega} = \frac{P_9 - P_{10}}{P_9 - p_9} \quad (\text{stator 1})$$

f) Loss parameter

$$\frac{\bar{\omega} \cos \beta'_8}{2\sigma} \quad (\text{rotor 1})$$

$$\frac{\bar{\omega} \cos \beta_{10}}{2\sigma} \quad (\text{stator 1})$$

g) Polytropic efficiency

$$1) \eta_p = \frac{\frac{\gamma-1}{\gamma} \ln \left[ \frac{P_8}{P_7} \right]}{\ln \left[ \frac{T_8}{T_0} \right]} \quad (\text{rotor 1})$$

$$2) \eta_p = \frac{\frac{\gamma-1}{\gamma} \ln \left[ \frac{P_{10}}{P_9} \right]}{\ln \left[ \frac{t_{10}}{t_9} \right]} \quad \text{(stator 1)}$$

h) Adiabatic efficiency

$$\eta_{ad} = \frac{\left[ \frac{P_8}{P_7} \right]^{\frac{\gamma-1}{\gamma}} - 1}{\left[ \frac{T_{10}}{T_0} \right] - 1} \quad \text{(rotor 1)}$$

$$\eta_{ad} = \frac{\left[ \frac{P_{10}}{P_6} \right]^{\frac{\gamma-1}{\gamma}} - 1}{\left[ \frac{T_{10}}{T_0} \right] - 1} \quad \text{(stage 1)}$$

i) Stall margin

$$SM = \left[ \left( \frac{P_{16}/P_6}{W\sqrt{\theta_6}/\delta_6} \right)_{\text{Stall}} \left( \frac{W\sqrt{\theta_6}/\delta_6}{P_{16}/P_6} \right)_{\text{Reference Point or Operating Point}} - 1 \right] 100$$

j) Flow coefficient  $\phi = \frac{V_z}{U_{\text{mean flow}}}$

k) Pressure coefficient  $\psi = \frac{\Delta H_{id}}{U_{m^2}}$   
 $= \frac{\eta_{ad} \Delta T_{\text{actual}} c_p J_{gc}}{U_{\text{mean flow}}^2}$

APPENDIX B

AIRFOIL GEOMETRY ON CONICAL SURFACES

The airfoil geometry on conical surfaces for rotor 1, stator 1, rotor 2 (unshrouded), rotor 2 (redesign), and stator 2 is presented in Tables XI to XV in this appendix. The information is provided in U. S. customary units and in S. I. units.

TABLE XI - AIRFOIL GEOMETRY ON CONICAL SURFACES - ROTOR 1

Multiple - Circular - Arc Airfoils, 28 Blades

	Hub	3.15	6.70	10.10	22.70	31.65	41.85	51.85	62.90	74.60	80.70	87.00	93.40	Tip
Percent Flow	0													100.0
X Span at Leading Edge	0.0	5.7	11.2	16.6	32.4	42.4	52.4	62.1	71.7	81.2	85.9	90.7	95.3	100.0
Average X Span	0.0	5.35	10.6	15.8	31.2	41.2	51.2	61.05	70.95	80.6	85.45	90.35	95.15	100.0
X Span at Trailing Edge	0.0	5.0	10.0	15.0	30.0	40.0	50.0	60.0	70.0	80.0	85.0	90.0	95.0	100.0

U. S. Customary Units, inches and degrees

	3.62	3.70	3.76	3.83	4.00	4.08	4.17	4.25	4.32	4.40	4.45	4.48	4.51	4.55
$\frac{c}{f}$	0.85	0.92	1.00	1.08	1.29	1.49	1.65	1.81	1.88	2.11	2.21	2.30	2.40	2.50
$\frac{s}{c}$ to max. t	52.8	53.0	53.5	54.0	55.5	56.5	57.6	59.0	60.5	62.0	62.6	63.5	64.3	64.8
$\frac{t}{c}$	0.518	0.520	0.522	0.525	0.535	0.540	0.544	0.550	0.570	0.600	0.605	0.614	0.629	0.648
$\frac{t}{s}$	0.0110	0.0139	0.0138	0.0135	0.0129	0.0120	0.0112	0.0106	0.0100	0.0092	0.0088	0.0083	0.0078	0.0073
$\frac{t}{s}$	0.0110	0.0139	0.0138	0.0135	0.0129	0.0120	0.0112	0.0106	0.0100	0.0092	0.0088	0.0083	0.0078	0.0073
$\frac{t}{s}$	44.6	46.4	47.8	48.9	51.4	52.9	54.4	55.9	57.2	58.4	59.0	59.7	60.4	61.0
$\frac{t}{s}$	39.8	41.8	43.5	44.8	47.9	49.9	51.8	53.6	55.3	56.3	57.6	58.4	59.2	59.9
$\frac{t}{s}$	79.5	82.7	83.2	84.3	88.2	89.1	91.4	93.6	95.3	96.3	97.6	98.4	99.2	100.0
$\frac{t}{s}$	70.0	68.9	69.0	69.5	72.3	73.0	74.8	76.5	78.5	80.5	81.5	82.5	83.5	84.5
$\frac{t}{s}$	8.5	8.4	8.2	8.0	7.9	7.8	7.7	7.5	7.4	7.3	7.2	7.1	7.0	6.9
$\frac{t}{s}$	6.9	6.88	6.7	6.6	6.0	5.5	5.2	4.9	4.7	4.5	4.4	4.3	4.2	4.1
$\frac{t}{s}$	20.3	18.3	16.2	14.3	8.9	5.5	2.3	-0.8	-1.9	-4.9	-8.4	-9.9	-11.4	-12.9
$\frac{t}{s}$	2.38	2.27	2.17	2.09	1.88	1.77	1.67	1.58	1.51	1.44	1.41	1.38	1.36	1.33

S. I. Units, meters and radians

	0.0919	0.0940	0.0955	0.0976	0.1016	0.1038	0.1059	0.1080	0.1097	0.1115	0.1130	0.1138	0.1146	0.1156
$\frac{c}{f}$	0.0216	0.0234	0.0251	0.0274	0.0328	0.0376	0.0419	0.0465	0.0503	0.0544	0.0581	0.0591	0.0609	0.0635
$\frac{s}{c}$ to max. t	52.8	53.0	53.5	54.0	55.5	56.5	57.6	59.0	60.5	62.0	62.6	63.5	64.3	64.8
$\frac{t}{c}$	0.000356	0.000353	0.000351	0.000343	0.000328	0.000305	0.000284	0.000269	0.000254	0.000234	0.000224	0.000211	0.000198	0.000185
$\frac{t}{s}$	0.779	0.811	0.834	0.853	0.899	0.921	0.949	0.977	0.999	1.019	1.029	1.042	1.053	1.064
$\frac{t}{s}$	0.695	0.731	0.761	0.783	0.837	0.871	0.905	0.936	0.966	0.992	1.003	1.019	1.032	1.045
$\frac{t}{s}$	1.316	1.217	1.102	0.984	0.669	0.398	0.174	0.281	0.215	-0.192	0.188	0.199	0.225	0.258
$\frac{t}{s}$	0.118	0.117	0.113	0.110	0.106	0.105	0.104	0.085	0.084	0.227	0.232	0.244	0.279	0.323
$\frac{t}{s}$	0.120	0.120	0.117	0.115	0.106	0.096	0.082	0.068	0.050	0.023	0.011	-0.025	-0.049	-0.070
$\frac{t}{s}$	0.354	0.320	0.283	0.250	0.155	0.096	0.040	-0.014	-0.068	-0.1203	-0.147	-0.178	-0.199	-0.225
$\frac{t}{s}$	2.38	2.27	2.17	2.09	1.88	1.77	1.67	1.58	1.51	1.44	1.41	1.38	1.36	1.33

PRECEDING PAGE BLANK NOT FILMED





## APPENDIX C

### DESIGN VALUES OF OVERALL PERFORMANCE AND BLADE-ELEMENT PARAMETERS FOR THE REDESIGNED STAGE

This appendix provides the design values of overall performance and blade-element parameters for the redesigned stage. Spans and diameters for the blade-element data are given in Table XVI, and the column headings in the data table are identified in Table XVII. Finally, the overall performance and blade-element parameters are presented in Table XVIII for rotor 1, stator 1, rotor 2, and stator 2. The information is given in U. S. customary units and in S.I. units.

TABLE XVI – SPANS AND DIAMETERS FOR BLADE-ELEMENT DATA (Design Values)

SL	Rotor 1 Inlet Diameter Span (inches) (%)		Rotor 1 Exit Diameter Span (inches) (%)		Stator 1 Inlet Diameter Span (inches) (%)		Stator 1 Exit Diameter Span (inches) (%)	
1	13.47	5.8	15.59	5.0	15.93	4.9	17.38	4.3
2	14.52	11.4	16.35	10.0	16.64	9.9	17.93	8.9
3	15.56	17.0	17.10	15.0	17.36	14.8	18.49	13.6
4	18.52	32.9	19.37	30.0	19.53	29.8	20.26	28.1
5	22.22	52.8	22.38	50.0	22.42	49.8	22.69	48.2
6	24.00	62.4	23.89	60.0	23.87	59.9	23.93	58.4
7	24.88	67.1	24.65	65.0	24.60	64.9	24.55	63.6
8	25.76	71.8	25.40	70.0	25.33	69.9	25.18	68.8
9	28.38	85.9	27.67	85.0	27.50	85.0	27.07	84.4
10	29.26	90.6	28.42	90.0	28.23	90.0	27.70	89.6
11	30.13	95.3	29.18	95.0	28.95	95.0	28.34	94.8

SL	Rotor 2 Inlet Diameter Span (inches) (%)		Rotor 2 Exit Diameter Span (inches) (%)		Stator 2 Inlet Diameter Span (inches) (%)		Stator 2 Exit Diameter Span (inches) (%)	
1	17.87	4.3	18.74	3.8	18.93	3.8	19.18	3.2
2	18.38	8.8	19.14	7.8	19.30	7.8	19.49	6.8
3	18.90	13.5	19.54	12.0	19.69	11.9	19.82	10.6
4	20.51	28.0	20.84	25.3	20.94	25.3	20.91	23.2
5	22.74	48.0	22.73	44.6	22.75	44.8	22.58	42.2
6	23.88	58.1	23.73	54.9	23.72	55.1	23.49	52.8
7	24.45	63.3	24.25	60.2	24.22	60.5	23.97	58.2
8	25.03	68.4	24.78	65.6	24.72	65.9	24.46	63.9
9	26.78	84.2	26.42	82.4	26.29	82.7	26.00	81.7
10	27.37	89.4	26.98	88.1	26.82	88.4	26.53	87.8
11	27.96	94.7	27.55	94.0	27.36	94.2	27.07	93.9

PRECEDING PAGE BLANK NOT FILMED

REPRODUCIBILITY OF THE  
ORIGINAL PAGE IS POOR

TABLE XVII – IDENTIFICATION OF OVERALL PERFORMANCE AND BLADE-ELEMENT DATA TABLE COLUMN HEADINGS

ROTOR 1

SL	EPSI-1 DEGREE	EPSI-2 DEGREE	V-1 FT/SEC	V-2 FT/SEC	VM-1 FT/SEC	VM-2 FT/SEC	V8-1 FT/SEC	V8-2 FT/SEC	B-1 DEGREE	B-2 DEGREE	M-1	M-2	U-1 FT/SEC	U-2 FT/SEC	M'-1	M'-2	V'-1 FT/SEC	V'-2 FT/SEC
*	$\epsilon_7$	$\epsilon_8$	$V_7$	$V_8$	$V_{m7}$	$V_{m8}$	$V_{87}$	$V_{88}$	$\beta_7$	$\beta_8$	$M_7$	$M_8$	$U_7$	$U_8$	$M'_7$	$M'_8$	$V'_7$	$V'_8$
SL	INCS DEGREE	INCM DEGREE	DEV DEGREE	TURN DEGREE	RHOVM-1	RHOVM-2	D-FAC	OMEGA-B TOTAL	LOSS-P TOTAL	PO2/ PO1	%EFF-P TOT	%EFF-A TOT	B'-1 DEGREE	B'-2 DEGREE	V8'-1 FT/SEC	V8'-2 FT/SEC	PO/PO INLET	
*	$i_{m7}$	$i_{m7}$	$\delta_8^0$	$\Delta\beta$	$\rho_7 V_{m7}$	$\rho_8 V_{m8}$	D	$\Omega$	$\frac{\omega \cos \beta'_8}{20}$	$\frac{P_8}{P_7}$	$\eta_p$	$\eta_{ad}$	$\beta'_7$	$\beta'_8$	$V'_{87}$	$V'_{811}$	$\frac{P_8}{P_0}$	
				TO/TO INLET	PO/PO INLET	EFF-AD INLET %	EFF-P INLET %	WC1/A1 LBM/SEC SQFT		TO2/TO1	PO2/PO1	EFF-AD ROTOR %	EFF-P ROTOR %					
				$\frac{T_8}{T_0}$	$\frac{P_8}{P_0}$	$\eta_{ad}$	$\eta_p$	$\frac{W\sqrt{\beta_7}}{\delta_7 A_7}$		$\frac{T_8}{T_7}$	$\frac{P_8}{P_7}$	$\eta_{ad8}$	$\eta_{p8}$					

STATOR 1

SL	EPSI-1 DEGREE	EPSI-2 DEGREE	V-1 FT/SEC	V-2 FT/SEC	VM-1 FT/SEC	VM-2 FT/SEC	V8-1 FT/SEC	V8-2 FT/SEC	B-1 DEGREE	B-2 DEGREE	M-1	M-2	PO/PO INLET	TO/TO INLET	PO/PO STAGE	TO2/ TO1
*	$\epsilon_9$	$\epsilon_{10}$	$V_9$	$V_{10}$	$V_{m9}$	$V_{m10}$	$V_{89}$	$V_{810}$	$\beta_9$	$\beta_{10}$	$M_9$	$M_{10}$	$\frac{P_{10}}{P_0}$	$\frac{T_{10}}{T_0}$	$\frac{P_{10}}{P_7}$	$\frac{T_{10}}{T_7}$
SL	INCS DEGREE	INCM DEGREE	DEV DEGREE	TURN DEGREE	RHOVM-1	RHOVM-2	D-FAC	OMEGA-B TOTAL	LOSS-P TOTAL	PO2/ PO1	%EFF-P STATC-ST	%EFF-A TOT-INLET	%EFF-P TOT-INLET	%EFF-A TOT-STG	%EFF-P TOT-STG	
*	$i_{m9}$	$i_{m9}$	$\delta_{10}^0$	$\Delta\beta$	$\rho_9 V_{m9}$	$\rho_{10} V_{m10}$	D	$\Omega$	$\frac{\omega \cos \beta_{10}}{20}$	$\frac{P_{10}}{P_9}$	$\eta_{p-st}$	$\eta_{ad}$	$\eta_p$	$\eta_{ad-st}$	$\eta_{p-st}$	
		NCORR INLET RPM	WCORR INLET LBM/SEC	TO/TO INLET	PO/PO INLET	EFF-AD INLET %	EFF-P INLET %		TO2/TO1	PO2/PO1	EFF-AD STAGE %				$\eta_{ad-st}$	
		$\frac{N}{\sqrt{\beta_7}}$	$\frac{W\sqrt{\beta_7}}{\delta_7}$	$\frac{T_{10}}{T_0}$	$\frac{P_{10}}{P_0}$	$\eta_{ad}$	$\eta_p$		$\frac{T_{10}}{T_7}$	$\frac{P_{10}}{P_9}$						

\* SEE TABLE XVI  
SUBSCRIPTS REFER TO CALCULATION STATIONS

REPRODUCIBILITY OF THIS  
ORIGINAL PAGE IS POOR



TABLE XVII (Cont'd) — IDENTIFICATION OF OVERALL PERFORMANCE AND BLADE-ELEMENT DATA TABLE COLUMN HEADINGS

ROTOR 2																		
SL	EPSI-1 DEGREE	EPSI-2 DEGREE	V-1 FT/SEC	V-2 FT/SEC	VM-1 FT/SEC	VM-2 FT/SEC	Vθ-1 FT/SEC	Vθ-2 FT/SEC	B-1 DEGREE	B-2 DEGREE	M-1	M-2	U-1 FT/SEC	U-2 FT/SEC	M'-1	M'-2	V'-1 FT/SEC	V'-2 FT/SEC
*	$\epsilon_{12}$	$\epsilon_{13}$	$V_{12}$	$V_{13}$	$V_{m12}$	$V_{m13}$	$V_{\theta 12}$	$V_{\theta 13}$	$\beta_{12}$	$\beta_{13}$	$M_{12}$	$M_{13}$	$U_{12}$	$U_{13}$	$M'_{12}$	$M'_{13}$	$V'_{12}$	$V'_{13}$
SL	INCS DEGREE	INCM DEGREE	DEV DEGREE	TURN DEGREE	RHOVM-1	RHOVM-2	D-FAC	OMEGA-B TOTAL	LOSS-P TOTAL	PO2/ PO1	%EFF-P TOT	%EFF-A TOT	B'-1 DEGREE	B'-2 DEGREE	Vθ'-1 FT/SEC	Vθ'-2 FT/SEC	PO/PO INLET.	
*	$i_{m12}$	$i_{m12}$	$\delta_{13}^c$	$\Delta\beta$	$\rho_{12} V_{m12}$	$\rho_{13} V_{m13}$	D	$\bar{\omega}$	$\frac{\bar{\omega} \cos \beta'_{13}}{2\sigma}$	$\frac{P_{13}}{P_{12}}$	$\eta_p$	$\eta_{ad}$	$\beta'_{12}$	$\beta'_{13}$	$V'_{\theta 12}$	$V'_{\theta 13}$	$\frac{P_{13}}{P_0}$	
				TO/TO INLET	PO/PO INLET	EFF-AD INLET %	EFF-P INLET %	WC1/A1 LBM/SEC SQFT		TO2/TO1	PO2/PO1	EFF-AD ROTOR %	EFF-P ROTOR %					
				$\frac{T_{13}}{T_0}$	$\frac{P_{13}}{P_0}$	$\eta_{ad}$	$\eta_p$	$\frac{W\sqrt{\theta}_{12}}{\delta_{12} A_{12}}$		$\frac{T_{13}}{T_{12}}$	$\frac{P_{13}}{P_{12}}$	$\eta_{ad13}$	$\eta_{p13}$					
STATOR 2																		
SL	EPSI-1 DEGREE	EPSI-2 DEGREE	V-1 FT/SEC	V-2 FT/SEC	VM-1 FT/SEC	VM-2 FT/SEC	Vθ-1 FT/SEC	Vθ-2 FT/SEC	B-1 DEGREE	B-2 DEGREE	M-1	M-2	PO/PO INLET	TO/TO INLET	PO/PO STAGE	TO2/ TO1		
*	$\epsilon_{14}$	$\epsilon_{15}$	$V_{14}$	$V_{15}$	$V_{m14}$	$V_{m15}$	$V_{\theta 14}$	$V_{\theta 15}$	$\beta_{14}$	$\beta_{15}$	$M_{14}$	$M_{15}$	$\frac{P_{15}}{P_0}$	$\frac{T_{15}}{T_0}$	$\frac{P_{15}}{P_{12}}$	$\frac{T_{15}}{T_{12}}$		
SL	INCS DEGREE	INCM DEGREE	DEV DEGREE	TURN DEGREE	RHOVM-1	RHOVM-2	D-FAC	OMEGA-B TOTAL	LOSS-P TOTAL	PO2/ PO1	%EFF-P STATC-ST	%EFF-A TOT-INLET	%EFF-P TOT-INLET	%EFF-A TOT-STG	%EFF-P TOT-STG			
*	$i_{m14}$	$i_{m14}$	$\delta_{15}$	$\Delta\beta$	$\rho_{14} V_{m14}$	$\rho_{15} V_{m15}$	D	$\bar{\omega}$	$\frac{\bar{\omega} \cos \beta_{15}}{2\sigma}$	$\frac{P_{15}}{P_{14}}$	$\eta_{p-st}$	$\eta_{ad}$	$\eta_p$	$\eta_{ad-st}$	$\eta_{p-st}$			
		NCORR INLET RPM	WCORR INLET LBM/SEC	TO/TO INLET	PO/PO INLET	EFF-AD INLET %	EFF-P INLET %		TO2/TO1	PO2/PO1	EFF-AD STAGE %							
		$\frac{N}{\sqrt{\theta}_{12}}$	$\frac{W\sqrt{\theta}_{12}}{\delta_{12}}$	$\frac{T_{15}}{T_0}$	$\frac{P_{15}}{P_0}$	$\eta_{ad}$	$\eta_p$		$\frac{T_{15}}{T_{12}}$	$\frac{P_{15}}{P_{14}}$	$\eta_{ad-st}$							

\* SEE TABLE XVI  
SUBSCRIPTS REFER TO CALCULATION STATIONS

REPRODUCIBILITY OF THIS  
ORIGINAL PAGE IS POOR









## APPENDIX D

### AIRFOIL COORDINATES FOR MANUFACTURING SURFACES FOR THE REDESIGNED ROTOR 2

In this appendix the airfoil coordinates on manufacturing surfaces for the redesigned rotor 2 are presented in Table XIX. The information is presented in inches (U.S. customary units) and in meters (S.I. units).

TABLE XIX - AIRFOIL COORDINATES ON MANUFACTURING SURFACES  
(Redesigned Rotor 2)

INCHES			METERS		
ZC	YP	YS	ZC	YP	YS
-.0099	-.0113	.013*	.0000	-.0003	.0001
.0092	-.0067	.0209	.0002	-.0001	.0006
.0647	.0387	.0806	.0016	.0010	.0020
.1294	.0859	.1443	.0033	.0022	.0037
.1940	.1299	.2053	.0049	.0033	.0052
.2587	.1709	.2635	.0066	.0043	.0067
.3234	.2089	.3193	.0082	.0053	.0081
.3881	.2438	.3739	.0099	.0062	.0096
.4528	.2763	.4245	.0115	.0070	.0106
.5174	.3060	.4691	.0131	.0078	.0119
.5821	.3320	.5070	.0148	.0084	.0129
.6468	.3546	.5393	.0164	.0090	.0137
.7115	.3739	.5660	.0181	.0095	.0144
.7762	.3899	.5879	.0197	.0099	.0149
.8408	.4027	.6055	.0214	.0102	.0154
.9055	.4122	.6184	.0230	.0105	.0157
.9702	.4184	.6273	.0246	.0104	.0159
1.0349	.4212	.6316	.0263	.0107	.0160
1.0996	.4208	.6317	.0279	.0107	.0160
1.1643	.4171	.6274	.0294	.0104	.0159
1.2289	.4099	.6184	.0312	.0104	.0157
1.2936	.3991	.6050	.0329	.0101	.0154
1.3583	.3843	.5866	.0345	.0098	.0149
1.4230	.3657	.5634	.0361	.0093	.0143
1.4876	.3433	.5364	.0378	.0087	.0136
1.5523	.3167	.4994	.0394	.0080	.0127
1.6170	.2857	.4581	.0411	.0073	.0116
1.6817	.2499	.4095	.0427	.0063	.0104
1.7464	.2093	.3529	.0444	.0053	.0090
1.8110	.1633	.2871	.0460	.0041	.0073
1.8757	.1115	.2108	.0474	.0028	.0054
1.9404	.0536	.1210	.0493	.0014	.0031
2.0002	-.0050	.0244	.0508	-.0001	.0006
2.0051	-.0097	.0166	.0509	-.0002	.0004
RADIUS (INCHES) = 8.400			RADIUS (METERS) = .2134		
CHORD (INCHES) = 2.005			CHORD (METERS) = .0509		
XCSL (INCHES) = 1.0540			XCSL (METERS) = .0268		
YCSL (INCHES) = .4130			YCSL (METERS) = .0105		
RLE (INCHES) = .0098			RLE (METERS) = .000250		
RTE (INCHES) = .0089			RTE (METERS) = .000226		
X-AREA (SQ. IN.) = .3110			X-AREA (SQ. METERS) = .000201		
GAMMA-CHORD (DEG.) = 4.24			GAMMA-CHORD (RAU.) = .0739		

PRECEDING PAGE BLANK NOT FILMED

REPRODUCIBILITY OF THE  
ORIGINAL PAGE IS POOR







APPENDIX D

TABLE XIX (Cont'd) - AIRFOIL COORDINATES ON MANUFACTURING SURFACES  
(Redesigned Rotor 2)

INCHES			METERS			INCHES			METERS		
ZC	YP	YS	ZC	YP	YS	ZC	YP	YS	ZC	YP	YS
-.0000	-.0062	.0064	.0000	-.0002	.0002	.0000	-.0062	.0063	.0000	-.0002	.0002
-.0067	-.0042	.0074	.0009	-.0007	.0002	.0066	-.0061	.0072	.0002	-.0002	.0002
.0674	-.0057	.0165	.0017	-.0001	.0004	.0672	-.0040	.0156	.0007	-.0002	.0004
.1348	-.0053	.0261	.0034	-.0001	.0007	.1343	-.0060	.0245	.0014	-.0002	.0006
.2022	-.0050	.0352	.0051	-.0001	.0009	.2015	-.0061	.0330	.0021	-.0002	.0008
.2696	-.0048	.0438	.0068	-.0001	.0011	.2686	-.0062	.0409	.0028	-.0002	.0010
.3370	-.0048	.0518	.0085	-.0001	.0013	.3358	-.0065	.0483	.0035	-.0002	.0012
.4044	-.0049	.0593	.0103	-.0001	.0015	.4030	-.0068	.0551	.0042	-.0002	.0014
.4718	-.0051	.0661	.0120	-.0001	.0017	.4701	-.0072	.0615	.0049	-.0002	.0016
.5392	-.0054	.0724	.0137	-.0001	.0018	.5373	-.0078	.0674	.0056	-.0002	.0017
.6066	-.0059	.0782	.0154	-.0001	.0020	.6045	-.0084	.0728	.0063	-.0002	.0018
.6740	-.0065	.0835	.0171	-.0002	.0021	.6716	-.0091	.0777	.0070	-.0002	.0020
.7415	-.0072	.0882	.0188	-.0002	.0022	.7386	-.0098	.0821	.0077	-.0002	.0021
.8089	-.0080	.0923	.0205	-.0002	.0023	.8059	-.0107	.0860	.0084	-.0002	.0022
.8763	-.0088	.0959	.0223	-.0002	.0024	.8731	-.0115	.0894	.0091	-.0002	.0023
.9437	-.0096	.0997	.0240	-.0002	.0025	.9403	-.0124	.0921	.0098	-.0002	.0023
1.0111	-.0104	.1024	.0257	-.0003	.0026	1.0074	-.0131	.0940	.0105	-.0002	.0024
1.0785	-.0111	.1015	.0274	-.0003	.0026	1.0746	-.0137	.0949	.0112	-.0002	.0024
1.1459	-.0117	.1014	.0291	-.0003	.0026	1.1417	-.0143	.0949	.0119	-.0002	.0024
1.2133	-.0122	.1004	.0308	-.0003	.0026	1.2089	-.0149	.0941	.0126	-.0002	.0024
1.2807	-.0126	.0985	.0325	-.0003	.0025	1.2761	-.0150	.0924	.0133	-.0002	.0023
1.3481	-.0128	.0957	.0342	-.0003	.0024	1.3432	-.0151	.0896	.0140	-.0002	.0023
1.4155	-.0130	.0919	.0360	-.0003	.0023	1.4104	-.0152	.0863	.0147	-.0002	.0022
1.4829	-.0130	.0872	.0377	-.0003	.0022	1.4776	-.0150	.0819	.0154	-.0002	.0021
1.5503	-.0128	.0817	.0394	-.0003	.0021	1.5447	-.0147	.0768	.0161	-.0002	.0020
1.6177	-.0126	.0753	.0411	-.0003	.0019	1.6119	-.0142	.0709	.0168	-.0002	.0018
1.6851	-.0122	.0679	.0428	-.0003	.0017	1.6790	-.0136	.0640	.0175	-.0002	.0016
1.7525	-.0116	.0598	.0445	-.0003	.0015	1.7462	-.0128	.0564	.0182	-.0002	.0014
1.8199	-.0108	.0504	.0462	-.0003	.0013	1.8134	-.0118	.0479	.0189	-.0002	.0012
1.8873	-.0099	.0409	.0479	-.0003	.0010	1.8805	-.0106	.0384	.0196	-.0002	.0010
1.9547	-.0088	.0301	.0497	-.0002	.0008	1.9477	-.0092	.0285	.0203	-.0002	.0007
2.0221	-.0074	.0184	.0514	-.0002	.0005	2.0148	-.0076	.0177	.0210	-.0002	.0004
2.0895	-.0061	.0073	.0531	-.0002	.0002	2.0820	-.0060	.0061	.0217	-.0002	.0002
2.1569	-.0051	.0061	.0548	-.0002	.0002						
RADIUS (INCHES) = 12.212			RADIUS (METERS) = .3102			RADIUS (INCHES) = 12.343			RADIUS (METERS) = .3135		
CHORD (INCHES) = 2.090			CHORD (METERS) = .0531			CHORD (INCHES) = 2.082			CHORD (METERS) = .0529		
ZCSL (INCHES) = 1.0820			ZCSL (METERS) = .0275			ZCSL (INCHES) = 1.0785			ZCSL (METERS) = .0274		
YCSL (INCHES) = .6349			YCSL (METERS) = .0009			YCSL (INCHES) = .6313			YCSL (METERS) = .0008		
RLE (INCHES) = .0068			RLE (METERS) = .000172			RLE (INCHES) = .0047			RLE (METERS) = .000169		
RTE (INCHES) = .0067			RTE (METERS) = .000169			RTE (INCHES) = .0066			RTE (METERS) = .000167		
X-AREA (SQ. IN.) = .1614			X-AREA (SQ. METERS) = .000104			X-AREA (SQ. IN.) = .1555			X-AREA (SQ. METERS) = .000100		
GAMMA-CHORD (DEG.) = 46.46			GAMMA-CHORD (RAD.) = .8109			GAMMA-CHORD (DEG.) = 47.38			GAMMA-CHORD (RAD.) = .8269		



## APPENDIX E

### OVERALL PERFORMANCE AND BLADE-ELEMENT DATA WITH UNIFORM INLET FLOW

This appendix provides overall performance and blade-element data with uniform inlet flow. The information is presented for the redesigned fan. Fan overall performance is given in Table XX, and the overall performance and blade-element data for rotor 1, stator 1, rotor 2, and stator 2 are given in Table XXI. The column headings for Table XXI are identified in Table XVII of Appendix C. The information is present in U. S. customary units.

TABLE XX – FAN OVERALL PERFORMANCE (Uniform Inlet Flow)

Run Number	Speed Code	Point Number	$\frac{W\sqrt{\theta_0}}{\delta_0}$		$P_{11}/P_0$	$\eta_{ad 11}$	$P_{16}/P_0$	$\eta_{ad 16}$
			LBM/SEC	KG/SEC				
003	11	1	194.1	(88.0)	1.764	80.11	2.476	67.05
003	11	2	194.2	(88.1)	1.758	79.71	2.759	74.47
003	11	4	193.5	(87.8)	1.805	80.49	3.285	79.24
003	15	31	190.3	(86.3)	1.721	83.21	2.442	71.79
003	15	2	189.6	(86.0)	1.719	82.92	2.651	77.68
003	15	4	190.0	(86.2)	1.805	82.80	3.207	82.72
003	10	1	185.6	(84.2)	1.684	88.09	2.306	72.53
003	10	2	185.6	(84.2)	1.687	86.72	2.660	83.25
003	10	3	185.2	(84.0)	1.712	87.07	2.860	85.30
003	10	4	184.2	(83.5)	1.743	84.28	2.926	85.37
003	10	5	182.9	(82.9)	1.779	88.07	2.980	84.95
003	10	6	181.0	(82.1)	1.809	89.22	3.016	84.72
003	10	13	185.3	(84.0)	1.722	85.94	2.868	85.16
002	10	2	185.1	(83.9)	1.687	83.75	2.295	73.10
002	10	3	185.6	(84.2)	1.692	85.38	2.710	84.55
002	10	4	184.8	(83.8)	1.754	90.19	2.936	85.96
003	95	1	178.1	(80.8)	1.635	88.50	2.181	74.53
003	95	12	174.8	(79.3)	1.682	90.56	2.673	86.27
003	95	13	167.4	(75.9)	1.720	87.55	2.717	84.78
003	95	4	164.9	(74.8)	1.729	87.18	2.747	84.00
003	85	31	155.5	(70.5)	1.494	86.10	1.845	72.52
003	85	2	154.0	(69.8)	1.510	83.60	2.126	85.55
003	85	3	144.8	(65.7)	1.539	82.84	2.240	84.01
003	85	4	136.8	(62.0)	1.550	83.08	2.252	81.67
003	70	31	124.7	(56.6)	1.310	86.62	1.510	74.00
003	70	2	118.3	(53.7)	1.326	86.48	1.681	84.88
003	70	13	111.1	(50.4)	1.334	79.47	1.713	82.19
003	70	4	105.5	(47.8)	1.342	77.45	1.729	79.91
003	50	1	90.3	(41.0)	1.149	90.20	1.249	78.74
003	50	2	84.5	(38.3)	1.154	87.99	1.284	82.36
003	50	3	80.3	(36.4)	1.158	86.51	1.306	83.01
003	15	STALL	188.2	(85.4)			3.300	
003	10	STALL	178.8	(81.1)			3.035	
003	95	STALL	162.6	(76.9)			2.759	
003	85	STALL	133.8	(60.7)			2.269	
003	70	STALL	102.6	(46.5)			1.735	
003	50	STALL	67.6	(30.7)			1.319	

Speed Code	% Design Speed
50	50
70	70
85	85
90	90
95	95
10	100
15	105
11	110

REPRODUCIBILITY OF THE ORIGINAL PAGE IS POOR

PRECEDING PAGE BLANK NOT FILMED

TABLE XXI - OVERALL PERFORMANCE AND BLADE-ELEMENT DATA (Uniform Inlet Flow)

U. S. CUSTOMARY UNITS

ROTOR 1

Table with columns: SL, EPS1-1, EPS1-2, V-1, V-2, VM-1, VM-2, V0-1, V0-2, B-1, B-2, M-1, M-2, RUN NO, S, SPEED, CODE, SQ, POINT NO, U-1, U-2, M'-1, M'-2, V'-1, V'-2. Rows 1-11.

Table with columns: SL, INCS DEGREE, INCM DEGREE, DEV DEGREE, TURN DEGREE, RMQVM-1, RMQVM-2, D-FAC, OMEGA-B, LOSS-P, P02, XEFF-P, XEFF-A, B'-1, B'-2, V0'-1, V0'-2, PO/PO. Rows 1-11.

Summary table for Rotor 1 performance: TO/TO INLET, PO/PO INLET, EFF-AD INLET, EFF-P INLET, MCI/AI LBM/SEC, TO2/T01, P02/P01, EFF-AD RUTUR, EFF-P RUTUR.

STATOR 1

Table with columns: SL, CPS1-1, EPS1-2, V-1, V-2, VM-1, VM-2, V0-1, V0-2, B-1, B-2, M-1, M-2, RUN NO, S, SPEED, CODE, SQ, POINT NO, PO/PO, TO/TO, PD/PG, INLET, STAGE, TO2. Rows 1-11.

Table with columns: SL, INCS DEGREE, INCM DEGREE, DEV DEGREE, TURN DEGREE, RMQVM-1, RMQVM-2, D-FAC, OMEGA-B, LOSS-P, P02, XEFF-P, XEFF-A, B'-1, B'-2, V0'-1, V0'-2, PO/PO, TO2/T01, P02/P01, EFF-AD RUTUR, EFF-P RUTUR. Rows 1-11.

TABLE XXI (Cont'd) - OVERALL PERFORMANCE AND BLADE-ELEMENT DATA (Uniform Inlet Flow)

U. S. CUSTOMARY UNITS

ROTOR 2

Table with columns: SL, EPSI-1, EPSI-2, V-1, V-2, VM-1, VM-2, VO-1, VO-2, B-1, B-2, M-1, M-2, RUN NO, SPEED CODE, POINT NO, V'-1, V'-2. Rows 1-11.

Table with columns: SL, INCS, INCM, DEV, TURN, RHOVM-1, RHOVM-2, O-FAC, OMEGA-B, LOSS-P, POZ/P, XEFF-P, XEFF-A, B'-1, B'-2, VB'-1, VB'-2, PO/PO. Rows 1-11.

Summary table with columns: TO/TU, PO/PO, EFF-AD, EFF-P, WCI/A1, TO2/T01, P02/P01, EFF-AD, EFF-P. Values: 1.0833, 1.2749, 86.34, 86.77, 28.73, 1.0367, 1.1097, 82.24, 82.43.

STATOR 2

Table with columns: SL, EPSI-1, EPSI-2, V-1, V-2, VM-1, VM-2, VO-1, VO-2, B-1, B-2, M-1, M-2, RUN NO, SPEED CODE, POINT NO, PO/PO, TO/TU, PO/PO, TU/TU. Rows 1-11.

Table with columns: SL, INCS, INCM, DEV, TURN, RHOVM-1, RHOVM-2, O-FAC, OMEGA-B, LOSS-P, POZ/P, XEFF-P, XEFF-A, XEFF-P, XEFF-A, XEFF-P, XEFF-A. Rows 1-11.

Summary table with columns: WCORR, WCORR, TO/TU, PO/PO, EFF-AD, EFF-P, TO2/T01, P02/P01, EFF-AD. Values: 5380, 90.30, 1.0833, 1.2480, 78.74, 79.36, 1.0367, 0.9799, 85.69.













TABLE XXI (Cont'd) - OVERALL PERFORMANCE AND BLADE-ELEMENT DATA  
(Uniform Inlet Flow)

U. S. CUSTOMARY UNITS

ROTOR 2

Table with columns: SL, EPSI-1, EPSI-2, V-1, V-2, VM-1, VM-2, V0-1, V0-2, B-1, B-2, M-1, M-2, RUN NO, SPEED CODE, TO, POINT NO, V'-1, V'-2. Rows 1-11 showing performance data for Rotor 2.

Table with columns: SL, INCS, INCM, DEV, TURN, RHOVM-1, RHOVM-2, D-FAC, OMEGA-B, LOSS-P, PO2, XEFF-P, XEFF-A, B'-1, B'-2, V0'-1, V0'-2, PO/PO, INLET. Rows 1-11 showing blade element data for Rotor 2.

Summary table with columns: TO/TO INLET, PO/PO INLET, EFF-AD INLET, EFF-P INLET, MCI/AL LBM/SEC, X SOFT, T02/T01, PO2/P01, EFF-AD ROTOR, EFF-P ROTOR, X, Y. Values: 1.1687, 1.6207, 87.65, 88.45, 35.60, 1.0697, 1.2377, 89.95, 90.22, X, Y.

STATOR 2

Table with columns: SL, EPSI-1, EPSI-2, V-1, V-2, VM-1, VM-2, V0-1, V0-2, B-1, B-2, M-1, M-2, RUN NO, SPEED CODE, TO, POINT NO, PO/PO, TO/TO, PO/PO, TO/TO, PO/PO, TO/TO. Rows 1-11 showing performance data for Stator 2.

Table with columns: SL, INCS, INCM, DEV, TURN, RHOVM-1, RHOVM-2, D-FAC, OMEGA-B, LOSS-P, PO2, XEFF-P, XEFF-A, XEFF-P, XEFF-A, XEFF-P, NCCORR, MCMRR, TO/TO, PO/PO, EFF-AD, EFF-P, T02/T01, PO2/P01, EFF-AD, EFF-P. Rows 1-11 showing blade element data for Stator 2.

REPRODUCIBILITY OF THE ORIGINAL PAGE IS POOR







TABLE XXI (Cont'd) - OVERALL PERFORMANCE AND BLADE-ELEMENT DATA (Uniform Inlet Flow)

U. S. CUSTOMARY UNITS

ROTOR 2

Table with columns: SL, EPSI-1, EPSI-2, V-1, V-2, VM-1, VM-2, V0-1, V0-2, B-1, B-2, RUN NO, 3, SPEED, CODE, 70, POINT, NO 13, V'-1, V'-2. Rows 1-14.

Table with columns: SL, INCS, INCM, DEY, TURN, RHOVM-1, RHOVM-2, D-FAC, OMEGA-B, LOSS-P, PO2/, XEFF-P, XEFF-A, H'-1, B'-2, V0'-1, V0'-2, PO/PO. Rows 1-14.

Summary table for rotor data: TO/TO INLET, PO/PO INLET, EFF-AD INLET, EFF-P INLET, MCL/A1 INLET, LBM/SEC, % SQFT, TOZ/TOT, PO2/PO1, EFF-AD ROTOR, EFF-P ROTOR, %.

STATOR 2

Table with columns: SL, EPSI-1, EPSI-2, V-1, V-2, VM-1, VM-2, V0-1, V0-2, B-1, B-2, RUN NO, 3, SPEED, CODE, 70, POINT, NO 13, TOZ/, TO/TO, PO/PO, TOZ/TOT. Rows 1-11.

Table with columns: SL, INCS, INCM, DEY, TURN, RHOVM-1, RHOVM-2, D-FAC, OMEGA-B, LOSS-P, PO2/, XEFF-P, XEFF-A, H'-1, B'-2, V0'-1, V0'-2, PO/PO, TOZ/TOT, PO2/PO1, EFF-AD, EFF-P, MCL/A1, LBM/SEC, % SQFT. Rows 1-11.









TABLE XXI (Cont'd) - OVERALL PERFORMANCE AND BLADE-ELEMENT DATA  
(Uniform Inlet Flow)

U. S. CUSTOMARY UNITS

ROTOR 2

Table with 18 columns: SL, EPSI-1, EPSI-2, V-1, V-2, VM-1, VM-2, VO-1, VO-2, B-1, B-2, M-1, M-2, RUN NO, S, SPEED CODE, 85, POINT NO, V1, V2. Rows 1-11.

Table with 18 columns: SL, INCS, INCM, DEV, TLRN, RHQVM-1, RHQVM-2, C-FAC, OMEGA-B, LOSS-P, P02, EFF-P, EFF-A, B\*-1, B\*-2, V6\*-1, V6\*-2, PQ/PQ. Rows 1-11.

Summary table with 6 columns: TO/T0, PQ/PQ, EFF-AD, EFF-P, MC1/A1, T02/T01, PC2/P01, EFF-AD, EFF-P. Values: 1.2633, 1.5655, 80.77, 82.48, 39.76, 1.1070, 1.3157, 75.93, 76.82.

STATOR 2

Table with 18 columns: SL, EPSI-1, EPSI-2, V-1, V-2, VM-1, VM-2, VO-1, VO-2, B-1, B-2, M-1, M-2, RUN NO, S, SPEED CODE, 85, POINT NO, V1, V2. Rows 1-11.

Table with 18 columns: SL, INCS, INCM, DEV, TURN, RHQVM-1, RHQVM-2, C-FAC, OMEGA-B, LOSS-P, P02, EFF-P, EFF-A, BFF-P, EFF-A, EFF-P, TOT-STAT, TOT-STG. Rows 1-11.

Summary table with 6 columns: MCORR, MCORR, TO/T0, PQ/PQ, EFF-AD, EFF-P, T02/T01, P02/P01, EFF-AD. Values: 908.8, 155.50, 1.2633, 1.8449, 72.52, 74.75, 1.1070, 0.9386, 97.87.

TABLE XXI (Cont'd) – OVERALL PERFORMANCE AND BLADE-ELEMENT DATA  
(Uniform Inlet Flow)

U. S. CUSTOMARY UNITS

ROTOR 1

Table with columns: SL, EPSI-1, EPSI-2, V-1, V-2, VM-1, VM-2, V0-1, V0-2, B-1, B-2, M-1, M-2, RUN NO, SPEED CODE, POINT NO, and velocity/pressure values.

Table with columns: SL, INCS, INCM, DEV, TURN, RHGVN-1, RHGVN-2, D-PAC, OMEGA-B, LOSS-P, P01, XEFF-P, XEFF-A, B-1, B-2, V0-1, V0-2, and inlet values.

Summary table with columns: TC/TQ, PG/PO, EFF-AD, EFF-P, WCL/AI, TQ2/TQ1, P02/P01, EFF-AD, EFF-P, and numerical values.

STATOR 1

Table with columns: SL, EPSI-1, EPSI-2, V-1, V-2, VM-1, VM-2, V0-1, V0-2, B-1, B-2, M-1, M-2, RUN NO, SPEED CODE, POINT NO, and velocity/pressure values.

Table with columns: SL, INCS, INCM, DEV, TURN, RHGVN-1, RHGVN-2, D-PAC, OMEGA-B, LOSS-P, P01, XEFF-P, XEFF-A, XEFF-P, XEFF-A, XEFF-P, and inlet values.

Summary table with columns: W CORR, TO/TO, PG/PO, EFF-AD, EFF-P, TQ2/TQ1, P02/P01, EFF-AD, and numerical values.

TABLE XXI (Cont'd) - OVERALL PERFORMANCE AND BLADE-ELEMENT DATA  
(Uniform Inlet Flow)

U. S. CUSTOMARY UNITS

ROTOR 2

Table with columns: SL, EPSI-1, EPSI-2, V-1, V-2, VM-1, VM-2, V0-1, V0-2, B-1, B-2, M-1, M-2, RUN NO, S, SPEED CODE, S5, POINT NO 2, U-1, U-2, M'-1, M'-2, V'-1, V'-2. Rows 1-14.

Table with columns: SL, INCS, INCM, DEV, TURN, RHOVM-1, RHOVM-2, D-FAC, OMEGA-B, LOSS-P, PO2/, SEFF-P, SEFF-A, B\*-1, B\*-2, V8'-1, V8'-2, PU/PU. Rows 1-14.

Summary table with columns: TO/TO, PO/PO, EFF-AD, EFF-P, NCL/A1, TO2/T01, PO2/PO1, EFF-AD, EFF-P. Values: 1.2807, 2.1821, 88.80, 89.95, 39.11, 1.1142, 1.4453, 96.78, 96.93.

STATOR 2

Table with columns: SL, EPSI-1, EPSI-2, V-1, V-2, VM-1, VM-2, V0-1, V0-2, B-1, B-2, M-1, M-2, RUN NO, S, SPEED CODE, S5, POINT NO 2, TO/TO, PO/PO, TOT-INLET, TOT-STG, TOT-STG. Rows 1-11.

Table with columns: SL, INCS, INCM, DEV, TURN, RHOVM-1, RHOVM-2, D-FAC, OMEGA-B, LOSS-P, PO2/, SEFF-P, SEFF-A, SEFF-P, SEFF-A, SEFF-P. Rows 1-11.

Summary table with columns: NCGRR, HCGRR, TO/TO, PO/PO, EFF-AD, EFF-P, TO2/T01, PO2/PO1, EFF-AD, STAGE. Values: 9899, 13400, 1.2807, 2.1265, 85.95, 86.98, 1.1142, 0.9765, 89.67.

TABLE XXI (Cont'd) - OVERALL PERFORMANCE AND BLADE-ELEMENT DATA (Uniform Inlet Flow)

U. S. CUSTOMARY UNITS

ROTOR 1

Table for Rotor 1 performance data including columns for SL, C-PSI-1, C-PSI-2, V-1, V-2, VM-1, VM-2, VO-1, VO-2, B-1, B-2, M-1, M-2, RUN NO, 3, SPEED CODE 85, POINT NO 3, V-1, V-2, and various velocity/angle parameters in FT/SEC and DEGREE.

Table for Rotor 1 blade-element data including columns for SL, INCS, INCM, DEV, TURN, RHQVM-1, RHQVM-2, C-FAC, OMEGA-B, LOSS-P, PO2, XEFF-P, XEFF-A, B-1, B-2, VM-1, VM-2, PO/PO, TO2/TO1, PC2/PO1, EFF-AD, EFF-P, and INLET parameters.

STATOR 1

Table for Stator 1 performance data including columns for SL, C-PSI-1, C-PSI-2, V-1, V-2, VM-1, VM-2, VO-1, VO-2, B-1, B-2, M-1, M-2, RUN NO, 3, SPEED CODE 85, POINT NO 3, V-1, V-2, TO2/TO1, PO/PO, and various velocity/angle parameters.

















TABLE XXI (Cont'd) - OVERALL PERFORMANCE AND BLADE-ELEMENT DATA (Uniform Inlet Flow)

U. S. CUSTOMARY UNITS

ROTOR 1

Table with 20 columns: SL, EPSI-1, EPSI-2, V-1, V-2, VM-1, VM-2, V0-1, V0-2, B-1, B-2, M-1, M-2, RUN NO, SPEED, CODE 95, POINT NO 13, V'-1, V'-2. Rows 1-11 show performance metrics for rotor 1.

Table with 18 columns: SL, INCS, INCM, DEV, TURN, RHQVM-1, RHQVM-2, D-FAC, OMEGA-B, LOSS-P, P02, XEFF-P, XEFF-A, B'-1, B'-2, V0'-1, V0'-2, PQ/PD. Rows 1-11 show blade element data for rotor 1.

Summary table with 8 columns: TO/T0, PU/PD, EFF-AD, EFF-P, WCI/A1, TQ2/T01, P02/P01, EFF-AD, EFF-P. Values: 1.1913, 1.7622, 91.79, 92.40, 38.02, 1.1913, 1.7622, 91.79, 92.40.

STATOR 1

Table with 20 columns: SL, EPSI-1, EPSI-2, V-1, V-2, VM-1, VM-2, V0-1, V0-2, B-1, B-2, M-1, M-2, RUN NO, SPEED, CODE 95, POINT NO 13, V'-1, V'-2. Rows 1-11 show performance metrics for stator 1.

Table with 18 columns: SL, INCS, INCM, DEV, TURN, RHQVM-1, RHQVM-2, D-FAC, OMEGA-B, LOSS-P, P02, XEFF-P, XEFF-A, XEFF-P, XEFF-A, XEFF-P. Rows 1-11 show blade element data for stator 1.







TABLE XXI (Cont'd) - OVERALL PERFORMANCE AND BLADE-ELEMENT DATA (Uniform Inlet Flow)

U. S. CUSTOMARY UNITS

ROTOR 2

Table with columns: SL, EPSI-1, EPSI-2, V-1, V-2, VM-1, VM-2, V0-1, V0-2, B-1, B-2, M-1, M-2, RUN NO, 3, SPEED CODE, 95, POINT NO, 4, U-1, U-2, M'-1, M'-2, V'-1, V'-2. Rows 1-11.

Table with columns: SL, INCS, INCM, DEV, TURN, RHOVM-1, RHOVM-2, D-FAC, CMEGA-B, LOSS-P, PO2/, XEFF-P, XEFF-A, B'-1, B'-2, VB'-1, VB'-2, PC/PC. Rows 1-11.

Summary table with columns: TO/TO, PO/PO, EFF-AD, EFF-P, WCL/#1, TO2/TO1, PC2/PC1, EFF-AD, EFF-P. Values: 1.3570, 2.8007, 85.85, 87.72, 37.27, 1.1699, 1.6198, 86.38, 87.28.

STATOR 2

Table with columns: SL, EPSI-1, EPSI-2, V-1, V-2, VM-1, VM-2, V0-1, V0-2, B-1, B-2, M-1, M-2, RUN NO, 3, SPEED CODE, 95, POINT NO, 4, PO/PO, TO/TO, PC/PO, TC2/. Rows 1-11.

Table with columns: SL, INCS, INCM, DEV, TURN, RHOVM-1, RHOVM-2, D-FAC, CMEGA-B, LOSS-P, PO2/, XEFF-P, XEFF-A, XEFF-P, XEFF-A, XEFF-P. Rows 1-11.

Summary table with columns: NCORR, WCORR, TO/TO, PO/PO, EFF-AD, EFF-P, TO2/TO1, PO2/#01, EFF-AD. Values: 10158, 164.90, 1.3570, 2.7472, 84.00, 86.08, 1.1699, 0.9809, 82.70.

REPRODUCIBILITY OF THE ORIGINAL PAGE IS POOR













APPENDIX E

TABLE XXI (Cont'd) -- OVERALL PERFORMANCE AND BLADE-ELEMENT DATA (Uniform Inlet Flow)

U. S. CUSTOMARY UNITS

ROTOR 1

Table with 16 columns: V-1, V-2, VM-1, VM-2, V0-1, V0-2, B-1, B-2, M-1, M-2, RUN NO, S, SPEEL, CLDE, ID, POINT NO, U-1, U-2, U-1, U-2, V-1, V-2. Includes sub-headers for INCM, DEV, TURN, KHCVM, O-FAC, OMEGA, LOSS-P, P02, XEFF-P, XEFF-A, XEFF-P, XEFF-A, XEFF-P, XEFF-A, PC/PU, and INLET.

Summary table with 6 columns: TC/TD INLET, PC/PG INLET, EFF-AD INLET, EFF-P INLET, XCI/A,1 LBM/SEC, X SQFT, TQ2/TQ1, PC2/PC1, XEFF-A RUTOR, XEFF-P RUTOR, X, X.

STATOR 1

Table with 16 columns: V-1, V-2, VM-1, VM-2, V0-1, V0-2, B-1, B-2, M-1, M-2, RUN NO, S, SPEEL, CLDE, ID, POINT NO, U-1, U-2, U-1, U-2, V-1, V-2. Includes sub-headers for INCM, DEV, TURN, KHCVM, O-FAC, OMEGA, LOSS-P, P02, XEFF-P, XEFF-A, XEFF-P, XEFF-A, XEFF-P, XEFF-A, PC/PU, and INLET.







TABLE XXI (Cont'd) - OVERALL PERFORMANCE AND BLADE-ELEMENT DATA  
(Uniform Inlet Flow)

U. S. CUSTOMARY UNITS

ROTOR 2

Table with columns for blade elements (1-11), velocity components (V-1 to V-2), angles (B-1 to B-2), and performance metrics (3, SPEED CODE 10, POINT NC 13).

Table with columns for blade elements (1-11), incidence (INCS), incidence (INCH), deviation (DEV), turn (TURN), and various performance metrics (RHCVM-1, RHCVM-2, D-FAC, OMEGA-B, LCSS-P, etc.).

Summary table with columns: TO/TO INLET, PO/PO INLET, EFF-AD INLET, EFF-P INLET, WCI/A1 LBM/SEC SOFT, TO2/T01, PC2/P01, EFF-AD ROTOR, EFF-P ROTOR.

STATOR 2

Table with columns for blade elements (1-11), velocity components (V-1 to V-2), angles (B-1 to B-2), and performance metrics (3, SPEED CODE 10, POINT NC 13).

Table with columns for blade elements (1-11), incidence (INCS), incidence (INCH), deviation (DEV), turn (TURN), and various performance metrics (RHCVM-1, RHCVM-2, D-FAC, OMEGA-B, LCSS-P, etc.).

Summary table with columns: NCORR INLET, WCORR INLET, TO/TO INLET, PO/PO INLET, EFF-AD INLET, EFF-P INLET, TO2/T01, PC2/P01, EFF-AD STAGE, EFF-P STAGE.

REPRODUCIBILITY OF THE ORIGINAL PAGE IS POOR

TABLE XXI (Cont'd) - OVERALL PERFORMANCE AND BLADE-ELEMENT DATA  
(Uniform Inlet Flow)

U. S. CUSTOMARY UNITS

ROTOR 1

BL	CPSI-1	CPSI-2	V-1	V-2	VM-1	VM-2	V0-1	V0-2	B-1	B-2	M-1	M-2	RUN NO	SPEED	CODE	POINT NO	J	U-1		U-2		V1-1	V1-2
																		U-1	U-2	M-1	M-2		
1	10000	10000	10000	10000	10000	10000	10000	10000	10000	10000	10000	10000	10000	10000	10000	10000	10000	10000	10000	10000	10000	10000	10000

BL	INCS	INCM	DEV	TURN	RHOVM-1	RHOVM-2	C-FAC	OMEGA-8	LCSS-P	PO2/	XEFF-P	XEFF-A	B-1	B-2	V0-1	V0-2	PG/PU	INLET	PG/PU	INLET	EFF-AD	EFF-P	WCI/A1	T02/T01	PG2/PU1	EFF-A1	EFF-P		
																												TOTAL	TOTAL
1	2.33	15.73	56.54	41.29	51.34	0.4008	0.0051	0.0140	1.6743	96.55	96.24	44.31	-12.23	-62.92	145.1	1.0743	1.7345	89.78	90.52	42.15	1.0743	1.7345	89.78	90.52	42.15	1.0743	1.7345	89.78	90.52

STATOR 1

BL	CPSI-1	CPSI-2	V-1	V-2	VM-1	VM-2	V0-1	V0-2	B-1	B-2	M-1	M-2	RUN NO	SPEED	CODE	POINT NO	J	U-1		U-2		V1-1	V1-2	
																		U-1	U-2	M-1	M-2			FT/SEC
1	10000	10000	10000	10000	10000	10000	10000	10000	10000	10000	10000	10000	10000	10000	10000	10000	10000	10000	10000	10000	10000	10000	10000	10000











TABLE XXI (Cont'd) — OVERALL PERFORMANCE AND BLADE-ELEMENT DATA  
(Uniform Inlet Flow)

U. S. CUSTOMARY UNITS

ROTOR 2

SL	CP1-1	CP1-2	V-1	V-2	VM-1	VM-2	VO-1	VO-2	B-1	B-2	M-1	M-2	RUN NO	2, SPEED CODE 10,	POINT NO 4	U-1	U-2	M'-1	M'-2	V'-1	V'-2
DEGREE	DEGREE	FT/SEC	FT/SEC	FT/SEC	FT/SEC	FT/SEC	FT/SEC	DEGREE	DEGREE				FT/SEC	FT/SEC					FT/SEC	FT/SEC	
1	11.055	748.0	1048.2	739.0	721.3	-402.5	788.0	-7.9	47.4	0.0350	0.8521	834.3	875.1	1.0152	0.5795	1193.6	726.5				
2	9.762	754.6	1057.4	750.9	708.0	-74.1	765.3	-5.6	47.9	0.0432	0.8444	857.9	893.4	1.0203	0.5719	1196.9	716.2				
3	8.553	770.4	1047.1	749.8	654.9	-50.6	703.3	-2.3	48.3	0.0562	0.8378	882.2	912.4	1.0202	0.5655	1194.1	706.8				
4	7.226	793.7	968.1	742.2	706.5	-48.4	661.8	-3.5	43.1	0.0807	0.7725	937.7	973.1	1.0983	0.6181	1280.6	772.1				
5	6.034	748.4	837.6	747.0	597.4	-46.3	587.1	-3.5	44.5	0.0391	0.6606	1061.6	1061.1	1.1412	0.6015	1336.3	762.6				
6	4.016	680.1	749.6	682.5	546.9	-66.9	541.5	-5.6	44.7	0.5028	0.6053	1114.8	1107.9	1.1593	0.6172	1364.9	787.4				
7	2.128	691.3	761.0	688.1	547.5	-65.6	528.6	-5.4	43.9	0.5884	0.5970	1141.6	1132.1	1.1826	0.6392	1369.6	814.8				
8	0.214	712.2	772.3	710.6	553.3	-74.4	538.9	-5.8	44.2	0.6081	0.6006	1168.5	1156.8	1.2025	0.6514	1408.3	829.4				
9	0.130	759.0	791.1	758.5	573.7	-27.1	544.6	-2.0	43.4	0.6481	0.6180	1250.4	1233.4	1.2687	0.7002	1485.7	896.4				
10	0.078	762.7	792.9	760.6	597.3	-53.5	521.6	-4.0	41.0	0.6484	0.6158	1277.9	1259.0	1.3037	0.7374	1533.5	949.4				
11	0.400	754.2	770.9	749.1	593.8	-66.2	491.7	-6.7	39.5	0.6393	0.5947	1305.5	1286.4	1.3411	0.7653	1582.3	992.0				

SL	INCL	INCM	DEV	TURN	RHCVM-1	RHCVM-2	D-FAC	OMEGA-B	LOSS-P	PQ2/	EFF-P	EFF-A	B'-1	B'-2	VO'-1	VO'-2	PQ/PO
DEGREE	DEGREE	DEGREE	DEGREE					TOTAL	TOTAL	PQ1	TOT	TOT	DEGREE	DEGREE	FT/SEC	FT/SEC	INLET
1	6.466	27.26	44.77	68.74	86.27	0.5644	0.1567	0.0355	1.7943	88.50	87.51	51.62	6.86	-936.9	-67.1	3.1746	
2	5.59	22.46	42.45	69.98	86.19	0.5718	0.1373	0.0317	1.7942	89.77	88.09	51.09	8.05	-932.1	-108.1	3.1960	
3	4.07	18.03	39.34	71.84	86.24	0.5738	0.1037	0.0244	1.7572	92.10	91.42	49.86	10.50	-912.9	-129.2	3.2259	
4	4.85	14.22	28.03	73.68	90.85	0.5405	0.0868	0.0190	1.7409	92.76	92.17	51.81	23.78	-1006.1	-311.3	3.1495	
5	7.12	10.21	17.58	68.66	77.54	0.5631	0.1039	0.0231	1.6855	89.81	89.03	56.02	38.43	-1108.1	-474.0	2.9417	
6	5.93	9.77	13.49	62.21	70.88	0.5551	0.0962	0.0198	1.6898	90.41	89.67	59.47	45.98	-1181.8	-366.5	2.8349	
7	5.50	8.48	12.56	63.01	71.36	0.5435	0.1045	0.0214	1.6898	89.30	88.48	60.30	47.73	-1207.2	-603.5	2.8328	
8	4.27	8.10	5.77	11.58	65.51	72.56	0.5410	0.1180	0.0247	1.6621	87.73	86.80	59.67	48.09	-1215.9	-617.9	2.8654
9	2.47	5.10	2.98	9.15	70.10	75.30	0.5294	0.1550	0.0347	1.6591	83.10	81.86	59.23	50.08	-1277.5	-688.7	2.9246
10	2.42	5.14	4.20	5.28	65.77	77.77	0.5146	0.1626	0.0373	1.6594	81.95	80.63	60.16	50.88	-1331.4	-738.0	2.9508
11	4.83	7.45	8.54	68.43	76.57	0.5098	0.1849	0.0428	1.6465	78.69	77.15	61.64	53.11	-1343.7	-794.7	2.6930	

TC/TO	PQ/PO	EFF-AD	EFF-P	WC1/A1	TO2/TO1	PC2/PO1	EFF-AD	EFF-P
INLET	INLET	INLET	INLET	LBM/SEC			RTGR	RTGR
1	1	1	1	1	1	1	1	1
1.4176	2.9531	87.73	89.44	41.15	1.1883	1.7064	87.01	87.94

STATOR 2

SL	CP1-1	CP1-2	V-1	V-2	VM-1	VM-2	VO-1	VO-2	B-1	B-2	M-1	M-2	RUN NO	2, SPEED CODE 10,	POINT NO 4	U-1	U-2	M'-1	M'-2	V'-1	V'-2
DEGREE	DEGREE	FT/SEC	FT/SEC	FT/SEC	FT/SEC	FT/SEC	FT/SEC	DEGREE	DEGREE				FT/SEC	FT/SEC					FT/SEC	FT/SEC	
1	0.865	1097.6	719.7	772.2	719.7	780.0	-1.4	49.6	-0.1	0.8791	0.5528	3.6176	1.4464	1.7061	1.2004	1.2004					
2	0.811	1004.9	735.2	755.8	735.2	778.3	0.5	46.1	0.0	0.8690	0.5666	3.6551	1.4404	1.7205	1.2047	1.2047					
3	0.616	1073.3	760.6	740.0	760.6	777.4	1.0	46.6	0.1	0.6617	0.5893	3.6448	1.4329	1.7380	1.1993	1.1993					
4	0.139	992.1	734.8	741.4	734.8	659.2	-5.4	41.7	-0.4	0.7941	0.5722	3.6877	1.4312	1.7048	1.2055	1.2055					
5	0.118	860.9	627.3	629.9	628.7	586.8	-26.2	43.0	-2.4	0.6800	0.4656	2.6119	1.4052	1.6601	1.1802	1.1802					
6	0.710	793.1	549.4	579.1	549.3	546.9	-34.1	43.1	-3.0	0.6230	0.4432	2.6021	1.4045	1.6614	1.1813	1.1813					
7	0.675	784.5	545.6	579.3	549.7	529.0	-31.6	42.4	-3.3	0.6167	0.4408	2.6977	1.3999	1.6738	1.1823	1.1823					
8	0.554	754.2	565.6	585.1	565.1	540.0	-23.8	42.7	-2.4	0.6027	0.4370	2.8231	1.3987	1.6657	1.1869	1.1869					
9	0.042	619.7	628.3	610.2	628.3	547.4	1.9	41.9	0.2	0.6421	0.4443	2.8982	1.4069	1.6654	1.1866	1.1866					
10	0.205	824.9	637.0	636.6	636.9	524.5	5.4	39.5	0.5	0.6426	0.4484	2.9003	1.4335	1.6421	1.1917	1.1917					
11	0.209	608.6	602.9	619.6	602.8	495.1	10.2	37.8	1.0	0.6262	0.4589	2.8411	1.4464	1.6172	1.1974	1.1974					

SL	INCL	INCM	DEV	TURN	RHCVM-1	RHCVM-2	D-FAC	OMEGA-B	LOSS-P	PQ2/	EFF-P	EFF-A	B'-1	B'-2	VO'-1	VO'-2	PQ/PO
DEGREE	DEGREE	DEGREE	DEGREE					TOTAL	TOTAL	PQ1	STATC-ST	TOT-INLET	TOT-INLET	TOT-INLET	TCT-STG	TCT-STG	INLET
1	-1.433	11.71	45.67	50.50	98.99	0.5049	0.1238	0.0280	0.9510	82.87	82.73	85.16	79.30	60.79			
2	-1.26	11.29	46.02	50.27	102.02	0.4870	0.1104	0.0254	0.9570	83.90	84.67	81.32	82.08				
3	-1.05	10.52	46.32	50.20	106.90	0.4618	0.0866	0.0203	0.9666	86.35	86.61	89.91	85.28	86.39			
4	-0.82	9.49	42.13	53.95	104.76	0.4400	0.0657	0.0163	0.9775	88.30	91.00	89.81	88.14	88.99			
5	-0.70	7.51	45.34	80.81	88.49	0.4692	0.0571	0.0153	0.9445	89.67	87.78	89.45	86.04	87.00			
6	-0.58	6.45	46.61	74.21	76.61	0.4513	0.0537	0.0146	0.9876	90.79	84.30	87.69	86.55	87.35			
7	-0.47	6.45	45.68	74.65	76.31	0.4505	0.0480	0.0134	0.9892	91.59	85.13	87.09	86.89	87.61			
8	-0.37	6.85	45.68	74.65	79.41	0.4884	0.0524	0.0149	0.9879	90.43	86.45	85.03	86.06				
9	-0.28	7.31	45.05	75.65	87.63	0.4292	0.0356	0.0125	0.9514	92.18	84.67	86.93	81.82				
10	-0.21	8.12	39.06	81.61	87.71	0.4151	0.0430	0.0127	0.9856	90.42	81.07	86.16	78.85	80.26			
11	-0.14	12.90	36.87	81.01	81.67	0.4342	0.0798	0.0226	0.9824	84.73	77.52	80.52	74.13	75.60			

WCORR	WCORR	TO/TO	PQ/PC	EFF-AD	EFF-P	TO2/TO1	PC2/PO1	EFF-AD	EFF-P
INLET	INLET	INLET	INLET	INLET	INLET			STAGE	STAGE
1	1	1	1	1	1	1	1	1	1
1.0700	1.84.80	1.4176	2.9365	85.96	87.89	1.1883	0.9811	83.66	

TABLE XXI (Cont'd) – OVERALL PERFORMANCE AND BLADE-ELEMENT DATA  
(Uniform Inlet Flow)

U. S. CUSTOMARY UNITS

ROTOR 1

SL	EPSI-1	EPSI-2	V-1	V-2	VM-1	VM-2	V0-1	V0-2	B-1	B-2	M-1	M-2	3, SPEED CODE	10, POINT NO 5	V*-1	V*-2		
DEGREE	DEGREE	FT/SEC	FT/SEC	FT/SEC	FT/SEC	FT/SEC	FT/SEC	FT/SEC	DEGREE	DEGREE			U-1	U-2	FT/SEC	FT/SEC		
1	16.789	18.297	623.8	1056.9	623.8	612.5	0.0	861.3	0.0	34.6	0.5768	0.9363	630.7	730.2	0.8203	0.5549	887.1	626.4
2	14.411	15.912	637.0	1013.7	637.0	614.4	0.0	806.3	0.0	52.7	0.5899	0.8934	680.1	785.5	0.8629	0.5427	931.9	615.8
3	12.183	13.701	650.0	989.9	650.0	627.2	0.0	765.9	0.0	50.7	0.6028	0.8658	728.6	800.8	0.9054	0.5519	976.4	628.1
4	8.367	1.867	880.3	909.7	880.3	607.9	0.0	676.7	0.0	48.1	0.6331	0.7900	867.4	906.9	1.0259	0.5645	1102.3	650.0
5	0.647	1.444	659.0	814.8	659.0	559.1	0.0	592.4	0.0	46.7	0.6520	0.6981	1040.6	1048.1	1.1693	0.6182	1253.6	721.3
6	-0.676	-1.315	702.4	750.0	702.4	498.9	0.0	560.0	0.0	48.3	0.6554	0.6375	1124.0	1118.0	1.2367	0.6367	1325.4	749.1
7	-1.021	-2.580	703.6	755.5	703.6	532.4	0.0	536.0	0.0	45.2	0.6566	0.6433	1165.1	1154.1	1.2703	0.6496	1361.1	815.7
8	-2.816	-3.800	704.1	762.5	704.1	563.3	0.0	514.5	0.0	42.4	0.6571	0.6508	1206.3	1189.4	1.3035	0.7499	1396.7	879.1
9	-7.304	-7.491	695.0	773.1	695.0	591.9	0.0	497.2	0.0	40.0	0.6479	0.6571	1329.0	1295.4	1.3982	0.8446	1499.8	993.7
10	-8.968	-8.796	687.7	782.5	687.7	592.8	0.0	510.7	0.0	40.7	0.6406	0.6624	1370.0	1330.8	1.4278	0.8566	1532.9	1011.9
11	-10.651	-10.171	678.3	783.2	678.3	594.1	0.0	510.5	0.0	40.6	0.6311	0.6615	1410.8	1366.1	1.4565	0.8797	1565.4	1041.6

SL	INCS	INCM	DEV	TURN	RHOVM-1	RHOVM-2	D-FAC	OMEGA-8	LOSS-P	P02/	EFF-P	EFF-A	B*-1	B*-2	V0*-1	V0*-2	PC/PC
DEGREE	DEGREE	DEGREE	DEGREE	DEGREE				TOT #1	TOTAL	P01	TOT	TOT	DEGREE	DEGREE	FT/SEC	FT/SEC	INLET
1	-1.27	3.33	15.86	57.21	40.61	49.10	0.5236	0.0269	0.0058	1.8865	98.60	98.48	45.11	-12.10	-630.7	131.1	1.8865
2	-1.15	3.15	15.81	50.47	41.17	50.44	0.5506	0.0301	0.0069	1.8623	98.27	98.12	46.87	-3.80	-680.1	40.8	1.8623
3	-0.95	3.18	14.71	44.90	41.71	52.63	0.5540	0.0110	0.0026	1.8680	99.31	99.26	48.08	3.18	-728.6	-34.9	1.8680
4	0.29	3.76	11.05	31.08	42.90	53.09	0.5787	0.0475	0.0118	1.8342	96.36	96.05	51.79	20.73	-867.4	-230.2	1.8342
5	1.54	4.27	8.91	16.92	43.59	50.27	0.5675	0.1026	0.0239	1.7791	90.54	85.76	56.10	35.18	-1040.6	-455.7	1.7791
6	2.00	4.34	10.90	9.75	43.71	45.15	0.5667	0.1486	0.0313	1.7282	85.27	84.12	58.00	48.24	-1124.0	-558.8	1.7282
7	2.27	4.38	8.95	9.60	43.76	48.87	0.5260	0.1106	0.0234	1.7557	88.76	87.86	58.86	49.26	-1165.1	-618.1	1.7557
8	2.40	4.44	7.29	9.55	43.77	52.43	0.4898	0.0741	0.0158	1.7846	92.24	51.60	59.70	50.15	-1206.3	-674.9	1.7846
9	3.24	4.72	6.59	8.95	43.45	56.07	0.4519	0.0679	0.0144	1.8385	92.55	51.90	62.34	53.39	-1329.0	-798.2	1.8385
10	3.61	4.90	7.06	9.23	43.18	56.04	0.4576	0.0949	0.0202	1.8579	89.67	88.75	63.29	54.06	-1370.0	-820.0	1.8579
11	3.93	5.09	8.78	9.15	42.83	56.16	0.4523	0.1075	0.0227	1.8656	88.18	87.12	64.27	55.12	-1410.8	-855.6	1.8656

TO/TO	PC/PO	EFF-AD	EFF-P	WCI/AI	T02/T01	PC2/PC1	EFF-AD	EFF-P
INLET	INLET	INLET	INLET	LBM/SEC			ROTOR	ROTOR
		%	%	% SQFT			%	%
1.2029	1.8206	91.92	92.56	41.54	1.2029	1.8206	91.92	92.56

STATOR 1

SL	EPSI-1	EPSI-2	V-1	V-2	VM-1	VM-2	V0-1	V0-2	B-1	B-2	M-1	M-2	3, SPEED CODE	10, POINT NO 5	V0*	V0*
DEGREE	DEGREE	FT/SEC	FT/SEC	FT/SEC	FT/SEC	FT/SEC	FT/SEC	FT/SEC	DEGREE	DEGREE			INLET	INLET	STAGE	T01
1	18.100	14.749	1061.0	642.3	644.0	637.6	643.1	-77.8	52.8	-6.9	0.9405	0.5401	1.7857	1.2017	1.7857	1.2017
2	15.734	12.857	1022.1	641.1	646.2	638.2	792.0	-60.9	50.9	-5.4	0.9020	0.5399	1.7914	1.1979	1.7914	1.1979
3	13.604	11.003	1001.5	647.5	658.5	646.7	754.5	-31.0	48.9	-2.7	0.8814	0.5458	1.8028	1.1968	1.8028	1.1968
4	8.040	6.248	926.9	657.9	639.3	657.6	671.2	-18.6	46.4	-1.6	0.8069	0.5551	1.8159	1.1969	1.8159	1.1969
5	1.599	0.446	834.5	625.4	588.7	624.5	591.4	-34.2	45.1	-3.1	0.7108	0.5256	1.7638	1.1954	1.7638	1.1954
6	-1.743	-2.364	771.3	572.0	529.8	571.0	560.6	-34.3	46.6	-3.4	0.6572	0.4783	1.7009	1.2007	1.7009	1.2007
7	-2.882	-3.621	777.5	584.5	562.4	583.2	536.9	-39.1	43.7	-3.8	0.6637	0.4699	1.7114	1.1977	1.7114	1.1977
8	-3.934	-4.621	784.8	616.5	591.3	615.0	516.0	-42.8	41.2	-4.0	0.6711	0.5185	1.7435	1.1960	1.7435	1.1960
9	-4.582	-7.228	797.1	663.2	620.5	663.2	500.4	-11.1	39.0	-1.0	0.6794	0.5574	1.7930	1.2071	1.7930	1.2071
10	-7.424	-7.946	807.7	673.9	622.7	673.9	514.4	-2.4	39.7	-0.2	0.6857	0.5640	1.8023	1.2188	1.8023	1.2188
11	-8.299	-8.595	809.9	674.5	625.6	674.5	514.5	-1.6	39.4	-0.1	0.6861	0.5633	1.8020	1.2238	1.8020	1.2238

SL	INCS	INCM	DEV	TURN	RHOVM-1	RHOVM-2	D-FAC	OMEGA-8	LOSS-P	P02/	EFF-P	EFF-A	B*-1	B*-2	V0*-1	V0*-2	PC/PC
DEGREE	DEGREE	DEGREE	DEGREE	DEGREE				TOTAL	TOTAL	P01	STAG-ST	TOT-INLET	TOT-INLET	TOT-INLET	TOT-STG	TOT-STG	INLET
1	0.25	2.36	5.45	59.69	51.45	62.88	0.5654	0.1225	0.0249	0.9468	89.23	89.28	56.10	89.28	89.28	90.10	
2	0.05	2.45	5.83	56.30	52.69	63.34	0.9639	0.0934	0.0197	0.9618	88.07	91.49	92.15	91.49	92.15	93.66	
3	-0.58	2.20	7.67	51.67	54.78	64.47	0.5208	0.0875	0.0193	0.9653	88.24	93.13	93.66	93.13	93.66	94.31	
4	0.63	3.09	7.66	47.99	55.16	65.70	0.4674	0.0263	0.0064	0.9908	95.66	94.31	94.75	94.31	94.75	95.09	
5	-0.40	4.65	6.18	48.24	52.29	61.38	0.4503	0.0198	0.0054	0.9945	95.98	88.21	89.05	88.21	89.05	89.09	
6	1.60	7.22	5.92	50.07	47.37	55.31	0.4769	0.0648	0.0185	0.9837	87.35	81.60	82.90	81.60	82.90	83.87	
7	-1.04	4.78	5.54	47.55	51.03	56.68	0.4657	0.1163	0.0339	0.9701	77.10	83.87	85.02	83.87	85.02	86.68	
8	-3.44	2.71	5.44	45.16	54.39	60.15	0.4268	0.0991	0.0293	0.9741	77.91	87.78	88.68	87.78	88.68	89.54	
9	-5.64	1.24	9.59	39.94	57.99	64.79	0.3705	0.0965	0.0301	0.9743	73.36	87.54	88.54	87.54	88.54	89.54	
10	-5.26	1.79	11.57	35.88	58.02	65.32	0.3712	0.1132	0.0359	0.9694	68.41	83.71	84.98	83.71	84.98	86.48	
11	-6.06	1.09	13.18	35.70	58.25	65.12	0.3736	0.1268	0.0406	0.9658	64.74	81.78	83.20	81.78	83.20	84.20	

NCORR	MCCR	T0/T0	PC/PO	EFF-AD	EFF-P	T02/T01	P02/P01	EFF-AD
INLET	INLET	INLET	INLET	INLET	INLET			STAG
APM	LBM/SEC			%	%			%
10731.0	182.90	1.2029	1.7789	88.07	88.98	1.2029	0.4771	88.07



TABLE XXI (Cont'd) — OVERALL PERFORMANCE AND BLADE-ELEMENT DATA  
(Uniform Inlet Flow)

U. S. CUSTOMARY UNITS

ROTOR 1

SL	EPI-2		V-1		VM-1		VM-2		V0-1		V0-2		B-1		B-2		M-1		M-2		RUN NO	S, SPEED CODE 10,		POINT NO 6														
	DEGREE	DEGREE	FT/SEC	FT/SEC	FT/SEC	FT/SEC	FT/SEC	FT/SEC	FT/SEC	FT/SEC	FT/SEC	FT/SEC	DEGREE	DEGREE	DEGREE	DEGREE	DEGREE	DEGREE	DEGREE	DEGREE		DEGREE	DEGREE	FT/SEC	FT/SEC	M-1	M-2	V-1	V-2									
1	100.78	100.78	603.5	1034.7	603.5	588.3	0.0	831.1	0.0	53.4	0.5568	0.9145	629.7	72.0	0.8068	0.5311	872.2	600.3																				
2	140.40	140.40	617.1	592.4	617.1	589.3	0.0	798.5	0.0	51.6	0.5702	0.8727	679.0	76.3	0.8478	0.5191	927.5	590.3																				
3	222.1	222.1	630.5	960.0	630.5	597.4	0.0	761.7	0.0	50.9	0.5834	0.8483	727.4	79.5	0.8908	0.5246	902.6	598.6																				
4	305.0	305.0	603.3	843.2	603.3	586.7	0.0	673.5	0.0	49.0	0.6166	0.7744	866.0	90.5	1.0131	0.5469	1090.8	630.6																				
5	37.0	37.0	606.5	809.9	606.5	590.7	0.0	603.0	0.0	46.1	0.6394	0.6927	1039.0	104.4	1.0598	0.5900	1252.3	699.2																				
6	92.0	92.0	652.0	759.9	652.0	606.5	0.0	577.1	0.0	49.7	0.6049	0.6403	1222.2	117.0	1.0286	0.6385	1318.4	726.8																				
7	170.0	170.0	654.2	759.1	654.2	582.2	0.0	556.7	0.0	46.9	0.6070	0.6447	1183.3	115.2	1.0267	0.6716	1390.9	790.9																				
8	277.0	277.0	695.3	772.2	695.3	547.1	0.0	535.1	0.0	44.3	0.6485	0.6507	1204.3	118.7	1.0195	0.7400	1340.6	851.4																				
9	330.0	330.0	680.7	772.9	680.7	575.8	0.0	515.6	0.0	41.0	0.6416	0.6548	1320.5	129.3	1.0392	0.8199	1495.0	967.7																				
10	400.0	400.0	682.3	783.6	682.3	578.5	0.0	528.6	0.0	42.3	0.6351	0.6664	1307.7	132.6	1.0428	0.8332	1526.5	987.2																				
11	460.0	460.0	673.6	785.7	673.6	582.6	0.0	527.1	0.0	42.0	0.6263	0.6617	1408.5	136.9	1.04518	0.8587	1561.3	1059.6																				

SL	INC		DEV	TURN	RHOVM-1		RHOVM-2		U-FAC	OMEGA-B		LCSS-P	PO2/		EFF-P		EFF-A	B-1		B-2		V0-1	V0-2		PO/PU
	DEGREE	DEGREE			DEGREE	DEGREE	TOTAL	TOTAL		PO1	TOT		DEGREE	DEGREE	FT/SEC	FT/SEC		INLET	STAGE	INLET	TOT		INLET	STAGE	
1	10.37	10.37	46.20	57.76	57.76	35.70	48.05	0.5419	0.0067	0.0024	1.0885	99.06	99.06	90.01	-11.75	-629.7	122.0	1.0885	99.06	99.06	90.01	34.3	1.8635	1.8635	1.8635
2	30.49	30.49	16.27	50.86	40.31	49.27	0.3691	0.0109	0.0025	1.0865	99.39	99.39	47.33	-3.33	-679.0	122.0	1.0865	99.39	99.39	47.33	34.3	1.8635	1.8635	1.8635	
3	40.00	40.00	15.16	45.28	40.00	51.03	0.3767	0.0004	-0.0030	1.0887	100.02	100.04	48.90	3.65	-727.4	122.0	1.0887	100.02	100.04	48.90	34.3	1.8635	1.8635	1.8635	
4	40.00	40.00	11.90	30.86	40.00	52.30	0.5906	0.0227	0.0056	1.0850	98.30	98.16	50.66	21.56	-860.0	-231.9	1.0850	98.30	98.16	50.66	34.3	1.8635	1.8635	1.8635	
5	20.32	20.32	9.09	17.17	43.14	49.62	0.5040	0.0865	0.0201	1.0816	92.27	91.66	56.53	35.38	-1039.0	-443.4	1.0816	92.27	91.66	56.53	34.3	1.8635	1.8635	1.8635	
6	20.32	20.32	10.83	16.36	40.34	44.96	0.5834	0.1339	0.0604	1.0779	87.24	86.19	58.34	47.57	-1222.2	-539.9	1.0779	87.24	86.19	58.34	34.3	1.8635	1.8635	1.8635	
7	20.32	20.32	8.75	10.10	41.42	48.53	0.5466	0.1006	0.0214	1.0823	90.17	89.34	59.16	45.06	-1163.3	-597.5	1.0823	90.17	89.34	59.16	34.3	1.8635	1.8635	1.8635	
8	20.32	20.32	7.85	5.97	43.40	51.09	0.5125	0.0697	0.0149	1.0830	92.59	92.39	59.97	30.01	-1204.3	-652.5	1.0830	92.59	92.39	59.97	34.3	1.8635	1.8635	1.8635	
9	30.47	30.47	6.62	5.10	43.22	55.63	0.4719	0.0636	0.0134	1.0838	93.27	92.05	62.52	52.42	-1326.9	-777.7	1.0838	93.27	92.05	62.52	34.3	1.8635	1.8635	1.8635	
10	30.70	30.70	7.06	9.39	42.98	55.63	0.4763	0.0685	0.0158	1.0907	90.71	89.44	63.44	54.04	-1367.7	-800.0	1.0907	90.71	89.44	63.44	34.3	1.8635	1.8635	1.8635	
11	40.00	40.00	8.70	9.35	42.05	56.31	0.4689	0.0777	0.0207	1.0916	89.62	88.64	64.39	55.04	-1408.5	-836.7	1.0916	89.62	88.64	64.39	34.3	1.8635	1.8635	1.8635	

TC/TO	PC/PO	EFF-AD	EFF-P	WCL/AL	TO2/TOT	PC2/PO1	EFF-AD	EFF-P
INLET	INLET	%	INLET	INLET	%	INLET	INLET	%
1.2067	1.8538	93.23	93.78	41.11	1.2067	1.8538	93.23	93.78

STATOR 1

SL	EPI-1		EPI-2		V-1		V-2		VM-1		VM-2		V0-1		V0-2		B-1		B-2		M-1		M-2		RUN NO	S, SPEED CODE 10,		POINT NO 6									
	DEGREE	DEGREE	FT/SEC	FT/SEC	FT/SEC	FT/SEC	FT/SEC	FT/SEC	FT/SEC	FT/SEC	FT/SEC	FT/SEC	FT/SEC	FT/SEC	FT/SEC	FT/SEC	DEGREE	DEGREE	DEGREE	DEGREE	DEGREE	DEGREE	DEGREE	DEGREE		DEGREE	DEGREE	FT/SEC	FT/SEC	M-1	M-2	V-1	V-2				
1	100.212	100.212	14.926	1030.4	613.0	618.3	611.3	833.2	-45.2	53.7	-4.2	0.9163	0.5147	1.7912	1.1990	1.7912	1.1990	1.7912	1.1990	1.7912	1.1990	1.7912	1.1990	1.7912	1.1990	1.7912	1.1990	1.7912	1.1990	1.7912	1.1990	1.7912	1.1990	1.7912	1.1990	1.7912	1.1990
2	130.90	130.90	13.182	598.4	609.4	617.6	608.2	784.4	-37.4	51.9	-3.5	0.8787	0.5122	1.7948	1.1956	1.7948	1.1956	1.7948	1.1956	1.7948	1.1956	1.7948	1.1956	1.7948	1.1956	1.7948	1.1956	1.7948	1.1956	1.7948	1.1956	1.7948	1.1956	1.7948	1.1956	1.7948	1.1956
3	130.90	130.90	11.511	577.2	612.3	626.0	610.4	750.3	-47.7	50.2	-4.4	0.8575	0.5149	1.8030	1.1954	1.8030	1.1954	1.8030	1.1954	1.8030	1.1954	1.8030	1.1954	1.8030	1.1954	1.8030	1.1954	1.8030	1.1954	1.8030	1.1954	1.8030	1.1954	1.8030	1.1954	1.8030	1.1954
4	40.07	40.07	8.888	908.5	626.0	615.7	625.2	668.0	-32.0	47.3	-2.9	0.7893	0.5269	1.8239	1.1957	1.8239	1.1957	1.8239	1.1957	1.8239	1.1957	1.8239	1.1957	1.8239	1.1957	1.8239	1.1957	1.8239	1.1957	1.8239	1.1957	1.8239	1.1957	1.8239	1.1957	1.8239	1.1957
5	20.175	20.175	1.315	828.5	604.2	569.9	602.7	602.0	-42.6	46.6	-4.0	0.7105	0.5061	1.7924	1.2026	1.7924	1.2026	1.7924	1.2026	1.7924	1.2026	1.7924	1.2026	1.7924	1.2026	1.7924	1.2026	1.7924	1.2026	1.7924	1.2026	1.7924	1.2026	1.7924	1.2026	1.7924	1.2026
6	30.901	30.901	1.451	775.8	580.4	517.9	555.2	577.6	-76.1	48.1	-7.8	0.6596	0.4669	1.7440	1.2070	1.7440	1.2070	1.7440	1.2070	1.7440	1.2070	1.7440	1.2070	1.7440	1.2070	1.7440	1.2070	1.7440	1.2070	1.7440	1.2070	1.7440	1.2070	1.7440	1.2070	1.7440	1.2070
7	20.287	20.287	2.670	780.3	575.7	547.7	573.5	555.8	-50.6	45.4	-5.0	0.6649	0.4807	1.7584	1.2046	1.7584	1.2046	1.7584	1.2046	1.7584	1.2046	1.7584	1.2046	1.7584	1.2046	1.7584	1.2046	1.7584	1.2046	1.7584	1.2046	1.7584	1.2046	1.7584	1.2046	1.7584	1.2046
8	30.955	30.955	3.680	786.7	600.0	575.2	599.8	536.7	-14.1	43.1	-1.3	0.6705	0.5022	1.7832	1.2037	1.7832	1.2037	1.7832	1.2037	1.7832	1.2037	1.7832	1.2037	1.7832	1.2037	1.7832	1.2037	1.7832	1.2037	1.7832	1.2037	1.7832	1.2037	1.7832	1.2037	1.7832	1.2037
9	40.412	40.412	6.512	797.4	650.5	605.7	650.1	518.7	-24.1	40.7	-2.1	0.6775	0.5444	1.8416	1.2142	1.8416	1.2142	1.8416	1.2142	1.8																	

TABLE XXI (Cont'd) – OVERALL PERFORMANCE AND BLADE-ELEMENT DATA  
(Uniform Inlet Flow)

U. S. CUSTOMARY UNITS

ROTOR 2

SL	EPSI-1		EPSI-2		V-1		V-2		VM-1		VM-2		VO-1		VO-2		B-1		B-2		M-1		M-2		RUN NO	3% SPEED	CODE	10% POINT NO	6	V1-1	V1-2					
	DEGREE	DEGREE	FT/SEC	FT/SEC	FT/SEC	FT/SEC	FT/SEC	FT/SEC	FT/SEC	FT/SEC	FT/SEC	FT/SEC	FT/SEC	FT/SEC	FT/SEC	FT/SEC	DEGREE	DEGREE	DEGREE	DEGREE	DEGREE	DEGREE	DEGREE	DEGREE								FT/SEC	FT/SEC	FT/SEC	FT/SEC	FT/SEC
1	11.003	11.103	664.8	1048.9	663.3	600.3	-44.0	660.1	-3.8	55.0	0.5607	0.0328	835.4	876.6	0.9291	0.4768	110.0	600.0																		
2	10.725	9.866	668.9	1038.3	677.9	610.0	-38.4	640.3	-3.1	53.9	0.5052	0.8251	859.0	894.6	0.9440	0.4860	117.0	612.4																		
3	9.950	8.666	679.3	1027.2	677.9	659.5	-40.5	767.5	-3.9	53.9	0.5749	0.8177	883.4	913.0	0.9737	0.5340	120.0	612.0																		
4	6.200	5.174	708.1	947.4	707.4	637.4	-31.6	700.9	-2.6	47.7	0.6007	0.7510	959.0	974.4	1.0327	0.5496	124.0	612.0																		
5	1.414	1.288	692.0	854.7	690.7	567.3	-42.3	612.3	-3.5	43.2	0.5843	0.6537	1063.2	1062.5	1.1008	0.5009	130.0	612.0																		
6	-0.865	653.4	781.6	648.9	648.9	564.9	-70.2	540.1	-6.7	43.7	0.5486	0.6004	1146.3	1109.4	1.1399	0.6243	135.0	612.0																		
7	-2.810	-2.062	664.9	776.7	663.0	547.7	-50.5	550.0	-4.3	43.1	0.5593	0.6048	1143.1	1100.3	1.1483	0.6227	136.0	612.0																		
8	-3.962	-3.096	664.9	776.7	664.5	530.3	-43.7	576.6	-1.4	47.3	0.5774	0.6104	1170.0	1100.3	1.1532	0.6133	136.0	612.0																		
9	-6.759	-6.136	730.3	802.7	729.9	575.3	-24.3	559.8	-1.9	44.1	0.6158	0.6210	1232.0	1235.0	1.2359	0.6809	140.0	612.0																		
10	-7.663	-7.243	739.4	806.3	738.9	592.2	-28.1	547.2	-2.2	42.6	0.6209	0.6218	1274.0	1261.2	1.2613	0.7153	150.0	612.0																		
11	-8.573	-8.495	739.6	789.4	737.2	585.7	-59.2	529.2	-4.6	42.0	0.6198	0.6043	1307.2	1288.0	1.3014	0.7330	155.0	612.0																		

SL	INCS	INCM	DEV	TLRN	RHCVM-1	RHCVM-2	C-FAC	OMEGA-8	LGSS-P	PO2/PO1	%EFF-P	%EFF-A	B1-1	B1-2	V1-1	V1-2	PC/PG
DEGREE	DEGREE	DEGREE	DEGREE					TOTAL	TOTAL	PO1	TGT	TGT	DEGREE	DEGREE	FT/SEC	FT/SEC	INLET
1	3.43	7.75	21.93	51.38	65.06	72.91	0.6456	0.2208	0.0503	1.7809	85.77	84.57	52.41	1.53	-879.4	-16.1	3.1897
2	3.32	7.77	12.89	48.21	65.06	75.47	0.6370	0.1904	0.0443	1.7942	87.45	86.38	53.28	5.07	-895.4	-54.3	3.2190
3	3.59	8.16	18.33	43.14	66.63	83.29	0.5906	0.1328	0.0315	1.8037	90.73	89.93	53.94	10.80	-929.5	-120.1	3.2500
4	2.70	7.56	13.66	31.25	69.33	83.29	0.5858	0.1105	0.0280	1.7419	90.37	89.39	54.51	23.22	-990.0	-273.5	3.2775
5	4.34	5.11	10.22	19.57	66.74	75.17	0.5855	0.1320	0.0293	1.8088	87.63	86.91	58.01	38.44	-1103.4	-50.1	3.3022
6	7.05	11.39	8.98	16.24	61.95	74.97	0.5427	0.1017	0.0213	1.8039	90.07	89.31	61.42	45.19	-1192.4	-50.2	2.9507
7	6.05	10.13	7.67	14.19	63.55	73.10	0.5482	0.1105	0.0231	1.8085	89.04	86.11	60.92	46.73	-1193.5	-50.2	2.9629
8	4.34	8.35	5.25	12.35	66.00	71.23	0.5394	0.1212	0.0256	1.8078	87.91	87.00	59.92	47.57	-1183.7	-561.0	2.9906
9	3.32	6.03	2.34	10.72	70.51	77.37	0.5340	0.1611	0.0366	1.8624	82.55	81.05	60.16	49.44	-1276.4	-675.2	3.0594
10	3.64	5.42	3.52	10.25	70.90	79.32	0.5197	0.1563	0.0303	1.8599	83.06	81.82	60.44	50.19	-1307.6	-714.0	3.0702
11	4.04	5.74	6.56	9.34	70.62	77.63	0.5219	0.1970	0.0456	1.8404	78.35	76.60	61.55	52.22	-1366.4	-758.6	3.0431

TC/TO	PC/PG	EFF-AD	EFF-P	W1/W1	TO2/TO1	PC2/PO1	EFF-AD	EFF-P
INLET	INLET	INLET	INLET	LB/SEC			ROTOR	ROTOR
%	%	%	%	%	%	%	%	%
1.4357	3.0801	86.61	88.52	35.31	1.1898	1.7067	85.85	86.87

STATOR 2

SL	EPSI-1		EPSI-2		V-1		V-2		VM-1		VM-2		VO-1		VO-2		B-1		B-2		M-1		M-2		RUN NO	3% SPEED	CODE	10% POINT NO	6	V1-1	V1-2				
	DEGREE	DEGREE	FT/SEC	FT/SEC	FT/SEC	FT/SEC	FT/SEC	FT/SEC	FT/SEC	FT/SEC	FT/SEC	FT/SEC	FT/SEC	FT/SEC	FT/SEC	FT/SEC	DEGREE	DEGREE	DEGREE	DEGREE	DEGREE	DEGREE	DEGREE	DEGREE								FT/SEC	FT/SEC	FT/SEC	FT/SEC
1	11.003	11.103	664.8	1048.9	663.3	600.3	-44.0	660.1	-3.8	55.0	0.5607	0.0328	835.4	876.6	0.9291	0.4768	110.0	600.0																	
2	10.725	9.866	668.9	1038.3	677.9	610.0	-38.4	640.3	-3.1	53.9	0.5052	0.8251	859.0	894.6	0.9440	0.4860	117.0	612.4																	
3	9.950	8.666	679.3	1027.2	677.9	659.5	-40.5	767.5	-3.9	53.9	0.5749	0.8177	883.4	913.0	0.9737	0.5340	120.0	612.0																	
4	6.200	5.174	708.1	947.4	707.4	637.4	-31.6	700.9	-2.6	47.7	0.6007	0.7510	959.0	974.4	1.0327	0.5496	124.0	612.0																	
5	1.414	1.288	692.0	854.7	690.7	567.3	-42.3	612.3	-3.5	43.2	0.5843	0.6537	1063.2	1062.5	1.1008	0.5009	130.0	612.0																	
6	-0.865	653.4	781.6	648.9	648.9	564.9	-70.2	540.1	-6.7	43.7	0.5486	0.6004	1146.3	1109.4	1.1399	0.6243	135.0	612.0																	
7	-2.810	-2.062	664.9	776.7	663.0	547.7	-50.5	550.0	-4.3	43.1	0.5593	0.6048	1143.1	1100.3	1.1483	0.6227	136.0	612.0																	
8	-3.962	-3.096	664.9	776.7	664.5	530.3	-43.7	576.6	-1.4	47.3	0.5774	0.6104	1170.0	1100.3	1.1532	0.6133	136.0	612.0																	
9	-6.759	-6.136	730.3	802.7	729.9	575.3	-24.3	559.8	-1.9	44.1	0.6158	0.6210	1232.0	1235.0	1.2359	0.6809	140.0	612.0																	
10	-7.663	-7.243	739.4	806.3	738.9	592.2	-28.1	547.2	-2.2	42.6	0.6209	0.6218	1274.0	1261.2	1.2613	0.7153	150.0	612.0																	
11	-8.573	-8.495	739.6	789.4	737.2	585.7	-59.2	529.2	-4.6	42.0	0.6198	0.6043	1307.2	1288.0	1.3014	0.7330	155.0	612.0																	

SL	INCS	INCM	DEV	TLRN	RHCVM-1	RHCVM-2	C-FAC	OMEGA-8	LGSS-P	PO2/PO1	%EFF-P	%EFF-A	B1-1	B1-2	V1-1	V1-2	PC/PG
DEGREE	DEGREE	DEGREE	DEGREE					TOTAL	TOTAL	PO1	STATC-ST	TGT-INLET	TGT-INLET	FT/SEC	FT/SEC	INLET	
1	4.04	8.07	13.77	51.00	77.62	89.86	0.5850	0.1348	0.0305	0.9490	83.34	82.10	64.62	76.32	77.99		
2	4.03	6.65	13.08	50.22	79.62	93.06	0.5589	0.1216	0.0240	0.9547	84.17	84.20	66.45	78.75	80.29		
3	1.77	4.28	12.63	46.63	86.87	99.45	0.5198	0.1001	0.0235	0.9332	86.03	87.29	69.13	83.00	84.44		
4	3.75	4.62	12.16	44.47	80.34	98.42	0.4866	0.0702	0.0174	0.9770	87.00	90.03	91.47	85.88	86.90		
5	4.01	6.32	10.26	45.76	78.22	85.25	0.5108	0.0625	0.0167	0.9635	89.80	86.39	86.21	86.29	86.29		
6	-2.04	3.70	9.67	42.86	77.95	78.53	0.5179	0.0557	0.0134	0.9868	90.88	84.43	86.35	86.35	87.49		
7	-0.80	5.40	9.66	44.13	76.29	77.61	0.										

TABLE XXI (Cont'd) — OVERALL PERFORMANCE AND BLADE-ELEMENT DATA  
(Uniform Inlet Flow)

U. S. CUSTOMARY UNITS

ROTOR 1

SL	LPSI-1	EP51-2	V-1	V-2	VM-1	VM-2	V0-1	V0-2	B-1	B-2	M-1	M-2	3, SPEED	CODE	15, POINT	NO. 31	V1-1	V1-2
	DEGREE	DEGREE	FT/SEC	FT/SEC	FT/SEC	FT/SEC	FT/SEC	FT/SEC	DEGREE	DEGREE							FT/SEC	FT/SEC
1	16.540	18.386	666.7	1154.5	666.7	732.8	0.0	892.2	0.0	50.6	0.6194	1.0317					660.9	765.1
2	13.275	16.033	683.1	1119.3	683.1	734.1	0.0	844.9	0.0	49.0	0.6359	0.9946					712.7	802.2
3	11.362	13.844	695.0	1093.6	695.0	740.0	0.0	805.3	0.0	47.4	0.6520	0.9678					763.5	839.2
4	4.619	8.029	735.7	966.3	735.7	702.0	0.0	692.9	0.0	44.6	0.6893	0.8604					908.9	950.3
5	-1.069	1.386	753.3	757.4	753.3	582.4	0.0	544.6	0.0	43.1	0.7075	0.6844					1098.3	1098.3
6	-2.451	-1.682	755.1	700.9	755.1	505.9	0.0	485.1	0.0	43.8	0.7094	0.5977					1177.8	1172.4
7	-2.755	-2.970	756.0	739.4	756.0	573.8	0.0	466.6	0.0	39.1	0.7103	0.6336					1221.0	1209.4
8	-3.054	-4.194	755.7	774.5	755.7	627.5	0.0	454.6	0.0	35.9	0.7100	0.6662					1264.0	1246.4
9	-6.569	-7.633	740.0	800.7	740.0	662.4	0.0	449.8	0.0	34.2	0.6937	0.6861					1392.7	1351.5
10	-10.291	-9.112	729.6	797.7	729.6	651.3	0.0	460.6	0.0	35.2	0.6831	0.6801					1435.6	1394.5
11	-11.604	-10.384	718.2	759.7	718.2	586.8	0.0	482.4	0.0	39.3	0.6715	0.6405					1478.4	1431.5

SL	INCS	INCM	DEV	TURN	RHCVM-1	RMCVM-2	D-FAC	CMEGA-B	LOSS-P	PO2/	%EFF-P	%EFF-A	B*-1	B*-2	VB*-1	VB*-2	PC/PC
	DEGREE	DEGREE	DEGREE	DEGREE				TOTAL	TOTAL	PO1	TOT	TOT	DEGREE	DEGREE	FT/SEC	FT/SEC	INLET
1	-1.68	2.73	18.10	54.36	42.38	56.89	0.4348	0.0054	-0.0012	2.0050	100.28	100.32	44.51	-9.85	-660.9	127.1	2.0050
2	-1.00	2.42	16.27	49.27	43.01	58.40	0.4678	0.0039	0.0009	1.9890	99.78	99.76	45.94	-3.33	-712.7	42.7	1.9890
3	-1.75	2.35	14.26	44.63	43.59	60.12	0.4848	0.0027	0.0006	1.9856	99.82	99.81	47.25	2.63	-763.5	-33.9	1.9856
4	-0.67	2.60	10.46	30.69	44.84	58.91	0.5276	0.0740	0.0185	1.8792	93.90	93.36	50.83	20.14	-908.9	-257.4	1.8792
5	0.85	3.53	13.28	11.81	45.39	49.49	0.5207	0.1635	0.0356	1.6602	82.27	81.01	55.36	43.55	-1090.5	-553.7	1.6602
6	1.42	3.70	16.31	3.70	45.44	43.15	0.5018	0.1951	0.0366	1.5681	76.83	75.14	57.35	53.65	-1177.8	-687.3	1.5681
7	1.91	3.86	8.76	5.91	45.47	49.82	0.4516	0.1366	0.0271	1.6265	83.47	82.33	56.24	52.32	-1221.0	-742.8	1.6265
8	2.99	4.41	7.05	7.91	45.46	55.31	0.4156	0.0888	0.0183	1.6849	89.18	88.37	59.12	51.61	-1264.0	-791.8	1.6849
9	3.41	4.71	8.06	8.19	44.97	58.82	0.3881	0.0940	0.0197	1.7388	88.29	87.36	62.04	53.85	-1392.7	-907.6	1.7388
10	3.77	4.93	11.84	8.04	44.64	57.34	0.3959	0.1303	0.0270	1.7326	83.83	82.58	63.10	55.06	-1435.6	-933.9	1.7326
11	3.77	4.93	11.84	5.92	44.26	50.57	0.4285	0.2133	0.0415	1.6764	73.70	71.76	64.11	58.19	-1478.4	-949.1	1.6764

TO/TO	PO/PO	EFF-AD	EFF-P	NC1/A1	TO2/TO1	PC2/PO1	EFF-AD	EFF-P
INLET	INLET	INLET	INLET	LBM/SEC			ROTOR	ROTOR
		%	%				%	%
1.2015	1.7667	87.55	88.49	43.22	1.2015	1.7667	87.55	88.49

STATOR 1

SL	EP51-1	EP51-2	V-1	V-2	VM-1	VM-2	V0-1	V0-2	B-1	B-2	M-1	M-2	3, SPEED	CODE	15, POINT	NO. 31	V1-1	V1-2
	DEGREE	DEGREE	FT/SEC	FT/SEC	FT/SEC	FT/SEC	FT/SEC	FT/SEC	DEGREE	DEGREE							FT/SEC	FT/SEC
1	18.226	14.923	1166.1	818.4	122.7	818.3	873.4	-6.9	48.7	-0.5	1.0442	0.6954					1.8814	1.2188
2	15.956	13.226	1135.4	817.5	174.8	817.5	829.9	8.9	47.1	0.6	1.0118	0.6951					1.8866	1.2172
3	13.478	11.667	1113.0	825.1	180.7	824.6	793.2	28.1	45.5	1.9	0.9682	0.7024					1.9000	1.2168
4	8.436	7.480	1011.3	793.5	741.7	793.5	687.5	4.5	42.8	0.3	0.8654	0.6750					1.8384	1.2102
5	1.764	1.834	824.3	656.5	619.5	654.8	543.8	-67.8	41.3	-5.7	0.7097	0.5557					1.6318	1.1898
6	-1.608	-1.370	729.5	598.2	545.0	595.3	485.4	-59.0	41.7	-5.7	0.6243	0.5034					1.5556	1.1818
7	-3.159	-2.814	766.7	622.3	607.6	620.3	467.5	-49.9	37.6	-4.6	0.6588	0.5270					1.5746	1.1813
8	-3.994	-3.932	800.6	670.6	658.0	669.5	454.2	-39.1	34.8	-3.3	0.6904	0.5701					1.6206	1.1828
9	-6.169	-6.608	828.4	741.2	663.9	740.4	452.6	-35.4	33.2	-2.7	0.7122	0.6307					1.6588	1.1965
10	-6.920	-7.412	827.1	737.0	685.0	736.0	463.6	-37.6	34.2	-2.9	0.7077	0.6240					1.6515	1.2066
11	-7.920	-8.267	761.9	695.5	625.1	694.2	486.2	-41.0	36.0	-3.4	0.6700	0.5825					1.6384	1.2215

SL	INCS	INCM	DEV	TURN	RHCVM-1	RMCVM-2	D-FAC	CMEGA-B	LOSS-P	PO2/	%EFF-P	%EFF-A	B*-1	B*-2	VB*-1	VB*-2	PC/PC
	DEGREE	DEGREE	DEGREE	DEGREE				TOTAL	TOTAL	PO1	STATC-ST	TOT	INLET	TOT	INLET	TOT	STG
1	-3.84	-1.73	11.85	49.18	59.35	76.69	0.4451	0.1227	0.0251	0.9389	82.72	90.34	51.25	90.34	91.15	91.15	
2	-3.74	-1.34	11.85	46.48	60.76	76.93	0.4263	0.1079	0.0229	0.9485	83.74	91.44	52.15	91.44	92.15	92.15	
3	-3.58	-1.19	12.34	43.40	62.38	77.83	0.4029	0.0913	0.0201	0.9577	85.16	92.74	93.36	92.74	93.36		
4	-4.10	-0.45	9.60	42.51	61.10	74.11	0.3682	0.0335	0.0082	0.9864	93.29	96.30	91.07	96.30	91.07		
5	-4.23	6.80	5.14	45.42	51.82	59.03	0.3798	0.0087	0.0024	0.9972	97.77	78.88	60.23	78.88	60.23		
6	-3.32	2.30	3.70	47.36	45.82	52.90	0.4047	0.0906	0.0258	0.9771	79.69	73.97	75.51	73.97	75.51		
7	-7.19	-1.31	4.78	42.22	52.01	55.21	0.3948	0.1701	0.0495	0.9560	59.12	76.34	77.77	76.34	77.77		
8	-9.82	-3.67	6.68	38.13	57.16	59.91	0.3491	0.1511	0.0448	0.9587	57.76	80.83	82.06	80.83	82.06		
9	-11.43	-4.55	7.80	35.94	60.59	66.38	0.2909	0.0800	0.0244	0.9770	66.74	83.14	84.33	83.14	84.33		
10	-10.77	-3.72	8.84	37.10	59.28	65.40	0.3019	0.0797	0.0252	0.9774	67.34	78.49	79.99	78.49	79.99		
11	-7.65	-6.50	9.92	41.37	52.92	60.43	0.3366	0.0865	0.0277	0.9775	67.76	68.34	70.42	68.34	70.42		

NCORR	TO/TO	PO/PO	EFF-AD	EFF-P	TO2/TO1	PO2/PO1	EFF-AD	EFF-P
INLET	INLET	INLET	INLET	INLET			STAGE	STAGE
			%	%			%	%
11245.0	190.30	1.2015	1.7210	83.21	84.42	1.2015	0.9742	83.21

TABLE XXI (Cont'd) - OVERALL PERFORMANCE AND BLADE-ELEMENT DATA  
(Uniform Inlet Flow)

U. S. CUSTOMARY UNITS

ROTOR 2

SL	EPSI-1	EPSI-2	V-1	V-2	VM-1	VM-2	V0-1	V0-2	B-1	B-2	M-1	M-2	3, SPEED CODE	15, POINT NO	31	U-1	U-2	M*-1	M*-2	V*-1	V*-2	
DEGREE	DEGREE	FT/SEC	FT/SEC	FT/SEC	FT/SEC	FT/SEC	FT/SEC	FT/SEC	DEGREE	DEGREE						FT/SEC	FT/SEC			FT/SEC	FT/SEC	
1	11.628	11.400	523.5	1257.3	523.5	532.2	-6.8	843.8	-0.4	42.1	0.7953	1.0223	876.9	919.7	1.1007	0.7604	1278.2	935.2				
2	10.937	10.421	927.5	1234.6	927.5	905.8	8.1	838.8	0.5	42.8	0.7998	1.0006	901.6	958.9	1.1105	0.7366	1287.9	911.3				
3	10.225	9.457	937.7	1196.3	937.3	871.0	27.1	823.0	1.7	43.4	0.8099	0.9681	927.2	958.9	1.1224	0.7122	1299.5	881.5				
4	7.795	6.457	921.5	1068.3	921.5	850.9	5.6	678.4	0.4	38.7	0.7965	0.8760	1006.5	1022.7	1.1759	0.7589	1360.5	918.0				
5	2.580	2.803	800.0	930.9	758.6	770.7	-46.4	522.2	-3.3	34.1	0.6872	0.7452	1115.9	1115.2	1.2115	0.7784	1410.2	972.4				
6	-1.030	0.139	735.0	816.1	732.6	677.3	-59.2	455.3	-4.6	33.9	0.6291	0.6500	1171.6	1164.4	1.2260	0.7810	1432.4	980.6				
7	-2.735	-1.196	748.3	769.5	746.7	637.2	-50.1	431.4	-3.8	34.0	0.6417	0.6121	1199.8	1189.7	1.2484	0.7879	1455.9	990.5				
8	-4.042	-2.431	784.4	778.0	783.4	656.3	-39.3	417.8	-2.9	32.4	0.6748	0.6204	1228.1	1215.7	1.2818	0.8240	1489.9	1033.1				
9	-7.122	-6.033	837.5	818.1	836.8	712.1	-35.8	402.7	-2.4	29.4	0.7206	0.6505	1314.1	1296.2	1.3664	0.9085	1588.2	1142.5				
10	-7.944	-7.251	830.9	808.6	830.0	704.0	-38.0	397.9	-2.6	29.4	0.7111	0.6393	1343.0	1323.8	1.3789	0.9193	1611.3	1163.2				
11	-8.754	-8.513	791.4	760.4	750.3	654.9	-41.5	386.5	-3.0	30.4	0.6696	0.5947	1372.0	1391.9	1.3702	0.9123	1619.5	1166.5				

SL	INCS	INCM	DEV	TURN	RHOVM-1	RHOVM-2	D-FAC	CMEGA-B	LCSS-P	PO2/	%EFF-P	%EFF-A	B*-1	B*-2	V0*-1	V0*-2	PC/PC
DEGREE	DEGREE	DEGREE	DEGREE	TOTAL	TOTAL	TOTAL	TOTAL	TOTAL	PO1	TOT	TOT	DEGREE	DEGREE	FT/SEC	FT/SEC	INLET	
1	-5.81	-1.50	25.04	39.03	80.93	92.13	0.4234	0.3092	0.0703	1.6219	73.64	71.60	43.67	4.64	-883.7	-75.9	3.0511
2	-6.02	-1.57	20.11	37.64	81.34	90.82	0.4464	0.3182	0.0739	1.6108	72.46	70.57	43.93	6.30	-893.6	-100.1	3.0366
3	-6.46	-1.88	16.40	35.03	82.21	88.57	0.4693	0.3299	0.0781	1.5754	70.41	68.48	43.90	8.87	-900.1	-135.9	2.9862
4	-4.24	0.35	12.53	25.42	79.53	90.92	0.4489	0.2529	0.0603	1.5386	73.97	72.36	47.51	22.09	-1006.9	-344.3	2.8562
5	2.06	6.64	9.39	17.92	66.94	85.85	0.4222	0.1313	0.0295	1.5971	85.35	84.36	55.53	37.61	-1162.3	-593.0	2.6434
6	4.84	5.18	10.07	12.94	60.95	75.56	0.4203	0.1167	0.0239	1.5782	86.15	85.24	55.21	46.28	-1230.5	-709.1	2.4584
7	4.24	6.32	10.64	9.22	62.42	71.08	0.4195	0.1403	0.0275	1.5192	82.20	81.13	55.11	44.90	-1249.9	-758.3	2.3852
8	2.86	6.67	8.16	7.76	66.02	73.68	0.4018	0.1458	0.0291	1.4851	80.27	75.15	58.24	50.48	-1267.3	-797.9	2.4045
9	1.33	4.01	4.22	6.83	70.97	79.58	0.3762	0.1718	0.0375	1.4526	74.99	73.65	58.14	51.32	-1349.9	-893.5	2.4677
10	1.71	3.89	5.94	8.29	69.95	77.77	0.3756	0.1814	0.0400	1.4444	73.38	71.98	58.91	52.62	-1361.0	-925.9	2.4455
11	3.19	4.88	10.08	4.97	65.42	70.83	0.3789	0.1808	0.0385	1.4398	73.38	71.95	60.70	55.74	-1413.5	-965.4	2.3600

TO/TO	PO/PC	EFF-AD	EFF-P	MCI/41	TO2/T01	PC2/PC1	EFF-AD	EFF-P
INLET	INLET	INLET	INLET	LBM/SEC	%	%	ROTOR	ROTOR
1.4034	2.6292	78.56	81.22	43.34	1.1680	1.5277	76.69	77.46

STATOR 2

SL	EPSI-1	EPSI-2	V-1	V-2	VM-1	VM-2	V0-1	V0-2	B-1	B-2	M-1	M-2	3, SPEED CODE	15, POINT NO	31	PO/PO	TO/TO	PO/PC	TC2/
DEGREE	DEGREE	FT/SEC	FT/SEC	FT/SEC	FT/SEC	FT/SEC	FT/SEC	FT/SEC	DEGREE	DEGREE						INLET	INLET	STAGE	TOT
1	8.905	0.919	1305.6	581.1	1003.5	979.8	835.2	-51.2	40.1	-3.0	1.0702	0.7671	2.5290	1.4665	1.3446	1.3446	1.2046		
2	8.070	0.945	1281.0	954.7	974.7	988.8	831.2	-108.7	40.7	-6.3	1.0461	0.7792	2.5766	1.4679	1.3649	1.2054			
3	7.152	0.684	1244.4	1010.6	937.6	1004.3	818.1	-112.8	41.3	-6.4	1.0125	0.7944	2.6261	1.4641	1.3859	1.2032			
4	4.447	0.423	1130.5	588.2	905.2	983.3	677.2	-98.9	36.5	-5.7	0.9152	0.7835	2.6155	1.4346	1.3991	1.1823			
5	1.955	-0.117	972.8	925.3	820.1	924.4	523.2	-38.8	32.5	-2.4	0.7825	0.7387	2.5152	1.3978	1.4919	1.1697			
6	0.824	-0.444	862.3	856.8	731.5	849.3	456.8	-112.7	32.0	-7.5	0.6899	0.6839	2.3958	1.3785	1.5333	1.1652			
7	0.050	-0.639	812.7	802.3	688.2	797.3	432.3	-88.8	32.1	-6.3	0.6491	0.6355	2.3075	1.3675	1.4856	1.1581			
8	-0.940	-0.814	815.9	801.1	704.9	800.0	418.7	-43.0	30.7	-3.1	0.6566	0.6404	2.3087	1.3604	1.4372	1.1512			
9	-3.594	-1.262	863.3	864.1	762.7	866.0	404.6	-5.7	27.9	-0.4	0.6898	0.6908	2.3979	1.3769	1.4116	1.1518			
10	-4.467	-1.362	855.7	841.8	760.8	840.0	400.3	-54.4	27.8	-3.7	0.6833	0.6675	2.3449	1.3901	1.3836	1.1530			
11	-5.482	-1.254	820.7	798.5	722.5	757.5	389.2	-38.7	26.4	-2.9	0.6456	0.5931	2.1586	1.4064	1.3415	1.1514			

SL	INCS	INCM	DEV	TURN	RHOVM-1	RHOVM-2	D-FAC	CMEGA-B	LCSS-P	PO2/	%EFF-P	%EFF-A	B*-1	B*-2	V0*-1	V0*-2	PC/PC
DEGREE	DEGREE	DEGREE	DEGREE	TOTAL	TOTAL	TOTAL	TOTAL	TOTAL	PO1	STAG-ST	TOT-INLET	TOT-INLET	TOT-STG	TOT-STG			
1	-8.39	-6.83	8.83	43.65	65.19	97.69	0.4024	0.3322	0.0750	0.8286	44.05	64.45	68.70	42.81	45.10		
2	-6.71	-4.69	4.98	46.58	94.07	99.40	0.3946	0.3088	0.0707	0.8444	43.56	65.87	44.90	47.22			
3	-5.33	-2.83	4.44	47.72	62.00	102.10	0.3706	0.2667	0.0622	0.8699	44.72	67.95	47.71	50.02			
4	-8.68	-4.81	4.58	42.62	93.87	102.63	0.3077	0.2087	0.0516	0.9112	37.51	72.46	75.85	54.86	56.92		
5	-12.18	-6.87	7.50	34.53	89.23	98.17	0.2246	0.1839	0.0492	0.9366	-9.49	75.52	78.43	70.91	72.48		
6	-12.44	-6.66	2.67	39.50	79.83	90.25	0.2164	0.1563	0.0428	0.9551	-84.23	74.66	77.52	78.18	79.44		
7	-12.13	-6.14	3.62	38.44	75.07	84.50	0.1986	0.1374	0.0383	0.9658	-236.54	73.13	76.04	75.28	76.61		
8	-13.38	-7.18	7.03	33.74	77.43	85.24	0.1803	0.1464	0.0415	0.9635	-239.49	74.71	77.45	71.79	73.18		
9	-15.85	-5.16	9.76	28.32	83.23	91.62	0.1392	0.1057	0.0310	0.9712	-357.26	75.08	77.85	67.79	69.30		
10	-16.68	-5.80	7.07	31.48	81.91	87.48	0.1787	0.1582	0.0467	0.9578	-248.98	70.46	73.71	63.13	64.76		
11	-17.35	-10.26	9.02	31.29	75.91	76.40	0.2317	0.2802	0.0835	0.9317	-68.95	61.90	65.77	57.43	59.14		

NCORR	WCORR	TO/TO	PO/PO	EFF-AD	EFF-P	TO2/T01	PO2/PO1	EFF-AD
INLET	INLET	INLET	INLET	INLET	INLET	%	%	STAGE
11245	19030	1.4034	2.4425	71.79	75.03	1.1680	0.9290	62.20

REPRODUCIBILITY OF THE ORIGINAL PAGE IS POOR

TABLE XXI (Cont'd) -- OVERALL PERFORMANCE AND BLADE-ELEMENT DATA  
(Uniform Inlet Flow)

U. S. CUSTOMARY UNITS

ROTOR 1

SL	EPSI-1	EPSI-2	V-1	V-2	VN-1	VN-2	VO-1	VO-2	B-1	B-2	M-1	M-2	3, SPEED	CODE 15,	POINT NO 2	V*-1	V*-2	
DEGREE	DEGREE	FT/SEC	FT/SEC	FT/SEC	FT/SEC	FT/SEC	FT/SEC	DEGREE	DEGREE				U-1	U-2	M*-1	M*-2	FT/SEC	FT/SEC
1	16.519	18.362	663.7	1153.3	663.7	728.6	0.0	894.0	0.0	50.9	0.6164	1.0302	660.4	764.5	0.8696	0.6611	936.3	740.1
2	13.843	16.020	680.0	1114.6	680.0	726.7	0.0	845.1	0.0	49.3	0.6328	0.9897	712.1	801.5	0.9163	0.6464	904.7	728.4
3	11.345	13.819	695.9	1062.1	695.9	727.3	0.0	801.2	0.0	47.0	0.6488	0.9563	762.9	838.5	0.9627	0.6435	1032.6	728.4
4	4.671	7.948	732.0	981.2	732.0	698.2	0.0	689.4	0.0	44.6	0.6856	0.8537	908.2	949.5	1.0925	0.6498	1166.5	745.1
5	-1.488	1.219	748.6	788.0	748.6	572.1	0.0	541.9	0.0	43.4	0.7026	0.6760	1089.6	1097.5	1.2408	0.6841	1322.0	797.5
6	-2.126	-1.898	749.9	697.2	749.9	502.8	0.0	483.0	0.0	43.9	0.7039	0.5946	1176.9	1171.4	1.3100	0.7270	1395.5	852.5
7	-2.497	-3.176	750.3	741.2	750.3	575.7	0.0	466.8	0.0	39.0	0.7044	0.6351	1220.0	1208.4	1.3446	0.8045	1432.2	938.5
8	-3.657	-4.375	749.5	775.9	749.5	626.5	0.0	457.8	0.0	36.2	0.7036	0.6649	1263.0	1248.4	1.3787	0.8650	1468.7	1006.4
9	-8.441	-7.932	733.0	802.7	733.0	662.2	0.0	453.7	0.0	34.4	0.6866	0.6875	1391.6	1356.4	1.4732	0.9588	1572.8	1119.5
10-10.185	-9.185	722.5	802.0	722.5	653.1	0.0	465.6	0.0	35.4	0.6758	0.6835	1434.4	1393.4	1.5024	0.9670	1606.1	1134.6	
11-11.538	-10.424	711.1	766.7	711.1	590.1	0.0	489.5	0.0	39.6	0.6643	0.6460	1477.2	1430.4	1.5314	0.9358	1639.5	1110.6	

SL	INCS	INCN	DEV	TURN	RHOVN-1	RHOVN-2	D-FAC	OMEGA-B	LOSS-P	PO2/P01	ZEFF-P	ZEFF-A	B*-1	B*-2	VO*-1	VO*-2	PO/PO	PO/PO
DEGREE	DEGREE	DEGREE	DEGREE	DEGREE				TOTAL	TOTAL	TOT	TOT	TOT	DEGREE	DEGREE	FT/SEC	FT/SEC	INLET	INLET
1	-1.77	2.83	17.86	54.70	42.26	56.69	0.4376	-0.0067	-0.0015	2.0075	100.34	100.39	44.61	-10.09	-660.4	129.5	2.0075	2.0075
2	-1.77	2.52	16.17	49.48	42.89	57.90	0.4737	0.0092	0.0021	1.9841	99.46	99.42	46.04	-3.44	-712.1	43.6	1.9841	1.9841
3	-1.65	2.46	14.47	44.42	43.48	59.12	0.4942	0.0168	0.0040	1.9666	98.92	98.82	47.36	2.93	-762.9	-37.3	1.9666	1.9666
4	-0.55	2.92	10.75	30.52	44.72	58.75	0.5275	0.0713	0.0178	1.8756	94.13	93.61	50.95	20.43	-908.2	-260.2	1.8756	1.8756
5	0.99	3.67	13.88	11.36	45.24	48.68	0.5235	0.1678	0.0361	1.6512	81.86	80.57	55.51	44.15	-1089.6	-555.5	1.6512	1.6512
6	1.57	3.85	16.53	3.64	45.28	42.99	0.4999	0.1930	0.0360	1.5677	76.95	75.48	57.51	53.07	-1176.9	-688.5	1.5677	1.5677
7	1.82	3.93	11.88	6.21	45.29	50.11	0.4494	0.1327	0.0264	1.6319	84.07	82.96	58.41	52.19	-1220.0	-741.7	1.6319	1.6319
8	2.09	4.04	8.66	7.79	45.27	55.29	0.4169	0.0904	0.0187	1.6892	89.10	88.29	59.31	51.52	-1263.0	-787.6	1.6892	1.6892
9	3.19	4.61	6.92	8.52	44.75	58.83	0.3897	0.0965	0.0203	1.7437	88.11	87.16	62.23	53.71	-1391.6	-902.7	1.7437	1.7437
10	3.61	4.90	7.81	8.48	44.41	57.53	0.3978	0.1328	0.0277	1.7403	83.73	82.44	63.29	54.81	-1434.4	-927.8	1.7403	1.7403
11	3.97	5.13	11.48	8.49	44.02	50.87	0.4317	0.2168	0.0426	1.6867	73.65	71.68	64.31	57.82	-1477.2	-940.9	1.6867	1.6867

TO/TO	PO/PO	EFF-AD	EFF-P	WC1/A1	TO2/T01	PO2/P01	EFF-AD	EFF-P
INLET	INLET	INLET	INLET	LBM/SEC	%	%	ROTOR	ROTOR
		%	%				%	%
1.2017	1.7657	87.37	88.32	43.06	1.2017	1.7657	87.37	88.32

STATOR 1

SL	EPSI-1	EPSI-2	V-1	V-2	VN-1	VN-2	VO-1	VO-2	B-1	B-2	M-1	M-2	3, SPEED	CODE 15,	POINT NO 2	PO/PO	TO/TO	PO/PO	TO2/	
DEGREE	DEGREE	FT/SEC	FT/SEC	FT/SEC	FT/SEC	FT/SEC	FT/SEC	DEGREE	DEGREE				U-1	U-2	M*-1	M*-2	INLET	INLET	STAGE	T01
1	18.220	14.918	1166.0	806.6	770.5	806.6	875.2	0.0	48.8	0.0	1.0440	0.6844	1.8795	1.2191	1.8795	1.2191	1.8795	1.2191	1.8795	1.2191
2	15.933	13.192	1132.2	805.6	769.8	805.4	830.2	17.2	47.3	1.2	1.0084	0.6841	1.8853	1.2170	1.8853	1.2170	1.8853	1.2170	1.8853	1.2170
3	13.817	11.568	1103.1	808.0	770.6	807.4	789.3	29.8	45.8	2.1	0.9783	0.6869	1.8914	1.2153	1.8914	1.2153	1.8914	1.2153	1.8914	1.2153
4	8.347	7.113	1007.3	781.2	739.6	781.2	684.0	9.2	42.8	0.7	0.8820	0.6640	1.8332	1.2090	1.8332	1.2090	1.8332	1.2090	1.8332	1.2090
5	1.593	1.113	814.6	646.6	609.1	644.6	541.0	-31.2	41.6	-4.5	0.7010	0.5471	1.6227	1.1887	1.6227	1.1887	1.6227	1.1887	1.6227	1.1887
6	-2.001	-2.181	725.9	594.8	541.6	592.1	483.4	-37.2	41.8	-5.5	0.6209	0.5025	1.5513	1.1813	1.5513	1.1813	1.5513	1.1813	1.5513	1.1813
7	-3.286	-3.584	767.6	624.3	608.6	622.7	467.8	-44.0	37.6	-4.1	0.6597	0.5267	1.5745	1.1816	1.5745	1.1816	1.5745	1.1816	1.5745	1.1816
8	-4.098	-4.597	801.2	674.9	636.4	674.1	459.3	-33.7	35.0	-2.9	0.6906	0.5737	1.6220	1.1839	1.6220	1.1839	1.6220	1.1839	1.6220	1.1839
9	-6.229	-7.061	828.9	748.0	691.8	747.1	458.6	-38.1	33.5	-2.9	0.7121	0.6366	1.7036	1.1980	1.7036	1.1980	1.7036	1.1980	1.7036	1.1980
10	-6.966	-7.757	829.4	746.7	684.3	745.8	468.8	-37.4	34.5	-2.9	0.7092	0.6324	1.6985	1.2085	1.6985	1.2085	1.6985	1.2085	1.6985	1.2085
11	-7.946	-8.460	796.7	707.5	625.6	706.5	493.3	-37.4	38.4	-3.0	0.6736	0.5925	1.6460	1.2245	1.6460	1.2245	1.6460	1.2245	1.6460	1.2245

SL	INCS	INCN	DEV	TURN	RHOVN-1	RHOVN-2	D-FAC	OMEGA-B	LOSS-P	PO2/P01	ZEFF-P	ZEFF-A	B*-1	B*-2	VO*-1	VO*-2	PO/PO	PO/PO		
DEGREE	DEGREE	DEGREE	DEGREE	DEGREE				TOTAL	TOTAL	TOT	STATC-ST	TOT-INLET	TOT-INLET	TOT-STG	TOT-STG			INLET	INLET	
1	-3.71	-1.60	12.33	48.84	59.25	76.02	0.4541	0.1264	0.0259	0.9370	82.61	90.08	90.91	90.08	90.08	90.91	90.08	90.91	90.08	90.91
2	-3.54	-1.14	12.64	46.08	60.39	76.28	0.4330	0.1026	0.0218	0.9512	84.88	91.43	92.14	91.43	91.43	92.14	91.43	92.14	91.43	92.14
3	-3.76	-0.97	12.49	43.67	61.53	76.70	0.4115	0.0806	0.0178	0.9633	87.17	92.67	93.28	92.67	92.67	93.28	92.67	93.28	92.67	93.28
4	-4.24	-0.52	9.94	42.09	61.03	73.32	0.3760	0.0356	0.0087	0.9856	93.17	90.35	91.12	90.35	91.12	90.35	91.12	90.35	91.12	90.35
5	-3.92	1.13	4.77	46.12	51.01	58.10	0.3868	0.0195	0.0053	0.9951	94.89	78.35	79.72	78.35	79.72	78.35	79.72	78.35	79.72	78.35
6	-3.26	2.36	3.84	47.28	45.68	52.56	0.4059	0.1057	0.0301	0.9737	75.21	73.70	73.70	73.70	73.70	73.70	73.70	73.70	73.70	73.70
7	-7.21	-1.36	5.33	41.64	52.27	55.36	0.3903	0.1795	0.0523	0.9536	56.31	76.19	77.63	76.19	77.63	76.19	77.63	76.19	77.63	76.19
8	-9.56	-3.42	6.56	37.91	57.14	60.24	0.3433	0.1564	0.0464	0.9572	55.01	80.62	81.67	80.62	81.67	80.62	81.67	80.62	81.67	80.62
9	-11.12	-4.24	7.62	36.43	60.51	66.86	0.2855	0.0802	0.0250	0.9770	64.19	83.00	84.21	83.00	84.21	83.00	84.21	83.00	84.21	83.00
10	-10.44	-3.39	8.89	37.39	59.31	66.12	0.2944	0.0818	0.0259	0.9768	63.87	78.41	79.93	78.41	79.93	78.41	79.93	78.41	79.93	78.41
11	-7.26	-0.11	10.26	41.41	53.04	61.28	0.3271	0.0917	0.0293	0.9760	63.15	68.08	70.20	68.08	70.20	68.08	70.20	68.08	70.20	68.08

NCORR	NCORR	TO/TO	PO/PO	EFF-AD	EFF-P	TO2/T01	PO2/P01	EFF-AD
INLET	INLET	INLET	INLET	INLET	INLET	%	%	STAGE
RPM	LBM/SEC			%	%			%
11236	189.60	1.2017	1.7190	82.92	84.15	1.2017	0.9735	82.92









TABLE XXI (Cont'd) - OVERALL PERFORMANCE AND BLADE-ELEMENT DATA (Uniform Inlet Flow)

U. S. CUSTOMARY UNITS

ROTOR 1

Table with columns: S/C, EPSI-1, EPSI-2, V-1, V-2, VM-1, VM-2, V0-1, V0-2, B-1, B-2, M-1, M-2, KUN NU, S, SPEED, CODE, II, POINT, NU 1, V1-1, V1-2. Rows include performance data for various stages.

Table with columns: S/C, INCS, INCM, DEV, TURN, RHQVM-1, RHQVM-2, C-FAC, OMEGA-B, LOSS-P, PG2, XEFF-P, XEFF-A, B1-1, B1-2, V0-1, V0-2, PG/PU, INLET. Rows include detailed blade element data.

Summary table with columns: TO/TU, PU/PO, EFF-AD, EFF-P, WCI/WL, TO2/T01, PG2/PO1, XEFF-AD, XEFF-P. Values: 1.2194, 1.0135, 84.40, 85.83, 44.09, 1.2194, 1.0135, 84.40, 85.83.

STATOR 1

Table with columns: S/C, EPSI-1, EPSI-2, V-1, V-2, VM-1, VM-2, V0-1, V0-2, B-1, B-2, M-1, M-2, KUN NU, S, SPEED, CODE, II, POINT, NU 1, V1-1, V1-2. Rows include performance data for stator stages.

Table with columns: S/C, INCS, INCM, DEV, TURN, RHQVM-1, RHQVM-2, C-FAC, OMEGA-B, LOSS-P, PG2, XEFF-P, XEFF-A, B1-1, B1-2, V0-1, V0-2, PG/PU, INLET. Rows include detailed blade element data for stator.

Summary table with columns: WCI/WL, WCI/WL, TO/TU, PG/PO, EFF-AD, EFF-P, TO2/T01, PG2/PO1, XEFF-AD, XEFF-P. Values: 1.1709, 1.0410, 1.2194, 1.7635, 80.11, 81.62, 1.2194, 0.9724, 80.11.



TABLE XXI (Cont'd) — OVERALL PERFORMANCE AND BLADE-ELEMENT DATA  
(Uniform Inlet Flow)

U. S. CUSTOMARY UNITS

ROTOR 1

SL	EPI-1		EPSI-2		V-1		V-2		VM-1		VM-2		VO-1		VO-2		B-1		B-2		M-1		M-2		RUN NO	SPEED CODE		POINT NO 2				
	DEGREE	DEGREE	FT/SEC	FT/SEC	FT/SEC	FT/SEC	FT/SEC	FT/SEC	DEGREE	DEGREE	FT/SEC	FT/SEC	DEGREE	DEGREE	FT/SEC	FT/SEC	DEGREE	DEGREE	FT/SEC	FT/SEC	FT/SEC	FT/SEC	FT/SEC	FT/SEC		FT/SEC	FT/SEC	FT/SEC	FT/SEC	FT/SEC		
1	18.408	18.408	691.6	1236.4	691.6	776.3	0.0	960.7	0.0	5.0	0.6445	1.1067	0.92.5	801.7	0.9120	0.7110	978.7	794.4														

SL	INCS		INCM		DEV		TURN		RHOVM-1		RHOVM-2		D-FAC		OMEGA-B		LOSS-P		PO2/P01		EFF-P		EFF-A		B*-1		B*-2		VM*-1		VM*-2		PO/PO				
	DEGREE	DEGREE	DEGREE	DEGREE	DEGREE	DEGREE	DEGREE	DEGREE	TOTAL	TOTAL	TOTAL	TOTAL	TOTAL	TOTAL	TOTAL	TOTAL	TOTAL	TOTAL	TOTAL	TOTAL	TOTAL	TOTAL	TOTAL	TOTAL	TOTAL	TOTAL	TOTAL	TOTAL	TOTAL	TOTAL	TOTAL	TOTAL	TOTAL	TOTAL	TOTAL		
1	18.408	18.408	3.01	16.39	50.35	43.32	59.17	0.4232	0.0274	0.0059	2.1443	98.61	98.46	44.79	-11.56	-692.5	159.0	2.1443																			

TO/TD INLET	PO/PO INLET	EFF-AD INLET	EFF-P INLET	HCI/A1 LBM/SEC	SOFT	TO2/T01	PO2/P01	EFF-AD ROTOR	EFF-P ROTOR
1.2191	1.8104	84.24	85.48	44.11		1.2191	1.8104	84.24	85.48

STATOR 1

SL	EPI-1		EPSI-2		V-1		V-2		VM-1		VM-2		VO-1		VO-2		B-1		B-2		M-1		M-2		RUN NO	SPEED CODE		POINT NO 2							
	DEGREE	DEGREE	FT/SEC	FT/SEC	FT/SEC	FT/SEC	FT/SEC	FT/SEC	DEGREE	DEGREE	FT/SEC	FT/SEC	DEGREE	DEGREE	FT/SEC	FT/SEC	DEGREE	DEGREE	FT/SEC	FT/SEC	FT/SEC	FT/SEC	FT/SEC	FT/SEC		FT/SEC	FT/SEC	FT/SEC	FT/SEC	FT/SEC	FT/SEC				
1	18.408	18.408	691.6	1236.4	691.6	776.3	0.0	960.7	0.0	5.0	0.6445	1.1067	0.92.5	801.7	0.9120	0.7110	978.7	794.4																	

SL	INCS		INCM		DEV		TURN		RHOVM-1		RHOVM-2		D-FAC		OMEGA-B		LOSS-P		PO2/P01		EFF-P		EFF-A		B*-1		B*-2		VM*-1		VM*-2		PO/PO			
	DEGREE	DEGREE	DEGREE	DEGREE	DEGREE	DEGREE	DEGREE	DEGREE	TOTAL	TOTAL	TOTAL	TOTAL	TOTAL	TOTAL	TOTAL	TOTAL	TOTAL	TOTAL	TOTAL	TOTAL	TOTAL	TOTAL	TOTAL	TOTAL	TOTAL	TOTAL	TOTAL	TOTAL	TOTAL	TOTAL	TOTAL	TOTAL	TOTAL	TOTAL		
1	18.408	18.408	3.01	16.39	50.35	43.32	59.17	0.4232	0.0274	0.0059	2.1443	98.61	98.46	44.79	-11.56	-692.5	159.0	2.1443																		

NCUMK INLET	NCUMK INLET	TU/TU INLET	PO/PO INLET	EFF-AD INLET	EFF-P INLET	TO2/T01	PO2/P01	EFF-AD STAGE
1.1783	1.9420	1.2191	1.7577	79.71	81.23	1.2191	1.8104	79.71

TABLE XXI (Cont'd) - OVERALL PERFORMANCE AND BLADE-ELEMENT DATA (Uniform Inlet Flow)

U. S. CUSTOMARY UNITS

ROTOR 2

Table with columns: SL, EPSI-1, EPSI-2, V-1, V-2, VM-1, VM-2, VO-1, VO-2, B-1, B-2, M-1, M-2, RUN NO, S, SPEC, CLDE, POINT NO, 2, U-1, U-2, V-1, V-2. Rows 1-11.

Table with columns: SL, INCX, INCM, DEV, TURN, RHOVM-1, RHOVM-2, C-FAC, OMEGA-B, LGSS-P, P02/P01, EFF-P, EFF-A, B-1, B-2, V-1, V-2, P0/P0, INLET. Rows 1-11.

Summary table with columns: TD/T0, PD/P0, EFF-AD, EFF-P, WCI/A1, T02/T01, P02/P01, EFF-AD, EFF-P. Values: 1.4497, 2.8955, 78.57, 81.47, 43.65, 1.1891, 1.0474, 80.4, 81.75.

STATOR 2

Table with columns: SL, EPSI-1, EPSI-2, V-1, V-2, VM-1, VM-2, VO-1, VO-2, B-1, B-2, M-1, M-2, RUN NO, S, SPEC, CLDE, POINT NO, 2, P0/P0, INLET, TGT, INLET, STAGE, T01. Rows 1-11.

Table with columns: SL, INCX, INCM, DEV, TURN, RHOVM-1, RHOVM-2, C-FAC, OMEGA-B, LGSS-P, P02/P01, EFF-P, EFF-A, B-1, B-2, V-1, V-2, P0/P0, INLET, TGT, INLET, STAGE, T01. Rows 1-11.

Summary table with columns: WQRR, WQRR, T0/T0, P0/P0, EFF-AD, EFF-P, T02/T01, P02/P01, EFF-AD, EFF-P. Values: 1178.3, 194.20, 1.4497, 2.7590, 74.47, 77.77, 1.1891, 0.9529, 72.14.







**APPENDIX F**

**OVERALL PERFORMANCE AND BLADE-ELEMENT DATA  
WITH TIP RADIALLY DISTORTED INLET FLOW**

This appendix provides the overall performance and blade-element data for the redesigned fan stage with tip radially distorted inlet flow. Fan overall performance is presented in Table XXII, and overall performance and blade-element data for rotor 1, stator 1, rotor 2, and stator 2 are provided in Table XXIII. The column headings for Table XXIII are identified in Table XVII of Appendix C. The 1st-stage pressure and temperature data used in calculating the parameters shown are from radial traverses corrected through the use of the correlations described in the section on data reduction techniques. The data is provided in U. S. customary units.

**TABLE XXII – FAN OVERALL PERFORMANCE (Tip Radially Distorted Inlet Flow)**

Run Number	Speed Code	Point Number	$w\sqrt{\theta_6} / \delta_6$		P <sub>11</sub> /P <sub>6</sub>	$\eta_{ad11}$	P <sub>16</sub> /P <sub>6</sub>	$\eta_{ad16}$
			LBM/SEC	KG/SEC				
006	10	31	186.3	(84.5)	1.71	88.6	2.35	74.6
006	10	32	186.4	(84.5)	1.72	88.2	2.68	83.9
006	10	34	182.5	(82.8)	1.84	89.9	3.04	85.7
006	85	31	157.0	(71.2)	1.52	90.5	1.94	79.8
006	85	32	154.4	(70.0)	1.53	89.4	2.18	88.3
006	85	34	144.7	(65.6)	1.55	86.3	2.26	84.8
006	70	31	125.4	(56.9)	1.33	88.8	1.59	82.0
006	70	32	114.9	(52.1)	1.34	86.2	1.71	84.8
006	70	34	108.6	(49.3)	1.32	78.9	1.69	81.2
006	10	stall	177.7	(80.6)			3.089	
006	85	stall	144.2	(65.4)			2.261	
006	70	stall	96.9	(43.9)			1.650	

Speed Code	% Design Speed
50	50
70	70
85	85
90	90
10	100
15	105
11	110

**REPRODUCING PAGE BLANK NOT FILMED**





TABLE XXIII (Cont'd) - OVERALL PERFORMANCE AND BLADE-ELEMENT DATA  
(Tip Radially Distorted Flow)

U. S. CUSTOMARY UNITS

ROTOR 1

Table with 20 columns: SL, EPSI-1, EPSI-2, V-1, V-2, VM-1, VM-2, VO-1, VO-2, B-1, B-2, M-1, M-2, RUN NO, S. SPEED, CODE, TO, POINT NO, V-1, V-2. Rows 1-5.

Table with 20 columns: SL, INCS, INCH, DEV, TURN, RHOVM-1, RHOVM-2, D-FAC, OMEGA-B, LOSS-P, PO2, XEFF-P, XEFF-A, B\*-1, B\*-2, VO\*-1, VO\*-2, PO/PU. Rows 1-5.

Table with 8 columns: TO/TO, PO/PO, EFF-AD, EFF-P, WCI/AL, TO2/T01, PO2/PO1, EFF-AD, EFF-P. Rows 1-2.

STATOR 1

Table with 20 columns: SL, EPSI-1, EPSI-2, V-1, V-2, VM-1, VM-2, VO-1, VO-2, B-1, B-2, M-1, M-2, RUN NO, S. SPEED, CODE, TO, POINT NO, V-1, V-2. Rows 1-5.

Table with 20 columns: SL, INCS, INCH, DEV, TURN, RHOVM-1, RHOVM-2, D-FAC, OMEGA-B, LOSS-P, PO2, XEFF-P, XEFF-A, B\*-1, B\*-2, VO\*-1, VO\*-2, PO/PU. Rows 1-5.

Table with 8 columns: NCORR, WCORR, TO/TO, PO/PO, EFF-AD, EFF-P, TO2/T01, PO2/PO1, EFF-AD. Rows 1-2.

ROTOR 2

Table with 20 columns: SL, EPSI-1, EPSI-2, V-1, V-2, VM-1, VM-2, VO-1, VO-2, B-1, B-2, M-1, M-2, RUN NO, S. SPEED, CODE, TO, POINT NO, V-1, V-2. Rows 1-5.

Table with 20 columns: SL, INCS, INCH, DEV, TURN, RHOVM-1, RHOVM-2, D-FAC, OMEGA-B, LOSS-P, PO2, XEFF-P, XEFF-A, B\*-1, B\*-2, VO\*-1, VO\*-2, PO/PU. Rows 1-5.

Table with 8 columns: TO/TO, PO/PO, EFF-AD, EFF-P, WCI/AL, TO2/T01, PO2/PO1, EFF-AD, EFF-P. Rows 1-2.

STATOR 2

Table with 20 columns: SL, EPSI-1, EPSI-2, V-1, V-2, VM-1, VM-2, VO-1, VO-2, B-1, B-2, M-1, M-2, RUN NO, S. SPEED, CODE, TO, POINT NO, V-1, V-2. Rows 1-5.

Table with 20 columns: SL, INCS, INCH, DEV, TURN, RHOVM-1, RHOVM-2, D-FAC, OMEGA-B, LOSS-P, PO2, XEFF-P, XEFF-A, B\*-1, B\*-2, VO\*-1, VO\*-2, PO/PU. Rows 1-5.

Table with 8 columns: NCORR, WCORR, TO/TO, PO/PO, EFF-AD, EFF-P, TO2/T01, PO2/PO1, EFF-AD. Rows 1-2.











TABLE XXIII (Cont'd) - OVERALL PERFORMANCE AND BLADE-ELEMENT DATA (Tip Radially Distorted Flow)

U. S. CUSTOMARY UNITS

ROTOR 1

Table with 23 columns: SL, EPSI-1, EPSI-2, V-1, V-2, VM-1, VM-2, V0-1, V0-2, B-1, B-2, M-1, M-2, RUN NO, S, SPEED CODE 10, POINT NO 32, U-1, U-2, M-1, M-2, V-1, V-2. Rows 1-5 contain performance data for Rotor 1.

Table with 18 columns: SL, INCS, INCM, DEV, TURN, RHOVM-1, RHOVM-2, D-FAC, CMEGA-B, LOSS-P, P02, XEFF-P, XEFF-A, B-1, B-2, V0-1, V0-2, PC/PO. Rows 1-5 contain detailed performance data for Rotor 1.

Summary table for Rotor 1 with 6 columns: TO/TO INLET, PO/PO INLET, EFF-AD INLET, EFF-P INLET, WCI/A1 LB/SEC, TO2/T01, P02/P01, EFF-AD ROTOR, EFF-P ROTOR. Values: 1.1699, 1.7518, 91.41, 92.04, 42.31, 1.1699, 1.7509, 91.31, 91.95.

STATOR 1

Table with 23 columns: SL, EPSI-1, EPSI-2, V-1, V-2, VM-1, VM-2, V0-1, V0-2, B-1, B-2, M-1, M-2, RUN NO, S, SPEED CODE 10, POINT NO 32, U-1, U-2, M-1, M-2, V-1, V-2. Rows 1-5 contain performance data for Stator 1.

Table with 18 columns: SL, INCS, INCM, DEV, TURN, RHOVM-1, RHOVM-2, D-FAC, CMEGA-B, LOSS-P, P02, XEFF-P, XEFF-A, B-1, B-2, V0-1, V0-2, PC/PO. Rows 1-5 contain detailed performance data for Stator 1.

Summary table for Stator 1 with 6 columns: WCORR INLET, WCORR INLET, TO/TO INLET, PO/PO INLET, EFF-AD INLET, EFF-P INLET, TO2/T01, P02/P01, EFF-AD STAGE, EFF-P STAGE. Values: 10731, 186.40, 1.1899, 1.7215, 48.33, 89.17, 1.1899, 0.9827, 88.24.

ROTOR 2

Table with 23 columns: SL, EPSI-1, EPSI-2, V-1, V-2, VM-1, VM-2, V0-1, V0-2, B-1, B-2, M-1, M-2, RUN NO, S, SPEED CODE 10, POINT NO 32, U-1, U-2, M-1, M-2, V-1, V-2. Rows 1-5 contain performance data for Rotor 2.

Table with 18 columns: SL, INCS, INCM, DEV, TURN, RHOVM-1, RHOVM-2, D-FAC, CMEGA-B, LOSS-P, P02, XEFF-P, XEFF-A, B-1, B-2, V0-1, V0-2, PC/PO. Rows 1-5 contain detailed performance data for Rotor 2.

Summary table for Rotor 2 with 6 columns: TO/TO INLET, PO/PO INLET, EFF-AD INLET, EFF-P INLET, WCI/A1 LB/SEC, TO2/T01, P02/P01, EFF-AD ROTOR, EFF-P ROTOR. Values: 1.3870, 2.7865, 87.99, 89.22, 42.24, 1.1656, 1.6187, 88.52, 89.28.

STATOR 2

Table with 23 columns: SL, EPSI-1, EPSI-2, V-1, V-2, VM-1, VM-2, V0-1, V0-2, B-1, B-2, M-1, M-2, RUN NO, S, SPEED CODE 10, POINT NO 32, U-1, U-2, M-1, M-2, V-1, V-2. Rows 1-5 contain performance data for Stator 2.

Table with 18 columns: SL, INCS, INCM, DEV, TURN, RHOVM-1, RHOVM-2, D-FAC, CMEGA-B, LOSS-P, P02, XEFF-P, XEFF-A, B-1, B-2, V0-1, V0-2, PC/PO. Rows 1-5 contain detailed performance data for Stator 2.

Summary table for Stator 2 with 6 columns: WCORR INLET, WCORR INLET, TO/TO INLET, PO/PO INLET, EFF-AD INLET, EFF-P INLET, TO2/T01, P02/P01, EFF-AD STAGE, EFF-P STAGE. Values: 10731, 186.40, 1.3870, 2.4829, 83.88, 85.92, 1.1656, 0.9628, 81.11.



## APPENDIX G

### OVERALL PERFORMANCE AND BLADE-ELEMENT DATA WITH HUB RADIALLY DISTORTED INLET FLOW

This appendix provides overall performance and blade-element data with hub radially distorted inlet flow. The information presented is for the redesigned stage. Fan overall performance is given in Table XXIV, and the overall performance and blade-element data for rotor 1, stator 1, rotor 2, and stator 2 are given in Table XXV for 70 percent, 85 percent, and 100 percent of design speed. The column headings for Table XXV are identified in Table XVIII of Appendix C. The 1st-stage pressure and temperature data used in calculating the parameters shown are from radial traverses corrected using the correlations described in the section on data reduction techniques. The information is presented in U. S. customary units.

TABLE XXIV – FAN OVERALL PERFORMANCE (Hub Radially Distorted Flow)

Run Number	Speed Code	Point Number	$w\sqrt{\theta_6} / \delta_6$					
			LBM/SEC	KG/SEC	$P_{11}/P_6$	$\eta_{ad\ 11}$	$P_{16}/P_6$	$\eta_{ad\ 16}$
005	10	1	179.2	(81.3)	1.66	88.4	2.25	73.9
005	10	4	179.7	(81.5)	1.67	88.4	2.34	77.4
005	10	3	178.1	(80.8)	1.69	87.6	2.73	84.4
005	85	1	152.3	(69.1)	1.48	87.5	1.83	74.9
005	85	4	140.8	(63.9)	1.48	81.8	2.17	84.5
005	70	11	123.2	(55.9)	1.30	85.7	1.53	79.2
005	70	3	116.6	(52.9)	1.30	82.4	1.66	86.6
005	70	13	110.4	(50.1)	1.30	80.6	1.69	85.3
005	70	4	100.5	(45.6)	1.30	73.6	1.70	78.8
005	10	stall	176.2	(79.9)			2.815	
005	85	stall	134.8	(61.1)			2.167	
005	70	stall	94.7	(42.9)			1.701	

Speed Code	% Design Speed
50	50
70	70
85	85
90	90
95	95
10	100
15	105
11	110





TABLE XXV (Cont'd) – OVERALL PERFORMANCE AND BLADE-ELEMENT DATA  
(Hub Radially Distorted Flow)

U. S. CUSTOMARY UNITS

ROTOR 1

SL	EPI-1	EPI-2	V-1	V-2	VM-1	VM-2	VO-1	VO-2	B-1	B-2	M-1	M-2	RUN NO		S. SPEED		CODE	TO	POINT	NO 13	V'-1	V'-2
													U-1	U-2	U-1	U-2						
1	4.000	4.913	281.0	835.0	281.0	311.3	0.0	556.4	0.0	60.0	0.2533	0.5811	474.2	533.7	0.4967	0.2753	551.2	312.0	1.02718	1.3085	1.2716	1.3085
2	4.000	4.913	281.0	835.0	281.0	311.3	0.0	556.4	0.0	60.0	0.2533	0.5811	474.2	533.7	0.4967	0.2753	551.2	312.0	1.02718	1.3085	1.2716	1.3085
3	4.000	4.913	281.0	835.0	281.0	311.3	0.0	556.4	0.0	60.0	0.2533	0.5811	474.2	533.7	0.4967	0.2753	551.2	312.0	1.02718	1.3085	1.2716	1.3085
4	4.000	4.913	281.0	835.0	281.0	311.3	0.0	556.4	0.0	60.0	0.2533	0.5811	474.2	533.7	0.4967	0.2753	551.2	312.0	1.02718	1.3085	1.2716	1.3085
5	4.000	4.913	281.0	835.0	281.0	311.3	0.0	556.4	0.0	60.0	0.2533	0.5811	474.2	533.7	0.4967	0.2753	551.2	312.0	1.02718	1.3085	1.2716	1.3085

STATOR 1

SL	EPI-1	EPI-2	V-1	V-2	VM-1	VM-2	VO-1	VO-2	B-1	B-2	M-1	M-2	RUN NO	S. SPEED		CODE	TO/TO	POINT	NO 13	V'-1	V'-2
														U-1	U-2						
1	4.000	4.913	281.0	835.0	281.0	311.3	0.0	556.4	0.1	58.0	0.2528	0.5808	1.2585	1.0950	1.0950	1.2585	1.0950	1.2585	1.0950	1.0950	1.0950
2	4.000	4.913	281.0	835.0	281.0	311.3	0.0	556.4	-1.0	52.0	0.2515	0.5808	1.2532	1.0942	1.0942	1.2532	1.0942	1.2532	1.0942	1.0942	1.0942
3	4.000	4.913	281.0	835.0	281.0	311.3	0.0	556.4	-2.0	46.0	0.2499	0.5808	1.2469	1.0932	1.0932	1.2469	1.0932	1.2469	1.0932	1.0932	1.0932
4	4.000	4.913	281.0	835.0	281.0	311.3	0.0	556.4	-3.0	40.0	0.2483	0.5808	1.2409	1.0922	1.0922	1.2409	1.0922	1.2409	1.0922	1.0922	1.0922
5	4.000	4.913	281.0	835.0	281.0	311.3	0.0	556.4	-4.0	34.0	0.2467	0.5808	1.2350	1.0912	1.0912	1.2350	1.0912	1.2350	1.0912	1.0912	1.0912

ROTOR 2

SL	EPI-1	EPI-2	V-1	V-2	VM-1	VM-2	VO-1	VO-2	B-1	B-2	M-1	M-2	RUN NO		S. SPEED		CODE	TO/TO	POINT	NO 13	V'-1	V'-2
													U-1	U-2	U-1	U-2						
1	4.000	4.913	281.0	835.0	281.0	311.3	0.0	556.4	0.1	48.7	0.2699	0.6741	599.9	624.7	0.6380	0.4441	735.4	521.0	1.0759	1.0759	1.0759	1.0759
2	4.000	4.913	281.0	835.0	281.0	311.3	0.0	556.4	-1.0	42.3	0.2684	0.6741	609.7	600.5	0.7112	0.4471	688.5	552.0	1.0759	1.0759	1.0759	1.0759
3	4.000	4.913	281.0	835.0	281.0	311.3	0.0	556.4	-2.0	37.3	0.2669	0.6741	620.4	574.0	0.7864	0.5119	802.0	608.0	1.0759	1.0759	1.0759	1.0759
4	4.000	4.913	281.0	835.0	281.0	311.3	0.0	556.4	-3.0	31.0	0.2654	0.6741	631.1	548.0	0.8599	0.6013	943.0	710.5	1.0759	1.0759	1.0759	1.0759
5	4.000	4.913	281.0	835.0	281.0	311.3	0.0	556.4	-4.0	25.0	0.2639	0.6741	641.8	522.0	0.9093	0.6845	1044.4	770.7	1.0759	1.0759	1.0759	1.0759

STATOR 2

SL	EPI-1	EPI-2	V-1	V-2	VM-1	VM-2	VO-1	VO-2	B-1	B-2	M-1	M-2	RUN NO		S. SPEED		CODE	TO/TO	POINT	NO 13	V'-1	V'-2
													U-1	U-2	U-1	U-2						
1	4.000	4.913	281.0	835.0	281.0	311.3	0.0	556.4	0.3	46.3	0.2894	0.5567	1.7999	1.2146	1.2146	1.7999	1.2146	1.7999	1.2146	1.2146	1.2146	
2	4.000	4.913	281.0	835.0	281.0	311.3	0.0	556.4	-1.0	40.8	0.2879	0.5567	1.7773	1.1989	1.1989	1.7773	1.1989	1.7773	1.1989	1.1989	1.1989	
3	4.000	4.913	281.0	835.0	281.0	311.3	0.0	556.4	-2.0	35.3	0.2864	0.5567	1.7547	1.1832	1.1832	1.7547	1.1832	1.7547	1.1832	1.1832	1.1832	
4	4.000	4.913	281.0	835.0	281.0	311.3	0.0	556.4	-3.0	29.8	0.2849	0.5567	1.7321	1.1675	1.1675	1.7321	1.1675	1.7321	1.1675	1.1675	1.1675	
5	4.000	4.913	281.0	835.0	281.0	311.3	0.0	556.4	-4.0	24.3	0.2834	0.5567	1.7095	1.1518	1.1518	1.7095	1.1518	1.7095	1.1518	1.1518	1.1518	









TABLE XXV (Cont'd) - OVERALL PERFORMANCE AND BLADE-ELEMENT DATA (Hub Radially Distorted Flow)

U. S. CUSTOMARY UNITS

ROTOR 1

Table with columns: SL, EPI-1, EPI-2, V-1, V-2, VM-1, VM-2, V0-1, V0-2, B-1, B-2, M-1, M-2, RUN NO, S, SPEED, CODE, IG, POINT NO, 1, V-1, V-2, U-1, U-2, W-1, W-2, W-1, W-2. Rows 1-5.

Table with columns: SL, INCS, INCM, DEV, TURN, RHOVM-1, RHOVM-2, D-FAC, CREGA-B, LOSS-P, POZ/PO1, XEFF-P, XEFF-A, B-1, B-2, W-1, W-2, PC/PC, TCZ/TCT, INLET, INLET, INLET, INLET, LBM/SEC, SOFT, TOZ/TOT, POZ/PO1, EFF-AD, EFF-P, PC/TOR, PC/TOR. Rows 1-5.

STATOR 1

Table with columns: SL, EPI-1, EPI-2, V-1, V-2, VM-1, VM-2, V0-1, V0-2, B-1, B-2, M-1, M-2, RUN NO, S, SPEED, CODE, IG, POINT NO, 1, V-1, V-2, U-1, U-2, W-1, W-2, W-1, W-2. Rows 1-5.

Table with columns: SL, INCS, INCM, DEV, TURN, RHOVM-1, RHOVM-2, D-FAC, CREGA-B, LOSS-P, POZ/PO1, XEFF-P, XEFF-A, B-1, B-2, W-1, W-2, PC/PC, TCZ/TCT, INLET, INLET, INLET, INLET, LBM/SEC, SOFT, TOZ/TOT, POZ/PO1, EFF-AD, EFF-P, PC/TOR, PC/TOR. Rows 1-5.

ROTOR 2

Table with columns: SL, EPI-1, EPI-2, V-1, V-2, VM-1, VM-2, V0-1, V0-2, B-1, B-2, M-1, M-2, RUN NO, S, SPEED, CODE, IG, POINT NO, 1, V-1, V-2, U-1, U-2, W-1, W-2, W-1, W-2. Rows 1-5.

Table with columns: SL, INCS, INCM, DEV, TURN, RHOVM-1, RHOVM-2, D-FAC, CREGA-B, LOSS-P, POZ/PO1, XEFF-P, XEFF-A, B-1, B-2, W-1, W-2, PC/PC, TCZ/TCT, INLET, INLET, INLET, INLET, LBM/SEC, SOFT, TOZ/TOT, POZ/PO1, EFF-AD, EFF-P, PC/TOR, PC/TOR. Rows 1-5.

STATOR 2

Table with columns: SL, EPI-1, EPI-2, V-1, V-2, VM-1, VM-2, V0-1, V0-2, B-1, B-2, M-1, M-2, RUN NO, S, SPEED, CODE, IG, POINT NO, 1, V-1, V-2, U-1, U-2, W-1, W-2, W-1, W-2. Rows 1-5.

Table with columns: SL, INCS, INCM, DEV, TURN, RHOVM-1, RHOVM-2, D-FAC, CREGA-B, LOSS-P, POZ/PO1, XEFF-P, XEFF-A, B-1, B-2, W-1, W-2, PC/PC, TCZ/TCT, INLET, INLET, INLET, INLET, LBM/SEC, SOFT, TOZ/TOT, POZ/PO1, EFF-AD, EFF-P, PC/TOR, PC/TOR. Rows 1-5.



TABLE XXV (Cont'd) - OVERALL PERFORMANCE AND BLADE-ELEMENT DATA (Hub Radially Distorted Flow)

U. S. CUSTOMARY UNITS

ROTOR 1

Table with 16 columns: SL, EPSI-1, EPSI-2, V-1, V-2, VM-1, VM-2, VO-1, VO-2, B-1, B-2, M-1, RUN NO, S, SPEED CODE, 10, POINT NO, 4, V1-1, V1-2. Contains 5 rows of data.

Table with 16 columns: SL, INCS, INCM, DEV, TURN, RHCVM-1, RHCVM-2, C-FAC, MEGA-B, LOSS-P, PO2, REFF-P, REFF-A, B-1, B-2, V0-1, V0-2, PO/PU. Contains 5 rows of data.

Table with 8 columns: TO/TO, PO/PU, EFF-AD, EFF-P, MCI/AI, TQ2/TQ1, PC2/PO1, EFF-AD, EFF-P. Contains 1 row of data.

STATOR 1

Table with 16 columns: SL, EPSI-1, EPSI-2, V-1, V-2, VM-1, VM-2, VO-1, VO-2, B-1, B-2, M-1, RUN NO, S, SPEED CODE, 10, POINT NO, 4, V1-1, V1-2. Contains 5 rows of data.

Table with 16 columns: SL, INCS, INCM, DEV, TURN, RHCVM-1, RHCVM-2, C-FAC, MEGA-B, LOSS-P, PO2, REFF-P, REFF-A, B-1, B-2, V0-1, V0-2, PO/PU. Contains 5 rows of data.

Table with 8 columns: TO/TO, PO/PU, EFF-AD, EFF-P, MCI/AI, TQ2/TQ1, PC2/PO1, EFF-AD, EFF-P. Contains 1 row of data.

ROTOR 2

Table with 16 columns: SL, EPSI-1, EPSI-2, V-1, V-2, VM-1, VM-2, VO-1, VO-2, B-1, B-2, M-1, RUN NO, S, SPEED CODE, 10, POINT NO, 4, V1-1, V1-2. Contains 5 rows of data.

Table with 16 columns: SL, INCS, INCM, DEV, TURN, RHCVM-1, RHCVM-2, C-FAC, MEGA-B, LOSS-P, PO2, REFF-P, REFF-A, B-1, B-2, V0-1, V0-2, PO/PU. Contains 5 rows of data.

Table with 8 columns: TO/TO, PO/PU, EFF-AD, EFF-P, MCI/AI, TQ2/TQ1, PC2/PO1, EFF-AD, EFF-P. Contains 1 row of data.

STATOR 2

Table with 16 columns: SL, EPSI-1, EPSI-2, V-1, V-2, VM-1, VM-2, VO-1, VO-2, B-1, B-2, M-1, RUN NO, S, SPEED CODE, 10, POINT NO, 4, V1-1, V1-2. Contains 5 rows of data.

Table with 16 columns: SL, INCS, INCM, DEV, TURN, RHCVM-1, RHCVM-2, C-FAC, MEGA-B, LOSS-P, PO2, REFF-P, REFF-A, B-1, B-2, V0-1, V0-2, PO/PU. Contains 5 rows of data.

Table with 8 columns: TO/TO, PO/PU, EFF-AD, EFF-P, MCI/AI, TQ2/TQ1, PC2/PO1, EFF-AD, EFF-P. Contains 1 row of data.

## APPENDIX H

### OVERALL PERFORMANCE AND VELOCITY VECTOR PARAMETERS FOR CIRCUMFERENTIALLY DISTORTED INLET FLOW

This appendix provides overall performance and velocity vector parameters for circumferentially distorted inlet flow. The information presented is for the redesigned fan. Fan overall performance is given in Table XXVI. Tables XXVII, XXVIII, and XXIX give velocity vector parameters at rotor 1 inlet, stator 1 exit, and stator 2 exit, respectively. Table XXX gives 1st-stage total temperature ratios, and Table XXXI gives fan total pressure and total temperature ratios. Velocity calculations are based on standard day inlet plenum conditions, and the velocity vector data (i.e.  $V$ ,  $V_m$ , and  $V_\theta$ ) are presented in U.S. customary units (ft/sec). The circumferential reference position is TDC looking forward. The relative position of the circumferential-distortion screen is  $246^\circ - 336^\circ$  (hub) and  $246^\circ - 326^\circ$  (tip). Tip is 100 percent span.  $\beta^\circ$  is defined as  $\tan^{-1} (\tan \beta / \cos \epsilon)$ , where  $\epsilon$ 's are design values.

**TABLE XXVI - FAN OVERALL PERFORMANCE**  
(Circumferentially Distorted Inlet Flow)

Run Number	Speed Code	Point Number	Screen Positions	$\frac{W\sqrt{\theta_6}}{\delta_6}$		$P_{11}/P_6$	$\eta_{ad 11}$	$P_{16}/P_6$	$\eta_{ad 16}$
				LBM/SEC	KG/SEC				
007	10	31	2	185.0	(83.9)	1.717	91.5	2.342	71.8
007	10	02	6	184.6	(83.7)	1.732	86.4	2.678	80.9
007	10	03	6	176.0	(79.8)	1.831	88.3	2.877	81.8
007	90	01	2	167.4	(75.9)	1.587	93.1	2.109	77.6
007	90	02	2	148.8	(67.5)	1.628	87.4	2.430	81.7
007	90	03	6	145.8	(66.1)	1.637	81.2	2.439	80.2
007	70	01	2	123.9	(56.2)	1.327	91.4	1.608	80.9
007	70	02	2	113.8	(51.6)	1.334	82.3	1.712	79.9
007	70	13	6	106.6	(48.3)	1.331	78.9	1.728	80.6
007	10	STALL		171.3	(77.7)			2.883	
007	90	STALL		142.6	(64.7)			2.438	
007	70	STALL		102.6	(46.5)			1.723	
				<b>Speed Code</b>	<b>% Design Speed</b>				
				50	50				
				70	70				
				85	85				
				90	90				
				95	95				
				10	100				
				15	105				
				11	110				

TABLE XXVII - VELOCITY VECTOR PARAMETERS AT ROTOR 1 INLET  
(Circumferentially Distorted Inlet Flow)

FIRST ROTOR INLET CIRCUMFERENTIAL DISTRIBUTIONS - WEDGE PROBE STATION 6

	$P_6/P_0$	$\rho_6/\rho_0$	$90 - \beta'$	M	V	$V_m$	$V_0$	$90 - \beta'$		$P_6/P_0$	$\rho_6/\rho_0$	$90 - \beta'$	M	V	$V_m$	$V_0$	$90 - \beta'$
	72°									72°							
10	.493	.928	92.7	.29	318.	317.	-15.	35.8		.983	.941	92.1	.25	281.	281.	-10.	32.8
30	.485	.911	91.5	.34	372.	371.	-10.	33.0		.985	.926	91.3	.30	332.	332.	-8.	30.2
50	.490	.905	91.6	.35	387.	387.	-11.	24.0		.985	.917	91.0	.32	356.	356.	-6.	26.2
70	.484	.900	90.8	.35	383.	383.	-5.	24.5		.984	.920	90.8	.31	346.	346.	-5.	22.4
90	.480	.891	91.4	.30	331.	331.	-8.	18.4		.982	.935	90.6	.27	297.	297.	-3.	16.9
MR	.483	.913	91.4	.33	362.	362.	-9.			.984	.925	91.0	.30	327.	327.	-6.	
	162°									162°							
10	.484	.927	86.2	.28	312.	312.	10.	36.9		.983	.942	85.7	.25	276.	276.	6.	33.4
30	.484	.910	88.2	.33	364.	364.	12.	33.5		.984	.925	88.2	.29	326.	325.	10.	30.6
50	.494	.903	88.2	.35	385.	385.	12.	28.7		.986	.917	88.0	.32	356.	356.	12.	26.9
70	.481	.905	88.2	.34	379.	379.	12.	24.7		.985	.921	88.1	.31	345.	345.	12.	22.8
90	.480	.890	89.0	.30	335.	335.	6.	19.1		.984	.925	88.5	.26	289.	289.	7.	16.7
MR	.481	.911	88.4	.33	367.	367.	10.			.985	.925	88.2	.29	324.	324.	10.	
	252°									252°							
10	.472	.901	76.1	.33	366.	355.	88.	46.8		.473	.922	76.6	.28	311.	302.	72.	40.6
30	.450	.893	77.7	.32	358.	350.	77.	35.8		.460	.914	78.3	.27	294.	288.	60.	29.9
50	.457	.895	79.9	.34	371.	365.	65.	29.3		.448	.905	81.0	.28	309.	305.	48.	24.6
70	.464	.887	80.1	.35	383.	378.	66.	26.1		.467	.907	81.1	.30	336.	332.	52.	23.0
90	.478	.899	80.2	.35	384.	379.	65.	22.7		.430	.915	79.8	.31	346.	341.	62.	20.5
MR	.467	.893	79.2	.34	375.	369.	70.			.468	.912	79.7	.29	325.	320.	58.	
	342°									342°							
10	.474	.894	100.4	.35	382.	376.	-69.	37.3		.478	.921	100.6	.29	326.	321.	-60.	33.6
30	.477	.884	99.1	.38	418.	413.	-66.	33.4		.480	.914	99.7	.34	376.	371.	-63.	30.8
50	.479	.879	97.5	.39	434.	430.	-56.	29.1		.483	.904	97.9	.35	385.	382.	-53.	26.4
70	.481	.880	96.9	.39	432.	429.	-52.	25.8		.485	.907	97.8	.34	381.	377.	-52.	23.1
90	.480	.898	98.8	.36	398.	396.	-47.	21.2		.484	.922	97.7	.30	337.	334.	-45.	18.2
MR	.479	.887	97.7	.38	416.	412.	-56.			.483	.912	98.4	.33	364.	361.	-53.	

PT. 7-70-01  $W\sqrt{\theta/\delta} = 123.9$  lbm/sec (56.2 kg/sec)

$P_{16}/P_6 = 1.561$

$P_0 = 1754$  lbf/ft<sup>2</sup> (83,900 N/m<sup>2</sup>)

$T_0 = 509.4$  R (283 K)

PT. 7-70-02  $W\sqrt{\theta/\delta} = 113.8$  lbm/sec (51.6 kg/sec)

$P_{16}/P_6 = 1.670$

$P_0 = 1802$  lbf/ft<sup>2</sup> (86,100 N/m<sup>2</sup>)

$T_0 = 496.0$  R (275 K)

REPRODUCIBILITY OF THE ORIGINAL PAGE IS POOR

TABLE XXVII (Cont'd) - VELOCITY VECTOR PARAMETERS AT ROTOR 1 INLET  
(Circumferentially Distorted Inlet Flow)

FIRST ROTOR INLET CIRCUMFERENTIAL DISTRIBUTIONS - WEDGE PROBE STATION 6

	$P_6/P_0$	$p_6/P_0$	90- $\beta$ °	M	V	$V_m$	$V_0$	90- $\beta$ °	$P_6/P_0$	$p_6/P_0$	90- $\beta$ °	M	V	$V_m$	$V_0$	90- $\beta$ °	$P_6/P_0$	$p_6/P_0$	90- $\beta$ °	M	V	$V_m$	$V_0$	90- $\beta$ °	
12°																									
10	.983	.984	97.9	.24	255	263	36	29.6	.987	.989	93.4	.24	263	252	36	30.8	.985	.989	91.8	.23	256	256	36	30.8	
FR	.986	.983	96.3	.29	326	324	35	28.4	.987	.932	92.6	.29	318	315	35	28.9	.987	.937	91.3	.27	304	304	35	28.3	
50	.985	.986	96.3	.30	329	327	39	23.5	.987	.930	92.7	.29	325	325	35	28.0	.986	.938	89.7	.29	323	323	35	28.3	
70	.986	.933	94.7	.28	312	311	26	19.8	.987	.945	91.5	.28	313	313	35	28.0	.986	.938	89.6	.28	308	308	35	28.0	
90	.984	.966	94.7	.24	263	262	21	14.7	.986	.945	92.2	.24	262	241	30	19.9	.983	.947	89.7	.23	256	256	35	14.8	
MR	.985	.935	95.6	.27	302	301	30		.987	.935	92.3	.27	300	300	30	12		.986	.939	90.0	.26	293	293	35	0
42°																									
102°																									
10	.982	.984	91.4	.24	266	266	7	31.7	.985	.935	88.2	.23	252	252	4	31.1	.986	.944	89.7	.24	263	263	2	31.9	
FR	.984	.974	91.8	.28	313	313	10	28.8	.986	.936	88.1	.27	302	304	19	28.9	.985	.935	90.9	.27	302	302	0	28.3	
50	.986	.929	92.4	.29	325	325	13	24.8	.986	.931	88.4	.28	304	304	9	24.7	.987	.927	90.9	.29	332	332	0	24.8	
70	.987	.933	91.6	.28	315	315	9	20.8	.988	.945	88.4	.28	312	312	9	20.7	.986	.931	90.3	.29	315	315	2	20.9	
90	.985	.946	91.7	.24	268	268	8	15.3	.986	.949	88.5	.24	264	241	7	15.2	.985	.944	90.3	.28	274	274	1	15.8	
MR	.987	.937	91.8	.27	301	301	9		.987	.939	88.5	.27	296	295	8		.986	.936	90.3	.27	302	302	1		
132°																									
162°																									
10	.982	.984	81.4	.24	266	266	7	31.7	.985	.935	88.2	.23	252	252	4	31.1	.986	.944	89.7	.24	263	263	2	31.9	
FR	.984	.974	81.8	.28	313	313	10	28.8	.986	.936	88.1	.27	302	304	19	28.9	.985	.935	90.9	.27	302	302	0	28.3	
50	.986	.929	92.4	.29	325	325	13	24.8	.986	.931	88.4	.28	304	304	9	24.7	.987	.927	90.9	.29	332	332	0	24.8	
70	.987	.933	91.6	.28	315	315	9	20.8	.988	.945	88.4	.28	312	312	9	20.7	.986	.931	90.3	.29	315	315	2	20.9	
90	.985	.946	91.7	.24	268	268	8	15.3	.986	.949	88.5	.24	264	241	7	15.2	.985	.944	90.3	.28	274	274	1	15.8	
MR	.987	.937	91.8	.27	301	301	9		.987	.939	88.5	.27	296	295	8		.986	.936	90.3	.27	302	302	1		
192°																									
222°																									
10	.985	.947	85.6	.24	265	264	8	33.0	.985	.944	81.4	.23	274	270	44	35.5	.976	.934	78.6	.25	278	272	55	35.8	
FR	.984	.934	85.5	.28	307	306	24	29.4	.985	.931	81.1	.28	310	308	48	30.8	.962	.927	81.2	.23	258	255	40	25.7	
50	.983	.927	86.8	.29	322	322	18	24.7	.984	.925	81.0	.29	310	308	39	26.3	.963	.922	83.5	.25	279	277	32	21.8	
70	.986	.932	87.1	.29	317	317	16	21.4	.987	.929	85.3	.31	309	308	29	22.2	.972	.921	83.1	.28	307	305	37	20.7	
90	.982	.942	87.5	.24	270	270	12	19.4	.986	.942	85.5	.24	273	263	22	16.6	.981	.932	82.1	.27	302	299	42	17.7	
MR	.984	.935	86.7	.27	300	299	17		.986	.933	84.0	.28	311	303	32		.972	.927	82.0	.26	290	287	40		
252°																									
312°																									
10	.948	.930	85.0	.17	187	186	16	24.6	.966	.924	101.5	.22	244	239	49	26.8	.980	.937	101.5	.26	285	279	57	30.1	
FR	.949	.920	85.0	.19	207	207	12	20.7	.949	.921	99.6	.23	230	227	38	20.7	.982	.943	98.1	.30	332	329	47	28.4	
50	.942	.916	87.1	.20	223	223	12	17.6	.943	.925	98.9	.19	208	207	32	17.5	.987	.920	96.5	.29	323	319	46	24.8	
70	.943	.918	86.9	.20	218	218	12	14.8	.942	.923	94.4	.17	188	186	28	14.2	.984	.928	94.3	.29	323	321	36	20.3	
90	.942	.929	87.0	.18	181	181	9	10.7	.951	.930	104.2	.18	201	194	49	10.8	.984	.944	95.8	.24	273	270	27	16.1	
MR	.943	.921	86.9	.18	205	205	12		.944	.925	100.7	.19	212	209	39		.984	.930	97.1	.28	315	313	39		

REPRODUCIBILITY OF THIS ORIGINAL PAGE IS POOR

PT. 7-70-13  $W\sqrt{\theta/\delta} = 106.6 \text{ lbm/sec (48.3 kg/sec)}$   
 $P_{16}/P_6 = 1.692$   
 $P_6 = 1868 \text{ lbf/ft}^2 (89,200 \text{ N/m}^2)$   
 $T_0 = 512.5^\circ \text{R (284 K)}$



TABLE XXVII (Cont'd) - VELOCITY VECTOR PARAMETERS AT ROTOR 1 INLET  
(Circumferentially Distorted Inlet Flow)

FIRST ROTOR INLET CIRCUMFERENTIAL DISTRIBUTIONS - WEDGE PROBE STATION 6

72°							72°							72°								
P <sub>0</sub> /P <sub>6</sub>	p <sub>6</sub> /P <sub>0</sub>	90 - β'	M	V	V <sub>m</sub>	V <sub>θ</sub> 90 - β'	P <sub>0</sub> /P <sub>0</sub>	p <sub>6</sub> /P <sub>0</sub>	90 - β'	M	V	V <sub>m</sub>	V <sub>θ</sub> 90 - β'	P <sub>0</sub> /P <sub>0</sub>	p <sub>6</sub> /P <sub>0</sub>	90 - β'	M	V	V <sub>m</sub>	V <sub>θ</sub> 90 - β'		
10	.960	.840	92.8	.45	491.	491.	.971	.872	91.2	.40	435.	435.	.990	38.3	.954	.801	95.2	.51	552.	549.	.50	39.8
30	.967	.852	91.3	.51	552.	552.	.970	.842	88.4	.48	497.	497.	.999	35.0	.959	.745	88.5	.61	657.	657.	.17	39.9
50	.959	.801	91.4	.53	575.	575.	.975	.837	89.8	.47	517.	517.	.960	29.8	.960	.758	93.8	.59	638.	638.	.42	30.6
70	.966	.817	91.3	.51	559.	559.	.970	.841	89.3	.41	446.	446.	.952	25.1	.952	.774	88.8	.55	598.	598.	.47	28.4
90	.965	.823	91.3	.46	508.	508.	.964	.851	90.0	.44	482.	482.	.956	19.8	.956	.766	91.7	.57	618.	618.	.12	23.5
PR	.985	.815	91.5	.50	541.	541.	.970	.849														
162°							162°							162°								
10	.961	.848	89.5	.43	468.	468.	.977	.876	87.4	.38	423.	423.	.992	35.0	.952	.799	89.0	.51	552.	552.	.91	42.7
30	.962	.819	88.4	.49	530.	530.	.965	.848	86.7	.44	478.	478.	.952	29.4	.952	.764	88.2	.57	615.	615.	.20	38.1
50	.959	.805	89.1	.52	562.	562.	.979	.840	88.0	.46	505.	505.	.959	24.1	.959	.749	84.9	.60	652.	651.	.13	32.8
70	.963	.812	89.9	.50	545.	545.	.972	.852	88.8	.44	482.	482.	.955	19.0	.955	.754	84.9	.59	638.	638.	.12	28.4
90	.969	.834	90.4	.45	492.	492.	.964	.859	89.2	.39	428.	428.	.952	18.9	.952	.785	90.3	.53	578.	578.	.03	22.6
PR	.983	.822	89.8	.48	524.	524.	.969	.856	88.2	.43	466.	466.	.954		.954	.768	89.2	.57	612.	612.	.91	
252°							252°							252°								
10	.948	.813	77.8	.46	504.	493.	.948	.851	79.5	.42	459.	451.	.984	44.6	.924	.758	78.3	.54	585.	573.	118.	49.5
30	.915	.794	79.7	.46	499.	491.	.917	.817	81.0	.41	449.	443.	.992	34.5	.992	.734	80.6	.54	581.	579.	95.	39.0
50	.915	.751	81.9	.48	526.	521.	.922	.810	83.2	.43	477.	473.	.994	29.0	.994	.720	82.1	.56	610.	604.	84.	32.7
70	.927	.786	82.1	.49	536.	531.	.933	.809	83.8	.44	487.	484.	.994	26.2	.994	.718	82.3	.58	629.	623.	84.	29.3
90	.951	.807	82.1	.49	534.	529.	.957	.851	82.3	.45	497.	492.	.938	22.8	.938	.752	82.3	.57	618.	613.	83.	25.1
PR	.931	.776	81.2	.48	524.	517.	.937	.821	82.1	.44	481.	477.	.912		.912	.736	81.5	.56	609.	603.	90.	
342°							342°							342°								
10	.948	.796	100.1	.51	551.	542.	.964	.861	104.4	.41	445.	431.	.934	33.2	.934	.746	99.3	.58	623.	615.	-100.	41.0
30	.957	.769	97.2	.57	615.	610.	.953	.836	102.4	.45	497.	485.	.944	30.3	.944	.712	98.1	.65	700.	693.	-99.	37.6
50	.961	.760	95.7	.59	635.	632.	.973	.830	99.3	.48	526.	520.	.952	27.3	.952	.701	96.7	.68	722.	717.	-84.	32.9
70	.963	.764	95.5	.58	632.	629.	.973	.842	99.2	.46	501.	495.	.955	23.2	.955	.705	96.4	.67	719.	714.	-80.	29.3
90	.961	.795	96.6	.53	572.	568.	.958	.863.	99.1	.41	450.	444.	.953	18.8	.953	.743	96.3	.61	654.	650.	-72.	24.0
PR	.959	.776	96.6	.56	605.	601.	.963	.856	100.3	.44	487.	479.	.950		.950	.720	97.1	.64	689.	683.	-85.	

PT. 7-90-01  $W\sqrt{\theta/\delta} = 167.4$  lbm/sec (75.9 kg/sec)  
 $P_{16}/P_6 = 1.994$   
 $P_{10} = 1575$  lbf/ft<sup>2</sup> (75,300 N/m<sup>2</sup>)  
 $T_{10} = 509.2$  R (283 K)

PT. 7-90-02  $W\sqrt{\theta/\delta} = 148.8$  lbm/sec (67.4 kg/sec)  
 $P_{16}/P_6 = 2.324$   
 $P_{10} = 1643$  lbf/ft<sup>2</sup> (78,600 N/m<sup>2</sup>)  
 $T_{10} = 509.8$  R (283 K)

PT. 7-10-31  $W\sqrt{\theta/\delta} = 185.0$  lbm/sec (83.8 kg/sec)  
 $P_{16}/P_6 = 2.180$   
 $P_{10} = 1481$  lbf/ft<sup>2</sup> (70,800 N/m<sup>2</sup>)  
 $T_{10} = 503.2$  R (279 K)

TABLE XXVII (Cont'd) - VELOCITY VECTOR PARAMETERS AT ROTOR 1 INLET  
(Circumferentially Distorted Inlet Flow)

FIRST ROTOR INLET CIRCUMFERENTIAL DISTRIBUTIONS - WEDGE PROBE STATION 6

	$P_6/P_0$	$p_6/P_0$	$90-\beta^*$	M	V	$V_m$	$V_a$	$90-\beta^*$	$P_6/P_0$	$p_6/P_0$	$90-\beta^*$	M	V	$V_m$	$V_a$	$90-\beta^*$	$P_6/P_0$	$p_6/P_0$	$90-\beta^*$	M	V	$V_m$	$V_a$	$90-\beta^*$
	42°																							
	12°																							
10	.972	.884	87.7	.37	405.	406.	-55.	34.1	.978	.891	91.7	.37	406.	406.	-12.	36.3	.974	.885	90.0	.36	396.	396.	0.	36.0
30	.978	.871	87.0	.41	450.	447.	-55.	30.0	.979	.874	91.9	.41	446.	446.	-15.	31.4	.975	.870	88.6	.41	447.	446.	11.	32.2
50	.977	.864	96.0	.42	463.	460.	-48.	25.5	.978	.867	92.2	.42	458.	458.	-17.	26.2	.976	.863	89.3	.42	465.	465.	6.	27.0
70	.976	.872	95.3	.40	444.	442.	-41.	21.7	.977	.876	91.5	.40	437.	436.	-11.	22.1	.975	.871	89.3	.40	444.	444.	3.	22.6
90	.972	.885	94.6	.37	404.	403.	-33.	17.5	.970	.891	91.1	.35	386.	386.	-8.	17.2	.960	.884	90.3	.34	380.	380.	-2.	17.0
MR	.975	.875	95.8	.40	435.	433.	-44.		.976	.879	91.6	.39	427.	427.	-12.		.971	.875	89.5	.39	429.	429.	4.	
	102°																							
10	.974	.886	89.6	.37	408.	406.	3.	37.1	.973	.889	87.5	.36	399.	399.	17.	37.3	.974	.877	87.3	.39	429.	429.	20.	39.4
30	.974	.858	90.2	.42	456.	456.	-1.	32.4	.978	.868	86.8	.41	452.	452.	25.	33.2	.967	.854	87.4	.43	467.	466.	21.	33.8
50	.975	.855	90.2	.44	481.	481.	-1.	27.7	.977	.858	87.7	.43	477.	476.	19.	28.1	.973	.866	88.9	.45	495.	495.	10.	28.6
70	.974	.862	90.2	.42	462.	462.	-1.	23.4	.976	.867	87.8	.42	456.	456.	18.	23.5	.979	.853	88.4	.44	478.	478.	6.	24.4
90	.965	.877	90.3	.37	409.	409.	-2.	18.2	.964	.881	87.8	.36	399.	398.	8.	17.9	.967	.871	88.8	.39	427.	427.	9.	19.1
MR	.973	.868	90.1	.41	446.	446.	-1.		.973	.871	87.8	.40	440.	439.	17.		.970	.869	88.3	.42	461.	461.	14.	
	162°																							
10	.975	.878	84.7	.39	429.	428.	40.	40.3	.973	.872	81.4	.40	439.	434.	65.	42.3	.954	.854	80.0	.40	441.	441.	77.	43.0
30	.976	.859	84.9	.43	472.	470.	42.	34.8	.972	.860	81.8	.44	484.	479.	69.	36.5	.928	.835	81.7	.39	430.	426.	62.	33.0
50	.979	.849	87.2	.44	486.	486.	22.	28.5	.979	.843	85.4	.47	511.	509.	41.	30.2	.929	.823	83.4	.42	460.	457.	53.	27.9
70	.977	.855	87.4	.44	483.	482.	22.	24.7	.978	.851	87.0	.45	493.	493.	26.	25.4	.933	.827	83.4	.44	479.	476.	55.	25.2
90	.964	.872	88.0	.38	421.	421.	15.	18.9	.971	.870	87.8	.40	439.	438.	17.	19.7	.959	.846	83.4	.43	469.	466.	54.	21.4
MR	.972	.862	86.7	.42	460.	460.	26.		.975	.856	85.3	.43	476.	474.	39.		.944	.836	82.7	.42	460.	457.	58.	
	222°																							
10	.905	.845	86.0	.32	349.	348.	25.	33.8	.933	.845	102.7	.38	417.	417.	-89.	32.9	.964	.865	103.7	.40	435.	423.	-103.	33.1
30	.893	.827	88.5	.33	370.	369.	9.	27.5	.911	.830	101.8	.37	405.	397.	-83.	26.4	.965	.847	100.6	.42	477.	469.	-88.	30.2
50	.892	.813	88.4	.37	403.	403.	14.	24.1	.895	.815	99.2	.36	396.	391.	-63.	21.8	.974	.844	98.7	.46	499.	493.	-76.	26.4
70	.891	.818	88.2	.35	387.	387.	12.	20.1	.843	.823	98.9	.34	377.	373.	-58.	18.4	.971	.853	98.7	.43	475.	470.	-72.	22.4
90	.882	.835	88.7	.28	313.	313.	7.	14.2	.897	.833	102.0	.33	363.	355.	-76.	15.1	.965	.869	98.1	.39	429.	425.	-60.	18.0
MR	.891	.826	88.1	.33	366.	366.	12.		.903	.829	100.8	.35	388.	381.	-73.		.968	.856	99.4	.42	465.	458.	-76.	
	282°																							
10	.905	.845	86.0	.32	349.	348.	25.	33.8	.933	.845	102.7	.38	417.	417.	-89.	32.9	.964	.865	103.7	.40	435.	423.	-103.	33.1
30	.893	.827	88.5	.33	370.	369.	9.	27.5	.911	.830	101.8	.37	405.	397.	-83.	26.4	.965	.847	100.6	.42	477.	469.	-88.	30.2
50	.892	.813	88.4	.37	403.	403.	14.	24.1	.895	.815	99.2	.36	396.	391.	-63.	21.8	.974	.844	98.7	.46	499.	493.	-76.	26.4
70	.891	.818	88.2	.35	387.	387.	12.	20.1	.843	.823	98.9	.34	377.	373.	-58.	18.4	.971	.853	98.7	.43	475.	470.	-72.	22.4
90	.882	.835	88.7	.28	313.	313.	7.	14.2	.897	.833	102.0	.33	363.	355.	-76.	15.1	.965	.869	98.1	.39	429.	425.	-60.	18.0
MR	.891	.826	88.1	.33	366.	366.	12.		.903	.829	100.8	.35	388.	381.	-73.		.968	.856	99.4	.42	465.	458.	-76.	

ORIGINAL PAGE IS POOR QUALITY OF THE

PT. 7-90-03  $W\sqrt{\theta/\delta} = 145.8 \text{ lbm/sec (66.1 kg/sec)}$   
 $P_{16}/P_0 = 2.338$   
 $P_0 = 1669 \text{ lbf/ft}^2 (79,750 \text{ N/m}^2)$   
 $T_0 = 508.8 \text{ R (282 K)}$

TABLE XXVII (Cont'd) - VELOCITY VECTOR PARAMETERS AT ROTOR 1 INLET  
(Circumferentially Distorted Inlet Flow)

FIRST ROTOR INLET CIRCUMFERENTIAL DISTRIBUTIONS - WEDGE PROBE STATION 6

	12°									42°									72°								
	$P_0/P_0$	$p_6/P_0$	$90-\beta$	M	V	$V_m$	$V_0$	$90-\beta'$		$P_0/P_0$	$p_6/P_0$	$90-\beta$	M	V	$V_m$	$V_0$	$90-\beta'$		$P_0/P_0$	$p_6/P_0$	$90-\beta$	M	V	$V_m$	$V_0$	$90-\beta'$	
10	.944	.771	95.2	.55	59.7	58.8	63	41.4		.961	.783	92.5	.55	59.4	59.3	26	43.4		.984	.795	93.1	.52	56.3	56.8	30	41.4	
30	.961	.736	95.2	.63	67.6	67.3	61	38.1		.961	.750	92.5	.61	65.4	65.3	28	38.4		.981	.761	91.1	.59	63.3	63.3	12	37.9	
50	.956	.725	94.3	.64	68.7	68.6	52	32.6		.957	.724	92.1	.63	67.4	67.4	28	33.0		.962	.748	91.2	.61	65.7	65.7	14	32.4	
70	.954	.729	93.3	.63	67.9	67.8	39	28.9		.958	.741	92.1	.62	66.4	66.4	24	28.8		.957	.752	91.0	.60	64.4	64.4	11	28.1	
90	.955	.766	93.3	.57	61.6	61.5	35	23.5		.958	.775	92.5	.56	60.2	60.1	26	23.2		.952	.744	92.0	.53	57.7	57.7	20	22.3	
MR	.955	.744	94.1	.61	65.5	65.3	47.			.958	.755	92.3	.59	64.0	64.0	26.			.957	.767	91.5	.57	61.8	61.8	17.		

	102°									132°									162°								
	$P_0/P_0$	$p_6/P_0$	$90-\beta$	M	V	$V_m$	$V_0$	$90-\beta'$		$P_0/P_0$	$p_6/P_0$	$90-\beta$	M	V	$V_m$	$V_0$	$90-\beta'$		$P_0/P_0$	$p_6/P_0$	$90-\beta$	M	V	$V_m$	$V_0$	$90-\beta'$	
10	.950	.750	90.2	.54	58.1	58.1	2	43.8		.954	.752	90.7	.51	55.6	55.6	7	41.8		.997	.751	88.8	.53	57.4	57.4	12	44.1	
30	.961	.756	90.1	.59	64.2	64.2	1	38.8		.957	.757	89.3	.57	61.7	61.7	8	37.8		.991	.762	89.0	.57	61.9	61.9	11	38.1	
50	.957	.741	90.4	.62	66.3	66.3	5	33.0		.960	.751	89.9	.60	64.9	64.9	1	32.3		.960	.742	89.4	.62	65.5	65.5	7	33.3	
70	.964	.743	90.5	.60	65.1	65.1	5	28.6		.958	.755	89.9	.59	63.8	63.8	1	28.1		.958	.749	89.4	.60	65.0	65.0	7	28.8	
90	.954	.760	91.5	.55	59.1	59.1	16	22.9		.953	.744	90.9	.53	57.4	57.4	9	22.2		.955	.752	90.5	.54	58.9	58.9	5	23.0	
MR	.954	.742	90.6	.58	62.8	62.8	7.			.955	.771	90.1	.56	61.0	61.0	1.			.956	.763	89.6	.58	62.3	62.3	5.		

	192°									222°									252°								
	$P_0/P_0$	$p_6/P_0$	$90-\beta$	M	V	$V_m$	$V_0$	$90-\beta'$		$P_0/P_0$	$p_6/P_0$	$90-\beta$	M	V	$V_m$	$V_0$	$90-\beta'$		$P_0/P_0$	$p_6/P_0$	$90-\beta$	M	V	$V_m$	$V_0$	$90-\beta'$	
10	.959	.799	86.9	.52	56.5	56.4	31	44.5		.953	.754	82.6	.53	57.3	56.8	74	47.0		.923	.754	78.5	.54	58.3	57.1	116	49.4	
30	.952	.767	87.0	.56	61.1	61.0	32	38.4		.947	.757	82.8	.58	62.2	61.7	78	40.6		.954	.725	80.2	.54	58.2	57.4	99	39.3	
50	.952	.748	87.8	.60	64.4	64.3	25	32.9		.950	.740	85.9	.62	66.9	66.7	48	34.6		.926	.721	82.3	.56	61.1	6.6	82	32.8	
70	.958	.755	88.7	.59	63.5	63.5	14	28.4		.962	.750	87.3	.61	65.3	65.3	31	29.5		.906	.724	82.7	.57	62.2	6.7	79	29.0	
90	.944	.786	90.3	.52	56.3	56.3	3	22.1		.955	.750	86.5	.55	59.2	59.2	15	23.5		.939	.753	82.7	.57	61.7	6.2	78	26.1	
MR	.952	.770	88.4	.56	60.6	60.6	17.			.956	.762	86.0	.58	62.6	62.5	43.			.914	.738	81.7	.56	60.7	6.0	87.		

	282°									312°									342°								
	$P_0/P_0$	$p_6/P_0$	$90-\beta$	M	V	$V_m$	$V_0$	$90-\beta'$		$P_0/P_0$	$p_6/P_0$	$90-\beta$	M	V	$V_m$	$V_0$	$90-\beta'$		$P_0/P_0$	$p_6/P_0$	$90-\beta$	M	V	$V_m$	$V_0$	$90-\beta'$	
10	.847	.743	83.1	.43	46.6	46.3	56	40.2		.945	.731	96.7	.49	54.0	53.6	53	34.8		.935	.752	97.6	.57	61.3	6.7	83	41.4	
30	.824	.726	87.0	.43	47.1	47.0	24	31.2		.924	.705	93.8	.49	53.1	53.0	35	32.3		.948	.733	98.3	.62	66.6	6.9	96	36.3	
50	.824	.737	86.6	.48	52.0	51.9	31	27.7		.921	.692	93.0	.50	54.5	54.4	28	27.3		.957	.684	91.2	.70	74.9	7.8	15	35.8	
70	.826	.712	87.1	.45	50.5	50.7	25	23.8		.914	.694	93.0	.49	53.6	53.5	28	23.8		.955	.700	90.4	.68	72.8	7.8	5	31.3	
90	.825	.729	87.8	.42	46.4	46.4	17	18.8		.921	.714	94.2	.45	49.3	49.2	37	19.0		.952	.757	97.9	.56	61.1	6.5	8	22.4	
MR	.828	.722	86.7	.44	48.7	48.7	28.			.927	.706	93.9	.48	52.6	52.5	36.			.951	.727	94.7	.63	67.9	6.7	56.		

PT. 7-10-02  $W\sqrt{\theta/\delta} = 184.6 \text{ lbm/sec (83.7 kg/sec)}$   
 $P_{16}/P_6 = 2.494$   
 $P_0 = 1488 \text{ lbf/ft}^2 (71,000 \text{ N/m}^2)$   
 $T_0 = 500.4^\circ\text{R} (278^\circ\text{K})$

TABLE XXVII (Cont'd) - VELOCITY VECTOR PARAMETERS AT ROTOR 1 INLET  
(Circumferentially Distorted Inlet Flow)

FIRST ROTOR INLET CIRCUMFERENTIAL DISTRIBUTIONS - WEDGE PROBE STATION 6

10	30	50	70	90	MR	12°						42°						72°									
						P <sub>6</sub> /P <sub>0</sub>	p <sub>6</sub> /P <sub>0</sub>	90 - β°	M	V	V <sub>m</sub>	V <sub>o</sub>	90 - β'	P <sub>6</sub> /P <sub>0</sub>	p <sub>6</sub> /P <sub>0</sub>	90 - β°	M	V	V <sub>m</sub>	V <sub>o</sub>	90 - β'	P <sub>6</sub> /P <sub>0</sub>	p <sub>6</sub> /P <sub>0</sub>	90 - β°	M	V	V <sub>m</sub>
.954	.963	.962	.959	.947	.943	.989	.47	5.4	5.9	.72	36.7	.961	.974	.917	.47	5.7	5.7	.15	40.0	.963	.976	.917	.45	5.6	5.9	.15	38.8
.963	.962	.963	.961	.954	.951	.985	.47	5.8	5.7	.72	33.6	.962	.976	.916	.45	5.7	5.7	.18	35.0	.962	.978	.911	.45	5.7	5.7	.18	35.9
.962	.962	.962	.964	.954	.951	.985	.47	5.8	5.8	.72	28.4	.963	.971	.913	.45	5.7	5.7	.19	29.3	.962	.977	.902	.45	5.4	5.4	.20	30.3
.959	.959	.959	.953	.954	.951	.985	.45	5.8	5.8	.72	25.2	.963	.970	.913	.45	5.6	5.6	.12	25.1	.964	.970	.902	.45	5.6	5.6	.12	25.6
.960	.960	.960	.953	.950	.949	.985	.45	5.4	5.4	.72	20.7	.957	.962	.913	.45	5.6	5.6	.11	20.4	.957	.962	.904	.47	5.5	5.5	.30	20.5
.960	.960	.960	.952	.952	.949	.985	.45	5.4	5.4	.72	20.7	.960	.967	.916	.45	5.5	5.5	.15	20.5	.962	.967	.902	.45	5.5	5.5	.20	20.5

10	30	50	70	90	MR	102°						132°						162°									
						P <sub>6</sub> /P <sub>0</sub>	p <sub>6</sub> /P <sub>0</sub>	90 - β°	M	V	V <sub>m</sub>	V <sub>o</sub>	90 - β'	P <sub>6</sub> /P <sub>0</sub>	p <sub>6</sub> /P <sub>0</sub>	90 - β°	M	V	V <sub>m</sub>	V <sub>o</sub>	90 - β'	P <sub>6</sub> /P <sub>0</sub>	p <sub>6</sub> /P <sub>0</sub>	90 - β°	M	V	V <sub>m</sub>
.962	.967	.963	.964	.957	.950	.987	.44	5.2	5.2	.12	41.9	.957	.968	.892	.44	5.0	5.0	.70	40.2	.956	.962	.877	.45	5.0	5.0	.22	43.3
.967	.959	.963	.977	.902	.890	.984	.44	5.4	5.4	.11	36.7	.959	.955	.882	.45	5.0	5.0	.17	36.2	.957	.954	.873	.44	5.4	5.4	.28	37.2
.964	.964	.964	.964	.956	.950	.984	.44	5.0	5.0	.14	30.9	.965	.978	.885	.45	5.0	5.0	.16	31.3	.965	.969	.880	.45	5.2	5.2	.22	32.0
.964	.958	.964	.967	.902	.890	.984	.44	5.0	5.0	.12	26.9	.962	.978	.885	.45	5.0	5.0	.16	27.1	.963	.972	.889	.45	5.7	5.7	.12	27.7
.962	.958	.962	.967	.902	.890	.984	.44	5.4	5.4	.12	21.6	.958	.961	.892	.45	5.3	5.3	.18	21.6	.963	.960	.889	.45	5.2	5.2	.10	22.6
.962	.958	.962	.967	.902	.890	.984	.44	5.4	5.4	.12	21.6	.960	.977	.887	.45	5.6	5.6	.13	21.6	.962	.966	.883	.45	5.5	5.5	.17	21.6

10	30	50	70	90	MR	192°						222°						252°									
						P <sub>6</sub> /P <sub>0</sub>	p <sub>6</sub> /P <sub>0</sub>	90 - β°	M	V	V <sub>m</sub>	V <sub>o</sub>	90 - β'	P <sub>6</sub> /P <sub>0</sub>	p <sub>6</sub> /P <sub>0</sub>	90 - β°	M	V	V <sub>m</sub>	V <sub>o</sub>	90 - β'	P <sub>6</sub> /P <sub>0</sub>	p <sub>6</sub> /P <sub>0</sub>	90 - β°	M	V	V <sub>m</sub>
.962	.957	.957	.957	.950	.948	.982	.45	5.4	5.4	.45	44.0	.954	.959	.818	.45	5.5	5.5	.79	46.4	.954	.974	.784	.45	5.2	5.2	.11	49.0
.957	.978	.955	.965	.885	.872	.988	.45	5.8	5.8	.46	38.3	.946	.965	.820	.45	6.0	6.0	.84	40.1	.958	.970	.818	.45	5.8	5.8	.79	37.7
.957	.965	.955	.965	.885	.872	.988	.45	5.8	5.8	.37	33.3	.964	.978	.800	.45	6.0	6.0	.45	33.7	.959	.974	.830	.45	5.9	5.9	.73	31.9
.964	.970	.955	.965	.885	.872	.988	.45	5.4	5.4	.23	27.8	.965	.975	.803	.45	6.4	6.4	.41	29.3	.916	.971	.830	.45	6.0	6.0	.72	28.4
.948	.978	.955	.965	.885	.872	.988	.45	5.4	5.4	.12	21.7	.959	.970	.878	.45	6.0	6.0	.22	23.1	.947	.970	.824	.45	5.8	5.8	.80	24.4
.956	.973	.955	.965	.885	.872	.988	.45	5.8	5.8	.29	21.7	.959	.972	.884	.45	6.2	6.2	.49	21.7	.921	.974	.821	.45	6.4	6.4	.81	21.7

10	30	50	70	90	MR	282°						312°						342°										
						P <sub>6</sub> /P <sub>0</sub>	p <sub>6</sub> /P <sub>0</sub>	90 - β°	M	V	V <sub>m</sub>	V <sub>o</sub>	90 - β'	P <sub>6</sub> /P <sub>0</sub>	p <sub>6</sub> /P <sub>0</sub>	90 - β°	M	V	V <sub>m</sub>	V <sub>o</sub>	90 - β'	P <sub>6</sub> /P <sub>0</sub>	p <sub>6</sub> /P <sub>0</sub>	90 - β°	M	V	V <sub>m</sub>	V <sub>o</sub>
.862	.835	.843	.841	.877	.841	.983	.44	4.8	4.8	.38	34.7	.855	.859	.101	.44	5.3	5.3	.10	36.8	.946	.976	.104	.43	.50	5.4	5.3	.13	35.6
.835	.835	.835	.835	.877	.877	.983	.44	4.7	4.7	.16	31.6	.857	.828	.980	.44	5.3	5.3	.74	31.2	.954	.963	.993	.43	.57	6.2	6.3	.10	34.2
.843	.835	.835	.835	.877	.877	.983	.44	5.1	5.1	.27	27.8	.843	.817	.981	.44	5.3	5.3	.56	28.3	.966	.970	.979	.43	.61	6.5	6.5	.09	30.4
.841	.835	.835	.835	.877	.877	.983	.44	5.6	5.6	.28	23.5	.838	.821	.981	.44	5.0	5.0	.84	22.2	.962	.971	.969	.43	.61	6.5	6.5	.07	27.0
.841	.835	.835	.835	.877	.877	.983	.44	5.6	5.6	.18	18.6	.850	.841	.981	.44	4.9	4.9	.74	18.6	.961	.978	.972	.43	.64	6.8	6.8	.04	21.8
.841	.835	.835	.835	.877	.877	.983	.44	5.6	5.6	.23	18.6	.852	.832	.978	.44	5.6	5.6	.70	18.6	.959	.977	.984	.43	.57	6.2	6.1	.09	18.6

REPRODUCIBILITY OF THE ORIGINAL PAGE IS POOR

PT. 7-10-03  $W\sqrt{\theta/\delta} = 176.0$  lbm/sec (79.8 kg/sec)  
 $P_{16}/P_6 = 2.701$   
 $P_0 = 1530$  lbf/ft<sup>2</sup> (73,050 N/m<sup>2</sup>)  
 $T_0 = 509.6$  °R (283 K)

324

TABLE XXVIII - VELOCITY VECTOR PARAMETERS AT STATOR 1 EXIT  
(Circumferentially Distorted Inlet Flow)

FIRST STATOR EXIT CIRCUMFERENTIAL DISTRIBUTIONS - COMBO PROBE STATION 11

	86°					86°												
	P11/P0	p11/p0	90- $\beta$	M	V	V <sub>u</sub>	V <sub>w</sub>	V <sub>o</sub>	90- $\beta$	P11/P0	p11/p0	90- $\beta$	M	V	V <sub>u</sub>	V <sub>w</sub>	V <sub>o</sub>	90- $\beta$
10	1.344	1.094	91.46	.55	625.	625.	-18.	45.4		1.328	1.137	92.1	.48	547.	597.	-20.	41.5	
30	1.337	1.079	91.48	.56	637.	637.	-20.	42.6		1.351	1.122	91.1	.52	596.	596.	-11.	41.1	
50	1.296	1.064	94.46	.52	586.	584.	-37.	35.4		1.308	1.126	94.5	.47	535.	533.	-42.	34.2	
70	1.309	1.078	94.0	.53	597.	595.	-42.	34.7		1.327	1.124	92.2	.49	564.	564.	-21.	34.0	
90	1.319	1.113	91.15	.50	567.	567.	-15.	32.0		1.327	1.148	91.5	.46	527.	527.	-13.	30.3	
HR	1.320	1.092	92.46	.53	600.	599.	-27.			1.329	1.133	92.2	.48	553.	552.	-21.		

		176°					176°												
		P11/P0	p11/p0	90- $\beta$	M	V	V <sub>u</sub>	V <sub>w</sub>	V <sub>o</sub>	90- $\beta$	P11/P0	p11/p0	90- $\beta$	M	V	V <sub>u</sub>	V <sub>w</sub>	V <sub>o</sub>	90- $\beta$
10	1.315	1.102	91.3	.51	580.	580.	-13.	43.4		1.297	1.143	91.7	.43	496.	496.	-15.	39.9		
30	1.331	1.093	91.3	.54	611.	610.	-14.	41.7		1.344	1.126	89.9	.50	576.	576.	-1.	40.0		
50	1.299	1.064	94.11	.51	574.	573.	-11.	37.2		1.309	1.134	91.5	.48	539.	529.	-44.	34.9		
70	1.289	1.072	91.10	.52	589.	589.	0.	35.8		1.322	1.127	91.3	.48	550.	550.	-23.	33.9		
90	1.303	1.115	89.18	.48	544.	544.	0.	31.5		1.322	1.155	89.3	.44	508.	508.	6.	29.9		
HR	1.309	1.095	90.46	.51	577.	577.	-6.			1.320	1.149	90.4	.46	533.	533.	-4.			

		266°					266°												
		P11/P0	p11/p0	90- $\beta$	M	V	V <sub>u</sub>	V <sub>w</sub>	V <sub>o</sub>	90- $\beta$	P11/P0	p11/p0	90- $\beta$	M	V	V <sub>u</sub>	V <sub>w</sub>	V <sub>o</sub>	90- $\beta$
10	1.223	1.032	90.0	.49	554.	554.	-9.	42.8		1.188	1.097	88.1	.34	388.	388.	-13.	33.5		
30	1.224	1.021	89.3	.52	580.	580.	-7.	41.1		1.257	1.089	90.0	.46	520.	520.	0.	37.8		
50	1.194	1.016	89.1	.49	547.	548.	2.	35.6		1.247	1.094	91.2	.44	497.	497.	-10.	33.4		
70	1.200	1.014	89.6	.50	558.	558.	4.	34.4		1.263	1.093	89.2	.46	523.	523.	7.	32.9		
90	1.211	1.092	88.8	.45	512.	512.	11.	30.2		1.269	1.119	89.9	.43	487.	487.	0.	28.8		
HR	1.210	1.090	89.3	.49	547.	547.	7.			1.251	1.101	89.8	.43	493.	493.	2.			

		356°					356°												
		P11/P0	p11/p0	90- $\beta$	M	V	V <sub>u</sub>	V <sub>w</sub>	V <sub>o</sub>	90- $\beta$	P11/P0	p11/p0	90- $\beta$	M	V	V <sub>u</sub>	V <sub>w</sub>	V <sub>o</sub>	90- $\beta$
10	1.402	1.112	91.12	.59	667.	667.	-14.	47.4		1.373	1.152	91.5	.51	584.	584.	-15.	43.6		
30	1.377	1.095	91.6	.58	660.	659.	-18.	43.7		1.370	1.132	90.8	.53	606.	606.	-8.	41.7		
50	1.315	1.095	93.2	.52	590.	588.	-23.	38.7		1.300	1.135	94.2	.45	520.	519.	-38.	32.5		
70	1.313	1.092	94.2	.52	590.	590.	-44.	34.4		1.330	1.128	91.5	.49	563.	563.	-14.	34.1		
90	1.325	1.118	93.3	.50	588.	587.	-32.	31.8		1.311	1.153	91.2	.44	503.	503.	-18.	29.0		
HR	1.340	1.104	92.9	.54	613.	612.	-31.			1.337	1.141	91.9	.48	554.	554.	-18.			

PT. 7-70-01  $W\sqrt{\theta}/\delta = 123.9 \text{ lbm/sec (56.2 kg/sec)}$  $P_{16}/P_6 = 1.561$  $P_0 = 1754 \text{ lbf/ft}^2 (83,900 \text{ N/m}^2)$  $T_0 = 509.4 \text{ R (283 K)}$ PT. 7-70-02  $W\sqrt{\theta}/\delta = 113.8 \text{ lbm/sec (51.6 kg/sec)}$  $P_{16}/P_6 = 1.670$  $P_0 = 1802 \text{ lbf/ft}^2 (86,100 \text{ N/m}^2)$  $T_0 = 496.0 \text{ R (275 K)}$

TABLE XXVIII (Cont'd) - VELOCITY VECTOR PARAMETERS AT STATOR 1 EXIT  
(Circumferentially Distorted Inlet Flow)

FIRST STATOR EXIT CIRCUMFERENTIAL DISTRIBUTIONS - COMBO PROBE STATION 11

	26°					56°					86°										
	P11/P0	p11/P0	90-β*	M	V	Vm	V0 90-β*	P11/P0	p11/P0	90-β*	M	V	Vm	V0 90-β*	P11/P0	p11/P0	90-β*	M	V	Vm	V0 90-β*
10	1.330	1.167	91.2	.44	50.4	50.3	-11.39.6	1.325	1.172	91.6	.44	50.3	50.2	-9.38.2	1.327	1.162	91.5	.44	46.2	46.2	-12.37.1
30	1.343	1.181	91.7	.47	54.5	54.4	-15.38.4	1.359	1.184	90.9	.51	58.1	58.1	-9.40.5	1.352	1.149	91.0	.49	55.5	55.5	-10.39.4
50	1.316	1.149	92.1	.44	50.9	50.9	-11.33.8	1.318	1.152	93.8	.45	51.7	51.6	-35.33.5	1.322	1.134	92.2	.45	51.2	51.2	-20.33.9
70	1.327	1.162	92.8	.44	56.6	56.6	-18.31.3	1.327	1.159	90.9	.47	54.3	54.3	-9.33.3	1.341	1.147	89.0	.48	54.6	54.6	-9.34.1
90	1.328	1.170	92.8	.43	48.1	48.1	-57.24.0	1.326	1.159	99.9	.39	44.8	44.3	-77.28.6	1.316	1.175	93.1	.40	46.7	46.6	-26.27.0
MR	1.317	1.160	93.2	.43	49.5	49.4	-28.	1.319	1.147	94.2	.45	51.9	51.7	-38.	1.327	1.158	91.4	.44	51.1	51.1	-13.

	116°					146°					176°										
	P11/P0	p11/P0	90-β*	M	V	Vm	V0 90-β*	P11/P0	p11/P0	90-β*	M	V	Vm	V0 90-β*	P11/P0	p11/P0	90-β*	M	V	Vm	V0 90-β*
10	1.333	1.152	92.5	.45	51.6	51.6	-23.39.6	1.319	1.153	92.4	.44	50.9	50.8	-21.39.4	1.284	1.120	92.9	.38	44.2	44.1	-16.38.7
30	1.335	1.136	91.2	.45	57.3	57.3	-12.39.9	1.345	1.137	91.2	.50	56.6	56.6	-11.39.7	1.345	1.121	92.9	.48	54.6	54.6	-9.38.8
50	1.315	1.143	93.6	.45	51.8	51.8	-33.33.6	1.318	1.146	93.5	.48	51.6	51.6	-32.33.7	1.321	1.121	90.0	.45	51.3	51.3	-18.28.9
70	1.336	1.170	91.1	.48	55.0	55.0	-11.33.5	1.334	1.139	90.9	.48	54.9	54.9	-9.33.7	1.337	1.149	89.0	.47	53.8	53.8	-7.33.6
90	1.318	1.154	95.5	.43	49.0	48.1	-47.27.4	1.319	1.165	94.5	.42	48.8	48.6	-38.27.7	1.325	1.174	91.3	.42	48.1	48.1	-14.
MR	1.322	1.148	92.9	.46	52.8	52.8	-27.	1.327	1.149	92.6	.46	52.5	52.4	-26.	1.325	1.168	91.0	.44	50.7	50.7	-19.

	206°					236°					266°										
	P11/P0	p11/P0	90-β*	M	V	Vm	V0 90-β*	P11/P0	p11/P0	90-β*	M	V	Vm	V0 90-β*	P11/P0	p11/P0	90-β*	M	V	Vm	V0 90-β*
10	1.304	1.149	92.1	.43	49.3	49.2	-18.38.5	1.254	1.148	90.7	.36	41.2	41.2	-5.34.4	1.186	1.126	95.8	.27	31.5	31.3	-32.26.5
30	1.337	1.133	91.0	.49	56.1	56.1	-10.39.5	1.322	1.140	91.4	.46	53.1	53.1	-13.37.8	1.247	1.103	93.0	.42	48.1	48.0	-25.34.6
50	1.316	1.143	93.5	.45	51.2	51.1	-32.33.4	1.305	1.143	90.9	.44	50.5	50.5	-8.33.9	1.256	1.114	94.8	.41	47.4	47.3	-4.31.1
70	1.327	1.138	91.1	.48	54.4	54.4	-11.33.4	1.324	1.139	89.1	.47	53.6	53.6	-9.33.6	1.249	1.108	93.4	.42	47.7	47.6	-29.29.5
90	1.318	1.161	94.4	.43	49.3	49.1	-37.28.0	1.312	1.166	90.9	.42	47.7	47.7	-7.28.1	1.239	1.126	101.1	.37	42.6	41.8	-82.23.3
MR	1.320	1.145	92.6	.45	52.1	52.0	-23.	1.308	1.149	90.5	.43	49.9	49.8	-5.	1.240	1.115	98.0	.39	44.9	44.6	-47.

	296°					326°					356°										
	P11/P0	p11/P0	90-β*	M	V	Vm	V0 90-β*	P11/P0	p11/P0	90-β*	M	V	Vm	V0 90-β*	P11/P0	p11/P0	90-β*	M	V	Vm	V0 90-β*
10	1.173	1.146	92.3	.48	21.2	21.2	-8.19.7	1.210	1.152	93.2	.39	44.8	44.7	-25.35.7	1.357	1.149	97.0	.44	50.6	50.2	-6.37.2
30	1.292	1.140	95.9	.38	44.3	44.1	-46.31.7	1.362	1.171	91.1	.47	54.3	54.3	-10.38.6	1.355	1.155	92.9	.48	55.5	55.2	-28.38.4
50	1.229	1.146	95.8	.42	48.4	48.1	-49.21.2	1.337	1.170	91.0	.44	51.0	51.0	-9.33.2	1.298	1.130	94.1	.42	48.5	48.3	-35.31.8
70	1.301	1.155	95.8	.41	47.9	47.7	-48.21.8	1.349	1.165	89.1	.46	53.6	53.6	-9.33.6	1.308	1.143	91.3	.44	51.0	51.0	-12.31.6
90	1.229	1.152	97.1	.39	44.9	44.5	-56.25.2	1.288	1.166	100.5	.34	40.2	39.6	-73.22.4	1.257	1.157	101.8	.34	40.0	39.2	-82.22.0
MR	1.279	1.140	96.0	.41	47.3	47.1	-49.	1.330	1.174	93.0	.43	49.3	49.3	-26.	1.313	1.158	95.5	.43	49.3	49.1	-47.

PT. 7-70-13 W $\sqrt{\theta/\delta}$  = 106.6 lbm/sec (48.3 kg/sec)

P<sub>16</sub>/P<sub>6</sub> = 1.692

P<sub>0</sub> = 1868 lbf/ft<sup>2</sup> (89,200 N/m<sup>2</sup>)

T<sub>0</sub> = 512.5°R (284 K)

TABLE XXVIII (Cont'd) - VELOCITY VECTOR PARAMETERS AT STATOR 1 EXIT  
(Circumferentially Distorted Inlet Flow)

FIRST STATOR EXIT CIRCUMFERENTIAL DISTRIBUTIONS - COMBO PROBE STATION 11

86°					86°					86°														
P <sub>11</sub> /P <sub>0</sub>	p <sub>11</sub> /P <sub>0</sub>	90-β°	M	V	V <sub>m</sub>	V <sub>0-90</sub>	90-β°	M	V	V <sub>m</sub>	V <sub>0-90</sub>	90-β°	M	V	V <sub>m</sub>	V <sub>0-90</sub>	90-β°							
10	1.468	1.209	92.1	65	753	752	-27	43.3	1.463	1.270	92.7	45	534	534	-25	33.8	1.469	1.275	93.8	70	820	818	-51	82.0
30	1.457	1.178	91.9	66	761	760	-25	40.5	1.454	1.228	93.5	60	695	693	-42	37.4	1.472	1.223	92.3	72	834	834	-34	40.0
50	1.439	1.158	92.5	64	738	737	-32	36.6	1.454	1.220	94.0	37	666	665	-47	33.4	1.455	1.157	95.4	66	774	770	-73	34.1
70	1.450	1.225	92.5	66	762	762	-34	35.0	1.458	1.229	90.9	61	715	715	-12	33.9	1.482	1.132	92.5	74	847	846	-37	35.1
90	1.483	1.204	91.2	64	737	736	-16	32.4	1.461	1.222	90.9	59	685	685	-10	30.6	1.479	1.151	91.4	73	837	837	-21	32.9
MR	1.472	1.174	91.9	65	749	748	-25		1.455	1.232	92.1	58	673	673	-25	30	1.472	1.192	92.8	71	826	825	-40	
176°					176°					176°														
10	1.456	1.168	94.3	59	689	687	-51	40.2	1.444	1.224	94.8	51	596	594	-50	36.1	1.454	1.225	94.7	58	684	682	-80	36.0
30	1.454	1.152	92.8	65	747	746	-38	39.9	1.450	1.240	92.7	61	702	701	-33	36.3	1.474	1.237	94.2	67	781	779	-57	37.4
50	1.439	1.134	92.1	64	734	733	-27	37.0	1.454	1.223	92.5	60	689	689	-30	35.1	1.481	1.222	90.6	72	828	828	-9	37.7
70	1.430	1.150	90.4	70	822	822	-6	37.8	1.456	1.238	91.4	62	715	715	-18	34.0	1.489	1.126	94.1	72	828	826	-59	33.9
90	1.450	1.181	90.6	65	746	745	-8	33.2	1.456	1.236	89.7	60	701	701	-4	31.8	1.445	1.078	89.0	80	912	912	-16	36.0
MR	1.424	1.144	91.8	65	747	747	-23		1.458	1.235	91.8	59	682	688	-21		1.465	1.144	92.3	72	830	830	-33	
266°					266°					266°														
10	1.424	1.060	89.9	67	658	658	1	40.5	1.424	1.154	88.9	24	285	285	5	20.4	1.439	1.089	92.0	58	675	675	-24	37.5
30	1.431	1.031	89.6	64	726	726	5	40.2	1.449	1.174	93.2	56	643	642	-36	35.5	1.458	1.074	90.3	65	772	772	-4	38.7
50	1.437	1.000	89.3	63	712	712	9	38.8	1.447	1.155	93.9	54	627	628	-42	32.6	1.484	1.021	90.1	67	768	768	-2	35.8
70	1.437	1.030	88.5	65	736	736	19	35.5	1.447	1.152	90.7	59	685	685	-8	32.9	1.475	1.053	89.9	74	839	839	1	35.7
90	1.459	1.012	86.2	66	747	745	80	34.2	1.451	1.127	91.4	56	648	647	-5	29.3	1.426	1.018	88.8	71	808	808	17	32.8
MR	1.437	1.016	88.9	64	723	722	21		1.442	1.149	91.6	60	688	687	-19		1.437	1.025	90.0	69	783	783	0	
356°					356°					356°														
10	1.483	1.242	92.8	67	785	784	-38	44.4	1.461	1.315	93.9	55	646	645	-44	38.0	1.479	1.282	94.7	70	826	824	-67	41.7
30	1.450	1.190	92.9	68	786	785	-40	41.3	1.446	1.259	90.8	60	706	706	-10	39.2	1.479	1.240	92.2	72	844	843	-32	40.3
50	1.457	1.166	92.7	66	786	785	-38	37.5	1.457	1.252	91.5	58	684	684	-18	38.1	1.460	1.174	92.9	69	808	807	-41	36.1
70	1.436	1.140	93.1	67	767	766	-42	35.3	1.457	1.278	89.9	62	729	729	1	35.0	1.469	1.130	93.6	73	838	837	-53	34.4
90	1.452	1.144	92.2	64	740	739	-28	32.5	1.481	1.328	90.0	59	698	698	0	31.8	1.451	1.178	92.1	71	821	820	-30	32.2
MR	1.459	1.183	92.7	65	764	764	-36		1.449	1.303	91.0	59	694	694	-12		1.485	1.201	93.0	71	827	826	-43	

PT. 7-90-01  $W\sqrt{\theta}/\delta = 167.4 \text{ lbf}/\text{sec} (75.9 \text{ kg}/\text{sec})$   
 $P_{16}/P_6 = 1.994$   
 $P_0 = 1575 \text{ lbf}/\text{ft}^2 (75,300 \text{ N}/\text{m}^2)$   
 $T_0 = 509.2 \text{ R} (283 \text{ K})$

PT. 7-90-02  $W\sqrt{\theta}/\delta = 148.8 \text{ lbf}/\text{sec} (67.4 \text{ kg}/\text{sec})$   
 $P_{16}/P_6 = 2.324$   
 $P_0 = 1643 \text{ lbf}/\text{ft}^2 (78,600 \text{ N}/\text{m}^2)$   
 $T_0 = 509.8 \text{ R} (283 \text{ K})$

PT. 7-10-31  $W\sqrt{\theta}/\delta = 185.0 \text{ lbf}/\text{sec} (83.8 \text{ kg}/\text{sec})$   
 $P_{16}/P_6 = 2.180$   
 $P_0 = 1481 \text{ lbf}/\text{ft}^2 (70,800 \text{ N}/\text{m}^2)$   
 $T_0 = 503.2 \text{ R} (279 \text{ K})$

TABLE XXVIII (Cont'd) - VELOCITY VECTOR PARAMETERS AT STATOR 1 EXIT  
(Circumferentially Distorted Inlet Flow)

FIRST STATOR EXIT CIRCUMFERENTIAL DISTRIBUTIONS - COMBO PROBE STATION 11

	P11/P0	p11/P0	90-β°	M	V	Vm	Vθ	90-β°		P11/P0	p11/P0	90-β°	M	V	Vm	Vθ	90-β°		P11/P0	p11/P0	90-β°	M	V	Vm	Vθ	90-β°
	26°																									
10	1.484	1.235	93.7	.39	467.	466.	.30	30.4	1.434	1.291	90.5	.39	463.	463.	.44	31.1	1.422	1.291	91.7	.37	445.	445.	.13	29.7		
30	1.439	1.231	97.2	.48	566.	561.	.71	31.1	1.49b	1.273	95.3	.48	573.	569.	.62	31.8	1.549	1.270	95.0	.54	635.	632.	.58	34.7		
50	1.400	1.211	93.6	.54	641.	640.	.40	32.8	1.511	1.269	97.5	.51	597.	592.	.78	32.0	1.581	1.267	94.8	.54	638.	636.	.51	32.7		
70	1.445	1.236	92.3	.58	690.	689.	.27	32.8	1.578	1.275	94.0	.58	662.	661.	.46	31.3	1.601	1.286	90.9	.60	705.	704.	.12	32.7		
90	1.451	1.242	94.8	.56	660.	658.	.55	28.9	1.576	1.281	98.5	.54	641.	634.	.95	27.3	1.635	1.306	91.2	.58	676.	676.	.14	30.4		
MR	1.460	1.242	94.3	.53	630.	628.	.47.		1.534	1.280	96.0	.51	608.	605.	.64.		1.575	1.280	92.5	.55	649.	648.	.28.	30		
	56°																									
10	1.444	1.241	92.6	.42	492.	492.	.22	31.9	1.442	1.269	93.6	.43	508.	507.	.32	32.5	1.442	1.283	94.5	.43	509.	507.	.40	32.2		
30	1.554	1.249	93.6	.57	666.	665.	.42	36.4	1.584	1.235	92.3	.61	704.	703.	.28	38.5	1.598	1.267	92.0	.60	691.	690.	.24	38.0		
50	1.554	1.257	94.6	.56	653.	651.	.52	32.9	1.570	1.248	92.9	.58	677.	676.	.35	34.5	1.570	1.248	92.1	.58	677.	677.	.28	34.7		
70	1.597	1.251	91.7	.60	703.	702.	.21	33.3	1.590	1.235	91.0	.61	713.	713.	.13	34.0	1.590	1.241	90.4	.61	705.	705.	.10	33.7		
90	1.630	1.285	90.9	.58	683.	683.	.11	30.7	1.618	1.245	90.6	.58	682.	682.	.8	30.8	1.628	1.291	89.4	.58	680.	680.	.7	31.0		
MR	1.575	1.269	92.4	.58	660.	659.	.28		1.577	1.287	91.8	.58	675.	674.	.21.		1.580	1.269	91.3	.57	670.	670.	.15.			
	86°																									
10	1.444	1.241	92.6	.42	492.	492.	.22	31.9	1.442	1.269	93.6	.43	508.	507.	.32	32.5	1.442	1.283	94.5	.43	509.	507.	.40	32.2		
30	1.554	1.249	93.6	.57	666.	665.	.42	36.4	1.584	1.235	92.3	.61	704.	703.	.28	38.5	1.598	1.267	92.0	.60	691.	690.	.24	38.0		
50	1.554	1.257	94.6	.56	653.	651.	.52	32.9	1.570	1.248	92.9	.58	677.	676.	.35	34.5	1.570	1.248	92.1	.58	677.	677.	.28	34.7		
70	1.597	1.251	91.7	.60	703.	702.	.21	33.3	1.590	1.235	91.0	.61	713.	713.	.13	34.0	1.590	1.241	90.4	.61	705.	705.	.10	33.7		
90	1.630	1.285	90.9	.58	683.	683.	.11	30.7	1.618	1.245	90.6	.58	682.	682.	.8	30.8	1.628	1.291	89.4	.58	680.	680.	.7	31.0		
MR	1.575	1.269	92.4	.58	660.	659.	.28		1.577	1.287	91.8	.58	675.	674.	.21.		1.580	1.269	91.3	.57	670.	670.	.15.			
	116°																									
10	1.444	1.241	92.6	.42	492.	492.	.22	31.9	1.442	1.269	93.6	.43	508.	507.	.32	32.5	1.442	1.283	94.5	.43	509.	507.	.40	32.2		
30	1.554	1.249	93.6	.57	666.	665.	.42	36.4	1.584	1.235	92.3	.61	704.	703.	.28	38.5	1.598	1.267	92.0	.60	691.	690.	.24	38.0		
50	1.554	1.257	94.6	.56	653.	651.	.52	32.9	1.570	1.248	92.9	.58	677.	676.	.35	34.5	1.570	1.248	92.1	.58	677.	677.	.28	34.7		
70	1.597	1.251	91.7	.60	703.	702.	.21	33.3	1.590	1.235	91.0	.61	713.	713.	.13	34.0	1.590	1.241	90.4	.61	705.	705.	.10	33.7		
90	1.630	1.285	90.9	.58	683.	683.	.11	30.7	1.618	1.245	90.6	.58	682.	682.	.8	30.8	1.628	1.291	89.4	.58	680.	680.	.7	31.0		
MR	1.575	1.269	92.4	.58	660.	659.	.28		1.577	1.287	91.8	.58	675.	674.	.21.		1.580	1.269	91.3	.57	670.	670.	.15.			
	146°																									
10	1.444	1.241	92.6	.42	492.	492.	.22	31.9	1.442	1.269	93.6	.43	508.	507.	.32	32.5	1.442	1.283	94.5	.43	509.	507.	.40	32.2		
30	1.554	1.249	93.6	.57	666.	665.	.42	36.4	1.584	1.235	92.3	.61	704.	703.	.28	38.5	1.598	1.267	92.0	.60	691.	690.	.24	38.0		
50	1.554	1.257	94.6	.56	653.	651.	.52	32.9	1.570	1.248	92.9	.58	677.	676.	.35	34.5	1.570	1.248	92.1	.58	677.	677.	.28	34.7		
70	1.597	1.251	91.7	.60	703.	702.	.21	33.3	1.590	1.235	91.0	.61	713.	713.	.13	34.0	1.590	1.241	90.4	.61	705.	705.	.10	33.7		
90	1.630	1.285	90.9	.58	683.	683.	.11	30.7	1.618	1.245	90.6	.58	682.	682.	.8	30.8	1.628	1.291	89.4	.58	680.	680.	.7	31.0		
MR	1.575	1.269	92.4	.58	660.	659.	.28		1.577	1.287	91.8	.58	675.	674.	.21.		1.580	1.269	91.3	.57	670.	670.	.15.			
	176°																									
10	1.444	1.241	92.6	.42	492.	492.	.22	31.9	1.442	1.269	93.6	.43	508.	507.	.32	32.5	1.442	1.283	94.5	.43	509.	507.	.40	32.2		
30	1.554	1.249	93.6	.57	666.	665.	.42	36.4	1.584	1.235	92.3	.61	704.	703.	.28	38.5	1.598	1.267	92.0	.60	691.	690.	.24	38.0		
50	1.554	1.257	94.6	.56	653.	651.	.52	32.9	1.570	1.248	92.9	.58	677.	676.	.35	34.5	1.570	1.248	92.1	.58	677.	677.	.28	34.7		
70	1.597	1.251	91.7	.60	703.	702.	.21	33.3	1.590	1.235	91.0	.61	713.	713.	.13	34.0	1.590	1.241	90.4	.61	705.	705.	.10	33.7		
90	1.630	1.285	90.9	.58	683.	683.	.11	30.7	1.618	1.245	90.6	.58	682.	682.	.8	30.8	1.628	1.291	89.4	.58	680.	680.	.7	31.0		
MR	1.575	1.269	92.4	.58	660.	659.	.28		1.577	1.287	91.8	.58	675.	674.	.21.		1.580	1.269	91.3	.57	670.	670.	.15.			
	206°																									
10	1.444	1.241	92.6	.42	492.	492.	.22	31.9	1.442	1.269	93.6	.43	508.	507.	.32	32.5	1.442	1.283	94.5	.43	509.	507.	.40	32.2		
30	1.554	1.249	93.6	.57	666.	665.	.42	36.4	1.584	1.235	92.3	.61	704.	703.	.28	38.5	1.598	1.267	92.0	.60	691.	690.	.24	38.0		
50	1.554	1.257	94.6	.56	653.	651.	.52	32.9	1.570	1.248	92.9	.58	677.	676.	.35	34.5	1.570	1.248	92.1	.58	677.	677.	.28	34.7		
70	1.597	1.251	91.7	.60	703.	702.	.21	33.3	1.590	1.235	91.0	.61	713.	713.	.13	34.0	1.590	1.241	90.4	.61	705.	705.	.10	33.7		
90	1.630	1.285	90.9	.58	683.	683.	.11	30.7	1.618	1.245	90.6	.58	682.	682.	.8	30.8	1.628	1.291	89.4	.58	680.	680.	.7	31.0		
MR	1.575	1.269	92.4	.58	660.	659.	.28		1.577	1.287	91.8	.58	675.	674.	.21.		1.580	1.269	91.3	.57	670.	670.	.15.			
	236°																									
10	1.444	1.241	92.6	.42	492.	492.	.22	31.9	1.442	1.269	93.6	.43	508.	507.	.32	32.5	1.442	1.283	94.5	.43	509.	507.	.40	32.2		
30	1.554	1.249	93.6	.57	666.	665.	.42	36.4	1.584	1.235	92.3	.61	704.	703.	.28	38.5	1.598	1.267	92.0	.60	691.	690.	.24	38.0		
50	1.554	1.257	94.6	.56	653.	651.	.52	32.9	1.570	1.248	92.9	.58	677.	676.	.35	34.5	1.570	1.248	92.1	.58	677.	677.	.28	34.7		
70	1.597	1.251	91.7	.60	703.	702.	.21	33.3	1.590	1.235	91.0	.61	713.	713.	.13	34.0	1.590	1.241	90.4	.61	705.	705.	.10	33.7		
90	1.630	1.285	90.9	.58	683.	683.	.11	30.7	1.618	1.245	90.6	.58	682.	682.	.8	30.8	1.628	1.291	89.4	.58	680.	680.	.7	31.0		
MR	1.575	1.269	92.4	.58	660.	659.	.28		1.577	1.287	91.8	.58	675.	674.	.21.		1.580	1.269	91.3	.57	670.	670.	.15.			
	266°																									
10	1.444	1.241	92.6	.42	492.	492.	.22	31.9	1.442	1.269	93.6	.43	508.	507.	.32	32.5</										



TABLE XXVIII (Cont'd) - VELOCITY VECTOR PARAMETERS AT STATOR 1 EXIT  
(Circumferentially Distorted Inlet Flow)

FIRST STATOR EXIT CIRCUMFERENTIAL DISTRIBUTIONS - COMBO PROBE STATION 13

	$P_{11}/P_0$	$p_{11}/P_0$	$90-\beta^*$	M	V	$V_m$	$V_0$	$90-\beta^*$	$P_{11}/P_0$	$p_{11}/P_0$	$90-\beta^*$	M	V	$V_m$	$V_0$	$90-\beta^*$	$P_{11}/P_0$	$p_{11}/P_0$	$90-\beta^*$	M	V	$V_m$	$V_0$	$90-\beta^*$
	26°								56°								86°							
10	1.775	1.254	94.8	.70	820.	817.	83.	41.8	1.763	1.255	93.4	.69	858.	864.	88.	41.7	1.703	1.257	95.5	.67	790.	788.	78.	40.2
30	1.833	1.314	91.9	.71	832.	831.	28.	40.2	1.787	1.283	91.0	.72	841.	841.	14.	40.7	1.730	1.258	92.9	.69	808.	804.	41.	38.9
50	1.928	1.372	86.5	.63	732.	728.	83.	32.5	1.867	1.374	85.0	.66	768.	764.	77.	33.8	1.553	1.144	94.3	.68	788.	783.	89.	38.0
70	1.825	1.116	92.5	.75	865.	864.	38.	35.8	1.822	1.144	92.9	.72	836.	835.	43.	34.5	1.621	1.149	94.1	.72	829.	827.	89.	34.1
90	1.644	1.159	92.1	.72	835.	835.	30.	32.8	1.466	1.194	92.0	.71	817.	817.	28.	32.1	1.672	1.083	89.0	.81	928.	918.	16.	36.6
MR	1.688	1.233	93.2	.71	823.	822.	46.		1.675	1.206	92.8	.70	817.	816.	40.		1.659	1.144	92.5	.73	843.	842.	37.	
	116°								146°								176°							
10	1.695	1.249	94.8	.68	794.	791.	84.	40.8	1.619	1.222	95.1	.65	766.	763.	88.	39.7	1.558	1.220	99.0	.60	709.	707.	81.	37.7
30	1.717	1.222	92.2	.71	831.	830.	33.	40.0	1.696	1.212	92.5	.71	829.	828.	37.	39.9	1.674	1.237	94.4	.67	783.	781.	80.	37.5
50	1.800	1.169	93.6	.69	799.	797.	50.	35.7	1.610	1.168	92.3	.69	811.	811.	32.	36.7	1.589	1.179	93.1	.67	777.	776.	42.	35.1
70	1.621	1.141	92.7	.73	838.	837.	40.	34.8	1.613	1.137	92.7	.72	842.	841.	40.	35.1	1.590	1.027	90.1	.82	930.	930.	2.	38.5
90	1.672	1.192	91.2	.71	823.	823.	17.	32.7	1.655	1.186	91.5	.71	823.	822.	21.	32.7	1.649	1.193	92.1	.70	805.	804.	29.	31.8
MR	1.682	1.193	92.6	.70	819.	818.	38.		1.641	1.184	92.6	.70	817.	817.	37.		1.618	1.168	92.7	.70	810.	809.	38.	
	206°								236°								266°							
10	1.574	1.144	94.6	.64	749.	747.	80.	39.3	1.507	1.185	94.0	.60	700.	698.	89.	37.8	1.499	1.074	93.4	.63	723.	722.	43.	38.8
30	1.668	1.190	92.2	.71	821.	820.	32.	39.7	1.628	1.143	90.6	.73	840.	840.	9.	40.9	1.667	1.058	90.7	.70	795.	795.	10.	39.4
50	1.598	1.156	91.7	.67	804.	803.	24.	36.6	1.533	1.082	90.2	.72	833.	833.	4.	37.9	1.405	1.038	91.3	.67	768.	768.	18.	35.5
70	1.890	1.117	93.0	.73	836.	835.	44.	34.7	1.547	1.080	93.2	.73	839.	838.	47.	34.6	1.388	.999	91.6	.70	796.	796.	23.	33.9
90	1.643	1.163	91.1	.72	822.	822.	16.	32.7	1.604	1.047	88.9	.60	913.	913.	17.	36.0	1.444	1.042	90.1	.70	790.	790.	1.	31.9
MR	1.618	1.164	92.3	.70	811.	811.	33.		1.571	1.096	91.0	.74	845.	845.	14.		1.423	1.001	91.2	.68	779.	779.	18.	
	296°								326°								356°							
10	1.236	1.055	95.8	.48	565.	563.	57.	31.7	1.663	1.251	98.1	.65	774.	767.	103.	38.6	1.798	1.299	94.2	.70	829.	821.	80.	41.9
30	1.428	1.164	93.3	.67	779.	778.	45.	37.9	1.640	1.178	93.5	.72	850.	849.	52.	40.2	1.778	1.251	92.0	.72	840.	839.	30.	40.3
50	1.382	1.027	93.5	.67	773.	771.	47.	34.9	1.580	1.126	92.5	.71	845.	844.	37.	37.7	1.661	1.202	92.0	.70	814.	813.	28.	36.7
70	1.397	.974	92.3	.74	850.	850.	34.	35.4	1.615	1.148	94.4	.72	849.	848.	55.	34.7	1.638	1.160	92.9	.72	834.	833.	43.	34.8
90	1.446	.993	89.7	.77	881.	881.	5.	34.9	1.711	1.017	91.1	.89	1035.	1034.	20.	38.9	1.640	1.207	91.5	.71	820.	820.	21.	32.4
MR	1.407	1.015	92.2	.70	809.	808.	31.		1.661	1.119	93.4	.77	903.	901.	54.		1.706	1.221	92.4	.71	826.	825.	34.	

PT. 7-10-02  $W\sqrt{\theta/\delta} = 184.6 \text{ lbm/sec (83.7 kg/sec)}$   
 $P_{16}/P_0 = 2.494$   
 $P_0 = 1488 \text{ lbf/ft}^2 (71,000 \text{ N/m}^2)$   
 $T_0 = 500.4^\circ \text{R (278}^\circ \text{K)}$

TABLE XXVIII (Cont'd) - VELOCITY VECTOR PARAMETERS AT STATOR 1 EXIT  
(Circumferentially Distorted Inlet Flow)

FIRST STATOR EXIT CIRCUMFERENTIAL DISTRIBUTIONS - COMBO PROBE STATION 11

	P11/P0	p11/P0	90-β°	M	V	Vn	V0	90-β°		P11/P0	p11/P0	90-β°	M	V	Vn	V0	90-β°		P11/P0	p11/P0	90-β°	M	V	Vn	V0	90-β°
	26°									56°									86°							
10	1.688	1.334	95.2	0.53	635.	632.	0.58	34.9	1.609	1.352	102.6	0.50	603.	589.	-13.	32.3	1.556	1.281	92.0	0.54	644.	644.	-22.	36.3		
30	1.786	1.403	93.1	0.60	714.	713.	-38.	35.7	1.699	1.444	98.4	0.59	695.	688.	-10.	34.4	1.733	1.492	92.8	0.66	773.	772.	-58.	37.8		
50	1.764	1.376	94.8	0.61	727.	724.	-61.	33.0	1.706	1.367	93.8	0.63	742.	740.	-49.	35.2	1.664	1.428	94.6	0.62	726.	724.	-58.	32.9		
70	1.821	1.477	86.7	0.73	867.	865.	0.	38.0	1.832	1.466	95.1	0.61	727.	724.	-65.	32.0	1.684	1.474	87.8	0.74	857.	857.	-33.	37.1		
90	1.873	1.528	85.6	0.72	849.	847.	-6.	35.3	1.848	1.461	94.0	0.63	742.	740.	-52.	32.7	1.734	1.428	87.6	0.69	804.	803.	-33.	33.1		
MR	1.840	1.446	89.9	0.66	786.	786.	1.		1.791	1.462	85.5	0.69	813.	812.	-21.		1.689	1.427	90.4	0.66	776.	775.	-8.			
	116°									146°									176°							
10	1.584	1.202	94.6	0.59	694.	692.	-56.	37.3	1.574	1.242	94.9	0.59	696.	694.	-60.	37.3	1.542	1.256	95.2	0.58	654.	651.	-6.	36.6		
30	1.731	1.257	91.1	0.69	804.	804.	-16.	39.6	1.732	1.245	91.6	0.70	814.	814.	-23.	39.8	1.708	1.292	94.5	0.64	752.	750.	-58.	36.6		
50	1.671	1.248	92.0	0.66	771.	770.	-27.	35.3	1.659	1.230	91.4	0.67	779.	779.	-19.	35.9	1.641	1.292	94.1	0.69	803.	803.	-2.	34.3		
70	1.671	1.211	91.3	0.69	808.	808.	-19.	34.4	1.654	1.194	92.0	0.70	808.	808.	-29.	34.2	1.644	1.175	92.7	0.71	821.	820.	-39.	34.4		
90	1.726	1.259	90.6	0.68	791.	790.	-8.	31.8	1.707	1.242	91.0	0.69	799.	799.	-13.	32.1	1.710	1.217	90.2	0.71	826.	826.	-3.	33.2		
MR	1.686	1.249	91.6	0.67	781.	781.	-22.		1.674	1.232	91.9	0.68	788.	787.	-27.		1.653	1.223	92.1	0.68	787.	787.	-29.			
	206°									236°									266°							
10	1.552	1.227	94.9	0.59	693.	690.	-59.	37.2	1.522	1.231	94.4	0.56	656.	654.	-51.	36.1	1.376	1.171	93.4	0.49	570.	569.	-34.	32.7		
30	1.714	1.239	91.4	0.70	811.	811.	-20.	39.8	1.668	1.227	91.1	0.67	780.	780.	-15.	38.9	1.541	1.149	90.9	0.66	759.	759.	-12.	38.1		
50	1.643	1.216	91.2	0.67	779.	779.	-16.	36.0	1.602	1.192	91.1	0.66	771.	770.	-15.	35.8	1.500	1.192	92.7	0.63	729.	728.	-34.	33.6		
70	1.651	1.182	92.2	0.71	818.	818.	-32.	34.5	1.608	1.113	90.1	0.74	855.	855.	-2.	36.5	1.300	1.134	93.5	0.65	744.	743.	-46.	31.6		
90	1.705	1.225	91.0	0.70	813.	813.	-14.	32.5	1.676	1.237	91.6	0.67	781.	780.	-22.	31.4	1.554	1.164	90.2	0.66	756.	756.	-3.	30.7		
MR	1.664	1.218	91.9	0.68	793.	793.	-26.		1.626	1.201	91.8	0.67	780.	779.	-21.		1.511	1.154	91.8	0.63	730.	730.	-23.			
	296°									326°									356°							
10	1.583	1.276	114.9	0.53	604.	604.	-44.	61.0	1.551	1.225	104.8	0.16	192.	186.	-49.	11.7	1.712	1.472	98.2	0.47	573.	570.	-62.	32.0		
30	1.533	1.248	92.6	0.65	806.	808.	-98.	31.8	1.492	1.242	100.5	0.37	458.	450.	-84.	23.6	1.728	1.440	96.4	0.48	580.	577.	-65.	29.8		
50	1.618	1.274	95.6	0.59	707.	703.	-69.	31.9	1.583	1.244	98.5	0.53	644.	637.	-95.	29.0	1.615	1.468	96.3	0.56	681.	677.	-74.	30.9		
70	1.506	1.244	94.2	0.62	732.	730.	-64.	31.0	1.548	1.249	93.1	0.62	764.	763.	-42.	32.4	1.929	1.430	92.5	0.67	802.	802.	-36.	34.6		
90	1.677	1.303	92.4	0.61	728.	728.	-31.	29.3	1.698	1.252	90.6	0.67	816.	816.	-9.	32.7	1.948	1.431	91.9	0.68	814.	814.	-27.	34.9		
MR	1.599	1.264	96.0	0.69	810.	803.	-84.		1.590	1.209	94.7	0.61	744.	742.	-61.		1.975	1.455	90.0	0.68	809.	809.	-1.			

PT. 7-10-03  $W\sqrt{\theta/\delta} = 176.0$  lbm/sec (79.8 kg/sec)  
 $P_{16}/P_6 = 2.701$   
 $P_0 = 1530$  lbf/ft<sup>2</sup> (73,050 N/m<sup>2</sup>)  
 $T_0 = 509.6$  °R (283 °K)

TABLE XXIX - VELOCITY VECTOR PARAMETERS AT FAN EXIT  
(Circumferentially Distorted Inlet Flow)

SECOND STATOR EXIT CIRCUMFERENTIAL DISTRIBUTIONS - WEDGE PROBE STATION 16

	P16/P0	p16/P0	90-β°	M	V	V <sub>u</sub>	V <sub>o</sub>	90-β°												
43°																				
10	1.589	1.180	90.0	.67	787.	787.	0.	90.7												
30	1.679	1.155	91.1	.75	868.	868.	-17.	90.4												
50	1.564	1.170	92.3	.66	761.	761.	-30.	89.0												
70	1.525	1.173	93.5	.62	724.	723.	-44.	89.1												
90	1.540	1.173	90.3	.64	742.	742.	-33.	89.3												
MR	1.579	1.170	91.5	.67	779.	779.	-20.													
133°																				
10	1.622	1.189	89.9	.69	810.	810.	2.	91.5												
30	1.662	1.159	90.9	.74	849.	849.	-13.	90.0												
50	1.546	1.170	91.8	.64	744.	744.	-3.	89.0												
70	1.510	1.171	93.0	.61	709.	708.	-37.	89.8												
90	1.524	1.174	90.4	.62	721.	721.	-5.	89.5												
MR	1.572	1.171	91.1	.66	769.	768.	-15.													
226°																				
10	1.465	1.250	96.5	.65	774.	769.	-87.	86.8												
30	1.672	1.239	98.8	.67	783.	773.	-120.	83.8												
50	1.534	1.225	99.6	.58	676.	666.	-113.	87.6												
70	1.504	1.221	100.3	.55	646.	636.	-115.	84.5												
90	1.511	1.222	96.3	.56	658.	654.	-73.	84.8												
MR	1.573	1.230	98.3	.60	708.	701.	-103.													
316°																				
10	1.264	1.267	94.2	.66	778.	772.	-70.	87.7												
30	1.458	1.232	97.7	.67	778.	768.	-104.	84.0												
50	1.545	1.221	98.8	.59	687.	681.	-103.	84.8												
70	1.577	1.217	99.8	.57	662.	653.	-112.	85.3												
90	1.534	1.221	94.8	.58	680.	678.	-87.	86.3												
MR	1.580	1.228	97.8	.61	715.	709.	-90.													
43°																				
10	1.439	1.406	87.8	.63	751.	751.	32.	90.8												
30	1.725	1.404	90.5	.55	655.	655.	-6.	89.9												
50	1.521	1.403	90.4	.46	551.	551.	-3.	89.9												
70	1.420	1.401	90.9	.46	552.	552.	-9.	89.9												
90	1.620	1.405	88.2	.46	549.	549.	17.	89.8												
MR	1.489	1.404	89.5	.52	623.	623.	6.													
133°																				
10	1.831	1.409	87.8	.62	741.	741.	29.	90.4												
30	1.724	1.405	90.4	.55	651.	651.	-5.	89.9												
50	1.524	1.402	90.3	.46	551.	551.	-3.	89.9												
70	1.420	1.401	91.1	.46	552.	552.	-11.	89.8												
90	1.620	1.405	88.1	.46	549.	549.	18.	89.8												
MR	1.689	1.404	89.5	.52	620.	620.	5.													
226°																				
10	1.402	1.445	94.8	.57	684.	684.	-57.	84.6												
30	1.715	1.428	97.4	.52	620.	615.	-8.	88.6												
50	1.525	1.429	98.2	.44	521.	519.	-7.	89.2												
70	1.511	1.423	98.4	.43	511.	506.	-7.	89.8												
90	1.620	1.428	95.9	.43	528.	524.	-5.	89.6												
MR	1.671	1.429	97.4	.48	575.	571.	-7.													
316°																				
10	1.747	1.441	94.5	.53	640.	638.	-5.	89.1												
30	1.684	1.432	97.3	.49	600.	598.	-7.	89.1												
50	1.528	1.431	98.0	.43	548.	543.	-2.	89.0												
70	1.529	1.429	98.0	.44	549.	546.	-7.	89.0												
90	1.628	1.431	95.4	.45	546.	543.	-5.	89.0												
MR	1.663	1.432	96.7	.47	560.	556.	-6.													

PT. 7-70-01  $W\sqrt{\theta/\delta} = 123.9 \text{ lbf/sec (56.2 kg/sec)}$   
 $P_{16}/P_0 = 1.561$   
 $P_0 = 1754 \text{ lbf/ft}^2 (83,900 \text{ N/m}^2)$   
 $T_0 = 509.4 \text{ R (283 K)}$

PT. 7-70-02  $W\sqrt{\theta/\delta} = 113.8 \text{ lbf/sec (51.6 kg/sec)}$   
 $P_{16}/P_0 = 1.670$   
 $P_0 = 1802 \text{ lbf/ft}^2 (86,100 \text{ N/m}^2)$   
 $T_0 = 496.0 \text{ R (275 K)}$

TABLE XXIX (Cont'd) - VELOCITY VECTOR PARAMETERS AT FAN EXIT  
(Circumferentially Distorted Inlet Flow)

SECOND STATOR EXIT CIRCUMFERENTIAL DISTRIBUTIONS - WEDGE PROBE STATION 16

	$P_{16}/P_0$	$p_{16}/P_0$	$90 - \beta^*$	M	V	$V_m$	$V_0$	$90 - \beta^*$	$P_{16}/P_0$	$p_{16}/P_0$	$90 - \beta^*$	M	V	$V_m$	$V_0$	$90 - \beta^*$	$P_{16}/P_0$	$p_{16}/P_0$	$90 - \beta^*$	M	V	$V_m$	$V_0$	$90 - \beta^*$
	16°								43°								76°							
10	1.578	1.448	93.5	55	59.1	65.0	-42	45.7	1.444	1.382	85.0	60	71.6	71.3	63	50.9	1.250	1.202	95.6	55	66.6	66.6	-65	62.5
30	1.726	1.483	96.3	47	56.5	56.0	-62	36.8	1.734	1.464	91.2	50	60.2	60.2	-13	40.2	1.726	1.477	95.6	48	57.2	56.9	-56	37.3
50	1.544	1.483	99.1	38	46.1	48.4	-73	29.0	1.542	1.474	91.6	40	49.2	47.7	-18	31.8	1.544	1.483	99.9	40	47.9	47.7	-77	29.8
70	1.433	1.483	98.3	38	45.7	45.2	-66	27.4	1.426	1.469	91.0	38	46.4	46.3	-8	29.5	1.432	1.480	98.2	40	48.2	47.7	-68	28.6
90	1.539	1.483	95.9	38	46.8	45.5	-48	27.0	1.526	1.464	87.0	39	47.4	47.3	25	29.3	1.556	1.482	95.3	40	49.1	48.8	-46	28.2
MR	1.700	1.483	96.5	45	53.8	53.4	-61		1.704	1.482	89.0	47	56.8	56.5	10		1.703	1.484	96.7	45	54.1	53.7	-63	
	103°								136°								163°							
10	1.439	1.445	85.0	50	71.2	7.9	6.1	50.7	1.838	1.494	94.3	55	86.1	85.9	-5	44.4	1.433	1.465	87.6	58	68.4	68.2	28	47.9
30	1.748	1.474	92.5	50	59.6	59.6	-26	39.4	1.728	1.486	98.3	47	56.2	55.6	-8	35.8	1.743	1.462	89.8	51	60.3	60.3	2	40.8
50	1.447	1.474	92.5	41	48.5	48.5	-72	32.6	1.446	1.483	98.7	40	48.1	48.1	-73	30.1	1.444	1.467	90.4	41	48.7	48.7	-4	32.6
70	1.433	1.445	90.1	40	47.9	47.9	-11	32.5	1.437	1.482	98.2	40	48.8	48.1	-7	34.7	1.439	1.466	90.3	40	48.4	48.4	-3	30.6
90	1.433	1.464	87.2	40	48.2	48.2	24	29.7	1.464	1.482	96.2	41	49.8	49.8	-48	28.7	1.468	1.465	86.7	41	49.0	48.9	28	30.1
MR	1.706	1.463	89.0	47	56.9	56.8	10		1.704	1.480	97.0	46	53.9	53.5	-64		1.700	1.465	88.9	47	56.3	56.3	11	
	193°								226°								251°							
10	1.432	1.443	87.0	57	67.7	67.6	35	48.1	1.817	1.492	94.5	54	84.5	84.3	-5	43.8	1.777	1.461	86.2	54	64.3	64.3	42	46.9
30	1.738	1.483	90.1	50	60.0	60.0	-1	40.6	1.729	1.483	97.4	46	55.6	55.2	-7	35.9	1.704	1.463	87.2	47	56.8	56.8	25	40.0
50	1.444	1.483	90.2	40	48.3	48.3	-2	34.6	1.446	1.483	99.2	39	46.8	46.2	-7	32.3	1.458	1.472	89.4	37	44.5	44.5	-4	28.0
70	1.432	1.465	89.4	40	48.7	48.7	5	31.1	1.431	1.482	98.3	40	47.8	47.3	-6	28.3	1.468	1.470	89.4	36	43.9	43.9	-4	28.2
90	1.438	1.465	86.6	40	48.8	48.7	29	36.1	1.459	1.481	95.2	41	49.6	49.4	-45	28.5	1.461	1.471	86.7	37	45.0	44.9	26	28.1
MR	1.699	1.464	88.6	47	56.0	56.0	14		1.694	1.484	96.9	44	53.1	52.7	-84		1.689	1.467	87.7	43	52.3	52.2	81	
	286°								313°								346°							
10	1.721	1.494	94.3	45	55.0	54.8	-4	38.1	1.733	1.477	89.7	44	54.1	54.1	-3	42.2	1.402	1.492	94.3	53	63.0	62.8	-47	42.6
30	1.674	1.494	96.8	41	49.1	48.8	-5	33.1	1.714	1.479	90.2	47	55.9	55.9	2	38.4	1.713	1.488	97.2	45	54.0	53.7	-68	35.2
50	1.609	1.488	99.1	31	44.8	44.8	-4	24.1	1.633	1.479	91.7	38	45.2	45.2	-13	30.8	1.664	1.484	99.2	38	45.5	45.2	-73	28.7
70	1.600	1.486	97.4	37	44.3	43.9	-5	26.9	1.624	1.468	88.5	38	46.0	46.0	12	30.0	1.639	1.483	98.1	38	45.9	45.4	-64	27.4
90	1.640	1.488	95.1	38	46.1	45.9	24	26.9	1.639	1.469	87.4	39	45.3	45.3	22	29.0	1.653	1.485	95.6	40	48.1	47.8	-46	27.6
MR	1.655	1.491	96.0	39	47.1	46.8	-5		1.670	1.473	89.4	43	51.4	51.4	5		1.686	1.486	96.8	43	51.6	51.2	-61	

PT. 7-70-13  $W\sqrt{\theta/\delta} = 106.6$  lbfm/sec (48.3 kg/sec)  
 $P_{16}/P_0 = 1.692$   
 $P_0 = 1868$  lbf/ft<sup>2</sup> (89,200 N/m<sup>2</sup>)  
 $T_0 = 512.5$  °R (284 °K)

REPRODUCIBILITY OF THIS ORIGINAL PAGE IS POOR

TABLE XXIX (Cont'd) - VELOCITY VECTOR PARAMETERS AT FAN EXIT  
(Circumferentially Distorted Inlet Flow)

SECOND STAGE EXIT CIRCUMFERENTIAL DISTRIBUTIONS - WEDGE PROBE STATION 16

43°										43°										43°									
P16/P0	p16/p0	90-β	M	V	Vx	Vy	90-β	P16/P0	p16/p0	90-β	M	V	Vx	Vy	90-β	P16/P0	p16/p0	90-β	M	V	Vx	Vy	90-β						
10	1.916	1.168	95.6	87	1087	1045	-188	46.0	2.532	1.932	87.1	83	796	795	4.0	46.8	2.445	1.240	97.1	1.00	1263	1263	-156	49.3					
30	2.23b	1.241	99.3	96	1131	1116	-183	46.1	2.219	1.932	87.3	86	723	722	28	39.8	2.456	1.209	93.9	1.06	1270	1267	-86	49.4					
50	2.063	1.118	92.3	98	1147	1146	-46	48.6	2.231	1.929	88.7	86	584	584	13	31.6	2.170	1.249	99.7	92	1123	1107	-189	41.0					
70	2.027	1.106	92.9	97	1130	1129	-87	45.9	2.284	1.927	88.8	88	608	608	13	30.7	2.004	1.227	96.8	87	1051	1043	-124	39.0					
90	2.100	1.185	95.2	96	1121	1116	-102	42.7	2.299	1.928	84.7	81	650	648	40	31.7	2.242	1.186	92.1	1.03	1222	1220	-66	43.0					
MR	2.077	1.159	96.5	95	1121	1116	-106		2.352	1.928	87.3	84	683	682	32		2.243	1.211	95.9	99	1193	1186	-122						
133°										133°										133°									
10	1.481	1.142	99.8	86	1041	1026	-172	48.7	2.515	1.964	86.9	87	758	757	42	43.9	2.533	1.266	100.0	1.06	1273	1263	-221	47.7					
30	2.224	1.171	97.6	99	1156	1145	-183	47.4	2.443	1.970	87.4	86	704	703	32	38.9	2.446	1.210	94.5	1.06	1258	1254	-99	48.8					
50	2.054	1.229	97.5	89	1046	1037	-137	43.0	2.268	1.974	88.6	85	568	568	14	30.6	2.222	1.277	101.5	93	1113	1091	-222	39.9					
70	2.021	1.131	92.3	93	1042	1041	-42	44.7	2.270	1.965	88.4	88	582	582	16	29.7	1.932	1.145	96.0	90	1072	1066	-112	39.9					
90	2.078	1.098	89.3	1.00	1151	1151	14	46.1	2.325	1.960	85.1	80	635	633	54	30.7	2.084	1.093	92.3	1.01	1190	1189	-48	42.6					
MR	2.062	1.163	94.7	94	1104	1100	-90		2.369	1.966	87.2	82	659	658	32		2.240	1.194	96.6	99	1187	1179	-137						
226°										226°										226°									
10	1.627	1.268	102.1	61	768	749	-160	37.7	2.473	1.966	94.4	87	721	719	66	39.8	2.132	1.247	104.9	90	1121	1083	-288	42.2					
30	2.163	1.171	102.3	90	1080	1058	-220	43.6	2.364	1.969	96.7	92	654	649	77	34.1	2.411	1.279	104.3	1.00	1210	1172	-299	42.3					
50	2.017	1.278	101.6	83	993	979	-201	40.2	2.240	1.966	97.8	84	583	584	76	28.2	2.276	1.240	105.6	97	1174	1130	-320	39.1					
70	1.937	1.285	101.8	79	943	925	-187	37.9	2.274	1.968	98.2	86	586	580	84	27.5	1.969	1.225	106.1	85	1036	998	-287	34.8					
90	1.977	1.330	99.1	80	959	952	-119	37.9	2.331	1.963	94.4	80	642	640	69	29.0	2.205	1.156	101.7	1.00	1198	1176	-243	38.4					
MR	1.980	1.283	100.8	81	980	964	-181		2.333	1.968	96.3	80	634	630	69		2.209	1.230	104.3	95	1158	1125	-287						
316°										316°										316°									
10	1.560	1.334	96.6	48	608	604	-70	34.4	2.211	2.029	96.6	84	316	313	-36	20.2	1.789	1.381	99.8	82	864	793	-133	37.8					
30	2.049	1.335	98.3	81	972	962	-140	43.0	2.228	2.022	95.1	82	534	532	-48	29.5	2.315	1.379	100.0	85	1096	1079	-190	42.6					
50	1.938	1.344	99.0	73	884	873	-139	38.3	2.299	2.014	97.9	81	518	513	-72	26.3	2.072	1.353	100.4	81	988	971	-178	37.9					
70	1.956	1.347	99.8	72	863	851	-147	35.6	2.356	2.007	96.2	88	612	609	-66	28.8	2.108	1.358	99.8	82	990	976	-168	36.8					
90	1.933	1.352	95.8	73	883	878	-90	36.1	2.433	2.016	94.1	83	669	667	-47	29.8	2.108	1.364	95.2	81	997	993	-90	36.8					
MR	1.916	1.443	98.0	73	884	876	-123		2.430	2.015	95.7	86	585	582	-58		2.116	1.365	98.7	82	1004	992	-182						

PT. 7-90-01  $W\sqrt{\theta/\delta} = 167.4$  lbm/sec (75.9 kg/sec)  
 $P_{16}/P_0 = 1.994$   
 $P_0 = 1575$  lbf/ft<sup>2</sup> (75,300 N/m<sup>2</sup>)  
 $T_0 = 509.2$  R (283 K)

PT. 7-90-02  $W\sqrt{\theta/\delta} = 148.8$  lbm/sec (67.4 kg/sec)  
 $P_{16}/P_0 = 2.324$   
 $P_0 = 1643$  lbf/ft<sup>2</sup> (78,600 N/m<sup>2</sup>)  
 $T_0 = 509.8$  R (283 K)

PT. 7-10-31  $W\sqrt{\theta/\delta} = 185.0$  lbm/sec (83.8 kg/sec)  
 $P_{16}/P_0 = 2.180$   
 $P_0 = 1481$  lbf/ft<sup>2</sup> (70,800 N/m<sup>2</sup>)  
 $T_0 = 503.2$  R (279 K)

TABLE XXIX (Cont'd) - VELOCITY VECTOR PARAMETERS AT FAN EXIT  
(Circumferentially Distorted Inlet Flow)

SECOND STATOR EXIT CIRCUMFERENTIAL DISTRIBUTIONS - WEDGE PROBE STATION 16

	P <sub>16</sub> /P <sub>0</sub>	p <sub>16</sub> /P <sub>0</sub>	50-β°	M	V	V <sub>m</sub>	V <sub>0</sub>	90-β°	P <sub>16</sub> /P <sub>0</sub>	p <sub>16</sub> /P <sub>0</sub>	90-β°	M	V	V <sub>m</sub>	V <sub>0</sub>	90-β°	P <sub>16</sub> /P <sub>0</sub>	p <sub>16</sub> /P <sub>0</sub>	90-β°	M	V	V <sub>m</sub>	V <sub>0</sub>	90-β°												
	16°												43°												76°											
10	2.447	2.031	84.3	.52	663.	651.	.49.	37.6	2.496	1.999	86.2	.57	725.	724.	.48.	43.0	2.512	2.044	94.5	.55	702.	699.	.55.	38.9												
30	2.334	2.037	96.0	.46	579.	576.	.61.	31.4	2.299	2.007	87.5	.45	568.	567.	.25.	33.1	2.382	2.034	96.2	.48	613.	610.	.66.	32.7												
50	2.221	2.030	98.4	.37	474.	469.	.69.	24.6	2.258	2.007	86.9	.41	529.	529.	.28.	29.4	2.275	2.029	98.1	.38	481.	486.	.69.	25.3												
70	2.291	2.029	97.2	.39	500.	496.	.62.	24.4	2.288	1.999	86.5	.44	569.	568.	.35.	29.4	2.277	2.034	97.1	.41	518.	514.	.64.	25.1												
90	2.307	2.024	93.7	.44	563.	562.	.37.	26.2	2.269	1.996	88.5	.43	557.	557.	.15.	26.4	2.329	2.033	94.0	.45	573.	571.	.40.	26.5												
HR	2.314	2.029	95.8	.44	560.	557.	.56.		2.325	2.001	87.1	.47	599.	598.	.30.		2.347	2.034	95.9	.46	584.	581.	.60.													
	103°												136°												163°											
10	2.547	1.987	85.7	.61	764.	762.	.45.	44.5	2.492	2.027	94.4	.55	699.	697.	.54.	38.8	2.504	1.985	87.1	.59	738.	737.	.37.	43.1												
30	2.381	1.987	87.4	.52	649.	649.	.29.	37.0	2.364	2.017	96.4	.48	610.	606.	.68.	32.5	2.438	1.988	87.3	.55	686.	685.	.30.	38.4												
50	2.271	1.992	87.4	.44	555.	554.	.25.	30.6	2.255	2.018	98.5	.40	513.	507.	.76.	26.1	2.280	1.989	88.1	.48	563.	563.	.19.	31.2												
70	2.264	1.987	87.4	.44	557.	557.	.26.	28.9	2.294	2.017	96.9	.43	552.	548.	.67.	26.5	2.270	1.984	88.2	.44	563.	563.	.18.	28.8												
90	2.286	1.983	87.4	.46	583.	583.	.26.	28.3	2.337	2.016	93.7	.46	597.	595.	.39.	27.4	2.326	1.977	86.0	.49	620.	618.	.44.	30.0												
HR	2.355	1.987	87.2	.50	633.	632.	.31.		2.336	2.018	95.9	.47	596.	593.	.61.		2.368	1.984	87.3	.51	643.	642.	.31.													
	193°												226°												253°											
10	2.499	1.993	87.0	.58	727.	726.	.38.	42.8	2.484	2.040	94.4	.54	684.	682.	.52.	38.3	2.421	1.999	86.3	.53	676.	675.	.43.	40.9												
30	2.454	1.993	87.5	.56	697.	697.	.30.	38.9	2.374	2.034	96.3	.49	618.	614.	.68.	32.8	2.414	2.005	86.5	.52	662.	661.	.40.	37.7												
50	2.284	1.994	88.2	.45	571.	571.	.18.	31.1	2.285	2.023	98.4	.42	532.	533.	.79.	27.2	2.267	2.004	86.2	.42	541.	540.	.35.	31.1												
70	2.296	1.991	88.2	.46	583.	583.	.18.	29.8	2.316	2.025	96.9	.44	567.	563.	.68.	27.0	2.243	2.001	86.4	.42	541.	540.	.34.	28.2												
90	2.345	1.981	85.1	.50	636.	633.	.54.	31.0	2.365	2.028	93.5	.48	614.	612.	.38.	28.1	2.319	2.007	85.0	.46	591.	589.	.51.	29.0												
HR	2.380	1.990	87.1	.51	650.	650.	.33.		2.362	2.027	95.8	.47	605.	602.	.61.		2.339	2.002	88.1	.48	608.	605.	.42.													
	286°												313°												346°											
10	2.304	2.025	95.9	.31	407.	405.	.42.	25.5	2.262	2.033	85.2	.14	184.	183.	.15.	12.8	2.226	2.018	94.5	.38	482.	480.	.38.	29.5												
30	2.271	2.035	93.9	.40	509.	508.	.34.	29.0	2.292	2.009	84.7	.41	518.	516.	.48.	31.3	2.248	2.026	97.8	.39	493.	488.	.66.	27.1												
50	2.256	2.032	97.1	.39	496.	492.	.81.	25.8	2.314	1.988	85.6	.47	596.	595.	.45.	32.8	2.219	2.023	97.8	.37	466.	461.	.63.	24.3												
70	2.279	2.033	97.1	.41	522.	518.	.65.	25.3	2.296	1.978	88.2	.47	594.	593.	.18.	30.1	2.332	2.029	97.4	.44	580.	575.	.75.	27.4												
90	2.345	2.035	93.6	.46	586.	584.	.37.	27.1	2.395	1.990	85.3	.53	672.	670.	.55.	32.3	2.367	2.011	94.1	.48	619.	618.	.44.	28.2												
HR	2.281	2.033	95.3	.41	524.	522.	.49.		2.309	1.998	86.0	.50	638.	636.	.45.		2.296	2.021	96.2	.43	549.	546.	.60.													

PT. 7-90-03 W $\sqrt{\theta/\delta}$  = 145.8 lbm/sec (66.1 kg/sec)  
P<sub>16</sub>/P<sub>0</sub> = 2.338  
P<sub>0</sub> = 1669 lbf/ft<sup>2</sup> (79,750 N/m<sup>2</sup>)  
T<sub>0</sub> = 508.8° R (282° K)

TABLE XXIX (Cont'd) - VELOCITY VECTOR PARAMETERS AT FAN EXIT  
(Circumferentially Distorted Inlet Flow)

SECOND STATOR EXIT CIRCUMFERENTIAL DISTRIBUTIONS - WEDGE PROBE STATION 16

	$P_{16}/P_0$	$P_{16}/P_0$	$90-\beta^\circ$	M	V	$V_m$	$V_0$	$90-\beta^\circ$		$P_{16}/P_0$	$P_{16}/P_0$	$90-\beta^\circ$	M	V	$V_m$	$V_0$	$90-\beta^\circ$		$P_{16}/P_0$	$P_{16}/P_0$	$90-\beta^\circ$	M	V	$V_m$	$V_0$	$90-\beta^\circ$
	16°									43°									76°							
10	2.652	2.110	95.8	.64	832.	827.	-98.	39.7		2.685	1.912	83.8	.71	916.	916.	-19.	48.6		2.660	2.009	95.2	.65	837.	834.	-75.	40.5
30	2.675	1.984	97.7	.67	850.	843.	-114.	37.6		2.665	1.900	90.1	.71	905.	905.	.1.	42.1		2.614	1.990	97.2	.64	813.	806.	-102.	36.6
50	2.335	1.954	100.6	.51	651.	650.	-122.	28.7		2.327	1.902	90.7	.55	701.	701.	.9.	32.8		2.328	1.958	100.2	.50	643.	633.	-114.	28.2
70	2.411	1.963	98.8	.55	707.	698.	-108.	29.1		2.418	1.902	89.8	.60	759.	759.	.2.	33.3		2.427	1.986	98.8	.56	702.	694.	-108.	28.9
90	2.402	1.964	94.7	.55	709.	706.	-58.	28.8		2.396	1.903	86.6	.58	750.	749.	.4.	32.0		2.354	1.964	95.1	.54	693.	690.	-62.	28.1
MR	2.495	1.974	97.6	.59	759.	752.	-100.			2.504	1.904	89.1	.64	817.	817.	.12.			2.481	1.976	97.3	.58	740.	734.	-94.	
	103°									136°									163°							
10	2.699	1.912	84.5	.72	923.	922.	-24.	45.8		2.685	2.003	95.3	.65	831.	827.	-76.	44.2		2.684	1.913	88.3	.71	908.	903.	-27.	45.8
30	2.677	1.894	89.7	.72	910.	909.	.5.	42.4		2.667	1.994	97.3	.66	831.	825.	-106.	37.1		2.671	1.899	89.6	.72	895.	895.	.7.	42.1
50	2.314	1.901	91.0	.54	688.	686.	-12.	32.0		2.332	1.953	100.1	.51	648.	638.	-114.	28.3		2.304	1.902	91.6	.53	673.	673.	-19.	31.8
70	2.414	1.897	90.1	.56	752.	752.	.2.	32.8		2.420	1.964	98.8	.58	697.	689.	-105.	28.7		2.403	1.898	90.0	.59	742.	742.	.1.	32.6
90	2.382	1.998	86.3	.58	743.	742.	.47.	31.7		2.401	1.983	95.0	.55	697.	694.	-61.	28.2		2.382	1.902	86.5	.58	736.	737.	.45.	31.7
MR	2.507	1.900	89.0	.64	815.	814.	.14.			2.493	1.975	97.2	.59	746.	744.	-94.			2.497	1.903	89.1	.64	804.	804.	.13.	
	193°									226°									253°							
10	2.681	1.922	88.1	.71	907.	906.	-30.	45.8		2.641	2.007	94.5	.64	829.	826.	-66.	40.4		2.644	1.934	87.4	.69	882.	881.	-40.	45.2
30	2.664	1.898	89.2	.71	905.	905.	.13.	42.7		2.630	1.997	97.2	.64	821.	814.	-102.	36.8		2.665	1.928	84.7	.65	828.	828.	.19.	40.3
50	2.303	1.906	91.6	.53	680.	680.	-19.	31.9		2.308	1.954	100.0	.49	635.	626.	-110.	27.9		2.218	1.929	90.3	.45	578.	578.	.03.	28.2
70	2.432	1.903	90.1	.59	750.	750.	.2.	33.0		2.430	1.968	94.8	.53	685.	677.	-108.	28.3		2.420	1.923	89.0	.51	640.	640.	.11.	29.2
90	2.379	1.904	86.1	.57	739.	737.	.50.	31.9		2.386	1.968	95.4	.53	691.	688.	-65.	27.9		2.317	1.923	85.8	.52	661.	659.	.48.	29.0
MR	2.494	1.906	88.9	.63	809.	809.	.15.			2.470	1.979	97.1	.57	738.	732.	-92.			2.421	1.927	88.1	.58	738.	738.	.25.	
	286°									313°									346°							
10	2.435	2.007	84.2	.53	699.	697.	-51.	36.0		2.412	1.950	86.9	.56	725.	724.	.39.	39.5		2.577	2.027	95.3	.64	829.	826.	-76.	40.2
30	2.443	2.006	95.1	.54	696.	693.	-62.	33.3		2.401	1.935	88.0	.52	780.	780.	.28.	38.8		2.644	2.002	97.1	.64	813.	806.	-100.	36.6
50	2.274	1.996	94.6	.44	562.	556.	-84.	25.6		2.310	1.929	89.3	.51	653.	653.	.8.	31.4		2.338	1.976	99.2	.53	677.	667.	-108.	29.6
70	2.324	1.989	96.2	.48	612.	609.	-66.	26.4		2.391	1.930	89.1	.54	678.	678.	.10.	30.6		2.449	1.981	99.3	.56	705.	696.	-115.	28.8
90	2.366	1.994	94.0	.50	648.	646.	-45.	26.7		2.429	1.931	85.0	.58	736.	733.	.64.	32.0		2.477	1.987	95.0	.57	730.	727.	-63.	29.3
MR	2.370	1.994	95.6	.50	646.	643.	-62.			2.425	1.933	87.6	.57	719.	716.	.31.			2.524	1.993	97.1	.59	752.	746.	-93.	

PT. 7-10-02  $W\sqrt{\theta}/\delta = 184.6 \text{ lbm/sec (83.7 kg/sec)}$   
 $P_{16}/P_0 = 2.494$   
 $P_0 = 1488 \text{ lbf/ft}^2 (71,000 \text{ N/m}^2)$   
 $T_0 = 500.4^\circ \text{R (278}^\circ \text{K)}$

TABLE XXIX (Cont'd) - VELOCITY VECTOR PARAMETERS AT FAN EXIT  
(Circumferentially Distorted Inlet Flow)

SECOND STATOR EXIT CIRCUMFERENTIAL DISTRIBUTIONS - WEDGE PROBE STATION 16

	P16/P0	P10/P0	90-β*	M	V	V <sub>u</sub>	V <sub>0</sub>	90-β*	P16/P0	P10/P0	90-β*	M	V	V <sub>u</sub>	V <sub>0</sub>	90-β*	P16/P0	P10/P0	90-β*	M	V	V <sub>u</sub>	V <sub>0</sub>	90-β*
	16°								43°								76°							
10	2.853	2.229	94.6	57	736	733	59	37.5	2.867	2.240	86.0	61	590	788	86	42.8	2.923	2.310	94.3	59	774	772	58	38.9
30	2.706	2.277	96.3	50	652	648	72	31.6	2.764	2.242	86.8	58	720	719	40	37.1	2.776	2.291	95.9	53	495	490	71	33.3
50	2.531	2.274	99.5	39	517	510	85	23.9	2.604	2.242	86.7	47	613	612	38	30.8	2.555	2.279	98.3	43	565	559	82	28.0
70	2.461	2.272	97.0	45	594	590	73	25.8	2.604	2.230	86.8	48	624	623	35	29.2	2.633	2.278	95.3	46	598	594	85	26.1
90	2.480	2.271	93.5	50	657	656	40	27.3	2.691	2.234	85.4	52	687	685	55	30.2	2.691	2.280	93.4	49	648	644	38	26.9
MR	2.679	2.276	95.9	49	639	635	66		2.709	2.235	86.3	53	693	692	46		2.718	2.287	95.5	50	688	685	63	
	103°								136°								161°							
10	2.924	2.228	86.9	64	815	818	45	43.4	2.915	2.201	94.3	59	755	759	58	35.6	2.884	2.217	87.0	63	801	800	42	42.5
30	2.867	2.230	88.7	58	748	747	43	38.2	2.795	2.288	94.3	54	699	698	71	33.4	2.836	2.223	86.9	60	780	789	40	38.5
50	2.683	2.230	87.1	44	611	600	30	30.0	2.590	2.277	98.7	44	568	564	88	25.9	2.582	2.223	87.7	47	602	601	24	29.7
70	2.604	2.210	87.3	49	696	696	30	29.8	2.640	2.265	96.6	47	613	613	71	26.6	2.634	2.218	87.8	50	646	646	25	29.7
90	2.701	2.220	83.9	54	699	696	74	31.0	2.702	2.266	93.4	51	665	664	40	27.8	2.714	2.213	83.9	55	706	702	78	31.1
MR	2.731	2.224	86.3	55	711	710	44		2.726	2.277	94.6	50	666	663	48		2.738	2.224	86.6	55	713	711	43	
	193°								226°								253°							
10	2.856	2.226	86.5	61	782	781	44	42.0	2.896	2.212	94.3	58	757	755	47	38.3	2.784	2.249	85.6	55	726	724	55	40.2
30	2.809	2.234	86.8	59	759	757	42	38.8	2.779	2.292	98.5	53	695	692	86	33.8	2.726	2.259	85.1	63	688	685	59	38.3
50	2.661	2.233	87.9	44	605	605	22	29.9	2.589	2.253	98.2	43	563	558	81	26.0	2.550	2.258	86.6	42	552	551	32	27.9
70	2.611	2.213	88.1	50	647	647	22	29.7	2.658	2.282	97.0	47	613	609	76	26.8	2.580	2.250	86.7	45	581	580	34	27.4
90	2.711	2.221	84.2	54	707	704	71	31.2	2.708	2.282	93.6	50	660	658	41	27.4	2.671	2.245	84.2	51	655	652	66	29.9
MR	2.723	2.225	84.6	55	709	708	42		2.721	2.289	95.6	50	661	658	64		2.663	2.252	85.6	50	647	645	50	
	286°								313°								346°							
10	2.357	2.235	95.7	10	210	214	22	13.1	2.320	2.296	91.3	12	160	160	44	9.9	2.414	2.259	96.1	31	409	407	43	23.3
30	2.464	2.286	94.5	32	481	482	33	22.8	2.330	2.287	83.4	16	215	213	25	12.4	2.528	2.282	100.1	38	497	489	87	24.8
50	2.606	2.236	97.8	43	559	559	76	25.9	2.541	2.253	82.8	42	545	540	68	28.1	2.538	2.287	97.0	39	506	502	61	24.0
70	2.634	2.233	97.1	46	600	596	74	26.1	2.730	2.219	87.8	65	710	710	27	32.1	2.729	2.274	96.8	52	685	681	76	28.3
90	2.744	2.234	93.1	45	670	669	37	27.9	2.680	2.223	86.7	62	803	801	47	33.9	2.769	2.279	96.8	54	697	692	82	27.7
MR	2.628	2.234	95.8	44	580	578	55		2.701	2.236	86.2	53	684	682	45		2.645	2.278	97.3	47	607	602	77	

PT. 7-10-03  $W\sqrt{\theta/\delta} = 176.0$  lbm/sec (79.8 kg/sec)  
 $P_{16}/P_0 = 2.701$   
 $P_{10} = 1530$  lbf/ft<sup>2</sup> (73,050 N/m<sup>2</sup>)  
 $T_0 = 509.6$  R (283 K)

REPRODUCIBILITY OF THE  
ORIGINAL PAGE IS POOR



TABLE XXX - FIRST-STAGE TOTAL TEMPERATURE RATIO  
(Circumferentially Distorted Inlet Flow)

COMBINATION PROBE -  $T_{11}/T_0$

Circumferential Position - Degrees

% Span	86°	176°	266°	356°	% Span	86°	176°	266°	356°	% Span	86°	176°	266°	356°
10	1.2081	1.1879	1.1560	1.2263	10	1.1694	1.1624	1.1276	1.1900	10	1.1599	1.1589	1.1261	1.1908
30	1.1987	1.1850	1.1434	1.2031	30	1.1560	1.1484	1.1123	1.1645	30	1.1611	1.1555	1.1390	1.1864
50	1.1857	1.1817	1.1359	1.1919	50	1.1513	1.1446	1.1061	1.1586	50	1.1603	1.1522	1.1330	1.1845
70	1.1770	1.1713	1.1364	1.1744	70	1.1450	1.1396	1.1101	1.1519	70	1.1728	1.1616	1.1446	1.1899
90	1.1963	1.1856	1.1481	1.1912	90	1.1685	1.1554	1.1201	1.1623	90	1.1812	1.1737	1.1538	1.2054
MR	1.1934	1.1825	1.1440	1.1916	MR	1.1644	1.1524	1.1158	1.1646	MR	1.1729	1.1624	1.1434	1.1932

PT. 7-10-31  $\sqrt{D/\delta} = 185.0 \text{ lbm/sec (83.8 kg/sec)}$ ;  $P_{16}^*/P_0^* = 2.180$ ;  $T_0 = 503.2^\circ \text{R (279 K)}$   
 $P_0 = 1481 \text{ lbf/ft}^2 \text{ (70,800 N/m}^2)$

PT. 7-90-01  $\sqrt{D/\delta} = 167.4 \text{ lbm/sec (75.9 kg/sec)}$ ;  $P_{16}^*/P_0^* = 1.984$ ;  $T_0 = 509.2^\circ \text{R (283 K)}$   
 $P_0 = 1575 \text{ lbf/ft}^2 \text{ (75,300 N/m}^2)$

PT. 7-90-02  $\sqrt{D/\delta} = 14.88 \text{ lbm/sec (67.4 kg/sec)}$ ;  $P_{16}^*/P_0^* = 2.324$ ;  $T_0 = 509.8^\circ \text{R (283 K)}$   
 $P_0 = 1843 \text{ lbf/ft}^2 \text{ (78,600 N/m}^2)$

% Span	86°	176°	266°	356°	% Span	86°	176°	266°	356°
10	1.1012	1.0982	1.0796	1.1128	10	1.1076	1.1033	1.0839	1.1165
30	1.0941	1.0920	1.0681	1.1025	30	1.1017	1.0996	1.0836	1.1125
50	1.0897	1.0872	1.0626	1.0958	50	1.0988	1.0976	1.0812	1.1071
70	1.0904	1.0880	1.0633	1.0957	70	1.0992	1.0982	1.0827	1.1050
90	1.1033	1.0875	1.0693	1.0952	90	1.1163	1.1100	1.0919	1.1250
MR	1.0965	1.0901	1.0663	1.1000	MR	1.1059	1.1026	1.0856	1.1141

PT. 7-70-01  $\sqrt{D/\delta} = 123.9 \text{ lbm/sec (56.2 kg/sec)}$ ;  $P_{16}^*/P_0^* = 1.861$ ;  $T_0 = 504.4^\circ \text{R (283 K)}$   
 $P_0 = 1754 \text{ lbf/ft}^2 \text{ (83,900 N/m}^2)$

PT. 7-70-02  $\sqrt{D/\delta} = 113.8 \text{ lbm/sec (51.6 kg/sec)}$ ;  $P_{16}^*/P_0^* = 1.670$ ;  $T_0 = 496.0^\circ \text{R (275 K)}$   
 $P_0 = 1802 \text{ lbf/ft}^2 \text{ (86,100 N/m}^2)$

% Span	26°	56°	86°	116°	146°	176°	206°	236°	266°	296°	326°	356°
10	1.2193	1.2139	1.2037	1.2104	1.2198	1.1976	1.1882	1.1838	1.1539	1.1562	1.2456	1.2330
30	1.2251	1.2079	1.1980	1.1971	1.2068	1.1899	1.1759	1.1761	1.1392	1.1812	1.2430	1.2110
50	1.1863	1.1952	1.1844	1.1925	1.2063	1.1843	1.1769	1.1759	1.1380	1.1782	1.2419	1.2036
70	1.1774	1.1818	1.1767	1.1801	1.1955	1.1783	1.1667	1.1669	1.1358	1.1847	1.2442	1.1855
90	1.1858	1.1977	1.1893	1.1974	1.2136	1.1879	1.1890	1.1802	1.1551	1.1999	1.2525	1.2029
MR	1.1971	1.1989	1.1900	1.1992	1.2086	1.1870	1.1796	1.1771	1.1455	1.1854	1.2467	1.2060

PT. 7-10-02  $\sqrt{D/\delta} = 184.6 \text{ lbm/sec (83.7 kg/sec)}$ ;  $P_{16}^*/P_0^* = 2.484$   
 $P_0 = 1488 \text{ lbf/ft}^2 \text{ (71,000 N/m}^2)$ ;  $T_0 = 500.4^\circ \text{R (278 K)}$

% Span	26°	56°	86°	116°	146°	176°	206°	236°	266°	296°	326°	356°
10	1.2241	1.2334	1.1926	1.1897	1.1889	1.1865	1.1867	1.1811	1.1614	1.1622	1.2344	1.2436
30	1.2279	1.1965	1.1930	1.1870	1.1820	1.1822	1.1812	1.1748	1.1502	1.2048	1.2572	1.2487
50	1.2363	1.2017	1.1972	1.1917	1.1867	1.1871	1.1837	1.1759	1.1512	1.2140	1.2740	1.2631
70	1.2383	1.2091	1.2037	1.1919	1.1833	1.1827	1.1800	1.1767	1.1558	1.2211	1.2942	1.2608
90	1.2554	1.2100	1.2135	1.2089	1.1977	1.1952	1.1946	1.1842	1.1713	1.2325	1.2978	1.2613
MR	1.2403	1.2129	1.2025	1.1961	1.1890	1.1880	1.1885	1.1792	1.1608	1.2177	1.2847	1.2610

PT. 7-10-03  $\sqrt{D/\delta} = 176.0 \text{ lbm/sec (79.8 kg/sec)}$ ;  $P_{16}^*/P_0^* = 2.701$   
 $P_0 = 1530 \text{ lbf/ft}^2 \text{ (73,050 N/m}^2)$ ;  $T_0 = 509.6^\circ \text{R (283 K)}$

% Span	26°	56°	86°	116°	146°	176°	206°	236°	266°	296°	326°	356°
10	1.1760	1.1650	1.1618	1.1549	1.1531	1.1534	1.1518	1.1489	1.1306	1.1378	1.1860	1.1932
30	1.1848	1.1715	1.1715	1.1651	1.1571	1.1578	1.1531	1.1516	1.1369	1.1677	1.2009	1.1956
50	1.1904	1.1750	1.1664	1.1619	1.1562	1.1567	1.1550	1.1499	1.1346	1.1844	1.2172	1.2066
70	1.2019	1.1873	1.1793	1.1710	1.1698	1.1684	1.1657	1.1614	1.1472	1.1942	1.2391	1.2153
90	1.2186	1.2186	1.2030	1.1983	1.1883	1.1834	1.1873	1.1772	1.1643	1.2113	1.2533	1.2347
MR	1.1998	1.1903	1.1820	1.1763	1.1691	1.1676	1.1668	1.1615	1.1479	1.1923	1.2316	1.2117

PT. 7-90-03  $\sqrt{D/\delta} = 145.8 \text{ lbm/sec (66.1 kg/sec)}$ ;  $P_{16}^*/P_0^* = 2.338$   
 $P_0 = 1689 \text{ lbf/ft}^2 \text{ (79,750 N/m}^2)$ ;  $T_0 = 508.8^\circ \text{R (282 K)}$

% Span	26°	56°	86°	116°	146°	176°	206°	236°	266°	296°	326°	356°
10	1.1113	1.1053	1.1050	1.1169	1.1044	1.0995	1.0982	1.0936	1.0795	1.1007	1.1111	1.1120
30	1.1079	1.1022	1.1029	1.0991	1.0962	1.1001	1.0970	1.0939	1.0831	1.1043	1.1163	1.1089
50	1.1033	1.0999	1.1005	1.0986	1.0965	1.0972	1.0949	1.0939	1.0844	1.1046	1.1156	1.1067
70	1.0987	1.0998	1.1006	1.0977	1.0967	1.0975	1.0953	1.0943	1.0853	1.1056	1.1217	1.1064
90	1.1190	1.1202	1.1156	1.1162	1.1105	1.1105	1.1126	1.1072	1.1003	1.1321	1.1369	1.1300
MR	1.1086	1.1064	1.1059	1.1041	1.1026	1.1021	1.1010	1.0983	1.0885	1.1169	1.1216	1.1135

PT. 7-70-13  $\sqrt{D/\delta} = 106.6 \text{ lbm/sec (48.3 kg/sec)}$ ;  $P_{16}^*/P_0^* = 1.892$   
 $P_0 = 1868 \text{ lbf/ft}^2 \text{ (89,200 N/m}^2)$ ;  $T_0 = 512.5^\circ \text{R (284 K)}$

Table XXXI Circumferential Distribution of Total Pressure Ratio and Total Temperature Ratio at The Second-Stage Stator Exit (Circumferentially Distorted Inlet Flow)

WAKE RAKE DATA

Circumferential Position - Degrees

PT. 7-10-31  $W\sqrt{\theta/\delta} = 185.0$  lbm/sec (83.8 kg/sec);  $P_{16}^*/P_6^* = 2.180$   
 $P_0 = 1481$  lbf/ft<sup>2</sup> (70,800 N/m<sup>2</sup>);  $T_0 = 503.2^\circ R$  (279 K)

Pressure Data					Temperature Data				
% Span	17°	110°	200°	287°	% Span	60°	117°	237°	330°
10	2.4088	2.4513	2.4032	2.1165	10	1.4554	1.4300	1.4186	1.4586
30	2.3862	2.3635	2.3268	2.1621	30	1.4044	1.3822	1.3665	1.4285
50	2.2928	2.2014	2.1679	1.9393	50	1.3731	1.3609	1.3444	1.4060
70	2.1776	2.1073	2.0656	1.8967	70	1.3388	1.3322	1.3199	1.3756
90	2.1531	2.1106	2.0744	1.9074	90	1.3749	1.3673	1.3579	1.4041
MR	2.277	2.240	2.201	2.002	MR	1.3866	1.3732	1.3600	1.4131

PT. 7-00-D1  $W\sqrt{\theta/\delta} = 167.4$  lbm/sec;  $P_{16}^*/P_6^* = 1.994$   
 $P_0 = 1675$  lbf/ft<sup>2</sup> (75,300 N/m<sup>2</sup>);  $T_0 = 509.2^\circ R$

Pressure Data					Temperature Data				
% Span	17°	110°	200°	287°	% Span	60°	117°	237°	330°
10	2.2103	2.1811	2.1453	1.8932	10	1.3582	1.3480	1.3379	1.3637
30	2.2521	2.1720	2.1509	1.9616	30	1.3201	1.3054	1.2937	1.3381
50	2.0822	2.0281	1.9940	1.7631	50	1.2981	1.2892	1.2735	1.3249
70	1.9735	1.9137	1.8888	1.7267	70	1.2723	1.2682	1.2573	1.3102
90	1.9702	1.9373	1.9232	1.7594	90	1.2954	1.2912	1.2796	1.3266
MR	2.098	2.041	2.015	1.819	MR	1.3072	1.2991	1.2871	1.3318

PT. 7-90-D2  $W\sqrt{\theta/\delta} = 148.8$  lbm/sec (67.4 kg/sec);  $P_{16}^*/P_6^* = 2.324$   
 $P_0 = 1643$  lbf/ft<sup>2</sup> (78,600 N/m<sup>2</sup>);  $T_0 = 509.8^\circ R$  (283 K)

Pressure Data					Temperature Data				
% Span	17°	110°	200°	287°	% Span	60°	117°	237°	330°
10	2.4936	2.5069	2.4878	2.2214	10	1.3637	1.3500	1.3461	1.3796
30	2.3770	2.4199	2.4178	2.2605	30	1.3395	1.3233	1.3212	1.3626
50	2.2430	2.2584	2.2804	2.2167	50	1.3105	1.3191	1.3216	1.3679
70	2.2833	2.2549	2.2778	2.2326	70	1.3611	1.3213	1.3249	1.3869
90	2.3147	2.2926	2.3195	2.2599	90	1.3949	1.3481	1.3535	1.4161
MR	2.346	2.349	2.358	2.244	MR	1.3618	1.3330	1.3344	1.3845

PT. 7-10-01  $W\sqrt{\theta/\delta} = 123.9$  lbm/sec (56.2 kg/sec);  $P_{16}^*/P_6^* = 1.561$   
 $P_0 = 1754$  lbf/ft<sup>2</sup> (83,900 N/m<sup>2</sup>);  $T_0 = 509.4^\circ R$  (283 K)

Pressure Data					Temperature Data				
% Span	17°	110°	200°	287°	% Span	60°	117°	237°	330°
10	1.6989	1.6828	1.6782	1.6360	10	1.2169	1.2138	1.2060	1.2213
30	1.7081	1.6710	1.6505	1.5786	30	1.1880	1.1790	1.1692	1.2021
50	1.5428	1.5282	1.5092	1.4627	50	1.1664	1.1655	1.1566	1.1856
70	1.4962	1.4799	1.4671	1.4402	70	1.1533	1.1533	1.1482	1.1743
90	1.5214	1.5100	1.4954	1.4615	90	1.1687	1.1710	1.1650	1.1920
MR	1.594	1.574	1.561	1.516	MR	1.1784	1.1762	1.1689	1.1952

PT. 7-70-02  $W\sqrt{\theta/\delta} = 113.8$  lbm/sec (51.6 kg/sec);  $P_{16}^*/P_6^* = 1.670$   
 $P_0 = 1802$  lbf/ft<sup>2</sup> (86,100 N/m<sup>2</sup>);  $T_0 = 496.0^\circ R$  (275 K)

Pressure Data					Temperature Data				
% Span	17°	110°	200°	287°	% Span	60°	117°	237°	330°
10	1.8659	1.8193	1.8012	1.7125	10	1.2265	1.2248	1.2193	1.2279
30	1.7260	1.7303	1.7243	1.6578	30	1.2016	1.1980	1.1943	1.2130
50	1.6247	1.6243	1.6197	1.5875	50	1.1913	1.1907	1.1865	1.2085
70	1.6142	1.6151	1.6129	1.5888	70	1.1883	1.1896	1.1885	1.2129
90	1.6065	1.6147	1.6131	1.5944	90	1.2158	1.2129	1.2120	1.2108
MR	1.694	1.684	1.677	1.629	MR	1.2057	1.2038	1.2007	1.2212

Table XXXI (Cont'd) Circumferential Distribution of Total Pressure Ratio and Total Temperature Ratio at The Second-Stage Stator Exit (Circumferentially Distorted Inlet Flow)

## WAKE RAKE DATA

Circumferential Position - Degree

PT. 7-10-02  $W\sqrt{\theta/\delta} = 184.6 \text{ lbn/sec (83.7 kg/sec)}$ ;  $P_{16}^*/P_6^* = 2.494$  $P_0 = 1488 \text{ lbf/ft}^2 (71,000 \text{ N/m}^2)$ ;  $T_0 = 500.4^\circ \text{R (278}^\circ \text{K)}$ 

## Pressure Data

% Span	20°	47°	77°	110°	137°	170°	197°	230°	260°	287°	320°	347°
10	2.7982	2.7648	2.7798	2.7695	2.7605	2.7577	2.7408	2.7261	2.5928	2.4782	2.5016	2.7267
30	2.7828	2.7351	2.7009	2.7184	2.6969	2.6768	2.6721	2.6396	2.4616	2.4390	2.5132	2.7328
50	2.3754	2.3997	2.3789	2.3580	2.3719	2.3373	2.3598	2.3178	2.2323	2.2778	2.3387	2.4446
70	2.4115	2.4236	2.4274	2.4042	2.4116	2.3808	2.3987	2.3676	2.2627	2.3134	2.3794	2.4385
90	2.3736	2.3696	2.3610	2.3623	2.3548	2.3529	2.3459	2.3342	2.2542	2.2947	2.4244	2.4397
MR	2.560	2.545	2.536	2.531	2.525	2.511	2.511	2.485	2.368	2.360	2.432	2.557

## Temperature Data

% Span	30°	57°	90°	120°	147°	180°	207°	240°	267°	297°	330°	357°
10	1.4714	1.4384	1.4538	1.4644	1.4421	1.4255	1.4347	1.4359	1.4105	1.4403	1.4624	1.4709
30	1.4220	1.3982	1.4066	1.4164	1.4004	1.3834	1.3920	1.3612	1.3631	1.4271	1.4406	1.4481
50	1.3852	1.3732	1.3773	1.3882	1.3762	1.3558	1.3730	1.3503	1.3516	1.4286	1.4353	1.3787
70	1.3612	1.3533	1.3603	1.3744	1.3632	1.3427	1.3611	1.3322	1.3467	1.4281	1.4284	1.3565
90	1.4172	1.4040	1.4126	1.4176	1.4043	1.3925	1.4087	1.3828	1.3893	1.4622	1.4597	1.4040
MR	1.4112	1.3941	1.4024	1.4125	1.3978	1.3804	1.3946	1.3687	1.3728	1.4375	1.4454	1.4028

PT. 7-10-03  $W\sqrt{\theta/\delta} = 176.0 \text{ lbn/sec (79.8 kg/sec)}$ ;  $P_{16}^*/P_6^* = 2.701$  $P_0 = 1530 \text{ lbf/ft}^2 (73,050 \text{ N/m}^2)$ ;  $T_0 = 609.6^\circ \text{R (283}^\circ \text{K)}$ 

## Pressure Data

% Span	20°	47°	77°	110°	137°	170°	197°	230°	260°	287°	320°	347°
10	2.9448	2.8400	2.9462	2.9424	2.9393	2.9123	2.9046	2.8761	2.6962	2.5387	2.5531	2.6699
30	2.6668	2.7379	2.7815	2.8010	2.8153	2.7958	2.8105	2.7752	2.6540	2.6267	2.6484	2.7033
50	2.5619	2.5910	2.5934	2.6009	2.6047	2.5907	2.5995	2.5835	2.5451	2.6037	2.6733	2.5812
70	2.6631	2.6316	2.6229	2.6272	2.6592	2.6208	2.6486	2.6167	2.5737	2.6325	2.7591	2.7080
90	2.6722	2.6761	2.6399	2.6735	2.6637	2.6690	2.6566	2.6567	2.6041	2.6660	2.8673	2.7410
MR	2.709	2.698	2.722	2.734	2.741	2.722	2.726	2.705	2.615	2.621	2.728	2.688

## Temperature Data

% Span	30°	57°	90°	120°	147°	180°	207°	240°	267°	297°	330°	357°
10	1.4593	1.4414	1.4307	1.4225	1.4287	1.4240	1.4219	1.4196	1.4097	1.4335	1.5064	1.5169
30	1.4241	1.4166	1.4101	1.3936	1.3974	1.3920	1.3966	1.3885	1.3810	1.4349	1.4882	1.4952
50	1.4187	1.4193	1.4028	1.3928	1.3960	1.3930	1.3925	1.3901	1.3900	1.4638	1.4814	1.4624
70	1.4533	1.4277	1.4111	1.3935	1.3928	1.3887	1.3898	1.3888	1.3868	1.4777	1.4908	1.4333
90	1.4811	1.4639	1.4568	1.4339	1.4287	1.4319	1.4277	1.4319	1.4232	1.5048	1.5187	1.4509
MR	1.4499	1.4353	1.4221	1.4083	1.4095	1.4067	1.4065	1.4035	1.3995	1.4646	1.4978	1.4651

PT. 7-90-03  $W\sqrt{\theta/\delta} = 145.8 \text{ lbn/sec (66.1 kg/sec)}$ ;  $P_{16}^*/P_6^* = 2.338$  $P_0 = 1669 \text{ lbf/ft}^2 (79, \text{N/m}^2)$ ;  $T_0 = 608.8^\circ \text{R (284}^\circ \text{K)}$ 

## Pressure Data

% Span	20°	47°	77°	110°	137°	170°	197°	230°	260°	287°	320°	347°
10	2.5084	2.4735	2.4992	2.5006	2.4851	2.4901	2.4697	2.4654	2.3520	2.2392	2.2835	2.4053
30	2.3237	2.3709	2.3873	2.3726	2.4006	2.3911	2.3981	2.3939	2.3152	2.3065	2.3251	2.3522
50	2.2187	2.2542	2.2566	2.2810	2.2856	2.2863	2.2797	2.2871	2.2490	2.2797	2.2999	2.2436
70	2.2861	2.2661	2.2727	2.2958	2.3035	2.2886	2.2964	2.2867	2.2590	2.3009	2.3483	2.3029
90	2.3106	2.2997	2.2995	2.3208	2.3160	2.3253	2.3197	2.3201	2.2941	2.3336	2.4012	2.3216
MR	2.335	2.336	2.347	2.356	2.359	2.358	2.353	2.351	2.294	2.297	2.339	2.328

## Temperature Data

% Span	30°	57°	90°	120°	147°	180°	207°	240°	267°	297°	330°	357°
10	1.3802	1.3779	1.3583	1.3524	1.3507	1.3465	1.3504	1.3465	1.3378	1.3570	1.3865	1.4039
30	1.3568	1.3607	1.3412	1.3308	1.3320	1.3240	1.3260	1.3185	1.3189	1.3528	1.3848	1.3910
50	1.3576	1.3567	1.3454	1.3326	1.3325	1.3273	1.3282	1.3230	1.3229	1.3711	1.3867	1.3796
70	1.3850	1.3744	1.3613	1.3503	1.3387	1.3407	1.3325	1.3353	1.3299	1.3669	1.4031	1.3742
90	1.4136	1.4002	1.3975	1.3837	1.3656	1.3731	1.3588	1.3648	1.3559	1.4071	1.4332	1.3955
MR	1.3809	1.3756	1.3626	1.3514	1.3447	1.3421	1.3399	1.3387	1.3338	1.3765	1.4015	1.3888

PT. 7-10-13  $W\sqrt{\theta/\delta} = 106.6 \text{ lbn/sec (48.3 kg/sec)}$ ;  $P_{16}^*/P_6^* = 1.692$  $P_0 = 1868 \text{ lbf/ft}^2 (89,200 \text{ N/m}^2)$ ;  $T_0 = 612.5^\circ \text{R (284}^\circ \text{K)}$ 

## Pressure Data

% Span	20°	47°	77°	110°	137°	170°	197°	230°	260°	287°	320°	347°
10	1.8557	1.8507	1.8382	1.8259	1.8216	1.8152	1.8088	1.7989	1.7458	1.7300	1.7681	1.8142
30	1.7369	1.7293	1.7297	1.7408	1.7278	1.7109	1.7177	1.7239	1.6854	1.6704	1.7044	1.7160
50	1.6519	1.6406	1.6457	1.6585	1.6495	1.6564	1.6443	1.6446	1.6249	1.6128	1.6504	1.6373
70	1.6374	1.6348	1.6418	1.6456	1.6474	1.6461	1.6438	1.6378	1.6286	1.6184	1.6487	1.6227
90	1.6281	1.6306	1.6340	1.6439	1.6415	1.6454	1.6391	1.6449	1.6262	1.6231	1.6431	1.6276
MR	1.708	1.704	1.702	1.706	1.701	1.704	1.694	1.693	1.660	1.656	1.683	1.688

## Temperature Data

% Span	30°	57°	90°	120°	147°	180°	207°	240°	267°	297°	330°	357°
10	1.2234	1.2236	1.2154	1.2126	1.2169	1.2117	1.2146	1.2084	1.2038	1.2093	1.2196	1.2295
30	1.2026	1.2017	1.1958	1.1937	1.1970	1.1925	1.1957	1.1882	1.1872	1.2015	1.2062	1.2079
50	1.1984	1.1954	1.1926	1.1902	1.1902	1.1899	1.1897	1.1899	1.1840	1.2011	1.2084	1.2016
70	1.2155	1.2075	1.2033	1.2002	1.1970	1.1986	1.1964	1.1965	1.1927	1.2107	1.2211	1.2179
90	1.2478	1.2336	1.2343	1.2275	1.2227	1.2260	1.2203	1.2236	1.2200	1.2323	1.2507	1.2299
MR	1.2184	1.2129	1.2089	1.2054	1.2054	1.2043	1.2039	1.2014	1.1984	1.2115	1.2236	1.2222

## DISTRIBUTION LIST

1. NASA-Lewis Research Center  
 21000 Brookpark Road  
 Cleveland, Ohio 44135  
 Attention:
 

Report Control Office	MS 5-5	1
Technical Utilization Office	MS 3-19	1
Library	MS 60-3	2
Fluid System Components Div.	MS 5-3	1
Compressor Branch	MS 5-9	5
W. L. Stewart	MS 3-5	1
R. S. Ruggeri	MS 5-9	1
M. J. Hartmann	MS 5-9	1
W. A. Benser	MS 5-9	1
D. M. Sandercock	MS 5-9	1
L. J. Herrig	MS 501-4	1
T. F. Gelder	MS 5-9	1
C. L. Ball	MS 5-9	1
L. Reid	MS 5-9	1
L. W. Schopen	MS 500-206	1
C. L. Meyer	MS 60-4	1
C. H. Winzig	MS 5-3	1
W. L. Beede	MS 5-3	1
D. W. Drier	MS 21-4	1
E. E. Bailey(AAMRDL)	MS 77-5	1
N. T. Musial	MS 500-311	1
  
2. NASA Scientific and Technical Information Facility  
 P. O. Box 33  
 College Park, Maryland 20740  
 Attention: Acquisitions Branch 10
  
3. NASA Headquarters  
 Washington, D. C. 20546  
 Attention: N. F. Rekos (RLC) 1

DISTRIBUTION LIST (Cont'd)

4. U. S. Army Aviation Material Laboratory  
Fort Eustis, Virginia 23604  
Attention: John White 1
  
5. Headquarters  
Wright-Patterson AFB, Ohio 45433  
Attention: A. J. Wennerstrom ARL/LF 1  
S. Kobelak, AFAPL/TBP 1  
R. P. Carmichael, ASD/XRHP 1
  
6. Department of the Navy  
Naval Air Systems Command  
Propulsion Division, AIR 536  
Washington, D. C. 20360 1
  
7. Department of Navy  
Bureau of Ships  
Washington, D. C. 20360  
Attention: G. L. Graves 1
  
8. NASA-Langley Research Center  
Technical Library  
Hampton, Virginia 23365  
Attention: Mark R. Nichols 1  
John V. Becker 1
  
9. The Boeing Company  
Commercial Airplane Group  
P. O. Box 3707  
Seattle, Washington 98124  
Attention: G. J. Schott, G-8410, MS 73-24 1

DISTRIBUTION LIST (Cont'd)

10. Douglas Aircraft Company  
3855 Lakewood Boulevard  
Long Beach, California 90801  
Attention: J. E. Merriman  
Technical Information Ctr. CI-250
11. Pratt & Whitney Aircraft  
Florida Research & Development Center  
P. O. Box 2691  
West Palm Beach, Florida 33402  
Attention: J. Brent  
H. D. Stetson  
W. R. Alley  
R. E. Davis  
R. W. Rockenbach  
B. A. Jones  
J. A. Fligg
12. Pratt & Whitney Aircraft  
400 Main Street  
East Hartford, Connecticut 06108  
Attention: R. E. Palatine  
T. G. Slaiby  
H. V. Marman  
M. J. Keenan  
B. B. Smyth  
A. A. Mikolajczak  
Library (UARL)  
W. M. Foley (UARL)
13. Allison Division, GMC  
Department 8894, Plant 8  
P. O. Box 894  
Indianapolis, Indiana 46206  
Attention: J. N. Barney U-26  
G. E. Holbrook T-22  
J. A. Korn T-26  
R. F. Alverson U-28  
Library S-5  
A. Medlock U-28  
P. Tramm U-23

DISTRIBUTION LIST (Cont'd)

14. Northern Research and Engineering  
219 Vassar Street  
Cambridge, Massachusetts 02139  
Attention: K. Ginwala 1
15. General Electric Company  
Flight Propulsion Division  
Cincinnati, Ohio 45215  
Attention: D. Prince H-79 1  
J. F. Klapproth H-42 1  
J. W. McBride H-44 1  
L. H. Smith H-50 1  
J. B. Taylor J-168 1  
Technical Information CTR. N-32 1  
Marlen Miller H-50 1  
C. C. Koch H-79 1
16. General Electric Company  
1000 Western Avenue  
Lynn, Massachusetts 01910  
Attention: D. P. Edkins - Bldg. 2-40 1  
F. F. Ehrich - Bldg. 2-40 1  
L. H. King - Bldg. 2-40 1  
R. E. Neitzel- Bldg. 2-40 1  
Dr. C. W. Smith - Library  
Bldg. 2-40M 1
17. Curtiss-Wright Corporation  
Wright Aeronautical  
Wood-Ridge, New Jersey 07075  
Attention: S. Lombardo 1  
G. Provenzale 1

DISTRIBUTION LIST (Cont'd)

18. AiResearch Manufacturing Company  
402 South 36th Street  
Phoenix, Arizona 85034  
Attention: Robert O. Bullock 1  
          W. F. Waterman 1  
          Jack Erwin 1  
          Don Seyler 1  
          Jack Switzer 1  
          G. L. Perrone 1
19. AiResearch Manufacturing Company  
2525 West 190th Street  
Torrance, California 90509  
Attention: R. Kobayashi 1  
          Bob Carmody 1  
          Library 1  
          R. Jackson 1
20. Union Carbide Corporation  
Nuclear Division  
Oak Ridge Gaseous Diffusion Plant  
P. O. Box "P"  
Oak Ridge, Tennessee 37830  
Attention: R. G. Jordan 1  
          D. W. Burton, K-1001, K-25 1
21. Avco Corporation  
Lycoming Division  
550 South Main Street  
Stratford, Connecticut 06497  
Attention: Clause W. Bolton 1
22. Teledyne CAE  
1330 Laskey Road  
Toledo, Ohio 43601  
Attention: Eli H. Benstein 1  
          Howard C. Walch 1



DISTRIBUTION LIST (Cont'd)

23. Solar  
San Diego, California 92112  
Attention: P. A. Pitt  
          J. Watkins  
1  
1
24. Goodyear Atomic Corporation  
Box 628  
Piketon, Ohio 45661  
Attention: C. O. Langebrake  
2
25. Iowa State University of Science & Tech.  
Ames, Iowa 50010  
Attention: Professor George K. Serovy  
          Dept. of Mechanical Engineering  
1
26. Hamilton Standard Division of United  
Aircraft Corporation  
Windsor Locks, Connecticut 06096  
Attention: Mr. Carl Rohrbach  
          Head of Aerodynamics and  
          Hydrodynamics  
1
27. Westinghouse Electric Corporation  
Small Steam and Gas Turbine Engineering B-4  
Lester Branch  
P. O. Box 9175  
Philadelphia, Pennsylvania 19113  
Attention: Mr. S. M. DeCorso  
1
28. Williams Research Corporation  
P. O. Box 95  
Walled Lake, Michigan 48088  
Attention: J. Richard Joy  
          Supervisor, Analytical Section  
1

**DISTRIBUTION LIST (Cont'd)**

29. Lockheed Missile and Space Company  
P. O. Box 879  
Mountain View, California 94040  
Attention: Technical Library 1
30. Eaton Research Center  
26201 Northwestern Highway  
Southfield, Michigan 48076  
ATTN: Librarian 1
31. Chrysler Corporation  
Research Office  
Dept. 9000  
P. O. Box 1118  
Detroit, Michigan 48231  
Attention: James Furlong (418-19-40) 1  
Ronald Pampreen (418-38-31) 1
32. Elliott Company  
Jeannette, Pennsylvania 15644  
Attention: J. Rodger Schields  
Director-Engineering 1
33. California Institute of Technology  
Pasadena, California 91109  
ATTN: Prof. Duncan Rannie 1

**DISTRIBUTION LIST (Cont'd)**

34. Massachusetts Institute of Technology  
Cambridge, Massachusetts 02139  
Attention: Dr. J. L. Kerrebrock 1
35. Caterpillar Tractor Company  
Peoria, Illinois 61601  
Attention: J. Wiggins 1
36. Penn State University  
Department of Aerospace Engineering  
233 Hammond Building  
University Park, Pennsylvania 16802  
Attention: Prof. B. Lakshminarayana 1
37. Texas A&M University  
Department of Mechanical Engineering  
College Station, Texas 77843  
Attention: Dr. Meherwan P. Boyce P.E. 1